STRENGTH AND COMPRESSIBILITY OF GRANULAR MATERIALS UNDER GENERALISED STRAIN CONDITIONS

VOLUME I

thesis submitted to the
University of London
Imperial College of Science and Technology

for the degree of

Doctor of Philosophy in the Faculty of Engineering
by

Gordon E. Green, B.Sc.(Durham), M.S. (Northwestern).

March 1969

ABSTRACT

An apparatus in which the 3 principal stresses acting on a cuboidal shaped sand specimen could be independently controlled was developed. Two pairs of principal stresses were applied through rigid flat plattens whereas the third pair were applied through the flexible rubber membrane sample sheath. To overcome the effects of friction at a rigid platten, a sandwich of two lubricated natural rubber membranes was interposed between it and the specimen. In this new independent stress control (ISC) apparatus the intermediate principal stress, σ_2' , was varied between σ_1' and σ_3'.

In order to justify the lubricated membrane technique applied to the ISC tests an extensive series of drained triaxial compression and extension tests on cylindrical and cuboidal specimens of varying proportions and degrees of end restraint were first performed. These tests showed that cylindrical specimens 4 ins diameter, 4 ins high and cuboidal specimens of dimensions; width, B = 3.0 ins, width C = 2.1 ins and height, H = 3.3 ins, were satisfactory for the Ham River sand used, provided 2/0.010 ins thick lubricated membranes were interposed at each rigid boundary.

The drained ISC tests on initially dense specimens in which σ_2' was varied show comparable strengths to the triaxial compression tests as $b \rightarrow 0$; where $b = (\sigma_2' - \sigma_3')/(\sigma_1' - \sigma_3')$. The strength rises rapidly by 5.0° up to plane strain, $0.2 < b < 0.3$, and thereafter remains constant as $b \rightarrow 1.0$. Cylindrical triaxial extension test specimens give a 2.0° higher ϕ' whereas the cuboidal triaxial extension test specimens give a 4.9° higher ϕ' than in triaxial compression, i.e. the ISC tests close to $b = 1$ show almost exactly the same increase in ϕ' above triaxial compression

as do the cuboidal triaxial extension tests. The linear and volumetric strains obtained by extrapolating the ISC test data to b = 0 and b = 1.0 indicate that the conventional triaxial compression and extension tests underestimate these strains by a factor of 2 or more.

The extended Tresca and extended von Mises failure criteria are shown to be entirely unacceptable. A potentially more useful theory is that due to Parkin, based on particulate mechanics, which predicts a variation in ϕ' similar in form to that observed. The Mohr-Coulomb criterion tends to underestimate the strength over most of the range of b values.

ACKNOWLEDGEMENTS

The research for this thesis was carried out in the Civil Engineering Department, headed by Professor A.W.Skempton, F.R.S., at Imperial College of Science and Technology, University of London. The writer was supervised by Professor A.W.Bishop.

During 1962 and 1963 the writer held a D.S.I.R. Research Studentship followed in 1964 by a Research Assistantship provided by the College. The research was completed and this thesis was written whilst the writer held the post of Lecturer in Civil Engineering at the college from 1965.

The writer is greatly indebted to Professor Bishop, his supervisor, colleague and friend, for his many helpful suggestions and discussions throughout the experimental work and whilst preparing this thesis.

Other members of the academic staff and research students who have contributed in stimulating discussions and comments include Dr.N.R. Morgenstern, Mr.A.E.Skinner and Mr.S.W.Smotrych. The assistance of the soils laboratory staff together with the main workshop staff is gratefully acknowledged in respect of development and construction of apparatus. Miss J.Gurr was responsible for photographs of the apparatus; those of failed specimens being taken by the writer. Dr.J.S.Tchalenko kindly provided the photomicrographs for Plate 5.1.

Many others have contributed directly and indirectly. The labour of checking the final text was greatly eased by the careful typing of Mrs.A.Nash.

List of Contents

		Page
	Title Page	i
	Abstract	ii
	Acknowledgements	iv
	List of Contents	v

VOLUME I

Chapter 1	Purpose and extent of the investigation	
1.1	The relevance to field problems of strength and deformation characteristics measured in laboratory tests.	1
1.2	The scope of this investigation.....	2
1.3	The research programme	4
1.4	Some aspects of the notation and method of presentation.	6
Chapter 2	The strength of granular materials under various 3-dimensional stress systems	
2.1	Non-uniformities and errors in conventional triaxial strength tests.	8
2.1.1	Piston friction.....	8
2.1.2	Sample sheath rigidity.....	8
2.1.3	Filter paper drains.....	9
2.1.4	Sample sheath penetration.....	9
2.1.5	Stress measurements.....	10
2.1.6	Pore pressure effects in clays	10
2.1.7	Platten friction	11
2.1.8	Stress and strain variations within a specimen	12
2.1.9	Stress gradients within a specimen	14
2.1.10	Axial loading condition.....	15
2.1.11	Equality of radial and tangential stresses.....	16
2.1.12	Initial non-uniformities due to difficulties in sample preparation.	19
2.1.13	Specimen anisotropy.....	20
2.2	Theories concerning platten friction	21
2.3	Experiments concerning platten friction and sample proportions.	25

2.3.1	Techniques which have been tried with varying degrees of success.	25
2.3.2	Some techniques tried for concrete and rock.....	27
2.3.3	Lubricated plattens and varying H/D ratio.....	28
2.3.3.1	Experiments on sands.....	29
2.3.3.2	Experiments on clays	32
2.4	Failure theories applied to soils	36
2.4.1	Theories based on continuum mechanics.....	37
2.4.1.1	Mohr-Coulomb, extended Tresca and extended von Mises theories.	37
2.4.1.2	Some other theories.....	38
2.4.2	Theories based on particulate mechanics.....	41
2.4.2.1	Some theories based on ordered packings of spheres.....	41
2.4.2.2	Stress-dilatancy theory	42
2.4.2.3	Some other theories.....	44
2.5	Comparative strengths in triaxial compression and extension.	44
2.5.1	Experiments on sands.....	45
2.5.2	Experiments on clays.....	49
2.6	Comparative strengths in triaxial compression and plane strain.	50
2.6.1	Experiments on sands.....	51
2.6.2	Experiments on clays.....	54
2.7	Comparative strengths as σ_2' is varied continuously between σ_1' and σ_3'.	56
2.7.1	Experiments on cuboidal specimens.....	57
2.7.1.1	Sands.....	57
2.7.1.2	Clays.....	61
2.7.2	Experiments on hollow cylindrical specimens.....	62
2.7.2.1	Sands.....	62
2.7.2.2	Clays.....	65
2.7.2.3	Torsion tests on solid cylinders.....	66
2.8	Important factors involved in developing an adequate independent stress control test.	66

Chapter 3	Preliminary study of the mode of deformation of cylindrical triaxial compression test samples	
3.1	Ideal shear test samples.....	69
3.2	Shape factor for a cylindrical triaxial compression sample.	69
3.3	Previous work.....	70
3.4	Test results.....	70
3.5	Review of mode of deformation.....	73
Chapter 4	Design, development and description of apparatus	
4.1	Triaxial cell for cylindrical compression tests.....	75
4.1.1	Introduction.....	75
4.1.2	Enlarged loading plattens.....	75
4.1.3	Sample sheath.....	76
4.1.4	Internal axial proving ring.....	76
4.1.5	Cell design.....	78
4.2	Triaxial cell for cylindrical extension tests.....	79
4.3	Triaxial cell for cuboidal compression and extension tests.	79
4.4	Independent stress control cell.....	80
4.4.1	Important factors in design.....	80
4.4.2	Cell.....	81
4.4.3	Internal axial proving ring.....	82
4.4.4	Axial loading plattens.....	83
4.4.5	Sample sheath.....	84
4.4.6	Independent stress control belt.....	84
4.4.6.1	Proving ring.....	84
4.4.6.2	Hydraulic ram.....	85
4.4.6.3	Belt and plattens.....	85
4.4.6.4	Suspension wires.....	86
4.4.6.5	Encapsulated dial gauges.....	86
4.5	General arrangement of testing apparatus.....	87
Chapter 5	Description of material tested	
5.1	Particle size analysis and specific gravity.....	88
5.2	Particle breakdown.....	89

Chapter 6	Test programme	
6.1	Introduction.....	90
6.2	Cylindrical triaxial compression test series, 4 ins diameter samples.	92
6.2.1	1st series.....	92
6.2.1.1	Type X, Tests X/1 & X/3 to X/13.....	92
6.2.1.2	Type A, Tests A/1 to A/16.....	92
6.2.1.3	Type B, Tests B/1 to B/9.....	92
6.2.1.4	Type C, Tests C/1 to C/7.....	93
6.2.1.5	Type D, Tests D/1 to D/3.....	93
6.2.1.6	Type B1, Tests B1/1 to B1/4.....	93
6.2.1.7	Type E, Tests E/1 to E/4.....	93
6.2.2	2nd series.....	93
6.2.2.1	Type SA, Tests SA/1 to SA/4.....	94
6.2.2.2	Type SB, Tests SB/1 to SB/5.....	94
6.2.2.3	Type SC, Tests SC/1 & SC/2.....	94
6.2.2.4	Type SD, Tests SD/1 & SD/2.....	94
6.2.2.5	Type SD1, Tests SD1/1 & SD1/2.....	94
6.2.2.6	Type SE, Tests SE/1 & SE/2.....	94
6.2.2.7	Type SF, Tests SF/1 & SF/2.....	95
6.3	Cylindrical triaxial compression and extension test series, 4 ins diameter specimens.	95
6.3.1	Type H, Tests H/1 to H/7, triaxial compression.....	95
6.3.2	Type HA, Tests HA/1 to HA/6, triaxial compression, decreasing σ_3'.	95
6.3.3	Type EX, Tests EX/1 to EX/12, triaxial extension.....	96
6.3.4	Type EL, Tests EL/1 to EL/3, triaxial extension	96
6.3.5	Type ELA, Tests ELA/1 to ELA/4, triaxial extension	96
6.4	Cuboidal triaxial compression and extension test series.	97
6.4.1	Type IB, Tests IB/1 to IB/6, cylindrical triaxial compression.	97
6.4.2	Type IA, Tests IA/1 to IA/10, triaxial compression.....	97
6.4.3	Type IC, Tests IC/1 to IC/4, triaxial compression	97
6.4.4	Type ICE, Tests ICE/2 & ICE/4 to ICE/10, triaxial extension.	98
6.5	Independent stress control test series, cuboidal samples.	98

6.5.1	Type ISC	98
6.5.1.1	Tests ISC/1 to ISC/3	98
6.5.1.2	Tests ISC/4 to ISC/7	99
6.5.1.3	Tests ISC/8 to ISC/18	99
6.5.1.4	Tests ISC/19 & ISC/20	99
6.5.2	Type IC, Tests IC/5 & IC/6	99
Chapter 7	Preparation of samples, test procedure and calculations	
7.1	Specimen preparation	100
7.1.1	Cylindrical samples	100
7.1.1.1	Normal sample	100
7.1.1.2	Two halves sample	102
7.1.2	Cuboidal samples	103
7.2	Test procedure	105
7.2.1	Cylindrical triaxial compression tests	105
7.2.2	Cylindrical triaxial extension tests	107
7.2.3	Cuboidal triaxial compression and extension tests	107
7.2.4	Independent stress control tests	108
7.3	Shear test calculations	111
7.3.1	All tests	111
7.3.2	Cylindrical samples	112
7.3.3	Cuboidal triaxial compression and extension samples	113
7.3.4	Cuboidal independent stress control samples	114
Chapter 8	Cylindrical triaxial compression test results and discussion	
8.1	Introduction	115
8.2	1st series of tests	116
8.2.1	Type X	116
8.2.2	Type A	117
8.2.3	Type B	118
8.2.4	Type C	118
8.2.5	Type D	119
8.2.6	Type E	119
8.2.7	Type B1	120
8.3	2nd series of tests	120

8.4	Comparison of stress-strain and volume change curves...	121
8.5	Comparison of residual strengths.....	124
8.6	Comparison of failure characteristics - 1st series of tests.	125
8.6.1	Comparison of peak strengths.....	127
8.6.2	Comparison of axial strains at failure	129
8.6.3	Comparison of volumetric strains at failure	130
8.6.4	Comparison of volumetric strain rates at failure	131
8.7	Comparison of failure characteristics - 2nd series of tests.	131
8.8	Influence of end restraint and H/D ratio	133

Chapter 9	Cylindrical triaxial compression and extension test results and discussion	
9.1	Introduction.....	136
9.1.1	Type H.....	138
9.1.2	Type HA.....	138
9.1.3	Type EX.....	139
9.1.4	Type EL	140
9.1.5	Type ELA	141
9.2	Comparison of stress-strain and volume change curves ..	141
9.3	Comparison of failure characteristics.....	143
9.4	Comparison of peak strengths.....	145
9.5	Comparison of axial and lateral strains at failure	148
9.6	Comparison of volumetric strains at failure	149
9.7	Comparison of volumetric strain rates at failure	149
9.8	Influence of end restraint, H/D ratio and stress path .	150

Chapter 10	Cuboidal triaxial compression and extension test results and discussion	
10.1	Introduction	152
10.1.1	Type IB	154
10.1.2	Type IA	154
10.1.3	Type IC	155
10.1.4	Type ICE	156
10.2	Comparison of stress-strain and volume change curves ..	157
10.3	Comparison of failure characteristics	158

10.4	Comparison of peak strengths	162
10.5	Comparison of axial and lateral strains at failure	165
10.6	Comparison of volumetric strains at failure	166
10.7	Comparison of volumetric strain rates at failure	167
10.8	Influence of end restraint and H/D ratio	167
Chapter 11	Independent stress control test results and discussion	
11.1	Introduction	170
11.2	Plane strain tests: ISC belt plattens fixed, $\Delta B/B_0 = 0$.	173
11.3	Belt plattens opening, $\Delta B/B_0 < 0$	175
11.4	ISC belt plattens closing, $\Delta B/B_0 > 0$	176
11.5	Plane strain tests: axial plattens fixed $\Delta H/H_0 \doteq 0$	179
11.6	Control tests, Type IC	179
11.7	Comparison of stress-strain and volume change characteristics.	180
11.8	Comparison of peak strengths	182
11.9	Comparison of axial and lateral strains at failure	187
11.10	Comparison of volumetric strains at failure	190
11.11	Comparison of volumetric strain rates at failure	191
11.12	Variation of the intermediate principal stress	193
11.13	Comparison of results with some failure theory predictions.	200
11.14	Stress paths in σ_3' = constant space	204
11.15	Correlation of stresses and strains	206
Chapter 12	Summary and conclusions	
12.1	Introduction	210
12.2	Preliminary tests	210
12.3	Cylindrical triaxial compression tests	210
12.4	Cylindrical triaxial compression and extension tests...	210
12.5	Cuboidal triaxial compression and extension tests	211
12.6	Independent stress control tests	212
	List of references	215

VOLUME II

Appendix A1	Equivalent coefficient of friction of lubricated plattens	
A1.1	Choice of lubricant and number of membranes	235
A1.2	Theoretical analysis	235
A1.3	Method of measurement of equivalent μ	236
A1.4	Test technique	237
A1.5	Test results	237
A1.6	Comparison with previous work	237
Appendix A2	Non-uniformity of initial sample porosity	
A2.1	Porosity measurements within samples	239
A2.2	Methods of sample preparation	240
A2.3	Porosity measurements using suction probe	240
A2.4	Test technique	240
A2.5	Test results	241
A2.6	Effect of initial porosity variations on shear behaviour.	242
Appendix A3	Calibration of apparatus	
A3.1	Electro-mechanical stability of proving rings ...	243
A3.1.1	Temperature effect	243
A3.1.2	Zero stability	244
A3.1.3	Long term stability	244
A3.2	Load calibration of proving rings and pressure gauge.	245
A3.2.1	Proving rings	245
A3.2.2	Proving ring calibrator	245
A3.2.3	Accuracy of calibration	246
A3.2.4	Calibration curves	247
A3.2.5	Lateral loads	247
A3.2.6	Ambient pressure	247
A3.2.7	Pressure gauge	248
A3.3	Compressibility of proving rings and lubricated membrane sandwiches.	248

A3.3.1	Axial proving ring in the triaxial cell	248
A3.3.2	Axial proving ring in the ISC cell	249
A3.3.3	ISC belt	250
Appendix A4	Isotropic compression of Belgium Sand	
A4.1	Introduction	251
A4.2	Testing technique	251
A4.3	Test results	251
A4.4	Relation to previous work	252
Appendix A5	Cylindrical triaxial compression tests on glass ballotini	
A5.1	Introduction	254
A5.2	Test programme	254
A5.3	Test results	255
Appendix A6	Sample sheath strength and platten friction corrections	
A6.1	Introduction	258
A6.2	Triaxial compression and extension tests	259
A6.3	Independent stress control tests	259
Appendix A7	Typical test computations	
A7.1	Cylindrical triaxial compression	262
A7.2	Cuboidal triaxial extension	264
A7.3	Independent stress control	266
Appendix A8	Graphical presentation of cylindrical triaxial compression test results	269
Appendix A9	Graphical presentation of cylindrical triaxial compression and extension test results	270
Appendix A10	Graphical presentation of cuboidal triaxial compression and extension test results	271
Appendix A11	Graphical presentation of independent stress control test results	272

"The experiment serves two purposes, often independent one from the other: it allows the observation of new facts, hitherto either unsuspected, or not yet well defined; and it determines whether a working hypothesis fits the world of observable facts." RENE J.DUBOS.

CHAPTER 1

PURPOSE AND EXTENT OF THE INVESTIGATION

1.1 The relevance to field problems of strength and deformation characteristics measured in laboratory tests

The cylindrical triaxial compression test is probably the most common laboratory test used to determine the strength and deformation characteristics of a soil. The information obtained is then used in an analysis of a field problem. It is of fundamental importance that we obtain the actual results that we set out to measure and that they are relevant to the problem in hand. Unfortunately this is by no means true at present. The stress or strain conditions that are applied to a soil in the laboratory are frequently different from those existing in the field. In addition there are imperfections in the design of the laboratory testing apparatus so that the stresses really acting on the sample are not those that are intended.

In an ideal cylindrical triaxial test the 3 principal effective stresses are known throughout the test, drainage conditions can be controlled and failure is not forced to occur on any predetermined surface. The intermediate principal stress, σ_2', is either equal to the minor principal stress, σ_3', a cylindrical triaxial compression test, or is equal to the major principal stress, σ_1', a cylindrical triaxial extension test. However symmetrical stress conditions exist in only a few field situations, for example, on the axis of square and circular footings or piles. In many practical cases an approximately plane strain condition, $e_2 = 0$ exists and σ_2' is not equal to either σ_1' or σ_3', for example in slopes, earth dams, retaining walls and strip footings. For these situations a laboratory plane strain test is clearly more relevant. However the triaxial test on a cylindrical specimen is a conveniently performed laboratory test whereas plane strain conditions are much more difficult to impose on a sample in the laboratory.

In addition to situations in which symmetrical stress or plane strain conditions obtain there exists the more general class of field problem in which the relative value of the intermediate principal stress, σ_2', is varying from point to point, for example beneath square or

circular footings or piles and excavations. It is also of great basic research interest to study the behaviour of a particulate material subjected to generalised strain conditions. It may not be possible at the present time to employ a rigorous analysis of a field problem involving a continuously varying intermediate principal stress. Before this can be done it is a prerequisite to establish what influence, if any, a variation of σ_2' between the limits σ_1' and σ_3' has on the behaviour of a soil sample. Triaxial compression, extension and plane strain are but particular cases of the more general problem, albeit they are very significant conditions. The laboratory behaviour of soils under these specific conditions is indicative of, and must correlate with, the behaviour in a test in which the 3 principal stresses are independently varied.

1.2 The scope of this investigation

The primary object of this investigation was to develop an apparatus in which the 3 principal stresses acting on a soil sample could be independently controlled. There are two significant problems to be solved. The first is to devise a method of applying known normal boundary stresses to the sample without undesirable shear stresses being imposed on it as well. The second is to be able to analyse the stresses within the sample with a reasonable degree of certainty since they can not easily be measured directly. Two basically different approaches appear to be possible. In the first a hollow cylindrical specimen is subjected to differential internal and external pressures plus an axial load or torsional load or both. This method was rejected since the stress analysis is non-rigorous and failure does not occur simultaneously throughout the specimen even in an ideal test. The second approach is to load a cuboidal shaped specimen such that the boundary stresses are principal stresses and the specimen can be said to possess point-like attributes. This was the method adopted.

For a cuboidal shaped specimen, there are three obvious methods of applying the boundary tractions, either through rigid flat plattens or flexible membranes or a combination of both. If either rigid flat plattens or flexible membranes are used alone it appears to be very difficult to avoid interference of adjacent loading systems along the 12 edges of the specimen. One advantage of using flexible membranes is that

the boundary stresses are uniform, independent of whether the sample is homogeneous or not, or whether its boundaries are slightly irregular or not. If non-tilting rigid flat plattens are used the sample must be sufficiently homogeneous, its boundaries must be sufficiently flat and, in addition, some method of reducing the boundary friction to an acceptable level is needed to ensure a relatively uniform normal stress across the boundary. The method selected was to interpose a sandwich of two thin natural rubber membranes lubricated with silicone grease between the specimen and a rigid, flat, polished stainless steel platten on two pairs of faces. On the third pair of faces the specimen was stressed by the cell fluid acting on the sample sheath. No mechanical difficulty arises at the junction of a flexible boundary and a rigid boundary. At the junction of two rigid boundaries it is possible by using slightly different sized plattens for the various types of test to arrange that there is always a small gap present throughout. The soil was able to arch across this gap whilst lateral expansion or contraction was not restricted.

In order to justify the lubricated membrane technique applied to the independent stress control tests, an extensive series of triaxial compression and extension tests on cylindrical and cuboidal specimens of varying proportions and degree of end restraint were first performed. In the conventional cylindrical triaxial test the effect of end restraint on the measured strength is minimised by using a height to diameter ratio, $H/D = 2$, or thereabouts. However there is evidence to suggest that strains are much more sensitive to inadequacies in the apparatus and that generally the strains required to reach failure in a conventional test are seriously underestimated. With reduced end restraint it should be possible to obtain much more uniform strains both up to and perhaps even beyond failure and to be able to justifiably reduce the H/D ratio to 1 or even lower. A similarly proportioned cuboidal specimen should also give acceptable results. Having reduced end restraint to an insignificant amount it is necessary to investigate as well the best method of conveniently preparing a specimen. An obvious criterion is to aim at a method which results in the most uniform lateral deformations up to and preferably beyond failure.

A basic difficulty in this research is that we are looking for small differences in strength and deformation characteristics between a number

of slightly varying test types. It is vital that extraneous errors are not present of a sufficient magnitude to significantly affect the measured changes. As far as possible all known factors affecting the results are quantitatively accounted for.

In essence the design and development of the independent stress control cell is a logical amalgamation of two existing ideas. It is a combination of the greased rubber membrane technique to reduce friction at a boundary, apparently first used in soil testing by Roscoe (1953), with the Imperial College plane strain apparatus devised by Bishop and Wood, Wood (1958).

Having obtained data on the strength and compressibility of the soil under generalised strain conditions it remains to examine the data in the light of currently available failure theories. These theories may be divided into two classes. There are those based on continuum mechanics which are largely adapted from theories initially developed for metals. These only relate to the strength (c', ϕ') at failure and do not encompass strains. Secondly there are the more fundamental theories based on particulate mechanics which aim at relating the stress-strain behaviour to the interparticle friction and type of packing etc.

1.3 The research programme

The main investigation was carried out on one material, saturated Ham River sand tested in shear under drained conditions. The results are strictly speaking only valid for this material. However there appears to be no reason to believe that it is atypical of sands or particulate materials, e.g. glass ballotini. The preliminary investigation described in Chapter 3 was on Belgian sand, Sable de Mol, Ladanyi (1960), Wade (1963), since the Ham River sand was not available at the time. This investigation was carried out to determine the influence of the method of preparation of the sample on the mode of deformation of 4 ins diameter, 4 ins high triaxial compression specimens with lubricated ends.

In the first stage of the main investigation, Chapter 8, the influence of the degree of end restraint, height to diameter ratio, H/D, and mode of sample preparation on the behaviour of cylindrical triaxial compression test specimens was studied. It was aimed at establishing

whether a specimen of H/D ratio equal to 1 with lubricated ends would give a satisfactory measure of the strength. In addition, it was of great interest to examine the influence on the measured strains and strain rates of modifying the specimen shape and of improving the degree of uniformity of the stresses applied to the sample.

Having established a satisfactory cylindrical triaxial compression test specimen shape and type of end condition, a similar investigation was carried out on cylindrical triaxial extension test specimens, Chapter 9. It is noted that both of these studies were on specimens having a wide range of initial porosities. It was found that a 4 ins diameter, 4 ins high sample with 2/0.010 ins thick lubricated membranes at each end was adequate for both types of test.

In the third stage of the investigation, Chapter 10, the influence of the degree of end restraint and sample proportions on the behaviour of cuboidal triaxial compression and extension test specimens was examined. The study was confined to initially dense samples due to difficulties in testing technique. It was found that a cuboidal specimen of approximate dimensions; width, B=3.0 ins, width, C=2.1 ins and height, H = 3.3 ins was most suitable. This size of specimen was therefore subsequently used in the independent stress control tests in which σ_2' was varied between its limits σ_1' and σ_3' ; again for initially dense specimens only.

The fourth stage of the investigation, Chapter 11, was concerned with the independent stress control (ISC) tests proper. Using the apparatus designed by the writer the strain in the e_2 direction was controlled such that σ_2' varied from σ_1' to σ_3' . The specimen size quoted above was used with 2/0.010 ins thick lubricated membranes on each axial platten and 1/0.010 ins thick lubricated membrane plus the sample sheath (0.013 ins thick) on each lateral - belt platten. The intermediate principal stress, σ_2', and strain, e_2, were measured throughout. The results were compared and contrasted with the cylindrical and cuboidal triaxial compression and extension test data. The results were, in addition, interpreted with reference to a number of failure theories of current interest.

1.4 Some aspects of the notation used and method of presentation

There is apparently unavoidable ambiguity in some of the terms used in this thesis. In soil testing the word 'triaxial' is associated with a shear test in which 3 principal stresses are applied to a soil sample. Two of the stresses are always equal although this is not explicit in the word 'triaxial'. To use the word 'triaxial' in describing a new test in which all three principal stresses may be different is considered to be inconvenient and is certainly confusing. One might use the term 'true triaxial' for the new test, but this is cumbersome. The description chosen for the new test in which all three principal stresses may be varied was the 'independent stress control test', which is conveniently abbreviated to the 'ISC' test.

In the conventional triaxial compression test specimen the axial boundary is strain-controlled whereas the intermediate and minor principal stresses, $\sigma_2' = \sigma_3'$, are applied directly by the cell pressure across a stress-controlled boundary. It is assumed that the axial stress, σ_1', is uniform and is not affected by the rigidity of the platten, especially when lubricated membranes are used. Similar conditions appertain in a triaxial extension test specimen but with $\sigma_1' = \sigma_2'$ and σ_3' as the axial stress. Both are mixed boundary conditions. In the ISC test two pairs of boundaries are strain-controlled and the third pair is stress-controlled. In all the tests, although they are in part strain-controlled, the analysis presumes 3 principal stresses to be acting. However since the ISC test is predominantly strain-controlled the title of the thesis refers to 'generalised strain conditions'.

The cylindrical samples are defined in a conventional manner by the diameter, D, and the height, H. The cuboidal samples are defined by the height, H, the width in the direction of the ISC belt, B, and the width in the direction of the pair of stress controlled boundaries (i.e. the cell pressure), C. For convenience these definitions for the cuboidal samples apply whether or not the ISC belt was actually used. Thus in the cuboidal triaxial compression tests we refer to the sample widths B & C.

It was considered that generally it was more convenient to denote strains by the symbols $\Delta H/H_0$, $\Delta B/B_0$, $\Delta C/C_0$, $\Delta D/D_0$, $\Delta V/V_0$, rather than to use e_1, e_2, e_3, e_v. By this means the readers attention is focussed

on the physical soil specimen rather than the more abstract strain co-ordinate system. On the other hand the stresses appear to be more conveniently denoted by σ_1', σ_2' & σ_3', dashes implying that they are effective stresses. In connection with the strains a sign convention is necessary and is as follows. Accepting compressive stresses as being positive then a reduction in a linear dimension gives rise to a positive linear strain and a reduction in volume to a positive volumetric strain. The latter is contrary to common practice but appears to be more logical. In order to aid the reader volumetric strain versus axial strain curves are plotted in the conventional manner so that the volumetric strain scale is negative upwards, e.g. see Fig A 8.1. The stress-strain and volume change curves for each test are included in the thesis to form as complete a record as possible.

CHAPTER 2

THE STRENGTH OF GRANULAR MATERIALS UNDER VARIOUS 3-DIMENSIONAL STRESS SYSTEMS

2.1 Non-uniformities and errors in conventional triaxial strength tests

The possible errors that may arise in the interpretation of a triaxial test on soil may be classified into two main groups. There are those which we are generally aware of and for which an allowance can be made with some degree of certainty. Secondly there are those that we may or may not be aware of but about which it is more difficult, if not impossible, to make a quantitative estimate.

2.1.1 Piston friction

Consider some of the former group. The error in the measured axial load due to piston friction in a fixed bushing may be reduced by making a nominal correction based on experiment, Rutledge (1947), Bishop & Henkel (1957), Olsen & Campbell (1967). The uncertainty may be reduced by using a rotating bushing, Wood (1958), Andreson & Simons (1960), Bishop et al (1965); or a ball bushing, Warlam (1960), Duncan & Seed (1967). Alternatively the error may be eliminated by measuring the load inside the cell, Taylor, (1941), Casagrande & Shannon (1948), Nash & Dixon (1960), Sparrow & Beatty (1964), Green (1964), Barden & Khayatt (1966). The second method is, in principle, a better method provided the device used to measure the axial load inside the cell is sufficiently insensitive to lateral loads.

2.1.2 Sample Sheath Rigidity

The rigidity of the rubber sample sheath contributes to the measured stresses and a correction should be made. Provided the sample deforms relatively uniformly, the method given by Henkel & Gilbert (1952) based on a no volume change condition may be used, Bishop & Henkel (1957), Shockley & Ahlvin (1960). Alternatively the volumetric strain may be accounted for, Duncan & Seed (1967), although the effect is small. Duncan & Seed (1967) also give equations for the sample sheath strength

corrections for a cuboidal plane strain test. The sample sheath strength may be minimised by (a) using a thin natural rubber latex sheath, (b) using a large sample, and (c) testing at a high stress level, see Appendix A6. If a single shear plane is formed the sample sheath will be subject to large localised strains, the analyses of which are conflicting, La Rochelle (1960,1967), Chandler (1966b), Blight (1967a).

2.1.3 Filter paper drains

Associated with the strength correction for the sample sheath is a strength correction for the filter paper drains used in a drained test on clay, Bishop & Henkel (1957), Olsen & Kiefer (1963), Duncan & Seed (1967). Drained extension tests on clays using filter paper drains are a particularly difficult problem, Sowa (1963). Furthermore the permeability of the filter paper drains relative to that of the sample may require consideration, Blight (1963a), Bishop & Gibson (1963). Sample sheath and filter paper drain corrections are both serious problems when testing small clay samples at low stress levels. Duncan & Seed (1967) show a striking example of the effect of applying corrections to triaxial test data in the analysis of the long term stability of a 16° slope of San Francisco Bay mud. An analysis based on uncorrected data gives a factor of safety of 1.64 whereas using corrected data gives 1.04

2.1.4 Sample sheath penetration

The volume changes measured on granular media coarser than about 0.1mm mean diameter will be significantly affected by penetration of the sample sheath into the interstices between the grains, Newland & Allely (1957,1959), Roscoe et al (1963). Approximate corrections may be made for this error based upon experiment or theory. During the shear stage in a drained test on sand in which the cell pressure is maintained constant this error does not occur so that in this thesis, with the exception of Type HA tests, the problem does not arise. For the Type HA tests the effect is neglected since it is so small, Lee (1966).

2.1.5 Stress measurements

A problem which is apparently not so commonly recognised is that of obtaining reliable and comparable load and pressure measurements, particularly if one is comparing triaxial compression and extension test results. The axial load measuring device is commonly calibrated against a standard proving ring or in a calibrated compression testing machine. The cell pressure may be measured with a bourdon gauge, manometer or a dead weight tester. There will be errors in these two measurements which in general will not be the same. Since the directions, and therefore the mode of measurement, of the major and minor principal stresses are reversed in the triaxial compression & extension tests, different errors in the calibrations will have a significant effect on the measured strengths. It is desirable to calibrate both devices against the same standard so that even if the 2 stresses are not absolutely correct their relative values are comparable, see Appendix A3.

2.1.6 Pore pressure effects in clays

Consider now some of the second class of errors about which less appears to be generally known. When testing clays the question of non-uniform pore water pressures within the sample arises due to the low permeability of clay. In an undrained test the pore water pressure is often measured at the ends of the sample whereas failure occurs near mid-height. During shear the pore water pressures will almost certainly vary within the sample due to the time lag in their equalisation, Bishop et al (1960 a,b), Barden & McDermott (1965), Blight (1965). The non-uniformity of the pore water pressure will also vary with the degree of end restraint imposed on the sample, Blight (1961, 1963a,b, 1965), Barden (1963), Casagrande & Poulos (1964) Barden & McDermott (1965). These are two quite separate sources of pore pressure non-uniformity, although in practice it is difficult to separate their effects. However a testing rate based solely on the degree of equalisation of pore water pressure with time as determined by Gibson (1961) will be inadequate. Also some materials may fail along a single narrow zone and give rise to additional pore water pressure non-uniformity, Bishop et al (1960a), Bishop & Henkel (1957). The rates of testing selected for a drained test will be simi-

larly affected by the above factors. A detailed discussion of these points is given by Bishop & Henkel (1957).

2.1.7 Platten friction

The difficulty in isolating pore water pressure effects from other possible test errors can be entirely overcome by testing a more permeable material, e.g. sand. In drained tests on Ham River Sand, Fig 5.1, the rate of dissipation of non-uniform excess pore water pressures is very rapid and an axial rate of strain of about 10% per hour for drained triaxial compression is more than sufficient to ensure complete drainage. Any non-uniformities in stress within the conventional triaxial test may now be attributed largely to platten friction which causes visible barrelling of the sample at large strains. It is usually assumed in soils triaxial testing that the effect of end restraint on the measured strength is reduced to negligible proportions by adopting a H/D ratio for the sample of about 2, Taylor (1941), Waterways Experiment Station (1947), Bishop & Henkel (1957), Hvorslev (1957, 1960). Similar proportions have been used for testing rocks and concrete, e.g. Nadi (1950), Newman & Lachance (1962). However, although the strengths measured may be reliable, the strains at which these strengths are developed are probably in error, Roscoe et al (1963a).

It is important to distinguish between the errors that may occur at failure and beyond failure at large strains. At large strains the sample may be so badly distorted, Newland & Allely (1957), Cornforth (1961), Roscoe et al (1963a), Sowa (1963), that the validity of any interpretation of the stresses may be doubtful. At failure the degree of non-uniformity will be much less severe in the case of triaxial compression, Bishop (1966), but may still be a significant problem in triaxial extension, Cornforth (1961), Sowa (1963). Since the axial load carried by every horizontal section through the sample is the same, it follows that the average stress acting on a horizontal section near the midheight must be less than on a similar section near the ends. Observations show that the failure occurs near midheight where the stresses are apparently minimum, Olsen (1962). It may be argued that for triaxial compression the area of a plane inclined at $(45-\phi'/2)$ degrees to the axis of the specimen. and passing through the

centre of the 'barrelled' portion, is closely equal to the average area based on a uniform deformation assumption. The error at failure is therefore considered to be small, Bishop & Henkel (1957), Olsen (1962), Bishop (1966), although opinion is by no means unanimous, Roscoe et al (1959). In triaxial extension tests the errors are generally more serious due to necking, Eldin (1951), Cornforth (1961), Sowa (1963), Barden & Khayatt (1966). It is possible to stop the test at, or close to, failure and to carefully measure the shape of the necked portion, Eldin (1951), Cornforth (1961), in order to get a better estimate of the axial stress. Alternatively one may continually monitor the lateral deformations by externally sighting through the transparent cell wall and cell fluid with a telescope, Escario & Uriel (1961), Sowa (1963), Roscoe et al (1963a), or by means of a series of lateral strain belts, Tschebotarioff et al (1956), Amirsolymani (1966 a,b). By marking a grid on the sample sheath and photographing it at various stages during shear, Shockley (1953) showed that the porosity increased at midheight and decreased near the ends, irrespective of the initial porosity. Clearly it is to our great advantage to try to avoid these difficulties by obtaining more uniform sample deformations.

2.1.8 Stress and strain variations within a specimen

Measurements of stress, strain and density variations within samples have been made which assist in clarifying the extent and magnitude of the non-uniformities. Shockley & Ahlvin (1960) embedded W.E.S. type stress meters in a 35.7 ins diameter, 70 ins high vacuum triaxial specimen of compacted sand. For a nominal axial effective stress of 30.3 psi, two stress profiles along a radius, R, are shown, one at midheight and one near the top of the specimen. At midheight the stress was about 30 psi at the centre, increasing to about 34 psi at $\frac{1}{2}$R, then decreasing to about 20 psi at the perimeter. In the latter case the average stress measured by the gauges is much lower than the nominal 30 psi. In view of the authors claim that the stress gauges may overestimate the stress, the data appears to be unreliable. Tests were also performed using strain gauges to measure vertical strain at points within a sample. The strains are generally larger at the centre than at the periphery and are greatest

near the base, decreasing towards the top of the sample. However these strains measured over individual elements are not in aggregate equal to the average overall strain. The data is presented in such a form that this is not apparent.

A small embedded strain gauge was used by Truesdale & Rusin (1963) to measure axial and lateral strains within triaxial compression samples of both sand and clay. Their results for sand, $\sigma_3' = 10$ psi, show that both the axial and lateral strains vary markedly within the sample being greater than average at midheight and below average at the ends. Two tests results are given for compacted clay. An unconfined compression test shows similar strains at midheight and adjacent to the base, both slightly less than the average for the whole sample. A second test, $\sigma_3' = 60$ psi, shows a smaller strain at the base than at midheight or at the upper quarter point of the sample. The authors fourth conclusion appears to be wrong. The same technique was used subsequently by Januskevicius & Vey (1965) together with a small piezoelectric stress gauge. Their strain gauge data agrees with Truesdale & Rusin's results. The stress gauge results are unreliable since the gauges were too sensitive to initial placement conditions, changes in the modulus of deformation of the surrounding soil and the lateral deformations of the triaxial specimens approaching failure.

Shockley & Ahlvin (1960) also measured density variations within a 2.8 ins diameter, 6.5 ins high triaxial compression specimen of sand by quick freezing, slicing and using a volumetric displacement technique. By stopping similar tests at different stages a composite volume change pattern was obtained and was compared with an identically sectioned unsheared specimen. Whereas a dense sample exhibited an overall increase in volume the central failure zone showed a much larger increase and the ends consistently decreased in volume. A different technique was used by Cornforth (1961) to measure porosity variations within cylindrical and cuboidal saturated sand samples. Water content samples from points within sheared and unsheared specimens were obtained by carefully peeling back the rubber sheath without disturbing the specimen and removing a small sample with a spoon. Variations in porosity of up to 2% were measured in unsheared specimens together with significantly varying

changes in porosity within the specimen due to shearing. The individual water content determinations, when averaged, correlated very well with that obtained from overall measurements. In spite of this agreement, the writer feels sceptical that it is possible to sample a saturated sand without disturbing it so that its water content changes. This technique deserves further study since, if reliable, it has the overwhelming merit of simplicity.

More recently Belshaw (1967), reported by Kirkpatrick (1967) and Kirkpatrick & Belshaw (1968), measured displacements within drained triaxial compression test specimens of medium dense sand by means of X-rays and embedded lead shot. These tests showed that in tests with lubricated ends (2 layers of greased membrane) relatively homogeneous strains existed whereas if rough plattens were employed non-uniform strain conditions exist adjacent to the plattens. It is inferred that if uniform strains exist in a specimen then homogeneous states of stress are possible and are perhaps probable.

Variations in volume change due to end restraint in triaxial samples of saturated clay are more easily determined by simply slicing up the sample. Pore water migration in a compacted clay shale during undrained triaxial compression tests were demonstrated by Bishop et al (1960b) who obtained water content differences up to 2% at 25% axial strain. Rowe & Barden (1964) obtained a well defined difference of about 1.3% water content between the centre and ends of an initially uniform conventional sample of clay consolidated from the liquid limit (better than 0.1% initial water content variation). A similar variation was observed by Barden & McDermott (1965) for a compacted clay.

2.1.9 Stress gradients within a specimen

In the preceding discussion it is suggested that non-uniform deformations are predominantly associated with end restraint. There are a number of other possibilities that merit some consideration. Phalen (1960) observed that the central bulge in a conventional triaxial compression specimen is almost always displaced towards the base of the sample, see also Shockley & Ahlvin (1960), Haythornthwaite (1963a), Bishop (1966).

Phalen pointed out that the self-weight of the test specimen is normally neglected in the analysis. Including the self-weight increases the stress at the base compared with the top of the sample. The effect is very small for a conventional 1.5 ins or 4 ins diameter specimen under a lateral effective stress greater than 30 psi (say). It is much larger, and very significant, for a 12 ins diameter, 24 ins high specimen under a low lateral effective stress of 5 psi (say). Haythornthwaite (1963a) used plasticity theory to investigate the kinematics of the triaxial test. Although in general the theory admits non-coincidence of the axes of principal stress and strain, for a particular case when the axes do coincide an asymmetric velocity profile was obtained which agreed reasonably well with experimental observations. However this could not be reconciled with other aspects of plasticity theory and Haythornthwaite concluded that plasticity theory cannot adequately describe the behaviour of a granular material.

2.1.10 Axial loading condition

The development of a single well defined slip zone beyond failure appears to be partly controlled by the rigidity of the triaxial cell plus loading frame and the manner of connection between the top loading platten and the piston. Conventionally a ball or half-ball is used, Bishop & Henkel (1957). In both cases the top platten may tilt during the test if the line of action of the axial load is sufficiently eccentric and/or if a lateral load of sufficient magnitude is developed to overcome friction in the ball seating. In addition if a half-ball is used it is not unknown for lateral translation of the top platten to occur, i.e. slip occurs between the flat face of the half-ball and the piston. Alternatively the top loading platten may be prevented from tilting but is allowed to translate by inserting a layer of small ball bearings between it and the piston, Penman (1953), Chandler (1966b), Tombs (1969). All of these devices favour the development of a single slip zone in a granular material, as shown by Penman (1953), Whittke (1962), Rowe (1962), Rowe & Barden (1964). More uniform deformations may possibly be obtained and predominant slip zones may be avoided by minimising tilting of the top loading plattens. This of course complicates the measurement of the

axial load but this difficulty can be overcome using the device described in this thesis.

Recent tests by Belshaw (1967), Kirkpatrick (1967) and Kirkpatrick & Belshaw (1968) suggest that even using non-tilting plattens and lubricated ends it may be difficult to obtain a perfectly axial loading condition.

2.1.11 Equality of radial and tangential stresses

For a triaxial test on soil it is normally assumed that, neglecting end effects and in particular at midsection sufficiently remote from the ends, the sample has "point like attributes". By this we mean that for the case of triaxial compression or extension, (a) the axial stress, σ_z, is constant over the cross-section, and (b) the lateral stress is homogeneous. In particular (b) implies that $\sigma_r = \sigma_\theta$ = constant, independent of r and θ; where σ_r = radial stress and σ_θ = tangential stress - the conventional cylindrical polar co-ordinate system, Haythornthwaite (1960b). This is the heuristic hypothesis of Haar & von Karman (1909) as applied to axially symmetric problems, Haythornthwaite (1960b,c) Cox et al (1961). Now for an elastic material compressed between frictionless plattens the assumption $\sigma_r = \sigma_\theta$ is correct, Haythornthwaite (1960b). For a non-elastic material compressed between frictionless plattens it is normally considered to be true as also for the same material compressed between frictional plattens provided that the height to diameter ratio is about 2 - $2\frac{1}{2}$ and that we only consider sections remote from the ends of the specimen.

Broms (1963) suggested that for a soil the assumption is incorrect and that, even assuming there is no end restraint, $\sigma_r \neq \sigma_\theta$ and both σ_r and σ_θ vary with the radius, r . Broms postulated that for a triaxial compression test there were two possibilities. If $\sigma_r > \sigma_\theta$ then both σ_r and σ_θ would decrease as r increases whereas if $\sigma_r < \sigma_\theta$ then both σ_r and σ_θ would increase as r increases. In order to test this hypothesis it was assumed that the central core of a conventional triaxial specimen of sand with restrained ends could be removed and be replaced by water, Casbarian & Jamal (1963), Jamal (1963), Broms & Jamal (1965), all at Cornell University. The new specimen consisted of a

hollow cylinder, the inner chamber being filled with water. Since no shear stresses are assumed to act on any soil element whatever the distribution of σ_r and σ_θ, a consolidated undrained test on the new specimen should give the same strength as a similar test on a normal solid specimen if (i) the cell pressure, σ_3, and inner chamber pressure are the same for the hollow specimen and (ii) $\sigma_r = \sigma_\theta$ = constant, independent of r and θ. The test results tended to support the thesis that $\sigma_r \neq \sigma_\theta$, in fact that $\sigma_r > \sigma_\theta$, i.e. the Haar-von Kármán assumption is incorrect. However in the writer's opinion there are a number of serious objections which invalidate this conclusion. Undrained tests on sands are notoriously difficult to perform since cavitation may occur in the pore water. In addition although the overall sample may be undrained, internal redistribution of pore water will occur due to non-uniform deformations caused by end restraint. Broms and Casbarian & Jamal compared solid cylindrical samples 3 ins diameter, 6 ins high, H/D = 2, with hollow cylindrical samples of two sizes, (a) $4\frac{1}{2}$ ins high, 6 ins O.D., 3 ins I.D., and (b) 12 ins high, 6 ins O.D., 3 ins I.D. The $4\frac{1}{2}$ ins high hollow samples were used initially but were found unsatisfactory and the height was increased to 12 ins. In the latter case the overall ratio H/D = 2 but the ratio of height, H, to wall thickness, W, is 8. It appears certain that failure of the hollow cylinder would be influenced by buckling even if no end restraint occurred. The additional effect of end restraint severely accentuates the buckling problem. Indeed Casbarian & Jamal (1963) admitted that end restraints affected the behaviour of the $4\frac{1}{2}$ ins high hollow specimens in which H/W = 3. In the writer's opinion, in any hollow cylinder test used to examine the Haar-von Kármán assumption it must clearly be shown that (a) it is undrained in every element as well as overall, (b) end restraint is of negligible importance, and (c) buckling does not influence the results.

A later series of tests at Cornell University, Bemben (1966), do not appear to clarify these problems. A hollow cylindrical sample with restrained ends, 4 ins O.D., 3 ins I.D., 8 ins high (H/D = 2, H/W = 16) was tested both in compression & extension. The sample wall thickness appears to be excessively thin. Some doubt exists concerning the air content of both the pore water and inner chamber water so that $B \neq 1$ and approximate corrections were applied to account for this. Bemben concludes

that it is virtually impossible to obtain true undrained behaviour in a consolidated undrained test due to cavitation of dissolved air, but that the true behaviour is automatically achieved by a consolidated constant volume test. The latter is incorrect unless end restraint and sample inhomogeneity are eliminated so that the overall behaviour is identical to that of an element; which was not the case in Bemben's tests.

The validity of the assumption that $\sigma_r = \sigma_\theta$ has also been discussed in his text book by Harr (1966). Harr (p 174) states, "that this deduction is in error (i.e. $\sigma_2 = \sigma_3$) is immediately apparent if we consider not a cylindrical but a prismatic shape of rectangular cross-section....." The subsequent argument does not suggest to the writer that such a deduction is in error at all. The argument appears to depend only on differences between a rectangular cartesian and a cylindrical polar co-ordinate system. Harr continues by arguing that since lateral bulging occurs, whether uniform or not; "it seems reasonable to expect that with bulging there is an associated decrease in tangential stress". Harr supports this contention by reference to unconfined compression tests on concrete cylinders, Jones (1952), Jones & Kaplan (1957), in which vertical tension cracks were observed. In neither of these two references is there any evidence to suggest that the vertical cracking was preferentially radial. In fact Jones (1952) states that for cylindrical specimens both "radial and circumferential cracks appeared". If $\sigma_\theta < \sigma_r$ then one might expect that vertical cracks would be preferentially radial, since they are not then Harrs thesis that $\sigma_r \neq \sigma_\theta$ must be considered to be illfounded.

More convincing evidence of the equality of radial and circumferential strains is given by Belshaw (1967), Kirkpatrick (1967), Kirkpatrick & Belshaw (1968). Embedded lead shot, monitored by transmission X-rays, were used to show that radial displacements were directly proportional to radial distances in triaxial compression tests on 9 ins diameter, 9 ins high specimens of medium dense dry sand, provided adequately lubricated plattens were used (2 greased rubber membranes). A constant radial strain implies, from the equations of equilibrium, that the radial and circumferential strains be equal. When a rough loading platten was used at one end of the sample the radial and circumferential strains were found to be no longer equal.

2.1.12 Initial non-uniformities due to difficulties in sample preparation

It is relatively easy to obtain an initially uniform clay sample for triaxial testing. A specimen having a variation in water content less than 0.2% may be cut from a larger block of natural or artificially prepared clay, Rowe & Barden (1964). Samples of sand generally have to be formed within a mould of a size and shape identical to the desired specimen size. It is very difficult, if not impossible, at the present time to conveniently form a uniform triaxial specimen of sand, i.e. better than 0.2% porosity variation, say. It is, in addition, a major problem to measure porosity variations within a prepared sand specimen. A sand sample for a triaxial test may be formed dry or saturated; it may be poured through a tube or special funnel fitted with baffles; it may be spooned into the mould in layers and compacted by tamping or vibration. All of these techniques have been tried with various degrees of success, each having particular advantages and disadvantages, Bishop & Henkel (1957).

If a sample is initially non-uniform it is likely that this will cause non-uniform deformations to occur in addition to those caused by end restraint. Shockley & Ahlvin (1960) obtained initial porosity variations of up to 1% by compacting dry sand in layers using a variable number of blows per layer. The specimens were saturated, consolidated, frozen and disected. It is not clear whether the variations were reproducible or not but they do not appear to have had a large effect upon the subsequent behaviour.

Cornforth (1961) using the technique previously described obtained quite large variations in initial porosity in 4 ins diameter, 8 ins high triaxial specimens and in 2 ins wide, 16 ins long, 4 ins high plane strain specimens of saturated sand. Vertical variations in 4 triaxial specimens varied from 1.8% to 3.3% maximum difference in porosity whereas there was little measurable horizontal variation. The variations do not appear to correlate with the different compaction methods used. The vertical variations in one plane strain specimen compacted in 4 layers were less, 0.9% maximum difference, whereas horizontal variations of up to 2.7% occurred. In spite of these apparent variations in initial porosity the failure characteristics correlated extremely well based on the average porosity.

The effect of the mode of deposition on the lateral deformation was

examined by Amirsolymani (1969a,b). The pattern of overall diametral strains varied slightly, depending on whether the specimen was formed (a) by spooning and tamping or (b) by deposition through a funnel set at a constant height above the cell base. Unfortunately the tests were stopped at an overall axial strain of 1.4% due presumably to the limited range of the lateral deformation gauges.

Roscoe et al (1963a) observed that axial strains were affected by porosity non-uniformities more than were lateral strains. Triaxial compression tests on saturated sand specimens showed significant random variations in axial strain throughout the test whereas the lateral strain variations were controlled by end restraint. Extension test behaviour was initially similar but was dominated by necking effects at and beyond failure. Non-uniform porosities are more serious in extension tests as they probably contribute to the increased scatter in the results when compared with triaxial compression. It is possible that prior to failure in triaxial compression, i.e. in a stable stress system, the sample deforms so as to tend towards a more homogeneous state and small initial porosity variations are therefore not too important. In triaxial extension, which is an inherently unstable stress system, failure will tend to occur in the initially loosest zone of the sample. Whereas conventional compression samples usually exhibit a uniform barrel shape at and beyond failure, e.g. Shockley & Ahlvin (1960), Bishop (1966), a convoluted deformation pattern was observed by Vesic & Clough (1968) and by Eldin (1951) for extension test samples. This appears to reflect deficiencies in the method of sample preparation although none of the authors comment on this.

2.1.13 Specimen anisotropy

A triaxial specimen of sand of relatively uniform porosity may not be isotropic and the shear strength characteristics may be significantly anisotropic. Little is known about this due largely to the extreme experimental difficulties involved in distinguishing the factors involved. Anisotropy in the specimen induced by the method of preparation is a separate property from stress-induced anisotropy caused by shearing , Ko (1966). We are only concerned with the former here. Initial structural anisotropy arises from the influence of gravity and particle shape on the deposition process, Horne (1965). Non-spherical particles will be orient-

ed with respect to gravity and, in addition, the spatial arrangement of the grains may vary. Hydrostatic compression tests by Biarez (1961) on glass ballotini gave a greater stiffness in the lateral direction than in the axial direction, by as much as 30%, according to Parkin et al (1968). However, Parkin et al (1968) hydrostatically compressed dry sand deposited in air and obtained an axial stiffness as much as 5 times the radial stiffness; attributing the difference to the sample preparation technique or to the sphericity of the grains. This difference in stiffness seems excessive. Unfortunately no details of the experimental technique are available on which to try to assess its validity. Whether these differences under hydrostatic compression involving very small strains have a significant effect on the shear behaviour which involves much larger strains is not yet resolved.

Ko (1966) using a new soil testing device, was able to rotate the stress axes with respect to the mode of deposition. Little or no difference in the stress-strain behaviour was observed and Ko concluded that the degree of anisotropy in the sample induced by the method of preparation was small. However, serious deficiencies in Ko's apparatus have been pointed out by the writer, Green (1967), and by Bell (1968), Arthur & Menzies (1968), which cast some doubt on this conclusion.

Whereas the structure of clays has been studied relatively extensively, e.g. Tchalenko (1967), less appears to be known about the structure of sands. Using a carbowax impregnation technique, photographic enlargements of vertical and horizontal sections were studied by Parkin et al (1968). The orientations of the long grain axes were determined and showed that air deposited grains adopted a strongly preferential orientation with the long axes aligned in the horizontal plane. Spatial arrangements of grains may be more difficult to define and measure.

2.2 Theories concerning platten friction

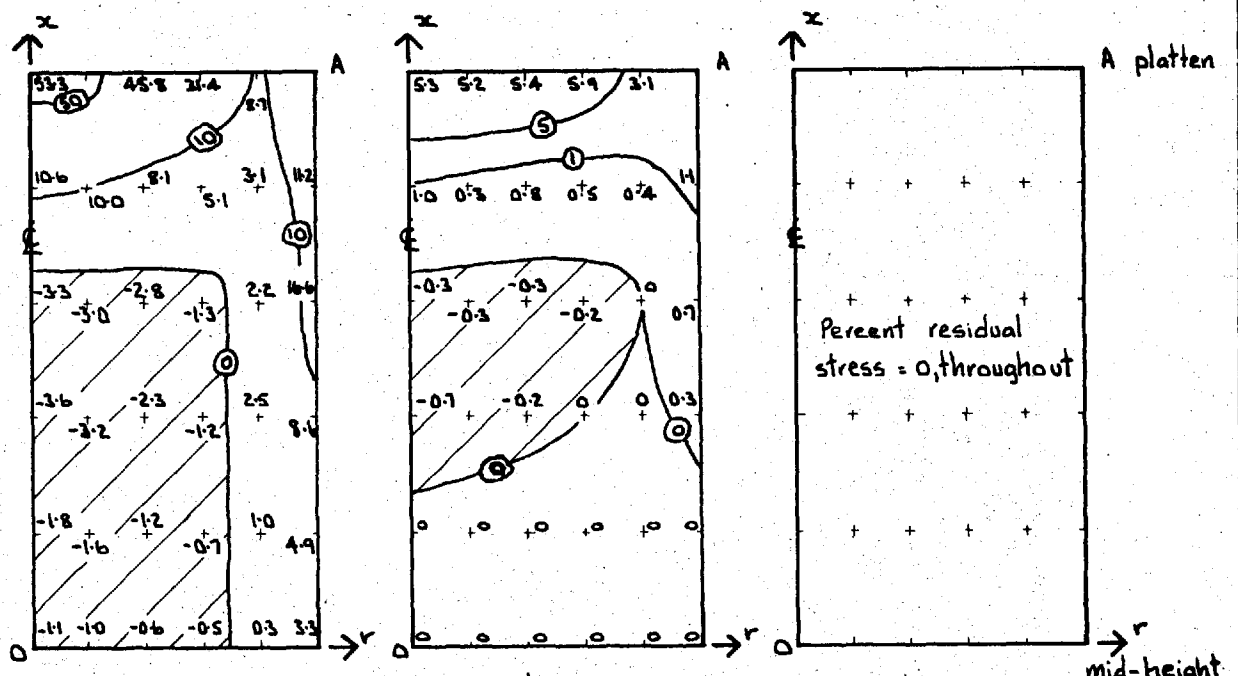
The stresses in an elastic circular cylinder compressed between perfectly smooth loading plattens of the same material and diameter as the cylinder under test will be uniform. This is true whether or not the sample is subject to an all round lateral stress. The conventional triaxial sample of soil, concrete or rock is subject to severe end restraints and it is of interest to examine theoretical solutions for such a cylinder

under differing end restraint conditions. The majority of these assume elasticity and a few extend elastic theory to include plastic domains controlled by a von Mises yield criterion. These solutions give an insight into the effect of end restraint on the stress distribution within a triaxial sample. They are however limited in as much as soil is not an elastic material and its behaviour may differ significantly from the ideal assumed.

Consider firstly those analyses involving elastic theory. Filon (1902) solved the problem of a restrained cylinder of H/D ratio $\pi/3$. The restraint imposed was a condition of zero lateral displacement of the curvilinear boundary at the two plattens (Point A in Fig 2.1). No restriction was placed on the lateral displacement of intermediate sample-platten contact points. Picket (1944) analysed a restrained cylinder of height, 2B, and radius, a, assuming that radial slipping at the ends does not occur using the Fourier method, i.e. the stresses and displacements at the boundary have a finite number of maxima and minima. Picket was unable to establish values for the stresses at the corners of the sample. He also stated the equations and indicated the method of solution for obtaining the stresses in a rectangular prism or cuboid. The same end restraint condition applied to a cylinder of H/D ratio 1:1 was studied by D'appolonia & Newmark (1951) using the lattice analogy method. The accuracy of this method is dependent on the mesh size chosen.

All the preceeding 3 solutions give similar stress patterns but are limited in two respects,(a) they are concerned only with an unconfined compression test, (b) varying degrees of end restraint can not be accounted for. The computed stresses are all based on a value for Poissons' ratio of $\frac{1}{4}$. The H/D ratio may be varied as also may Poissons' ratio, but not without difficulty as the computations must all be started again from scratch due to the basic influence of the former factor.

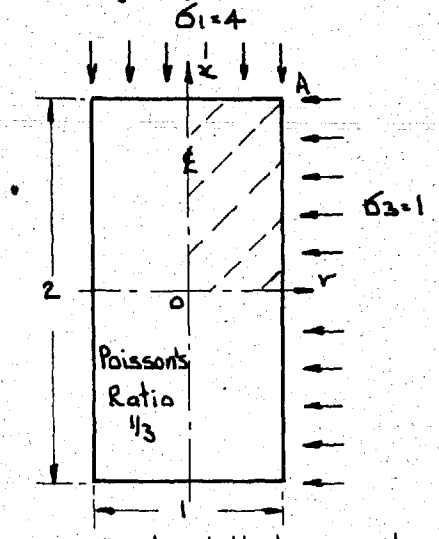
Balla (1957, 1960 a,b) obtained a solution for the stresses in an elastic cylindrical test specimen with any H/D ratio, subjected to axial and radial external stresses. The influence of end restraint was included as follows. The radial lateral displacement of the curvilinear boundary at the plattens (Point A in Fig 2.1), was assumed to vary inversely with the coefficient of surface friction and as a first approximation this variation was taken to be linear. If the plattens are perfectly smooth

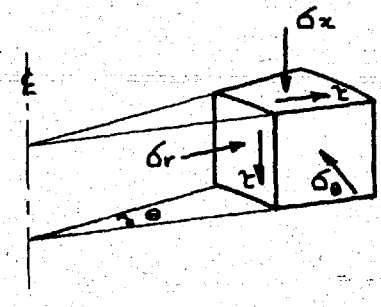


$\psi = 1.0$
Perfectly rough

$\psi = 0.1$

$\psi = 0$
Perfectly smooth





Co-ordinate system

Points plotted are % residual stress $= \dfrac{(\tau_o)_{\psi=0} - \tau_o}{(\tau_o)_{\psi=0}} \times 100\%$

where, $\tau_o = \left\{\frac{1}{6}\left[(\sigma x - \sigma r)^2 + (\sigma r - \sigma\theta)^2 + (\sigma\theta - \sigma x)^2\right] + \tau^2\right\}^{1/2}$

EFFECT OF VARYING END RESTRAINT ON THE STRESS DISTRIBUTION IN A TRIAXIAL COMPRESSION SPECIMEN

After Balla (1957, 1960 a,b)

FIG. 2.1

and frictionless the peripheral displacement attains its maximum value. If the coefficient of surface friction attains its maximum value then there is zero displacement of the peripheral boundary at the platten. These conditions were expressed as a roughness function:

$$\psi = f/f_{max} = 1 - \rho/\rho_{max}$$

where, f = coefficient of surface friction

ρ = radial displacement of peripheral boundary, of specimen at the platten.

Balla's analysis was repeated by the writer and found to be correct except for a number of apparent typographical errors which are listed in Fig 2.2. Balla failed to note the stress singularity at the peripheral boundary of the specimen at the platten, Point A, where the stresses are theoretically infinite. This in no way detracts from the value of the analysis.

Numerical solutions were only given for H/D = 2, Poisson's ratio = $\frac{1}{3}$ and for maximum roughness of the loading plattens. As with the previous solutions H/D may only be changed at the expense of complete recalculation whereas ψ may be easily varied. The effect of varying ψ is shown in Fig 2.1 using Balla's notation. It is seen that changing ψ from 1 to 0.1 results in a marked reduction in the percentage residual stress (as defined on Fig 2.1).

If $\psi = 0$ then of course the stresses are everywhere equal to σ_1 & σ_3 and the residual is zero. One may tentatively infer from these data that a reduction by a factor of 10 in the friction between a soil sample and loading plattens should significantly improve the degree of uniformity of the stress distribution within the sample, in particular adjacent to the plattens.

Balla (1960a) calculated the stress in a test specimen for H/D = 1, ψ = 1 for comparison with the I Appolonia and Newmark (1951) solution of the same problem. The agreement of the two solutions is remarkably good better than ± 4% although it is not clear whether the same value of Poissons' ratio was used in each ($\frac{1}{4}$ or $\frac{1}{3}$). Balla (1960a) also extended the elastic solution to include plastic failure according to a von Mises yield criterion for values of $1 \leq H/D \leq 2$ and $0 \leq \psi \leq 1$, for uniaxial compression. This solution suggests that even for a H/D ratio of 2, end

LIST OF APPARENT TYPOGRAPHICAL ERRORS IN BALLA'S ANALYSIS OF THE STRESS CONDITIONS IN THE TRIAXIAL COMPRESSION TEST.

This list applies to the paper first published in December 1960 in the Journal of the Soil Mechanics and Foundations Division as Proceedings Paper 2684 and reprinted in the Transactions of the American Society of Civil Engineers, 1960 as Paper 3218. There are some slight differences and this list refers specifically to the Transactions Paper No. 3218

Page 1077, equation (7) should read: $\sigma_\theta = \frac{\partial}{\partial x}\left[\mu \nabla^2 \phi - \frac{1}{r}\frac{\partial \phi}{\partial r}\right]$

Page 1079, equation (20) should read: $\frac{1}{1+\mu} E\rho = \frac{-\mu}{1+\mu}\sigma_1 r + \cdots$

Page 1081, equation (33): add bracket } after $+ J_0\left(i n \pi \frac{R}{H}\right)\Big]$

Page 1082, equation (39): add bracket } after $\cdots \frac{\cos^2 n\pi}{n^2}$

Page 1084, equation (46) should read: $E\rho_{H,R} = -\mu\sigma_1 R + \cdots$
and add bracket } after $- U_n \frac{i J_0(i n \pi R/H)}{J_1(i n \pi R/H)}\Big]$

Page 1085, equation (50) should read: $\cdots \frac{\cos n\pi}{n V_n} \frac{1}{\frac{1}{i} J_1\left(i n \pi \frac{R}{H}\right)}\Big[\cdots$

equation (51) should read: $\cdots \frac{1}{\frac{1}{i} J_1\left(i n \pi \frac{R}{H}\right)}\Big[\cdots$

Page 1086, equation (53) should read: $E\xi \frac{1}{H} = \frac{x}{H}\sigma_1 - 2\mu \frac{x}{H}\sigma_3 \cdots$
$\cdots \left\{6\mu \frac{(1-\mu)}{(1+\mu)}\frac{x}{H} - 4\left(\frac{H}{R}\right)^2\left(\frac{x}{H}\right) + \cdots\right.$

equation (54) should read: $E\rho\frac{1}{R} = -\mu\frac{r}{R}\sigma_1 + (1-\mu)\frac{r}{R}\sigma_3 - \left(\frac{\mu}{1-\mu}\sigma_1 - \sigma_3\right)\psi \cdots$

Page 1088, equation (69) should read: $\phi_\xi = Q\left[\frac{6(1-\mu)}{(1+\mu)}\mu\frac{x}{H} - 4\left(\frac{H}{R}\right)^2\frac{x}{H} + \cdots\right.$

equation (70) should read: $\cdots -12(1-\mu^2)\left(\frac{H}{R}\right)^2\left(\frac{x}{H}\right)^2\frac{r}{R} + \frac{3}{2}\left(1-\mu-2\mu^2\right)\left(\frac{r}{R}\right)^3 - \cdots$

Page 1089, equation (75) should read: $\xi = \frac{H}{E}\left\{\sigma_1\left[\frac{x}{H} - \psi\mu\frac{1+\mu}{1-\mu}\phi_\xi\right]\right.$
$\left. - \sigma_3\left[2\mu\frac{x}{H} - \psi(1+\mu)\phi_\xi\right]\right\}$

FIG. 2.2

restraint still has a small but significant influence.

The stresses in a cylindrical triaxial compression test specimen for different combinations of relative stiffness of the specimen and the end plattens and for different friction properties at the contact were obtained by Egger (1965), see also Leussink (1965). General approximate solutions were developed based on elasticity and a von Mises yield criterion. It was shown that the non-uniformity in the stress pattern was very small when the sample and the platten had comparable elastic properties and attempts were made to verify the theory by measuring the contact stresses. However in the writer's opinion the latter were not sufficiently close to the predicted values to justify Egger's claim of "a satisfying coincidence with the theory".

An analysis by Sinha et al (1961) of the unconfined compression test specimen with fully restrained ends is based on elasticity and Seth's law (Seth 1941). The latter is a yield criterion of the form:

$$\sigma_1 - \sigma_3 = K_2 - K_1 \ (\sigma_1 + \sigma_2 + \sigma_3)$$

No numerical results are given. The solution and assumptions made in deriving it are not fully understood. The existence of 2 constants, K_1 & K_2, in the yield criterion appears to present some difficulty.

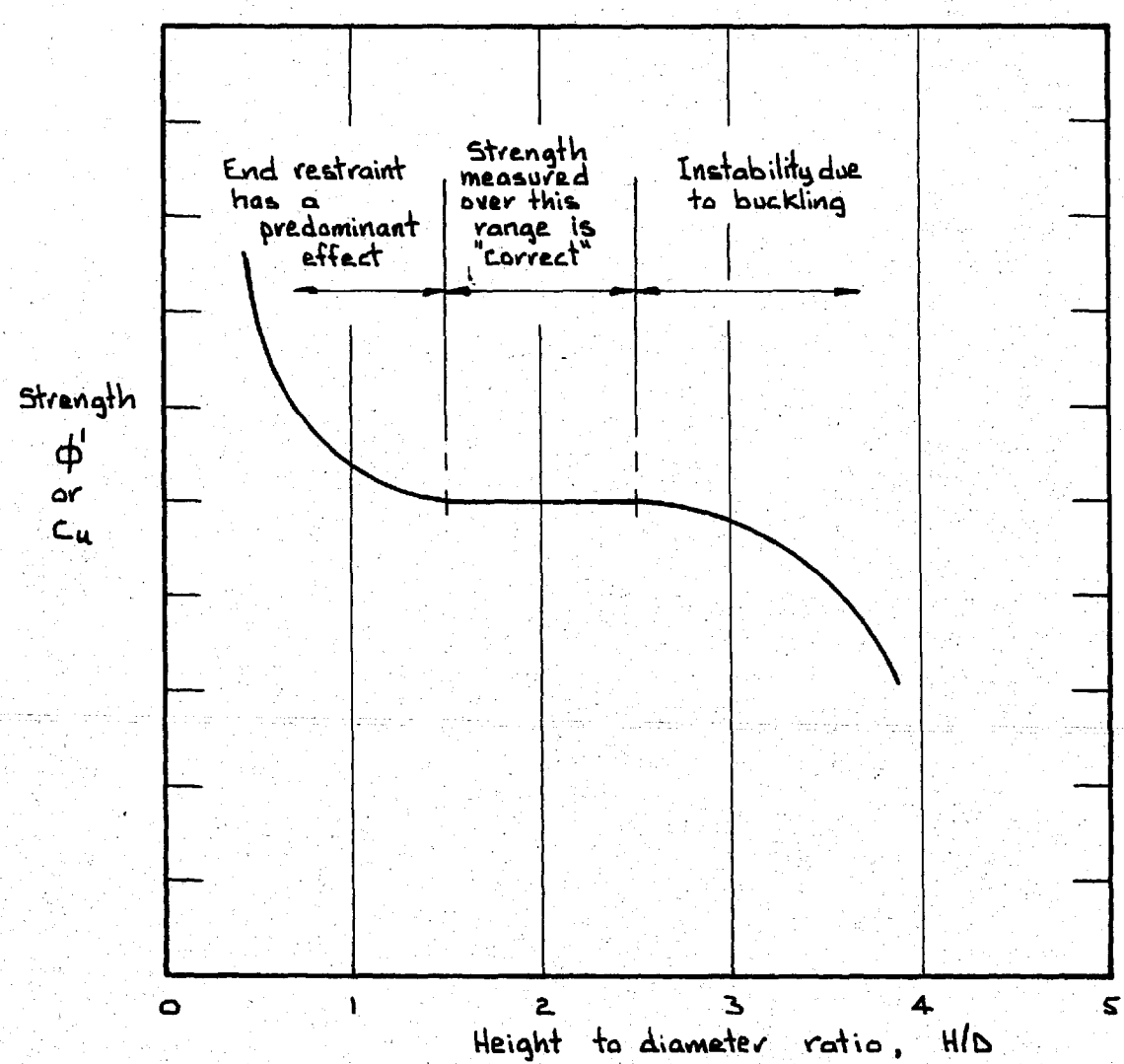
With the exception of the preceding theory, the solutions discussed all indicate that for a fully restrained cylinder of H/D = 2, stresses in the middle third are approximately uniform. If the degree of end restraint is reduced, Balla (1960a), then the uniformly stressed zone extends to form a larger portion of the specimen. This suggests that the H/D ratio could be reduced for such a sample without impairing its stress-strain behaviour. It is pertinent to note in passing that Saint-Venant's principle is frequently misinterpreted in compression testing theory. The principle, applied to the triaxial test, states that whatever distribution of the axial stress in the sample at the platten-sample interface; at a section remote from the platten the distribution of axial stress will be uniform. However the magnitude of the axial stress at points remote from the plattens will be affected by any additional shear stresses applied to the sample at the plattens due to friction. The effect may of course be small, but is not excluded by invoking Saint-Venant's principle.

2.3 Experiments concerning platten friction and sample proportions

It is conventional to test cylindrical triaxial compression specimens of soil of H/D ratio between 2 & 2.5. Current British practice favours the former ratio whereas North American practice tends towards the latter. The strength of shorter specimens will be significantly affected by end restraint and larger specimens may fail by buckling, Fig 2.3 . These proportions appear to be based on early tests summarised by Rutledge (1947) who suggested that a H/D ratio of 1.5 to 3.0 was satisfactory, together with numerous investigations of concrete and rock strength properties, e.g. Newman & Lachance (1962). In all these tests a frictional contact between specimen and platten obtained. Unpublished undrained tests by Northey at Imperial College (circa 1950) using rough non-tilting plattens, suggested that a H/D ratio between 1.5 & 2.5 would result in the 'correct' strength being measured. It is of course assumed that the horizontal portion of the curve in Fig 2.3 defines the 'correct' strength and although this is a very reasonable interpretation of the test data, it is not necessarily true that an ideally stressed test specimen would exhibit the same strength.

2.3.1 Techniques which have been tried with varying degrees of success

A number of attempts have been made in various testing devices to eliminate, or at least reduce, the frictional restraint at a soil-platten interface, Rowe & Barden (1964). A large number of slender rods loaded end-on were used by Kjellman (1936) and by Taylor (1941). The end of each rod in contact with the specimen was flat and the other end was spherical and in contact with a rigid platten. Kjellman's device was limited to about 3.2% compression strain across any loaded face due to the initial gaps between adjacent rods closing up. Both Kjellman's and Taylor's devices are, in principle, unsound in sustaining an extension across a loaded face as the rods are unstable, as Taylor observed. A segmented platten, each small segment being supported on ball bearings, was used by Tschebotarioff et al (1956) in a large triaxial cell. Little significant lateral expansion occurred as the specimen could only expand at the relatively few local joints between the rigid segments. An inferior design of segmental platten was later unsuccessfully tried by Freedman(1959).



IDEALISED RELATIONSHIP BETWEEN TRIAXIAL COMPRESSION STRENGTH AND H/D RATIO FOR SPECIMENS WITH CONVENTIONAL FRICTIONAL ENDS.

FIG. 2.3

The plattens were each divided radially into 6 equal segments or 'petal-leaves', supported on bearings. Freedman tried introducing a double layer of lead shot between a sand sample 4 ins diameter, 8 ins high and rigid plattens. Slight lateral expansion of the ends was obtained. Water-filled flexible rubber bags instead of rigid plattens were also used by Freedman. They were confined in a ring, the lateral expansion of which was controlled manually to achieve near uniform expansion of a vacuum triaxial compression sample. Slight but incomplete lateral expansion occurred. The difficulties in controlling the lateral expansion of the rubber bag and in measuring the axial strain render this technique unattractive. A related flexible membrane technique has more recently been used by Bell (1965) and Ko (1966), see Section 2.7.2.1.

Nonplaner plattens have been tried. Cooling & Golder (1940) used oiled conical plattens and Larew (1960) tried paraboloidal plattens. Conical plattens had been tried earlier for testing cylindrical specimens of rocks and concrete, Nadai (1950), the idea being that by inclining the face of the platten at an angle equal to the angle of friction between it and the specimen the resultant force on the specimen would be parallel to its axis. However for the large friction angles obtaining between sand and most metals, 30 - 40° at least, this is not a very satisfactory arrangement since the axial and lateral strains become very non-uniform.

There is an alternative approach, applicable only to a triaxial compression or extension test specimen. Amirsolymani (1966a,b) considered only the middle half of a 4 ins diameter, 8 ins high sand specimen and assumed that plane sections at the boundaries with the upper and lower specimen quarters remained plane throughout shear. This is tantamount to testing a 4 ins diameter, 4 ins high specimen between two 'sand plattens' each 4 ins diameter, 2 ins high; a technique borrowed from concrete testing and discussed later. The drawbacks to this method are that the volumetric strain of the 'specimen' cannot be measured directly and must be inferred from axial and lateral strain measurements over the middle half - no mean task. Undrained tests present special problems and the method does not appear to be capable of being extended to tests in which the three principal stresses are varied independently. Blight (1963b,1965) has used a variation of this technique suitable for undrained tests on clays. The central section of the test specimen was isolated from the end zones in

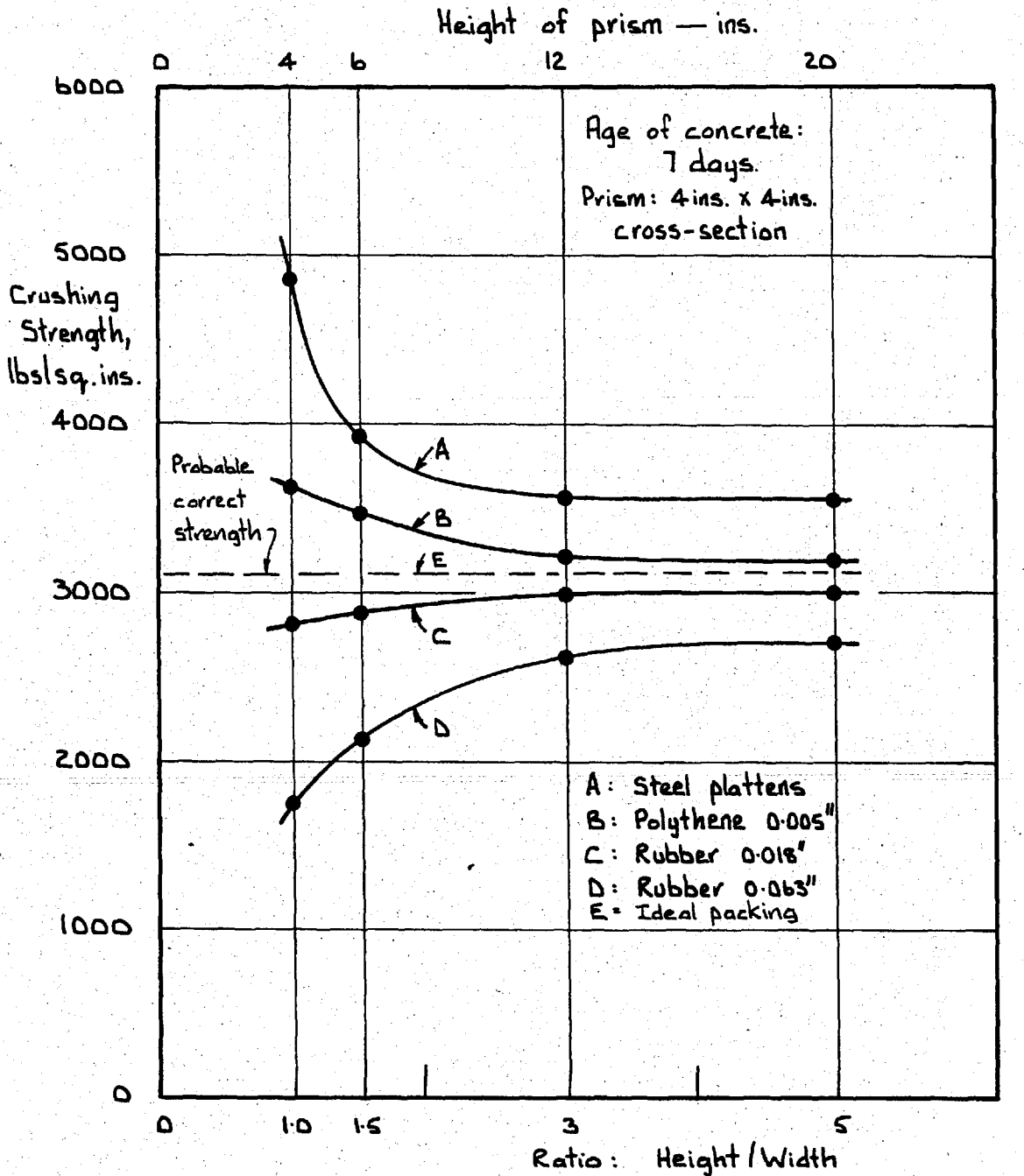
contact with the plattens. The latter were sealed in a thin coating of self-vulcanising rubber latex and were then enclosed with the central segment in a sample sheath in the usual manner. An axial sand filled hole in the lower end segment allowed pore water pressures in the central section to be measured. The technique appears to be successful for undrained tests but cannot easily be adapted to drained tests because the end segments are isolated and will remain undrained.

Direct sample contact with a low friction material has not proved altogether successful. Gray (1960) tried using Teflon (polytetrafluoroethylene) alone as a triaxial platten. Ostensibly a low friction material, it is so soft that sand grains become embedded and a high surface friction (17°) results. Limited success was obtained by Olsen & Campbell (1964) in testing clays. Polished Teflon plattens were used and the ends of the specimens were sprayed with a thin coating of Teflon. If the Teflon were unpolished and the spray coating were omitted then no improvement was obtained over the conventional test.

Unconfined compression tests on cubes of clay, Borowicka (1961), indicated that if the clay-platten interface were greased the cube deformed more uniformly and a conjugate set of visible slip zones formed. Tests on cylindrical clay specimens, Saada (1962) exhibited much more uniform strains if the ends of the samples were greased.

2.3.2 Some techniques tried for concrete and rock

There is an extensive literature pertaining to efforts to obtain uniform stresses in concrete and rock compression specimens, e.g. Newman & Lachance (1962). Consideration of some aspects of this work are relevant to the present problem. Because steel plattens and rock or concrete have different elastic properties, radial shear forces are developed at the interface, Mogi (1966). Steel being stiffer causes radial inward shear forces to act on the specimen and the introduction of a soft packing, e.g. lead, cardboard or rubber, at the interface may cause the direction of the shear forces to be reversed if the packing is squeezed out. Vertical tension cracks adjacent to the plattens are clear evidence of this. Increasing the H/D ratio will not necessarily eliminate the difficulty. Fig 2.4 shows data on concrete, Newman & Lachance (1962), which indicates that increasing the H/D ratio alone does not establish a unique strength.



VARIATION OF CRUSHING STRENGTH OF CONCRETE WITH HEIGHT OF SPECIMEN AND TYPE OF PACKING.

after Newman & Lachance (1962)

FIG. 2.4

One may speculate that the correct strength would be given by using a packing material such that the strength is independent of the H/D ratio, i.e. about 3,100 psi in this case. There appears to be no reason to believe that soil should not behave in a similar manner, if an appropriate packing were used. Experimental evidence given in Chapter 8 of this thesis indicates that this problem does not arise for the material tested at least for the stress range used.

Since rock and concrete are so stiff, irregularities at the platten-specimen interface may cause undesirable stress concentrations. This does not appear likely to occur with soil. Provided a height to width ratio of about 2 is maintained there appears to be little difference in strength between circular and square cross-sectioned concrete or rock samples although the evidence is conflicting, Newman & Lachance (1962), Berthier & Tourenq (1966). Waisted or dumb-bell shaped samples have frequently been used for testing rocks and concrete in an attempt to minimise end effects, particularly in extension tests . Their application to tests on soil, certainly on sand, seem very doubtful due to specimen preparation difficulties. A technique similar in approach to that of Blight (1963b,1965) and Amirsolymani (1966a,b) was suggested by Newman & Lachance (1962) in which a 6 ins test cube is sandwiched between 2 similar cubes which act as ideal plattens. All contact surfaces must be perfectly flat, no simple matter, and axial strains can only be measured at the exposed surface of the central cube.

2.3.3 Lubricated plattens and varying H/D ratio

The most promising technique appears to be that of interposing a thin rubber membrane between the sample and a polished plane stainless steel platten, the platten-membrane interface being lubricated with silicone grease. This was the method developed and used throughout the testing programme reported in this thesis. Roscoe (1953) used a 0.002 ins thick greased rubber membrane to reduce wall friction in the simple shear apparatus for tests on clay. More recent tests, Roscoe et al (1967), suggest that this technique was not suitable for coarse sands unless the membrane was undesirably thick. Friction at the σ_2 plattens was successfully reduced to negligible proportions, $\mu = 0.018$, in plane strain tests on cuboidal specimens by interposing a silicone grease

layer between the sample sheath and plane aluminium alloy plattens, Wood (1958), Cornforth (1961), Wade (1963), Duncan & Seed (1967). In an undrained triaxial compression test on a compacted soil Blight (1961) used a greased rubber membrane between polished brass plattens. A significant improvement in the uniformity of the pore pressure throughout the specimen was obtained.

The most extensive series of investigations on the use of a greased rubber membrane in contact with a polished metal platten to reduce end friction in triaxial tests have been performed at Manchester University, Rowe (1962), Rowe & Barden (1964).

2.3.3.1 Experiments on sands

Multiple slip zones at large strains, with little barrelling, were obtained in triaxial compression tests on 8 ins diameter, 8 ins high and 4 ins diameter, 4 ins high sand specimens by Freedman (1959) using a single thick membrane plus silicone grease (see also Fig 15 of Rowe (1962)). Gray (1960) tried different lubricants; soft soap giving the lowest effective angle of friction, 0.6°, at 14 psi normal stress. However, being water-soluble, soft soap is not a very practical proposition and silicone grease was deemed more suitable. Drained triaxial compression tests on 4 ins diameter, 4 ins high specimens of glass ballotini using silicone grease gave favourable results although interpretation of the stress-strain curve was complicated by "stick-slip" behaviour of the glass ballotini.

Rowe & Barden (1965) describe their technique for triaxial compression tests on 4 ins diameter, 4 ins high sand specimens. At each platten a thin rubber membrane (no thickness stated) plus silicone grease was used with a central $\frac{3}{4}$ ins diameter porous disc flush with the platten surface to facilitate drainage. Radial slits around the circumference of the membrane were claimed to be effective in promoting lateral expansion at large strains, but this appears to be a doubtful procedure. It was observed in early tests in which drainage was allowed at both ends of the specimen that, beyond failure, at large strains the base of the sample sometimes expanded laterally more than the top. Apparently this could often be corrected by closing the top drainage lead but for inexplicable reasons. Tests on Mersey River sand on 5 'short' specimens with lubricated plattens showed a 2° lower ϕ' value than 5 conventional 8 ins high samples,

together with larger linear and volumetric strains at failure. As the axial load was measured outside the cell and includes piston friction, which is likely to differ in the two tests, the results are subject to some uncertainty. A more limited series of tests on another sand in the same apparatus described by Freedman (1959) showed no significant difference in ϕ' between the two types of test.

Some of the difficulties associated with obtaining uniform large strains in triaxial compression specimens of sand, H/D = 1, with lubricated plattens were reviewed by Khayatt (1965). Lateral strains were found to be more uniform than with conventional specimens; dense and medium dense samples particularly so. Dense specimens expanded more at the base than at the top whereas loose specimens always expanded at the base and only marginally at the top (see also Smith (1965)). A single major slip zone did not occur, but beyond failure a conjugate set of slip zones were formed. The rate of testing had a slight influence on the uniformity of deformation as did, but to a greater degree, the method of sample preparation. Closing the top drainage lead improved the uniformity of deformation, c.f. Smith (1965), or, alternatively, so did applying a 1-2 psi back pressure.

Lee & Seed (1964) tried a number of lubricants including powdered molybdenum disulphide, molykote and silicone grease, the latter proving most effective. The thickness of the rubber was found to have a significant effect on the measured coefficient of friction. A 0.0025 ins thick membrane with fine to medium sand was unsatisfactory whereas a thickness of 0.015 ins gave a minimum measured shear strength. Increasing the thickness beyond 0.015 ins resulted in no further reduction in ϕ'. Friction tests on a 0.015 ins thick membrane plus a coarse sand gave a high ϕ' value and puncturing of the membrane was observed. The frictional resistance was found to increase if the normal load was maintained for some time. Triaxial compression tests on 50 - 100 U.S.sieve size sand in 1.4 ins diameter, 3.4 ins high specimens with and without lubricated plattens showed no significant difference in strength. Unfortunately the results of only 2 pairs of tests are shown and no "short", i.e. H/D = 1, specimens were tested.

Dense samples of medium-fine crushed feldspar were tested in drained triaxial compression, Lee (1966). Specimens were 4 ins diameter, 4 ins high with a 0.012-0.015 ins thick lubricated membrane with 3 radial slits

at each platten. The assembled plattens were preloaded to minimise subsequent bedding in the grease films. As observed by Khayatt (1965), specimens tended to expand laterally at the base more than at the top but closing the top drainage lead eliminated the difficulty. No comparisons with conventional specimens were given.

Barden & Khayatt (1966), using 4 ins diameter, 4 ins high drained sand specimens with lubricated plattens, compared behaviour in triaxial compression and extension. In extension the specimens deformed more uniformly up to failure than did conventional extension specimens. Although pre-failure necking was not eliminated the uncertainty concerning the area correction was greatly reduced. After failure a single slip zone formed, due to the unstable nature of the test, so that stress analysis is still very doubtful. The strains at failure in the extension specimens were noticeably greater than in a normal sample. Hence lubricated plattens appear to be especially advantageous in the extension test.

The strains within 9 ins diameter, 9 ins high triaxial compression specimens of dry sand were measured by Belshaw (1967), Kirkpatrick (1967), Kirkpatrick & Belshaw (1968), using embedded lead shot detected by X-rays. The displacement data obtained indicate that lubricated membranes resulted in relatively uniform strains within the specimen as compared to tests in which rough plattens were used. Some improvement was obtained with a single membrane whereas substantially uniform strains were obtained with a sandwich of two membranes at each platten.

A slightly different technique has been used in plane strain tests on rock-fill, Marsal et al (1965). Rigid plattens were used in both the σ_1' and σ_2' directions and friction between them and the rockfill (up to 3 ins gravel size particles) was reduced by interposing 3 layers of 1mm thick high-density polyethylene sheet lubricated with axle grease. The polyethylene was cut into square pieces with staggered joints to allow lateral expansion or contraction. An effective coefficient of friction, of 0.03 to 0.07 was obtained. Such a low value of μ is surprising considering the large particles and thin polyethylene sheet used.

Chapter 8 of this thesis was reported by Bishop & Green (1965).

2.3.3.2 Experiments on clays

Triaxial tests on clays using lubricated ends are more difficult to interpret than on sands due to complex pore pressure effects. Published results are conflicting due, in part, to an apparent lack of appreciation of this fact. Relatively uniform lateral deformations were obtained in an undrained triaxial compression test on compacted clay, H/D = 2, with single rubber membranes plus silicone grease and polished brass plattens, Blight (1961). It was shown theoretically, Blight (1963b), based on Filons' (1902) analysis that the pore pressure coefficient A could vary significantly in a triaxial specimen. Conventional undrained tests on a remoulded clay exhibited pore water pressures at midheight greater or less than at the ends depending on the strain and whether loading or unloading. Similar tests on a compacted clay indicated that if lubricated ends were used, the difference in pore water pressure between midheight and the ends was significantly reduced. The latter point was confirmed by Barden (1963).

Casagrande & Poulos (1964) obtained no significant improvement over conventional undrained triaxial tests when using lubricated ends. Canyon Dam clay passing a No.20 U.S. sieve was tested using one 0.002 ins thick rubber membrane and silicone grease on plattens having a 1° taper towards the centre. Friction measurements indicated unexpectedly high μ values dependent on the time of loading and initial grease film thickness. Isolated tests using a 0.010 ins thick membrane showed little improvement. It seems certain that both membranes were far too thin for the material being tested, the 0.002 ins thick membrane particularly so (see Appendix A1 of this thesis).

Undrained triaxial compression tests on weathered shale (50% clay fraction) consolidated from the liquid limit were carried out on $1\frac{1}{2}$ ins diameter, 3 ins high specimens by Rowe & Barden (1964), to study pore pressure response times. Three types of end plattens were used, (i) direct contact, (ii) a single greased rubber membrane, and (iii) identical to (ii) together with peripheral filter paper drains adjacent to the base. In all cases a $\frac{1}{8}$ ins diameter central ceramic probe in the base platten was used to measure the pore water pressure. After consolidation at 30 psi cell pressure, small incremental dead deviator loads were applied. Type (i) showed an initial high pore pressure increase which then decreased with time, type (ii) showed a slow rise in pore pressure, whereas (iii)

exhibited a rapid rise in pore pressure which subsequently remained at a constant value, to which (i) & (ii) also tended. Clearly from the point of view of pore pressure response the lubricated ends with peripheral filter paper drains are beneficial. The final pore pressures at failure were lower in type (ii) & (iii) compared with type (i) but the deviator stresses were approximately the same (no details were given). Lateral end expansion of types (ii) & (iii) occurred and in some tests one end expanded excessively so that the sample became unstable. This was reflected in water content profiles obtained after the tests. In additional constant rate of strain tests on two fissured clays the scatter in the measured undrained strengths was significantly reduced by using lubricated ends plus a slower rate of strain. Unfortunately it is not clear whether the reduced strain rate or lubrication was the major cause in minimising scatter.

Campbell (1963) and Olsen & Campbell (1964) tried various types of Teflon platten in consolidated undrained tests an $1\frac{1}{2}$ ins diameter, 3 ins high sodium kaolinite specimens (all material $<$ 20 microns). Rough Teflon, highly polished Teflon and highly polished Teflon together with a 0.0015 ins thick rubber membrane with a light coat of silicone oil were compared with conventional plattens. The degree of barrelling did not vary in any of the tests but a reduction of ϕ' of 3° was obtained using highly polished Teflon, both with and without a lubricated membrane. The failure characteristics in terms of total stresses were unaffected, the low friction plattens causing a lower shear induced excess pore water pressure. This is in agreement with Rowe & Barden (1964). Varying the H/D ratio from 1.2 to 3.6 for specimens with conventional rough ends indicated that if H/D $>$ 1.5 the reduction in ϕ' was marginal; based on either peak σ_1'/σ_3' or ($\sigma_1' - \sigma_3'$) failure criteria. However there was a difference in the absolute values of ϕ' for these two criteria of $3\text{-}3\frac{1}{2}^{\circ}$ for H/D $>$ 1.5. Unfortunately all these tests were performed at essentially the same machine rate of deformation 0.003 ins/min, i.e. the strain rate varied in the latter tests. Furthermore lubricated ends were not used, Rowe & Barden (1965). Calculations by the writer following Gibson (1961) based on coefficients of consolidation kindly supplied by Olsen (1965) of 6.4×10^{-3} and 2.1×10^{-2} cm^2/sec at 6 and 100 psi consolidation pressures respectively suggest that this

strain rate was too fast to achieve even 95% equalisation of excess pore water pressures in an ideally stressed 3 ins high specimen, Bishop & Henkel (1957). This being so Olsen & Campbell's conclusions must be treated with some reservation.

Undrained tests on silty clay using both lubricated plattens and segmental samples were performed by Blight (1965). The segmental specimens exhibited smaller pore water pressure differences between the midheight and ends than a conventional specimen. However the magnitudes of the pore water pressures in the segmental case were close to the value measured at the end in the conventional specimen and not at midheight as might be anticipated. This anomaly was not completely resolved. Evidence concerning failure behaviour appears to be conflicting. Blight's Fig 5 shows a 2° higher ϕ' for a segmental specimen and a 1° lower ϕ' for a specimen with lubricated ends, as compared with a conventional test. However the author claims later, his Fig 9, that there is no difference in strength between the different sample types.

Barden & McDermott (1965) performed undrained triaxial compression tests on 4 ins diameter, 4 ins & 8 ins high specimens of a compacted clay and of a N.C. and O.C. remoulded clay. Specimens with lubricated ends were compared with conventional samples, pore water pressures being measured at the ends and at midheight in both cases. The specimens were sheared at a slow strain rate based on 95% equalisation of excess pore water pressure, Gibson (1961), and at rates up to 70 times faster. Specimens with lubricated ends, both 4 ins & 8 ins high, gave similar pore water pressures at the ends and midheight even at the higher strain rates. The 8 ins high conventional specimens exhibited the same pore water pressure at the ends and midheight in the slow tests only; agreeing in magnitude with the lubricated ended specimens. At faster strain rates the pore water pressure at the ends and midheight differed by an increasing amount. However in contrast to Blight (1965) the end pore water pressure always agreed with that of the comparable lubricated ended specimen, i.e. tested at the same strain rate. Specimens 4 ins high tested slowly showed no significant difference in strength from similarly tested conventional 8 ins high specimens. However there was some uncertainty regarding piston friction (a fixed bushing was used) and furthermore, at failure, the effective stresses were very low due to the high pore water pressures developed.

A limited number of consolidated undrained tests on 1½ ins diameter, 1½ ins high samples of London clay with lubricated plattens showed slightly lower pore water pressures than conventional tests, but the effective stress failure envelope was unaffected, Webb(1966). Similar tests on undisturbed samples of Keuper Marl using a non-tilting top platten which could translate laterally gave an identical result, Chandler(1966a). Narain & Singh (1966) tested a saturated remoulded plastic clay in consolidated undrained compression with pore pressure measurements, obtaining apparently inconsistent results. Specimens 4 ins diameter, 8 ins high gave a $\phi' = 31.7^\circ$ in a conventional test and a $\phi' = 27.7^\circ$ when lubricated plattens were used. Conventional specimens 1½ ins diameter, 3 ins high gave a $\phi' = 30.5^\circ$ and short samples 1½ins diameter, 1½ ins high with lubricated plattens a $\phi' = 30.2^\circ$. In all cases $c' = 0$. No data is given on which a rational interpretation may be based.

Unconfined compression tests on boulder clay were reported by Jacobson (1967) using a rubber membrane on a glass platten lubricated with silicone grease. Varying the H/D ratio indicated that provided $1 < H/D < 2$ the strength was constant and equal to that of a conventional specimen. However the data is very scattered and the specimen was apparently only 3.5 cm diameter which seems far too small for a boulder clay with up to 20% small stones, 2-20 mm diameter, even assuming some of the larger stones were rejected.

The effect of platten restraint on both triaxial and plane strain compression test results was studied by Duncan & Dunlop (1968). Conventional test specimens were compared with the same sized specimens but with lubricated plattens. Unfortunately no 'short' samples were tested. Undrained tests on undisturbed San Francisco Bay mud at low stress levels (of the order of 1 kg/cm cell pressure) were performed on 1.4 ins diameter, 3.5 ins high triaxial specimens and on 1 ins x 2.8 ins wide, 2.8 ins high plane strain specimens. In both types of test lubricating the plattens apparently gave a 1° lower strength and increased the failure strains. No corrections were applied to the measured deviator stress to account for piston friction since it was argued that this correction would be the same for tests with or without lubricated plattens. This does not appear to the writer to be necessarily correct. The lateral load applied to the end of the loading piston inside the triaxial cell may be expected to be less

when lubricated plattens are used. Assuming Duncan & Dunlop used the ball bushing & piston shown in Fig 3 of Duncan & Seed (1967) and measured the piston friction by steadily driving the unloaded piston into the cell at various cell pressures as per Fig 3, then a large error seems likely. The piston used in the ball bushing was apparently $\frac{1}{4}$ ins diameter, 6 ins long. Under a very modest axial load this piston would tend to buckle and increase the frictional resistance. This would be greatly accentuated by any lateral load applied. Therefore Duncan & Seed's method of determining a piston friction correction appears to be erroneous and Duncan & Dunlop's interpretation of their data may be incorrect. Duncan & Dunlop (1968) also obtained an experimental relationship between the grease film thickness and its coefficient of friction, μ . Using Reynold's (1886b) relationship between the grease film thickness and time, they were able to relate μ with the testing time for 1.4 ins and 4 ins diameter specimens under different normal stresses. The results (their Fig 4) suggest that it is highly desirable to use 4 ins diameter samples which would maintain a μ value better than 2° for a testing time of up to 4 days. In tests lasting more than 1 or 2 days on 1.4 ins diameter specimens the value of μ becomes undesirably high.

It is clear from the foregoing review that a rubber membrane with a layer of silicone grease on a polished platten increases the uniformity of the pore water pressures and therefore of the effective stresses acting throughout a triaxial clay specimen. The strength is essentially unaltered when H/D = 1 and a significantly shorter testing time may be used without error, Blight (1967b), Barden & McDermott (1967). However caution will be required when testing small samples, e.g 1.5 ins diameter, at high stress levels and at slow testing rates as an excessive proportion of the grease film may be exuded.

2.4 Failure theories applied to soils

Supposing we know the three principal stresses σ_1', σ_2' & σ_3' acting at a point in a soil mass together with sufficient material properties of the soil to characterise its behaviour e.g. Coulomb angle of shearing resistance, ϕ'; angle of interparticle friction, ϕ_μ ; the state and type of packing of the particles. Given these, a theory of failure would predict whether at a particular point the stresses would or would not cause

failure, i.e. a failure criterion is an equation relating the stresses and material properties at failure. This and some other aspects of failure are discussed by Newmark (1960).

There are two types of criteria of current interest. Those based on continuum mechanics and developed for metals but which have been adapted to account for the particular behaviour of soils. Secondly there are tho those based on particulate mechanics, potentially more useful, but which involve difficult applied mechanics ideally to analyse the stresses in a disordered arrangement of irregular particles in contact. A crucial test of any failure theory is the degree of fit, or lack of it, with experimental data, and herein lies a fundamental problem. The difference in strength as the intermediate principal stress, σ_2', varies from σ_1' to σ_3' is likely to be small, say 3 or 4° for a sand. Clearly any test data ought to be reliable to 0.3 to 0.4°, say, otherwise comparisons may be of little worth. Unfortunately much of the available test data does not appear to fulfil this requirement. It is pointed out that none of the theories admit crushing and cracking of the grains although this is a well established phenomenon, even at low stress levels, Bishop (1965).

2.4.1 Theories based on continuum mechanics

These theories assume the soil to be a homogeneous, isotropic material possessing both friction and cohesion. The cohesion term may be excluded with little loss of generality and since the majority of experimental data are for sands this is convenient. Failure theories for soil take into account the increase in strength with an increase in mean normal stress, which is not a feature of the behaviour of metals. However, excepting the Cambridge critical state concept, the theories take no account of dilatancy, Reynolds (1885,1886a), a property of soils but not of metals - nor is this strictly necessary. The theories also assume that the principal axes of stress and strain coincide although there is evidence both theoretical and experimental to indicate that this is not necessarily correct for granular materials, De Josselin De Jong (1959).

2.4.1.1 Mohr-Coulomb, extended Tresca & extended von Mises theories

These three failures criteria are of current interest and are

conveniently considered together. A full discussion of the theories and their shortcomings is given in Chapter 11 of this thesis. The theories have been discussed by Kirkpatrick (1954, 1957), Hvorslev (1960), Roscoe et al (1963a), Bishop (1966). The shape of these surfaces on the reduced right section are (a) an irregular equal-sided hexagon, (b) a regular hexagon and (c) a circle respectively, Fig 2.5. Serious deficiencies of the extended Tresca and von Mises criteria were established by Bishop (1966), see also Barden & Khayatt (1966). The degree of fit of various experimental data to the theories was examined by Haythornthwaite (1960c,1963b), Gouze (1963), Saada (1963), Scott (1963b), Ladanyi (1967) in addition to the previously mentioned authors, and are referred to in appropriate subsequent sections.

2.4.1.2 Some other theories

A number of other failure theories have been proposed for soils. Johanson (1958) reported by Hvorslev (1960) used weighted values of the intermediate principal stress in equations similar to those of the extended Tresca and von Mises criteria. This gives a line on the reduced right section between the Mohr-Coulomb and extended von Mises lines, Fig 2.5. Although a strength in extension greater than that in compression can apparently be accommodated the form of the variation between these two limits is not clear at present.

An expression in terms of stress invariants for a curved and continuously convex failure surface passing through the 6 vertices of the Mohr-Coulomb hexagon was suggested by Coleman (1960), and may be written:

$$-3\Delta_2' = \left[\frac{2J_1'}{3} + \left(\frac{\Delta_3'}{2}\right)^{1/3}\right]^2 \sin^2\phi'$$

where J_1' = the first invariant of the effective stress tensor

$= (\sigma_1' + \sigma_2' + \sigma_3') = 3p'$

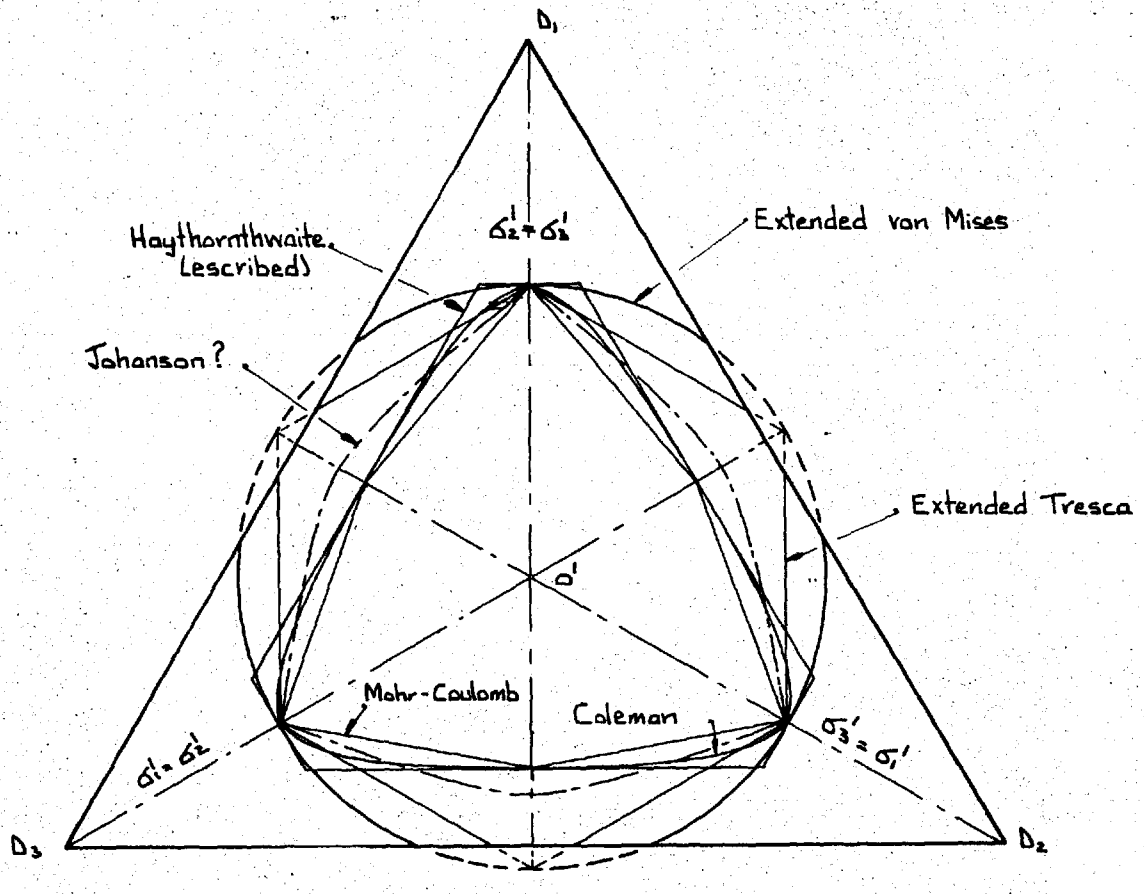
Δ_2' = the second invariant of the effective stress deviator tensor

$= (\sigma_1' - p')(\sigma_2' - p') + (\sigma_2' - p')(\sigma_3' - p') + (\sigma_3' - p')(\sigma_1' - p')$

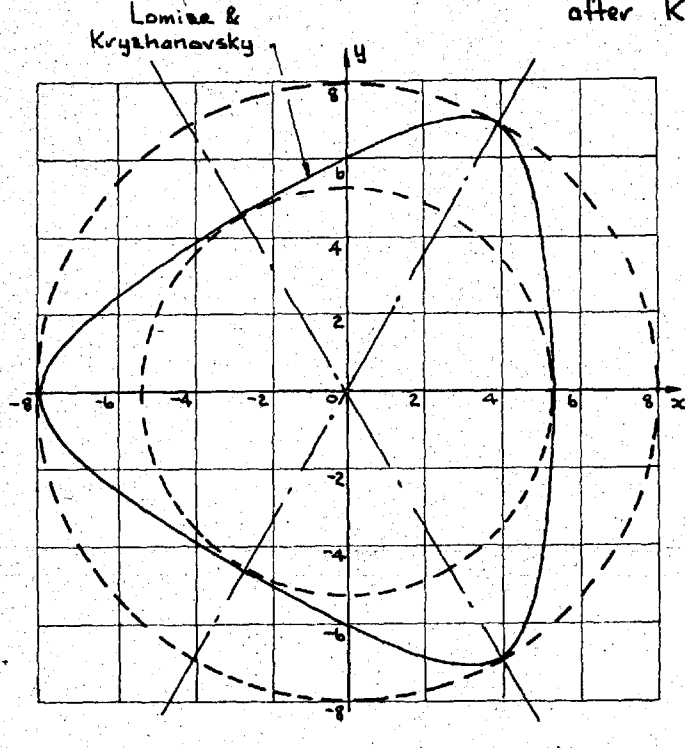
Δ_3' = the third invariant of the effective stress deviator tensor

$= (\sigma_1' - p')(\sigma_2' - p')(\sigma_3' - p')$

The theory implies that the strengths in compression and extension are equal minimum values but it is not clear whether the strength in plane



Reduced Right Section.
after Kirkpatrick (1957)



Batkins' Theory in transformed coordinates.
after Lomize & Kryzhanovsky (1966, 1967)

REPRESENTATION OF FAILURE CRITERIA IN PRINCIPAL EFFECTIVE STRESS SPACE

FIG. 2.5

strain constitutes the maximum value or whether the latter occurs at some other point. It is stated that the expression may be readily modified to account for differing ϕ' values in compression and extension and for a decrease in strength with increasing average normal stress.

Assuming soil to behave as a rigid-plastic, isotropic material with equal strength in compression and extension, Haythornthwaite considered two criteria based on inscribed and escribed straight line envelopes through these points on the reduced right section, Fig 2.5, Procter (1967), Barden (1968). The inscribed envelope is the largest symmetrical convex envelope that can be constructed. The equations for the escribed criterion are relatively cumbersome (they are given by Procter (1967)), due to the discontinuities remote from the axes of symmetry and as such are not mathematically convenient.

Finn & Mittal (1963) attempted to develop a failure theory for an elastic-plastic material which for a particular compression strength predicts an upper bound strength under a general stress system. It was postulated that if failure would occur at the same axial strain as in the triaxial compression test, then for plane strain:

$$\left[\left(\frac{\sigma_1'}{\sigma_3'}\right)_p - 1\right] \Big/ \left[\left(\frac{\sigma_1'}{\sigma_3'}\right)_p + 1\right] = \left[\left(\frac{\sigma_1'}{\sigma_3'}\right)_t - (1+\mu-2\mu^2)\right] \Big/ \left[\left(\frac{\sigma_1'}{\sigma_3'}\right)_t + (1-\mu)\right]$$

where subscripts 't' and 'p' refer to triaxial compression and plane strain respectively and μ is Poisson's ratio. For extension tests, where $\sigma_1' = \sigma_2'$, and failure is induced by reducing σ_3' the theory predicts the same strength as in compression. For a test where $\sigma_1' = \sigma_2'$ and failure is induced by increasing σ_1' & σ_2' with a constant σ_3', an apparently higher strength is predicted; an anomalous result.

Lomize & Kryzhanovsky (1966,1967) developed a theory for sands using principal stress invariants, based on extensions of concepts given by Botkin (1940) and Malyshev (1963). The theory gives a curvilinear triangle when plotted on the reduced right section in transformed co-ordinates, Fig 2.5. The transformed co-ordinate plot may be compared directly with the reduced right section by rotating the former through 30° clockwise. The failure criterion involves at least one experimentally determined coefficient, $\alpha_.$. It is not clear from the presentation whether a second parameter, the invariant Π_o^* is independently defined or can only be determined experimentally. Given measured values of ϕ'

in triaxial compression and extension the theory predicts intermediate ϕ' values, although the equations are complex. The curve shown in Fig. 2.5 is apparently the best fitting curve to particular experimental data, Lomize & Kryzhanovsky (1966). An empirical criterion was suggested by Malyshev (1967a) and in modified form, Malyshev (1967b). A generalisation of the Mohr-Coulomb theory, it allows for an increase in ϕ' in the region $0 < b < 1$ with equal ϕ' values at $b = 0$ and $b = 1$. The maximum increase in ϕ' occurs for $\sigma_2' = (\sigma_1' + \sigma_3')/2$ but the theory cannot predict this increase; it must be obtained experimentally and an empirical coefficient in the failure criterion evaluated. Depending on the form of the failure criterion equation chosen the variation between $0 < b < \frac{1}{2}$ and $\frac{1}{2} < b < 1$ may be curvilinear or linear on the reduced right section. It should be emphasised that, excepting Finn & Mittal's theory, none of the above failure theories say anything whatsoever about behaviour up to failure nor about strains.

The infinitely more difficult task of obtaining a generalised stress-strain relationship for soil up to and including failure has been studied at Cambridge by Roscoe and others. Based on an extension of Hvorslev's concepts for the shear strength of clay, Roscoe et al (1958,1959) evolved a three-dimensional yield surface together with the unique critical void ratio (CVR) state in which unlimited deformation can occur. Initially only applicable to triaxial compression tests, these concepts were developed and extended; Roscoe et al (1963b), Roscoe & Schofield (1963), Roscoe & Poorooshasb (1963), Schofield & Wroth (1968), finally to include generalised three-dimensional stress and strain conditions, Roscoe & Burland (1968). The latter paper considers a 'wet' clay as an isotropic work-hardening plastic material which can only yield when in a state corresponding to a point on the state boundary surface. It is shown that, assuming the Mohr-Coulomb failure criterion is valid throughout, i.e. ϕ' = constant, the strain behaviour under a general stress system may be predicted from three soil constants, M (or ϕ'), λ and κ obtained from triaxial compression tests. The important feature of this theory is that, accepting the limitations of the Mohr-Coulomb assumptions, it enables predictions of generalised strains in 'wet' clays to be predicted. Whether it can be extended to include sands is not at present clear. The writer would agree with Roscoe & Burlands' conclusion that, "the overall agreement between theory and

experiment is remarkable considering the assumptions that are made both in the theory and concerning the behaviour of the clay in the test equipment".

2.4.2 Theories based on particulate mechanics

There is an extensive literature pertaining to attempts to analyse the mechanics of an assemblage of particles in contact and this review will, of necessity, be brief. As noted by Gibson & Morgenstern (1963), the development of particulate theories of irreversible deformation is notoriously difficult, and an altogether satisfactory solution does not yet exist. It is necessary to proceed with caution in extending analyses of ordered arrays of ideal rods or spheres to real materials consisting of random accretions of irregular particles.

2.4.2.1 Some theories based on ordered packings of spheres

All of these theories are aimed at relating the angle of shearing resistance, ϕ', with the angle of interparticle friction, ϕ_μ acting between the grains. Caquot (1934) obtained the relationship $\tan \phi' = \frac{\pi}{2} \tan \phi_\mu$ for plane strain conditions. Bishop (1954) gave the relationship $\sin \phi' = 15 \tan \phi_\mu / (10 + 3 \tan \phi_\mu)$ for triaxial compression and for plane strain, assuming $\sigma_2' = [\sigma_1' + \sigma_3']/2$, the relationship $\sin \phi' = \frac{3}{2} \tan \phi_\mu$. Spencer (1961) claimed to have obtained a relationship between ϕ', ϕ_μ and the porosity, n, for a regular array of spheres in triaxial compression. However neither the equations nor their derivation was ever published.

Thurston & Deresiewicz (1959) analysed a face-centred cubic lattice of single-sized elastic spheres. Stress-strain relations for triaxial compression were obtained by integrating incremental relations given by Duffy & Mindlin based on Hertzian theory. Scott (1963a) following similar lines to Thurston & Deresiewicz showed that if $\tan \phi_\mu$ was varied from $0 - \frac{1}{2}$, that ϕ' was very insensitive to this variation, c.f. Skinner (1969). However Trollope & Parkin (1963) suggest that Thurston & Deresiewicz's paper contains a statical error.

The analysis of a rhombohedral packing, i.e. the densest possible state, in limiting equilibrium was investigated by Dantu (1961). A useful

review of the above and other solutions for triaxial compression is given by Farouki & Winterkorn (1964).

Extensive studies at Karlsruhe of regular packings of spheres are reported by Wittke (1962), Leussink & Wittke (1963) and Leussink (1965). Hexagonal and quadratic packings were analysed both in triaxial compression and in plane strain, theoretical relations between σ_1'/σ_3' and $\Delta H/H$ being given. For triaxial compression the failure criterion is similar to that obtained by Dantu (1961) and Rowe (1962). It is shown that ϕ' can be varied by up to 50% by varying the kind of packing without varying the porosity, i.e. the relation between ϕ' and porosity is not unique. Provided the analysis is correct, this is a very significant difference. As expected, plane strain conditions give higher strengths than do triaxial compression.

Parkin (1964,1965) following Rennie (1959) obtained a failure criterion for the densest packing of uniform rigid spheres over the complete stress range, $\sigma_1' \leqslant \sigma_2' \leqslant \sigma_3'$. The contacts may be frictional or frictionless and the applied stresses are rotated relative to the packing to give the most critical cases, i.e. minimum strengths. The latter degree of freedom is in contrast to the aforementioned theories, Trollope & Parkin (1967). Rennie (1959) showed that the failure mechanism is one of sliding between two contiguous close-packed planes of spheres, rather than a general dilatation. Parkin (1965, 1967) showed that triaxial compression gives the lowest strength, whereas plane strain (approximately) and triaxial extension give an equal maximum strength, the difference between these two limits increasing with the coefficient of interparticle friction, μ [or $\tan \phi_\mu$], see Fig 11.31 & Chapter 11 of this thesis.

2.4.2.2 Stress-dilatancy theory

Ordered arrays of single-sized rods in two dimensional compression and spheres in triaxial compression were analysed by Rowe (1962) on the basis of minimising the ratio of the work done by the major principal stress to the work done on the minor principal stress by the assembly; a so-called energy ratio. The orientation of the stresses relative to the packing was fixed and it was assumed that the results were valid, without further modification, for a random mass of irregular particles, e.g. sand. The theory was restated and amplified, Rowe (1963), and extended to include a

cohesion term for clays. A vigorous discussion followed, Gibson & Morgenstern (1963), Trollope & Parkin (1963), Scott (1964), Roscoe & Schofield (1964), replied to by Rowe (1964b), the outcome of which is far from clear. It appears that there was significant disagreement concerning the validity of the basis of the theory and over certain steps in the analysis. Clearly the extension per se to include materials such as sands is optimistic and for clays, very optimistic.

Additional discussion of the theory, Horne (1965) Part 1, in support of Rowe argues against the criticism raised by the above discussers, mainly concerning four points of issue, (i) the assumed mechanism of deformation, (ii) the assumed absence of rolling, (iii) the assumption that E (energy ratio) can be minimised in a random assembly and (iv) the significance of the α' planes. Horne obtained a more general energy equation based on a principle of maximum energy transmission and shows that Rowe's equation for triaxial compression is a particular case of this. A method is propounded, Horne (1965) Part II, for describing the anisotropy in an irregular assembly of uniform spheres and the concept of a continuously changing degree of anisotropy is used to obtain the stress-dilatancy equation by a different procedure.

The stress-dilatancy equation for the triaxial extension test was derived by Rowe et al (1964) together with some relevant work equations for the direct shear test. The relationship between stress-dilatancy concepts and earlier work by Taylor, Bishop and Roscoe were also discussed. Barden & Khayatt (1966) quoting unpublished work by Rowe derived the stress-dilatancy relation considering a random assembly of irregular rigid particles following Horne's assumptions. More recently the stress dilatancy theory has been extended to include both plane strain, and finally the general stress range $\sigma_1' \geq \sigma_2' \geq \sigma_3'$, Procter (1967), Barden (1968), Rowe (1969), Horne (1969).

A difficulty in the practical examination of the validity of the theory is that a reliable independent measurement of the angle of interparticle friction, ϕ_μ is needed. The measurement of ϕ_μ is very difficult for sands it being dependent on the surface preparation, possible surface contamination, presence of water, etc. and on the precise method of testing, see for example Horne & Deere (1962), Skinner (1969). The method used by Rowe was to replace the lower half of a conventional shear box by

a prepared block of intact material and to fill the upper half of the box with the particulate material. The mechanism obtaining at the contact seems to be of a speculative nature and, indeed, appears most unlikely to be that envisaged in the definition of ϕ_μ. Smith (1965) at Liverpool University using a similar technique to Rowe was apparently unable to obtain a unique value of ϕ_μ from the friction slider test, even when using Rowe's prepared quartz block.

2.4.2.3 Some other theories

Farouki & Winterkorn (1964) discuss Winterkorn's macromeritic systems failure theory. This states that a system of identical spheres is in a potentially liquid state when it has a void ratio of 0.62 or higher, the latter corresponding to the melting point of simple chemical substances. Unfortunately this theory requires theoretically negative void ratios in order to fit it to some experimental data on sands which inspires little confidence in its potential usefulness.

A theory for the mechanical behaviour of sand was developed by Brown (1964) based on two hypotheses. The first was an adaption for sand of Drucker's definition of a stable material and the second was that straining the sand aggregate causes it to transform from one randomly disordered configuration to another. Assuming an assembly of rough elastic grains these two hypotheses lead via a virtual work theorem to an incremental stress-strain theory valid up to failure; the dilation being shown to be path-independent.

2.5 Comparative strengths in triaxial compression & extension

The difficulties associated with assessing the validity, or otherwise, of experimental data should be well-known although the readiness of writers to quote, without criticism, data in an attempt to 'prove' their theories is, unfortunately, not unknown. The ϕ' value measured in triaxial extension has been variously reported as being as much as 6-8° above or below that measured in triaxial compression. There will of course be material differences but, granted this, it appears likely that all soils should behave in a similar manner. One may postulate that for sands the value in extension should be equal to that in compression for loose packings and greater than in compression for dense packings. Clays can reasonably be expected

to behave similarly although the influence of stress path and anisotropy of the soil structure are likely to be of greater importance, Bishop (1966). Triaxial extension strengths lower than in compression appear most unlikely to be correct, almost certainly so for sands.

Potential errors which affect a comparison of the values of ϕ' measured in compression and extension are of two types,(a) due to limitations in the apparatus and testing technique, and (b) due to uncertainties in interpretation of the test results. Some of the possible errors which are known to exist were extensively discussed in Section 2.1. They are emphasised and others will be noted as the occasion arises. Generally the quality of test data may be expected to improve with time as researchers become more aware of the problems involved and experimental methods are improved. Early test data must therefore be considered the least reliable in the absence of detailed evidence to the contrary. Furthermore, the data must be judged on the details known, or not known, concerning the method of testing and interpretation of the results. These remarks will apply equally to subsequent comparisons of plane strain tests and tests in which σ_2' was continuously varied.

Extension tests which are a particular case of more general tests in which σ_2' was continuously varied are,for convenience,discussed in Section 2.7.

2.5.1 Experiments on sands

Drained triaxial compression and extension tests on cylindrical and cuboidal saturated sand specimens at a range of densities are reported by Taylor (1941). Cuboidal compression specimens 1.0 x 1.0 x 2.6 ins high exhibited the same ϕ' - porosity relationship as cylindrical compression specimens 1.4 ins diameter,3 ins high. Similar specimens tested in extension gave different results. Both cylindrical and cuboidal loose specimens gave identical strengths, 3° lower than in compression. Dense cuboidal extension specimens showed a strength equal to that in compression but dense cylindrical specimens showed a 3° lower ϕ' value. Extension tests on larger cuboidal specimens were also performed but they appear to be less reliable. Taylor's results must be qualified by two noticeable experimental factors. The internal proving ring used may be expected to have been unstable and cause premature failure in compression.

No refined corrections for necking were apparently made to the extension test data.

Eldin (1951) reported by Bishop & Eldin (1953) performed drained comparison tests on 1.5 ins diameter, 3 ins high saturated sand specimens and obtained similar triaxial compression & extension strengths over a wide range of densities. Sample sheath strength corrections were applied together with a refined area correction for the necked extension specimens. However piston friction may have significantly affected the results since a fixed bushing was used. Furthermore Eldin analysed his test data on the basis of an assumed initial sample height of 3.0 ins rather than measure each sample. Clearly this is unsatisfactory.

Habib (1951, 1952, 1953) and later Peltier (1957), the latter summarising work at 3 French research establishments including Habib's, obtained lower strengths in extension than in compression. The average difference was about 7° varying from $6\frac{1}{2}^{\circ}$ to 9°. Habib did not measure the porosities. These abnormally low extension ϕ' values have never been explained, certainly their validity in the light of present knowledge appears to be doubtful. Tests on 1.5 ins diameter, 3 ins high specimens of saturated sand by Kirkpatrick (1954, 1957) showed similar strengths in compression and extension. Area corrections were applied (whether a refined neck correction was applied is uncertain) together with a sample sheath strength correction. Both Kirkpatrick's and the French test results are probably affected significantly by piston friction.

Unpublished tests reported by the Norwegian Geotechnical Institute (1953) showed similar strengths in compression and extension. Drained tests on 1.5 ins diameter specimens, placed dry and subsequently saturated, but based on an obscure definition of failure related to the slope of the stress-strain curve, gave higher strengths in compression than in extension according to Haythornthwaite (1960b). However the correlation between the initial porosity, n_i, and rate of dilation at failure is very poor in Haythornthwaite's tests. Furthermore, piston friction and a refined neck area correction in extension were apparently not accounted for and a somewhat arbitrary definition of failure was used, Kirkpatrick (1961).

Wu et al (1963) obtained identical ϕ' values in undrained triaxial compression and extension tests with pore pressure measurements on saturated sand samples of an unspecified size. It is not stated how the

specimens were formed. Hollow cylindrical specimens of sand reported in the same paper were formed by pouring dry sand into the former and saturating afterwards. If the same technique was used for the solid cylindrical specimens then the pore pressures subsequently measured are likely to be suspect due to the presence of air. Pore water pressures at failure as low as - 3.67 kg/cm^2 are apparently claimed which are inadmissable. However it is not clearly stated whether these are absolute values or changes.

More reliable drained test data on 4 ins diameter, 8 ins high saturated sand specimens was obtained by Cornforth (1961,1964) and later in a more limited series of tests using the same equipment by Wade (1963). Similar extension and compression strengths over a range of porosities were exhibited in tests in which a rotating bush was used to minimise ram friction and a refined neck area correction was applied in analysing the extension test results. Sample sheath strength corrections were almost insignificant at the stress levels involved.

A few (7) drained extension tests on 1.5 ins diameter, 3 ins high sand specimens over a range of porosities were performed by Thurairajah (1961), reported by Roscoe et al (1963a). The tests at 40 psi cell pressure (4) gave comparable ϕ' values to compression. The tests at 100 psi cell pressure (3) showed an increase in strength with a decrease in placement density, clearly unacceptable. One extension test at 40 psi cell pressure, whose local deformations were optically observed throughout shear (test 39) exhibited a $\phi' = 42.6^\circ$ based on a conventional analysis and a $\phi' = 48.5^\circ$ based on the minimum neck area. The use of the latter is unrealistic although it serves to show the limit of the error involved due to necking.

Tests on both solid and hollow cylindrical sand specimens by Esrig & Bemben (1965), Bemben (1966) present a confused view, Fig 2.6. The drained triaxial compression and extension tests on solid cylindrical specimens may be expected to be the most reliable. They show identical values at high porosities whereas at low porosities the extension ϕ' value is 5° higher than the value of ϕ' in compression. Remarkably, similar undrained tests gave the same results which, as noted by Bemben, casts great doubt on the validity of the undrained testing technique used. Constant volume compression and extension tests on solid cylindrical samples each give the same strength but are 1.5° lower than the drained

compression tests. Similar tests on hollow cylindrical samples in which the internal and external pressures were identical gave different strengths, the extension ϕ' value being 2° higher than the compression value, but both were different from all the other tests. The differences in the constant volume test results are not fully explained by Bemben, nor are they understood by the writer. Unfortunately consolidated drained compression and extension tests were not performed on hollow cylindrical samples, which would be crucial tests. As noted earlier, Section 2.1.11, end restraint is a serious problem in both undrained and constant volume tests. Furthermore Bemben did not apply a refined neck area correction to the extension test resuots nor were realistic piston friction corrections applied to the compression test data.

Khayatt (1965) and Barden & Khayatt (1966) obtained important comparisons of drained compression and extension tests on 4 ins diameter, 4 & 8 ins high sand specimens, the short samples having lubricated ends. An internal proving ring was used and it was observed that 4 ins high extension specimens deformed uniformly up to failure, thereafter necking and a single slip zone occurred. Extension and compression tests on 4 ins high specimens at different average stresses, i.e. $(\sigma_1' + \sigma_2' + \sigma_3')/3$, gave slightly different strengths (0.5° for loose samples and 2.0° for dense samples, extension being higher). When the average stresses were similar, identical ϕ' values were obtained. A few compression and extension tests on short samples following decreasing and increasing average stress paths respectively were performed and indicated that the path had little or no effect on the strength. Tests on 8 ins high dense specimens exhibited identical compression strengths to 4 ins high specimens and lower extension strengths (up to 6.0°) if no refined area correction was applied. After applying a neck area correction the extension strengths were close to those measured in compression. Subsequently, following suggestions by the writer to Barden, cubical samples with lubricated ends were tested in compression and extension, Bardon (1968). Dense cuboidal compression specimens gave the same compression strength as similar cylindrical samples but cubical extension specimens showed a strength some 4.0° higher. The reason for this increase is at present speculative. Barden (1968) is in agreement with the writer in believing that a plane strain mechanism obtains at failure but the evidence is scanty and conflicting.

Lambe (1967) quotes drained tests on a Libyan sand as giving a ϕ' value in compression of 41.4° and in extension of 44.5° but no details are given.

2.5.2 Experiments on clays

Early tests by Taylor (1950) and Taylor & Clough (1951) on undisturbed clay samples showed very slightly higher effective strengths in extension than in compression, as reinterpreted by Taylor (1955). Difficulties arose due to variability of batches of the undisturbed clay. Taylor & Clough (1951) observed that in a typical extension test the neck caused a 6% error in the area based on a uniform deformation assumption. Although the error in the shear stress on the failure plane is very small the error in ϕ' is 3.8°. Hirschfeld (1958) performed undrained triaxial compression and extension tests on undistrubed samples of 3 different clays. The strengths defined in terms of maximum σ_1'/σ_3', were so scattered due to the variability of the samples that no definite conclusions regarding the influence of σ_2' could be drawn.

Triaxial compression and extension tests following a variety of stress paths were performed by Gilbert (1954) and Parry (1956) on remoulded Weald Clay, reported by Henkel (1959,1960a, 1960b). Drained and undrained tests on normally consolidated specimens showed similar ϕ' values. Overconsolidated specimens gave a ϕ' in extension 0.5° lower than in compression, however the cohesion intercept was larger.

The above, together with other earlier tests by Rendulic, were reviewed by Hvorslev (1960).

Wu et al (1963) performed consolidated undrained tests with pore water pressure measurements on remoulded plastic clay samples of an unspecified size. There was apparently no difference in ϕ' between compression and extension. However all the tests were run at 3% axial strain per hour, which may be too fast for reliable pore water pressure measurements to be obtained. Compression tests on hollow cylindrical specimens, 4 ins O.D., 3 ins I.D. & 6 ins (?) high showed similar strengths, the samples being loaded incrementally to failure in about 6 hours. What corrections, if any, were applied in interpreting these results are unknown.

Isotropically consolidated undrained triaxial compression and extension tests on 1.5 ins diameter, 3 ins high samples of remoulded Weald clay were

performed by Sowa (1963). For the extension tests, both continuous and discontinuous spiral filter paper drains were used, the latter to reduce the filter paper strength correction, for which no adjustment was made. The lateral deformations in tests in which the spiral drains were used were continuously monitered optically during shear and a refined neck area correction applied. The ϕ' values measured in compression and extension were almost identical but an unduly large cohesion intercept was obtained in the extension tests which could not be explained. The issue was complicated by small variations in the test results due to a possible difference between the batches of clay. Subsequent tests on undisturbed Avonmouth clay using similar refined techniques, e.g. a slow testing rate and a rotating bush, exhibited slightly higher ϕ' values in extension than in compression, Smotrych (1968).

Ladd & Bailey (1964) obtained higher ϕ' values in extension based on K_o- consolidated undrained tests on normally consolidated undisturbed Kawasaki clay. Ladd & Varallyay (1965) observed that extension tests on isotropically consolidated samples gave suspect ϕ' values due to necking at the large strains encountered. In contrast, anisotropically consolidated samples were found to give more reliable results; an extension ϕ' value about 2.5° higher than in compression.

To summarise, both sands and clays show strengths in extension equal to or greater than those in compression. To discriminate differences in of 1 or 2°, careful experimental technique counts for everything.

2.6 Comparative strengths in triaxial compression & plane strain

Many of the difficulties discussed in comparing triaxial compression and extension test data are also relevant to plane strain tests. However since in the former comparison the major problems were associated with necking in the extension test the present comparisons are generally more reliable, provided the plane strain apparatus is well designed.

Intuitively one may postulate the plane strain ϕ' value to be at least equal to that in compression and probably to be a few degrees higher. All known experimental data supports this hypothesis. The plane strain tests discussed in this section were all performed on cuboidal specimens and, with two exceptions (Kummeneje (1957), Bjerrum & Kummeneje (1961) and Shibata & Karube (1967)) restrained rigid plattens were used to maintain a

plane strain condition, $e_2 = 0$.

Plane strain tests which are a particular case of more general tests in which σ_2' was continuously varied are, for convenience, discussed in Section 2.7.

2.6.1 Experiments on sands

A quasi-plane strain condition was induced in cuboidal dry sand specimens by Kummeneje (1957), Bjerrum & Kummeneje (1961) by making the specimen long enough that axial platten friction in the σ_2' direction was sufficient to maintain $e_2 = 0$ (approximately). Two sizes of specimen were tested, both 4cm wide & 12cm high, and of lengths 30cm & 60cm. The plane strain ϕ' was independent of the specimen length and was 3 to 4° higher than in corresponding triaxial compression tests on cylindrical specimens over a range of porosities. In both types of test a non-tilting contact was used between the upper platten and the loading piston. In an additional set of triaxial compression tests using a ball seating on two sizes of specimen, ϕ' values 1.0° lower than before were obtained.

Based on plane active earth pressure tests on dry sands, Christensen (1961) obtained ϕ' values in plane strain 4 to 5° higher than in triaxial compression for various initial porosities.

An extensive series of plane strain tests on two sands is reported by Bishop (1961), Cornforth (1961, 1964) and Wade (1963). K_o-consolidated saturated samples 2ins wide, 4ins high and 16ins long were tested in an elaborate apparatus, Cornforth (1964), maintaining a precise $e_2 = 0$ condition. Wade (1963) used a K_o-belt similar to that used for cylindrical triaxial specimens, Bishop & Henkel (1957). Drained plane strain tests over a range of porosities showed a marginal 0.5° difference from triaxial compression tests for loose samples, increasing to 4.0° for dense samples, plane strain strength being higher. In addition, both the linear and volumetric strains at failure were considerably smaller in plane strain than in triaxial compression, consequently little ambiguity arises in the stress calculations. It was also observed by Cornforth that the ultimate strengths were almost the same in triaxial compression as in plane strain, being 33.0° and 32.3° respectively, although these results are subject to some uncertainty in interpretation. A few quasi-plane strain tests were performed by Cornforth without the σ_2' end clamp and these exhibited similar

ϕ' values to the true plane strain tests supporting therefore the general validity of Kummeneje's tests.

In parallel with their theoretical analyses, see Section 2.4.2.1, Leussink & others have performed plane strain and triaxial compression tests on a sand at a range of porosities and on ordered packings of 1.5cm diameter steel and glass balls, Leussink & Wittke (1963), Leussink (1965), Leussink et al (1966). The plane strain specimens were 20 cm wide, 60cm high and 100cm long. The σ_2' platten-sample sheath interface was lubricated with soft soap, a vacuum being maintained to apply a confining pressure, σ_3'. Triaxial test specimens for the steel & glass balls were 20cm diameter and 50cm or 70cm high. The sand exhibited an essentially constant difference in ϕ' of 3.5 - 4.0° over a range of porosities, plane strain giving the higher strength. Very wide variations in ϕ' were obtained with the ordered packings. Hexagonally packed glass balls showed ϕ' values of 51.6° & 40.0° in plane strain and triaxial compression respectively, whereas quadratic packings at an identical porosity (26%) gave corresponding ϕ' values of 22.6° & 20.8°. Hexagonally packed steel balls showed ϕ' values of 40.4° & 37.4° in plane strain and triaxial compression respectively whereas quadratic packings at an identical porosity(26%) gave corresponding ϕ' values of 20.8° & 19.5°. The large disparity in ϕ' between the densely packed glass balls in plane strain and in triaxial compression is most likely due to the out of roundness of the glass balls.

Some aspects of the difference in volume change behaviour between plane strain and triaxial compression were studied by Finn et al (1967) following Leussink's notation, to correlate Wade's (1963) sand test data and a river sand tested at the University of California. Lorenz et al (1965) performed a series of plane strain tests on 10cm cubical specimens of dry sand contained in a rubber sheath. No directly comparable ϕ' values are given for triaxial compression although it is stated by Lorenz (1965) that the plane strain and triaxial compression strengths are different. The form in which the data is presented is obscure and an assessment of the results is difficult. The apparatus is only capable of imposing plane strain conditions and is not an independent stress control device, as incorrectly stated by Moretto (1965).

Rowe (1964a) and Rowe & Peaker (1965) quoted ϕ' for dry Mersey River sand of 33° & 34° when loose and 39.5° & 42° when dense, in triaxial

compression and plane strain respectively. Wightman (1967) performed drained plane strain tests on K_o - consolidated specimens 4 ins wide, 4ins high & 8ins long, of saturated River Welland sand, feldspar sand and glass ballotini. The River Welland sand showed a constant 4.0° higher plane strain ϕ' compared with triaxial compression tests by Khayatt (1967) there being some uncertainty in the behaviour of loose samples. Limited tests on feldspar sand showed a 4.0° higher plane strain ϕ' value on dense samples although the paucity of tests and their scatter is discouraging. Tests on glass ballotini suggest a ϕ' value 9.0° higher in plane strain based on one triaxial compression test for comparison. An isolated plane stra in test on dense zircon sand was suggestive of a 7.0° difference in ϕ'.

It is noticeable that whereas Leussink and Kummeneje both observed an increase in ϕ' in plane strain that was essentially independent of porosity, Cornforth, Wade, Rowe & Peaker and to a less certain extent Wightman, all obtained an increase in ϕ' in plane strain which was greatest for dense specimens and least (almost zero) for loose specimens. It appears unlikely that this is due to deficiencies in the apparatus. A plausible explanation is as follows. The one significant feature of the tests is that all of the former were at low stress levels, i.e. σ_3' was applied by means of a vacuum, whereas the latter were at a higher stress level σ_3' = 40 & 60 psi. As the average stress level is raised, dilatency is suppressed due to grain crushing, Bishop (1966), and the placement porosity at which the triaxial compression and plane strain ϕ' values are identical decreases. At very high stress levels, 10,000 psi perhaps, initially dense specimens may be expected to give the same compression & plane strain ϕ' values. Furthermore the ϕ' value has been shown to be independent of the initial placement porosity, e.g. Bishop (1966), Skinner (1969). At low stress levels it is well-nigh impossible to form specimens that are loose enough to achieve convergence of the two ϕ' – porosity curves.

A few plane strain tests on quarryblasted rockfill samples 75cm x 75cm wide & 180cm high, at low stress levels, i.e. σ_3' was applied by means of a vacuum, showed an increase of 13° in plane strain compared to triaxial compression, Marsal (1965). Subsequently, tests at higher stresses on an alluvial sand and gravel mixture and on a crushed basalt were performed, Marsal et al (1967). Unfortunately triaxial compression tests on the same

materials were not available so that a direct comparison was not possible. However Marsal et al concluded that the data were qualitatively similar to Cornforth's (1964) results.

2.6.2 Experiments on clays

Undrained tests with pore water pressure measurements on a compacted clay are reported by Mittal (1963) and Finn & Mittal (1963). Unfortunately the design of the plane strain device was such that plane strain was not obtained until 2% axial strain had taken place (due presumably to the sample being isotropically consolidated). The failure strains are therefore too large but the strengths are more likely valid. Triaxial compression tests on cylindrical and rectangular specimens showed similar ϕ' values but the failure strains were greater for the cylindrical specimens. The plane strain tests showed a 2.0° higher ϕ' value in tests at σ_3' = 60 psi and 4.2° higher at σ_3' = 75psi.

Wood (1958) performed K_o - consolidated undrained tests with pore water pressure measurements on a moraine (well-graded sandy gravel) compacted 3% wet of the Proctor optimum. In terms of effective stress the shear strength in plane strain was 15% higher than in triaxial compression. At maximum $(\sigma_1' - \sigma_3')$ the plane strain ϕ' value was 36.9° compared with 35.1° in triaxial compression. At maximum σ_1'/σ_3' the corresponding ϕ' values were 41.1° & 37.2°. For both failure criteria, cohesion intercepts of 1.8psi in plane strain and 0.5 psi in triaxial compression were obtained. Subsequently using the same apparatus Wade (1963) reported by Henkel & Wade (1966), performed similar tests on remoulded Weald clay. At maximum $(\sigma_1' - \sigma_3')$, K_o - consolidated plane strain tests showed a ϕ' of 27.1° compared with 25.9° for both isotropic and K_o - consolidated triaxial compression tests. At maximum σ_1'/σ_3' the corresponding ϕ' values were 27.4° & 26.2°. In all tests the cohesion intercept was zero. The strains required to reach failure, however defined, were very much reduced in plane strain. Wade also performed a few quasi-plane strain tests without the σ_2' end clamp which exhibited similar ϕ' values to the triaxial compression tests rather than the true plane strain strength, as was observed for sands. This was attributed to the relatively low frictional resistance of the clay-perspex platten interface.

Two types of anisotropically consolidated-undrained plane strain tests

on San Francisco Bay mud were performed to simulate undrained failure near the top and the toe of a slope, Duncan & Seed (1966). A specimen 1.1 ins wide, 2.78 ins high and 2.78 ins long was used and corrections were applied for the effects of the filter paper drains, rubber membranes, piston friction and platten friction, Duncan & Seed (1967). The ϕ' value measured in isotropically consolidated-undrained triaxial tests on undisturbed samples was 34.5°. The corresponding vertical plane strain (VPS) ϕ' value was 38.0° whereas horizontal plane strain (HPS) tests gave a ϕ' value of 35.0° , c' being zero for both types of test. Subsequently Duncan & Dunlop (1968) performed similar plane strain tests but with lubricated membranes on the axial plattens (the σ_2 plattens were always lubricated). It was difficult to distinguish any differences since they were small and of the same order as the scatter of the individual tests, however a reduction in ϕ' of 1.0° was just distinguishable when using lubricated ends in plane strain tests. A reduction in ϕ' of the same order was obtained when using lubricated ends in triaxial tests so that the difference in behaviour between plane strain and triaxial compression is unaffected.

Shibata & Karube (1967) obtained an unusually large increase in strength in plane strain tests on remoulded Osaka alluvial clay using apparatus described by Shibata & Karube (1965) and discussed subsequently in Section 2.7.2.2. Isotropic and K_o - consolidated samples exhibited similar behaviour in undrained tests with pore water pressure measurements. The value of ϕ' in plane strain varied from 39.0 to 47.0°and in triaxial compression from 35.0 to 38.0° (decreasing as the stress level increased), the average difference being about 7.0°. The variation in ϕ' with stress level seems rather high and is in contrast to earlier tests on the same material, Shibata & Karube (1965). The average increase of 7.0°in plane strain compared with triaxial compression is very high although the low clay fraction, 21%, may partly explain this.

With the exception of Shibata & Karube's tests all the data on clay is consistent and suggests an increase in ϕ' in plane strain of from 2.0 to 4.0° compared to triaxial compression.

2.7 Comparative strengths as σ_2' is varied continuously between σ_1' and σ_3'

In these tests all 3 principal stresses are varied independently so that the influence of the relative value of σ_2' on the behaviour may be obtained. It is convenient to denote the relative value of σ_2' by the parameter $b = (\sigma_2' - \sigma_3')/(\sigma_1' - \sigma_3')$. For triaxial compression, where $\sigma_2' = \sigma_3'$, then $b = 0$ and for triaxial extension, where $\sigma_1' = \sigma_2'$, then $b = 1$. For intermediate values of σ_2', then $0 < b < 1$; plane strain corresponding to a value of b equal to 0.2 or thereabouts, see Section 11.6. Cornforth's tests showed that b decreased from 0.24 to 0.19 as the initial density was varied from loose to dense, Bishop (1966). There is no evidence to suggest that b ever approaches 0.5 as predicted by plasticity theory.

The behaviour established for triaxial compression & extension and for plane strain, Sections 2.5 & 2.6, must be reconciled with any new independent stress control tests. The stress conditions in the former are particular cases of those in the new test and the results of ostensibly similar tests on the same soil in different apparatus are a crucial measure of the validity of the experiments. All known experimental data, both for sands and clays, indicates that the plane strain ϕ' value is at least equal to that in triaxial compression and is often a few degrees higher. Similarly the ϕ' value in triaxial extension is at least equal to, and frequently is greater than that in triaxial compression. We may postulate that, as b increases from zero, ϕ' increases until plane strain is reached, $b = 0.2$ or thereabouts. Between plane strain and $b = 1$ the value of ϕ' remains constant or it may decrease, possibly to the same value as at $b = 0$.

There are 2 main types of test which enable σ_2' to be continuously varied. In the first a cube or cuboidal shaped specimen is subject to 3 boundary stresses, each of which is assumed to be acting uniformly over its boundary face. These 3 stresses are principal stresses and are assumed to be the same on each and every element of the specimen. Provided the apparatus functions properly, i.e. the normal boundary stresses are uniform, shear stresses are not applied to the specimen at the boundaries and the 'corners' of the sample are correctly stressed, there is no further problem. In the second type of test a hollow cylindrical specimen is subjected to differential internal and external pressures and, in addition, an axial compressive load or a torsional load, or both may be applied. The stresses will vary across the wall of the cylinder and the form of this variation is

dependent on the relative wall thickness. Ideally the cylinder wall should be very thin so that stress variations are linear, but, whereas it is convenient to test thin walled metal tubes in tension, it is not practicable to test very thin walled cylindrical soil specimens in compression. The interpretation of the results for a soil relies heavily on a theoretical analysis of the stress distribution within a thick-walled hollow cylinder. Due to the stress variation across the wall failure will generally occur at the inner wall and progress outwards, so that even in any ideal specimen simultaneous failure throughout does not occur. However the pore water pressure will generally be uniform across the wall of the specimen. If it is desired to examine linear and volumetric strains it is necessary to somehow analyse (a) the linear strain variation across the wall of the specimen, and (b) the volumetric strains across the wall of the specimen, bearing in mind that only the overall volume change may be directly measured. This appears to be an exceedingly difficult proposition. Furthermore buckling may occur, the effect of which can not be accounted for theoretically. For these reasons the writer considers the hollow cylinder test as applied to failure of soils to be of limited value. However many experiments have been performed on hollow cylindrical specimens and some discussion is merited.

2.7.1 Experiments on cuboidal specimens

2.7.1.1 Sands

All the tests reported on sands are drained tests on either dry or saturated specimens.

Kjellman (1936) used apparatus described briefly in Section 2.3.1 to test dry sand in cubical specimens of 6.2cm side. A ϕ value of 35° was obtained in tests in which b = 0 whereas for tests in which b = 0.38 & 0.50 the value of ϕ' increased to 43°. However the validity of these results is limited by deficiencies in the apparatus. The multiple rods used to load each face of the specimen are inherently unstable in compression. Furthermore, sand grains (0.1cm) would become jammed into the 0.02 cm initial clearance between adjacent rods, so preventing contraction or accentuating expansion across a loaded face. For identical reasons, subsequent tests by Jakobson (1957) in the same apparatus must be considered to

be of limited value in defining the influence of the intermediate principal stress.

Tests were performed on 2 dry sands by Daniel (1954,1957) in a rigid-sided box $3\frac{1}{2}$ ins high, $1\frac{3}{4}$ ins square. The sides of the box were connected by a rubber sheet, folded inwards before filling with sand. The lateral stresses were applied by a lever and dead-weight system and remained constant during a shear test whilst the axial stress was varied. A comparison between conventional triaxial compression tests and tests at equal lateral stresses in the box showed reasonable agreement. When the lateral stresses were varied an increase in ϕ' of up to 16° was observed. Clearly the tests are grossly affected by sample-platten interfacial friction and arching at the corners so that the results are of little value.

An ingenious method of varying σ_2' on a cuboidal sample was suggested by Escario (1961). Steel shot were embedded in the sample sheath on the faces and an electromagnet was used to reduce the stress in the σ_2' direction. Difficulties arose in ensuring a uniform magnetic field normal to the σ_2' sample face and in keeping the electromagnet to a reasonable size. No results were given and it is not known whether the principle has proved to be workable.

Lenoe (1966) performed vacuum 3-dimensional stress tests on dry sand on cuboidal specimens of an unspecified size. The intermediate principal stress, σ_2', was applied through rubber membrane-faced boxes. No allowance was apparently made for edge effects around the σ_2' membrane 'pistons' and $(\sigma_2' - \sigma_3')$ was assumed to be equal to the air pressure in the boxes. The stress levels were very limited, particularly since $(\sigma_2' - \sigma_3')$ did not exceed 3 psi, so that the maximum value of b was only 0.10. Furthermore the stresses were based on the initial specimen geometry, no area corrections being applied, which, in view of the purpose of the experiments, was entirely inadequate. Lenoe obtained an apparent increase in ϕ' of 7.7° as b increased from 0 to 0.1. This seems far too large an increase in ϕ' for so small an increase in b and, particularly in view of the lack of any area correction in analysing the results, must be treated with considerable reservation. There appears to be no way of avoiding the difficulties inherent in this type of apparatus.

An elaborate and somewhat cumbersome apparatus was used by Bell (1965) to investigate the influence of σ_2' on failure. A dry sand specimen

16 ins square, 2 ins high contained in a rubber bag was sandwiched between 2 heavy steel plates faced with perspex (see also Ko & Scott (1967a)). The upper steel plate contained windows to enable the corners of the sample to be viewed. A flat rubber water-filled bag set in a recess in the lower plate was used to stress the sample. Four additional rubber water-filled bags were set around the edges of the specimen, being separated at the corners by adjustable hinged plates. The box and all the rubber bags were heavily greased on their contact surfaces. The specimen was stressed by pressurizing the water-filled rubber bags and the strains were measured by observing air-water interfaces in large burettes. The specimen was stressed incrementally, the corner separators being adjusted after each increment to prevent interference of the rubber bags at the corners. A triaxial compression test in this apparatus showed the same strength, about 37 to 38°, as in a conventional triaxial compression test. Tests approximating to plane strain gave a ϕ' value of about 50° and between plane strain and triaxial extension ϕ' remained virtually unchanged. The major objection to Bell's test is the ill-chosen specimen shape. The reasons for the 8:1 height to width ratio are not apparent, a cubical specimen would appear to be more suitable. Subsequent tests by Ko (1966) support this belief although they are deficient in other respects.

Tests on saturated Ottawa sand by Ko (1966) reported by Ko & Scott (1967a,b,c, 1968a,b) purport to define a failure envelope as σ_2' was varied whilst the average principal stress remained constant. A 4 ins cubical specimen was loaded at the boundaries by water-filled rubber bags contained in a rigid box. The apparatus incorporated an ingenious mechanical hydraulic analogue which was used to control the stresses. The author's drained tests did not reach failure in a conventional sense, i.e. maximum $(\sigma_1' - \sigma_3')$ or σ_1'/σ_3', a triaxial compression test being stopped at only 1.3% axial strain (test TCa - 1). Failure is obscurely defined as the point at which the deformations show an accelerated rate of increase with respect to the octahedral shear stress, Ko (1966), Ko & Scott (1968b). It was necessary to plot the deformations on a logarithmic scale in order to establish this point. Based upon this concept of failure, ϕ' values were obtained that were higher in triaxial extension, b = 1, than in triaxial compression, b = 0. The strength of a medium loose sample increased rapidly by 5° from b = 0 up to an approximate plane strain

condition and then increased very slightly by about 1°, between plane strain and triaxial extension, b = 1. A medium dense sample showed a similar increase of 6° from triaxial compression to a point beyond plane strain and afterwards a 2° decrease to triaxial extension.

Reference to Fig 13 of Ko & Scott (1967a) shows that a failure ϕ' of 38.5° was obtained in a conventional triaxial test on a cylindrical sample, Green (1967). A similar test in the new apparatus, test TCa-1, failed to define a peak ϕ' and at 1.3% axial strain a ϕ' of 46.2° was obtained. Extrapolation of the stress-strain curve for test TCa-1 given by the new apparatus in an attempt to define a peak ϕ' will result in an even greater, and most unlikely, deviation from the stress-strain curve for the conventional test. This disparity is believed to be largely due to the rigid spacing frame used to prevent interference of the rubber bags at the corners, Green (1967), although Ko & Scott (1968a) have disputed this with unconvincing arguments. Arthur & Menzies (1968) have provided even stronger evidence of the inadequacy of Ko's tests, if indeed additional evidence were needed. Using a modified version of Ko's apparatus they obtained results in close agreement with conventional tests. By preparing the specimen in a mould outside the test box a high degree of control over the sample shape was obtained. The specimen was transferred under a small suction and carefully positioned so as to be just clear of the rigid frame separating the rubber bags used to stress the specimen. Arthur & Menzies observed that, provided the sample did not contact the rigid frame, the same strength was observed in triaxial compression in the new apparatus as in a conventional triaxial compression test on a $1\frac{1}{2}$ ins diameter, 3 ins high sample. The strains required to reach failure were greater than in the conventional test, which is in almost exact agreement with tests on short lubricated samples presented in Chapters 8 & 10 of this thesis. Ko & Scott's tests have also been discussed by Bell (1968) using both theoretical arguments and experimental data to cast serious doubt on their validity.

An almost identical apparatus is briefly described by Lomize & Kryzhanovsky (1966,1967). A 2.8 ins cubical specimen was tested under various combinations of the 3 principal stresses with the average principal stress both constant and varying. The authors make no mention as to what happened at the corners where the rubber membranes are apparently in contact

The paper is largely concerned with a theory of failure, the 1967 version being essentially an English translation of the original 1966 Russian paper and as such the translation is not clear on certain points. Two sands were apparently tested, Volga sand showed an increase in ϕ' from 36° to 45° and Dnieper basin sand an increase in ϕ' from 36° to 58°, as b varied from 0 to 1 respectively. The latter increase of 22° appears to be far too large to be credible. It is not clear to what extent the experimental variation in ϕ' between triaxial compression and extension follows the theoretical curve of Fig 2.5, see also Section 2.4.1.2, so that agreement or disagreement with Ko's tests is uncertain.

A brief description of the ISC apparatus described in this thesis together with the type of results obtained was given by Bishop (1967).

2.7.1.2 Clays

Only a few sets of tests have been reported on cuboidal shaped clay samples. Buisson (1948) used a similar apparatus to Daniel (1954,1957), described in Section 2.7.2.1, to test a stiff clay. No details were given regarding the testing technique nor were any numerical experimental data presented. The author states that the strength was higher than that obtained from direct shear tests on the same material. Whether this increase is representative of the real behaviour of the clay or is solely due to friction in the apparatus is unknown.

An ingenious apparatus was used by Shibata & Karube (1965) to test normally consolidated remoulded Osaka alluvial clay in undrained tests in which σ_2' was varied. Specimens 2.0 x 3.5cm wide, 6.0cm high tested in triaxial compression & extension, b = 0 & 1, gave the same strength, $c' = 0.02$ kg/sq.cm and $\phi' = 33.7^\circ$. Two confined water-filled pressure bags were used to apply $(\sigma_2' - \sigma_3')$ in the 3.5 cm lateral direction. These bags consisted of a thin sheet of nylon cloth sandwiched between 2 rubber membranes. A correction was applied to $(\sigma_2' - \sigma_3')$ for edge effects due to squeezing out of the bags, Shibata (1966). The samples were isotropically consolidated, then equal increments of $(\sigma_1' - \sigma_3')$ and $(\sigma_2' - \sigma_3')$ were applied, after which $(\sigma_1' - \sigma_3')$ was increased at a constant rate of strain. A maximum increase in strength of about 5° was observed for b approximately equal to 0.5, independent of the consolidation pressure. The results are presented on a reduced right section, see Chapter 11, so

that the precise increase can not be easily determined. An average line drawn through the experimental points forms a smooth curve lying outside the Mohr-Coulomb hexagon. There is apparently some conflict with subsequently published plane strain data, Shibata & Karube (1967), see Section 2.6.2, where the measured strengths (c', ϕ') were dependent on the consolidation pressure.

An almost identical apparatus was used by Yong & McKyes (1967) to test remoulded kaolinite prepared from a slurry using specimens 1.5 x 2.0 ins wide, 4 ins high. The constraining effect on the specimen of the flexible σ_2- bags was found to be negligible provided their contact surfaces were adequately lubricated. Tests were performed using both incremental loading and a controlled rate of strain to apply ($\sigma_1' - \sigma_3'$) and differences in pore pressure response were obtained which were not entirely resolved. The experimental data reported is scant and is largely concerned with the incremental load tests. Identical strengths were apparently obtained in triaxial compression and extension, c' = 0.23 kg/sq cm and ϕ' = 24°. Higher strengths, by 4° or 5°, were obtained for intermediate values of σ_2'. The shape of the failure envelope was very similar to that obtained by Shibata & Karube (1965).

2.7.2 Experiments on hollow cylindrical specimens

2.7.2.1 Sands

Kirkpatrick (1954, 1957) used a specimen 2½ ins I.D., 4 ins O.D. and 6 ins high of medium-fine sand which was failed by increasing the internal pressure. The specimen geometry was such that at failure in a drained test the radial stress corresponded to σ_1', the axial stress to σ_2' and the tangential stress to σ_3'. Based on the average radial and tangential stresses a point was obtained for b = 0.5 (approx) corresponding to a ϕ' value about 2° higher than that obtained in triaxial compression and extension. By assuming, as a first approximation, the Mohr-Coulomb criterion to be valid the distribution of tangential stress was calculated and hence the strosses at the inner and outer wall. Assuming, apparently that failure occurred simultaneously throughout the wall (this point is not clear from the 1957 paper) two points were obtained on the reduced right section for b = 0.36 & 0.65 (approx) each corresponding to a 2° higher ϕ'

value than that predicted by Mohr-Coulomb. Two assumptions in Kirkpatrick's stress analysis make it non-rigorous. The ratio of the tangential stress to the radial stress was assumed to be constant, whereas in elastic theory their sum is constant, and failure was assumed to occur simultaneously across the wall. These assumptions are contrary to conventional thick walled cylinder theory and whether they are justifiable or not is uncertain.

Torsion and an axial compressive load combined with differing internal and external pressures were used by Haythornthwaite (1960a,c) in drained tests on a remoulded silt. A rapid rise in strength was obtained between b = 0 and b = 0.2 (approx), thereafter ϕ' decreased to b = 1, a lower ϕ' value than that for b = 0 being obtained. To what extent the results reflect the complex loading system and the uncertainties of the stress analysis is uncertain as few details of either are given.

Whitman & Luscher (1962) made the same assumptions as Kirkpatrick in analysing drained tests on medium sized Ottawa sand on specimens 1 ins I.D. 1½ & 2 ins O.D., 3 & 5 ins high. The sample was axially restrained so that plane strain conditions existed and the external pressure was increased to failure, hence the tangential stress corresponded to σ_1' and the radial stress to σ_3'. An increase in ϕ' of 6° above that in triaxial compression was obtained which was constant over a 6% porosity range and independent of the sample size. One might reasonably have expected the difference in ϕ' to decrease as the porosity increases. This discrepancy, together with the limitations of the method of analysis, suggest that the 6° increase must be treated with some reserve.

Hollow cylinders of sand 4 ins O.D., 3 ins I.D., 6 ins high were tested by Wu et al (1963) in an undrained condition with pore water pressure measurements. Two loading systems were used giving two groups of points on the failure surface. In the first the external pressure was raised in excess of the internal pressure and the specimen was then loaded axially to failure. In the second, an increment of axial stress was applied, then the outside pressure was increased to failure. A sophisticated elastic-plastic analysis was used, the validity of which is not easily assessed. In the theory yielding first occurs at the inner wall and an elastic-plastic boundary spreads outwards, failure being considered to occur when yielding reaches the outer wall. Values of ϕ' based on

the average stresses in the tangential and radial directions are about 5° higher than those in triaxial compression and extension (which were equal). The validity of this increase as also of earlier results was questioned by Haythornthwaite (1963b) who reiterates the problem of the stress variations within the specimen. The aforementioned papers were also reviewed by Harr (1966) who makes light of the difficulties in the stress analysis.

Esrig & Bemben (1965) and Bemben (1966) performed constant volume tests on hollow cylindrical specimens of fine sand. Their analysis was based on the average principal stresses within the specimen wall, after Kirkpatrick (1954, 1957) and Whitman & Luscher (1962). Bemben (1966) shows that the equations for the average radial and tangential stresses are the same whether based on elastic or plastic theory. However in his analysis he initially correctly states that the sum of the radial stress σ_r' and the tangential stress, σ_θ' is constant (p 42) whereas later (p 44) agreement with Whitman & Luscher's equation is obtained which supposes that the ratio $\sigma_r' / \sigma_\theta'$ is a constant, an apparent contradiction. Equal or slightly higher strengths were obtained in triaxial extension compared with triaxial compression, see Fig 2.6. A maximum increase in ϕ' of 5.5° to 6.0° occurred at about b = 0.5 over a porosity range of 2.6%. The failure envelope on the reduced right section formed a smooth, nearly symmetrical curve between these points.

A significant series of drained tests on a fine sand under varying stress conditions were performed by Procter (1967). Specimens 6 ins high 4 ins O.D., and 1½ & 2½ ins I.D. were used to try to ascertain if the wall thickness had any significant effect on the measured ϕ' value and to examine the possible errors in the analysis. Procter discusses extensively the limitations of the various assumptions that may be made in the stress analysis and opts for a linear radial stress distribution across the cylinder wall. Based upon average stresses the strength of dense specimens varied by up to 10½° as b was varied from 0 to 1. The thicker walled specimens (1½ ins I.D.) exhibited a 2° higher strength in extension than in compression whereas the thinner walled specimens (2½ ins I.D.) gave similar strengths. Both sized specimens gave similar strength in triaxial compression. An average increase in ϕ' for plane strain was 9½° for the 1½ ins I.D. specimens but was only 7° for the 2½ ins I.D. specimens, both maximum values. Plane strain tests on the same material by Wightman (1967),

see Section 2.6.1, showed only a 5° increase above triaxial compression. A difference of 2° or 4½° between the cuboidal sample and the hollow cylinder sample suggests that one or other is in error, most likely the hollow cylinder analysis. Clearly errors of so large a magnitude are highly undesirable and substantiate the inadequacy of the latter test.

2.7.2.2 Clays

Parallel with the tests on sand described in the previous section Wu et al (1963) performed similar undrained tests with pore water pressure measurements on a remoulded plastic clay. The authors claim that the data fit the Mohr-Coulomb criterion. However, assuming $c' = 0$, the results show a considerable scatter, the range of ϕ' values being from 26.7° to 35.2°, a difference of 8.5°. The distribution of the points on the failure envelope suggest that a large proportion of the scatter is associated with the mode of failure of the specimen together with the stress analysis used, see also Haythornthwaite (1963b).

Broms & Ratnam (1963) performed undrained tests with pore water pressure measurements on both isotropically and anisotropically consolidated remoulded kaolin. The specimens were 3 ins I.D., 6 ins O.D. and 4.5 ins high, with inner and outer sample sheaths 0.010 and 0.025 ins thick respectively. Analysis was based on the average stresses and failure was defined at maximum $(\sigma_1' - \sigma_3')$. Normally consolidated specimens exhibited a c' and ϕ' of 1.5 psi and 24.5° when isotropically consolidated and 2.0 psi and 28.5° when anisotropically consolidated. Overconsolidated specimens exhibited a c' and ϕ' of 4.0 psi and 23.0° when isotropically consolidated and 3.5 psi and 27.5° when anisotropically consolidated. The values of the cohesion intercept, c', appear to be rather high and may be due to the effect of the sample sheath, which, in aggregate, is very thick. The proportions of the specimen are such that the results are very likely affected by end restraint, but to what extent is uncertain. In a later series of tests on similar material Casbarian (1964) and Broms & Casbarian (1965) used a 10 ins high specimen of the same I.D. and O.D. as before. The shape of the $\phi' - b$ relationship was very similar to that obtained by the writer and reported in this thesis. In Series II C tests consolidated at 70 psi ϕ' increased from 29.2° to 36.0° as b varied from 0 to 1, an increase of nearly 7°. The value of ϕ' increased rapidly with increasing inter-

mediate principal stress for values of b less than about 0.25, thereafter the increase was small. The significance of these results is difficult to assess from the sparse information given by Broms & Casbarian (1965). It is noted that filter paper drains were placed on the inside and outside cylindrical surfaces of the specimen to aid drainage. The torque measurements were apparently corrected for the effects of the sample sheath and filter paper strength but the axial load was not.

The far more difficult problem of a cross-anisotropic clay in which the axis of the hollow cylinder corresponds to the axis of symmetry has been the subject of limited investigations by Suklje and Drnovsek (1965) and by Saada & Baah (1967). The former's studies were largely theoretical and little experimental data is given. The latter found that the intermediate principal stress should be included in the failure criterion and that as a first approximation, Hill's criterion for a cross-anisotropic material was found satisfactory, Hill (1950).

2.7.2.3 Torsion tests on solid cylinders

A torsion test on a solid cylindrical sample may be considered as a special case of a hollow cylinder test in which the inside diameter is reduced to zero. The stress distribution is, of course, particularly intractable. Habib (1951, 1952, 1953) used a dumb-bell shaped specimen to prevent failure occurring at the ends in a series of drained torsion tests on sand. Based on a plastic stress analysis, ϕ' increased from 33° for $b = 0.09$ to 36° for $b = 0.22$ and thereafter decreased to 27° for $b = 0.80$. Triaxial compression, $b = 0$, showed a $\phi' = 32^\circ$ and triaxial extension, $b = 1$, a $\phi' = 25^\circ$. The different types of test are self-consistent. However the lower ϕ' measured in extension compared to that in compression is contrary to the majority of other test data which suggests that they are equal or that the extension ϕ' is higher than the compression value.

2.8 Important factors involved in developing an adequate independent stress control test

The difficulties associated with pore water pressure equalisation and dissipation, filter paper drain strength and extended testing times are avoided by confining the investigation to drained tests on a saturated sand

or similar relatively permeable material. A number of common potential errors can be eliminated or reduced to what are believed to be negligible proportions by good apparatus design and careful attention to detailed testing technique. These include errors due to piston friction and proving ring calibration, pressure gauge calibration, sample sheath rigidity, sample sheath penetration and initial specimen non-uniformity or gross anisotropy or both.

It appears that the introduction of one or more greased rubber membranes of a suitable thickness at a sample/rigid platten boundary will significantly reduce the shear stresses applied to the sample due to friction. A number of experiments using greased rubber membranes to reduce end restraint indicate that they are generally successful. Explanations are available for those few tests which were unsuccessful, notably due to using too thin a membrane in relation to the sample particle size. In addition, Balla's theory suggests that a low friction contact will significantly increase the uniformity of the stresses within a triaxial sample. There is apparently no evidence available to indicate that the use of a lubricated rubber membrane causes premature failure of a soil sample due to the membrane being squeezed out from between it and the platten as has been observed for rocks and concrete, at least at the stress levels commonly used (up to $\sigma_1' = 300$ psi, say). Non-uniform deformations may still occur, particularly after failure, but the degree of non-uniformity is markedly reduced compared to a conventional shaped specimen.

This being so one should be able to modify the proportions of a cylindrical triaxial specimen to a H/D ratio of 1 without the measured strength (ϕ') being changed, presupposing of course that the conventional sample gives the 'correct' strength. At the same time the strains should be more uniform throughout the new specimen and therefore more realistic, and by inference so should the stresses. It should also be possible to obtain satisfactory triaxial compression and extension test data on cubical or cuboidal shaped samples using a similar technique. The essential steps in the investigation are as follows:-

(a) To vary H/D, and the degree of end restraint in cylindrical triaxial compression test specimens.

(b) To vary H/D and the degree of end restraint in cylindrical triaxial extension test specimens.

(c) A careful review of the data from (a) and (b) to determine the optimum sample shape and number & thickness of lubricated membranes required.

(d) To vary the sample geometry and the degree of end restraint in cuboidal triaxial compression and extension test specimens.

(e) A careful review of the data from (d) in the light of (a),(b),& (c) to try to obtain a suitably proportioned specimen for the independent stress control test.

(f) To examine the influence of continuously varying the intermediate principal stress, σ_2', between the limits of σ_1' and σ_3' as used in the triaxial compression and extension tests respectively.

(g) A careful review of the data from (f) and a comparison with that for the optimum shaped cylindrical and cuboidal triaxial compression and extension test specimens.

Taking ϕ' measured in triaxial compression, b = 0, as the basis, existing published evidence indicates that for sands the strength in triaxial extension, b= 1, is the same or is greater by up to 6-8°. The greatest increase is for dense specimens but loose specimens may also show a small increase. To what extent these conclusions hold for specimens other than cylindrical is largely unknown. The strength in plane strain, b= 0.2 or thereabouts, is found to be equal to that in triaxial compression for loose samples and is greater by up to 6-8° for dense samples. The form of the variation of ϕ' with b as the latter is continuously varied between the limits 0 and 1 is more controversial. The main uncertainty appears to be whether or not ϕ' increases, remains constant or decreases beyond plane strain as b is increased towards 1. Many of the tests which are used to examine this are of the hollow cylinder type against which a number of objections may be raised so that the data must be regarded as inconclusive.

Having obtained experimental data delineating the behaviour of the sand as b is continuously varied it remains to examine which, if any, of the failure theories currently available fit the observations. Those based on continuum mechanics can cope with most likely, and some unlikely, variations in strength as b is varied. Those based on particulate mechanics have barely reached a stage of development at which they can cope with a generalised stress system. In addition the degree of rigour of the proofs of some of the particulate theories is not yet well established. A detailed examination of these theories is outside the scope of this thesis.

CHAPTER 3

PRELIMINARY STUDY OF THE MODE OF DEFORMATION OF CYLINDRICAL TRIAXIAL COMPRESSION TEST SAMPLES

3.1 Ideal shear test samples

The ideal sample shape for a test in which the 3 principal stresses are independently varied appears to be a cube. Uniform normal boundary stresses would ideally be applied to 3 pairs of opposite faces. However the practical difficulties are very great in devising an apparatus capable of applying a set of stress-controlled boundary conditions. Likewise strain control on all boundaries is a very difficult proposition (this is currently being tried in a plane strain device by Roscoe at Cambridge). A mixed boundary solution appears to be much more tractable.

The corner problem is more acute at the junction of 2 stress-controlled boundaries than at the junction of 2 strain-controlled boundaries where the soil may be allowed to arch across a small gap. No corner problem arises at the junction of a rigid, strain-controlled boundary and a flexible stress-controlled boundary. In the conventional triaxial compression test the σ_1 boundary is strain-controlled whereas the $\sigma_2 = \sigma_3$ boundary is stress-controlled. In Ko's soil test box, Ko (1966), Ko & Scott (1967a), all 3 pairs of boundaries are stress-controlled. In the ISC cell described in this thesis, 2 pairs of boundaries are strain-controlled while the 3rd pair is stress-controlled.

3.2 Shape factor for a cylindrical triaxial compression sample

Before we can justify using a cubic sample it is necessary to see whether a cylindrical triaxial compression sample with H/D = 1 will give satisfactory results. The end restraint problem associated with testing compression samples between rigid loading plattens is well known. By using a sample with H/D = 2 or $2\frac{1}{2}$, the effect on the measured strength of the shear stress developed across the interface of the sample and the rigid loading platten is generally considered to be eliminated. If the H/D ratio is increased much beyond $2\frac{1}{2}$ or 3 the sample may fail by buckling

and will give a low apparent strength. If the interfaces between the sample and the plattens were perfectly frictionless we could reduce the H/D ratio below 2 to 1, say. Indeed we could, theoretically, reduce $H/D \rightarrow 0$ so that the sample became in effect a thin disc.

3.3 Previous work

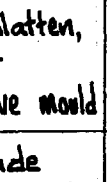
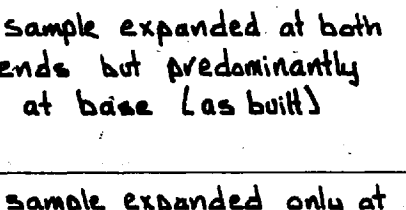
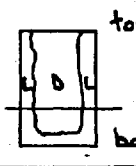
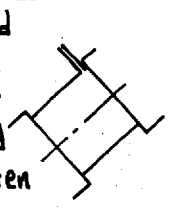
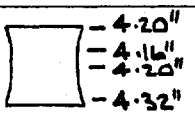
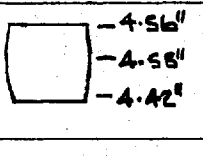
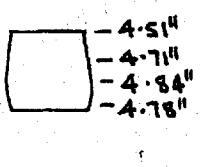
It had, at the time the present research was begun, 1963, been shown by Freedman (1959), Barnes (1960), Gray (1960), that a lubricated membrane inserted between the sample and a polished flat rigid platten reduced the effect of end restraint so that a H/D ratio of 1 could be justifiably used (see also Chapter 2). However the mode of deformation was still the subject of some uncertainty. At small strains, up to peak ϕ', the samples remained essentially cylindrical but beyond failure the samples expanded predominantly either at the top or at the base. It appeared to be very difficult, but not impossible, to obtain continued uniform lateral expansion throughout the whole of the shear test. In later papers, Rowe & Barden (1964), Lee (1966), it was suggested that the non-uniformity was associated with the drainage conditions and that by closing the top drainage lead more uniform lateral expansion could often be obtained.

3.4 Test results

In view of the uncertainty it was decided to perform a series of preliminary experiments to study the mode of deformation of 4 ins diameter samples, generally 4 ins high. The samples were sheared relatively rapidly (1% per minute) and no stress or strain measurements were made, Fig 3.1. All the compression tests were on Belgium sand, Sable de Mol, Ladanyi (1960), Wade (1963), generally with 1/0.010 ins thick lubricated membrane at each end of the sample.

The results of tests type P1 (4 tests), P2, P3 and P4 suggest that a medium dense or loose sample made in a conventional manner, i.e. by spooning or pouring, wet or dry, expands predominantly at the base. A circumferential slip zone just below the top platten suggests that a punching action frequently exists, i.e. an upper, relatively rigid, cone of sand displaces the lower portion of the sample outwards, see also Plate 8.3(a).

An extensive porosity gradient was formed in test type P5. The mode of deformation is remarkable in that the upper loose portion expanded non-

Test type	Dry or Sat.	Sample height	Density	Special features	Observations	Conclusions
P1	sat.	4" high	medium dense	4 tests, placed by spooning & tapping mould	sample expanded predominantly at base, slip zones visible, punching action	sample very reluctant to expand at top
P2	sat.	2" high	medium dense	placed by spooning & tapping mould	sample expanded predominantly at base, punching action, no slip zones visible	
P3	dry	2" high	loose	placed by pouring from funnel	sample expanded predominantly at base, no slip zones visible at $\Delta H/H_c$ = +30%	
P4	dry	4" high	loose	placed by pouring from funnel, extra thickness of sample sheath around base of sample 	sample expanded predominantly at base, trace of slip zone visible at $\Delta H/H_c$ = +30%	
P5	dry	4" high	loose/ dense	top half of sample- loose, by pouring from funnel, bottom half - dense, by extensive tamping	 $\Delta H/H_c$=+10% $\Delta H/H_c$=+30%	top half of sample equivalent to P3
P6	dry	4" high	dense	extensive tamping, top platten-lubricated, bottom platten-direct contact	no expansion at base, expansion at top	expansion at top will occur if forced
P7	dry	4" high	dense	surrounded by mercury to within "/2" of top of sample	sample expanded predominantly at base	gravity forces not significant
P8	dry	4" high	dense	3" deep solid top platten	sample expanded predominantly at base	normal top platten is sufficiently rigid
P9	dry	8" high	dense	vibrated, tested slowly, strain rate 0·0016 ins/min.	barrel-shaped, ends did not expand, single slip zone	lubricated ends have no significant effect on a conventional sample
P10	dry	4" high	dense	vibrated, triaxial cell inverted and clamped to load frame crosshead after pressurising	sample expanded at both ends, but predominantly at at base (as built)	gravity forces not significant
P11	dry	4" high	dense	sample made upsidedown on upturned top platten, inverted after part assembly, then remove mould	sample expanded at base and not at top (as built)	sample preparation is crucial factor
P12	dry	4" high	dense	6" high sample made upsidedown on upturned top platten, inverted, strike off 2" from base	sample expanded at both ends but predominantly at base (as built)	 no 'wall' effect
P13	dry	4" high	loose	lubricated membranes placed on both plattens at same time, σ_3' raised to 150 p.s.i. then reduced to 40 p.s.i.	sample expanded only at base, punching action	overconsolidation has no effect on deformation pattern
P14	dry	4" high	medium dense	compaction in 1/2" layers with 4" diam., 14lb static ram	sample expanded predominantly at base	Compaction in layers not significant
P15	dry	4" high	medium dense	compaction in "/2" layers with 4" diam., 14lb static ram, upsidedown as P11	sample expanded at base and not at top (as built)	
P16	sat.	4" high	medium dense	no top drainage, strain rate 0·0005 ins/min.	sample expanded predominantly at base	drainage conditions not significant
P17	sat.	4" high	medium dense	no bottom drainage, strain rate 0·0005 ins/min	sample expanded predominantly at base	
P18	dry sat.	4" high	medium dense	2 tests, sand poured through tube at corner of tilted mould with top platten in position 	mould not filled completely, sample expanded at both ends, complicated by tilting of top platten and void under edge of top platten	contact between sample and plattens is crucial factor
P19	dry	4" high	dense	vibrated, no top drainage	sample expanded at both ends, increased expansion at base late in test	
P20	dry	4" high	dense	vibrated, drainage at both ends	sample expanded at both ends, increased expansion at top late in test	
P21	dry	4" high	dense	vibrated, drainage at both ends, top loosened by striking off with straightedge	sample remained cylindrical till $\Delta H/H_c$ = 15%, base expansion predominant subsequently, no visible slip zones	
P22	dry	4" high	medium dense	compaction in 1/2" layers with 4" diam, 14lb static ram, top layer made dense by tamping	sample expanded predominantly at base	

RESULTS OF PRELIMINARY STUDY OF MODE OF DEFORMATION OF 4 INS. DIAMETER CYLINDRICAL TRIAXIAL COMPRESSION TEST SAMPLES

All tests on Belgium sand, Sable de Mol, G= 2·65 (Wade, 1963)
10·010 ins. thick lubricated membrane generally used at each end of sample.
Sample sheath 0·020 ins. thick. Drainage generally from both ends.
Strain rate generally about 1% per minute. σ_3' = 40 lbs/sq. ins.

FIG. 3.1

uniformly, the greatest expansion being at its junction with the dense lower portion of the sample. One might have expected expansion to occur predominantly at the top platten since, if the top 2 ins of the sample is considered to be equivalent to test type P3, its base is in contact with a relatively frictional boundary.

Omission of a lubricated membrane from the base of the sample in test type P6 was sufficient to reverse the mode of deformation; also observed by Lee (1966).

Surrounding the sample with mercury in test type P7 causes an increase in σ_3' at the base of the sample of 1.71 psi (compared with a normal pressure increase of 0.15 psi due to the water in the cell) but did not change the mode of deformation. We may postulate that the predominant base expansion was caused by the increase in vertical stress of 0.29 psi at the base of the sample due to its self-weight. If this were correct then one would have expected the base expansion of the sample surrounded by mercury to have been suppressed. Indeed, since the vertical pressure gradient due to mercury was 12.6 times that due to water one might expect the sample to have expanded predominantly at the top. This did not occur and therefore gravity forces do not appear to be very important.

Although it appeared very unlikely that the top loading platten was not sufficiently rigid it was replaced by a 3 ins deep solid brass platten in test type P8. No change in the deformation pattern was observed.

A conventional 8 ins high dense sample, test type P9, sheared slowly, failed by symmetrical barrelling with a single slip zone inclined at about 59° to the horizontal. There appeared to be no expansion at either platten contact. Freedman (1959) tested 8 ins diameter, 16 ins high samples and observed that a lubricated end was effective in allowing free lateral expansion of the sample but that they did not always fail as a cylinder. Often the top or bottom half would bulge at large strains and this was attributed to initial non-uniformities in the sample caused by the method of sample preparation.

In test type P10 the assembled triaxial cell was inverted and clamped to the load frame crosshead as a further check on a possible gravity effect, again with a negative result identical to test type P7.

Test type P11 was a crucial test. A dense dry sample was formed upside down on the upturned top platten. The cell base was inverted and clamped to the mould, the rubber membrane turned back and the O-rings

secured. The whole assembly was inverted by sliding it off the edge of the bench whilst supporting the top loading platten by hand. When sheared the sample expanded across the top platten, i.e. the base as built. This suggests that there is a significant difference in the form of contact between the top and bottom plattens. In the normal method of sample preparation the sand is poured onto the bottom platten and a relatively uniform, intimate contact may be inferred. The top of the sample is levelled with a straight edge using a tamping action similar to that used in screeding off concrete. The top loading platten is then carefully lowered into position so that one can envisage contact along a series of irregular ridges. It seems that this difference may be a major factor in causing the non-uniform lateral expansion.

The influence of a rigid boundary on the packing of particulate materials has received some attention in the past, e.g. Graton & Fraser (1935), Macrae & Gray (1961), Bernal (1962), Bernal et al (1964). Macrae & Gray suggest that variations extending only a few grain diameters from the rigid boundary occur when dry granular materials are poured into rigid containers. However they used $\frac{1}{8}$ ins diameter spherical particles poured into a 3 ins diameter cylinder so that there is a major scale difference to the present problem. Bernal and his colleagues have carried out a number of intriguing experiments directed primarily towards obtaining a model of the structure of a liquid. They show that "crystals" of ordered packings can grow within a random mass of steel spheres when subjected to cyclical shearing. A flat plate is shown to act as a nucleous for this crystal growth, see. Fig 16, Bernal (1962).

In tests type P12 to P15 inclusive, efforts were made to try to eliminate the suspected difference in sample contact, however none were successful. In test type P12, a 6 ins high sample was made (with the aid of a collar from a Proctor mould) on the upturned top platten similar to P11. After inverting, the 2 ins collar was removed and the sample struck off level. Uniform lateral expansion was not obtained. In test type P13 both lubricated membranes were made up at the same time in case the ageing of the grease film was significant, Roscoe (1953), Appendix A1. In addition the cell pressure was initially raised to 150 psi and then reduced to 40 psi in an attempt to bed the sample onto the platten, particularly the upper platten. No difference in the behaviour of the sample was observed.

The samples used in tests type P14 and P15 were compacted in $\frac{1}{2}$ ins layers, using an identical technique to that used in the suction probe experiments, see Appendix A2, Fig A2.1. No significant changes in their modes of deformation were observed.

As already noted, it has been suggested that by restricting drainage to the base of the sample a more uniform lateral expansion can be obtained although the reasons for this are not clear. In tests type P16 and P17 the top and bottom drainage leads respectively were closed but no significant changes were observed.

The suspected difference in contact at the ends of the sample was further pursued by attempting to prepare samples by pouring sand into the mould through a tube at the corner. A notch was made in the mould and both end plattens were clamped to the mould. The sample sheath was sealed to the bottom platten but remained turned back over the mould at the top. A flexible tube was inserted under the edge of the platten, the sample sheath forming an effective seal. Sand was poured through a funnel with the mould tilted up. By rocking the mould back and forth attempts were made to fill it as far as possible. Two tests type P18, one dry and one saturated, were performed. In both cases the sample appeared to expand uniformly at both ends but this was complicated by the sample being imperfect at the corner where the tube had been, causing the top platten to tilt upon applying the cell pressure. However the results tend to confirm that the contact difference is very important. Unfortunately the method of sample preparation used in test type P18 is impractical for general use as it appears to be impossible to avoid a cavity or a relatively loose portion at the top 'corner'.

A series of 3 vibrated (dense) samples were then tested, types P19, P20 & P21. The measured sample diameters indicate that lateral expansion occurred throughout the sample height, but that at large strains the degree of non-uniformity increased.

A final test on a medium dense sample, type P22, in which the top layer was carefully tamped to densify it gave no further significant information.

3.5 Review of mode of deformation

The major factor influencing the mode of deformation of 4 ins diameter,

4 ins high cylindrical triaxial compression samples appears to be the difference in the contact at the top and botton sample-platten interfaces. Generally the observations are in agreement with those made by researchers at Manchester University and summarised by Khayatt (1965). It was not possible to obtain any significant difference in the mode of deformation by restricting drainage to one or other ends of the sample; this is in contrast to Rowe and Barden (1964), Khayatt (1965), Lee (1966).

It was concluded that the sample preparation technique used in test type P18 was not a practical proposition and that the normal method would have to suffice. However during the initial stages of the first series of cylindrical triaxial compression tests S.W.Smotrych suggested that it might be possible to form a sample in two halves. After some initial tests the preparation technique described in Chapter 7 was finally used and generally resulted in a more uniform lateral expansion of the sample throughout the test.

CHAPTER 4

DESIGN, DEVELOPMENT AND DESCRIPTION OF APPARATUS

4.1 Triaxial cell for cylindrical compression tests

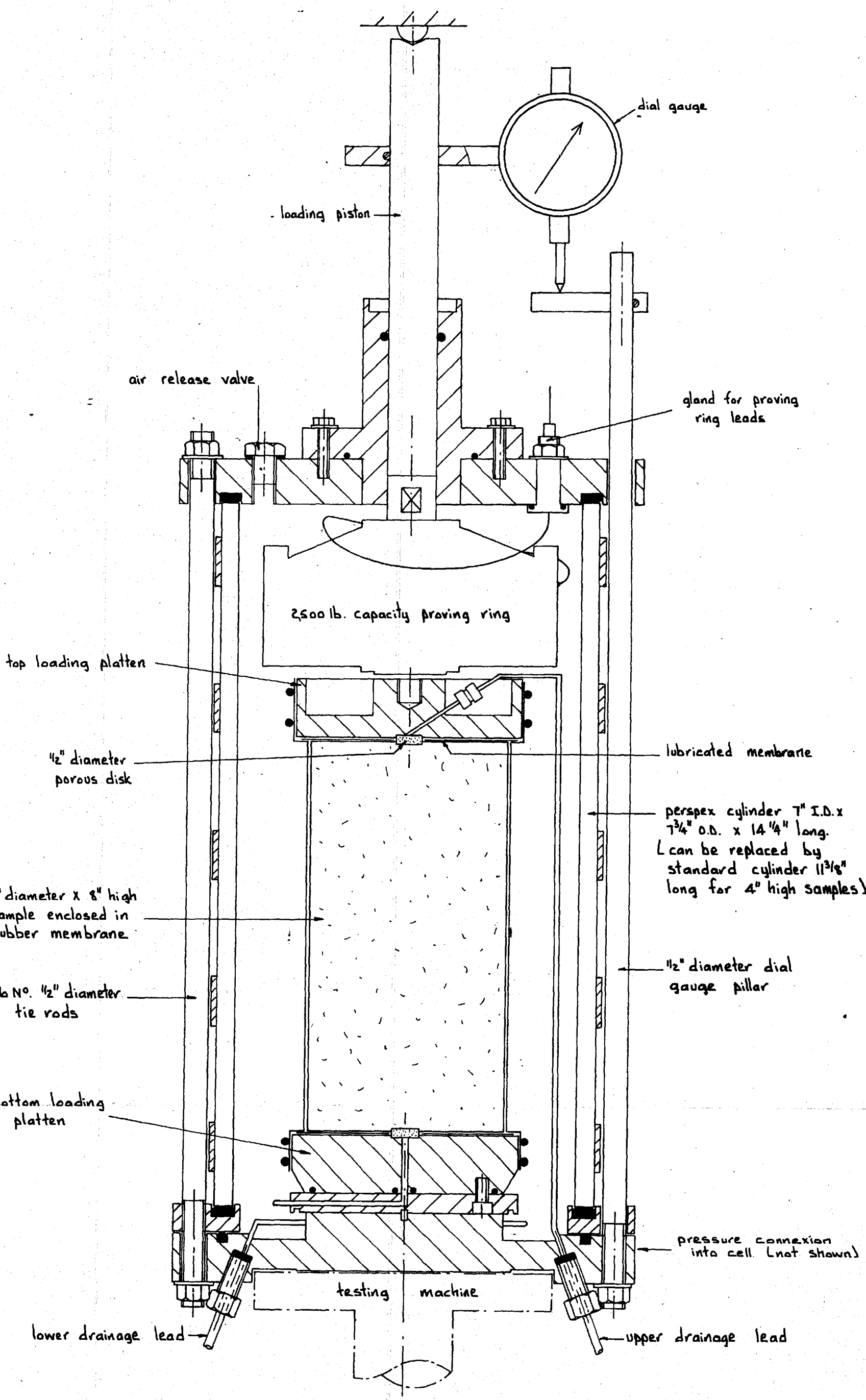
4.1.1 Introduction

A cross-section of the cell used for the cylindrical triaxial compression tests is shown in Fig 4.1 and two general views are shown in Plates 4.1 & 4.2. A conventional cell for 4 ins diameter specimens, Bishop & Henkel (1957), was modified to accommodate an internal axial proving ring mounted on the end of a 1 ins diameter loading piston. The piston passed through a heavy brass bushing bolted to the flat top of the triaxial cell. An O-ring seal to prevent leakage was incorporated in the bushing. Since the load was measured internally any frictional loss in the bushing was of no consequence. This is a marked improvement over the conventional external proving ring and fixed bushing, Bishop & Henkel (1957). It is also a significant improvement over the conventional external proving ring and rotating bushing, Wood (1958), Andresen & Simons (1960), Bishop et al (1965). A carefully made rotating bushing may function quite well initially but a little wear may cause the piston to oscillate and apply a fluctuating load to the sample. Internal electrically recorded load measurement is clearly better in every way provided a reliable system is used, in particular one that is insensitive to lateral loads.

4.1.2 Enlarged loading plattens

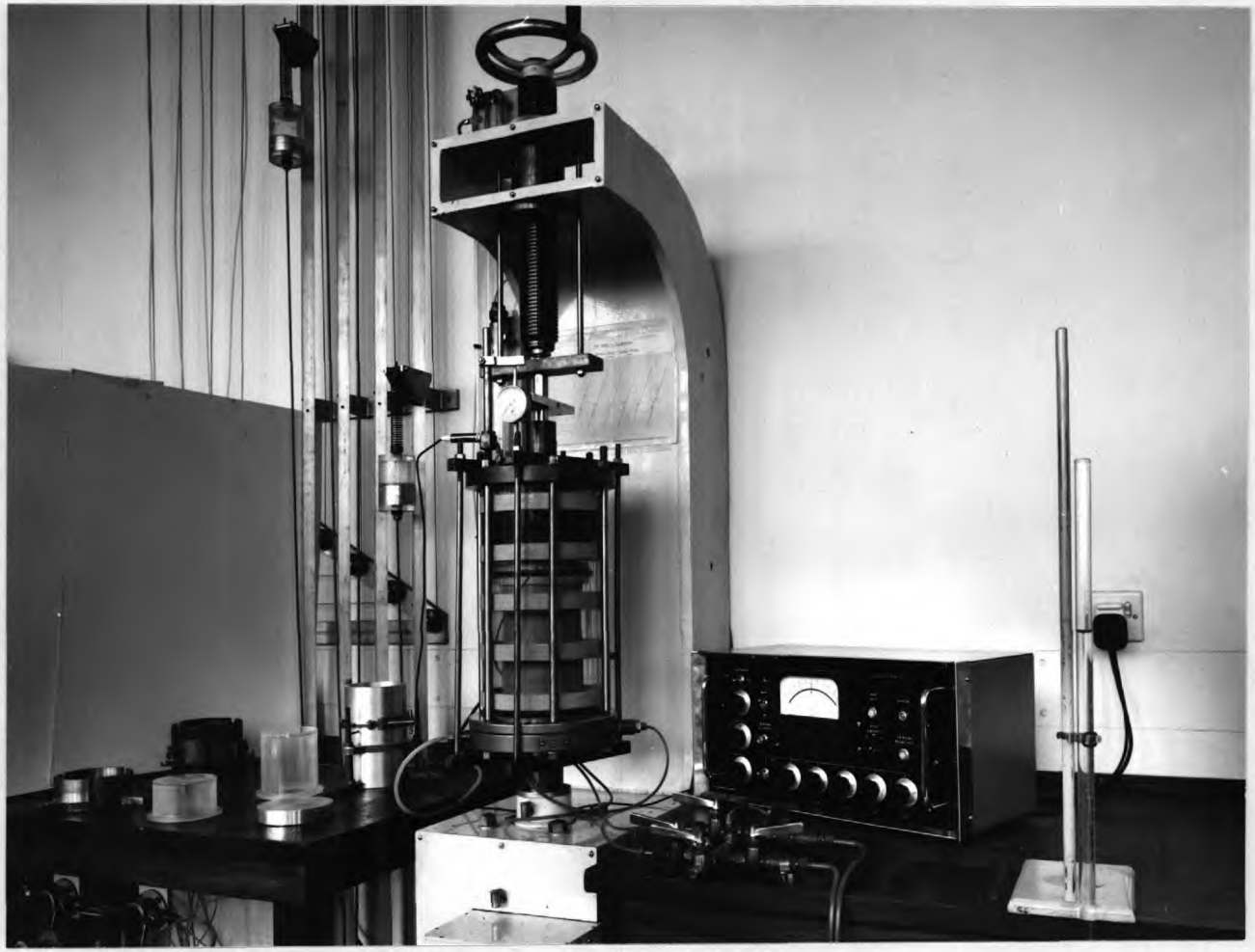
The conventional loading plattens were replaced by enlarged stainless steel plattens (EN58J) carefully machined flat and polished to a mirror finish. These enlarged plattens were 4.7 ins diameter which allowed a lateral expansion of up to -17% to occur before the sample overhung the edge. At the same time it was possible to stretch the sample sheath over the platten reasonably easily.

In order to facilitate the preparation of a sample in two halves, see Fig 7.1 it was required that the bottom platten be removable together with its drainage lead. This platten was bolted to an aluminium alloy disc which was located on a spigot on the cell base to ensure coaxiality. A



TRIAXIAL CELL FOR CYLINDRICAL COMPRESSION SAMPLE

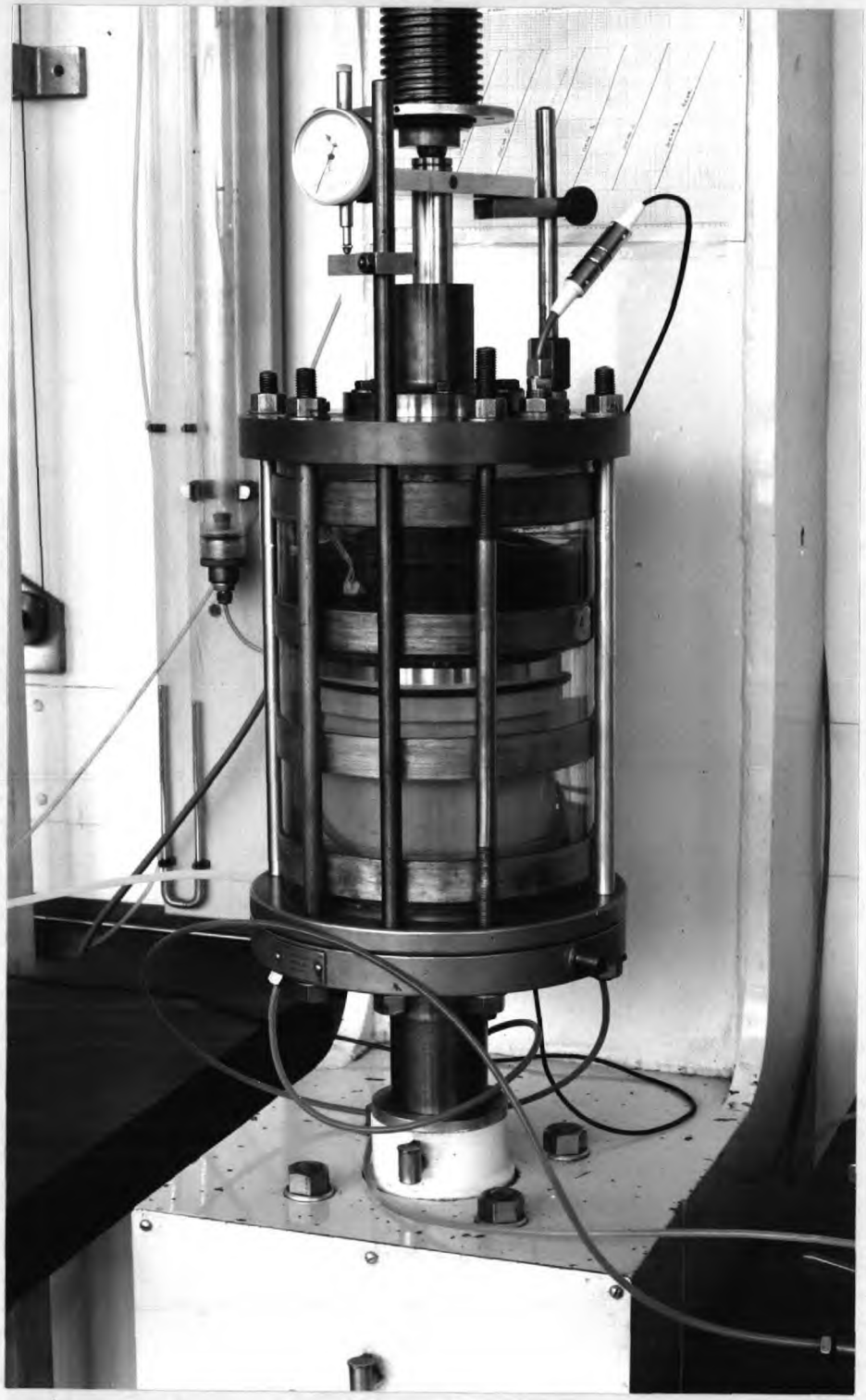
Scale: half full size.



GENERAL VIEW OF TRIAXIAL APPARATUS FOR CYLINDRICAL COMPRESSION AND EXTENSION SAMPLES.

The cell is set up for an extension test.

PLATE 4.1



TRIAXIAL CELL FOR CYLINDRICAL COMPRESSION SAMPLES.

PLATE 4.2

long flexible plastic lower drainage lead allowed the bottom loading platten to be placed on a bench adjacent to the cell base. A groove in the underside of the aluminium alloy disc served as an anchorage for the 3 clamping bars used to fix the mould during preparation of a sample in two halves, Fig 7.1. For samples prepared in a normal manner the bottom loading platten was bolted directly to the cell base, Fig 4.3.

Porous discs of vitrified bauxilite A80KV, $\frac{1}{2}$ ins diameter were used at both ends of the sample to permit drainage and to allow water to be circulated should any air bubbles be trapped in the leads after sample preparation. These discs were each mounted 1/16 ins proud of the surface of the platten to facilitate their removal. They also helped to stabilise the sample against bodily sliding out from between the plattens.

The anvil of the proving ring made direct contact with the top loading platten to ensure that the latter could not tilt and that uniform axial deformation was applied to the specimen during compression.

4.1.3 Sample sheath

A standard rubber sample sheath about 0.020 ins thick was used for all the 4 ins diameter samples. It was sealed to the enlarged plattens with soft grade O-rings of unstretched internal diameter $3\frac{1}{2}$ ins placed with the aid of a split ring. Little difficulty was encountered in stretching the sheath neatly over the plattens.

Attempts to use a thin sample sheath 0.010 ins thick, were discontinued as it was too easily punctured by the sand particles during sample preparation.

4.1.4 Internal axial proving ring

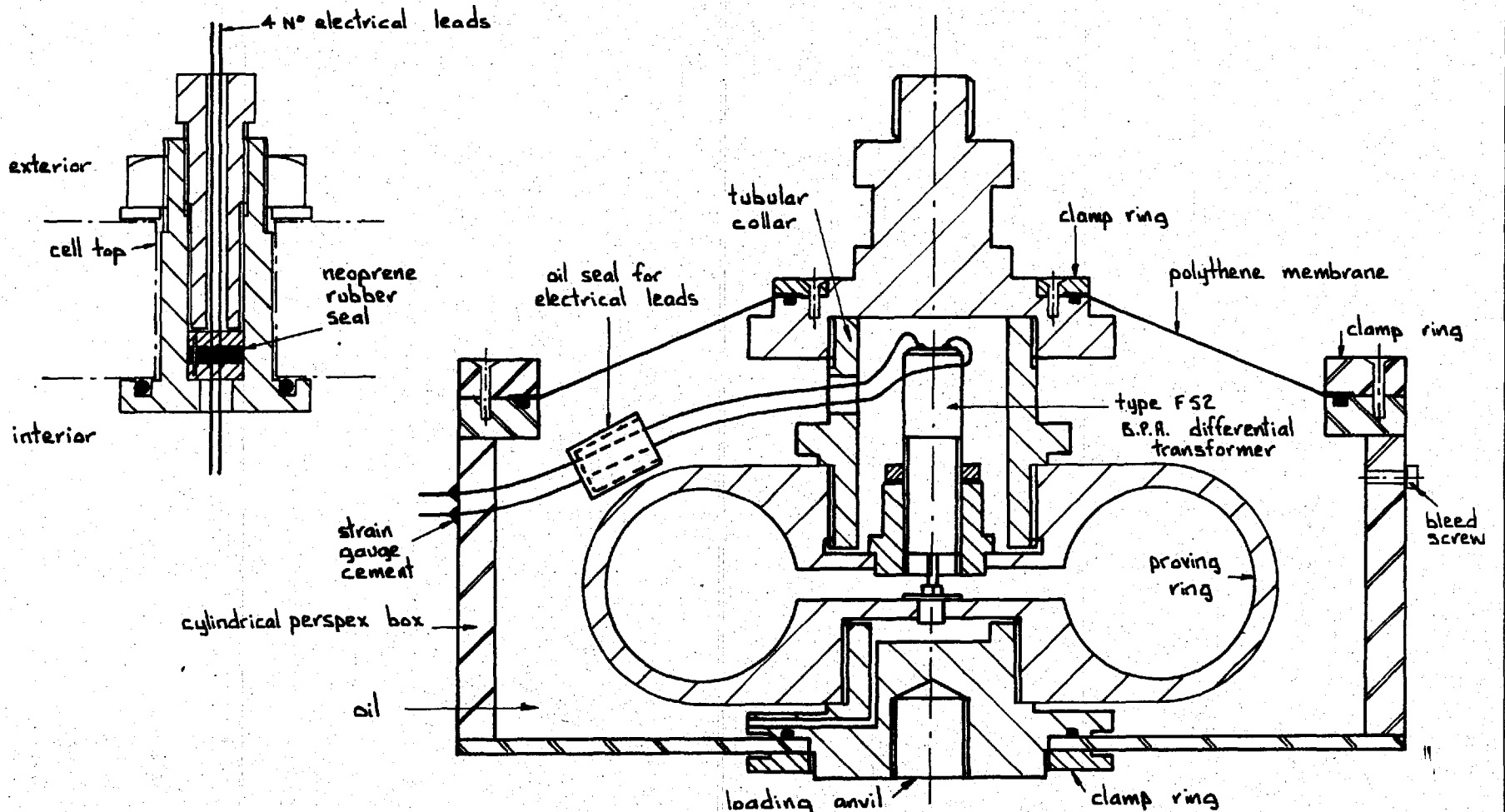
The suitability of a commercially available differential inductance displacement transducer coupled to a steel proving ring and associated measuring equipment was brought to the writer's attention by A.E.Skinner. Taylor (1941) used a conventional proving ring inside the triaxial cell, but above a free water surface, which was subjected to controlled air pressure. Difficulty was encountered with the stability of the system as the load was increased and also, apparently, with the migration of air through the rubber sample sheath. Casagrande & Shannon (1948) used an

internal proving ring fitted with electrical resistance strain gauges for studying the influence of high rates of loading. More recently internal load cells using electrical resistance strain gauges have been used in triaxial cells by Nash & Dixon (1960), Dunn (1964), Sparrow & Beaty (1964) and others. Electrical resistance strain gauges under stress over a long period of time have, in the past, often been unreliable. However developments in their design and improved adhesives make them more attractive in the immediate future.

The axial load was measured with a flat steel proving ring having a maximum working load of ± 2500 lbs and a maximum deflection of ± 0.025 ins, Fig 4.2 & Plate 4.3. The ring is comparatively stiff so that the post-peak portion of the stress-strain curve should be more accurately defined as the elasticity of the loading system is very much reduced. The deformation was recorded by a 4-arm differential inductance type displacement transducer, type F52, mounted on the axis of the ring. The body and the free armature of the transducer are separately threaded into brass bushes cemented to relatively stress-free portions of the proving ring. The brass loading anvil and tubular brass collar are shouldered to transmit the axial load directly into the ring to avoid stressing the displacement transducer mounting flanges. The ring is fixed to the loading piston by a heavy threaded brass boss.

The unit is enclosed in an oil-filled fabricated cylindrical perspex box to protect it, prevent corrosion and to ensure good electrical insulation. The cell pressure is transmitted to the oil through a polythene membrane. O-ring seals are used on appropriate joints, but serve only to retain the oil, there being no pressure differential across them. The loading anvil is threaded to permit a connection for extension tests to be screwed in.

The 4 electrical leads to the displacement transducer are fed through a detachable gland in the top of the triaxial cell which facilitates removal for calibration. The wires are threaded through 4 holes in a neoprene rubber disc which is compressed between two similar brass discs. To prevent air from being forced out along the interstices between the stranded wire leads and the plastic insulation a seal was made in the leads inside the perspex box. The wires were each bared and solder was run into the strands over a $\frac{1}{8}$ ins length. The leads were then potted in araldite



2,500 LB CAPACITY AXIAL PROVING RING AND GLAND FOR LEADS

Scale : full size

FIG. 4.2



2,500 LB. CAPACITY AXIAL PROVING RING AND B.P.A. TYPE C61 TRANSDUCER METER.

PLATE 4.3

using a perspex tubular former. This arrangement was completely successful in preventing leakage.

The coils of the 4-arm differential inductance displacement transducer are connected as the active arms of a bridge circuit. Movement of the armature varies their inductance differentially thus unbalancing the bridge and giving rise to an output signal at carrier frequency. The transducer is energised by the C61 null indicating transducer meter containing a built in oscillater which supplies a 5V.200 m A (max) at 2.5 kc/s signal. The out of balance signal is nulled by torroidal tapped transformers having a span of 10^5 digits.

The C61 meter was developed specifically for the electronic measurement of small physical quantities with observations extending over long periods of time. The null method of reading eliminates some errors completely, others are reduced by careful circuit design. The transducer meter, proving ring, and displacement transducer were supplied by Boulton Paul Aircraft Ltd.

Details of temperature effect, zero stability and long-term stability checks together with the appropriate load calibrations are given in Appendix A3.

4.1.5 Cell design

The conventional cell for 4 ins diameter specimens was large enough to accommodate a 4 ins high sample together with the internal axial proving ring. For 8 ins high samples the standard reinforced perspex cylinder Plate 4.2, was replaced by one 3 ins longer similarly reinforced with circumferential bands of resin-bonded glass fibre, Plate 4.1.

Axial deformation was measured with a 1 ins travel dial gauge reading to 0.001 ins mounted on an arm clamped to the loading piston and bearing against a rod fixed to the cell base.

Alignment of the loading piston with respect to the cell base required uniform peripheral tightening of 3 O-rings. The upper portion of the cell was adjusted after assembly so that the flat cell top was parallel to the annular clamping ring. Each time the cell was assembled the 6 nuts holding the upper portion of the cell to the cell base were tightened as evenly as possible. A metal to metal seal here, together with shouldered tie rods, would have been better (these were incorporated into the design of

the ISC cell).

As the axial proving ring was encapsulated in an oil-filled perspex box it was possible to fill the cell with de-aired water in a normal manner.

4.2 Triaxial cell for cylindrical extension tests

The apparatus used for the cylindrical triaxial compression tests was modified slightly to accommodate extension tests. The triaxial cell, set up for a 4 ins high extension test sample is shown in Fig 4.3 and for a 7.0 ins high extension test sample in Plate 4.1.

The standard reinforced perspex cylinder was adequate for the 4 ins high samples. The non-standard reinforced perspex cylinder was required for the 7.0 ins high samples. It was not possible to test a 8.0 ins high sample in extension as the bayonet-type extension fitting limited the headroom available within the cell.

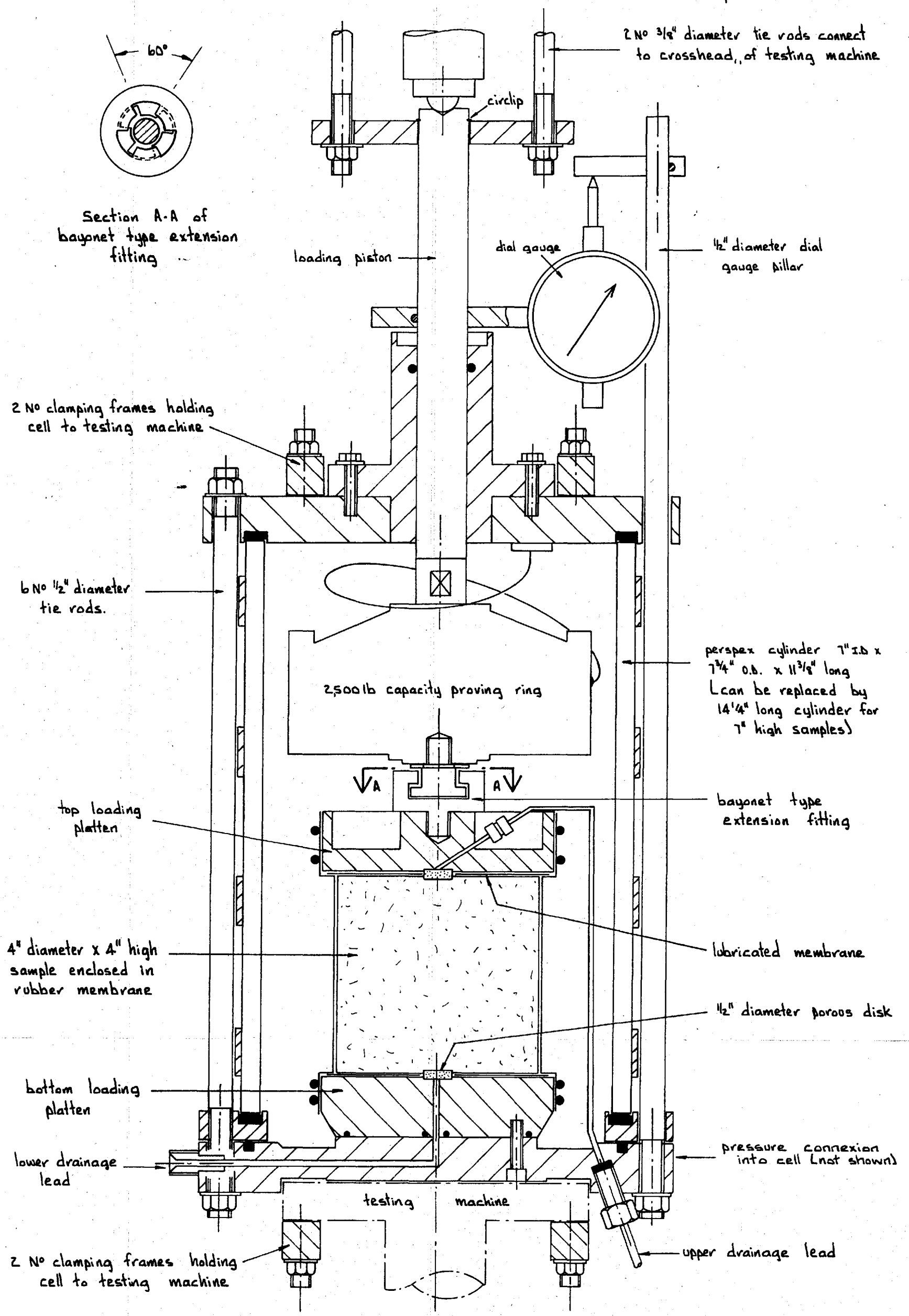
All the extension samples were built in a normal manner so that the bottom loading platten was bolted directly to the cell base. In order to prevent the cell lifting off the pedestal of the testing machine it was held down by two clamping frames. This is a relatively crude method which will tend to distort the alignment of the loading piston and the bottom loading platten. The arrangement used in the ISC cell is superior.

In order to apply a tensile load, the loading piston was clamped to the load frame crosshead by means of a crossarm, 2 tie-rods and a circlip. The dial gauge measuring axial deformation was inverted for convenience in the computations.

A stainless steel bayonet-type extension connection was made which ensured that uniform axial deformation was applied to the sample, Section A-A, Fig 4.3. Three projecting lugs on the upper boss engaged with three lugs in the lower boss. When rotated through 60° the upper boss could be withdrawn, there being large clearances all round to permit some initial lateral misalignment. Index marks were engraved on the two bosses to facilitate their correct engagement.

4.3 Triaxial cell for cuboidal compression & extension tests

Cuboidal triaxial compression and extension tests were performed in the independent stress control (ISC) cell described in Section 4.4. The ISC belt was omitted from the cell. The cell was connected to the testing



TRIAXIAL CELL FOR CYLINDRICAL EXTENSION SAMPLE

Scale: half full size

FIG. 4.3

machine pedestal by 6 bolts, see Fig 4.4. The loading piston was attached to the crosshead of the testing machine by the $2/\frac{3}{8}$ ins diameter tie rods shown in Fig 4.3 in an identical manner to that used for the cylindrical triaxial extension tests.

4.4 Independent stress control cell

The independent stress control (ISC) cell was conceived and designed by the writer. The general arrangement of the ISC apparatus is shown in Plate 4.4 and the cell itself, minus the cell body and two of the four main tie rods, is shown in Plate 4.5. A main sectional elevation of the cell appears in Fig 4.4 and two subsidiary cross-sections in Fig 4.5.

Before discussing, in detail, the construction and mode of operation of the ISC cell a review of some of the important factors considered in the design of the cell is given, not necessarily in order of priority.

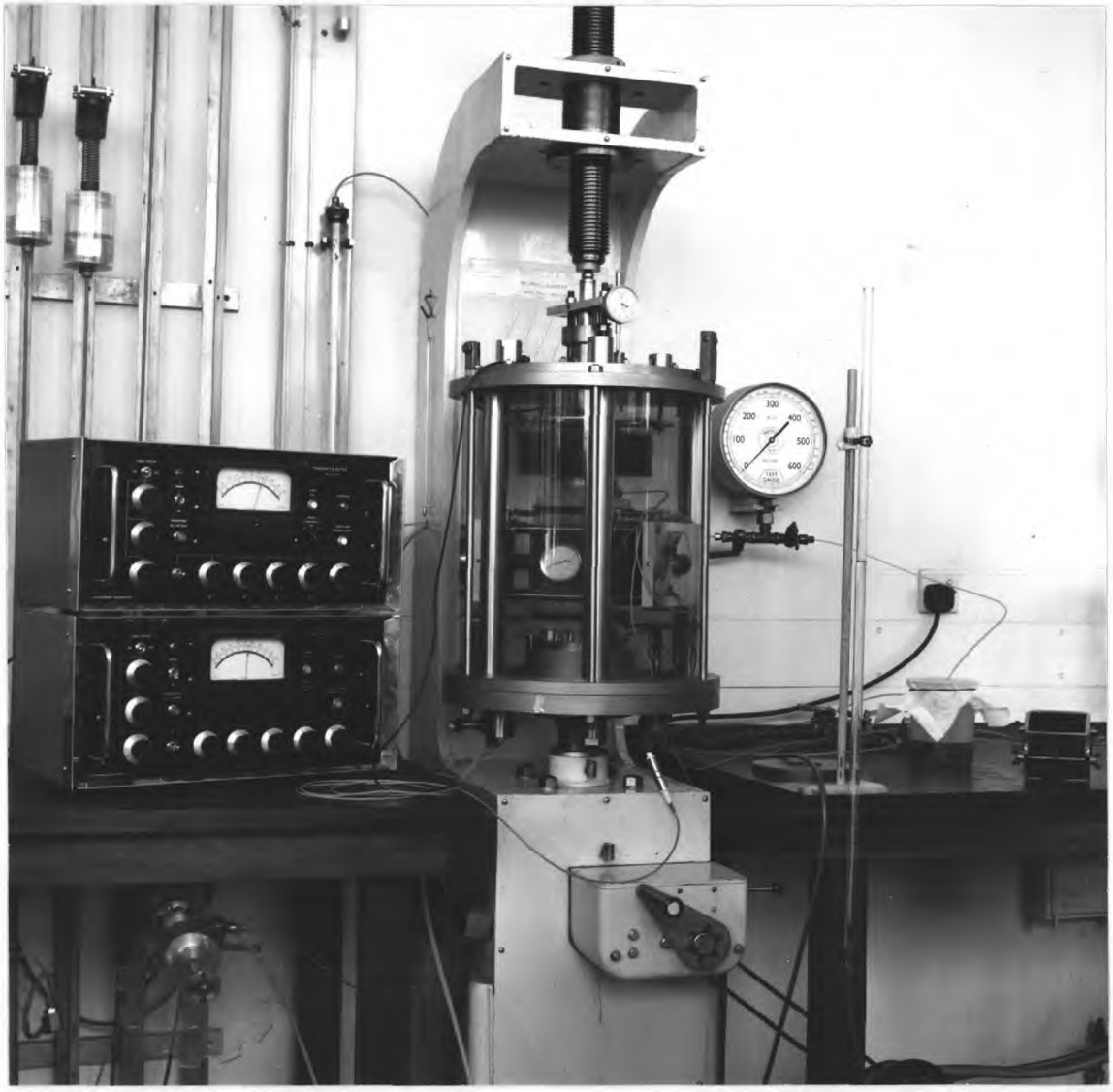
4.4.1 Important factors in design

(i) Rigid loading plattens with lubricated membranes are used in two of the principal stress directions. The principal stress in the third direction is applied by the cell pressure acting on the sample sheath. In effect, two pairs of boundaries are strain-controlled and the third pair is stress-controlled.

(ii) The sample is cuboidal in shape, but it is possible to easily vary the proportions to obtain an optimum sample geometry, i.e. to reduce the effect of boundary restraint to an insignificant amount.

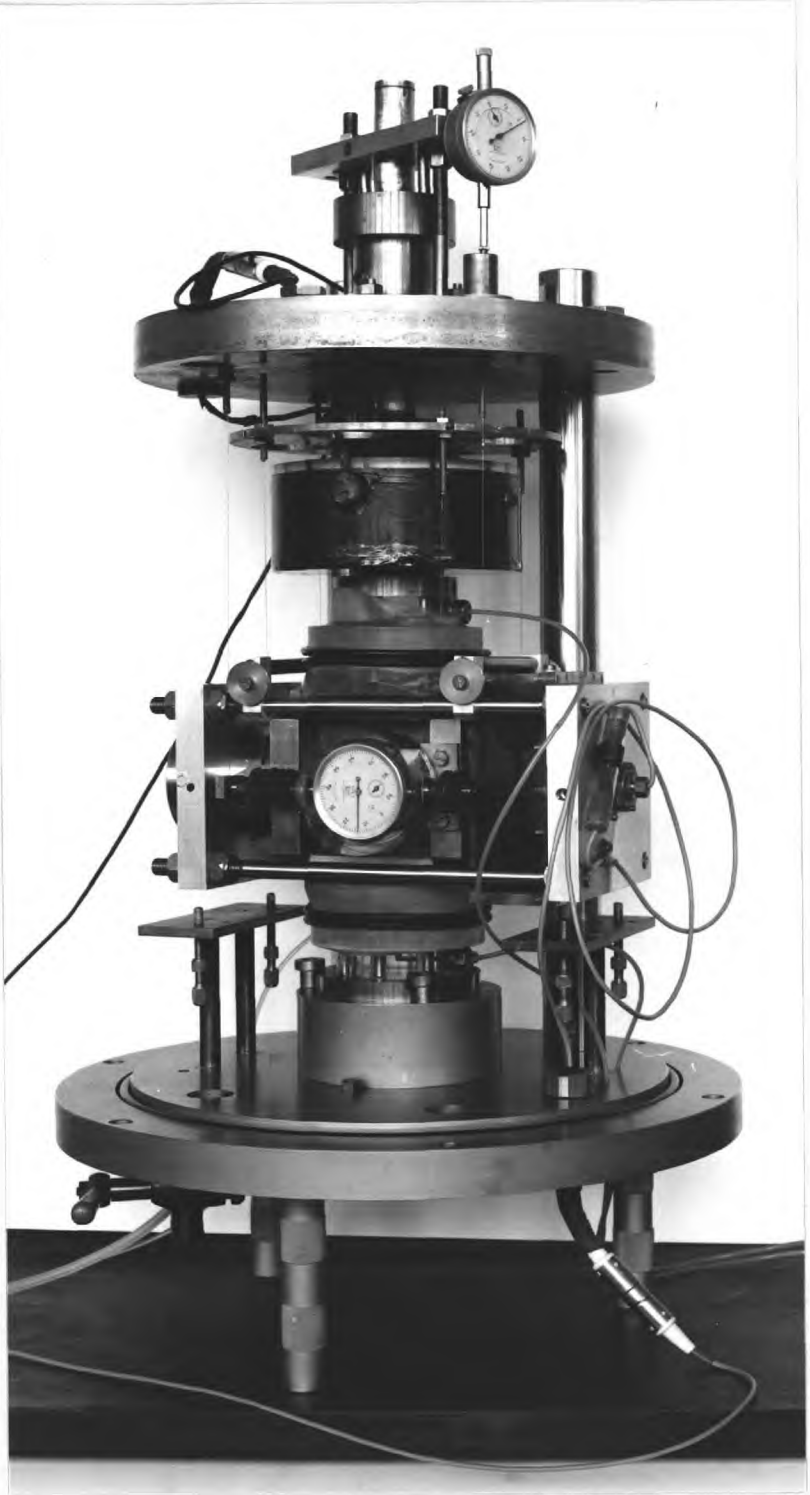
(iii) The sample arches across the gap at the junction of two adjacent rigid loading plattens. Belt plattens of differing dimensions are used for different types of tests to minimise the extent to which arching is necessary.

(iv) A cylindrical sample sheath is used, of a suitable diameter and thickness. This avoids the complications of making a specially pre-formed sheath. Using a particular size of sample sheath the geometry can still be varied a little, provided the perimeter of the sample remains constant. The cylindrical sample sheath is easily sealed on the cylindrical portion of the axial plattens by means of O-rings in the normal way and a transition



GENERAL VIEW OF
INDEPENDENT STRESS CONTROL
APPARATUS.

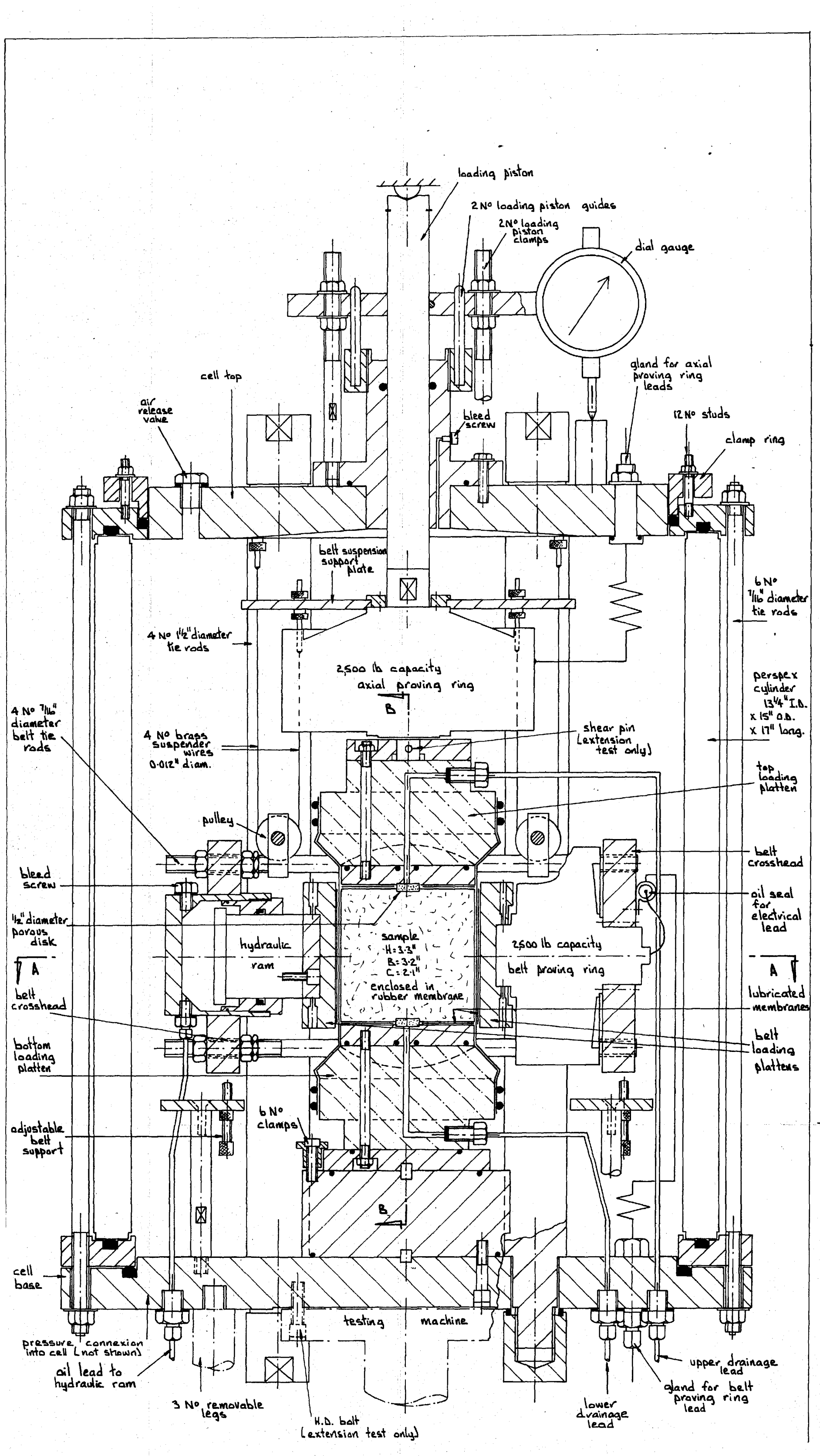
PLATE 4.4

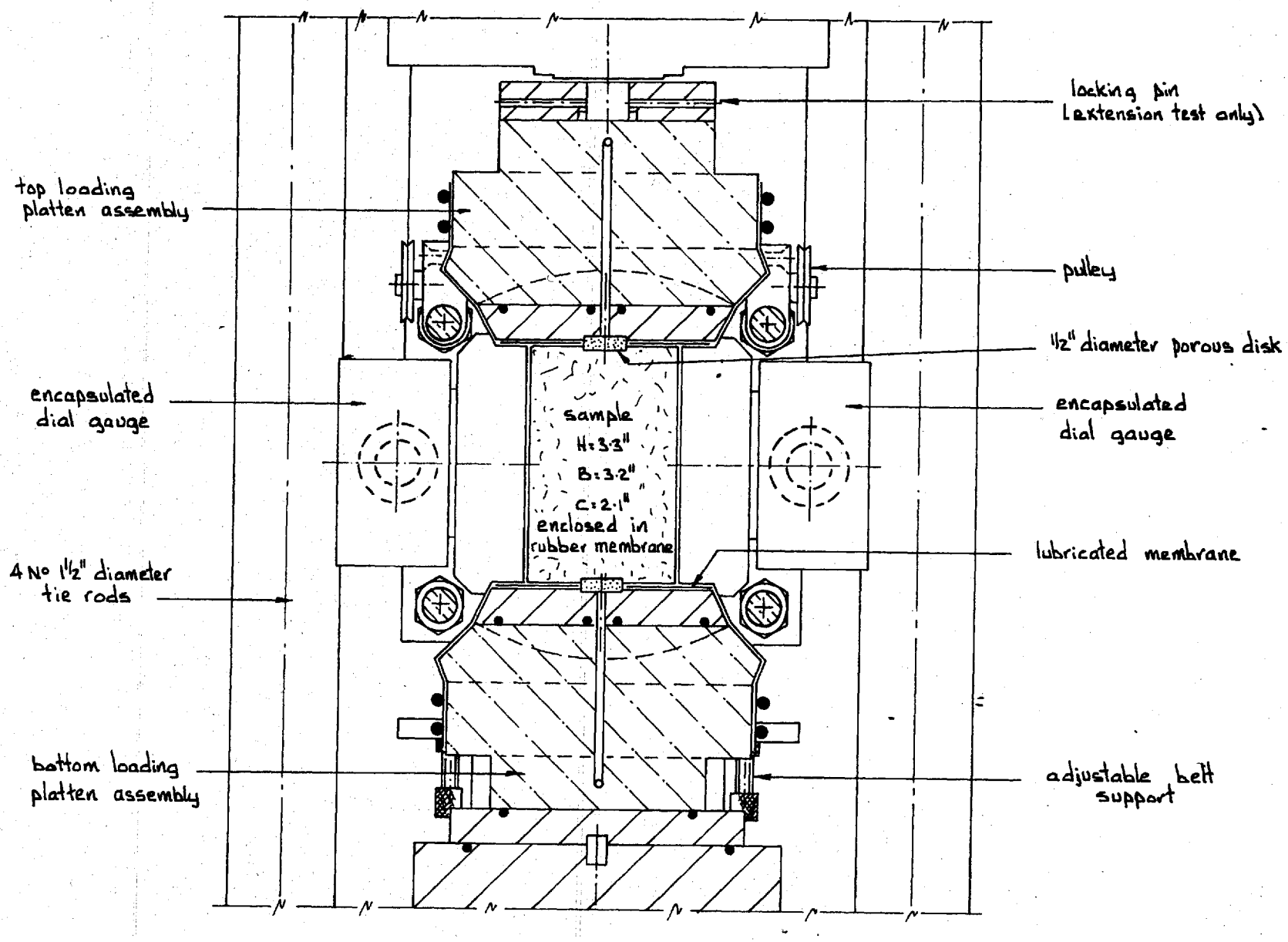


INDEPENDENT STRESS CONTROL CELL.

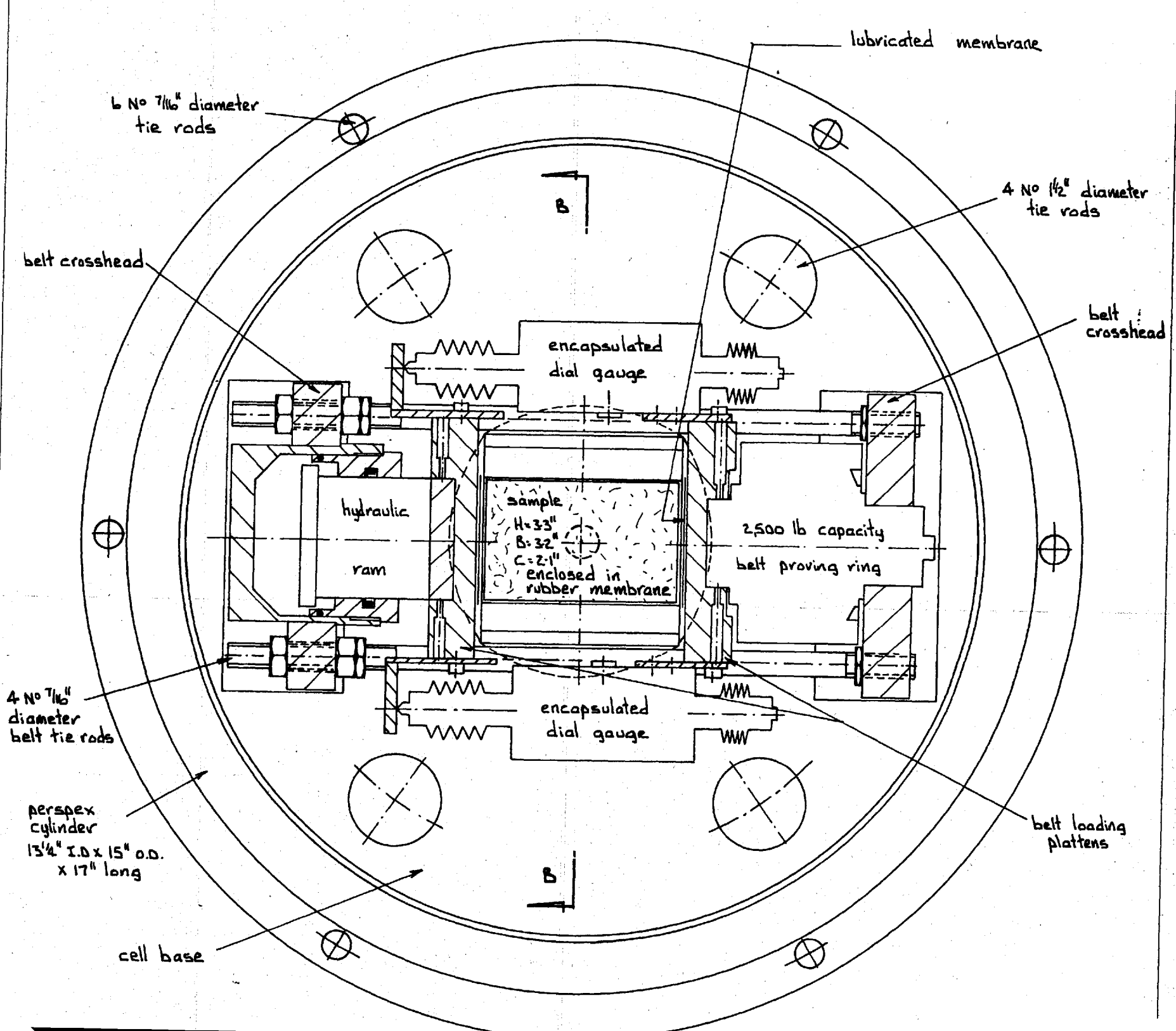
The cell wall and two of the four main tie rods are not shown.

PLATE 4.5


loading piston
2 N° loading piston guides
2 N° loading piston clamps
dial gauge
gland for axial proving ring leads
cell top
air release valve
bleed screw
12 N° studs
clamp ring
belt suspension support plate
6 N° 7/16" diameter tie rods
4 N° 1½" diameter tie rods
2,500 lb capacity axial proving ring
B
perspex cylinder 13¼" I.D. x 15" O.D. x 17" long.
4 N° 7/16" diameter belt tie rods
4 N° brass suspender wires 0·012" diam.
shear pin (extension test only)
top loading platten
pulley
belt crosshead
bleed screw
oil seal for electrical lead
½" diameter porous disk
hydraulic ram
sample H=3·3" B=3·2" C=2·1" enclosed in rubber membrane
2,500 lb capacity belt proving ring
A
A
lubricated membranes
belt crosshead
belt loading platens
bottom loading platten
6 N° clamps
adjustable belt support
B
cell base
testing machine
pressure connexion into cell (not shown)
oil lead to hydraulic ram
3 N° removable legs
H.D. bolt (extension test only)
lower drainage lead
upper drainage lead
gland for belt proving ring lead


locking pin (extension test only)
top loading platten assembly
pulley
½" diameter porous disk
encapsulated dial gauge
sample H=3·3" B=3·2" C=2·1" enclosed in rubber membrane
encapsulated dial gauge
lubricated membrane
4 No 1½" diameter tie rods
bottom loading platten assembly
adjustable belt support

SECTION B-B


lubricated membrane
6 No 7/16" diameter tie rods
4 No 1½" diameter tie rods
B
belt crosshead
belt crosshead
encapsulated dial gauge
hydraulic ram
sample H=3·3" B=3·2" C=2·1" enclosed in rubber membrane
2,500 lb capacity belt proving ring
4 No 7/16" diameter belt tie rods
encapsulated dial gauge
belt loading plattens
perspex cylinder 13¼" I.D x 15" O.D. x 17" long
B
cell base

section is incorporated in the loading plattens.

(v) The existing axial proving ring, loading piston and bushing is transferred from the triaxial cell and used in the ISC cell with minor modifications only.

(vi) A similar proving ring is used to measure the load in the ISC belt direction. A second C61 transducer meter is required to simplify recording.

(vii) A large diameter, short stroke, hydraulic ram is used to control the strain in the ISC belt direction since a mechanical system is difficult to control remotely.

(viii) The ISC belt is capable of maintaining zero strain in the sample in the belt direction or of applying a controlled rate of strain (positive or negative) to the sample.

(ix) The strain in the ISC belt direction is measured directly between the belt plattens.

(x) The strain in the ISC belt direction is controlled manually for a plane strain test, but automatically for other tests.

(xi) The rate of testing is chosen for convenience in recording, consistent with complete dissipation of excess pore pressures in the sample.

(xii) The ISC belt is assembled and finally adjusted and checked before the cell body is lowered into position and the cell filled with water. The cell top is independent of the cell wall.

(xiii) Visibility of the sample during the test is desirable.

(xiv) The cell is assembled on the bench top and lifted by crane into the testing machine after pressurization.

(xv) All the internal appurtenances can be removed so that the cell may be used for other unspecified purposes at a later date.

(xvi) It is possible to prepare a satisfactory sample reasonably easily.

(xvii) The cell is filled with water so that all the internal components must be resistant to corrosion.

(xviii) By removing the ISC belt the cell may be used to test cuboidal samples in triaxial compression & extension.

4.4.2 Cell

The cell base, cell top and 3 annular clamp rings were machined from

cast brass to avoid possible distortion problems. After plating they were found to be slightly porous, particularly the cell top, and were impregnated with a resin under pressure which cured this. The cell top and cell base were connected by four $1\frac{1}{2}$ ins diameter stainless steel shouldered tie rods with domed nuts incorporating a Dowty bonded seal. The underside of the cell top was dished slightly to assist in de-airing the cell.

The cylinder forming the cell body was fabricated from $\frac{7}{8}$ ins thick sheet perspex there being a single longitudinal butt joint. Two annular brass rings incorporating O-ring seals were clamped to the machined ends of the perspex cylinder by six 7/16 ins diameter tie rods. The cell body assembly was sealed and clamped separately to the base of the cell. A third clamp ring was required to precompress the O-ring seal between the upper end of the cell body and the cell top. The axial load due to the internal pressure is carried by the 4 heavy tie rods whereas the 6 light cell body tie rods serve only to maintain a seal. The 3 main O-ring seals were designed to give metal to metal, or metal to perspex contact to maintain good alignment. The O-ring rolling seal between the cell body and cell top permits some lateral mis-alignment in the cell components.

The cell is supported on 3 removable legs during assembly on the laboratory bench, Plate 4.5. Two lifting lugs replace the normal nuts on a diametral pair of cell body tie rods, Plate 4.4. The cell top and axial proving ring are lifted by a wire strap (not shown). A $\frac{1}{2}$ ton capacity crane serviced the working area. All services into the cell go directly through the cell base or cell top, generally with external Dowty bonded seals. The cell base could be bolted to the testing machine pedestal to permit the application of axial tensile loads, Fig 4.4. The axial deformation is measured on a 1 inch travel dial gauge reading to 0.001 ins mounted on a crossarm clamped to the loading piston and bearing directly onto the cell top.

4.4.3 Internal axial proving ring

The internal axial proving ring, loading piston and bushing used in the triaxial cell was modified slightly and transferred to the ISC cell. A bleed hole was drilled in the bushing to assist in de-airing the cell. Two guides were added to the bushing to prevent the loading piston from rotating and disturbing the assembled ISC belt. Two clamps were added to

locate, and provide controlled adjustment for, the loading piston during assembly and pressurization of the cell outside the testing machine.

A belt suspension support plate was fitted to the boss on the upper side of the proving ring. It was retained by a clamp ring but could rotate to allow adjustment.

4.4.4 Axial loading plattens

Each of the two axial loading plattens was composed of three components bolted together by 6 studs. The plattens proper were rectangular stainless steel plates (EN58J) carefully machined flat and polished to a mirror finish. There were two pairs of these, of slightly differing widths in the cell direction, to accommodate samples of differing dimensions. Only the smaller set, used for the main series of ISC tests, is shown. Sandwiched between the platten proper and a circular brass plate is a perspex block. This perspex block is cylindrical remote from the sample with a transition section to connect to the rectangular platten. Perspex was used to reduce their weight. O-rings were inserted where necessary to isolate the sample drainage connections from the cell fluid.

The bottom loading platten was clamped to a brass plinth which was bolted to the cell base. Additional space was provided in the ISC cell for future developments, hence the reason for the plinth. The clamps holding the bottom platten to the plinth were designed to permit a sample to be prepared remote from the cell base if required. In addition they made it much easier to strip down a sample after testing without the risk of losing part of the sample. The failed sample, still under a suction, was removed together with the plattens and placed in a dish before stripping.

The design of the drainage system is identical to that described in Section 4.1.2.

The loading anvil of the proving ring made direct contact with the top loading platten to ensure that the latter could not tilt and that essentially uniform overall axial deformation was applied to the specimen during compression.

In order to apply a tensile load a boss was screwed into the proving ring anvil. A spigot on the boss fitted into a hole in the circular brass plate of the top loading platten and a shear pin was inserted. Alternatively

the bayonet-type extension connection described in Section 4.2 was used. For this a threaded shouldered sleeve was inserted in the circular brass plate of the top loading platten (not shown).

4.4.5 Sample sheath

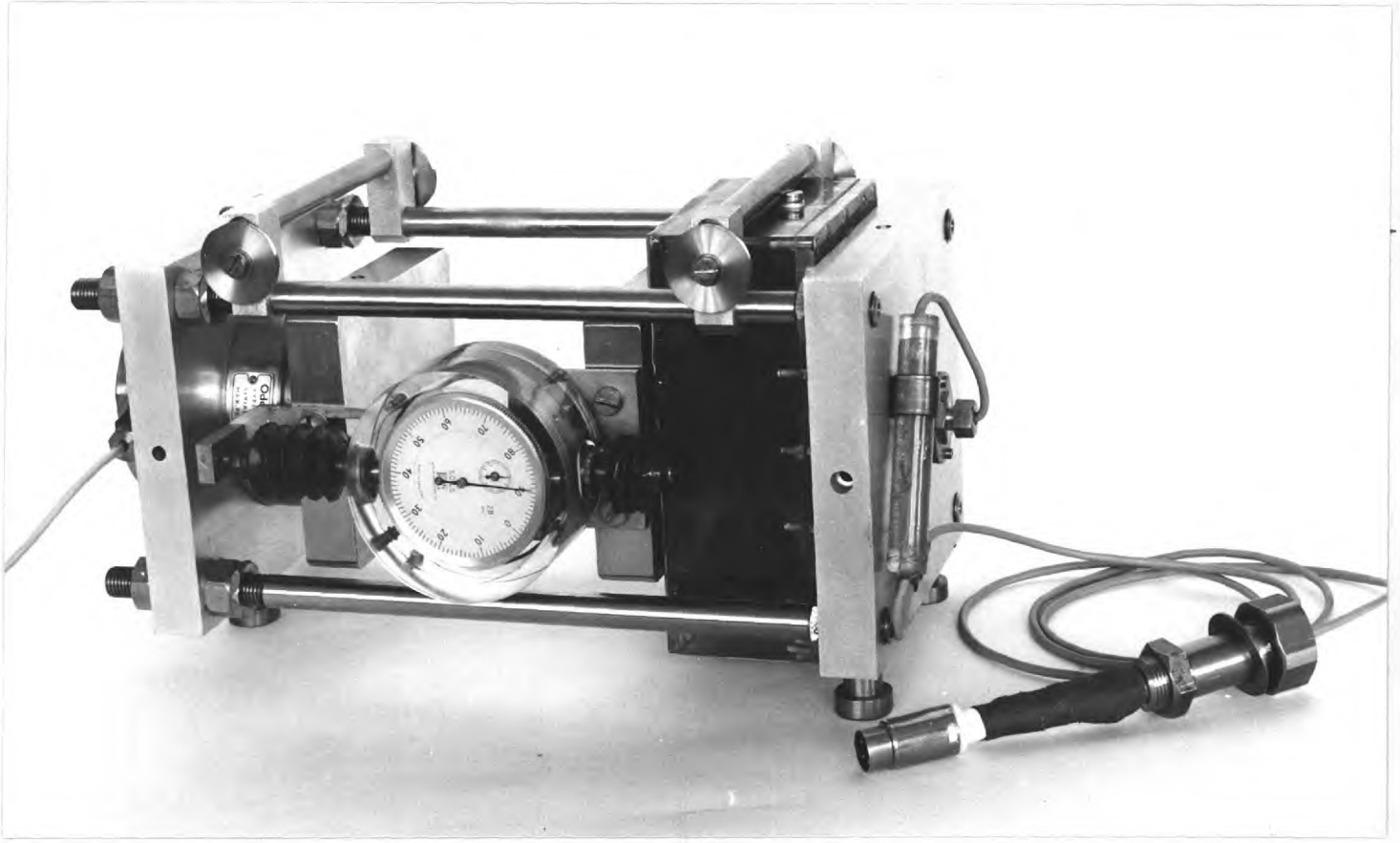
The standard 4 ins diameter nominal size sample sheath is in fact significantly undersize so that it is stretched when fitted over a 4ins diameter sample. It is possible by applying a vacuum to the inside of a conventional cylindrical sample mould, to stretch the sheath and hold it against the wall of the mould. The standard sheath when used for the initially designed cuboidal samples, B = 3.0, C = 3.1 ins, could not be fitted into the four vertical corners of the mould even though the cuboidal sample perimeter was equal to that of a 4 ins diameter sample. Clearly in trying to fit it the undersized cuboidal sheath is highly stressed at the sample corners but not on the faces whereas a cylindrical sheath is uniformly stressed. A special sheath of 4 ins finished diameter was obtained, 0.010 - 0.013 ins thick. Later when the sample cross-section was modified to B = 3.2, C = 2.1 ins a second special sheath was made of $3\frac{1}{2}$ ins finished diameter, 0.010 - 0.013 ins thick. It was necessary to limit the sheath thickness to 0.013 ins otherwise it was impossible to get it to fit around the various corners of the plattens, see Plates 11.1, 11.2 & 11.3.

4.4.6 Independent stress control belt

The ISC belt is shown separately in Plate 4.6. The load is measured on a 2500 lb capacity proving ring identical to the axial proving ring. The deformation is controlled by a hydraulic ram and its magnitude is measured directly between the loading plattens on 2 encapsulated dial gauges. Plate 4.6 shows a single dial gauge mounted on the plattens. In practice a second similar gauge was mounted between the plattens as well to check on possible tilting, Fig 4.5.

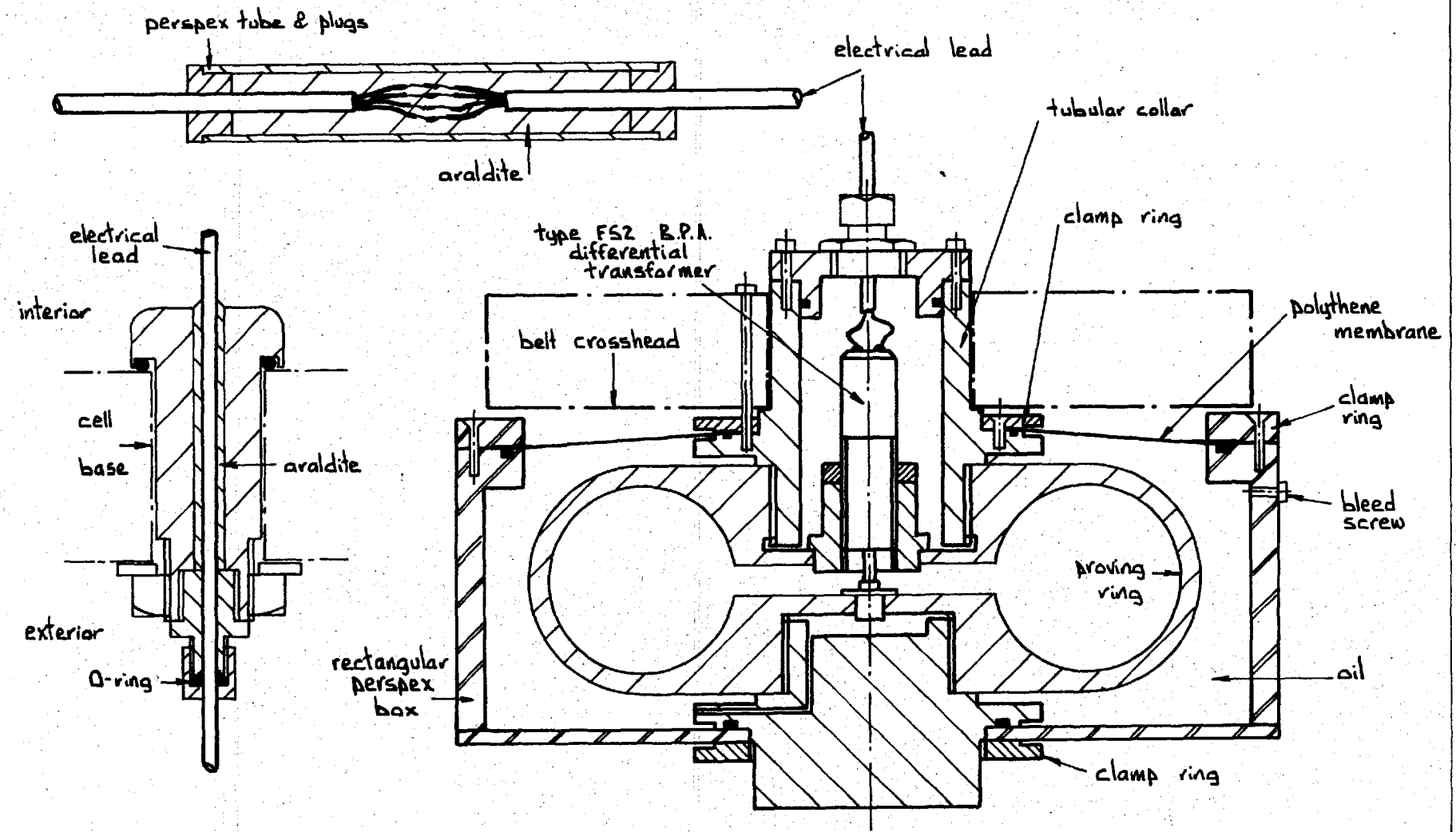
4.4.6.1 Proving ring

The design of the mountings for the ISC belt proving ring is very similar to that for the axial proving ring and is shown in Fig 4.6. The perspex box is rectangular instead of cylindrical. The tubular brass collar is a sliding fit in the duralumin belt crosshead and is held by 3 long retain-



INDEPENDENT STRESS CONTROL BELT.

PLATE 4.6



2,500 LB CAPACITY BELT PROVING RING AND GLAND FOR LEAD

Scale: full size

FIG. 4.6

ing screws. A heavy duty 4-core electrical cable is used to reduce the chance of damage. An araldite seal is provided in the lead external to the capsule to prevent oil escaping along the electrical lead. The detachable cell base gland incorporated a soft O-ring to seal onto the outer plastic cable covering, backed up by araldite. A similar soft O-ring seal was used at entry to the oil filled proving ring capsule.

The belt proving ring was energised by, and its output recorded on, a second C61 transducer meter, Mark II. There is no significant difference between the Mark I and Mark II instruments as far as the present tests are concerned.

4.4.6.2 Hydraulic ram

The 2 ins diameter, $\frac{3}{4}$ ins stroke stainless steel hydraulic ram runs in a brass bushing threaded into a stainless steel body. A rubber-ptfe seal provides a low friction leak-proof seal on the ram.

The ram is connected to a 1 ins I.D. control cylinder by $\frac{1}{8}$ ins diameter Saran tube, Fig 4.8. The control cylinder may be operated manually or a reversible electric motor and a variable speed gear box may be connected to provide an approximately constant rate of strain.

The hydraulic system was filled with a light mineral oil from a reservoir and could be bled at the hydraulic ram. The maximum working pressure in the ram for the present series of tests was about 500 psi. A 0-600 psi pressure gauge provided a rough check on the load.

A test on the efficacy of the ram seal was carried out as follows. The ISC belt was assembled and a steel block was placed between the plattens. A load of about 2000 lbs was induced in the system and it was left overnight. The load dropped overnight by about 15% which, considering the "hardness" of the system is very satisfactory. Moreover a small pressure increment applied by the control cylinder to the ram the following morning brought an immediate smooth increase in load as recorded on the proving ring.

4.4.6.3 Belt and plattens

The two belt crossheads were connected by 4 tie rods. The tie rods are screwed into the belt proving ring crosshead and are adjustable at the hydraulic ram crosshead. Locknuts permit the belt to be assembled in correct alignment during sample preparation.

The belt loading plattens were of stainless steel (EN58J) carefully machined flat and polished to a mirror finish. They are each a push fit on the belt proving ring anvil and on an extension piece screwed to the hydraulic ram, each being held in place by four locking screws. There were two pairs of these plattens of slightly differing widths in the axial direction to accommodate different test types. The type shown in Figs 4.4 & 4.5 are used for plane strain tests and for tests in which the belt opens. For tests in which the belt plattens moved inwards a narrower pair were used to prevent fouling at the corners.

4.4.6.4 Suspension wires

Four pulleys were mounted on the upper pair of belt tie rods. Hard drawn brass wires connected to the underside of the cell top passed around these pulleys and were connected to adjustable studs on the belt suspension support plate. During a test the ISC belt is freely suspended on these wires which maintain the line of action of the belt thrust on the centre-line of the sample during axial deformation.

Adjustable supports on the cell base are used whilst setting up a sample, being retracted after fitting and tensioning the four suspension wires.

4.4.6.5 Encapsulated dial gauges

Two encapsulated dial gauges were made, Plate 4.7 and Fig 4.7.

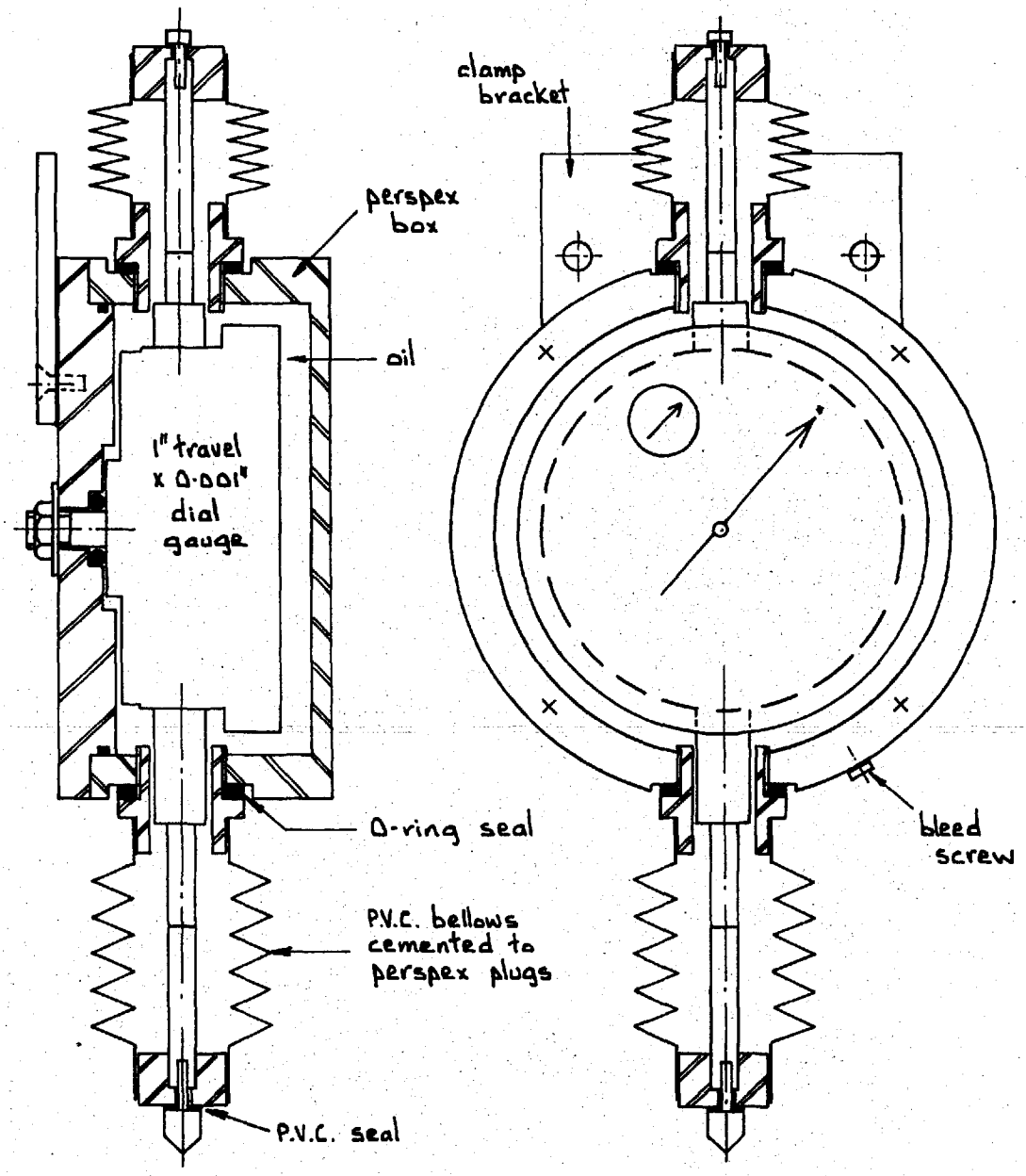
A 1 ins travel dial gauge reading to 0.001 ins is placed inside a cylindrical perspex box. The return spring in the dial gauge was removed and replaced by a stronger spring to overcome the stiffness of the PVC bellows. The transparent plastic face of the gauge was removed and holes were drilled in the back plate to ventilate the gauge. The bezel locking device was removed.

Two PVC bellows cemented to perspex plugs serve to enclose the dial gauge spindle to which appropriate extension rods are added. The box and dial gauge are filled with light mineral oil. Great care was taken to remove all air from the system so that the bellows would not collapse under the cell pressure. Appropriate seals serve only to contain the oil within the capsule.



ENCAPSULATED DIAL GAUGE.

PLATE 4.7



ENCAPSULATED DIAL GAUGE

Scale: full size

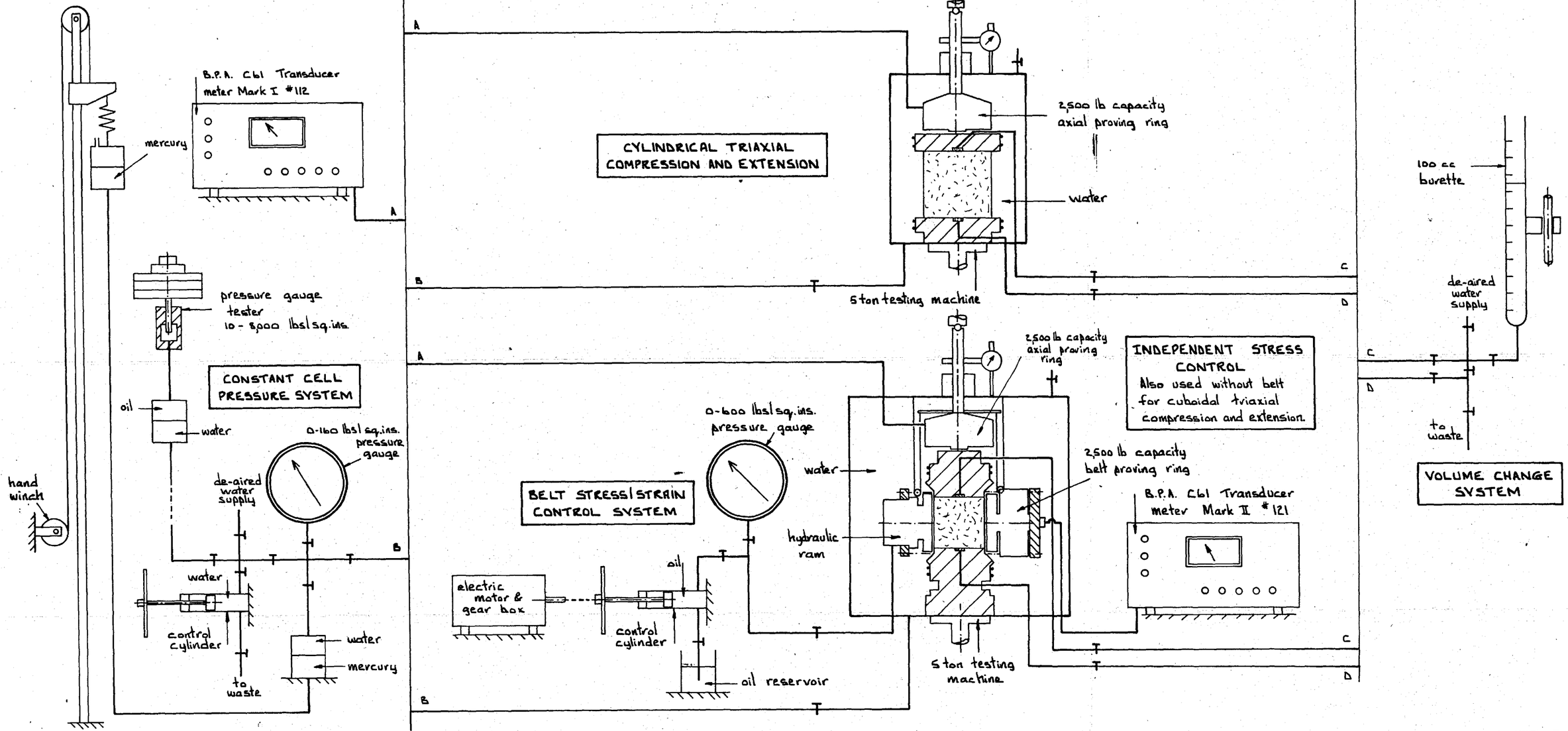
FIG. 4.7

4.5 General arrangement of testing apparatus

A diagrammatic layout of the apparatus used for all the drained shear tests is shown in Fig 4.8. The cell for cylindrical triaxial compression & extension tests was used interchangeably with the ISC cell. The latter, minus the ISC belt, was also used for the cuboidal triaxial compression and extension tests. The cells were loaded at a controlled rate of strain in a 5 ton capacity worm gear screw jack testing machine driven by an electric motor and gear-box. A Kopp variator in series with the gear box permits infinite speed variation from 0.05 ins/min to 0.000001 ins/min. The drive unit was mounted separately from the loading frame to reduce the risk of vibrations being transmitted to the sample, especially important in testing sand.

The cells were filled with de-aired water and maintained at the desired pressure with a self-compensating mercury control, Bishop & Henkel (1957). The pressure was generally measured on a 0 - 160 psi precision pressure gauge. For pressures in excess of this range a Budenberg dead-weight tester was connected directly into the system, see Appendix A3.

The volume change was measured directly on a 100 cc burette connected to the sample through a valve network that permitted the leads to be purged of air bubbles. The burette could be adjusted to maintain the meniscus level with the centre-line of the sample.



DIAGRAMMATIC LAYOUT OF APPARATUS FOR DRAINED SHEAR TESTS

FIG. 4.8

CHAPTER 5

DESCRIPTION OF MATERIAL TESTED

5.1 Particle size analysis and specific gravity

The material used in the experiments was Ham River sand supplied by the Building Research Station. It was a medium to fine uniform sand which was delivered and used in two batches. Similar material was used by Walker (1964) and Walker & Whitaker (1967) in model pile tests at the Building Research Station. Sands of similar gradings were used by Eldin (1951), Fraser (1957), Cornforth (1961) and Wade (1963) for shear strength research at Imperial College.

The first batch of about 200 lbs was used for the first series of cylindrical triaxial compression tests. This sand, as delivered, was considered to contain too high a proportion of fines passing a No.200 B.S.sieve and was therefore washed in an elutriating vessel to remove the fines, finally washed in distilled water, dried and thoroughly mixed to ensure initial homogeneity.

A second batch of about 300 lbs of a similar sand was used for all the subsequent tests. It was delivered in five 50 lbs bags and was stored in these bags until required. Samples of the second batch showed a lower proportion of fines passing a No.200 B.S.sieve. It was therefore considered not worthwhile to wash it as it was not anticipated that this would improve the consistency of the test results. Sieve analyses and rapid tilt tests on dry samples from each bag in the second batch suggested that there was no significant difference between their contents.

The specific gravities and maximum porosities of the two batches were as follows:

	Batch No.1	Batch No.2
Specific gravity	2.674	2.664
Porosity by rapid tilt test on dry sand*	48.4%	47.8%

*The procedure for this test is given by Kolbuszewski (1948a,b).

The particle size analysis of the two materials is shown in Fig 5.1.

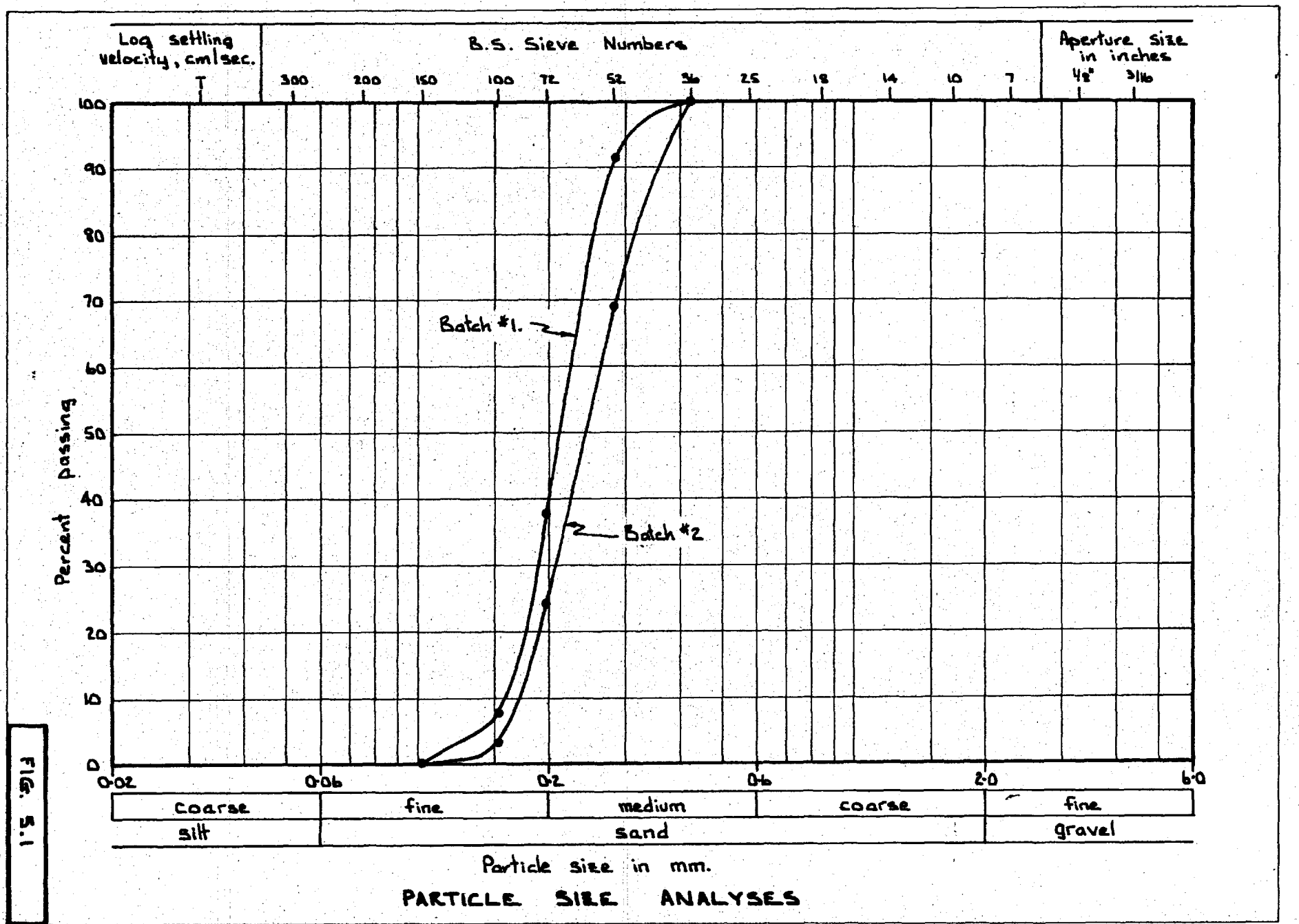


Fig. 5.1

PARTICLE SIZE ANALYSES

5.2 Particle breakdown

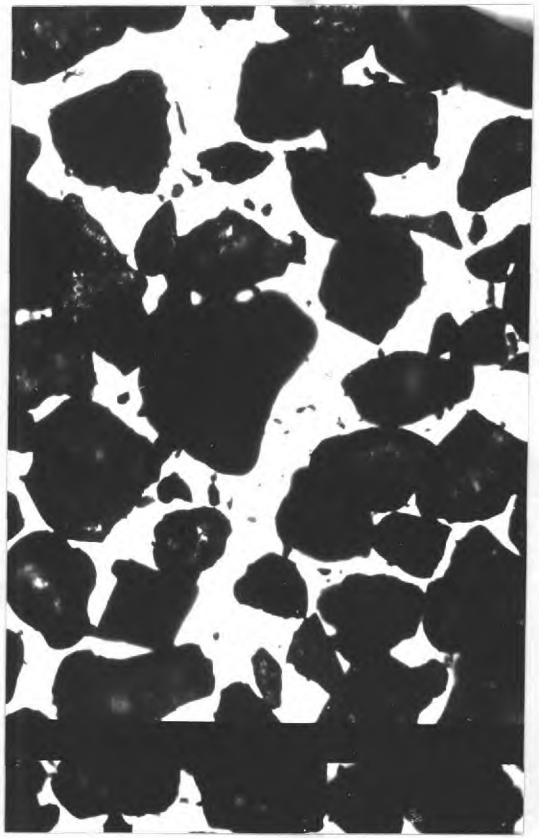
It is known that particle breakdown occurs during the application of a hydrostatic stress to a granular material and more so under a subsequent shear stress, Cornforth (1961), Bishop et al (1965), Bishop & Green (1965), Bishop (1966). This breakdown may affect the behaviour of samples of re-used material so that, ideally, a fresh sample should be used for each test. The amount of Brasted sand available to Cornforth was so limited that about 40% of the total was required for each of 63 tests. The tests were arranged in groups in an attempt to minimise the effect on the result and Cornforth states, "a consideration of all the test results does not suggest that there was any serious effect from this source". The quantity of material available to the writer was generally sufficient to enable a fresh sample to be taken for each shear test although a limited amount of material was re-used once in the later stages of parts of the test programme.

Microscopical examination of the sand grains before and after shearing clearly indicated that some fracturing of the grains had taken place, Plate 5.1. Under X5 magnification no apparent difference was discernible between the size and shape of a typical grain before and after shearing. However, after shearing a quantity of fines was present of a medium to coarse silt size, i.e. 0.01-0.04 mm grain size. Plate 5.1 illustrates the type of, and to a limited extent the quantity of, fines produced during test. Re-using the sand 3 times is seen to increase the quantity of fines present. A quantitative assessment of the samples shown is probably not valid due to the difficulty of preparing a truly representative microscope slide since the fines were easily lost on taking a small sample to place on the slide, Krumbein & Pettijohn (1938).

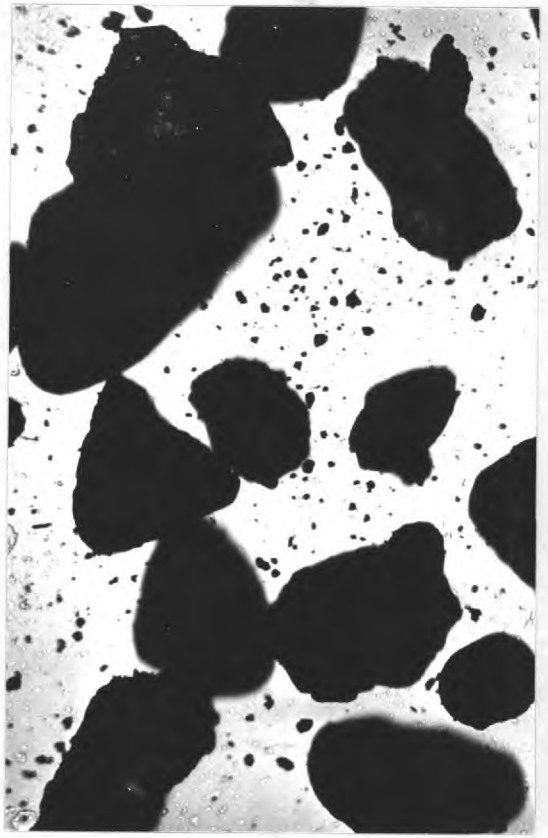
Measurements of particle breakdown due to shearing at high stress levels, up to $\sigma_3' = 4000$ psi, have been made by Skinner (1969) by sieving a complete sample before and after a test, also see Bishop (1966), Marsal (1965), Borg et al (1966), Vesic & Barksdale (1963). The effects of particle breakdown which are very significant at high stress levels are small at the stress levels used in the present work. This possible small effect was, in general, eliminated by using a fresh sample for each test. On occasions it was necessary to re-use the sand once.



Batch #2, Bag #1,
unwashed & unused.



Batch #1,
washed & used once.



Batch #2, Bag #5,
unwashed,
reused 3 times (test B1/4).

PHOTOMICROGRAPHS OF HAM RIVER SAND SHOWING PARTICLE BREAKDOWN.



Scale

PLATE S.1

CHAPTER 6

TEST PROGRAMME

6.1 Introduction

All tests reported in this thesis were fully drained tests carried out on saturated Ham River sand. This has the advantage that volume changes within the sample may be more easily measured and with greater accuracy than if the tests were on dry sand.

It is possible that a sample formed of dry sand may absorb small variable amounts of moisture from the atmosphere during sample preparation. These variations in surface moisture will affect the surface friction properties of the mineral grains, Hafiz (1950), Tschebotarioff & Welch (1948), Penman (1953), Horn & Deere (1962), Skinner (1969). Their effect on the measured shear strength of aggregates of sand grains is less well documented. Suffice it to say that saturating the sand eliminated this problem in the present work.

In all the tests, except Test X/5, the pore pressure in the sample was atmospheric and volume changes were measured on a 100 cc glass burette. In Test X/5 a back pressure was used necessitating using a paraffin volume gauge, Bishop & Donald (1961).

All the cylindrical compression and extension tests were carried out on 4 ins diameter samples to enable reasonably accurate measurements to be made. The area of the porous drain used at each end of the sample is much smaller than in the conventional triaxial test. However, as the permeability of the Ham River sand is relatively high, 3×10^{-2} cm/sec, the volume change response during consolidation was virtually instantaneous under a 5 psi cell pressure increment. A convenient testing rate of about 10% axial strain per hour was therefore chosen. A few tests at a much slower strain rate confirmed that there was no significant build-up of excess pore pressure in the sample during the shear stage.

The dimensions of the cuboidal samples were generally a little smaller than the cylindrical samples but still gave an acceptable accuracy of measurement. The drainage conditions are similar to those of the cylindrical samples and similar strain rates were therefore used.

For simplicity all the samples were isotropically consolidated. The

additional complication of introducing a K_o-belt, Bishop & Henkel (1957) to monitor a zero lateral strain consolidation condition was not considered to be warranted in the present series of tests. In contrast to the Imperial College plane strain apparatus the ISC belt may be brought into contact with the sample following isotropic consolidation so that K_o-consolidation is not vital for the ISC tests. Triaxial compression tests on sands consolidated under K_o-conditions and under isotropic conditions have been compared by Bishop & Eldin (1953), Fraser (1957), Bjerrum et al (1961). In all cases it was found that the shear strength parameters were unaffected by the method of consolidation. However in all these tests end restraint might have had a significant effect on the results and it remains to be shown that these conclusions still apply to short samples with lubricated ends and to the cuboidal ISC test samples.

The samples in the present tests were consolidated by raising the cell pressure in 5 psi increments and recording the volume change under each increment. This provided a useful check on the consistency of the sample preparation technique and was helpful in detecting leaks in the system.

The tests on cylindrical samples covered a range of initial porosities. These tests indicated, as has all the earlier research on granular materials, that any difference in behaviour under different test conditions is most marked in dense samples. In view of the difficulties involved in the preparation of a cuboidal sample, and in addition to reduce the number of variables involved in what was essentially a series of exploratory tests, only dense cuboidal samples were tested. This applies to both the cuboidal compression extension tests and the ISC tests.

Details of the test programme were developed as the research progressed. Conclusions drawn from tests completed at any stage guided the subsequent work, in particular with regard to the precise proportions of the cuboidal sample and the optimum number and thickness of lubricated membranes. The research was largely concerned with measuring small differences in behaviour between slightly different types of specimen and repeatability of a single test type was therefore vital. It was frequently necessary to repeat tests as controls to ensure that no changes had occurred in the calibration of the measuring system or the sand or the operators' technique. Small changes did occur which, had they remained undetected, could have caused errors in the interpretation of the test results.

Two separate batches of Ham River sand were used which were not quite identical. Hence some care is needed in comparing data obtained using the these separate batches. Adequate control tests were carried out on the second batch of sand to enable satisfactory comparisons to be drawn in the four major test series. The following programme of drained tests, summarised in Figs 6.1, 6.2 & 6.3, was carried out in chronological order.

6.2 Cylindrical Triaxial Compression Test Series, 4 ins Diameter Samples

6.2.1 1st Series

Ham River sand, Batch No.1 was generally used. The initial porosity of the samples was varied over as wide a range as could conveniently be placed, i.e. from 38.1%, dense-vibrated, to 45.5%, loose-spooned in under water. The samples were consolidated at a cell pressure of 40 psi which was maintained constant and the axial stress increased, generally using a nominal rate of deformation equivalent to 10% of the specimen height per hour, with drainage to a burette at atmospheric pressure.

6.2.1.1 Type X, Tests X/1 & X/3 to X/13

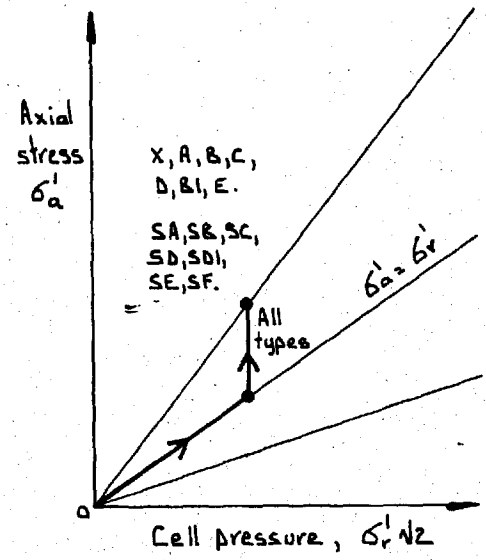
The samples were 4 ins high, built in the normal manner with lubricated ends. One 0.009 ins thick lubricated rubber membrane was used on each platten. In test X/5 a 40 psi back pressure was applied to the sample and the cell pressure was increased to 80 psi, the normal glass burette being replaced by a paraffin volume gauge, Bishop & Donald (1961). Tests X/9-13 were on re-used sand.

6.2.1.2 Type A, Tests A/1 to A/16

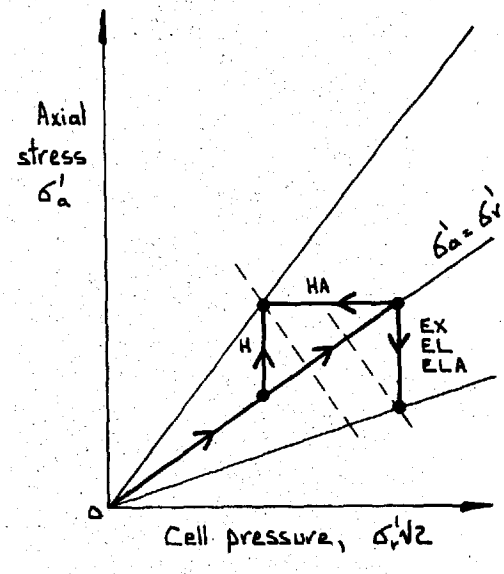
The samples were 4 ins high, built in two halves with lubricated ends. Normally 1/0.009 ins thick lubricated rubber membrane was used on each platten. In certain tests a sandwich of 2 or more 0.009 or 0.024 ins thick membranes was used, each interface being lubricated with silicone grease. Tests A/15 & 16 were on re-used sand.

6.2.1.3 Type B, Tests B/1 to B/9

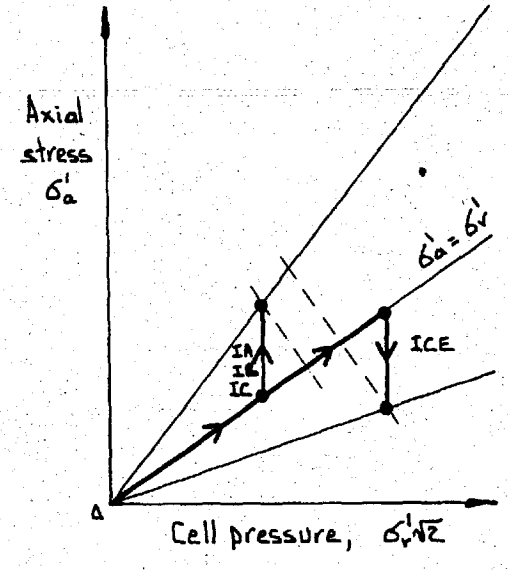
The samples were 8 ins high, built in two halves with non-lubricated



Cylindrical triaxial compression



Cylindrical triaxial compression & extension



Cuboidal triaxial compression & extension

The stress paths for these tests are shown on Figs. 11.32 to 11.36

Independent stress control

STRESS PATHS FOLLOWED TO FAILURE

FIG. 6.1

Type of sample / End conditions	Mode of sample preparation									
	Made in two halves		Normal							
	Cylindrical D = 4 ins		Cylindrical D = 4 ins				Cuboidal			
	H = 8 ins	H = 4 ins	H = 8 ins	H = 7 ins	H = 4 ins	H = 2 ins	H = 3·4 ins B = 3·0 ins C = 3·1 ins	H = 4·1 ins B = 3·0 ins C = 3·1 ins	H = 4·6 ins B = 3·0 ins C = 3·1 ins	H = 3·3 ins B = 3·1 ins C = 2·2 ins
Lubricated 1 | 0·009 ins or 1 | 0·010 ins	C SB	A SD			X SF	SE				
Lubricated 2 | 0·009 ins or 2 | 0·010 ins	C	H HA SDI		EL	EX IB		IA	IA ICE	IA	IC ICE ISC
Lubricated 3 or more membranes	C	A					IA		•	ICE
Non-lubricated Direct contact	B BI SA	D SC								
Non-lubricated 4 ins diameter porous disc (L + ½ ball)			E	ELA						

NOMINAL SAMPLE DIMENSIONS
MODE OF PREPARATION
&
END CONDITIONS

FIG. 6.2

Test type	Cylindrical triaxial compression	Cylindrical triaxial extension	Cuboidal triaxial compression	Cuboidal triaxial extension	Independent stress control
X	12				
A	16				
B	9				
C	7				
D	3				
BI	4				
E	4				
SA	4				
SB	5				
SC	2				
SD	2				
SDI	2				
SE	2				
SF	2				
H	7				
HA	6				
EX		12			
EL		3			
ELA		4			
IB		6			
IA			10		
IC			4		
ICE				8	
ISC					20
IC			2		
Total	87	25	16	8	20

TOTAL NUMBER OF SHEAR TESTS REPORTED IN THE THESIS IN APPROXIMATE CHRONOLOGICAL ORDER

FIG. 6.3

ends. The sand was in direct contact with the polished stainless steel loading plattens. Test B/9 was on re-used sand.

6.2.1.4 Type C, Tests C/1 to C/7

The samples were 8 ins high, built in two halves with lubricated ends. Normally 1/0.009 ins thick lubricated rubber membrane was used on each platten. In Tests C/3 & 4, sandwiches of 2/0.009 ins and 3/0.024 ins thick membranes were used respectively, each interface being lubricated with silicone grease.

6.2.1.5 Type D, Tests D/1 to D/3

The samples were 4 ins high, built in two halves with non-lubricated ends. The sand was in direct contact with the polished stainless steel loading plattens.

6.2.1.6 Type B1, Tests B1/1 to B1/4

The samples were 8 ins high, built in two halves with non-lubricated ends. The sand was in direct contact with the polished stainless steel loading plattens. Ham River sand, Batch No.2, Bag No.5 was used.

6.2.1.7 Type E, Tests E/1 to E/4

The samples were 8 ins high, built in the normal manner with non-lubricated ends. Conventional $\frac{1}{4}$ ins thick, 4 ins diameter porous discs were used on each platten. A $\frac{3}{4}$ ins diameter half-ball and seating was inserted between the top loading platten and the axial proving ring anvil in Tests E/1-3. In Test E/4 a nominal rate of deformation of 0.007 ins/min was used, equivalent to 5% of the specimen height per hour. All Type E tests were on re-used sand.

6.2.2 2nd Series

Generally these tests were similar tests to those in the 1st Series but were carried out over a $3\frac{1}{2}$ week period to reduce the likelihood of uncontrolled variables affecting the results. The second batch of Ham River sand was generally used, Bag No.3. The samples were consolidated at a cell pressure of 40 psi which was maintained constant and the axial stress

increased using a nominal rate of deformation equivalent to 10% of the specimen height per hour, with drainage to a burette at atmospheric pressure. The initial porosity was maintained as close as possible to 41.5%, i.e. medium dense, in all tests.

6.2.2.1 Type SA, Tests SA/1 to SA/4

The samples were 8 ins high, built in two halves with non-lubricated ends, similar to the 1st Series, Type B. The sand was in direct contact with the polished stainless steel loading plattens.

6.2.2.2 Type SB, Tests SB/1 to SB/5

The samples were 8 ins high, built in two halves with lubricated ends, similar to the 1st Series, Type C. One 0.009 ins thick lubricated membrane was used on each platten. In Test SB/5 sand from Bag No.4 was used.

6.2.2.3 Type SC, Tests SC/1 & SC/2

The samples were 4 ins high, built in two halves with non-lubricated ends, similar to the 1st Series, Type D. The sand was in direct contact with the polished stainless steel plattens.

6.2.2.4 Type SD, Tests SD/1 & SD/2

The samples were 4 ins high, built in two halves with lubricated ends, similar to the 1st Series, Type A. One 0.009 ins thick lubricated rubber membrane was used on each platten.

6.2.2.5 Type SD1, Tests SD1/1 & SD1/2

The samples were 4 ins high built in two halves with lubricated ends, similar to the 1st Series, Type A, modified. Two 0.009 ins thick lubricated rubber membranes were used on each platten.

6.2.2.6 Type SE, Tests SE/1 & SE/2

The samples were 2 ins high, built in the normal manner with lubricated ends. One 0.009 ins thick lubricated rubber membrane was used on each platten.

6.2.2.7 Type SF, Tests SF/1 & SF/2

The samples were 4 ins high, built in the normal manner with lubricated ends, similar to the 1st Series, Type X. One 0.009 ins thick lubricated rubber membrane was used on each platten.

6.3 Cylindrical Triaxial Compression & Extension Test Series, 4 ins Diameter Samples

Ham River sand, Batch No.2, Bag No.4 was used. The initial porosity of the samples was varied over as wide a range as could conveniently be placed, i.e. from 38.6%, dense-vibrated, to 45.9%, loose-spooned in under water.

6.3.1 Type H, Tests H/1 to H/7, Triaxial Compression

The samples were 4 ins high, built in two halves with lubricated ends. Two 0.010 ins thick lubricated rubber membranes were used on each platten. The samples were consolidated at a cell pressure of 40 psi which was maintained constant and the axial stress increased using a nominal rate of deformation equivalent to 10% of the specimen height per hour, with drainage to a burette at atmosphere pressure. Tests H/6 and 7 were on re-used sand.

6.3.2 Type HA, Tests HA/1 to HA/6, Triaxial Compression, Decreasing σ_3'

The samples were 4 ins high, built in two halves with lubricated ends. Two 0.010 ins thick lubricated rubber membranes were used on each platten. The samples were consolidated at a cell pressure of from 140-190 psi. The axial stress was maintained constant while the sample was strained at a nominal rate of deformation equivalent to 10% of the specimen height per hour with drainage to a burette at atmospheric pressure. In Tests HA/1, 2 & 5 the rate of deformation was halved during the early part of the test (the Kopp variator in the drive system permits smooth speed changes to be made during a shear test). The axial stress was maintained constant by reducing the cell pressure manually until it reached 40 psi when the self-compensating mercury control was switched in. The precise consolidation pressure was dependent on the initial porosity of the sample, being chosen to promote failure at σ_3' = 40 psi, assuming that the strength would be

similar to that of the Type H samples.

6.3.3 Type EX, Tests EX/1 to EX/12, Triaxial Extension

The samples were 4 ins high, built in the normal manner with lubricated ends. Two 0.010 ins thick lubricated rubber membranes were used on each platten. The samples were consolidated at a cell pressure of from 140-180 psi. The axial stress was decreased, axial extension test, generally using a nominal rate of deformation equivalent to either 10% or 5% of the specimen height per hour, with drainage to a burette at atmospheric pressure The precise consolidation pressure was dependent on the initial porosity of the sample, being designed to promote failure at $\sigma_3' =$ 40 psi. In Test EX/5 a nominal rate of deformation of 0.001 ins/min was used; equivalent to 1.5% of the specimen height per hour. Tests EX/10-12 were on re-used sand.

6.3.4 Type EL, Tests EL/1 to EL/3, Triaxial Extension

The samples were 7 ins high, built in the normal manner with lubricated ends. Two 0.010 ins thick lubricated rubber membranes were used on each platten. The samples were consolidated at a cell pressure of from 140-180 psi. The axial stress was decreased, axial extension test, using a nominal rate of deformation equivalent to 6.0% of the specimen height per hour, with drainage to a burette at atmospheric pressure. The precise consolidation pressure was dependent on the initial porosity of the sample, being designed to promote failure at $\sigma_3' =$ 40 psi. All Type EL tests were on re-used sand.

6.3.5 Type ELA, Tests ELA/1 to ELA/4, Triaxial Extension

The samples were 7 ins high, built in the normal manner with non-lubricated ends. Conventional $\frac{1}{4}$ ins thick, 4 ins diameter porous discs were used on each platten. The samples were consolidated at a cell pressure of from 140-180 psi. The axial stress was decreased, axial extension test, using a nominal rate of deformation equivalent to 6.3% of the specimen height per hour, with drainage to a burette at atmospheric pressure. The precise consolidation pressure was dependent on the initial porosity of the sample, being designed to promote failure at $\sigma_3' =$ 40 psi. All Type ELA tests were on re-used sand.

6.4 Cuboidal Triaxial Compression & Extension Test Series

Ham River sand, Batch No.2, Bags No.1 & 2 (mixed) were used. The initial porosity was maintained as close as possible to 39.0%, i.e. dense in all tests. Type IB cylindrical triaxial compression tests serve as control tests for comparison purposes.

6.4.1 Type IB, Tests IB/1 to IB/6, Cylindrical Triaxial Compression

The samples were 4 ins diameter, 4 ins high, built in the normal manner with lubricated ends. Two 0.010 ins thick lubricated rubber membranes were used on each platten. The samples were consolidated at a cell pressure of 30 psi which was maintained constant and the axial stress increased using a nominal rate of deformation equivalent to 5% of the specimen height per hour, with drainage to a burette at atmospheric pressure. These cylindrical compression tests serve as control tests.

6.4.2 Type IA, Tests IA/1 to IA/10, Triaxial Compression

The samples were cuboidal, B = 3.0, C = 3.1 ins, of varying height, H = 3.4, 4.1 & 4.6 ins, built in the normal manner with lubricated ends. Normally 2/0.010 ins thick lubricated rubber membranes were used on each platten. In Test IA/3 a sandwich of 3/0.010 ins thick membranes were used, each interface being lubricated with silicone grease. The samples were consolidated at a cell pressure of 30 psi which was maintained constant and the axial stress increased using a nominal rate of deformation varying from 5.1 to 9.1% of the specimen height per hour, with drainage to a burette at atmospheric pressure.

6.4.3 Type IC, Tests IC/1 to IC/4, Triaxial Compression

The samples were cuboidal, B=3.0, C=2.3 & H=3.3 ins, built in the normal manner with lubricated ends. Two 0.010 ins thick lubricated rubber membranes were used on each platten. The samples were consolidated at a cell pressure of 30 psi which was maintained constant and the axial stress increased using a nominal rate of deformation equivalent to 6.4% of the specimen height per hour, with drainage to a burette at atmospheric pressure.

6.4.4 Type ICE, Tests ICE/2 & ICE/4 to ICE/10, Triaxial Extension

The samples were cuboidal, either B = 3.2, C = 2.1 & H = 3.3 ins, or B = 3.0, C = 3.1 & H = 4.1 ins, built in the normal manner with lubricated ends. Normally 2/0.010 ins thick lubricated rubber membranes were used on each platten. In Test ICE/4 a sandwich of 3/0.010 ins thick membranes was used, each interface being lubricated with silicone grease. The samples were consolidated at a cell pressure of 140 psi which was maintained constant. The axial stress was decreased, axial extension test, using a nominal rate of deformation varying from 5.1 to 6.4% of the specimen height per hour, with drainage to a burette at atmospheric pressure. The consolidation pressure was designed to promote failure at $\sigma_3' = 40$ psi assuming ϕ' in extension is equal to ϕ' in compression. In fact this was not quite true for the cuboidal samples but this is not significant as far as the choice of the cell pressure is concerned.

6.5 Independent Stress Control Test Series, Cuboidal Samples

Ham River sand, Batch No.2, Bags No.1 & 2 (mixed) was used. The initial porosity was maintained as close as possible to 39%, i.e. dense, in all tests. The samples were consolidated at a cell pressure of 30 psi which was maintained constant and were sheared with drainage to a burette at atmospheric pressure.

6.5.1 Type ISC

The samples were cuboidal, B = 3.2, C = 2.1 & H = 3.3 ins, built in the normal manner with lubricated ends. Two 0.010 ins thick lubricated rubber membranes were used on each axial platten. One 0.010 ins thick membrane together with the sample sheath (0.010-0.013 ins thick) were used on each ISC belt platten, each interface being lubricated.

6.5.1.1 Tests ISC/1 to ISC/3

The axial stress was increased using a nominal rate of deformation equivalent to 3.6% of the specimen height per hour. The ISC belt plattens were maintained at a fixed distance apart - plane strain test.

6.5.1.2 Tests ISC/4 to ISC/7

The axial stress was increased using a nominal rate of deformation equivalent to 3.6% of the specimen height per hour. The ISC belt plattens were moved apart, belt opening, using nominal rates of strain selected to give suitably spaced points on the plots of the failure characteristics against $b = (\sigma_2' - \sigma_3')/(\sigma_1' - \sigma_3')$ at failure.

6.5.1.3 Tests ISC/8 to ISC/18

The axial stress was increased using a nominal rate of deformation varying from 2.7 to 3.6% of the specimen height per hour. The ISC belt plattens were moved together, belt closing, using nominal rates of strain selected to give suitably spaced points on the plots of the failure characteristics against $b = (\sigma_2' - \sigma_3')/(\sigma_1' - \sigma_3')$ at failure.

6.5.1.4 Tests ISC/19 & ISC/20

The ISC belt plattens were moved together, belt closing, using a nominal rate of strain equivalent to 2.8% of the specimen width in the belt direction per hour. The axial strain was maintained at zero except for the compression of the lubricated rubber membranes and the axial proving ring - nominally a plane strain test. This was much easier than trying to maintain zero axial deformation precisely, the deviation from true plane strain being small.

6.5.2 Type IC, Tests IC/5 & IC/6, Cuboidal Triaxial Compression

The samples were cuboidal, B = 3.2, C = 2.1 & H = 3.3 ins and B = 3.0, C = 2.3 & H = 3.3 ins respectively, built in the normal manner with lubricated ends. Two 0.010 ins thick lubricated rubber membranes were used on each axial platten. The axial stress was increased using a nominal rate of deformation equivalent to 3.6 and 6.4% of the specimen height per hour respectively. These 2 cuboidal triaxial compression tests serve as control tests.

CHAPTER 7

PREPARATION OF SPECIMENS, TEST PROCEDURE AND CALCULATIONS

7.1 Specimen Preparation

7.1.1 Cylindrical Samples

Some of the problems associated with preparing a satisfactory sample have been examined and are discussed in Chapter 3. The two basic methods of sample preparation finally used were as follows.

7.1.1.1 Normal Sample

A quantity of sand in a metal tray was dried overnight and weighed on a 7kg balance reading to 1 gm. Water was slowly added while the sand was still hot and the saturated sand was left to cool. This ensured more reproducible sample weights and minimised the chance of entrapped air bubbles being present on the surface of the sand grains. Two $\frac{1}{2}$ ins diameter porous discs were saturated by boiling in a dish of water and were left to cool in the dish.

A disc of rubber membrane slightly smaller than the platten diameter, with a central hole, was smeared with a thin film of silicone grease. The polished surface of the bottom loading platten was similarly greased and the membrane stuck down. Air bubbles and surplus grease were carefully removed with a straight-edge. If required, further greased membranes were added. The exposed membrane surface in contact with the sand was not greased. For tests in which the sample was in direct contact with the platten the above procedure was omitted.

The sample sheath was sealed to the platten with two O-rings. De-aired water was run into the sheath to a depth of 1 ins, entrapped air bubbles were removed, and a $\frac{1}{2}$ ins diameter porous disc was inserted into the recess in the platten, under water.

A three-part split mould of appropriate height held together with an encircling chain-link belt, Plate 4.1, was assembled on a surface table to ensure correct alignment. The mould was placed concentrically on the bottom loading platten and completely lined with a single rectangular sheet of paper towel. The sample sheath was turned back over the upper lip of

the mould and the mould was clamped to the cell base using clamps similar to those shown by Bishop & Henkel (1957), Fig 61, and by Cornforth (1961), Plate 6-5. Care was needed to prevent the mould sliding about on the platten surface and disturbing the greased membranes. A suction was applied to the mould, supplied by a vacuum pump, to hold the sample sheath securely against the inside of the mould.

In those few tests, Type E, where a conventional $\frac{1}{4}$ ins thick, 4 ins diameter porous disc was used on each platten the $\frac{1}{2}$ ins diameter porous disc was omitted and a saturated 4 ins diameter disc was inserted after applying a suction to the mould. This disc was made a close fit inside the mould so that sand grains could not penetrate between the sample sheath and the edge of the disc.

Saturated sand was spooned into the mould and tamped with a spatula or vibrated as required, being finally levelled off about 0.05 ins above the upper rim of the mould by tamping with a straight edge. The surface tension of the water was sufficient to prevent spillage at the edges, the water level being carefully controlled during the latter stages of sample preparation by bleeding the drainage system.

Lubricated rubber membranes were prepared on the top loading platten in a similar manner to those on the bottom loading platten. The drainage lead was purged of air bubbles and a $\frac{1}{2}$ ins diameter porous disc was inserted into the recess in the platten. The platten was carefully lowered onto the sample and the sample sheath turned back onto the platten and sealed with two O-rings. Air was easily trapped under the lip of the platten at this stage and a wash bottle was often useful in removing air bubbles by flooding with water. Great care was needed to avoid washing sand into the gap between the platten and the mould. Any air bubbles remaining probably had little effect upon a drained test beyond being a nuisance should they enter the drainage leads. However they would be much more serious in an undrained test.

In the Type E tests the sample was levelled off about $\frac{1}{8}$ ins below the upper rim of the mould and a conventional $\frac{1}{4}$ ins thick, 4 ins diameter porous disc, previously saturated, was carefully lowered into position on top of the sand. The top loading platten was placed on the porous disc and the sample sheath turned back onto the platten and sealed with two O-rings. No difficulties with air bubbles arose using this method of sample

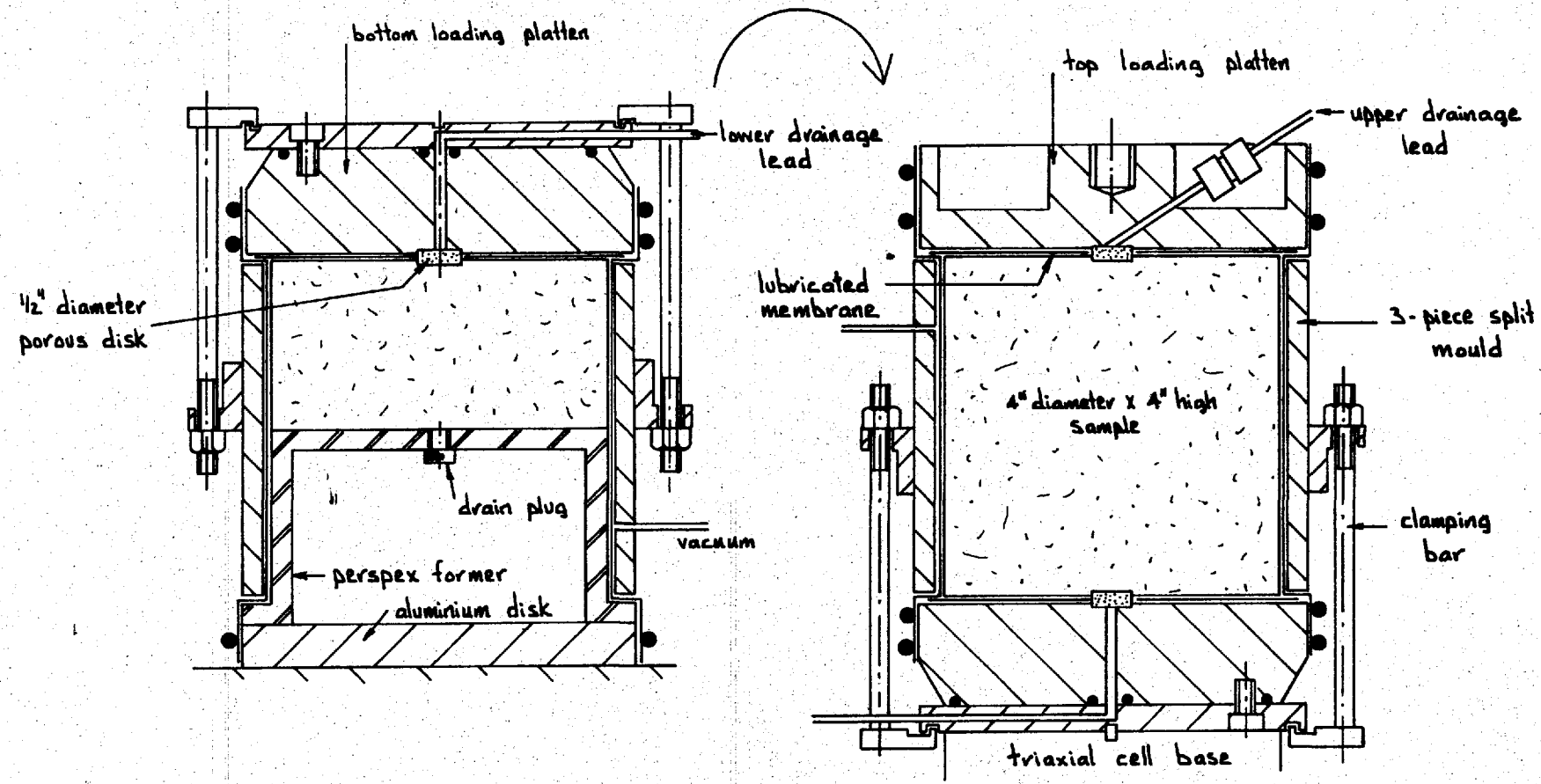
preparation. The sample was connected to the volume change burette and the meniscus pressure datum adjusted to correspond to the mid-height of the sample. The burette was lowered by 2 feet, thus applying a small effective stress to the sand. The sample was left, preferably for 1-2 hours, to check for leaks and to try to eliminate any small pockets of water trapped between the sample sheath and the plattens. The burette reading was noted and the three-part split mould dismantled. Provided the sample was not disturbed during assembly of the top platten, particularly if placed loose, removal of the mould was straightforward. Loose samples were easily densified, trapping the mould; which could sometimes be removed by lifting the top platten very slightly, otherwise the specimen was rebuilt. The burette reading was noted and the diameter of the specimen was measured at approximately 2 ins vertical intervals on each of two diameters. In the early tests the gauge described by Bishop & Henkel (1957), Fig 59, was used, reading to 0.001 ins. Later a vernier caliper gauge, reading to 0.001 ins, was used as it was found to be more convenient. The height of the sample was measured throughout with this same vernier caliper gauge at 4 points equidistant around its periphery, measuring between the platten loading surfaces. Due allowance was made in the calculations for the thickness of the sample sheath.

The burette reading was again noted, any change being indicative of disturbance or possible leaks. The remaining saturated sand not used in the sample was dried overnight and weighed whilst still hot.

7.1.1.2 Two Halves Sample

The procedure used in preparing a sample in two halves was similar in detail to that for a normal sample. However the mould was filled in two stages as shown in Fig 7.1.

The assembled mould was lined with paper towel, a sample sheath stretched over it, and a vacuum applied. The exposed surface of the sample sheath was thoroughly wetted. The close-fitting perspex former, Plate 4.1, was also wetted and pushed into the mould. The former was filled with water and an aluminium disc placed on it, the membrane turned back and sealed with an O-ring. The assembly was upturned and placed on the laboratory bench. De-aired water was run into the sheath to a depth of 1 ins and entrapped air bubbles were removed. The remaining half of the mould was



Stage 1. Sample half built.

Stage 2. Sample complete.

PREPARATION OF CYLINDRICAL SAMPLE IN TWO HALVES

Scale : half full size.

FIG. 7.1

filled with saturated sand at the required porosity, being levelled off flush with the rim of the mould. The water level in the sample was controlled by siphoning as there was no proper drainage connection at this stage. Care was needed during the final stages to prevent the water level falling below tho surface of the sand causing air bubbles to enter which were subsequently very difficult to remove. The detached bottom loading platten, Figs 4.1 & 7.1, was prepared and carefully lowered upside-down onto the sample. The sample sheath was turned back onto the platten and sealed. The platten was clamped to the mould with 3 clamping rods as shown in Fig 7.1 and a negative pore-water pressure applied to the sample by lowering the volume change burette. The assembly was inverted by sliding it off the edge of the bench whilst supporting the aluminium disc by hand and placed on the triaxial cell base spigot. Great care was needed to avoid jarring the sample.

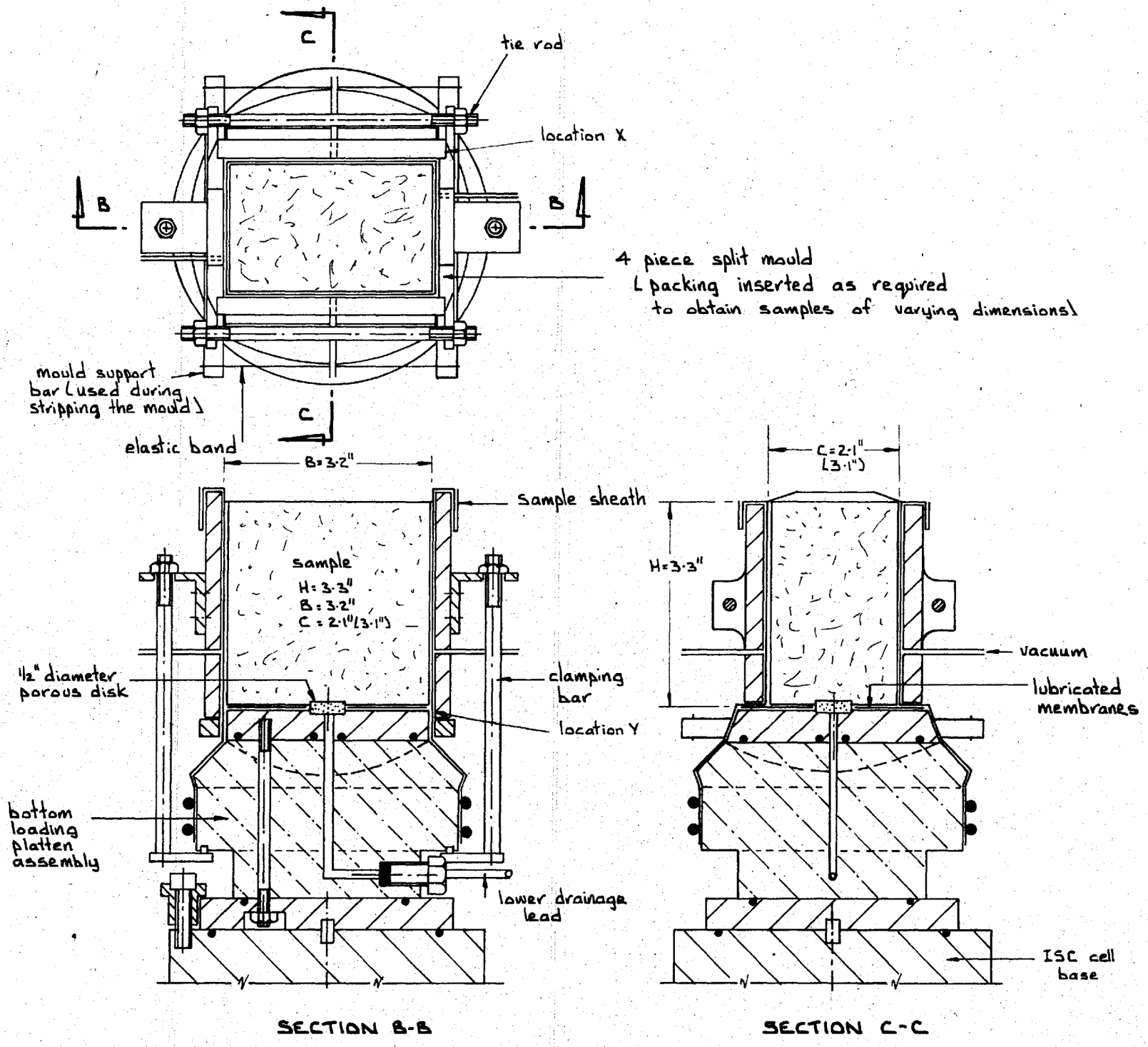
The burette was raised, removing the suction from the sample, the sample sheath seal was broken, the sheath turned back and the aluminium disc removed. Water was siphoned out of the perspex former and the drain plug removed. The former was slowly rotated and carefully extracted from the mould avoiding disturbance. The second half of the mould was filled with saturated sand at the required porosity, being levelled off about 0.05 ins above the upper rim of the mould by tamping with a straight-edge.

The sample was completed in an identical fashion to one built in a normal manner.

7.1.2 Cuboidal Samples

All the cuboidal samples were prepared in a normal manner by clamping the mould to the bottom loading platten, fixed to the cell base, and building the sample in one whole, Fig 7.2. The mould is composed of four brass plates held together by two tie rods. The plates were carefully machined so that when assembled on a surface table with the nuts evenly tightened the mould was absolutely square.

Two sets of mould side plates with clamping bar lugs were used, i.e. those corresponding to the ISC belt platten positions, one pair being approximately 1 ins wider than the other pair. The wider pair were used for all the cuboidal triaxial compression and extension tests. The narrow pair were subsequently made and used for all the ISC tests in which samples



PREPARATION OF CUBOIDAL SAMPLE

Scale: half full size

FIG. 7.2

of cell width, C = 2.1 ins were tested. Both of these pairs of mould side plates projected beyond the corners of the plattens to locate the mould with respect to the plattens, Section B-B of Fig 7.2.

The samples in Tests IA/4 - 10 were made by lining the mould with four $\frac{1}{8}$ ins thick machined brass plates projecting an appropriate amount above the mould rim to obtain the required increased sample height. The narrow samples used in the Type IC tests were obtained by inserting two $\frac{1}{2}$ ins thick machined perspex plates on the cell faces and two $\frac{1}{8}$ ins machined perspex plates on the belt faces of the mould respectively. These packings were held in place with sellotape and a hole drilled through each of them to line up with the vacuum lead which was provided on each of the four sides of the mould. The mould was completely lined with four rectangular sheets of paper towel.

Thus it was possible to conveniently build samples having a cell width C = 2,1 ins or C = 3.1 ins. As indicated in Chapter 4 two corresponding sets of stainless steel axial loading plattens were used. Fig 7.2 shows the smaller sample.

The method of sample preparation was similar to that used for the cylindrical samples made in the normal manner. Perseverance was required to fit the sample sheath around the loading plattens in order to minimise the quantity of water trapped between the sheath and the transition section of the plattens. Inevitably water was trapped, but most of it was expelled when the volume change burette was lowered, applying a small effective stress to the sand. The remainder was expelled during consolidation.

To prevent the sides of the mould slipping down and possibly damaging the membrane during dismantling,two mould support bars were fitted, held in place by elastic bands. The tie rod nuts were released and the tie rods were removed. The mould sections were lifted off one at a time, the remaining sections being supported to prevent them damaging the thin sample sheath stretched over the bottom loading platten transition section.

In some of the ISC tests it was necessary to adjust the width of the sample in the belt direction, B, very carefully so that a suitable clearance existed between the ISC belt loading plattens and the edges of the axial plattens, see Fig 4.4. To achieve this the mould was packed with narrow strips of cardboard at four locations X to increase the width in the belt direction, B, very slightly. To prevent sand from penetrating the result-

ant gap at four locations Y, similar narrow strips of cardboard were inserted and sellotaped to the mould.

The dimensions of the samples were measured with a vernier caliper gauge reading to 0.001 ins. The height and widths were each measured at 4 points adjacent to the corners of the sample.

7.2 Test Procedure

7.2.1 Cylindrical triaxial compression tests

The triaxial cell was assembled on the testing machine pedestal, Fig 4.1, care being taken to avoid disturbing the sample. The lead from the C61 transducer meter was connected to the axial proving ring by the line plug and socket adjacent to the cell top and the electrical system checked. De-aired water was run in to fill the cell through the cell base pressure connection, with the air release valve removed. The axial proving ring was lowered until the loading anvil was just clear of the top loading platten, by raising the testing machine pedestal by hand. The volume change burette reading was noted and the air release valve replaced. The cell pressure was raised to 2,3,4,5,10,15,20,25,30,35,40 psi etc., the burette reading being recorded for each pressure increment. At a cell pressure of 2 psi the burette was raised so that the meniscus was level with the mid-height of the sample. It was maintained at this pressure datum throughout the test. The sample was allowed to reach equilibrium under each pressure increment for 5-10 minutes. Having reached the desired consolidation pressure the self-compensating mercury control was switched in and the system left for at least 2-3 hours to check for leaks. No attempt was made to measure the change in height of the sample directly during consolidation. The reduction in height was obtained from the measured volume change by assuming isotropic consolidation. This was considered more reliable than trying to maintain contact between the proving ring anvil and the top loading platten. Using this latter method there was a risk of disturbing the sample and also the measurements could be significantly affected by cell distortion during the first few cell pressure increments even though a dial gauge pillar extending from the cell base was used, Fig 4.1. At the beginning of the shear stage the zero decade reading on the C61 transducer meter was noted and the proving ring anvil was brought

just into contact with the top loading platten. The dial gauge was adjusted to zero and the level of the meniscus adjusted to a convenient position within the burette.

The testing machine gear box was set to give the required nominal rate of deformation and the sample was sheared. Throughout the shear test readings were taken at intervals of the axial deformation dial gauge, C61 transducer meter decade setting and volume change burette. The tests were continued at least until the axial load decreased and many tests were continued further to large axial strains, up to +30% in certain tests.

At the end of the shear test the motor drive was stopped, the clutch disengaged and the sample unloaded by hand until the axial proving ring anvil was well clear of the top loading platten. The valves connecting the sample to the burette were closed, sealing off the sample. The self-compensating mercury control was disconnected and the cell pressure reduced to atmospheric pressure. The alternative method of relying on the suction provided by lowering the burette in order to sustain the sample during dismantling was not used. It was tried but it was found that the sample sheath wrinkled so badly under the large axial strain imposed that it was impossible to take sensible measurements of the diameter of the sample. Furthermore, satisfactory photographs could not be obtained. Since the main purpose of the post-shear diametral measurements was to determine the degree of non-uniformity of the lateral deformation of the sample the uncertainty as to the precise effective stress acting on the sample at the time of measurement was of little consequence. The cell was drained and carefully dismantled. The sample was sketched and the diameter measured at approximately 2 ins vertical intervals on each of two diameters with the vernier caliper gauge. Photographs were taken of certain samples. The sample was removed from the sample sheath onto a metal tray either away from the cell base or by tipping up the cell base onto the tray. Great care was needed to collect all the sand especially any adhering to the greasy rims of the loading plattens and around the $\frac{1}{2}$ ins diameter porous discs. The sand recovered was dried overnight to determine its dry weight. The apparatus was cleaned and the drainage leads flushed out in preparation for the next test. The sample sheath and lubricated rubber membranes were washed in warm, soapy water, dried and generally powdered with French chalk.

7.2.2 Cylindrical triaxial extension tests

The procedure for the cylindrical triaxial extension tests was similar to that for the cylindrical triaxial compression tests with the following modifications. The male and female bosses forming the stainless steel bayonet-type extension connection were screwed into the proving ring anvil and top loading platten respectively. The triaxial cell was assembled, Fig 4.3, and the lead from the C61 transducer meter connected. De-aired water was run in to fill the cell, with the air release valve removed. The axial proving ring was rotated by the dial gauge arm clamped to the loading piston until the two index marks on the extension connection were aligned. The axial proving ring was slowly lowered by raising the testing machine pedestal by hand, until a load was registered on the C61 transducer meter. The testing machine pedestal was lowered a fraction to remove the load and the loading piston was rotated through 60° to engage the connector lugs. The two tie rods connecting the loading piston to the crosshead of the testing machine were assembled as also were the two clamping frames holding the cell to the pedestal. The sample was consolidated at the required cell pressure and was left for at least 2-3 hours to check for leaks. At the high cell pressures involved, 140-190 psi, leaks occurred more frequently than with the compression test samples consolidated at 40 psi. The sample was sheared at an appropriate rate of strain, see Chapter 5. The majority of the extension tests were stopped as soon after failure as possible to determine the extent to which necking had occurred and its possible influence on the measured value of ϕ' at failure, Bishop (1966), Cornforth (1961). The necking becomes very pronounced beyond the peak strength in an extension test, Roscoe et al (1963a), and may be very misleading as far as the accuracy of the measured ϕ' at failure is concerned. The remainder of the procedure is similar to that for the cylindrical triaxial compression tests.

7.2.3 Cuboidal triaxial compression & extension tests

The cuboidal triaxial compression and extension tests were performed in the ISC cell with the ISC belt removed. The general method of assembly of the cell is described in the next section, 7.2.4. In addition the following features not already covered in Sections 7.2.1 & 7.2.2 for the cylindrical triaxial compression and extension tests are to be noted. For

an extension test the ISC cell was bolted to the testing machine pedestal with 6 screws inserted from the underside of the pedestal, Fig 4.4. The loading piston was clamped to the crosshead of the testing machine by the 2 tie rods shown in Fig 4.3. The top loading platten was connected to the proving ring anvil by a shear pin, Fig 4.4, as described in Chapter 4. The test procedure was generally similar to that for the cylindrical triaxial compression and extension tests, described in Sections 7.2.1 & 7.2.2. Difficulty was experienced with the extension test samples lifting off the plattens as failure was approached. The overall test success rate was only about 50% and was probably due to the difficulty in forming a perfect sample; particularly in getting the membrane to fit at the sample platten junction on the belt face, see Plates 10.1 & 10.2.

7.2.4 Independent stress control tests

The ISC belt was preassembled and the inner nuts and locknuts adjusted so that the two belt crossheads were parallel to one another and at a suitable distance apart. The tie rod linking the two suspender pulley assemblies adjacent to the hydraulic ram, Plate 4.6, was removed to allow these two assemblies to be rotated so as not to foul the top loading platten during assembly. The hydraulic ram and control cylinder were bled and the ram adjusted so that the belt plattens would clear the sample when assembled. The two encapsulated dial gauges were adjusted to a convenient zero position. All the preceding adjustments were, in part, controlled by the particular type of ISC test to be subsequently performed, i.e. plane strain, belt opening or closing. A rectangular sheet of 0.010 ins thick rubber membrane was smeared with a thin film of silicone grease. The polished surfaces of the ISC belt loading plattens were similarly greased and the membranes stuck down. Air bubbles and surplus grease were carefully removed with a straight-edge. The exposed surfaces of each of the two membranes were greased as were the two belt faces of the sample sheath. The 4 adjustable belt support screws were set up to an appropriate position. The ISC belt minus the hydraulic ram & crosshead was threaded over the sample. The hydraulic ram and crosshead was then slid over the 4 belt tie rods and the nuts threaded on and tightened. Throughout the assembly of the belt it was necessary to avoid disturbing the sample and care was required. The tie rod linking the two suspender pulley assemblies adjacent

to the hydraulic ram was assembled. The assembled ISC belt was adjusted in line and level with respect to the sample by means of the 4 adjustable belt support screws. The lead from the C61 transducer meter, Mark II, was connected to the belt proving ring by the line plug and socket adjacent to the cell and the electrical system checked.

The 4 heavy shouldered tie rods were slipped into the cell base and the cell top lowered into position. The loading piston had been previously retracted far enough to avoid fouling the top loading platten. The domed tie rod nuts and seals were threaded on and tightened (the nuts and tie rods were numbered as they were not interchangeable). The lead from the C61 transducer meter was connected to the axial proving ring by the line plug and socket adjacent to the cell and the electrical system checked. The axial proving ring was lowered until the loading anvil was just clear of the top loading platten by adjusting the loading piston clamp nuts. The four brass suspender wires were attached by their threaded pins and adjusted until they were all just taut. The belt support screws were retracted so that the ISC belt was freely suspended on the 4 wires. The belt was again checked for line and level, and minor adjustments made. The drainage and electrical leads were positioned so as not to interfere with the operation of the cell and a final overall check was made. The cell body was carefully lowered over the cell on to the cell base, care being taken to avoid knocking the belt or trapping one of the leads. The 6 tie rod nuts were attached at the underside of the cell base and tightened down to ensure a metal to metal contact between the cell body and cell base. The cell body clamp ring was tightened down evenly, by means of the 12 small nuts, to prestress the O-ring seal between the cell body and the cell top. The air release valve and bleed screw were removed and the cell was filled with de-aired water. The air release valve was replaced and when water issued from the air bleed screw hole the supply was turned off. The volume change burette reading was recorded, the air bleed screw replaced, and the cell pressure was raised to 2,3,4,5,10,15,20,25 & 30 psi, the burette reading being recorded for each pressure increment. At a cell pressure of 2 psi the burette was raised so that the meniscus was level with the mid-height of the sample. It was maintained at this pressure datum throughout the test. The sample was allowed to reach equilibrium under each pressure increment for 5-10 minutes. Having reached the desired

consolidation pressure the self-compensating mercury control was switched in and the pressurised cell was lifted into the testing machine and left for at least 2-3 hours to check for leaks. As with the triaxial samples, the reductions in the sample dimensions after consolidation were obtained from the measured volume change assuming isotropic consolidation. The testing machine pedestal was raised by hand until the loading piston was in contact with the crosshead via a half-ball. The loading piston clamping nuts were slackened off and the lower nuts run down well clear of the dial gauge cross arm. At the beginning of the shear stage the zero decade reading on the C61 transducer meter was noted and the axial proving ring anvil was brought just into contact with the top loading platten. The dial gauge was adjusted to zero and the level of the meniscus was adjusted to a convenient position within the burette. The ISC belt plattens were brought into contact with the sample by means of the oil-filled control cylinder and generally a small initial load was applied to bed the plattens. Readings were taken on the two encapsulated dial gauges during this process to establish a reliable zero strain point. No significant volume change was observed in the sample.

The testing machine gear box was set to give the desired nominal rate of axial deformation and the sample was sheared. In the plane strain tests ISC/1,2,& 3,zero deformation was maintained in the belt direction on encapsulated dial gauge No.1 by very slight manual adjustment of the control cylinder during the test. The reading on encapsulated dial gauge No.2 was noted as a check on possible tilting of the hydraulic piston in its sleeve. In tests ISC/4 to 7 the ISC belt plattens were moved apart, belt opening, by driving the control cylinder at an appropriate rate with an electric motor through a gear box. In tests ISC/8 to 18 the ISC belt plattens were moved together, belt closing, by reversing the electric motor. In the plane strain tests ISC/19 & 20 the axial plattens were kept at a fixed nominal distance apart and the ISC belt plattens were moved together, belt closing.

The volume capacity of the control cylinder relative to that of the hydraulic ram was sufficient to cover the required continuous belt deformation without having to reset the control cylinder provided it was set initially in a suitable position. Throughout the shear test, readings were taken at intervals of the axial deformation dial gauge, the two C61 transducer meter decade readings, the two encapsulated dial gauges and the volume

change burette.

The tests were continued at least until the axial load decreased and generally until the axial and belt plattens appeared to interfere at the corners.

At the end of the shear test the motor drive(s) was stopped, the clutch disengaged and the sample unloaded by hand until the belt plattens and axial proving ring were clear of the sample and top loading platten respectively. The loading piston was clamped to the cell top, the testing machine pedestal lowered and the cell was lifted off the machine and on to the bench.

The valves connecting the sample to the burette were closed, sealing off the sample. The self-compensating mercury control was disconnected and the cell pressure reduced to atmospheric pressure. The cell was drained by means of the large Klinger valve in the cell base, Plates 4.4 & 4.5, and carefully dismantled. Care was needed in removing the ISC belt as the clearance between the 4 tie rods and the axial loading plattens, Fig 4.6, Section B-B, was reduced after shearing the specimen. The sample was sketched and the dimensions measured with the vernier caliper gauge. Photographs were taken of certain samples.

The sample was removed from the sample sheath onto a metal tray away from the cell base, care being taken to try to collect all the sand. The sand recovered was dried overnight to determine its dry weight. The apparatus was cleaned and the drainage leads flushed out in preparation for the next test. The sample sheath and lubricated rubber membranes were washed and the sample sheath was powdered with French chalk.

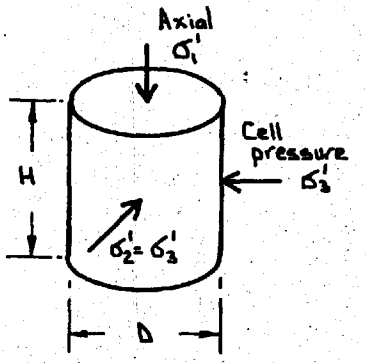
7.3 Shear Test Calculations

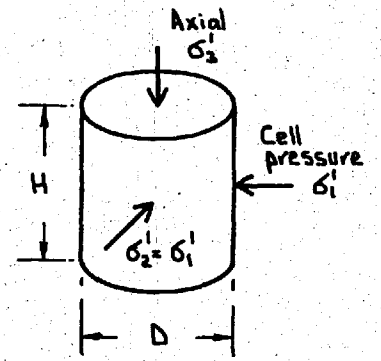
7.3.1 All tests

The dimensions of, and stresses acting on, the samples are denoted in Fig 7.3. All strains are engineers strains based on conditions at the end of consolidation.

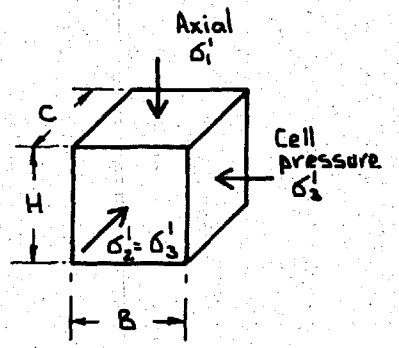
$\frac{\Delta H}{H_c}$ = axial strain, which is positive for a reduction in height (compression) and is negative for an increase in height (extension).

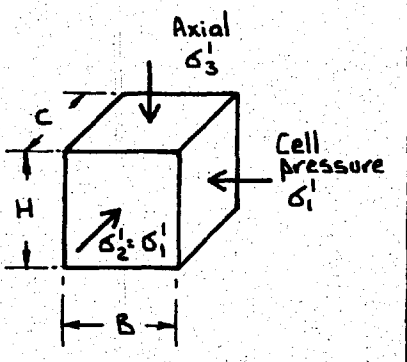
$\frac{\Delta V}{V_c}$ = volumetric strain, which is positive for a reduction in volume (consolidation) and is negative for an increase in volume (dilatation).



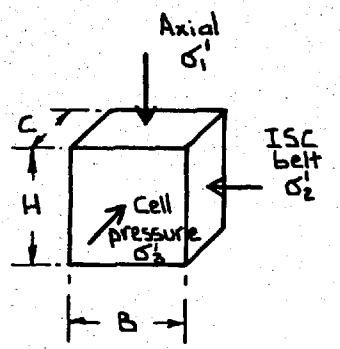


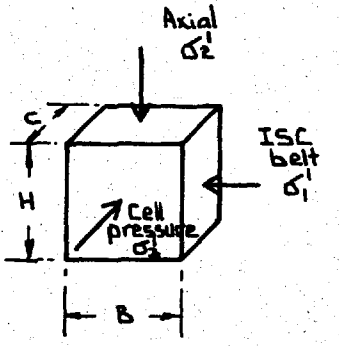
Cylindrical triaxial compression,
1st series.
2nd series.
Cylindrical triaxial
compression & extension.





Cuboidal triaxial
compression & extension.





Independent stress control.

STRESSES ACTING ON SAMPLES AT FAILURE

FIG. 7.3

The sign conventions used for linear and volumetric strains are chosen to be consistent with one another. Previous writers have used various conventions, e.g. Cornforth (1961) defines linear compression as positive but volume reduction as negative, which appears to be inconsistent.

Porosity was calculated as follows:

$$\text{Porosity, } n = 1 - \frac{W_s}{G\ \gamma_w\ V}$$

where W_s = average dry weight of sand in specimen.

V = volume of specimen.

G = specific gravity of sand.

γ_w = unit weight of water.

Axial deviator stress was calculated as follows:

$$(\sigma_1' - \sigma_3') = \frac{\text{Net load}}{A_s}$$

where $(\sigma_1' - \sigma_3')$ = axial deviator stress.

A_s = average axial cross-sectional area of specimen.

$$= \frac{A_c\ (1 - \Delta V/V_c)}{(1 - \Delta H/H_c)}$$

where A_c = average axial cross-sectional area of specimen at end of consolidation.

Net load = L + W

where L = load measured on axial proving ring, which is positive in compression and is negative in extension

W = weight of top loading platten, etc.

7.3.2 Cylindrical Samples

Average lateral strain was calculated as follows:

$$\left(1 - \frac{\Delta D}{D_c}\right) = \left[\frac{1 - \Delta V/V_c}{1 - \Delta H/H_c}\right]^{\frac{1}{2}}$$

where $\frac{\Delta D}{D_o}$ = average lateral strain, which is positive for a reduction in diameter and is negative for an increase in diameter.

Volumetric strain rate was calculated as follows:

$$\frac{d(\Delta V/V_o)}{d(\Delta H/H_c)} = \frac{(\Delta V/V_c)_2 - (\Delta V/V_c)_1}{(\Delta H/H_c)_2 - (\Delta H/H_c)_1}$$

where $\frac{d(\Delta V/V_c)}{d(\Delta H/H_c)}$ = volumetric strain rate with respect to specimen height.

$$\frac{d(\Delta V/V_c)}{d(\Delta D/D_c)} = \frac{(\Delta V/V_c)_2 - (\Delta V/V_c)_1}{(\Delta D/D_c)_2 - (\Delta D/D_c)_1}$$

$$= \frac{(\Delta V/V_c)_2 - (\Delta V/V_c)_1}{\left[\frac{1-(\Delta V/V_c)_1}{1-(\Delta H/H_c)_1}\right]^{1/2} - \left[\frac{1-(\Delta V/V_c)_2}{1-(\Delta H/H_c)_2}\right]^{1/2}}$$

where $\frac{d(\Delta V/V_c)}{d(\Delta D/D_c)}$ = volumetric strain rate with respect to specimen diameter.

The computations for a typical cylindrical triaxial compression test are given in Appendix A7.

7.3.3 Cuboidal Triaxial Compression & Extension Samples

Average lateral strain was calculated as follows:

$$(1 - \Delta B/B_c) = (1 - \Delta C/C_c) = \left[\frac{1 - \Delta V/V_c}{1 - \Delta H/H_c}\right]^{1/2}$$

where $\frac{\Delta B}{B_c} = \frac{\Delta C}{C_c}$ = average lateral strain in the B and C directions respectively, which are positive for a reduction in width and are negative for an increase in width.

Volumetric strain rate was calculated as follows:

$$\frac{d(\Delta V/V_c)}{d(\Delta H/H_c)} = \frac{(\Delta V/V_c)_2 - (\Delta V/V_c)_1}{(\Delta H/H_c)_2 - (\Delta H/H_c)_1}$$

where $\frac{d(\Delta V/V_c)}{d(\Delta H/H_c)}$ = volumetric strain rate with respect to specimen height.

$$\frac{d(\Delta V/V_c)}{d(\Delta B/B_c)} = \frac{d(\Delta V/V_c)}{d(\Delta C/C_c)} = \frac{(\Delta V/V_c)_2 - (\Delta V/V_c)_1}{\left[\frac{1-(\Delta V/V_c)_1}{1-(\Delta H/H_c)_1}\right]^{1/2} - \left[\frac{1-(\Delta V/V_c)_2}{1-(\Delta H/H_c)_2}\right]^{1/2}}$$

where $\frac{d(\Delta V/V_c)}{d(\Delta B/B_c)} = \frac{d(\Delta V/V_c)}{d(\Delta C/C_c)}$ = volumetric strain rate with respect to specimen widths B and C respectively.

The computations for a typical cuboidal triaxial extension test are given in Appendix A7.

7.3.4 Cuboidal Independent Stress Control Samples

ISC belt deviator stress was calculated as follows:

$$(\sigma_2' - \sigma_3') = \frac{\text{Net load}}{A_s^*}$$

where $(\sigma_2' - \sigma_3')$ = ISC belt deviator stress.

A_s^* = average ISC belt cross-sectional area of specimen.

$$= \frac{(A_c^* - \Delta V/B_c)}{(1 - \Delta B/B_c)}$$

where A_c^* = average ISC belt cross-sectional area of specimen at end of consolidation.

Net load = load measured on ISC belt proving ring which is positive in compression.

Average lateral - cell strain was calculated as follows:

$$(1 - \Delta C/C_c) = \frac{(1 - \Delta V/V_c)}{(1 - \Delta H/H_c)(1 - \Delta B/B_c)}$$

where $\frac{\Delta C}{C_c}$ = average lateral-cell strain, which is positive for a reduction in width and is negative for an increase in width.

$\frac{\Delta B}{B_c}$ = ISC belt strain, which is positive for a reduction in width (belt closing) and is negative for an increase in width (belt opening).

Volumetric strain rate was calculated as follows:

$$\frac{d(\Delta V/V_c)}{d(\Delta H/H_c)} = \frac{(\Delta V/V_c)_2 - (\Delta V/V_c)_1}{(\Delta H/H_c)_2 - (\Delta H/H_c)_1}$$

where $\frac{d(\Delta V/V_c)}{d(\Delta H/H_c)}$ = volumetric strain rate with respect to specimen height.

The computations for a typical independent stress control test are given in Appendix A7.

CHAPTER 8

CYLINDRICAL TRIAXIAL COMPRESSION TEST RESULTS AND DISCUSSION

8.1 Introduction

The primary purpose of the present research was to compare the failure characteristics of variously shaped samples under different stress systems. Many of the cylindrical triaxial compression tests were continued to large strains well beyond failure to try to define an ultimate or residual strength. However the latter is of secondary interest in this thesis and is not discussed in great detail. It had been hoped, optimistically in retrospect, to induce samples to deform uniformly well beyond the peak strength so that the ultimate strength would be more well defined, free from the usual qualifications concerning sample distortion and non-uniform stresses. This was not possible, although significant improvements were made.

The maximum angle of shearing resistance, ϕ', at failure, is based on a linear Mohr envelope tangent to the stress circle corresponding to the measured stress difference and passing through the origin. The average cross-sectional area of the sample, obtained by assuming the sample deforms uniformly, is used in calculating the axial stress. The density of the sand is expressed in terms of the initial porosity, n_i, as determined from the weight and linear dimensions of the sample under a 0.7 psi suction immediately prior to consolidation in the triaxial cell. Strains are engineers strains, expressed with respect to the dimensions of the sample at the end of consolidation. The stress-strain and volume change curves for each test are plotted in a normal manner but with sign conventions as defined in Chapter 7.

Before comparing all the test data, the results for each test type will be examined separately. The stress-strain and volume change curves for the individual cylindrical triaxial compression tests are given in Appendix A8. Tests which were clearly unreliable due to leaks are excluded from the thesis; indicated by a gap in the referencing sequence. Each test is numbered, firstly according to its type, and secondly, bracketed, its sequence in the particular series, e.g. Test X/9(41). The sequence number is of importance in detecting uncontrolled variations in

the testing techniques which were unfortunately present in the 1st Series of 56 tests spread over a period of 10 months.

For most tests the sample was sketched, after dismantling the cell, to record the general mode of deformation and the presence, or otherwise, of slip zones. Frequently the sample diameter was measured at suitable points to indicate quantitatively the non-uniform lateral expansion. The diameters given are each the mean of two diameters and are corrected for the thickness of the sample sheath.

The basic test characteristics and failure stresses etc. are tabulated in Figs 8.1, 8.2 & 8.3.

8.2 1st Series of Tests

8.2.1 Type X

These were samples 4 ins high, built in the normal manner with lubricated ends. One 0.009 ins thick lubricated rubber membrane was used on each platten. All the samples expanded predominantly at the base but measurements made in Tests X/7, 8, 9, 12 & 13 indicate that the top of the sample expanded also. Visual observation during a test by sighting the vertical edge of the sample against a triaxial cell tie rod suggested that most of the movement of the top of the sample occurred before peak deviator stress. Beyond this, expansion appeared to occur mainly at the base. These visual observations were complicated by distortion due to refraction and are not considered to be very reliable.

Slip zones were observed in the medium dense and dense samples, Tests X/3, 7, 8 & 9; whereas the loose samples did not exhibit any slip zones, Tests X/4, 5 & 6. In addition, for some of the dense samples a circumferential slip zone was visible just below the top platten, Tests X/3,8 & 9, which suggests that a punching action frequently occurred, i.e. an upper relatively rigid cone of sand displaced the lower portion of the sample outwards. The slip zones were never visible before the peak deviator stress had been reached and in some tests on dense samples a particularly good set of slip zones were formed, e.g. Test X/9. There was never any observed tendency for samples to fail on a single well defined surface so often associated with conventional dense sand samples, e.g. see Fig 6(b) of Rowe and Barden (1964).

Date	Test number	Sequence number	Porosity, n %			Stresses at failure psi		Strains at failure %			Volumetric strain rate at failure		ϕ' degrees		Material	End condition	Nominal axial strain rate ins/min	Mode of sample preparation	Notes
			Initial n_i	After consolidation	At failure	Axial σ_1'	Cell $\sigma_2' = \sigma_3'$	Axial $\Delta H/H_c$	Mean lateral $\Delta D/D_c$	Volumetric $\Delta V/V_c$	$\frac{d(\Delta V/V_c)}{d(\Delta H/H_c)}$								
TYPE X D=3.9 ins, H=4.1 ins																			
9/2/64	X/1	1	39.9	39.6	41.6	192.6	40.0	+8.6	-6.4	-3.5	-0.50		40.9		Batch 1	1/0.009 ins thick lubricated membrane	+0.007	Normal	
15/2/64	X/3	3	38.3	38.0	40.4	206.4	40.0	+7.5	-5.9	-3.9	-0.70		42.5						
19/2/64	X/4	4	45.4	44.7	45.4	155.2	40.0	+21.2	-13.1	-0.9	-0.07		36.2						
22/2/64	X/5	5	44.8	44.3	45.0	157.0	40.0	+23.0	-14.8	-1.4	-0.07		36.4						40 psi back pressure
28/2/64	X/6	6	43.4	42.8	44.6	163.5	40.0	+15.0	-10.1	-3.0	-0.20		37.3						
1/3/64	X/7	7	41.9	41.4	43.3	171.5	40.0	+10.6	-7.5	-3.3	-0.37		38.4						
15/10/64	X/8	39	40.9	40.4	41.9	169.1	39.1	+7.8	-5.5	-2.5	-0.46		38.6						
22/10/64	X/9	41	40.2	39.8	41.6	172.2	39.1	+8.6	-6.2	-3.1	-0.53		39.1		Batch 1 Reused				
23/11/64	X/10	47	41.1	40.6	42.4	170.2	39.1	+9.4	-6.7	-3.1	-0.46		38.8						
1/12/64	X/11	50	40.8	40.3	41.8	169.1	39.1	+8.6	-5.9	-2.6	-0.43		38.6						
3/12/64	X/12	51	41.0	40.6	42.1	171.1	39.1	+9.4	-6.4	-2.6	-0.44		38.9						
21/12/64	X/13	52	41.1	40.7	42.3	169.2	39.1	+8.6	-6.0	-2.8	-0.46		38.6						
TYPE A D=3.9 ins, H=4.1 ins																			
13/4/64	A/1	9	39.8	39.4	41.3	185.2	40.0	+7.6	-5.7	-3.1	-0.58		40.1		Batch 1	1/0.009 ins thick lubricated membrane	+0.007	Two halves	
7/4/64	A/2	10	44.7	44.1	44.7	155.5	40.0	+15.6	-9.5	-1.2	-0.15		36.2						
22/4/64	A/3	11	40.9	40.4	42.3	181.3	40.0	+9.4	-6.8	-3.3	-0.48		39.7						
25/4/64	A/4	12	42.5	41.9	43.3	167.8	40.0	+9.4	-6.3	-2.3	-0.36		37.9						
28/4/64	A/5	13	39.4	39.0	41.1	192.8	40.0	+7.6	-5.8	-3.6	-0.63		41.0						
2/4/64	A/6	14	38.5	38.1	40.4	202.3	40.0	+7.2	-6.4	-3.9	-0.72		42.1						Photo
4/9/64	A/7	30	44.0	43.6	44.5	153.2	39.1	+12.0	-7.5	-1.7	-0.21		36.4						
19/3/64	A/8	8	40.8	40.3	42.1	177.2	40.0	+8.8	-6.2	-3.0	-0.60		39.2						
13/9/64	A/9	33	41.0	40.6	42.4	167.8	39.1	+7.6	-5.8	-3.2	-0.54		38.4			3/0.024 ins			
20/9/64	A/10	35	40.8	40.3	42.1	166.3	39.1	+9.0	-6.4	-3.1	-0.48		38.2			5/0.024 ins			
30/9/64	A/11	36	44.5	43.8	44.5	146.2	39.1	+12.2	-7.4	-1.3	-0.20		35.3			2/0.009 ins			
4/10/64	A/12	37	38.3	37.9	40.2	188.2	39.1	+7.5	-5.9	-3.8	-0.74		41.1						
11/10/64	A/13	38	42.9	42.4	43.6	160.0	39.1	+10.0	-6.5	-2.1	-0.29		37.3			1/0.009 ins			
18/10/64	A/14	40	40.4	40.0	41.8	168.9	39.1	+8.5	-6.2	-3.1	-0.54		38.6			2/0.009 ins			
28/11/64	A/15	48	40.7	40.2	42.0	172.8	39.1	+9.0	-6.4	-3.1	-0.48		39.1		Batch 1 Reused	1/0.009 ins			
30/11/64	A/16	49	41.1	40.6	42.2	172.4	39.1	+8.2	-5.8	-2.7	-0.45		39.0						

CYLINDRICAL TRIAXIAL COMPRESSION TESTS, 1ST SERIES RESULTS

FIG. 8.1

Date	Test number	Sequence number	Porosity, n %			Stresses at failure psi		Strains at failure %			Volumetric strain rate at failure		ϕ' degrees		Material	End condition	Nominal axial strain rate ins/min	Mode of sample preparation	Notes
			Initial n_i	After consolidation	At failure	Axial σ_1'	Cell $\sigma_2' = \sigma_3'$	Axial $\Delta H/H_c$	Mean lateral $\Delta D/D_c$	Volumetric $\Delta V/V_c$	$\frac{d(\Delta V/V_c)}{d(\Delta H/H_c)}$								
TYPE B D=4.0 ins, H=8.1 ins																			
22/5/64	B/1	15	45.1	44.5	44.6	140.8	40.0	+11.6	-6.5	-0.2	-0.11		33.8		Batch 1	Direct contact	+0.014	Two halves	
1/6/64	B/2	18	39.7	39.3	40.7	184.4	40.0	+5.2	-3.9	-2.3	-0.62		40.0						
9/6/64	B/3	20	42.1	41.6	42.4	162.9	40.0	+6.8	-4.3	-1.5	-0.37		37.3						
11/6/64	B/4	21	43.1	42.6	43.4	155.7	40.0	+7.6	-4.6	-1.1	-0.23		36.2						
17/6/64	B/5	22	40.2	39.8	40.9	175.9	40.0	+6.0	-4.1	-2.0	-0.51		39.0						
22/6/64	B/6	23	38.1	37.6	39.0	197.9	40.0	+4.7	-4.2	-2.3	-0.75		41.6						
23/6/64	B/7	24	38.7	38.4	39.7	189.6	40.0	+5.2	-3.9	-2.3	-0.67		40.7						
25/6/64	B/8	25	44.4	43.9	44.1	143.8	40.0	+9.4	-5.3	-0.5	-0.13		34.3						
27/10/64	B/9	42	39.4	39.0	40.3	175.2	39.1	+6.1	-4.3	-2.1	-0.55		39.4		Batch 1 Reused				
TYPE C D=4.0 ins, H=8.1 ins																			
25/5/64	C/1	16	45.5	44.7	44.7	138.2	40.0	+11.8	-6.5	0	-0.08		33.4		Batch 1	1 | 0.009 ins	+0.014	Two halves	
28/5/64	C/2	17	39.4	39.1	41.9	184.2	40.0	+6.0	-4.6	-2.8	-0.66		40.0						
4/6/64	C/3	19	41.9	41.4	42.6	163.0	40.0	+7.6	-5.0	-1.9	-0.41		37.2			2 | 0.009 ins			Photo
28/6/64	C/4	26	42.9	42.4	43.4	156.1	40.0	+8.3	-5.3	-1.7	-0.30		36.2			3 | 0.024 ins			
10/7/64	C/5	27	38.6	38.3	40.1	191.1	40.0	+6.0	-4.7	-3.0	-0.70		40.8			1 | 0.009 ins			
10/8/64	C/6	28	44.2	43.6	44.0	145.8	39.4	+9.5	-5.4	-0.7	-0.19		35.1						
1/9/64	C/7	29	40.6	40.2	41.6	169.8	39.1	+6.8	-4.8	-2.4	-0.51		38.7						
TYPE D D=3.9 ins, H=4.1 ins																			
8/9/64	D/1	31	44.5	44.0	44.3	168.1	39.1	+11.0	-6.2	-0.4	-0.13		38.5		Batch 1	Direct contact	+0.007	Two halves	
11/9/64	D/2	32	39.1	38.8	40.1	235.0	39.1	+5.5	-3.9	-2.2	-0.64		45.9						
13/9/64	D/3	34	41.0	40.6	41.7	203.0	39.1	+7.3	-4.9	-2.0	-0.44		42.6						
TYPE B1 D=4.0 ins, H=8.1 ins																			
2/11/64	B1/1	43	40.3	39.6	40.8	164.0	39.1	+7.0	-4.8	-2.0	-0.45		37.9		Batch 2 Bag 5	Direct contact	+0.014	Two halves	
7/11/64	B1/2	44	40.2	39.8	40.9	165.0	39.1	+6.3	-4.2	-1.8	-0.46		38.1						
16/11/64	B1/3	45	40.7	40.3	41.2	160.5	39.1	+6.6	-4.3	-1.7	-0.41		37.5						
19/11/64	B1/4	46	40.1	39.6	40.7	163.1	39.1	+6.7	-4.4	-1.9	-0.43		37.8						
TYPE E D=4.0 ins, H=7.6 ins																			
2/1/65	E/1	53	42.7	42.1	42.7	154.6	39.1	+7.0	-4.2	-1.0	-0.29		36.6		Batch 1 Reused	4 ins diam. porous discs	+0.014	Normal	3/4 ins diam half ball seating
5/1/65	E/2	54	39.2	38.8	40.1	187.8	39.1	+4.7	-3.4	-2.0	-0.66		40.9						
7/1/65	E/3	55	45.3	44.4	44.3	139.0	39.1	+8.5	-4.4	+0.2	-0.13		34.1				+0.007		
10/1/65	E/4	56	39.8	39.3	40.4	173.1	39.1	+6.1	-4.1	-1.9	-0.53		39.1						

CYLINDRICAL TRIAXIAL COMPRESSION TESTS, 1ST SERIES RESULTS

FIG. 8.2

Date	Test number	Sequence number	Porosity, n %			Stresses at failure p.s.i.		Strains at failure %			Volumetric strain rate at failure		ϕ' degrees		Material	End condition	Nominal axial strain rate ins/min	Mode of sample preparation	Notes
			Initial n_i	After consolidation	At failure	Axial σ_1'	Cell $\sigma_2' = \sigma_3'$	Axial $\Delta H/H_c$	Mean lateral $\Delta D/D_c$	Volumetric $\Delta V/V_c$	$\frac{d(\Delta V/V_c)}{d(\Delta H/H_c)}$								
TYPE SA D = 4·0 ins, H = 8·1 ins																			
18/1/65	SA/1	1	41·5	40·8	41·8	162·6	39·4	+7·1	−4·5	−1·6	−0·38		37·5		Batch 2 Bag 3	Direct contact	+0·014	Two halves	
28/1/65	SA/2	8	41·6	41·0	41·8	162·2	39·4	+7·2	−4·6	−1·5	−0·37		37·5						
6/2/65	SA/3	15	41·6	41·1	41·8	163·4	39·4	+7·1	−4·5	−1·5	−0·39		37·7						
10/2/65	SA/4	18	41·2	40·6	41·6	164·8	39·4	+6·8	−4·4	−1·6	−0·43		37·8						Photo
TYPE SB D = 4·0 ins, H = 8·1 ins																			
19/1/65	SB/1	2	41·4	40·8	42·0	163·3	39·4	+8·2	−5·5	−2·1	−0·41		37·6		Batch 2 Bag 3	10·009 ins thick lubricated membrane	+0·014	Two halves	
29/1/65	SB/2	9	41·6	41·0	42·1	166·2	39·4	+8·0	−5·3	−1·9	−0·41		38·1						
4/2/65	SB/3	14	42·0	41·4	42·3	161·6	39·4	+7·8	−4·9	−1·6	−0·37		37·4						
7/2/65	SB/4	16	41·4	40·8	41·9	166·2	39·4	+8·0	−5·3	−2·0	−0·42		37·9						Photo
11/2/65	SB/5	19	41·2	40·6	41·7	159·3	39·4	+7·7	−5·1	−1·9	−0·40		37·1		Batch 2 Bag 4				
TYPE SC D = 3·9 ins, H = 4·1 ins																			
20/1/65	SC/1	3	40·8	40·3	41·4	197·4	39·4	+7·8	−4·9	−1·7	−0·39		41·8		Batch 2 Bag 3	Direct contact	+0·007	Two halves	
1/2/65	SC/2	11	41·6	41·1	41·9	189·4	39·4	+7·9	−5·0	−1·5	−0·35		40·9						
TYPE SD D = 3·9 ins, H = 4·1 ins																			
21/1/65	SD/1	4	41·2	40·7	42·2	172·0	39·4	+9·7	−6·6	−2·6	−0·39		38·8		Batch 2 Bag 3	10·009 ins	+0·007	Two halves	Photo
30/1/65	SD/2	10	41·6	40·9	42·5	169·5	39·4	+10·4	−7·1	−2·7	−0·40		38·5						
TYPE SD1 D = 3·9 ins, H = 4·1 ins																			
26/1/65	SD1/1	6	41·3	40·8	42·3	165·0	39·4	+9·1	−6·2	−2·7	−0·43		37·9		Batch 2 Bag 3	2/10·009 ins	+0·007	Two halves	
2/2/65	SD1/2	12	41·4	40·7	42·2	163·5	39·4	+9·5	−6·4	−2·4	−0·42		37·7						Photo
TYPE SE D = 3·9 ins, H = 2·1 ins																			
23/1/65	SE/1	5	41·6	41·1	42·7	178·2	39·4	+10·0	−6·9	−2·9	−0·41		39·6		Batch 2 Bag 3	1/10·009 ins	+0·0035	Normal	Failure "defined" at $\Delta H/H_c$ = 10%
3/2/65	SE/2	13	42·2	41·6	42·9	173·6	39·4	+10·0	−6·7	−2·4	−0·39		39·0						
TYPE SF D = 3·9 ins, H = 4·1 ins																			
27/1/65	SF/1	7	41·8	41·2	42·8	169·3	39·4	+10·9	−7·4	−2·9	−0·35		38·4		Batch 2 Bag 3	1/10·009 ins	+0·007	Normal	
8/2/65	SF/2	17	41·4	40·7	42·3	174·7	39·4	+10·6	−7·2	−2·9	−0·41		39·2						

CYLINDRICAL TRIAXIAL COMPRESSION TESTS, 2ND SERIES RESULTS

FIG. 8.3

In Test X/5 a 40 psi back pressure was applied to the sample. No significant difference in behaviour, on an effective stress basis, was observed from the other tests in this series and it was therefore inferred that nothing was to be gained by using a back pressure in any of the subsequent tests.

8.2.2 Type A

These samples were similar to Type X, 4 ins high with lubricated ends, but were built in two halves. It was hoped to obtain more uniform lateral expansions by using this method of sample preparation. Normally 1/0.009 ins thick lubricated rubber membrane was used on each platten but in certain tests, A/9-12 & 14, the number and thickness were increased.

The samples generally appeared to expand more uniformly up to peak than the Type X test samples, as seen by the naked eye. Caliper or belt gauges at the top and bottom of the sample to monitor the lateral deformations would have been useful to clarify this point. They were not available and the anticipated time required for their design and development was not considered justified.

Many slip zones were observed beyond peak ϕ' in the dense samples, Tests A/1, 3, 5, 6, 8, 14 & 15, and a lesser number in the medium dense samples, Tests A/4, 9, 10 & 16. The loose samples, Tests A/2 & 11, were generally free of visible slip zones although a few were apparent in Test A/7. Most samples expanded laterally predominantly at the bottom, beyond peak ϕ'. However in Tests A/3,5 & 9, the samples expanded at both ends taking on the conventional barrel-shaped appearance. This latter test, although medium dense, exhibited no visible slip zones.

Plate 8.1 (a) shows the sample in Test A/6 after dismantling. The sample had an initial porosity of 38.5% (i.e. dense) and failed at an axial strain of +7.2%. The test was continued up to an axial strain of +29.8%. A well defined regular pattern of slip zones can be seen. That the sample expanded at both plattens is clearly seen by the lip formed in the membrane at each platten.

In Test A/8, a series of horizontal rings were drawn on the sample sheath with a ballpoint pen. Slip zones were indicated by clearly defined discontinuities in these lines. It was possible to see the slip zones with the naked eye in the normal way. However no discontinuities were



(a) TEST A16.
cylindrical compression,
n_i = 38·5%, 4·1 ins high,
sample made in two halves,
1 0·009 ins thick membrane,
test stopped at $\Delta H/H_c$ = +29·8%,
$(\Delta H/H_c)_f$ = +7·2%.



(b) TEST C13.
cylindrical compression,
n_i = 41·9%, 8·1 ins high,
sample made in two halves,
2 0·009 ins thick membranes,
test stopped at $\Delta H/H_c$ = +27·6%,
$(\Delta H/H_c)_f$ = +7·6%.

PLATE 8.1

observed until after the peak ϕ' was reached.

8.2.3. Type B

These samples were 8 ins high, built in two halves with non-lubricated ends. The sand was in direct contact with the polished stainless steel loading plattens. The samples deformed in a well-known manner. A central bulge occurred in the loose samples with little or no expansion at the ends, Tests B/1 & 8. In Test B/1 slip zones were formed in a symmetrical pattern. The dense samples, Tests B/2, 3, 7 & 9, barrelled and a number of slip zones were formed, one or two of which were usually very well developed and passed through, or close to, the edges of the sample-platten interfaces. The first and second predominant slip zones (planes) were observed to intersect on a common strike line so that the samples exhibited some degree of symmetry. These predominant slip zones were always concave downwards suggesting a non-homogeneity in the sample or, as seems more likely, that the top platten had rotated very slightly. The loading piston was not a tight fit in the bushing and the axial proving ring, although relatively rigid, could rotate a little under an eccentric load. No spherical seating was used between the top loading platten and the axial proving ring anvil.

The latter portion of the stress-strain curves of some of the dense samples, e.g. Test B/7, was erratic due to irregular movements along particular slip zones.

The sample in Test B/4 was offset on the bottom platten so that it was loaded eccentrically by about 3/16 ins. A single predominant slip zone (plane) was formed dipping in the direction of the eccentricity, as one would clearly expect.

In the later stages of Test B/6 an electro-magnetic vibrator was inadvertently switched on adjacent to the testing machine. The resulting discontinuity in the stress-strain curve is clearly seen. This re-emphasised to the writer the importance of the slightest vibration in any loading test on sand, Green (1961).

8.2.4 Type C

These samples were similar to Type B, 8 ins high, built in two halves but with lubricated ends. Normally 1/0.009 ins thick lubricated rubber

membrane was used on each platten but in certain tests, C/3 & 4, the number and thickness were increased.

There is little detectable difference in the mode of failure from the Type B samples. There was little or no lateral expansion of the loose samples at the plattens, Tests C/1 & 6, and a very small lateral expansion of the dense samples, Tests C/2, 3 & 5. Again, predominant slip zones were formed in dense samples and more symmetrical multiple slip zones in the looser samples. Tests C/3 & 4 in which additional and thicker lubricated rubber membranes were used showed no significantly different behaviour.

Plate 8.1(b) shows the sample in Test C/3 in which 2/0.009 ins thick lubricated rubber membranes were used on each platten. The sample had an initial porosity of 41.9% (medium dense) and failed at an axial strain of +7.6%. The test was continued up to an axial strain of +27.6%. Major slip zones can be seen and there is some evidence of lateral expansion at the plattens.

8.2.5 Type D

These samples were 4 ins high, built in two halves with non-lubricated ends. Only 3 samples were tested, one dense, one medium dense and one loose, since the increase in the measured strength over the Type X,A,B & C samples was large.

All three samples barrelled severely, multiple slip zones being formed. The loose sample, Test D/1, deformed particularly symmetrically, the slip zone pattern being quite regular. There appeared to be no lateral expansion at the plattens in any of the tests but it was not possible to measure the diameter adjacent to the platten with any accuracy due to the severe barrelling. The latter part of the stress-strain curves for Tests D/2 &3 began to rise again beyond +18% axial strain due, presumably , to the effect of platten friction.

8.2.6 Type E

These samples were 8 ins high, built in the normal manner with non-lubricated ends. Conventional $\frac{1}{4}$ ins thick, 4 ins diameter porous discs were used on each platten and in Tests E/1 - 3 a $\frac{3}{4}$ ins diameter half-ball plus seating was inserted between the top loading platten and the axial proving ring anvil. In these three tests the top loading platten tilted

by 2,5 & 9 degrees respectively as measured after the tests. The sample in Test E/1, medium dense, bulged and a number of slip zones were formed. Test E/2, a dense, vibrated sample, formed a single slip zone, first observed just beyond peak ϕ' . The sample in Test E/3 failed catastrophically due to rotation of the top platten which commenced before peak ϕ' . A single slip zone was formed and the volume changes beyond about +12% axial strain were very erratic. A lateral translation of about $\frac{1}{4}$ ins was observed between the half-ball seating and the top loading platten, implying a fairly large lateral thrust (Webb,1966).

The normal non-tilting direct contact was reverted to in Test E/4 and two predominant slip zones were formed possessing a common strike line.

8.2.7 Type B1

These were similar to the Type B tests but on a portion of the 2nd batch of sand. The mode of deformation was similar to the Type B test samples. Tests B1/3 & 4 were on material re-used once and twice respectively.

8.3 2nd Series of Tests

All the tests were on medium dense samples at an initial porosity of approximately 41.5%. The mode of deformation and failure characteristics in the tests were similar to the relevant tests in the 1st Series and are not discussed further.

An additional test type was included, Type SE. These 2 samples were 2 ins high, built in the normal manner with lubricated ends. One 0.009 ins thick lubricated rubber membrane was used on each platten. Each sample expanded at both ends, but predominantly at the base. The stress-strain curves,Figs A 8.71 & A 8.72, failed to define a peak and failure was arbitrarily defined at + 10% axial strain for the purpose of comparing the different test types. This choice has no significant effect on the interpretation of the test results.

Plate 8.2(a) shows the sample in Test SA/4 after dismantling. The sample had an initial porosity of 41.2% (i.e. medium dense) and failed at an axial strain of +6.8%. The test was continued up to an axial strain of +22.5%. Two well defined slip zones are seen.

Plate 8.2(b) shows the sample in Test SB/4 after dismantling. The



(a) TEST SA14.
cylindrical compression,
n_i = 41·2 %, 8·1 ins high,
sample made in two halves,
direct contact with platens,
test stopped at $\Delta H/H_c$ = +22·5%,
$(\Delta H/H_c)_f$ = +6·8 %.



(b) TEST SB14.
cylindrical compression,
n_i = 41·4 %, 8·1 ins high,
sample made in two halves,
10·009 ins thick membrane,
test stopped at $\Delta H/H_c$ = +15·6%,
$(\Delta H/H_c)_f$ = +8·0 %.

PLATE 8.2

sample had an initial porosity of 41.4% (i.e. medium dense) and failed at an axial strain of +8.0%. The photograph shows the sample well beyond failure at +15.6% axial strain at which point a slip zone is clearly visible on the surface of the sample. The sample has barrelled with the maximum cross-sectional area occurring exactly at mid-height (c.f. Fig 2, Shockley & Ahlvin (1960) and also Fig 3, Bishop (1966)). The ends, although lubricated (each having 1/0.009 ins thick membrane) have expanded by a negligible amount.

Plate 8.3(a) & (b) show samples in Tests SD/1 & SD/2, respectively, after dismantling. The two samples have virtually identical initial porosities of 41.2 and 41.4% respectively, but differing degrees of end restraint. The sample in Test SD/1 had 1/0.009 ins thick lubricated rubber membrane at each end, the test being stopped at an axial strain of +19.2%. The sample in Test SD1/2 had 2/0.009 ins thick lubricated rubber membranes at each end and was stopped at an axial strain of +22.5%. The latter suggests that a reduced tendency to develop visible slip zones is associated with a decreased degree of end restraint.

8.4 Comparison of stress-strain & volume change curves

The stress-strain & volume change characteristics of selected tests from both the 1st and 2nd Series are shown in Figs 8.4, 8.5 & 8.6. In correlating data on samples possessing differing ratios of height to diameter and degrees of end restraint, it is important to compare only those samples that possess, as near as possible, the same initial porosity since small differences in porosity of about $\frac{1}{2}$% or more may completely mask any differences due to the type of test. It is also necessary to select representative samples from each category to minimise the influence of the natural scatter of the results.

Fig 8.4 shows a series of results for initially dense samples taken fromthe 1st Series. Any differences in behaviour between the test types should be most noticeable for dense samples. The 4 ins high sample in direct contact with the loading plattens, Test D/2, gives the highest peak and residual strengths, as one would clearly expect. The two 4 ins high samples with lubricated ends, 1/0.009 ins thick membrane, give very similar stress-strain & volume change curves, Tests A/6 & X/3. The sample made in two halves, Test A/6, shows a slightly lower strength associated with more

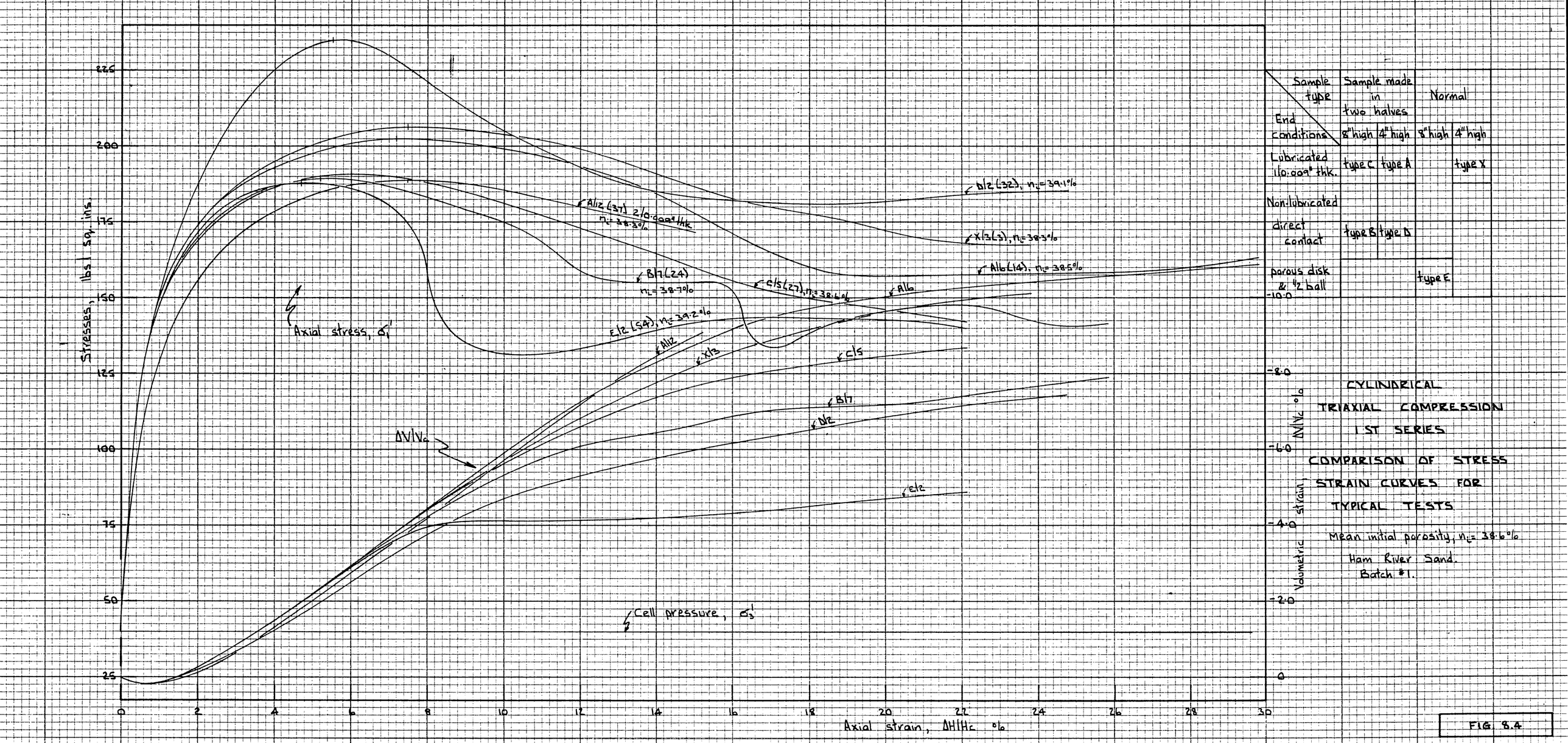


(a) TEST SD11.
cylindrical compression,
n_i = 41·2 %, 4·1 ins high,
sample made in two halves,
1 10·009 ins thick membrane,
test stopped at $\Delta H/H_c$ = +19·2 %,
$(\Delta H/H_c)_f$ = +9·7 %.



(b) TEST SD12.
cylindrical compression,
n_i = 41·4 %, 4·1 ins high,
sample made in two halves,
2 10·009 ins thick membranes,
test stopped at $\Delta H/H_c$ = +22·5 %,
$(\Delta H/H_c)_f$ = +9·5 %.

PLATE 8.3


Stresses, lbs/sq. ins.
Axial strain, ΔH/Hc %
Volumetric strain, ΔV/Vc %
Axial stress, σ1'
Cell pressure, σ3'
ΔV/Vc
A1/2 (37) 2/0.009" thk. n_i = 38.3%
B1/7 (24) n_i = 38.7%
C1/5 (27), n_i = 38.6%
D1/2 (32), n_i = 39.1%
E1/2 (59), n_i = 39.2%
X1/3 (3), n_i = 38.3%
A1/6 (14), n_i = 38.5%
A1/6
A1/2
X1/3
C1/5
B1/7
D1/2
E1/2
Sample type
End conditions
Sample made in two halves
Normal
8" high
4" high
8" high
4" high
Lubricated 1/0.009" thk.
type C
type A
type X
Non-lubricated direct contact
type B
type D
porous disk & ½" ball
type E
CYLINDRICAL TRIAXIAL COMPRESSION 1ST SERIES
COMPARISON OF STRESS STRAIN CURVES FOR TYPICAL TESTS
Mean initial porosity, n_i = 38.6%
Ham River Sand.
Batch #1.
FIG. 8.4

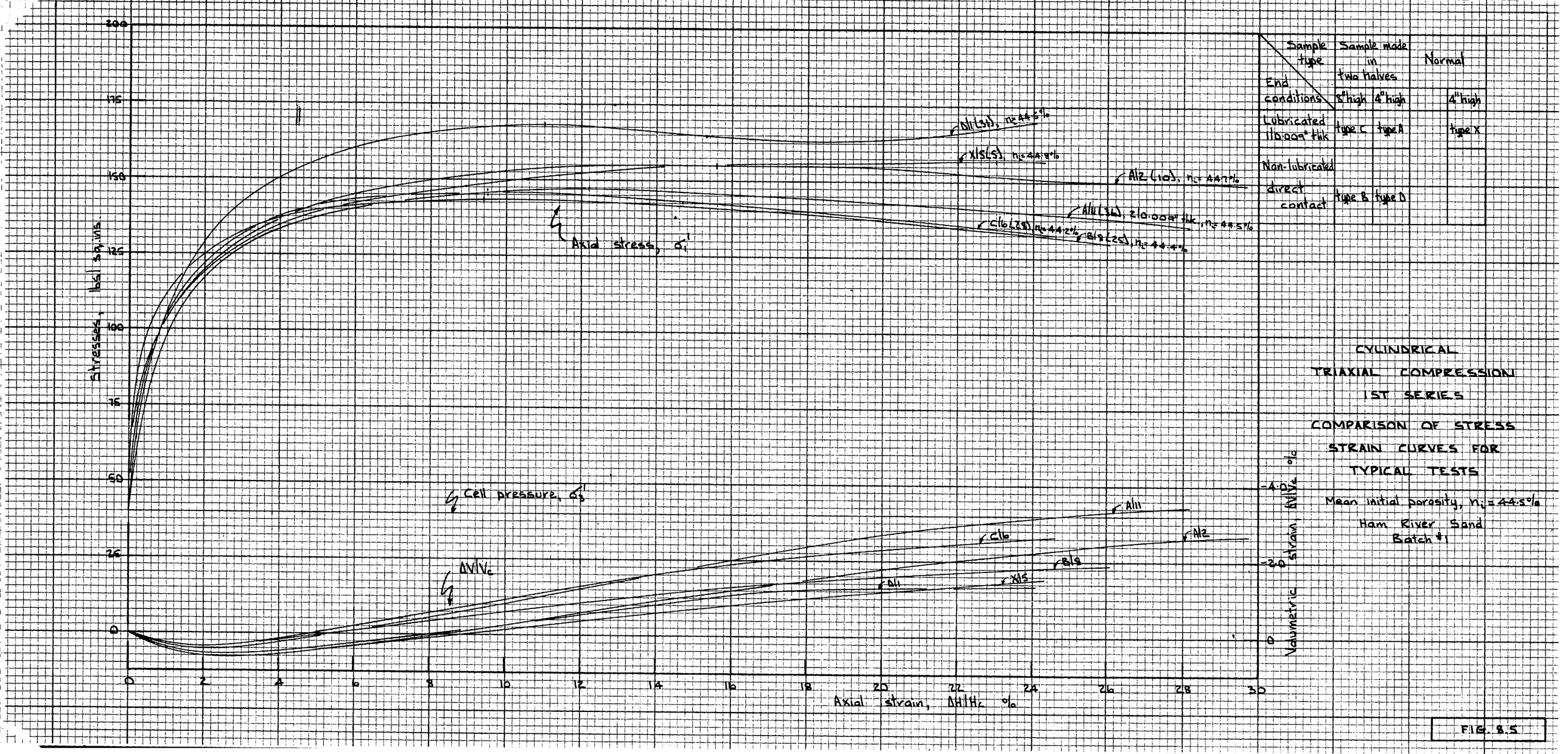

Sample type
Sample made in two halves
Normal
End conditions
8" high
4" high
4" high
Lubricated (10.009" thk
type C
type A
type X
Non-lubricated direct contact
type B
type D
CYLINDRICAL TRIAXIAL COMPRESSION 1ST SERIES
COMPARISON OF STRESS STRAIN CURVES FOR TYPICAL TESTS
Mean initial porosity, n_i = 44.5%
Ham River Sand
Batch #1
A11 (3H), n_i=44.5%
X15 (5), n_i=44.8%
A12 (10), n_i=44.7%
A14 (3H), 10.009" thk, n_i=44.5%
C16 (28), n_i=44.2%
B19 (25), n_i=44.4%
Axial stress, σ_1'
Cell pressure, σ_3'
$\Delta V/V_c$
A111
C16
A12
B19
A11
X15
Stresses, lbs/sq.ins.
Volumetric strain, $\Delta V/V_c$ %
Axial strain, $\Delta H/H_c$ %
0
25
50
75
100
125
150
175
200
-4.0
-2.0
0
2
4
6
8
10
12
14
16
18
20
22
24
26
28
30

FIG. 8.5

Sample type / End conditions	Sample made in two halves		Normal	
	8" high	4" high	2" high	4" high
Lubricated 1 to 0.09" thk.	type SB	type SD	type SE	type SF
2 to 0.09" thk.		type SDI		
Non-lubricated direct contact	type SA	type SC		

CYLINDRICAL TRIAXIAL COMPRESSION 2ND SERIES

COMPARISON OF STRESS STRAIN CURVES FOR TYPICAL TESTS

Mean initial porosity, n_i = 41.5%

Ham River Sand
Batch #2, Bag #3

Stresses, lbs/sq. ins.

Axial stress, σ_1'

Cell pressure, σ_3'

SE1 (5), n_i = 41.6%

SC1/2 (11), n_i = 41.6%

SF1/2 (17), n_i = 41.4%

SD1/2 (10), n_i = 41.6%

SD1/2 (12), n_i = 41.4%

SA1 (4), n_i = 41.6%

SB1 (12), n_i = 41.4%

SE1

SD1 & SF1/2

SD1/2

SC1

SB1

SC1/2

$\Delta V/V_c$

Volumetric strain, $\Delta V/V_c$ %

Axial strain, $\Delta H/H_c$ %

FIG. 8.6

uniform lateral expansion. The sample in Test X/3 was made in a normal manner.

The three 8 ins high samples, Tests B/7, C/5 & E/2, give similar peak strengths lower than any of the above-mentioned 4 ins high samples. The major difference between these three test results is in the shape of the stress-strain curve beyond peak deviator stress. Test E/2, the conventional type of triaxial compression test in which porous discs and a spherical seating are used, shows a sharp drop from peak to residual, associated with tilting of the top platten (ultimately by 5°) and formation of a predominant slip zone, see Fig A 8.53. With the sample in direct contact with a non-tilting top loading platten, Test B/7, the rate of reduction of the deviator stress beyond peak was much lower. The stress-strain curve was very erratic beyond about +12% axial strain due to irregular movement on differing slip zones. In contrast Test C/5, in which 1/0.009 ins thick lubricated rubber membrane was used on each platten, shows a much smoother transition from the peak to the residual state. Clearly the shape of the stress-strain curve beyond peak is very strongly dependent on stiffness of the loading system and on the sample end conditions. It is possible that the latter portions of the stress-strain curves for undisturbed London clay shown by Bishop et al (1965), Figs 3 & 4, are similarly dependent on the exact test conditions. The low stress level results show a very rapid reduction beyond peak which may be due to the strain energy stored in the testing machine and to tilting of the top loading platten.

The differences in the present test results are also reflected in the shape of the volume change curves, the curve for Test E/2 flattening off very sharply at +8% axial strain. The slope of the other two curves is not reduced so rapidly. The curve for Test C/5 lies above that for Test B/7, as one would expect.

By using a sandwich of 2/0.009 ins thick lubricated rubber membranes the strength of the 4 ins high samples was reduced to that of the 8 ins high samples, Test A/12. However increasing the number of membranes had little or no effect on the volume change, c.f. Tests A/12 & A/6.

Fig 8.5 shows a similar series of results for initially loose samples taken from the 1st Series. Here the differences in behaviour are much less marked. The 4 ins high sample in direct contact with the loading platten gives the highest strength. The two 4 ins high samples with

1/0.009 ins thick lubricated membrane at each end give similar stress-strain curves, Test A/2 (made in two halves) giving a slightly lower peak and residual deviator stress than Test X/5 (made in a normal manner). The stress-strain curves for Tests C/6 and B/8, an 8 ins high sample with 1/0.009 ins thick lubricated membrane and an 8 ins high sample in direct contact respectively, are almost indistinguishable right up to +25% axial strain. The volume changes are slightly larger for the sample with lubricated ends, as one might expect. The addition of a second membrane at each platten for the 4 ins high sample, Test A/11, lowers the stress-strain curve towards the lower bound set by the two 8 ins high samples. However the volume change is increased and differs significantly from that of the 8 ins high samples.

As with the dense samples, the strains at which peak strength is reached are much larger for the short samples than for the conventional size samples.

Fig 8.6 shows a series of results from the 2nd Series of tests on initially medium dense samples, which may be expected to lie somewhere between the previous two sets of data. Reference to Figs 8.4 & 8.5 shows that this is in fact so. An additional test type, 2 ins high with 1/0.009 ins thick lubricated membrane at each end, Test SE/1, is also shown. The stress-strain curve fails to reach a peak value, which is not at all surprising. That it lies well below the peak strength obtained in Test SC/2, 4 ins high sample in direct contact, clearly indicates the marked effect of the lubricated rubber membrane at each end. No tests were carried out on 2 ins high samples in direct contact with the loading platten; had they been done it is reasonable to expect very high strengths due to a predominant boundary restraint effect. It is noticeable that Test SE/1 exhibited a greater volume change than all other test types in this series.

The stress-strain and volume change curves for similar tests on Mersey River sand given by Rowe & Barden (1964) are not at first sight consistent with the present series of tests. The apparent strength of their short lubricated samples, H/D = 1, is lower than that of the long unlubricated samples, H/D = 2, by about 2° in the value of ϕ' at the peak stress. As the axial load was measured outside the cell and included piston friction (a rotating bush was not used), which is likely to be less when lubrication of the platten minimises lateral forces, their results are subject to some uncertainty. A more limited series of tests on another sand in the same

apparatus described by Freedman (1959) showed no significant difference between the two types of test.

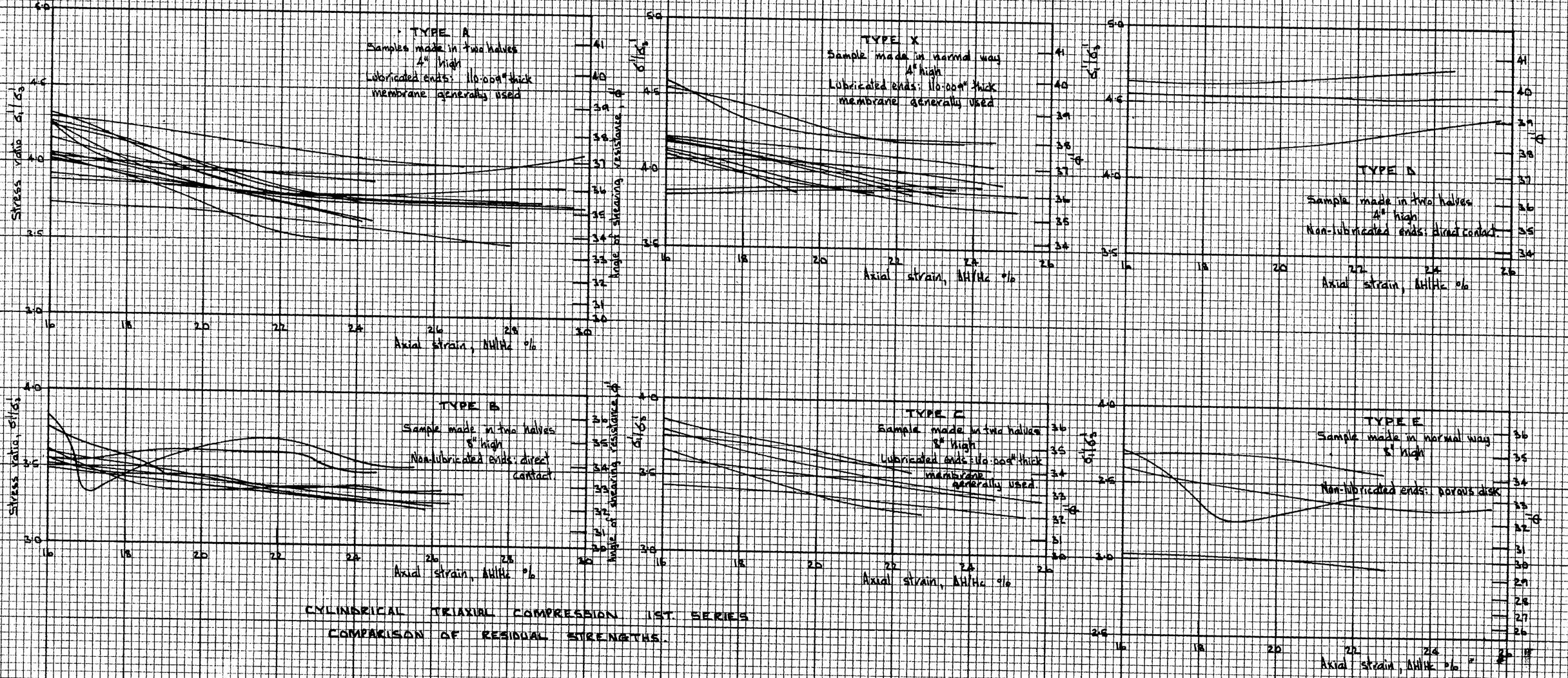
8.5 Comparison of residual strengths

The axial strains required to reach the residual (ultimate) strength were so large that interpretation of the results is very difficult . The area correction may be calculated according to various assumptions; Roscoe et al (1959), Webb (1966), Petley (1966), all of which are open to serious question. Moreover it does not appear possible at present to prove their validity experimentally. The curves shown in Fig 8.7 were obtained using the conventional right circular cylinder assumption, Bishop & Henkel (1957), Due to the further difficulty in defining the axial strain at which the residual strength was reached, the stress-strain curves beyond +16% axial strain are superimposed to define a range of possible residual strengths.

The observed residual strengths are independent of the initial porosities of the samples, but are dependent on the sample size and end conditions. Data for 4 ins high samples are shown in the upper portion of the figure and that for the 8 ins high samples in the lower portion. The 4 ins high samples in direct contact with the loading plattens, Type D, give an apparent residual ϕ' of from 38 - 40°; high values due to platten friction. The 4 ins high samples with 1/0.009 ins thick lubricated membrane at each end, built in a normal manner, Type X, give apparent residual strengths of from 35 - 38°. By forming the samples in two halves the residual strengths were lowered to 34 - 37°, Type A.

There is no significant difference between the observed residual strengths for the 8 ins high samples with and without lubricated ends, Type C & B respectively; from 32-34°. The stress-strain curves are much smoother for the Type C tests than for the Type B tests, suggesting more uniform deformation within the samples. Lubricating the ends of an 8 ins high sample appears to reduce the tendency for predominant slip zones to be formed within the sample.

The more conventional 8 ins high samples Type E built in a normal manner with a porous disc at each end show a relatively large scatter in residual strength of from 30-35° (there are admittedly only four test results of this type). The lowest stress-strain curve, Test E/2, is for an initially dense sample which failed catastrophically along a single slip



CYLINDRICAL TRIAXIAL COMPRESSION 1ST. SERIES
COMPARISON OF RESIDUAL STRENGTHS.

FIG. 8.1

zone beyond peak deviator stress, see Fig A 8.53.

Comparison of the Type A with the Type B & C tests indicates that the latter gives a lower apparent residual strength, 32-34°, compared with 34 - 37°. Clearly the short samples will not give as conservative a measure of the residual strength as the conventional samples, on a normal area correction basis.

The measurement of residual strength in the triaxial test is so open to question that the above comments must be treated with caution. It will be of interest to compare the present data with data on the same Ham River sand tested in the new ring shear apparatus which should give a much more reliable measure of the residual strength.

8.6 Comparison of Failure Characteristics - 1st Series of Tests

For each test type the failure characteristics are plotted against the initial porosity, Fig 8.8 to 8.13. The correlation between the tests at different porosities, for a particular test type, is clearly seen to be good considering only Tests X/1(1) to C/7(29). There was good reason to believe that between Tests C/7(29) and A/7(30) the calibration of the pressure gauge changed by $\frac{1}{2}$ - 1 psi which would give an error in the value of ϕ' of 0.2° to 0.4°. Although not noticed at the time this was deduced from subsequent recalibrations of the pressure gauge (see Appendix A3) and due allowance was made in Tests A/7(30) to E/4(56). The mean lines drawn through the experimental points are based on the initial 29 tests. The volumetric strain rate curves for each test type are drawn parallel to one another, c.f. Bishop & Green (1965) where a single line was drawn through all the test results.

The observed strengths of the latter half of the Type X tests, Fig 8.8 all lie about 1° below their expected values. These tests also show a tendency to fail at a slightly smaller axial strain than expected. The greatest disparity appears in the volumetric strains, whereas the volumetric strain rates hardly deviate from their expected values, based on Tests X/1(1) to X/7(7).

The observed strengths of the 4 ins high samples made in two halves with lubricated ends, Type A, are all consistent if we exclude, for the moment, those tests in which two or more lubricated membranes were used at each end of the sample, Fig 8.9. The points for the latter tests all lie

Maximum angle of shearing resistance, ϕ'

Volumetric strain at failure, $\Delta V/V_c$ %

Axial strain at failure, $\Delta H/H_c$ %

$\frac{d(\Delta V/V_c)}{d(\Delta H/H_c)}$

Volumetric strain rate at failure, $\frac{d(\Delta V/V_c)}{d(\Delta H/H_c)}$

Initial porosity, n_i

ϕ'

$\Delta H/H_c$

$\Delta V/V_c$

$\frac{d(\Delta V/V_c)}{d(\Delta H/H_c)}$

Sample made in normal way.
4" high
Lubricated ends : 10·000" thick membrane used
Ham River Sand, Batch #1.

CYLINDRICAL TRIAXIAL COMPRESSION.
1ST. SERIES, TYPE X.

A16 (4)
A12 (37) 2lo·009"
A15 (15)
A1 (9)
A13 (11)
A18 (8)
A115 (48)
A116 (49)
A14 (40) 2lo·009"
A19 (33) 3lo·024"
A110 (35) 5lo·024"
A14 (12)
A113 (38)
A17 (30)
A12 (10)
A110
A12
A111 (36) 2lo·009"
A16
A110
A16
A110
A16

ϕ'

$\Delta H/H_c$

$\Delta V/V_c$

$\frac{d(\Delta V/V_c)}{d(\Delta H/H_c)}$

Maximum angle of shearing resistance, ϕ' °

Volumetric strain at failure, $\Delta V/V_c$ %

Axial strain at failure, $\Delta H/H_c$ %

$\frac{d(\Delta V/V_c)}{d(\Delta H/H_c)}$ at failure

Initial porosity, n_i %

Sample made in two halves
4" high
Lubricated ends : 110·009" thick membrane generally used
Ham River Sand, Batch #1.

CYLINDRICAL TRIAXIAL COMPRESSION.
1ST. SERIES, TYPE A.

FIG 8.9

B16 (23)
B17 (24)
B12 (18)
B10 (17)
B15 (22)
B13 (20)
B14 (21)
B9 (25)
B11 (15)
$\Delta H/H_c$
$\Delta V/V_c$
$\frac{d(\Delta V/V_c)}{d(\Delta H/H_c)}$
ϕ'
Maximum angle of shearing resistance, ϕ'
Volumetric strain at failure, $\Delta V/V_c$ %
Axial strain at failure, $\Delta H/H_c$ %
Rate of failure, $\frac{d(\Delta V/V_c)}{d(\Delta H/H_c)}$
Initial porosity, n_i %
Sample made in two halves.
8" high.
Non-lubricated ends: direct contact
Ham River Sand, Batch #1

CYLINDRICAL TRIAXIAL COMPRESSION.
1ST SERIES, TYPE B.

FIG. 8.10

C15(27)

C12(11)

C17(29)

ϕ'

C13(19)
2 @ 0.009"

C14(26)
3 @ 0.024"

C16(28)

C11(16)

$\Delta H/H_c$

$\Delta V/V_c$

$\frac{d(\Delta V/V_c)}{d(\Delta H/H_c)}$

Maximum angle of shearing resistance, ϕ'

Volumetric strain at failure, $\Delta V/V_c$ %

Axial strain at failure, $\Delta H/H_c$ %

Volumetric strain rate at failure, $\frac{d(\Delta V/V_c)}{d(\Delta H/H_c)}$

Initial porosity, n_i %

Sample made in two halves.
8" high.
Lubricated ends: 1 @ 0.009" thick membrane generally used.
Ham River Sand, Batch #1.

CYLINDRICAL TRIAXIAL COMPRESSION.
1ST. SERIES, TYPE C.

FIG. 8.11

D12 (32)

D13 (34)

D11 (31)

ϕ'

$\Delta H/H_c$

$\Delta V/V_c$

$\frac{d(\Delta V/V_c)}{d(\Delta H/H_c)}$

Sample made in two halves.
4" high.
Non-lubricated ends: direct contact.
Ham River Sand, Batch #1.

Maximum angle of shearing resistance, ϕ' — 46, 45, 44, 43, 42, 41, 40

Volumetric strain at failure, $\Delta V/V_c$ °/o — 39, 38, -0.5, +0, -1.0, -1.5, -2.0, -2.5

Axial strain at failure, $\Delta H/H_c$ °/o — +12, +10, +8, +6, +4, +2, 0, -0.2, -0.3, -0.4, -0.5, -0.6, -0.7

Volumetric strain rate at failure, $\frac{d(\Delta V/V_c)}{d(\Delta H/H_c)}$

38.0 39.0 40.0 41.0 42.0 43.0 44.0 45.0

Initial porosity, n_i °/o

CYLINDRICAL TRIAXIAL COMPRESSION.
1ST SERIES, TYPE D.

FIG. 8.12.

E12 (54)

E14 (56)

φ'

Fresh samples

B12 (44)

B11 (43)

B14 (46)
Reused twice

B13 (45)
Reused once

E11 (53)

ΔH/H_c

E13 (55)

Type B1, Sample made in two halves.
8" high.
Non-lubricated ends: direct contact.
Ham River Sand, Batch #2, Bag #5.

Type E, Sample made in normal way.
8" high
Non-lubricated ends:
1-3 porous disk & ½ ball.
4 porous disk
Ham River Sand, Batch #1, reused

ΔV/V_c

d(ΔV/V_c) / d(ΔH/H_c)

Maximum angle of shearing resistance, φ'

Angle of shearing resistance at failure, φ'

Volumetric strain at failure, ΔV/V_c %

Axial strain at failure, ΔH/H_c %

Volumetric strain rate at failure, d(ΔV/V_c) / d(ΔH/H_c)

Initial porosity, n_i %

CYLINDRICAL TRIAXIAL COMPRESSION.
1ST. SERIES, TYPES B1, E.

FIG. 8.13

about 1° below the mean line for the tests in which 1/0.009 ins thick lubricated membrane was used at each end of the sample. The correlations of axial strain and volumetric strain rate at failure are not greatly affected by increasing the number and/or thickness of the lubricated membrane.

All the experimental points for the 8 ins high samples with non-lubricated ends, Type B, lie close to the mean lines with the possible exception of Test B/9(42) which gave a strength about $\frac{1}{2}^{\circ}$ lower than average, Fig 8.10. This test was the only Type B test from the latter half of the 1st Series and was, as is discussed later, suspect.

The data for the 8 ins high samples with 1/0.009 ins thick lubricated membrane at each end, Type C gave exceptionally good correlations for each of the 4 porosities plotted, Fig 8.11. This may of course be fortuitous, but on the other hand it may reasonably be expected since these samples should be freer of any boundary restraint than any of the other types tested. It should be noted that the number and thickness of lubricated membranes used was increased in Test C/3(19) to 2/0.009 ins and in Test C/4(26) to 3/0.024 ins, but that this had no appreciable effect on the measured failure characteristics.

The results of 3 tests on short samples with non-lubricated ends, Type D, are shown in Fig 8.12. These correlations are reasonable but must be treated with some caution on account of the paucity of data.

The results of Type E and Type B1 tests are shown together on Fig 8.13 for brevity. Tests E/1-3 were on 8 ins high samples with a porous disc at each end together with a spherical seating between the top loading platten and the proving ring anvil, the mean line being drawn through these 3 tests. In Test E/4 the spherical seating was omitted - the normal case in the tests reported in this thesis - and the failure characteristics for this test differed slightly from the other three. In particular the ϕ' value was about 1° lower for Test E/4.

The group of four Type B1 tests were included to study the effect of retesting the same sand a number of times and to give a link with subsequent tests on the second batch of Han River sand. These results are discussed in subsequent sections.

It appears that the peak ϕ' is the most sensitive indicator of a test results deviation from its expected value. The volumetric strain rate does not appear to be as markedly affected by slight test variations as is sometimes thought.

8.6.1 Comparison of Peak Strengths

The peak strengths of all the tests in the 1st Series are compared in Fig 8.14. For clarity only the sequence number with respect to time is indicated for each test since only this is essential to the discussion.

There is no apparent difference between the strength - porosity relationships for samples 8 ins high with or without lubricated ends, Types C or B respectively. As the degree of end restraint was potentially decreased by using 2/0.009 ins thick or even 3/0.024 ins thick lubricated membranes no difference in the strength - porosity relationship is apparent, Tests C/3(19) and C/4(26). There is a significant increase of from 1° for dense specimens to 2° for loose specimens in the strength of the 4 ins high samples with 1/0.009 ins thick lubricated membrane at each end, Type A, as compared with the 8 ins high samples. These remarks apply only to samples made in two halves. The strength - porosity relationship for 4 ins high specimens with 1/0.009 ins thick lubricated membrane for samples built in the normal way, Type X, is very slightly higher than that for samples built in two halves, Type A.

From the preliminary tests discussed in Chapter 3 together with the porosity measurement reported in Appendix A2 it might appear that the mode of deformation of a sample should be dependent on any initial porosity variations within it. In order to achieve initial porosities below about 39% it was necessary to vibrate the samples whereas samples above 39% initial porosity were achieved with various degrees of tamping. One might expect a discontinuity in the strength - porosity relation at about 39% initial porosity. This is clearly not the case and suggests that initial porosity variations within the cylindrical triaxial compression samples are eliminated before peak ϕ' is reached.

As the test programme continued beyond Test C/7(29) the new experimental points apparently lay below their expected values. These test results were corrected for a subsequently deduced change in the pressure gauge calibration. Tests A/7(30) and A/13(38) lie sufficiently close to their expected values, based on the first 29 tests, to infer that the results of intermediate tests D/1(31) to A/12(37) are significant. Tests D/1(31), D/2(32), D/3(34) are on 4 ins high samples in direct contact with the loading plattens and, as might be expected, give markedly higher ϕ' values due to the effect of end restraint on the short samples.

Sample type / End conditions	Sample made in two halves		Normal	
	8" high	4" high	8" high	4" high
Lubricated 110:000" thk.	⊙ type C	⊡ type A		⊡ type X
Non-lubricated direct contact	● type B	■ type D		
	◆ type B1			
porous disk & ½ ball			◆ E11-3	
porous disk			◆ E14	

Ham River Sand
Batch #1 generally used.
Type B1, Batch #2, Bag #5.

Maximum angle of shearing resistance, ϕ_{max}

Initial porosity, n_i %

CYLINDRICAL TRIAXIAL COMPRESSION.

COMPARISON OF PEAK STRENGTHS, 1ST. SERIES.

FIG. 8.14

Tests A/9(33), A/10(35), A/11(36) and A/12(37) were on 4 ins high samples made in two halves with two or more membranes at either end. Tests A/11(36) and A/12(37) with 2/0.009 ins thick lubricated membranes at each end, at opposite ends of the porosity scale, gave strengths close to those of the 8 ins high lubricated or non-lubricated samples. Tests A/9(33) and A/10(35) with 3/0.024 ins and 5/0.024 ins thick lubricated membranes respectively, also gave strengths identical to the 8 ins high samples.

By increasing the number and/or thickness of lubricated membranes one may apparently approach a lower limit strength - porosity relationship but beyond a certain point, in this case 2/0.009 ins thick membranes, the increase in the number or thickness of membranes has no significant effect on strength. As noted in Appendix A1, if the membrane thickness is small compared with the particle size the sand grains will squeeze the grease and a portion of the membrane into the pore-space between them and the effective coefficient of friction of the lubricated platten will be markedly reduced. It appears that lubricated and non-lubricated samples having a H/D ratio of 2 gave identical strengths and that below 2 the influence of end restraint becomes increasingly important.

The samples used in Tests X/8(39) and A/14(40) were taken from the remaining portion of the first batch of sand, after which it was necessary to re-use the material. Relative to the other tests in this series, Test X/8(39) gives a significantly low ϕ' value. Test A/14(40), in which 2/0.009 ins thick lubricated membranes were used shows rather less deviation from the value anticipated from the earlier tests. As the sand for these two tests had been taken from the bottom of the bin the possibility of segregation cannot be excluded.

Tests X/9(41) and B/9(42) are on samples of re-used material taken after remixing the whole of the first batch of sand. They both give values about 1° lower than would be expected.

Tests B1/1(43) to B1/4(46) were on samples taken from the second batch of unused sand. Tests B1/(43) and B1/2(44) were on fresh samples of the second batch and show good agreement with each other. Test B1/3(45) was on material from Test B1/2(44) re-used and shows no significant change in the strength-porosity relationship. When, in Test B1/4(46), the same material was tested a third time a very small reduction in ϕ' was observed. Whether this reduction in ϕ' is significant or not is debatable. At the

time the 1st and 2nd Series of tests were being analysed for publication, Bishop & Green (1965), it was felt that re-used material gave a slightly lower ϕ'. This hypothesis helped to explain the observed discrepancies in the data. However subsequent tests suggest that the Ham River sand could be re-used at least once without the breakdown of the particles having a significant effect on the observed test data. Since the grading of the second batch of Ham River sand was slightly different from that of the first batch there is no a priori reason to presume that they should exhibit exactly the same strengths. These 4 tests serve as a link with the subsequent test programme reported in Chapters 9,10 & 11.

Further tests were carried out on re-used material from the first batch of sand maintaining, as closely as possible, a constant initial placement density, Tests X/10(47) to X/13(52). With the exception of Test A/16(49) they all show a variation from the initial 29 tests.

The results of the tests on more conventional type samples, Tests E/1 (55) to E/4(56), give slightly higher ϕ' values than the established lower limit if the top platten is allowed to tilt (3 tests). When the top platten was prevented from tilting, the norm in all the tests reported in this thesis, the strength lay below the line for the Types B & C, 8 ins high samples.

A review of all of the results at this stage suggested one or more of a number of possibilities, (i) that the calibrations of the pressure gauge and proving ring might have changed during the tests, (ii) that the operator's technique of sample manufacture might have changed, or (iii) that the surface properties of the sand might have altered during the 11-month period after elutriation. To clarify the position a second batch of similar Ham River sand was obtained and the 2nd Series of 19 tests carried out on fresh unwashed samples over a $3\frac{1}{2}$-week period.

8.6.2 Comparison of Axial Strains at Failure

The axial strain at failure varied considerably with the sample height and degree of end restraint. The results of all the tests in the 1st Series are shown in Fig 8.15, again only the sequence number with respect to time is given by each point.

The failure strain for 8 ins high non-lubricated samples, Type B, varied from +5% for initially dense samples up to +12% for initially loose samples.

Sample type / End conditions	Sample made in two halves		Normal	
	8" high	4" high	8" high	4" high
Lubricated 10.009" thk.	⊙ type C	⊡ type A		⊡ type X
Non-lubricated direct contact	● type B	■ type D		
	● type B1			
porous disk & ½ ball			● E11-3	
porous disk			✱ E14	

Ham River Sand
Batch #1 generally used.
Type B1, Batch #2, Bag #5

Axial strain at failure, $\Delta H/H_c$ %

Initial porosity, n_i %

CYLINDRICAL TRIAXIAL COMPRESSION.

COMPARISON OF AXIAL STRAINS AT MAXIMUM ϕ', 1ST. SERIES.

FIG. 8.15

Reduction in end restraint by using 1/0.009 ins thick lubricated membrane at each end, Type C, increased the axial strain to failure to +6% for dense samples but had little or no effect on the loose samples. Additional lubricated membranes, up to 3/0.024 ins thick, appear to have no significant effect.

The tests on 4 ins high lubricated samples with a single membrane gave higher strains to failure. Samples made in two halves, Type A, varied from +7% at the dense end to about 16% at the loose end of the porosity range. Tests on 4 ins high lubricated samples made in a normal way, Type X, exhibited even higher strains to failure, +7½% and +22% at the dense and loose ends of the porosity range respectively (these were not distinguished between by Bishop & Green (1965).

Many of the tests in the latter half of the 1st Series deviate from their expected values in a similar manner to the peak strengths, but these are not discussed in detail.

The three tests, E/1(53), E/1(54) & E/1(55), in which normal 4 ins diameter vitrified bauxilite discs were used at each end of the specimen together with a spherical seating, gave significantly lower failure strains than the Type B or C tests. In contrast, Test E/4(56) in which a spherical seating was not used, agrees more closely with the Type C tests. Thus it appears that in the more conventional test the sample fails prematurely due to the formation of a single predominant slip zone, strongly associated with tilting of the top loading platten.

8.6.3 Comparison of Volumetric Strains at Failure

The volumetric strains at failure are shown in Fig 8.16 and are complementary to the axial strains at failure. The 4 ins high samples with lubricated ends show the greatest volumetric strains at failure, there being a 1% difference over the mid-section of the porosity range between samples made in a normal manner, Type X, and those made in two halves, Type A. The reason for this mid-porosity range difference is not apparent. One might expect any differences in behaviour between the sample types to vary monotonically with porosity.

The 8 ins high non-lubricated samples, Type B, give the lowest volumetric strains at failure of the main group of tests, as might be expected. The 4 Type E samples gave slightly lower values, consistent with the minimum

Sample type / End conditions	Sample made in two halves		Normal	
	8" high	4" high	8" high	4" high
Lubricated ll0·000" thk.	⊙ type C	⊡ type A		⊡ type X
Non-lubricated direct contact	● type B	■ type D		
	♦ type B1			
porous disk & ½ ball			E11-3	
porous disk			E14	

Volumetric strain at failure, $\Delta V/V_c$ %

+0·5, 0, -0·5, -1·0, -1·5, -2·0, -2·5, -3·0, -3·5, -4·0, -4·5

38·0, 39·0, 40·0, 41·0, 42·0, 43·0, 44·0, 45·0

Initial porosity, n_i %

Ham River Sand
Batch #1 generally used
Type B1, Batch #2, Bag #5

CYLINDRICAL TRIAXIAL COMPRESSION.

COMPARISON OF VOLUMETRIC STRAINS AT MAXIMUM ϕ'; 1ST. SERIES.

FIG. 9.16

axial strains to failure noted in the preceding section.

The 8 ins high samples with lubricated ends, Type C, give volumetric strains at failure similar to the Type B tests at the loose end of the porosity range. However the dense samples exhibited a higher value by approximately -0.7%. Thus although the addition of lubricated membranes to an 8 ins high sample does not affect the ϕ' value measured it does have a small but significant effect on the failure strains, both linear and volumetric, of the denser samples.

The volumetric strains at failure of many of the latter tests in the 1st Series vary markedly from their expected values, the Type X tests in particular.

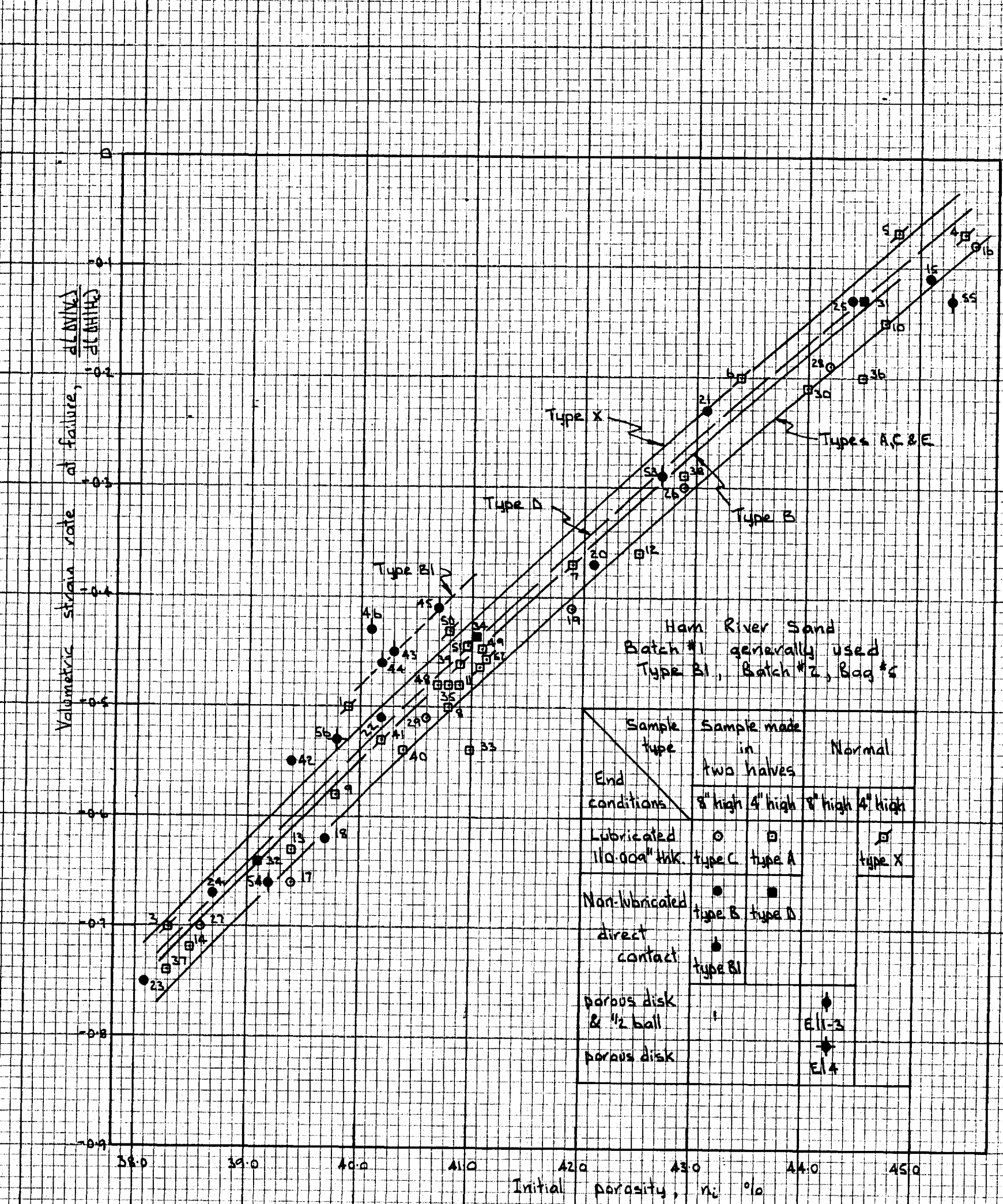
8.6.4 Comparison of Volumetric Strain Rates at Failure

The rate of dilatation at failure is defined here as the slope of the plot of volumetric strain against axial strain at the maximum stress difference. In the case of initially dense and medium dense samples this coincides with the maximum rate of dilatation whereas for loose samples the maximum rate of dilatation occurs before failure. The failure strain of a loose sample is more difficult to define as the peak is very flat and the interpretation of the results is less definite.

The variation of the rate of dilatation with porosity for all the tests in the 1st Series is shown in Fig 8.17. Excluding the Type B1 tests on the second batch of sand, the experimental points lie close to an almost unique line so that the relationship is apparently independent of the height to diameter ratio of the sample or of the degree of end restraint. This agreement seems remarkable in view of the wide variation in test conditions and suggests that either the rate of dilatation is very insensitive or it is a fundamental measure of the behaviour of the sand.

8.7 Comparison of Failure Characteristics - 2nd Series of Tests

On account of the variation of some of the later test results from their expected values in the 1st Series of tests a second group of tests were considered advisable. A second batch of similar Ham River sand was obtained and a 2nd Series of 19 tests carried out on fresh unwashed samples over a 3½ week period. Calibrations of the axial proving ring and pressure gauge were carried out before and after this series and these calibrations showed



CYLINDRICAL TRIAXIAL COMPRESSION.

COMPARISON OF VOLUMETRIC STRAIN RATES AT MAXIMUM ϕ', 1ST. SERIES.

FIG. 8.17

no change. The results of these tests are shown in Fig 8.18.

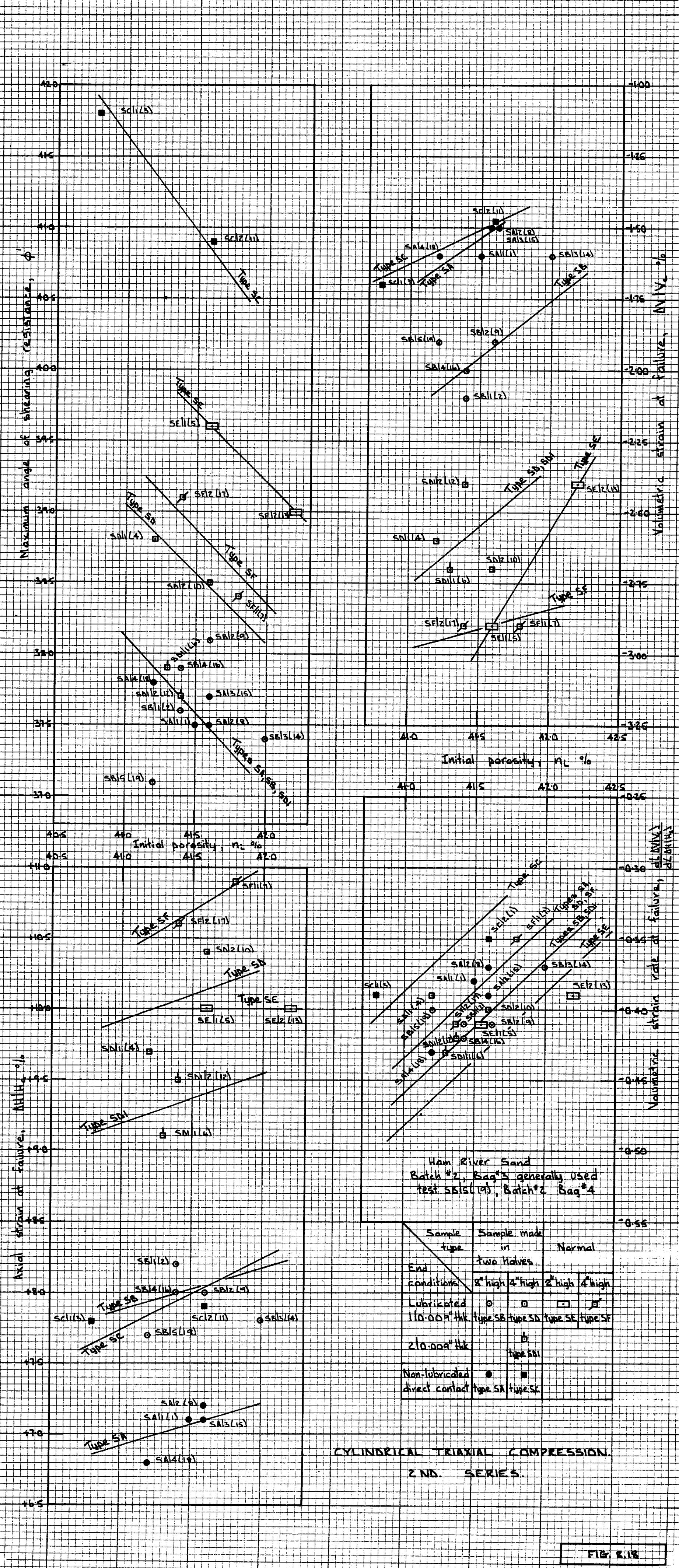
The initial porosity was maintained as close as possible to 41.5%, i.e. medium dense, and as some variation was inevitable the relevant slopes of the strength - porosity and strain - porosity relationships from the 1st Series were assumed to apply for purposes of comparison. Two consecutive sets of tests were completed on each type of sample and also on 2 ins high samples built in the normal way with 1/0.009 ins thick lubricated membrane at each end. Additional tests were carried out on the 8 ins high samples.

The 4 tests on the 8 ins high non-lubricated samples, Type SA, were very self-consistent. Of the 5 tests on 8 ins high lubricated samples, Tests SB/1(2) and SB/4(16) were consistent with the non-lubricated samples, as in the previous series, whereas Tests SB/2(9) and SB/3(14) gave values of 0.4° higher. In the 1st Series of tests and in Tests SB/1(2) and SB/4(16) the thin rubber discs were always washed in detergent after each test, dried and powdered with French chalk to prevent sticking. In Tests SB/2(9) and SB/3(14) the rubber discs were not powdered and these results show slightly higher strengths.

The first 18 tests of the 2nd Series were all on material from Bag No 3 whereas in Test SB/5(19) sand from Bag No 4 was used. There is clearly a small but significant difference between the two bags of supposedly similar Batch No 2 Ham River sand. This emphasises the caution needed in the present type of test programme.

Tests on 4 ins high lubricated samples made in two halves, Type SD, show a higher ϕ' when 1/0.009 ins thick lubricated membrane is used. When 2/0.009 ins thick lubricated membranes are used, Type SD1, the ϕ' values coincide with three of the 8 ins high samples. Increasing the number of membranes from 1 to 2 also affects the axial strain but not the volumetric strain at failure and also has a very marginal effect on the volumetric strain rate. Again tests on 4 ins high non-lubricated samples made in two halves, Type SC, give a markedly higher strength - porosity relationship. Also 4 ins high lubricated samples made in a normal manner Type SF, show a slightly higher ϕ' than those made in two halves, Type SD.

The tests on the lubricated 2 ins high samples, Type SE, were difficult to interpret since their stress-strain curves had no definite peak. The points shown correspond to an axial strain of +10%, being just beyond the



Ham River Sand
Batch #2, Bag #3 generally used
test SB1(19), Batch #2 Bag #4

Sample type / End conditions	Sample made in two halves		Normal	
	8" high	4" high	2" high	4" high
Lubricated 1/0.009" thk.	○ type SB	▭ type SD	▭ type SE	▭ type SF
2/0.009" thk		▭ type SD1		
Non-lubricated direct contact	● type SA	■ type SC		

CYLINDRICAL TRIAXIAL COMPRESSION.
2ND. SERIES.

FIG. 8.18

point at which the slope of the stress-strain curve began to flatten out rapidly, and probably represent a lower limit to possible values of ϕ' for these tests. The volumetric strain rates for the Type SE tests give remarkably good agreement with the other tests. The scales used in this particular plot are very open so that the range of values bounded by the Type SC and SE test is, in fact, very small indeed.

The differences in failure characteristics measured on the various types of sample in this series of 19 tests appear to confirm the general conclusions drawn from the 1st Series of tests. They also clearly indicate that it is possible, if appropriate precautions are taken, to achieve very repeatable test results which enable a precise discrimination between tests carried out under slightly differing conditions.

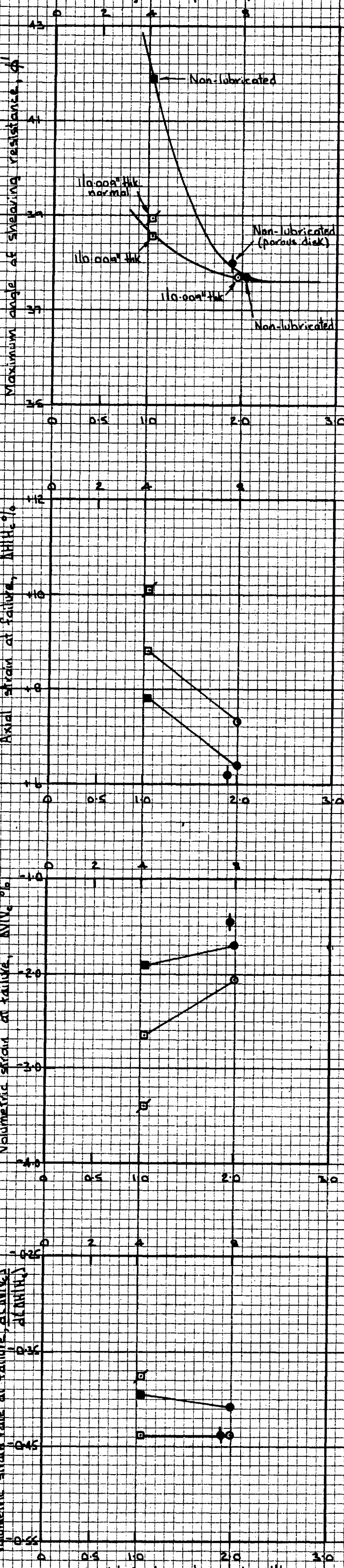
8.8 Influence of end restraint and H/D ratio

The results of the 1st and 2nd Series of tests are shown side by side in Fig 8.19. The points plotted are interpolated from the test data to correspond to an initial porosity of 41.5% in each case. There is very little difference between the two sets of results. Depending on the failure strain, the position of the points for the 2 ins high sample, Type SE, in the 2nd Series may vary. The points shown correspond to an axial strain at failure of +10% together with the possible limiting values of ϕ' and volumetric strain rate. Limiting values of axial strain and volumetric strain at failure cannot be defined.

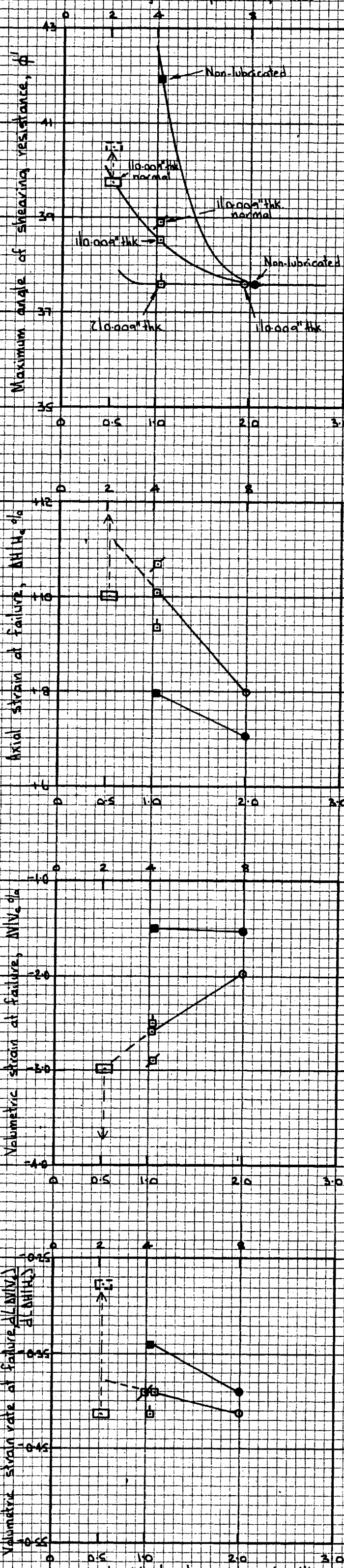
Corrections for the strength of the sample sheath have not been applied to any of the cylindrical triaxial compression test results. The correction is similar for all the tests and in any case, as is shown in Appendix A 6, is so small at the stress levels used as to be negligible.

For the type of sand and end plattens used, the reduction in end restraint by lubrication has no significant effect on the observed strength of samples having the usual H/D ratio of 2. For lower ratios the influence becomes increasingly important. For a H/D ratio of 1 very efficient lubrication, represented by a sandwich of 2/0.009 ins thick greased membranes is necessary to reduce the strength to that of the samples having a H/D ratio of 2. Additional membranes do not appear to reduce the strength below this value.

The accuracy with which this conclusion can be drawn depends on the



1ST SERIES.
n_i = 41·5 %



2ND. SERIES.
n_i = 41·5 %

CYLINDRICAL TRIAXIAL COMPRESSION.

INFLUENCE OF HEIGHT TO DIAMETER RATIO ON THE FAILURE CHARACTERISTICS OF SAMPLES HAVING VARIOUS DEGREES OF END RESTRAINT.

Plotted points are interpolated mean values.

FIG. 8.19

accuracy with which the stresses can be evaluated in samples which do not deform strictly as right circular cylinders. Samples with lubricated ends having a H/D ratio of 1 do not depart very far from a right circular cylindrical shape up to the strain corresponding to peak strength. The calculation of stress on the basis of the average cross-sectional area can therefore be considered to be subject to very little error.

If we assume that the short sample expands at the base only and that the σ_3' boundary is a parabola perpendicular to any base diameter, then an assessment of the error may be made. For a typical specimen, e.g. Test SD/1, the value of ϕ' may be evaluated in at least two ways, (i) on the basis of the average cross-sectional area, for which $\phi' = 38.8^\circ$, (ii) on the basis of the cross-sectional area at the base (the maximum area) of an equivalent sample of parabolic form, for which $\phi' = 37.8^\circ$. The second assumption gives an extreme lower limit to the possible value of the measured strength and is an unrealistic assumption. The first assumption is much more reasonable.

However, samples having a H/D ratio of 2 did not expand significantly at the ends whether lubricated or not. This is in contrast to the observation reported by Lee & Seed (1964) that samples of dense sand having a H/D ratio of 2.4 deformed approximately as right cylinders when lubricated ends were used. The explanation may lie in the fact that the samples used by Lee & Seed were only 1.4 ins in diameter, whereas the samples in the present series are 4.0 ins in initial diameter. The relative thickness of the rubber sample sheath may have an influence on the failure strain and on the deformed shape of the sample, although the reported results are difficult to reconcile, Waterways Experiment Station (1947), Chen (1948). In the present case the use of an average cross-sectional area in the stress calculation is more open to criticism, although it may be justified on the grounds that the slip zone which often forms after failure cuts the sample diagonally almost from corner to corner in elevation.

The probable range of uncertainty in the interpretation of tests on long samples can be estimated by assuming that the elevation of the sample is symmetrical about mid-height and parabolic in form. For a typical 8 ins high sample, e.g. Test SA/1, the value of ϕ' may be evaluated in three ways, (i) on the basis of the average cross-sectional area over the full height of the sample, for which $\phi' = 37.5^\circ$, (ii) on the basis of the aver-

age cross-sectional area of the middle half of the sample, for which the H/D ratio is 1 as in the short samples, this gives $\phi' = 37.0^{\circ}$, and (iii) on the basis of the cross-sectional area at mid-height, Roscoe et al (1959). The latter value is an extreme lower limit and gives $\phi' = 36.8^{\circ}$. The use of the second or third methods would suggest that even the most efficient lubrication did not quite reduce the strength of a 1 to 1 sample to that of a 2 to 1 sample, though the difference is only just significant. Whether this difference, if real, is due to the inhibition of zone failure by the rigid plattens in the short samples, or due to the departure of the actual stress conditions from those assumed in a barrelling sample, is a matter for speculation. The smallness of the difference is perhaps the most significant feature and comparing the results on a basis of the average cross-sectional area appears to give a consistent pattern. If the errors due to the type of area correction used are large then they appear to fortuitously cancel out which is most unlikely. It seems much more probable, and the above two examples, Tests SA/1 and SD/1, together with other tests analysed in a similar manner but not reported clearly support this, that the errors are very small and may be neglected.

The axial and volumetric strains to failure, which are complementary to one another, (i) increase as the end restraint is decreased, (ii) increase as the sample gets shorter, and (iii) increase if the 4 ins high sample is built in a normal way rather than in two halves.

The rate of change of volume at failure hardly varies for the different type of test; the scale in Fig 8.19 is very open. The data published by Rowe & Barden (1964) suggests that the rate of volume change at failure may be slightly less in a sample with lubricated ends, whereas that published by Lee and Seed (1964) for a long lubricated sample suggests that it may be greater. The differences are quoted for individual tests and are probably within the natural scatter of typical results. The tests by Taylor (1941) with reduced end restraint on a long sample similarly showed little difference.

CHAPTER 9

CYLINDRICAL TRIAXIAL COMPRESSION AND EXTENSION TEST RESULTS AND DISCUSSION

9.1 Introduction

In the first part of the research programme, reported in Chapter 8, it was established that a cylindrical triaxial compression sample of height to diameter ratio, H/D = 1, and with adequate lubrication of the ends, in this case 2/0.009 ins thick greased rubber membranes, gave the same strength as a conventional size sample, H/D = 2, tested in a triaxial compression. The second part of the work, described in this chapter, was aimed at determining whether a similarly shaped short sample would give a satisfactory measure of the strength in triaxial extension. At first sight it appears that a short sample having a H/D ratio of 1 should be more than adequate. The central portion of a cylindrical triaxial compression test sample in which failure principally occurs may be considered to be D.cot $(45^\circ - \phi'/2)$ in height, the angle $(45^\circ - \phi'/2)$ being measured from the vertical axis of the specimen. In the cylindrical triaxial extension test this height is reduced to D.cot $(45^\circ + \phi'/2)$, so that the portion of the sample required to be free from the possible influence of end restraint should be less.

As has been shown by Cornforth (1961), Sowa (1963) & Roscoe et al (1963a), the triaxial extension test is a more difficult test to perform and the results may be expected to show a greater scatter than corresponding triaxial compression tests. In addition the interpretation of the triaxial extension test data is subject to greater uncertainty due to necking of the sample causing the stresses and strains in the failing portion to be significantly different from those obtained assuming that the sample deforms as a right circular cylinder. Local instability or necking cannot occur in a compression test sample due to the nature of the stress system. In the initial analysis of the triaxial compression and extension test data no correction has been applied for the strength of the sample sheath and the sample has been assumed to deform as a right circular cylinder. The possible effect of these two factors is discussed in detail later.

The extension tests were generally stopped as close to failure as possible. By measuring the diameters of the sample at different positions

along its axis, after dismantling the triaxial cell, it was possible to assess the effect of necking on the measured strength. In retrospect, the tests should have been stopped closer to failure since the degree of necking has a greater effect on the measured ϕ' value than was realised at the time. Clearly as the difference between the failure strain and the strain at which the test was stopped increases, so does the degree of uncertainty in the interpretation of the results. One or two tests were continued beyond peak ϕ' to determine the subsequent mode of deformation. However the precise interpretation of the later portion of the stress-strain and volume change curves for these tests is very dubious. Consequently no attempt was made to obtain an ultimate or residual strength in triaxial extension.

Since a second batch of Ham River sand was used for the cylindrical triaxial extension tests a series of compression tests on 4 ins high samples with 2/0.010 ins thick lubricated membranes at each end, Type H, were performed concurrently as controls. Thus the triaxial compression and extension test series form a self-contained set. No apparent difficulties were encountered in obtaining repeatable results in this series of 32 tests due to a combination of experience, time scale and, no doubt, luck.

It was not practicable with the present apparatus to form samples in two halves for subsequent cylindrical triaxial extension tests as the bottom loading platten could not be conveniently fixed to the cell base after preparing the sample. Also, as shown in Chapter 8, the difference in strength between a 4 ins high sample made in two halves and one made in a normal manner is very small, Figs 8.14 & 8.18. The differences in the failure strains, both axial and volumetric, are a little larger but, since strength is the primary criterion on which tests are being compared, these small differences must perforce be neglected. Clearly in a perfect comparison both stress and strain must agree whereas in the present mixed-boundary situation it is optimistic to presume that concurrent agreement would be achieved. That the correlation is as good as it in fact is, is a very promising sign.

The definitions of stress, strain, ϕ' and porosity are identical to those given in Chapter 8, as is the method of presentation of the results. The stress - strain and volume change curves for the individual cylindrical triaxial compression and extension tests are given in Appendix

A9, and the basic test characteristics and failure stresses etc are tabulated in Fig 9.1.

9.1.1 Type H

These samples were 4 ins high built in two halves with lubricated ends. Two 0.010 ins thick lubricated rubber membranes were used on each platten. With the exceptions of Tests H/1 & 3 the tests were terminated at, or soon after, peak deviator stress. Consequently the possible formation of slip zones could not be studied. No slip zones were observed in Tests H/1 & 3, Figs A9.1 & A9.3, both medium dense samples, which confirms the results of Chapter 8. All the samples expanded predominantly at the base, however up to peak ϕ' the differences in the top, centre and base diameters were small. The sample in Test H/3 expanded very uniformly even well beyond peak ϕ'. This sample failed at an axial strain of +9.7% and the test was stopped at an axial strain of +19.4%. The measured diameters of the sample at the end of the test were 4.30, 4.51 & 4.38 ins at the top, middle and bottom of the sample respectively. The difference between the top and bottom diameters is very small indeed considering the relatively large axial strain involved. Test H/5 was stopped very close to the peak ϕ' and the measured diameters were 4.11 & 4.14 ins at the top and bottom respectively, whereas the central diameter was only 4.16 ins. The error in assuming the sample to deform as a right cylinder is 0.1° based on the maximum midheight cross-sectional area, which is negligible.

9.1.2 Type HA

These samples were identical to the Type H samples. The sample was consolidated at a cell pressure of from 140 - 190 psi, which was decreased during the shear stage, while the axial stress was maintained constant manually, Fig 6.1. In the early part of the shear stage it was difficult to maintain the deviator stress at the value required to give a constant σ_1' particularly as the value of σ_3' approached 40 psi. However as soon as the cell pressure had been reduced manually to 40 psi it was transferred to the self-compensating mercury control system. Thus it was possible to define the peak deviator stress and volumetric strain rate at failure fairly well whereas the axial and volumetric strain at failure cannot be defined accurately and are therefore not plotted, see Figs A 9.8 to A 9.13.

Date	Test number	Sequence number	Porosity, n %			Stresses at failure psi		Strains at failure %			Volumetric strain rate at failure		ϕ' degrees	Corrected ϕ' degrees	Material	End condition	Nominal axial strain rate ins/min	Mode of sample preparation	Notes
			Initial n_i	After consolidation	At failure	Axial σ_1'	Cell $\sigma_2' = \sigma_3'$	Axial $\Delta H/H_c$	Mean lateral $\Delta D/D_c$	Volumetric $\Delta V/V_c$	$\frac{d(\Delta V/V_c)}{d(\Delta H/H_c)}$	$\frac{d(\Delta V/V_c)}{d(\Delta D/D_c)}$							
TYPE H D=3·9 ins, H=4·1 ins, compression																			
27/6/65	H/1	1	41·3	40·7	42·3	163·2	40·0	+10·0	-6·8	-2·7	-0·39		37·3	37·1	Batch 2 Bag 4	2/0·010 ins thick lubricated membranes	+0·007	Two halves	
7/7/65	H/2	2	41·9	41·2	42·5	156·1	40·0	+9·2	-6·0	-2·1	-0·37		36·3	36·1					
11/7/65	H/3	3	40·4	39·8	41·6	168·2	40·0	+9·7	-6·9	-3·1	-0·50		38·0	37·8					
29/8/65	H/4	8	44·4	43·7	44·3	143·5	40·0	+14·2	-8·4	-1·1	-0·15		34·3	34·1					
31/8/65	H/5	9	38·6	38·1	40·2	184·1	40·0	+7·7	-5·9	-3·6	-0·71		40·0	39·8					
20/10/65	H/6	24	45·3	44·6	44·6	139·2	40·0	+17·4	-10·0	0	-0·09		33·6	33·4	Batch 2 Bag 4 Reused				
22/10/65	H/7	25	40·1	39·5	41·2	167·1	40·0	+8·2	-5·8	-2·8	-0·51		37·8	37·6					
TYPE HA D=3·9 ins, H=4·1 ins, compression, decreasing σ_1																			
11/7/65	HA/1	4	40·4	39·3		171·3	40·0				-0·50		38·4	38·2	Batch 2 Bag 4	2/0·010 ins thick lubricated membranes	+0·0035 / +0·007	Two halves	
13/7/65	HA/2	5	40·4	39·3		170·5	40·0				-0·51		38·3	38·1			+0·0035 / +0·007		
15/7/65	HA/3	6	45·2	43·8		143·6	40·0				-0·14		34·3	34·1			+0·007		
23/7/65	HA/4	7	44·0	42·7		150·2	40·0				-0·22		35·4	35·2					
2/9/65	HA/5	10	38·8	37·7		183·1	40·0				-0·69		39·9	39·7			+0·0035 / +0·007		
6/9/65	HB/6	11	42·4	41·3		160·1	40·0				-0·36		36·9	36·7			+0·007		
TYPE EX Cell $\sigma_1' = \sigma_2'$ Axial σ_3' D=3·9 ins, H=4·1 ins, extension																			
11/9/65	EX/1	12	41·4	40·3	40·4	160·0	40·8	-5·5	+2·6	-0·1	+0·20	-0·54	36·4	37·4	Batch 2 Bag 4	2/0·010 ins thick lubricated membranes	-0·007	Normal	
14/9/65	EX/2	13	41·5	40·3		162·0	40·3	-6·2	+3·0				36·9	37·9			-0·0035		
16/9/65	EX/3	14	41·4	40·4	40·6	162·0	39·4	-5·8	+2·6	-0·4	+0·21	-0·60	37·5	38·5			-0·007		
18/9/65	EX/4	15	41·4	40·3	40·3	160·0	40·6	-5·2	+2·5	0	+0·18	-0·48	36·5	37·5			-0·001		
20/9/65	EX/5	16	42·5	41·2	41·1	150·0	39·3	-6·4	+3·1	+0·2	+0·15	-0·41	35·7	36·7			-0·0035		
23/9/65	EX/6	17	39·1	38·3	38·7	180·0	40·5	-4·2	+1·7	-0·7	+0·30	-0·93	39·2	40·2			-0·007		
25/9/65	EX/7	18	45·5	43·9	43·2	140·0	42·8	-8·3	+4·6	+1·3	+0·07	-0·14	32·1	33·1					Photo
27/9/65	EX/8	19	45·9	44·4	43·5	130·0	39·3	-9·9	+5·3	+1·5	+0·05	-0·10	32·4	33·4					
3/10/65	EX/9	20	43·8	42·3	42·3	140·0	35·7	-10·2	+4·7	0	+0·16	-0·42	36·5	37·5			-0·0035		
5/10/65	EX/10	21	42·5	41·4	41·5	150·0	38·4	-8·1	+3·8	-0·1	+0·25	-0·51	36·3	37·3	Batch 2 Bag 4 Reused				
11/10/65	EX/11	22	42·5	41·4	41·2	150·0	42·0	-5·8	+2·8	+0·2	+0·14	-0·37	34·2	35·2					
16/10/65	EX/12	23	39·6	38·7	39·1	170·0	37·0	-5·3	+2·3	-0·7	+0·28	-0·84	40·0	41·0					
TYPE EL Cell $\sigma_1' = \sigma_2'$ Axial σ_3' D=3·9 ins, H=7·1 ins, extension																			
2/11/65	EL/1	26	41·0	40·0	40·2	160·0	38·2	-6·5	+2·9	-0·3	+0·22	-0·62	37·9		Batch 2 Bag 4 Reused	2/0·010 ins thick lubricated membranes	-0·007	Normal	
6/11/65	EL/2	27	38·8	38·0	38·4	180·0	40·2	-4·6	+1·9	-0·6	+0·29	-0·89	39·4						Photo
11/11/65	EL/3	28	45·3	44·0	42·9	140·0	42·7	-8·7	+4·8	+1·7	+0·04	-0·10	32·2						
TYPE ELA Cell $\sigma_1' = \sigma_2'$ Axial σ_3' D=3·9 ins, H=6·7 ins, extension																			
15/11/65	ELA/1	29	39·4	38·4	38·9	180·0	38·4	-7·1	+3·0	-0·9	+0·29	-0·90	40·4		Batch 2 Bag 4 Reused	4 ins diam. porous discs	-0·007	Normal	Photo
18/11/65	ELA/2	30	45·2	43·7	42·7	140·0	43·6	-7·7	+4·3	+1·6	+0·05	-0·12	31·7						
22/11/65	ELA/3	31	40·4	39·2	39·6	170·0	39·2	-6·9	+3·0	-0·4	+0·23	-0·66	38·7						
26/11/65	ELA/4	32	42·3	41·0	40·7	150·0	40·5	-6·7	+3·4	+0·4	+0·15	-0·39	35·4						

CYLINDRICAL TRIAXIAL COMPRESSION AND EXTENSION TEST SERIES RESULTS

FIG. 9.1

At the beginning of Test HA/1, the porosity was initially miscalculated so that the sample was consolidated at 160 rather than 170 psi; required to fit in with $\sigma_3' = 40$ psi. Hence the curve for σ_1' rises sharply when the cell pressure was transferred to the self-compensating mercury control.

No visible slip zones were apparent in any of the tests and the bottom of the sample expanded laterally in excess of the top in all the tests. In Tests HA/1 & 3 the sample barrelled slightly, in all the other tests it deformed more like a frustum of a cone. Due to the rapid reduction of the high cell pressure during the initial $+\frac{1}{2}\%$ axial strain the samples expanded, so that the initial portion of the volume change curve is displaced upwards. A similar effect was observed by Cornforth (1961).

9.1.3 Type EX

These samples were 4 ins high built in the normal manner with lubricated ends. Two 0.010 ins thick lubricated rubber membranes were used on each platten. The sample was consolidated at a cell pressure of from 140-180 psi and the axial stress was decreased to failure, Fig 6.1. The tests were stopped as soon after peak deviator stress had been reached as was possible. About 50% of the tests were stopped within 0 to 1% axial strain beyond the failure point so that subsequent measurements of the diameters of these samples, at different points over the height, could be used with a fair degree of accuracy to assess the possible range in the value of the peak ϕ'.

Plate 9.1 shows the sample in Test EX/8 after dismantling. The sample had an initial porosity of 45.9% (i.e. loose) and failed at an axial strain of -9.9%; at which point the test was stopped. Slight necking is clearly seen. This sample was carefully measured up with a travelling microscope to enable an exact determination of the neck area, the results of which are presented later in this chapter. When considering failure in a triaxial extension sample it should be recognised that, whereas the degree of necking at large strains will be very pronounced, the extent to which necking influences the measured strength at failure is much smaller. Thus the extension specimen of sand shown by Roscoe et al (1963) is misleading in view of the title of their paper. This misleading photograph is also shown by Barden & Khayatt (1966).

The lateral contraction of the samples was generally greatest at the



TEST Ex18.

cylindrical extension,
$n_i = 45.9\%$, 4.1 ins high,
2 10.010 ins thick membranes,
test stopped at $\Delta H/H_c = -9.9\%$,
$(\Delta H/H_c)_f = -9.9\%$.

PLATE 9.1

bottom compared with the top and in Tests EX/1, 11 & 12 a single slip zone was formed soon after failure. In Test EX/9 a central neck was formed and faint traces of 2 opposing slip zones were observed, Fig A 9.20. It appears that the dense and medium dense samples fail close to the base and that the looser samples neck in a more traditional manner. In retrospect, the triaxial cell could usefully have been modified to allow samples made in two halves to be tested in cylindrical triaxial extension. Although there is no reason to believe that the present samples built in a normal manner, gave spurious results when tested in triaxial extension, a reduction in the number of variables would be an advantage. It is possible but by no means certain that samples made in two halves would neck at the mid-height more frequently. The samples all expanded very slightly during the initial rapid reduction in axial stress, in a similar manner to the Type HA samples.

A small leak occurred in the sample sheath in Test EX/2 so that the measured volume changes were unreliable. Data from Test EX/3 was used to calculate the stresses, the error being negligible as the initial porosities of the two samples were within 0.1% of one another.

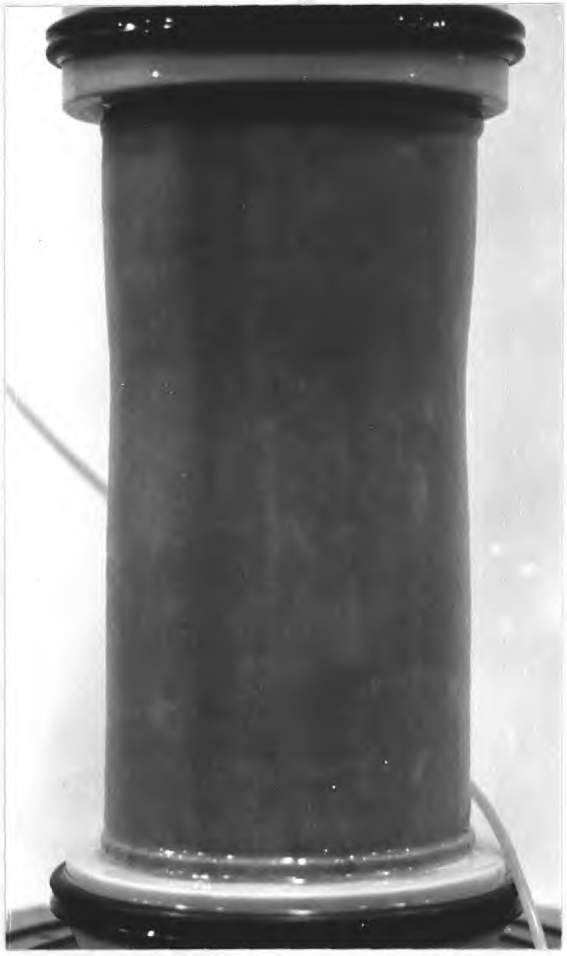
9.1.4 Type EL

These samples were 7 ins high built in the normal manner with 2/0.010 ins thick lubricated rubber membranes used on each platten. The samples were consolidated at a cell pressure of from 140-180 psi and the axial stress was decreased to failure, similar to Type EX, Fig 6.1.

All these samples formed necks centred at the lower third point. Tests EL/1 & 3 were stopped within -2% axial strain beyond failure and no slip zones were visible. Test EL/2 initially vibrated to a dense state was continued to -3.3% axial strain beyond failure, Plate 9.2(a). The sample was formed by filling the mould in 4 lifts, each lift being vibrated for 2 or 3 minutes. It appears that the 3 horizontal discontinuities formed in the sample and first observed just beyond the peak deviator stress are the junctions between the 4 lifts. Vibration does not eliminate these boundaries as one might have expected. This phenomenon was never observed in dense compression samples formed in a similar manner. It is not thought that the measured peak strength was greatly affected by these discontinuities. The single inclined slip zone formed at the neck in Test EL/2 was



(a) TEST EL12.
cylindrical extension,
n_i = 38·8%, 7·1 ins high,
2 lo·010 ins thick membranes,
test stopped at $\Delta H/H_c = -7·9\%$,
$(\Delta H/H_c)_f = -4·6\%$.



(b) TEST ELA11.
cylindrical extension,
n_i = 39·4%, 6·7 ins high,
porous disc at each end,
test stopped at $\Delta H/H_c = -8·4\%$,
$(\Delta H/H_c)_f = -7·1\%$.

PLATE 9.2

first observed after the 3 horizontal discontinuities were seen, in fact it intersects the lower discontinuity (not shown in Plate 9.2(a), see Fig A 9. 24). Multiple necking has been obtained in extension tests on $1\frac{1}{2}$ ins diameter samples, Eldin (1951), probably due to the mode of sample formation.

9.1.5 Type ELA

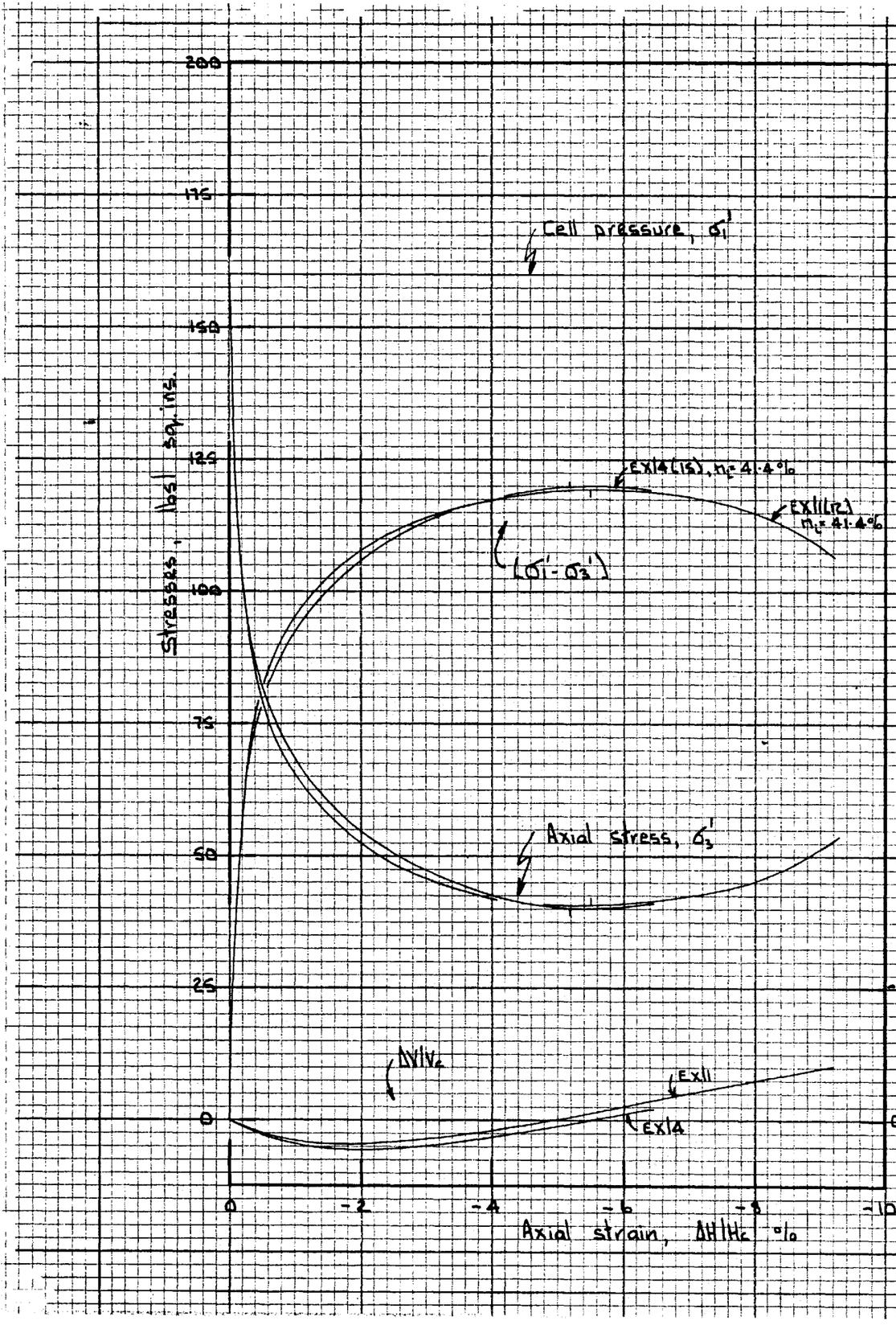
These samples were 7 ins high built in the normal manner with conventional vitrified bauxilite A80KV porous discs , 4 ins diameter and $\frac{1}{4}$ins thick, at each platten. The samples were consolidated at a cell pressure of from 140-180 psi and the axial stress was decreased to failure, similar to Type EX, Fig 6.1. All four tests were stopped at, or close to, failure. They all exhibited a slight neck just above midheight in contrast to the Type EL samples which necked at the lower third point. This was almost certainly due to the differing degree of end restraint in the two types of sample.

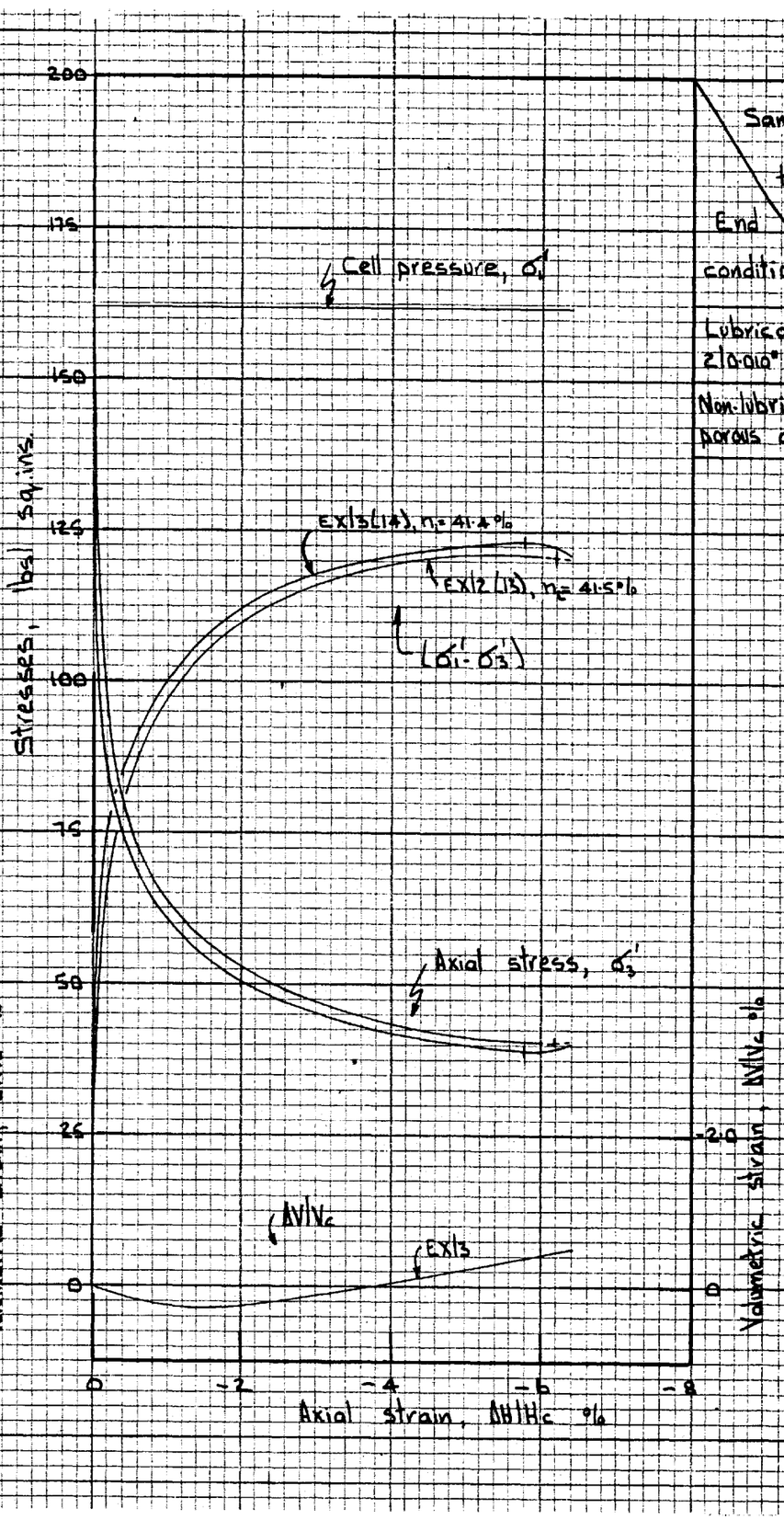
Plate 9.2(b) shows the sample in Test ELA/1 after dismantling. The sample failed at an axial strain of -7.1% and the test was stopped at -8.4%. Measurements of the sample diameter after dismantling the cell indicate that slip had occurred between the ends of the sample and the porous discs Fig A 9.26. The 2 other samples on which measurements were made behaved in a similar manner. No slip zones were observed in any of the tests, but since they were all stopped at or just after peak ϕ' this may be expected. The sample in Test ELA/1 was vibrated in one lift to avoid the formation of discontinuities similar to those in Test EL/2. The end of test measurements in Tests ELA/2 & 3 were made with the sample under a suction of 0.7 psi in contrast to the normal method used of sealing the sample off under a cell pressure of 40 psi to ensure that the sample sheath does not subsequently wrinkle.

The general modes of deformation of all the extension samples, including Types EX and EL are in agreement with similar tests reported by Barden & Khayatt (1966).

9.2 Comparison of stress-strain and volume change curves

The stress-strain and volume change characteristics of selected extension tests are shown in Figs 9.2, 9.3 & 9.4. Only a limited number of Type EL & ELA tests were performed so that valid comparisons with the





Sample type / End conditions	Normal Extension
Lubricated 2 [illegible] thk	4" high type EX
Non-lubricated porous disk	

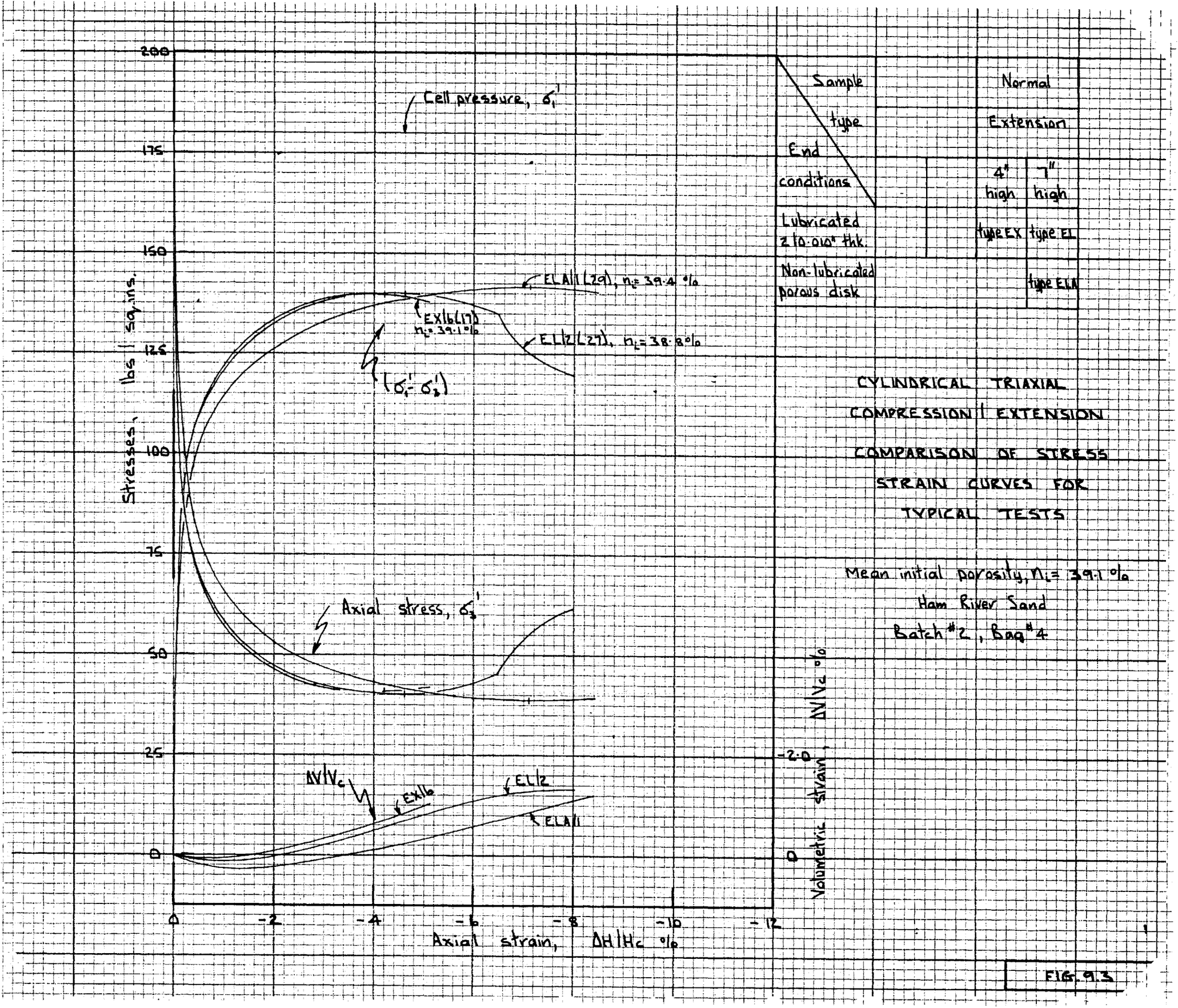
CYLINDRICAL TRIAXIAL COMPRESSION / EXTENSION

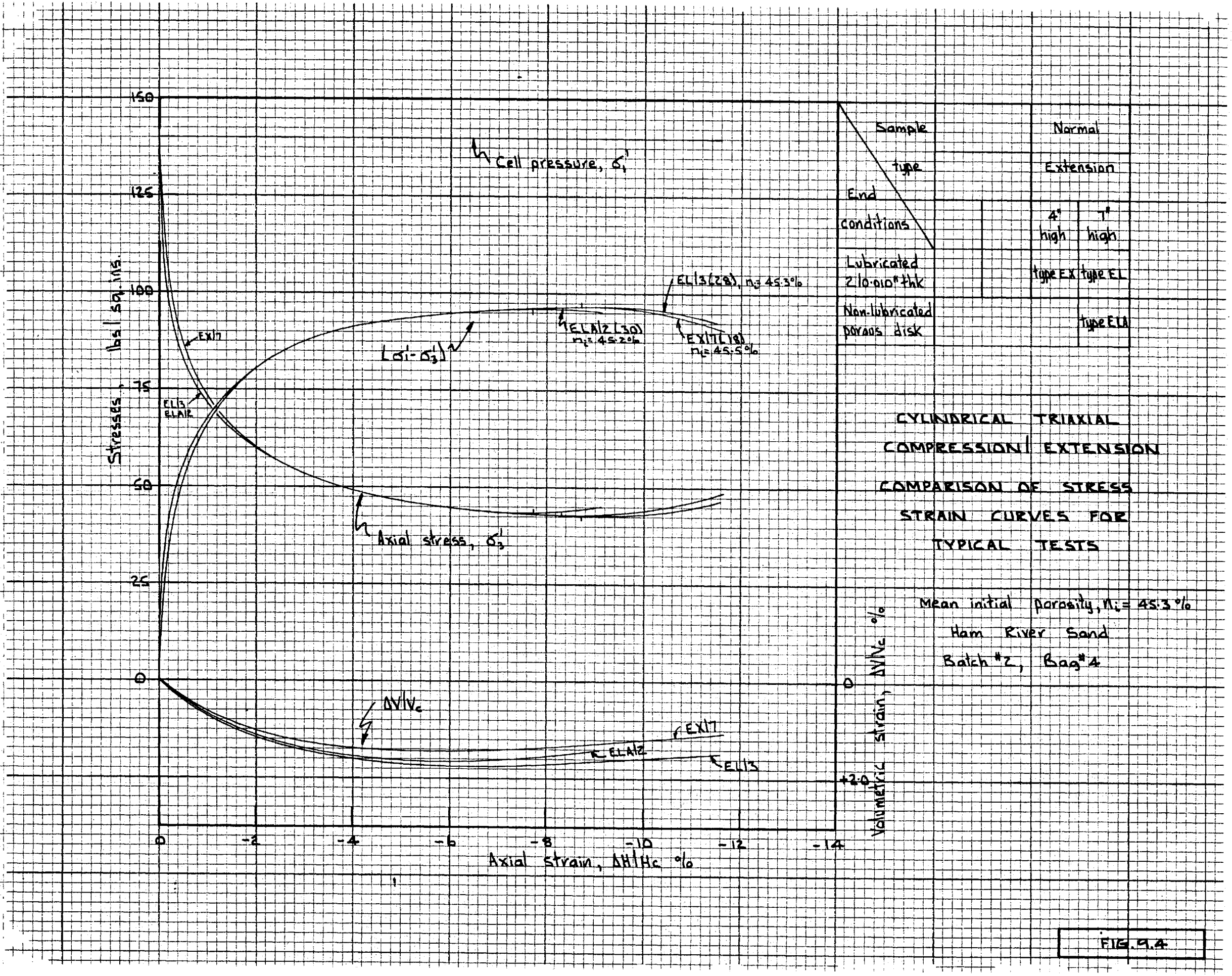
COMPARISON OF STRESS STRAIN CURVES FOR TYPICAL TESTS

Mean initial porosity, n_c = 41.4 %

Ham River Sand
Batch #2, Bag #4

FIG. 9.2


Cell pressure, σ_1'
EL A/1 (Z9), n_i = 39.4 %
EX 1b (L7) n_i = 39.1 %
EL 1Z (Z7), n_i = 38.8 %
$(\sigma_1' - \sigma_3')$
Axial stress, σ_3'
$\Delta V/V_c$
EX 1b
EL 1Z
EL A/1
Stresses, lbs/sq.ins.
200
175
150
125
100
75
50
25
0
0
-2
-4
-6
-8
-10
-12
Axial strain, $\Delta H/H_c$ %
Volumetric strain, $\Delta V/V_c$ %
-2.0
0
Sample type
End conditions
Normal Extension
4" high
7" high
Lubricated 2 to 0.010" thk.
type EX
type EL
Non-lubricated porous disk
type ELN
CYLINDRICAL TRIAXIAL COMPRESSION / EXTENSION
COMPARISON OF STRESS STRAIN CURVES FOR TYPICAL TESTS
Mean initial porosity, n_i = 39.1 %
Ham River Sand
Batch #2, Bag #4
FIG. 9.3



Sample type / End conditions	Normal Extension	
	4" high	7" high
Lubricated 2 lo·010" thk	type EX	type EL
Non-lubricated porous disk		type ELA

CYLINDRICAL TRIAXIAL COMPRESSION/EXTENSION COMPARISON OF STRESS STRAIN CURVES FOR TYPICAL TESTS

Mean initial porosity, n_i = 45.3 %

Ham River Sand

Batch #2, Bag #4

FIG. 9.4

Type EX tests are rather hard to draw.

Fig 9.2 shows two pairs of results for medium dense, 4 ins high samples with lubricated ends, Type EX. The cell pressures are slightly different for each pair. The two pairs of test results are self-consistent. The peak strengths of the four tests vary from 36.4 to 37.5° and indicate good repeatability. The volume change curves are also very consistent.

Fig 9.3 shows a series of results for dense samples, for which one might expect any differences in behaviour to be relatively large. The two samples with lubricated ends, Tests EX/6 (17) & EL/2(27), failed at similar strains whereas the axial strain at failure for the 7 ins high sample, in contact with porous discs, was nearly 3% higher, Test ELA/1(29). The reason for this is not clear, it would at first sight appear more reasonable that the reverse be true. The axial strain in Test EL/2(27) may be spurious due to the method used to build the sample, so that definite conclusions are not possible.

A different result was obtained in similar tests by Barden & Khayatt (1966). In their Fig 6 the results of two tests on dense samples of fine River Welland sand are given, a 4 ins x 4 ins sample with free ends and a 4 ins x 8 ins sample with fixed ends. The failure strain of the long fixed ended sample was about 4% whereas that of the short free ended sample was over 7%. Also the latter appears to give a higher strength even when the measured area corrections are accounted for. However a ball and socket joint was used between the loading piston and the top loading platten in these tests, which could account for the observed differences. It has been observed in the previous chapter of this thesis that a conventional compression sample fails at a smaller strain if a spherical seating is used, due to tilting of the top platten. What influence, if any, the spherical seating had in Khayatt's test is not known. It is quite probable that it would have a different effect on a 4 ins x 4 ins sample with free ends compared with a 4 ins x 8 ins sample with fixed ends. Furthermore these tests were performed at a lower stress level than the present tests so that the influence of the sample sheath on the results would have been greater; but no mention is made of this by Barden & Khayatt.

Fig 9.4 shows a similar series of results for loose samples where the differences in the shapes of the stress-strain and volume change curves are much smaller. As the stress-strain curves are very flat the failure

strains may be sensitive to the area correction used. On a uniform strain basis they are very similar for the 3 types of test. Unfortunately the sample in Test EX/7 was lost during dismantling. The other two tests were stopped at axial strains of -1.4% and -2.0% beyond failure so that precise comparisons are more difficult to make. The influence of the area corrections on the measured strength is further discussed in a subsequent section.

9.3 Comparison of failure characteristics

For each test type the failure characteristics are plotted against the initial porosity, Figs 9.5 to 9.10 . The correlation between the tests at different porosities for a particular test type is clearly seen to be good. To compare the extension tests with the compression tests it is necessary to plot the mean lateral strain and volumetric strain rate with respect to the mean lateral strain for the extension tests. The mean lateral strain is calculated from the measured values of the axial and volumetric strains and was not determined independently.

The Type H test results, 4 ins high samples with 2/0.010 ins thick lubricated membranes at each end, failed in triaxial compression are very self-consistent, Fig 9.5. The results of Tests H/6(24) & H/7(25) performed late in the series are in good agreement with the earlier five tests. Also shown are possible upper and lower bound ϕ' values for Test H/7(25) which failed at +8.2% and was stopped at +10.7% axial strain. The upper point, 38.3° is based on the sample being a frustum of a cone, Fig 9.16, the area at failure being the average cross-sectional area of the lower half of the frustum, A_2^*. The lower point, 37.3°, is based on the area at failure being the average cross-sectional area of the upper half of the frustum, A_3^* , see Fig 9.16. These two assumptions represent extreme cases. The inclination of a slip zone will be much steeper, $(45^\circ - \phi'/2)$, in a compression test than in the case of extension assumed in Fig 9.16. The potential slip zone will extend throughout the height of the sample so that the true ϕ' value is probably within a much closer range than that contained by these bounds. The ϕ' value obtained, based on the average cross-sectional area over the whole of the sample, 37.8°, is probably of the order 0.2° higher than the true strength.

The results for the Type HA tests on similar samples to the Type H tests, but with σ_3' decreasing to failure, are shown in Fig 9.6. There

H15(9)

H13(3)

H17(7.5)

H11(1)

H12(2)

H14(8)

H16(24)

$\Delta H/H_c$

$\Delta V/V_c$

$\frac{d(\Delta V/V_c)}{d(\Delta H/H_c)}$

ϕ'

Maximum angle of shearing resistance, ϕ'

Volumetric strain at failure, $\Delta V/V_c$ %

Axial strain at failure, $\Delta H/H_c$ %

Volumetric strain rate at failure $\frac{d(\Delta V/V_c)}{d(\Delta H/H_c)}$

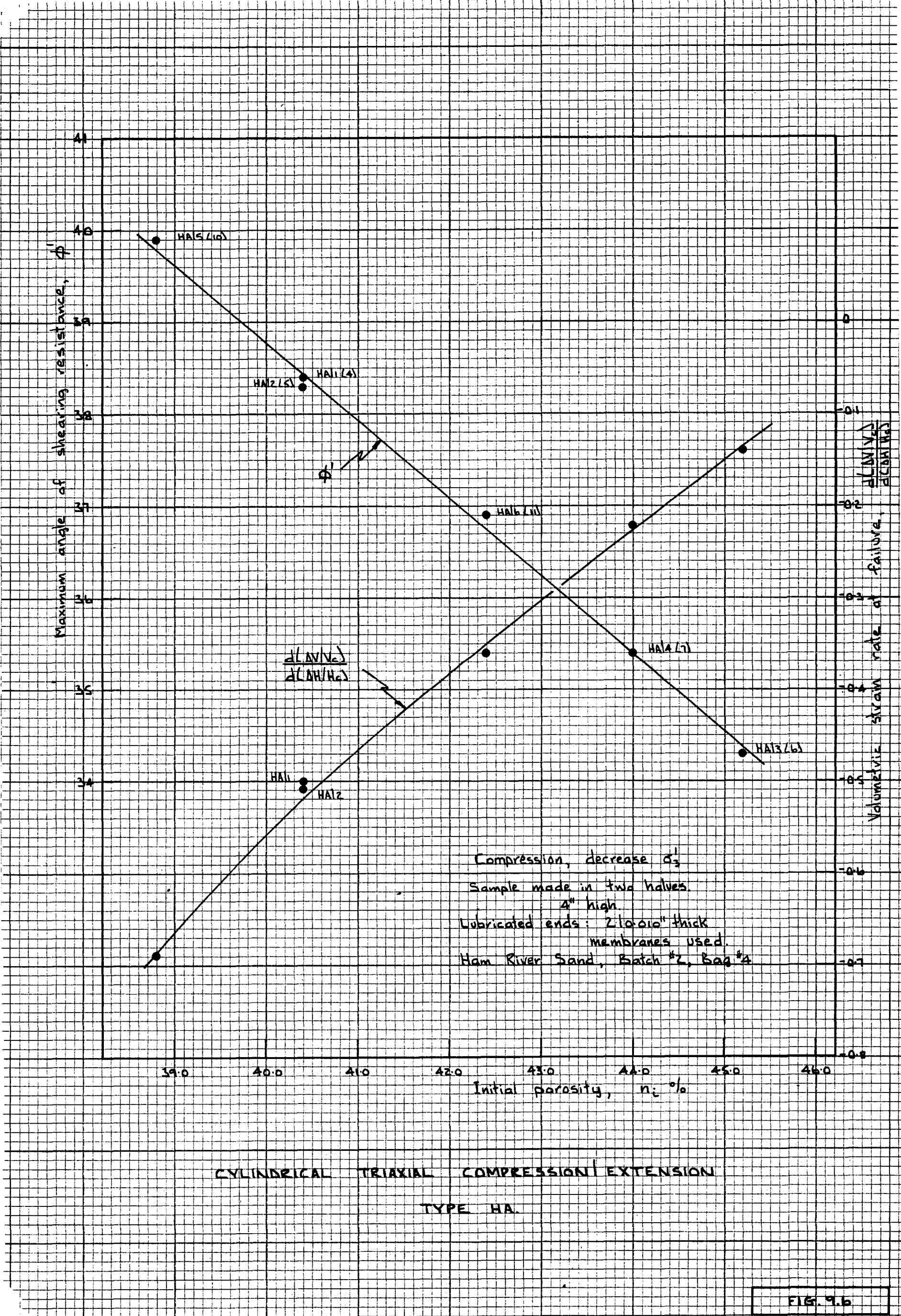
Initial porosity, n_i %

Compression, increase σ_1'

Sample made in two halves.
4" high.
Lubricated ends: 2 10 010" thick membranes used.
Ham River Sand, Batch #2., Bag #4

CYLINDRICAL TRIAXIAL COMPRESSION | EXTENSION.

TYPE H.



CYLINDRICAL TRIAXIAL COMPRESSION/EXTENSION

TYPE HA.

FIG. 9.6

Maximum angle of shearing resistance, ϕ'

41
40
39
38
37
36
35
34
33
32

EX|12 (23)
EX|6 (17)
EX|3 (14)
EX|2 (13)
EX|4 (15)
EX|1 (12)
EX|9 (20)
EX|10 (21)
EX|5 (16)
ϕ'
EX|11 (22)
$\Delta H/H_c$
EX|4
EX|1
EX|3
EX|11
EX|5
EX|7 (18)
EX|8 (19)
EX|10

Axial strain at failure, $\Delta H/H_c$ %

-4
-6
-8
-10
-12

Lateral strain at failure, $\Delta D/D_c$ %

+6
+4
+2
0

$\Delta D/D_c$
EX|10
EX|5
EX|11
EX|1
EX|3
EX|4

39·0 40·0 41·0 43·0 44·0 45·0 46·0

Initial porosity, n_i %

Extension
Sample made in a normal manner.
4·1" high
Lubricated ends: 2 | 0·010" thick membranes used
Ham River Sand, Batch #2, Bag #4

CYLINDRICAL TRIAXIAL COMPRESSION | EXTENSION.

TYPE EX.

FIG. 9.7

Volumetric strain at failure, $\Delta V/V_c$ %

+2·0 +1·5 +1·0 +0·5 0 -0·5 -1·0

$\Delta V/V_c$

Ex|8(19) Ex|7(18) Ex|11(22) Ex|5(16) Ex|4(15) Ex|11(12) Ex|9(20) Ex|10(21) Ex|3(14) Ex|6(17) Ex|12(23)

$\frac{d(\Delta V/V_c)}{d(\Delta B/D_c)}$

Ex|1 Ex|5 Ex|4 Ex|10 Ex|11 Ex|13

Extension
Sample made in a normal manner
4·1" high
Lubricated ends : 2 lb·010" thick membranes used
Ham River Sand, Batch #2, Bag #4

$\frac{d(\Delta V/V_c)}{d(\Delta H/H_c)}$

Ex|10 Ex|13 Ex|1 Ex|4 Ex|5 Ex|11

Volumetric strain rate at failure, $\frac{d(\Delta V/V_c)}{d(\Delta B/D_c)}$

-0·1 -0·2 -0·3 -0·4 -0·5 -0·6 -0·7 -0·8 -0·9 -1·0

Volumetric strain rate at failure, $\frac{d(\Delta V/V_c)}{d(\Delta H/H_c)}$

+0·3 +0·2 +0·1 0

39·0 40·0 41·0 42·0 43·0 44·0 45·0 46·0

Initial porosity, n_i %

CYLINDRICAL TRIAXIAL COMPRESSION/EXTENSION.

TYPE E.X.

FIG. 9.8

Extension
Sample made in a normal manner

Type EL ▲ 7:1" high
Lubricated ends: 2 lo-gio" thick membranes used.

Type ELA ■ 6:7" high
Non-lubricated ends: porous disk

Ham River Sand, Batch #2 Bag #4

43·6° 41·4° 41·0°

ELA/1/(29)

EL/2/(27)

ELA/3/(31)

EL/1/(26)

ELA/4/(32)

EL/3/(28)

ELA/2/(30)

Type EL

Type ELA

ϕ'

$\Delta H/H_c$

$\Delta D/D_c$

Maximum angle of shearing resistance, ϕ'

Lateral strain at failure, $\Delta D/D_c$ %

Axial strain at failure, $\Delta H/H_c$ %

Initial porosity, n_i %

CYLINDRICAL TRIAXIAL COMPRESSION/EXTENSION.

TYPES EL & ELA.

FIG. 9.9

Volumetric strain at failure, $\Delta V/V_c$ %

+2·0
+1·5
+1·0
+0·5
0
-0·5
-1·0

$\Delta V/V_c$

EL13(29)
ELA12(30)
ELA14(32)
ELA13(31)
EL11(28)
EL12(27)
ELA11(29)

Type ELA
Type EL

$\frac{d(\Delta V/V_c)}{d(\Delta N/N_c)}$

Type ELA
Type EL

Extension
Sample made in a normal manner.

Type EL ▲ 7·1" high
Lubricated ends: 2 lo·oio" thick membranes used.

Type ELA ■ 6·7" high
Non-lubricated ends: porous disk.

Ham River Sand, Batch#2, Bag#4

$\frac{d(\Delta V/V_c)}{d(\Delta N/N_c)}$

Type EL
Type ELA

Volumetric strain rate at failure, $\frac{d(\Delta V/V_c)}{d(\Delta N/N_c)}$

-0·1
-0·2
-0·3
-0·4
-0·5
-0·6
-0·7
-0·8
-0·9
-1·0

+0·3
+0·4
+0·1
0

39·0 40·0 41·0 42·0 43·0 44·0 45·0 46·0

Initial porosity, n_i %

CYLINDRICAL TRIAXIAL COMPRESSION/EXTENSION.

TYPES EL & ELA.

FIG. 9.10

is very good agreement between the strengths and volumetric strain rates for all the Type IIA tests. In view of the erratic initial portions of the stress-strain curves this would at first sight appear remarkable. It is probable that the initial high stresses, and in particular the large shearing stresses induced during the first 0.5% axial strain by the reduction in σ_3', cause the sample to become more homogeneous which results in more consistent ϕ' values. Although it was impossible to define a reliable failure strain, the slope of the volume change curves were virtually constant over a wide range of axial strains so that there is little ambiguity, Figs A 9.8 to A 9.13.

The Type EX extension results for 4 ins high samples are shown in Figs 9.7 & 9.8. The scatter in the results is greater than for the compression tests due to the limitations of the testing technique, Cornforth(1961), Roscoe et al (1963a), Barden & Khayatt (1966). Tests EX/9(2) gives results which differ by more than an acceptable amount from the others. As far as is known the test itself was satisfactory, however the sample used was prepared from the remaining contents of Bag No 4, after which test the sand was re-mixed and re-used. Thus segregation of the sand was possible and could explain the observed discrepancy. A similar problem arose in the Cylindrical Triaxial Compression, 1st Series, tests. Tests EX/10(21) & EX/11(22) give slightly inconsistent correlations whereas Test EX/12(23) gives data that correlates on all counts. The reasons for this are probably associated with variable necking in the failure zone.

The problem of a more appropriate area correction must be considered. Also shown in Fig 9.7 are adjusted ϕ' values for Tests EX/3,8,10 & 12. The adjustment to Test EX/8 is based on the shape of the neck as measured with a travelling microscope after dismantling, see Plate 9.1. Since the plan area of a plane inclined at $(45^\circ + \phi'/2)$ to the sample axis and centred at the neck is less than the average cross-sectional area of the whole of the sample, the adjusted ϕ' value is higher, by 1.3°. The adjustments to Tests EX/3,10 & 12 are made on the basis shown in Fig 9.16, since the measured shapes of the samples after the tests approximated closely to a frustum of a right circular cone. The area at failure is assumed to correspond to A_2. The adjusted values for the three tests are 0.8, 1.1 & 0.9° respectively, higher than those calculated assuming uniform deformation. It was not possible to apply reliable adjustments to the

remainder of the Type EX test data because either, (i) the sample was not measured up,or (ii) the test was not stopped sufficiently close to peak ϕ', or (iii) the observed shape does not fit a convenient theory. The magnitude of the increase in ϕ' does not appear to depend on the strain at which the test was stopped, Fig 9.17. The four tests give an average increase in ϕ' of 1.0° and there does not appear to be any reason to believe that they were atypical.

The Type EL and ELA extension test results on samples 7 ins high, Figs 9.9 & 9.10,are very limited in number so that any correlations can only be tentative. There does not appear to be a great difference between the results of the two types of test, i.e. with and without lubricated ends. This is in spite of the slight difference in the location of the neck, already referred to. The area correction problem appears to be much more acute for these two series of tests than for the short samples, Type EX. Five samples were measured up after dismantling the cell and a ϕ' value based on the average area within the necked zone was calculated, Fig 9.16, in a similar manner to Test EX/8. The calculated increases in ϕ' are relatively large, from 2.7 to 4.2°. However the tests were stopped between -0.7 & -2.4% axial strain beyond failure so that the shape of the neck when measured could be significantly different from that at failure. By plotting the differences in ϕ' against the axial strain differences, Fig 9.17, and extrapolating back to zero strain difference an increase of 2° is obtained. However, whereas the calculated increases in ϕ' appear to be independent of the axial strain difference in the Type EX tests they appear to be more reasonably interpreted as being dependent on the axial strain difference in the Type EL and ELA tests. Alternatively if we draw a horizontal line through the Type EL and ELA test points in Fig 9.16 we obtain a mean increase in ϕ' of 3.5°. Cornforth (1961) obtained increases in ϕ' of 0.40 to 3.15° (but mostly less than 1.0°) by similar methods, but his tests were stopped sooner after the peak ϕ' had been reached than the present tests. The test for which an increase of 3.15° was calculated (C-46) was stopped 0.4% axial strain beyond peak ϕ'. It seems likely that even in the best test a correction of from 1 to 3° must be applied to the value of ϕ' obtained assuming uniform deformation, clearly this is far from satisfactory.

9.4 Comparison of Peak Strengths

The peak strengths measured in the different tests are compared in Figs 9.11 to 9.14. For clarity and as an aid to discussion the five different test types are plotted both in separate groups, Figs 9.11 to 9.13, and together, Fig 9.14.

The effect of the stress path followed to failure in compression is shown in Fig 9.11, where the Type HA samples, in which σ_3' is decreased to failure, are compared with the Type H samples, in which σ_1' is increased to failure, see Fig 6.1. The medium dense and the loose samples give ϕ' values for the Type HA tests 0.7° higher than for the Type H tests, whereas the dense samples exhibit similar strengths. Analysis of the modes of deformation of the samples in the 2 types of test indicates that about half the Type H test samples barrelled and about half deformed as a frustum of a cone, whereas most of the Type HA test samples deformed as a frustum of a cone. Thus there appears to be no good reason to believe that the difference in strength is due to a differing mode of deformation. Cornforth (1961) obtained identical strengths when following stress paths similar to those followed by the Type H and HA samples. However his conventional 4 ins diameter, 8 ins high samples were all K_o-consolidated. Barden & Khayatt (1966) suggest that small differences occur even with their best test technique but do not give details, whereas Khayatt (1965) observed no differences, but in a limited number of tests. In tests on saturated Brasted sand Fraser (1957) obtained a higher strength (about 2°) when decreasing σ_1' & σ_3' to failure by increasing the pore water pressure as compared with a drained test in which σ_1' is increased to failure with σ_3' constant. Clearly this is not an altogether satisfactory comparison.

The effect on the strength, as measured in the 3 types of extension test, of sample size and end conditions is shown in Fig 9.12. All the points are based on uniform sample deformations. On this basis the short samples, Type EX, give the same strength as the long samples, Type EL and ELA. The strengths exhibited by the two types of long sample do not differ significantly from one another, as detailed earlier. However if we apply more appropriate area corrections to the test results we must, (i) increase all the Type EX ϕ' values by 1.0° and (ii) increase all the Type EL and ELA ϕ' values by at least 2° and maybe by 3.5°, Fig 9.17. This results in a net difference of from 1.0° to 2.5°, the Type EL & ELA tests exhibiting the higher strengths. Thus, if the preceding

Sample type	Sample made in two halves
End conditions	Compression 4" high
	increase σ_1' / decrease σ_3'
Lubricated 2 lo·olo" thk.	⊙ type H / ● type HA

Maximum angle of shearing resistance, ϕ'

42
41
40
39
38
37
36
35
34
33
32
31
30

Type HA

Type H

39·0 40·0 41·0 42·0 43·0 44·0 45·0 46·0

Initial porosity, n_i %

CYLINDRICAL TRIAXIAL COMPRESSION/ EXTENSION
COMPARISON OF PEAK STRENGTHS

Ham River Sand, Batch #2, Bag #4

FIG. 9.11

Sample type / End conditions	Normal Extension	
	4" high	7" high
Lubricated 2 lo-oil" thk.	⊡ type EX	▲ type EL
Non-lubricated porous disk		■ type ELA

Maximum angle of shearing resistance, ϕ

42
41
40
39
38
37
36
35
34
33
32
31
30

29 23 27 17 31 26 14 13 15 12 20 21 16 32 22 19 28 18 30

Type EX

Type EL

Type ELA

39·0 40·0 41·0 42·0 43·0 44·0 45·0 46·0

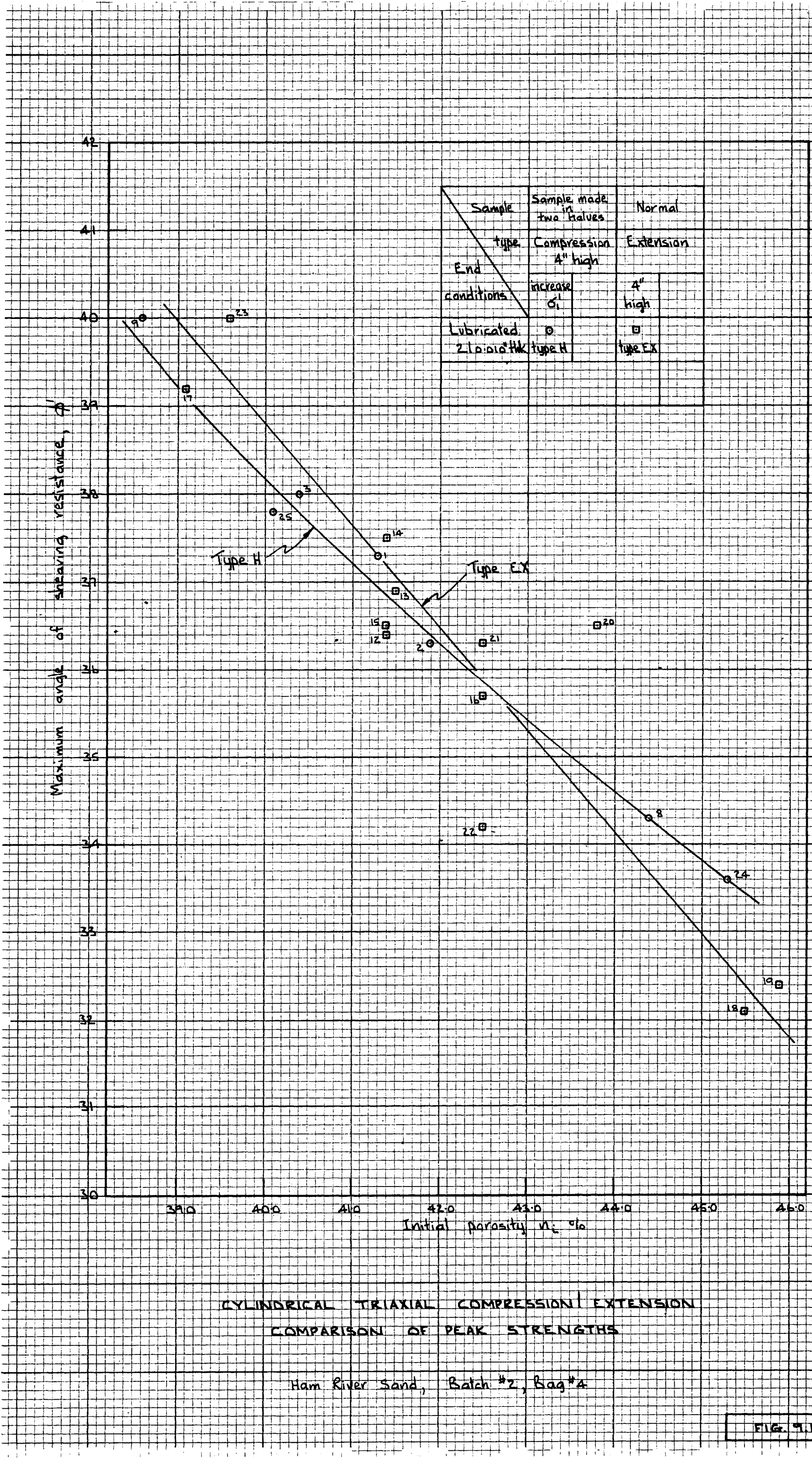
Initial porosity, n_i %

CYLINDRICAL TRIAXIAL COMPRESSION/EXTENSION
COMPARISON OF PEAK STRENGTHS

Ham River Sand, Batch #2, Bag #4

FIG. 9.12

Sample	Sample made in two Halves	Normal	
type	Compression 4" high	Extension	
End conditions	increase σ_1'		4" high
Lubricated 2 Lo:Lo"thk	○ type H		□ type EX



CYLINDRICAL TRIAXIAL COMPRESSION/EXTENSION

COMPARISON OF PEAK STRENGTHS

Ham River Sand, Batch #2, Bag #4

FIG. 9.13

Sample type / End conditions	Sample made in two halves		Normal	
	Compression 4" high		Extension	
	increase σ_1'	decrease σ_3'	4" high	7" high
Lubricated 2 10·010" thk.	⊙ type H	● type HA	⊡ type Ex	▲ type EL
Non-lubricated porous disk.				■ type ELA

Ham River Sand, Batch #2, Bag #4

Maximum angle of shearing resistance, ϕ'

Initial porosity, n_i %

Type ELA

Type HA

Type H

Type Ex

Type EL

CYLINDRICAL TRIAXIAL COMPRESSION / EXTENSION.

COMPARISON OF PEAK STRENGTHS.

FIG. 9.14

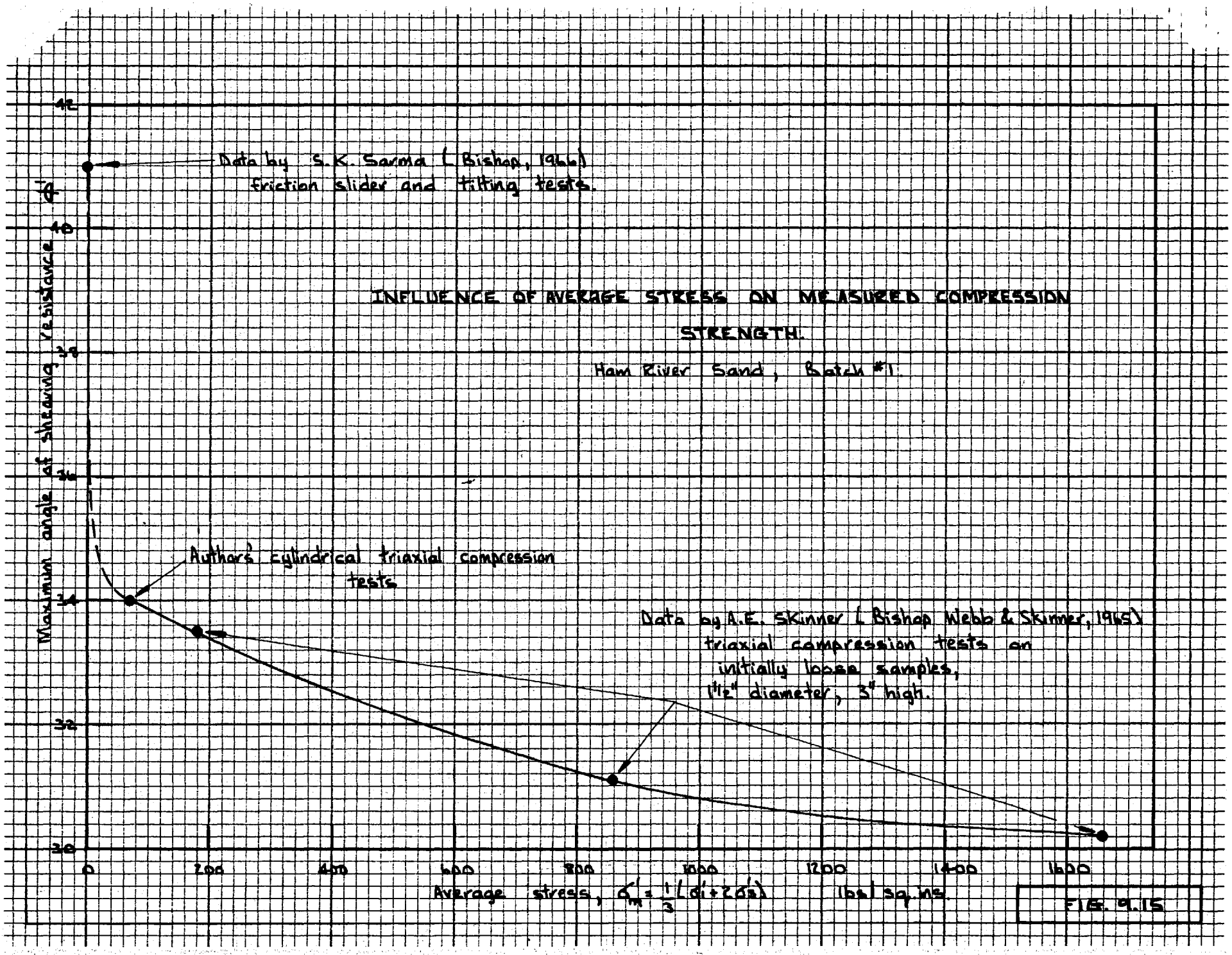
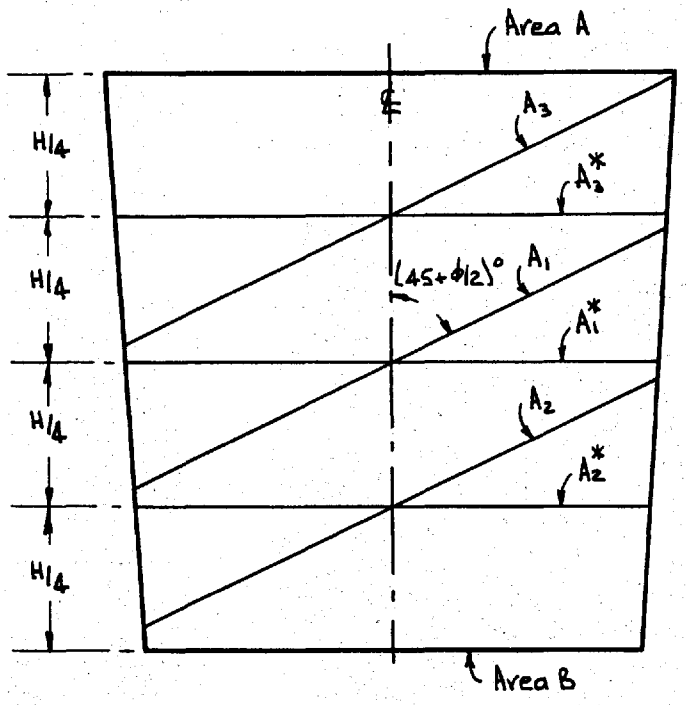

INFLUENCE OF AVERAGE STRESS ON MEASURED COMPRESSION STRENGTH.
Ham River Sand, Batch #1.
Data by S.K. Sarma (Bishop, 1966)
Friction slider and tilting tests.
Author's cylindrical triaxial compression tests.
Data by A.E. Skinner (Bishop Webb & Skinner, 1965)
triaxial compression tests on initially loose samples, 1½" diameter, 3" high.
Maximum angle of shearing resistance, φ'
42
40
38
36
34
32
30
0
200
400
600
800
1000
1200
1400
1600
Average stress, σ'm = 1/3 (σ'1 + 2σ'3)
lbs/sq.ins.

FIG. 9.15



$H/D \doteq 1$, where D = mean diameter
A > B and (A-B) is small

Consider a frustum of a right circular cone:
To a 1st. approx., $A_1^* = A_1 \sin(45+\phi/2)$
Similarly for A_2^* and A_3^*.

$$A_1^* = \frac{1}{2}(A+B)$$

$$\therefore A_2^* = \frac{1}{2}(A_1^*+B)$$

$$= \frac{1}{4}(A+3B)$$

Assuming failure occurs along slip zone A_2

$$\text{Corrected failure area in test} = \left(\text{Measured area based on right circular cylinder assumption}\right) \frac{A_2^*}{A_1^*}$$

$$= A_s \cdot \frac{\left(\frac{A}{B}+3\right)}{2\left(\frac{A}{B}+1\right)}$$

If failure occurs along slip zone A_3

$$\text{Corrected failure area in test} = A_s \cdot \frac{\left(3\frac{A}{B}+1\right)}{2\left(\frac{A}{B}+1\right)}$$

CROSS SECTIONAL AREA CORRECTION FOR 4INS. DIAMETER, 4 INS. HIGH SAMPLES DEFORMING AS A FRUSTUM OF A CONE IN EXTENSION.

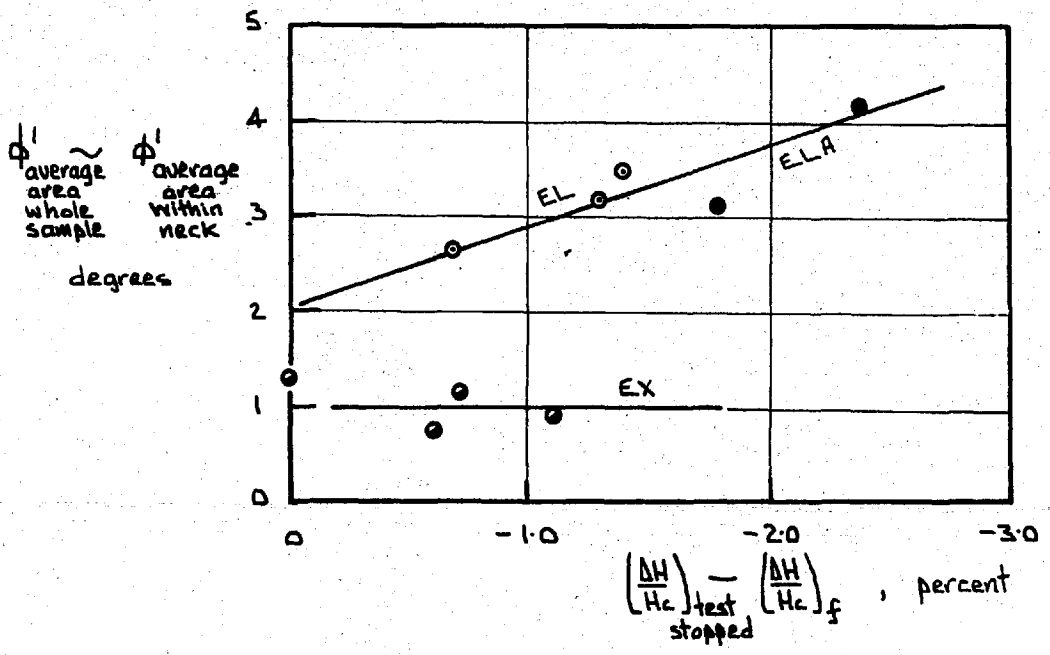
FIG. 9.16

Test No.	ϕ' based on average area of whole of sample.	ϕ' based on minimum area of neck.	ϕ' based on average area within neck	$\left(\frac{\Delta H}{H_c}\right)_{\text{test stopped}} - \left(\frac{\Delta H}{H_c}\right)_f$ %	Theory used
EX18	32·4	34·7	33·7 (1·3)	0	measured neck
EX13	37·5		38·3 (0·8)	−0·6	frustum of cone
EX110	36·3		37·4 (1·1)	−0·7	
EX112	40·0		40·9 (0·9)	−1·1	
EL11	37·9		41·0 (3·1)	−1·8	measured neck
EL13	32·9		37·1 (4·2)	−2·4	
ELA11	40·4		43·6 (3·2)	−1·3	measured neck
ELA12	31·7		35·2 (3·5)	−1·4	
ELA13	38·7		41·4 (2·7)	−0·7	

Notes:

(i) The average area within the neck is based on that part of the sample of height $D.\cot(45+\phi/2)$ and centred at the neck.

(ii) $(\Delta H/H_c)_f$ is based on the average area of the whole of the sample.



CYLINDRICAL TRIAXIAL EXTENSION TESTS
CORRECTIONS TO MEASURED STRENGTHS FOR VARIOUS ASSUMED CROSS-SECTIONAL AREAS OF SAMPLES

FIG. 9.17

arguments are valid, the Type EX test gives either, (i) a strength equal to that of a more conventional shaped sample, or (ii) a strength 1.0 to 2.5° lower than a conventional sample. It would therefore appear that the 4 ins high sample, Type EX, gives the most acceptable strength.

Similar types of test have been performed by Khayatt and are reported by Barden & Khayatt (1966). Their results appear to indicate that a 4 ins x 4 ins sample with lubricated ends tested in a cell with an internal proving ring gave the same strength in extension as a 4 ins x 8 ins sample tested in a cell with an external proving ring and no rotating bush, only if appropriate corrections were made in the latter tests for piston friction and the sample neck area. The measured corrections which were applied were +3, +6 and +8° in the 3 tests quoted for dense samples, which are very large indeed. This suggests to the writer that early published data obtained without using either an internal load measuring device or a rotating bush , and for which no piston friction or refined sample neck area corrections were applied, must be treated with considerable caution and in particular from a failure criterion point of view may be of limited value.

Having accepted the Type EX tests as giving the best estimate of the strength in triaxial extension we must now compare these with the Type H triaxial compression results, Fig 9.13. In this comparison uniform deformations are assumed as the basis of the points plotted. There is little difference in the strength observed in the two types of test, the compression and extension ϕ' values are essentially the same. However it is necessary to have a closer look at the possible effect of, (i) relative differences in mode of deformation, (ii) sample sheath strength corrections, (iii) variation in ϕ' with stress level, and (iv) accuracy of the basic measurements.

The last mentioned factor is the most difficult to assess precisely. Suffice it to say that it is thought that by using a large sized sample, a stable accurate proving ring and by calibrating this ring and the pressure gauge regularly, by interspersing the test types and by not re-using the sand too often these errors were reduced to an insignificant amount.

As shown in Appendix A6 the effect of the stiffness of the sample sheath on the value of ϕ' measured in compression is negligible. The deviation of the mode of deformation from that assumed lowers the value of ϕ' measured in compression by an amount of the order of 0.2°. Thus the

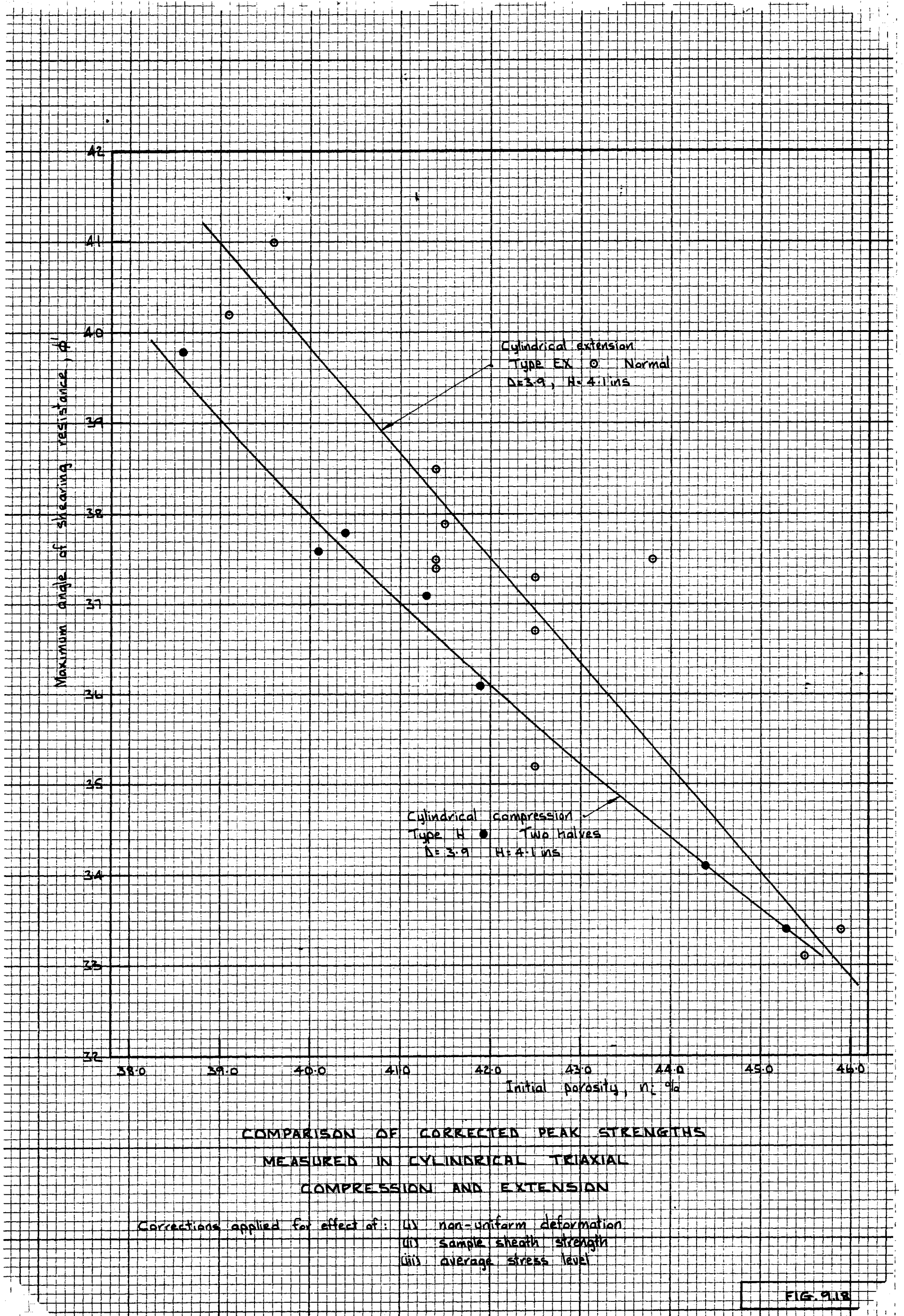
net effect of these two factors is to lower the value of ϕ' measured in compression by 0.2°.

The effect of the stiffness of the sample sheath on the value of ϕ' measured in extension is to lower its value by 0.1 to 0.2° below that measured. If we further assume that the axial strain in the neck is double the average axial strain, a pessimistic view, then ϕ' is lowered by about 0.3°. The deviation of the mode of deformation from that assumed has been shown to raise the ϕ' value by about 1.0° above that measured in triaxial extension. The cell pressure used in the extension test was chosen so that the major and minor principal stresses at failure would be the same as in the compression test. Hence the average stress in compression was about 90 psi whereas the average stress in extension was about 130 psi. The possible variation in ϕ' with average stress is shown in Fig 9.15, based on the author's test, tests by Skinner at higher stresses and tests by Sarma at very low stresses. The effect of a variation in the average stress is to lower the extension ϕ' by 0.3° compared with the compression ϕ' value. Hence the extension ϕ' value must be increased by 0.3° to put it on a comparable basis to the compression ϕ' value. Thus the net effect of these 3 factors is to raise the value of ϕ' measured in extension by $-0.3 + 1.0 + 0.3 = 1.0^{\circ}$, on average.

Combining these two sets of corrections results in raising the extension ϕ' values by an average of 1.2° relative to the compression ϕ' values. The Type EX and H test data with the average corrections applied are shown in Fig 9.18. The cylindrical compression and extension strengths are identical for initially loose samples and the extension tests give a gradually increasing strength rise of up to 2.0° for initially dense samples.

9.5 Comparison of Axial and Lateral Strains at Failure

The magnitudes of the axial strains at failure for the extension tests, Types EX, EL & ELA, are consistently less than those for compression tests, Type H, throughout the porosity range, Fig 9.19. The three different types of extension test give results which agree reasonably well with one another except for the dense samples. Here the 7 ins high, non-lubricated samples deviate significantly. The reason for this is not clear. The dense Type ELA samples, with porous discs at each end failed at higher



COMPARISON OF CORRECTED PEAK STRENGTHS MEASURED IN CYLINDRICAL TRIAXIAL COMPRESSION AND EXTENSION

Corrections applied for effect of: (i) non-uniform deformation
(ii) sample sheath strength
(iii) average stress level

FIG. 9.18

Sample type / End conditions	Sample made in two halves	Normal	
	Compression 4" high	Extension	
	increase σ_1'	4" high	7" high
Lubricated 2 | 0·010" thk	⊙ type H	□ type E.X	▲ type E.L
Non-lubricated porous disk			■ type E.L.N

Axial strain, $\Delta H/H_c$

Type H

Axial (Lateral) strain at failure %

$(-\Delta D/D_c$ %)

Lateral strain, $\Delta D/D_c$

Type E.L.A

Type E.L

Type E.X

Axial strain, $\Delta H/H_c$

Type E.X

Type E.L.A

Type E.L

Initial porosity n_i %

CYLINDRICAL TRIAXIAL COMPRESSION/EXTENSION.

COMPARISON OF AXIAL & LATERAL STRAINS AT MAXIMUM ϕ'.

Ham River Sand, Batch #2, Bag# 4.

FIG. 9.19

axial strains than the Type EL samples with lubricated ends. One might have expected the reverse to have occurred.

The observed general agreement between the extension tests, particularly for the looser samples, is in contrast to the cylindrical triaxial compression samples discussed in Chapter 8, see Fig 8.15. The derived mean lateral strains at failure for the extension tests vary from +2.0% to +5.0% which are about one-third of the axial strains in corresponding compression tests.

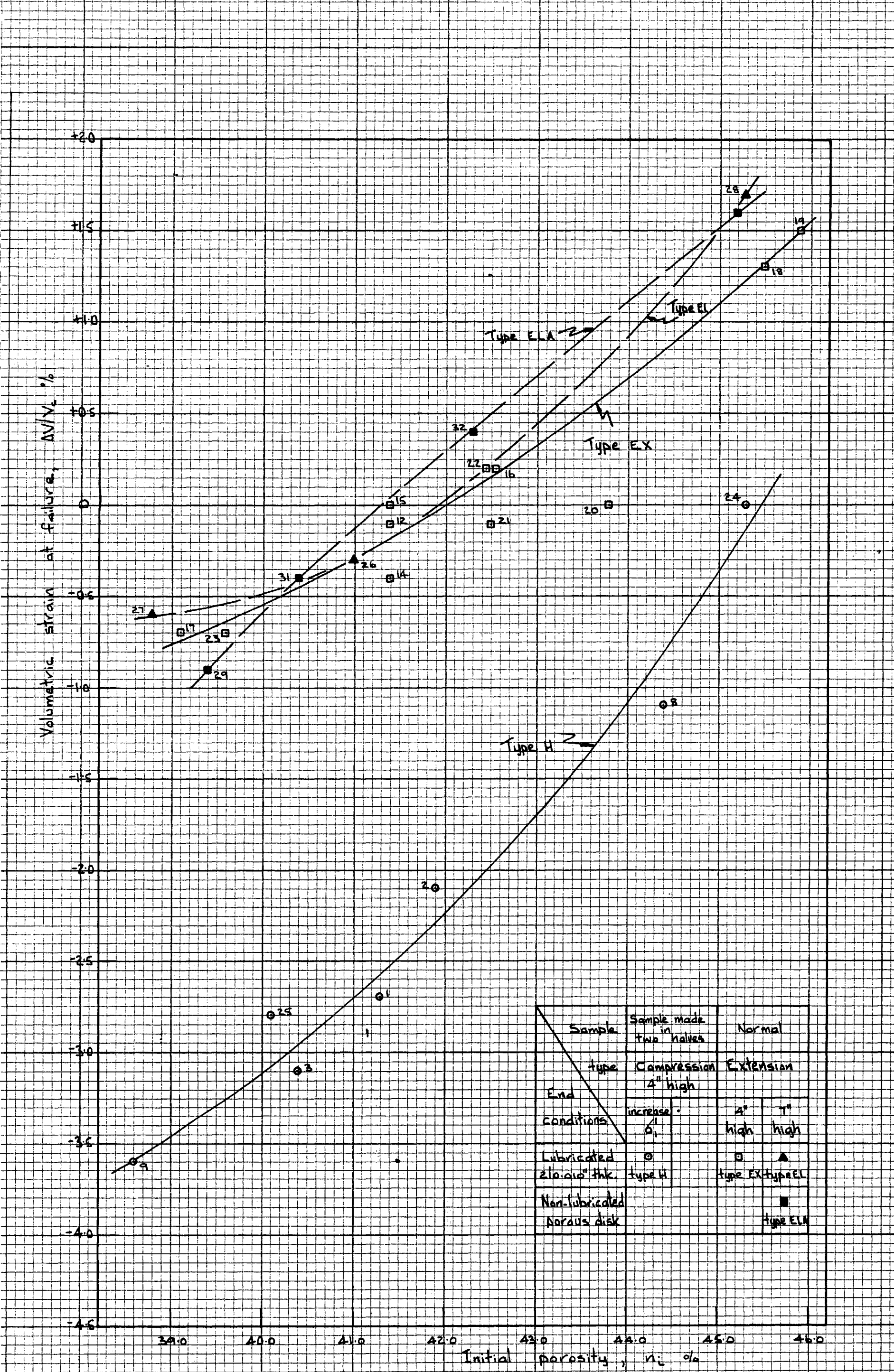
9.6 Comparison of Volumetric Strains at Failure

The volumetric strains at failure are shown in Fig 9.20 and are complimentary to the linear strains at failure. There is little significant difference in the behaviour of the three types of extension test samples. If different non-uniform deformations had occurred up to peak ϕ within the three types of extension test sample, then the volumetric strains at failure ought to be dissimilar. As previously noted, the Type EL samples exhibited necks of similar form to at least one Type EX sample, as measured up after the shear tests were completed. However they also showed relatively parallel sections, see Figs A 9.23 to A 9.25, at the ends. If this were a significant pre-failure feature then one might expect this to be reflected in the volume changes at failure, which they are not. Thus we may infer that relatively uniform volume changes occurred up to failure in all the extension test samples. This is in contrast to the behaviour of cylindrical triaxial compression test samples having different height to diameter ratios and degrees of end restraint, i.e. Types A, B & C, Fig 8.16. The volumetric strains in the extension tests are apparently less sensitive to the height to diameter ratio and degree of end restraint than in the compression tests.

The volumetric strains at failure are much lower in the extension tests than in the compression tests due partly to the higher average stress in the former case. The difference is greatest for the dense samples.

9.7 Comparison of Volumetric Strain Rates at Failure

The variation of the rate of dilatation with porosity for all the tests is shown in Fig 9.21. The influence of the stress path followed to failure in cylindrical triaxial compression is observed to be small; as

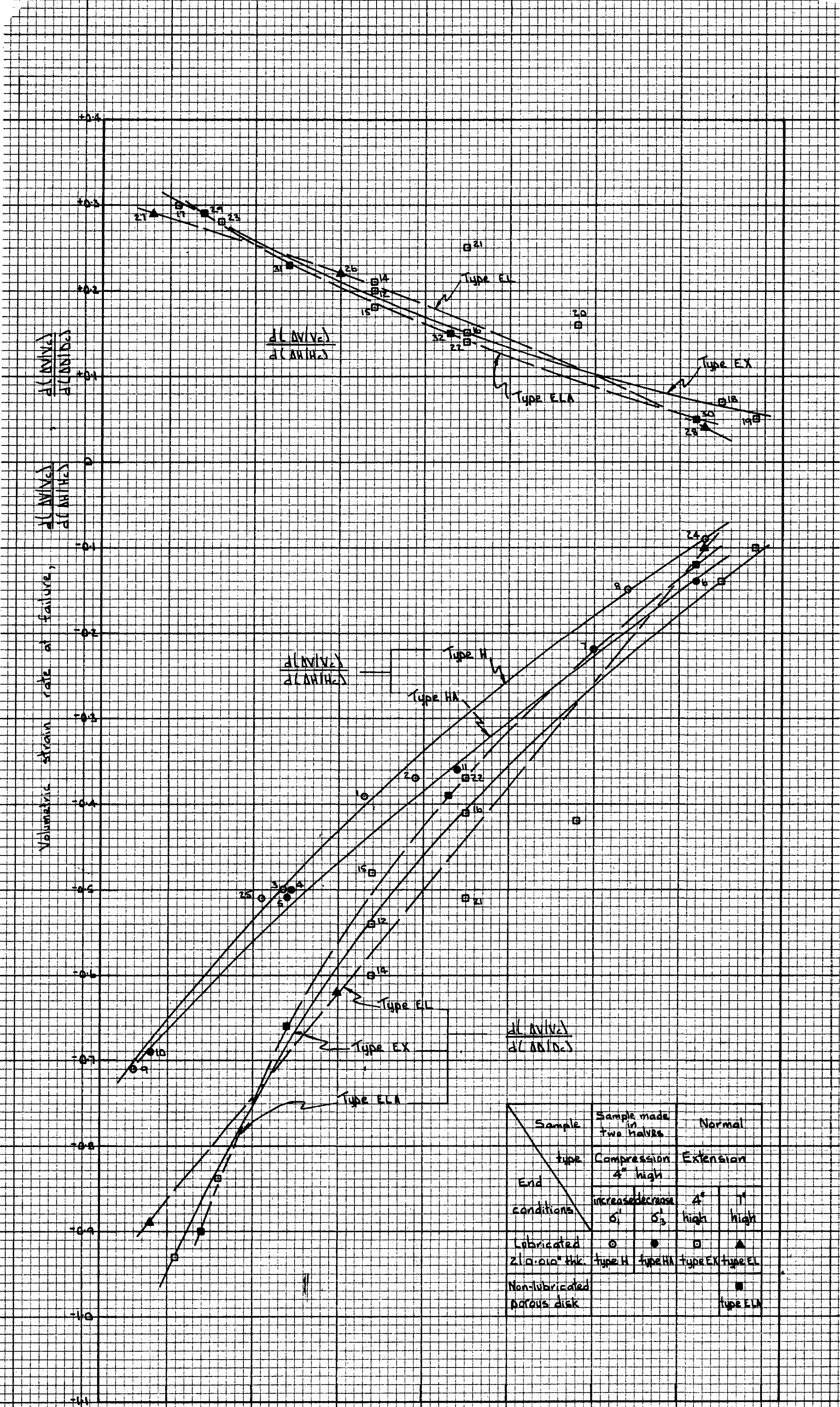


CYLINDRICAL TRIAXIAL COMPRESSION / EXTENSION.

COMPARISON OF VOLUMETRIC STRAINS AT MAXIMUM ϕ'.

Ham River Sand, Batch #2, Bag #4.

FIG. 9.20



CYLINDRICAL TRIAXIAL COMPRESSION/EXTENSION.

COMPARISON OF VOLUMETRIC STRAIN RATES AT MAXIMUM ϕ'.

Ham River Sand, Batch #2, Bag #4.

FIG. 9.21

shown by the Type H & HA test results. A mean line through these two sets of points (not shown) has a slope almost identical to that of the corresponding mean lines for the Cylindrical Triaxial Compression, 1st Series results, Fig 8.17.

There is no significant difference between the results of the three different types of extension test Type EX,EL & ELA. Thus the volumetric strain rate is independent of the H/D ratio and degree of end restraint, within the limits of the present tests.

The correlation between the volumetric strain rate with respect to mean lateral strain for the extension tests with the volumetric strain rate with respect to axial strain for the compression tests is very good at the loose end of the porosity scale. As the densities of the samples increase the results deviate, the extension tests showing numerically higher values. Little difference was observed in the behaviour of the earlier compression tests and it appears that all the extension test results follow, pretty closely, the same mean line with some deviation in the case of dense samples.

9.8 Influence of end restraint, H/D ratio and stress path

The strength and rate of dilatation at failure of cylindrical triaxial compression test samples of H/D = 1 is only slightly affected by the stress path followed. Failure under a decreasing average stress gives the same strength for dense samples and a 0.7° higher ϕ for loose samples than under an increasing average stress, Fig 9.11. The volumetric strain rates are almost identical, Fig 9.21 . These conclusions are not affected by uncertainties regarding corrections for non-uniform deformation, sample sheath strength or average stress level. The comparison of triaxial compression and extension failure characteristics should therefore not be greatly affected by the differing type of stress path followed, i.e. an increasing or decreasing average stress.

Of the 3 types of specimen tested in extension the short sample,H/D = 1, with 2/0.010 ins thick lubricated membranes at each end (Type EX) exhibited a similar strength to the two longer specimens assuming uniform deformations, Fig 9.12. However applying more appropriate area corrections to the test data results in a net difference of from 1.0 to 2.5°, the longer specimens (Type EL & ELA) giving the higher strengths. The precise magnitude of the difference is dependent on uncertainties in determining the most realistic

area correction for the Type EL & ELA tests. The Type EX specimens are therefore infered to be the most satisfactory in triaxial extension.

Comparing the corrected peak strengths measured in triaxial compression and extension for the most acceptable types of sample, Type H & EX, it is seen that the ϕ' values are identical for loose specimens and that the extension ϕ' value is 2^{o} higher for dense specimens, Fig 9.18. Corrections have been applied for non-uniform deformation, sample sheath strength and differences in average stress level. The only apparent differences remaining are the stress path type and the modes of sample preparation. The precise effect of these two factors is uncertain, they will probably tend to result in a slightly closer agreement between the two types of test than is shown, based on Type H & HA tests and on Type X & A tests.

We may conclude that, of the specimen types tested, a 4 ins diameter, 4 ins high specimen with adequately lubricated ends, in this case 2/0.010 ins thick membranes at each end, and preferably built in two halves, will give a minimum measured strength associated with the most uniform deformations. The deformations required to reach failure are generally greater than in similar tests on more conventional specimens.

Associated with similar strengths in cylindrical triaxial compression and extension the rates of dilatation with respect to the major principal strain, e_1 , are the same for loose samples but diverge slightly as the initial density is increased. For cylindrical triaxial extension the rate of dilatation is essentially unaffected by the sample proportions or degree of end restraint, as was also observed for cylindrical triaxial compression. The corresponding linear strains in cylindrical triaxial extension are about one third of those in cylindrical triaxial compression. The volume changes are also proportionally reduced.

CHAPTER 10

CUBOIDAL TRIAXIAL COMPRESSION AND EXTENSION TEST RESULTS AND DISCUSSION

10.1 Introduction

In the first two parts of the research programme, reported in the previous two chapters, it is shown that a cylindrical triaxial compression sample of H/D = 1 and with adequate lubrication of the ends, in this case 2/0.009 ins thick greased rubber membranes, gave the same strength as a conventional cylindrical sample tested in triaxial compression. Cylindrical triaxial extension tests give similar strengths to the cylindrical triaxial compression tests when compared on a conventional uniform deformation basis. After applying appropriate corrections to the strength results, most notably for the effect of necking in the extension test sample it is shown that the strength measured in extension is about 2.0° higher than that measured in compression for dense specimens, whereas for loose specimens the strengths are the same. The third part of the investigation, described in this chapter, was aimed at determining whether a cuboidal-shaped sample would give a satisfactory measure of the strength both in triaxial compression and extension.

At first sight it appears that a cubical sample should be the most suitable as it has a height to width ratio of 1 to 1. However, it is not clear what "width" to select in defining the specimen geometry of a cuboidal sample. A number are possible, (i) maximum width, or (ii) minimum width, or (iii) mean width, or (iv) width measured along a diagonal of the horizontal cross - section. For the specimen finally chosen for the ISC tests in which H = 3.3 ins, B = 3.2 ins and C = 2.1 ins, the H/D ratio is variously defined as (i) 1.0, (ii) 1.6, (iii) 1.2, and (iv) 0.9 respectively, clearly a significant variation, see Fig 8.19.

Two main series of cuboidal triaxial compression tests were performed: Type IA in which the widths B = 3.0 & C = 3.1 ins were constant and the height H was varied, 3.4, 4.1 & 4.6 ins; and Type IC in which B = 3.0, C = 2.3 & H = 3.3 ins. Based on the results of these tests two sample sizes were chosen for the extension tests, H = 3.3, B = 3.2 & C = 2.1 ins, and H = 4.1, B = 3.0 & C = 3.1 ins. In view of the limited number of test types it is not possible to conclude which of the definitions of specimen

geometry is most appropriate, c.f. the Cylindrical Triaxial Compression and Compression & Extension Tests.

All the tests on cuboidal specimens were on initially dense samples. Any differences in behaviour, particularly strength-wise, may be expected to be most marked for dense samples. It was, in addition, considered advisable to gain experience in forming dense cuboidal samples before tackling the more difficult problem of forming loose cuboidal samples.

The majority of the tests were stopped at peak strength, or as soon after as possible, the extension tests in particular, so that an ultimate or residual strength was generally not obtained.

A set of triaxial compression tests were performed as controls on short cylindrical samples, built in a normal manner, 4 ins high with 2/0.010 ins thick lubricated membranes at each end, Type IB.

Some difficulties arose in obtaining repeatable results due to what is believed to be a combination of a pressure gauge error together with an error in the caliper gauge used to measure up some of the samples. The resulting small difference in observed strengths has no major effect upon the interpretation of the results. Further details concerning this factor are given later.

Due to a combination of, (a) high cell pressure, σ_1', (b) a relatively thin sample sheath (0.010 - 0.013 ins thick), and (c) sample preparation difficulties, a number of the cuboidal extension tests, Type ICE, were unsatisfactory due to leaks in the sample sheaths, the sample lifting off the lower platten, or both. Test ICE/1 failed catastrophic - ally well before the peak strength had been reached due to the sample lifting off the lower platten which caused a leak so that the sample was destroyed. The sample in Test ICE/3 was lost due to a leak very early in the test. Neither of these two tests are reported. In Test ICE/6 the base of the sample lifted off the platten causing a premature failure, but no leak occurred. In Test ICE/9 the lower third of the sample was inadequately compacted so that a severe neck occurred and the sample exhibited a low strength. Both of these two test results are included for completeness but are considered separately from the main series of tests.

The interpretation of the results of the cuboidal triaxial extension tests is affected by similar factors to those described in the previous chapter for the cylindrical triaxial extension tests.

The definitions of stress, strain, ϕ' and porosity are identical to those given in Chapter 8. The cuboidal sample geometry is defined by the height in the axial direction, H, the width in the ISC belt direction, B, and the width in the cell direction, C. The stress-strain and volume change curves for the individual cylindrical triaxial compression and cuboidal triaxial compression & extension tests are given in Appendix A10. The basic test characteristics and failure stresses, etc, are tabulated in Fig 10.1.

10.1.1 Type IB

These were cylindrical samples, 4 ins high built in the normal manner with lubricated ends. Two 0.010 ins thick lubricated rubber membranes were used on each platten.

The samples were made in a normal manner to conform with the cuboidal samples. It was not considered feasible to form cuboidal samples in two halves on account of the difficulty in fitting the sample sheath into the mould and over the axial loading plattens. The majority of the tests were stopped close to failure but the sample was generally not measured up after dismantling the cell, except in Test IB/2.

The behaviour of the Type IB samples did not appear to differ significantly from the Types A,X & H samples. It should be noted that the difference observed between dense Type A & X samples, Fig 8.14 to 8.17 , was small so that, by inference, the mode of sample preparation is not likely to invalidate any conclusions subsequently drawn.

10.1.2 Type IA

These were cuboidal samples, B = 3.0, C = 3.1 ins, of varying height, H = 3.4, 4.1 & 4.6 ins, built in the normal manner with lubricated ends. Generally 2/0.010 ins thick lubricated rubber membranes were used at each end but in Test IA/3, 3/0.010 ins thick membranes were used instead.

Many of the tests were continued beyond the peak deviator stress up to a maximum of +20% axial strain (Test IA/3). Traces of multiple slip zones were visible above +12 to +14% axial strain, but no major slip zones were observed even at higher strains. The sample in Test IA/1, which failed at an axial strain of +7.7% and was measured up after stopping the test at an axial strain of+15.4% showed similar strains in the two lateral

Date	Test number	Sequence number	Porosity, n %			Stresses at failure psi		Strains at failure %			Volumetric strain rate at failure		ϕ' degrees	Corrected ϕ' degrees	Material	End condition	Nominal axial strain rate ins/min	Mode of sample preparation	Notes
			Initial n_i	After consolidation	At failure	Axial σ_1'	Cell $\sigma_2' = \sigma_3'$	Axial $\Delta H/H_c$	Mean lateral $\Delta D/D_c$	Volumetric $\Delta V/V_c$	$\frac{d(\Delta V/V_c)}{d(\Delta H/H_c)}$	$\frac{d(\Delta V/V_c)}{d(\Delta B/B_c)} = \frac{d(\Delta V/V_c)}{d(\Delta C/C_c)}$							
TYPE IB D=3·9 ins, H=4·1 ins, cylindrical Compression																			
25/2/66	IB/1	4	39·3	38·9	40·9	132·1	30·0	+7·7	−6·0	−3·3	−0·61		39·0	38·8	Batch 2 Bags 1&2 (mixed)	2/0·010 ins thick lubricated membranes	+0·0035	Normal	
26/2/66	IB/2	5	39·0	38·6	40·5	134·7	30·0	+7·4	−5·7	−3·2	−0·60		39·4	39·2					
1/3/66	IB/3	6	39·2	38·9	41·1	134·2	30·0	+7·8	−6·2	−3·4	−0·61		39·3	39·1					
23/4/66	IB/4	13	39·1	38·7	40·3	131·0	30·0	+7·2	−5·3	−2·8	−0·55		38·8	38·6					
26/4/66	IB/5	14	38·5	37·9	39·9	136·0	30·0	+7·1	−5·5	−3·3	−0·63		39·6	39·4					
13/5/66	IB/6	19	38·9	38·5	40·3	132·5	30·0	+7·7	−5·8	−3·1	−0·60		39·1	38·9					
TYPE IA cuboidal compression, H=3·4 ins, B=3·0 ins, C=3·1 ins																			
14/2/66	IA/1	1	39·7	39·2	41·0	135·6	30·0	+7·2	−5·5	−3·2	−0·59		39·6	39·4	Batch 2 Bags 1&2 (mixed)	2/0·010 ins	+0·0035	Normal	
17/2/66	IA/2	2	39·0	38·3	40·3	139·6	30·0	+6·8	−5·4	−3·4	−0·65		40·2	40·0					
22/2/66	IA/3	3	39·2	38·7	40·6	136·9	30·0	+6·7	−5·3	−3·3	−0·65		39·8	39·6		3/0·010 ins			
H=4·6 ins, B=3·0 ins, C=3·1 ins																			
7/3/66	IA/4	7	38·9	38·1	39·8	136·4	30·0	+6·7	−5·1	−2·9	−0·59		39·7	39·5		2/0·010 ins thick lubricated membranes	+0·007		
9/3/66	IA/5	8	38·8	38·1	39·8	137·8	30·0	+5·8	−4·5	−2·9	−0·64		39·9	39·7					
13/3/66	IA/6	9	39·5	38·9	40·5	132·2	30·0	+6·8	−4·9	−2·7	−0·57		39·1	38·9				Photo	
H=4·1 ins, B=3·0 ins, C=3·1 ins																			
15/3/66	IA/7	10	39·6	39·1	40·7	132·2	30·0	+6·7	−4·9	−2·7	−0·54		39·0	38·8					
20/3/66	IA/8	11	38·7	38·1	39·7	135·8	30·0	+6·7	−5·1	−3·0	−0·59		39·6	39·4					
22/3/66	IA/9	12	39·1	38·6	40·3	135·6	30·0	+7·4	−5·5	−3·0	−0·60		39·6	39·4			+0·0035		
14/7/66	IA/10	26	39·3	38·9	40·4	136·3	30·0	+6·7	−5·0	−2·8	−0·61		39·7	39·5					
TYPE IC cuboidal compression, H=3·3 ins, B=3·0 ins, C=2·3 ins																			
29/4/66	IC/1	15	39·7	39·3	40·9	137·0	30·0	+6·8	−5·2	−3·0	−0·61		39·8	39·6	Batch 2 Bags 1&2 (mixed)	2/0·010 ins	+0·0035	Normal	
6/5/66	IC/2	16	39·3	38·6	40·3	133·1	30·0	+7·2	−5·3	−2·9	−0·54		39·2	39·0					Photo
8/5/66	IC/3	17	38·9	38·2	40·3	132·4	30·0	+8·4	−6·2	−3·4	−0·59		39·1	38·9					
10/5/66	IC/4	18	38·6	38·1	40·0	136·2	30·0	+7·5	−5·8	−3·3	−0·62		39·7	39·5					
TYPE ICE cuboidal extension						Cell $\sigma_1' = \sigma_2'$	Axial σ_3'		$\Delta B/B_c : \Delta C/C_c$	H=3·3 ins, B=3·2 ins, C=2·1 ins										
22/5/66	ICE/2	20	39·1	37·9	38·3	140·0	27·3	−5·1	+2·1	−0·8	+0·31	−0·97	42·2	43·2	Batch 2 Bags 1&2 (mixed)	2/0·010 ins	−0·0035	Normal	
26/5/66	ICE/4	21	39·1	38·1	38·6	140·0	27·0	−4·8	+1·9	−0·8	+0·30	−0·97	42·5	43·5		3/0·010 ins			Photo
3/6/66	ICE/5	22	39·2	38·1	38·8	140·0	26·5	−5·5	+2·1	−1·1	+0·34	−1·13	42·9	43·9					
H=4·1 ins, B=3·0 ins, C=3·1 ins																			
8/6/66	ICE/7	23	39·2	38·2	38·7	140·0	26·8	−5·0	+2·0	−0·9	+0·32	−1·03	42·7	43·7		2/0·010 ins			
13/6/66	ICE/8	24	40·0	38·9	39·4	140·0	28·0	−5·0	+2·0	−0·9	+0·27	−0·81	41·7	42·7					
8/7/66	ICE/10	25	39·0	38·1	38·6	140·0	26·6	−4·6	+1·9	−0·8	+0·30	−0·96	42·9	43·9					
5/6/66	ICE/6		39·7	38·8	39·2	140·0	(30·5)	(−4·1)	(+1·7)	(−0·6)	(+0·28)	(−0·83)	(39·9)						
6/7/66	ICE/9		39·9	38·9	39·1	140·0	(32·0)	(−4·1)	(+1·8)	(−0·4)	(+0·27)	(−0·78)	(39·2)						

CUBOIDAL TRIAXIAL COMPRESSION AND EXTENSION TEST SERIES RESULTS.

FIG. 10.1

directions, Fig A 10.7. All the Type IA samples expanded at both ends but predominantly at the base. There was no apparent difference in the mode of deformation as the height of the sample was varied from 3.4 to 4.6 ins. It was generally difficult to remove the wrinkles in the sample sheath at the corners of the specimen so that a small error in the measured sample volume occurred, Plate 10.2. However, this was small enough so as to be negligible.

Plate 10.2(a) shows the sample in Test IA/6 after dismantling. The sample had an initial porosity of 39.5%, i.e. dense, and failed at an axial strain of +6.8%, the test being stopped at an axial strain of +10.7%. No slip zones are visible and the base has clearly expanded in excess of the top of the sample.

In Test IA/8 a small quantity of sand escaped adjacent to the two vertical edges of the top loading platten and was trapped between this edge and the sample sheath. The size of the resulting bulge was measured (approximately) and a correction of 0.2% applied to the initial porosity.

10.1.3 Type IC

These were cuboidal samples, B = 3.0, C = 2.3 & H = 4.1 ins, built in the normal manner with lubricated ends. Two 0.010 ins thick lubricated rubber membranes were used on each platten. The tests were stopped at or soon after failure had occurred and in Tests IC/1 & 3 the samples were measured up.

In the first test in this series, Test IC/1, an improvised cardboard and perspex packing was used inside the mould. The sample had an excessive initial taper, the base being about 0.050 ins wider than the top (in both the B and C directions). The observed lateral strains after dismantling at an axial strain +4.5% beyond that at which failure had occurred were very similar in the B and C directions, Fig A 10.17. In the subsequent 3 tests machined perspex packings were used throughout, which resulted in a much more uniform initial shape and, by inference, a more reliable result.

Plate 10.1 shows the sample in Test IC/3 after dismantling. The sample had an initial porosity of 38.9%, i.e. dense, and failed at an axial strain of +8.4%, the test being stopped at an axial strain of +9.0%. The measured strains in the B and C directions, Fig A 10.19, together with the two photographs , clearly show that, (a) the sample expanded throughout its



Cell face, C



Belt face, B

TEST IC13.

cuboidal compression,

n_i = 38.9%, H=3.3 ins, B=3.0 ins, C=2.3 ins,

2 | 0.010 ins thick membranes,

test stopped at $\Delta H/H_c$ = +9.0%,

$(\Delta H/H_c)_f$ = +8.4%.

PLATE 10.1



(a) TEST IA16.
cuboidal compression,
n_i = 39·5%, H = 4·6 ins, B = 3·0 ins, C = 3·1 ins,
2 10·010 ins thick membranes,
test stopped at $\Delta H/H_c$ = +10·7%,
$(\Delta H/H_c)_f$ = + 6·8%.



(b) TEST ICE14.
cuboidal extension,
n_i = 39·1%, H = 3·3 ins, B = 3·2 ins, C = 2·1 ins,
3 10·010 ins thick membranes,
test stopped at $\Delta H/H_c$ = - 5·5%,
$(\Delta H/H_c)_f$ = - 4·8%.

PLATE 10.2

height, (b) the base expanded more than the top, and (c) the strains in the B and C directions were almost identical.

The mode of deformation in Tests IC/2 & 4 was similar to that in Test IC/3. No slip zones were observed in any test in this series.

10.1.4 Type ICE

These cuboidal samples were of dimensions B = 3.2, C = 2.1 & H = 3.3 ins or B = 3.0, C = 3.1 & H = 4.1 ins, built in the normal manner with lubricated ends. Normally 2/0.010 ins thick lubricated rubber membranes were used on each platten but in Test ICE/4, 3/0.010 ins thick membranes were used instead. Tests ICE/2, 4 & 5 were on samples B = 3.2, C = 2.1 & H = 4.1 ins.

In Test ICE/6 the base of the sample lifted off the lower platten causing premature failure. The lateral strains measured after dismantling the cell suggest that a neck had begun to form at the base of the sample, but the test was stopped too early for it to be well defined, Fig A 10.24. The lateral strains in the B and C directions are virtually identical at corresponding positions along the height of the sample. In Test ICE/9 the lower third of the sample was inadequately compacted so that a severe neck occurred, Fig A 10.24. Again the lateral strains are very consistent in the two directions, even within the neck.

The samples in Tests ICE/2 & 5 were measured up after dismantling the cell, Figs A 10.21 & A 10.22, and show that (a) the upper portion had contracted uniformly, (b) a neck had formed at the base, and (c) the strains in the B and C directions were very similar.

Plate 10.2(b) shows the sample in Test ICE/4 after dismantling. The sample had an initial porosity of 39.7%, i.e. dense, and failed at an axial strain of -4.8%, the test being stopped at an axial strain of -5.5%. A well defined slip zone is seen at the top of the sample. Unfortunately, the sample was not measured up after dismantling the cell.

All the Type ICE tests were stopped at, or soon after, peak ϕ' and frequently the beginnings of a predominant slip zone were visible either at the base or at the top of the sample, e.g. Test ICE/4, Plate 10.2(b). The cuboidal extension samples never exhibited a central neck, c.f. Test EX/8, Plate 9.1 .

10.2 Comparison of stress-strain and volume change curves

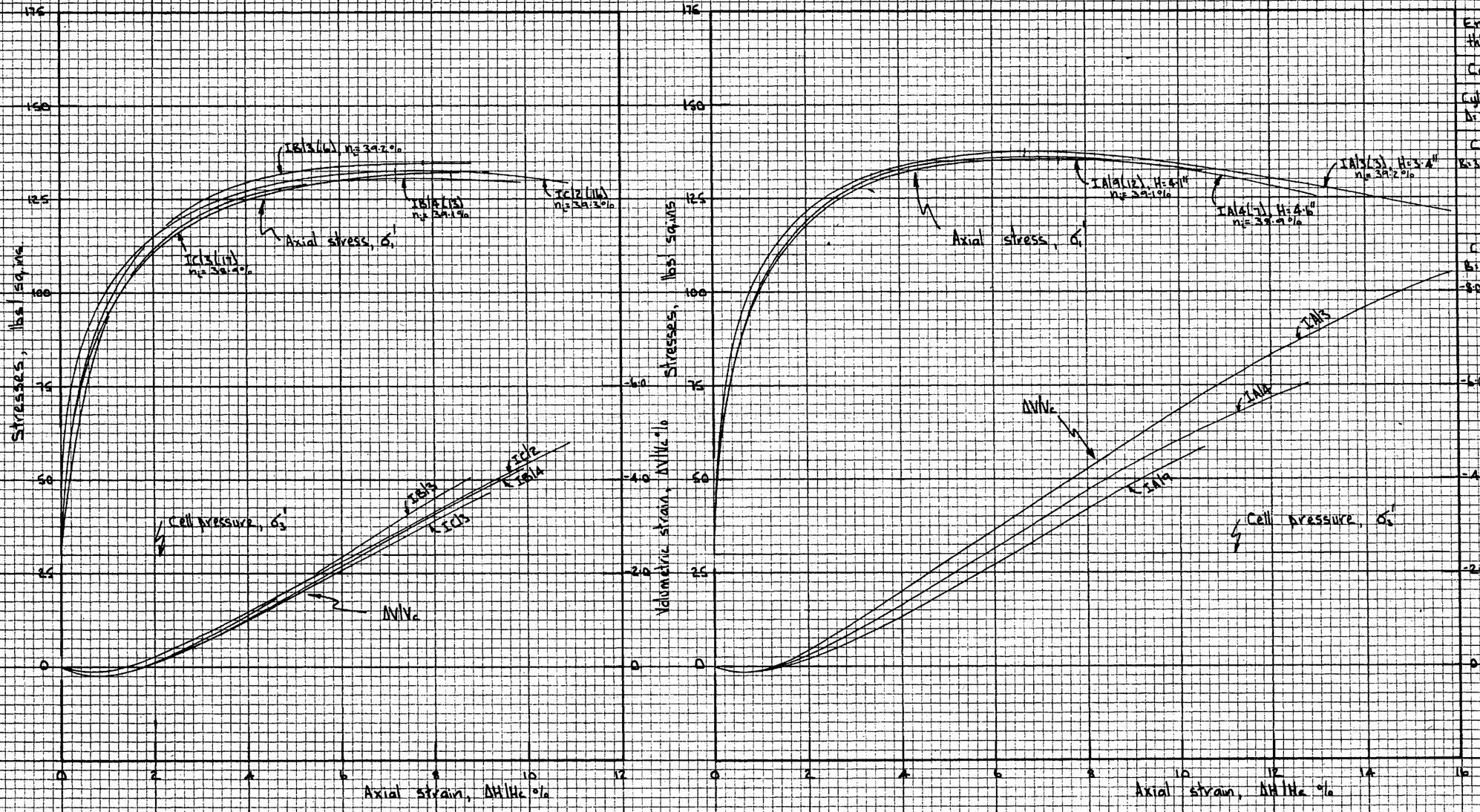
The stress-strain and volume change characteristics of selected tests are shown in Figs 10.2, 10.3, 10.4 & 10.5. All the tests were on initially dense samples so that any differences attributable to the sample shape should be readily distinguished.

Fig 10.2 shows a series of Type IA tests in which the sample cross-section was maintained constant whilst the height, H, was varied, 3.4, 4.1 & 4.6 ins. The stress-strain curve for the shortest sample, Test IA/3, lies slightly above those for the other two tests which are almost indistinguishable. The volume change curves show that the volume change of the shortest sample was greater than that in Tests IA/4 & 9, but that the latter two test results are the reverse of their expected order. The data for the Type IA cuboidal triaxial compression samples is compatible with that for similar cylindrical triaxial compression samples of varying H/D ratios, Tests A/12, X/3 & C/5 in Fig 8.4.

Fig 10.3 shows the results for the same three Type IA tests together with two Type IC tests in which the width of the sample in the coil direction, C, was reduced to 2.3 ins, c.f. Test IA/3. The stress-strain and volume change curves for the Type IA tests lie slightly above those for the Type IC tests and the axial strains at failure are marginally lower.

Thus it appears that for the sample sizes tested the effect of end restraint is minimum in cuboidal samples with B = 3.0, C = 2.3 & H = 3.3 ins, Type IC, so that this shape was chosen as the optimum. Fig 10.2 shows the Type IC test results together with the cylindrical triaxial compression control test, Type IB, results. There appears to be no significant difference between the stress-strain and volume change curves for the cuboidal triaxial compression samples, Type IC, and the cylindrical triaxial compression samples, Type IB.

The results of 3 cuboidal triaxial extension tests are shown in Fig 10.4. Tests ICE/4 & 5 were carried out on samples of a shape subsequently chosen for the ISC tests whereas Test ICE/7 was on the larger sample. There is no significant difference between the stress-strain and volume change behaviour of the 3 samples. Furthermore, in Test ICE/4, 3/0.010 ins thick lubricated rubber membranes were used at each platten rather than the normal 2/0.010 ins thick membranes. This appears to have had no effect on the value of the maximum deviator stress, although the slope of



End conditions: lubricated, 2 10.010" thk membranes generally used

Compression

Cylindrical D: 5.9", H: 4.1" type IB

Cuboidal B: 3.0", C: 5.1" type IA
H: 3.4"
H: 4.1"
H: 4.6"

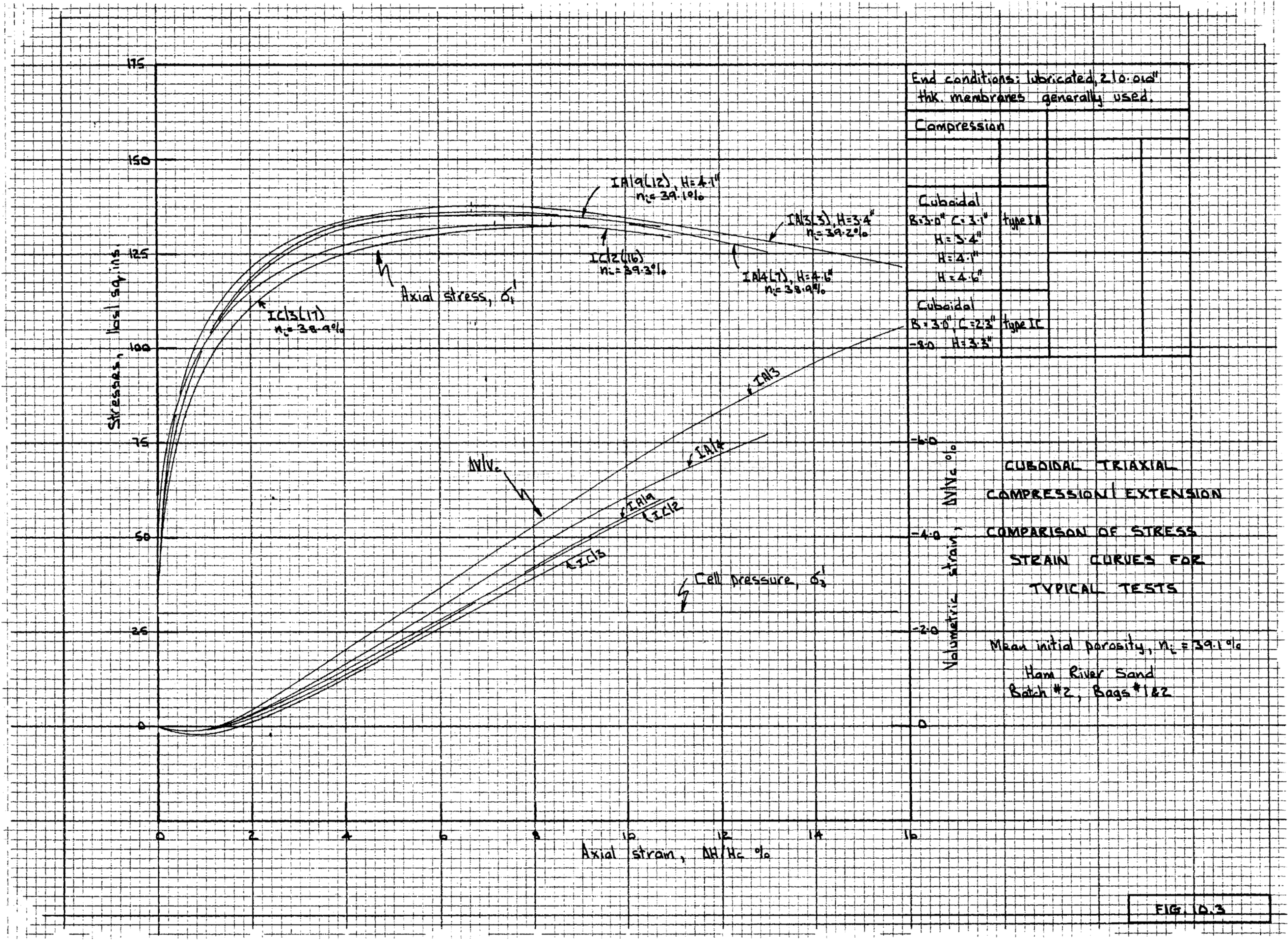
Cuboidal B: 3.0", C: 2.5" type IC
H: 3.3"

CUBOIDAL TRIAXIAL COMPRESSION / EXTENSION COMPARISON OF STRESS STRAIN CURVES FOR TYPICAL TESTS

Mean initial porosity, n_i = 39.1%

Ham River Sand
Batch #2, Bags # 1 & 2

FIG. 10.2



End conditions: lubricated, 2 10·010" thk. membranes generally used.

Compression

Cuboidal
B=3·0" C=3·1" type IA
H=3·4"
H=4·1"
H=4·6"

Cuboidal
B=3·0", C=2·3" type IC
H=3·3"

CUBOIDAL TRIAXIAL COMPRESSION/EXTENSION

COMPARISON OF STRESS STRAIN CURVES FOR TYPICAL TESTS

Mean initial porosity, n_i = 39·1%

Ham River Sand
Batch #2, Bags #1&2

FIG. 10.3

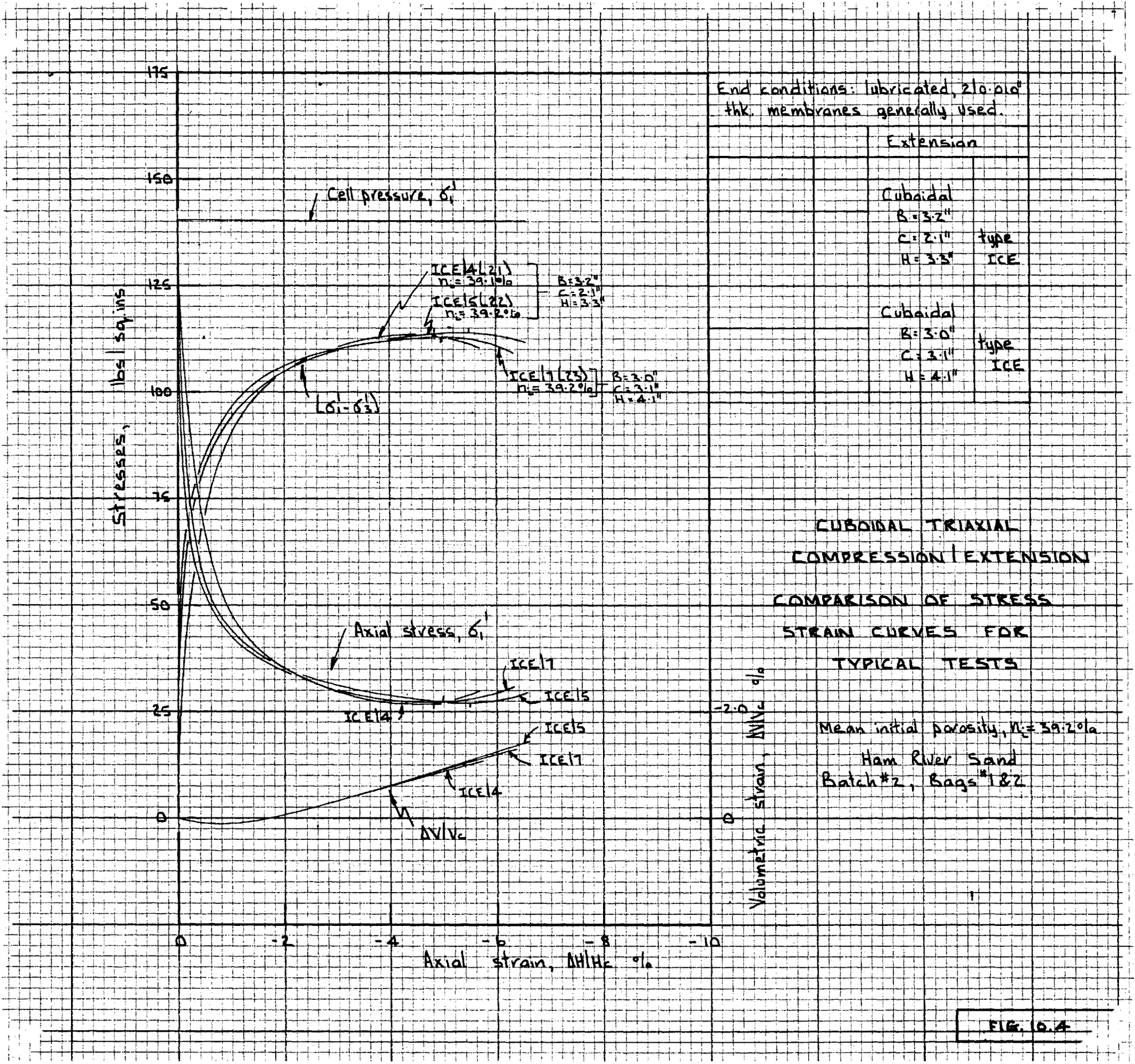

End conditions: lubricated, 2 to 0.01" thk. membranes generally used.
Extension
Cuboidal B = 3.2" C = 2.1" H = 3.3" type ICE
Cuboidal B = 3.0" C = 3.1" H = 4.1" type ICE
CUBOIDAL TRIAXIAL COMPRESSION / EXTENSION
COMPARISON OF STRESS STRAIN CURVES FOR TYPICAL TESTS
Mean initial porosity, n_c = 39.2%
Ham River Sand
Batch #2, Bags #1 & 2
Cell pressure, σ3'
Axial stress, σ1'
(σ1' - σ3')
ICE 4 (21) n_c = 39.1%
ICE 5 (22) n_c = 39.2%
ICE 7 (23) n_c = 39.2%
B = 3.2" C = 2.1" H = 3.3"
B = 3.0" C = 3.1" H = 4.1"
ICE 4
ICE 5
ICE 7
ΔV/Vc
Stresses, lbs / sq. ins
Axial strain, ΔH/Hc %
Volumetric strain, ΔV/Vc %
175
150
125
100
75
50
25
0
-2
-4
-6
-8
-10
-2.0

FIG. 10.4

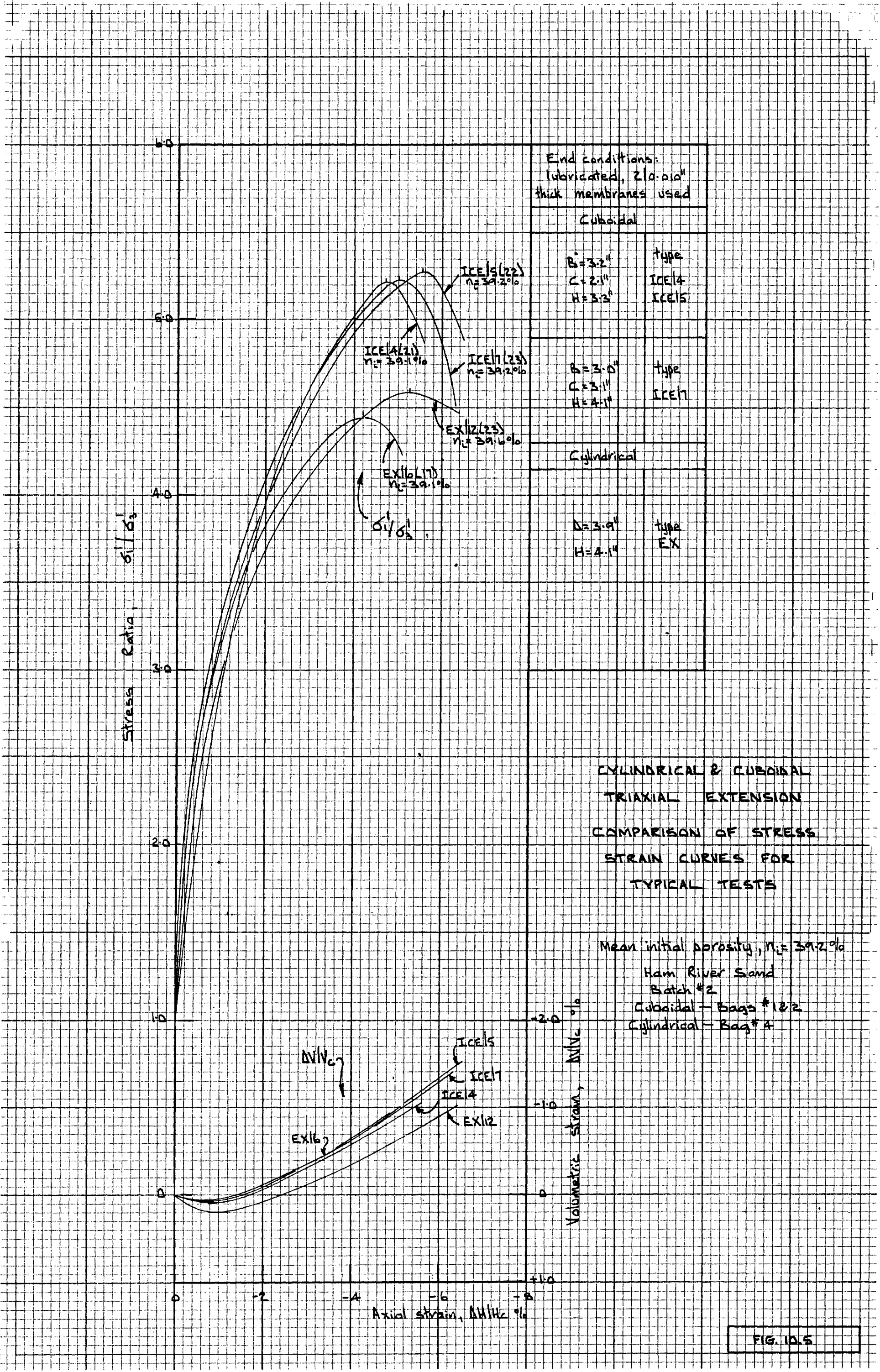

End conditions:
lubricated, 2 | 0.010" thick membranes used
Cuboidal
B = 3.2"
C = 2.1"
H = 3.3"
type
ICE 14
ICE 15
B = 3.0"
C = 3.1"
H = 4.1"
type
ICE 17
Cylindrical
D = 3.9"
H = 4.1"
type
EX
ICE 15 (22)
n_i = 39.2%
ICE 14 (21)
n_i = 39.1%
ICE 17 (23)
n_i = 39.2%
EX 12 (23)
n_i = 39.6%
EX 16 (17)
n_i = 39.1%
σ1'/σ3'
Stress Ratio, σ1'/σ3'
6.0
5.0
4.0
3.0
2.0
1.0
CYLINDRICAL & CUBOIDAL
TRIAXIAL EXTENSION
COMPARISON OF STRESS
STRAIN CURVES FOR
TYPICAL TESTS
Mean initial porosity, n_i = 39.2%
Ham River Sand
Batch #2
Cuboidal – Bags #1 & 2
Cylindrical – Bag #4
ΔV/V_c
ICE 15
ICE 17
ICE 14
EX 12
EX 16?
-2.0
-1.0
0
+1.0
Volumetric strain, ΔV/V_c %
0
-2
-4
-6
-8
Axial strain, ΔH/H_c %

FIG. 10.5

the initial portion of the stress-strain curve is significantly lower than in that in Tests ICE/5 & 7. This is consistent with the behaviour of the cylindrical triaxial compression test samples, e.g. Test A/12, Fig 8.4 and Test SD1/2, Fig 8.6.

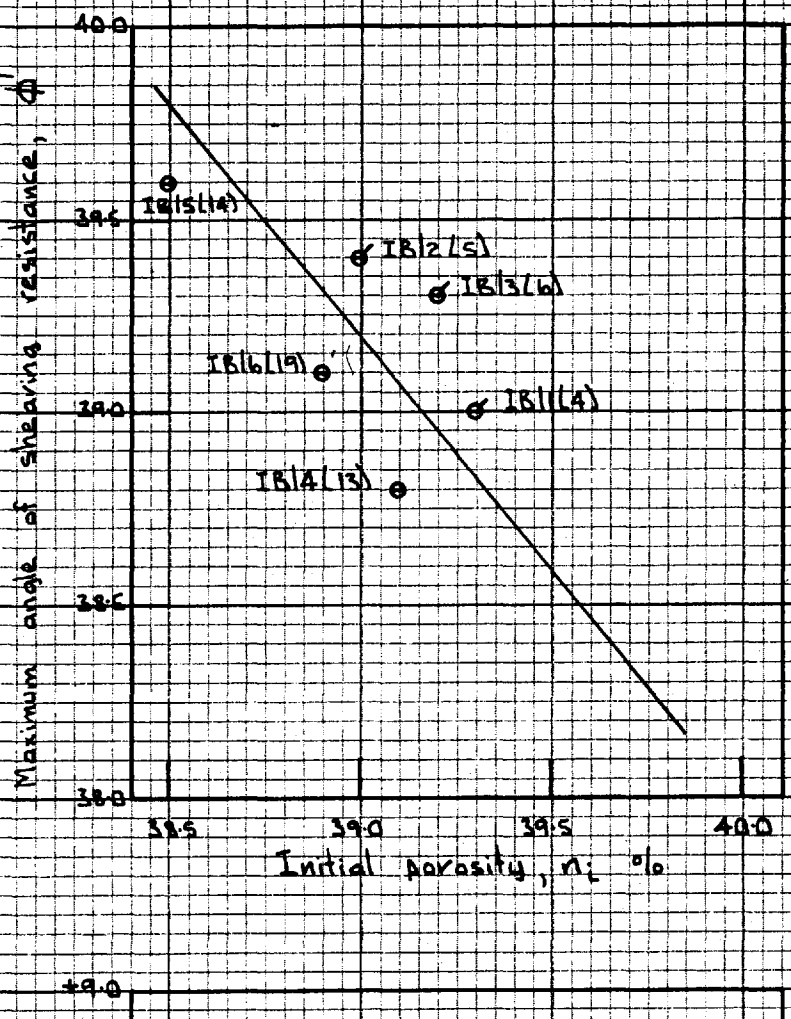
The stress-strain curves for the cuboidal triaxial extension tests are not directly comparable with those for the cylindrical triaxial extension tests since the minor principal stress, σ_3', was reduced from 40 to 30 psi for the cuboidal and ISC tests in order to reduce the stress in the perspex wall of the ISC cell. The 3 cuboidal triaxial extension test results are therefore compared with the results of 2 cylindrical triaxial extension tests, EX/6 & 12 (Fig A 9.17) on a principal stress ratio, σ_1'/σ_3', basis, Fig 10.5. There is little difference between the volume change characteristics of the two types of test whereas the cuboidal samples clearly show a significantly higher strength. Sand from different numbered bags was used for the two series of tests. However, there appears to be no difference between the peak compression strengths of the two materials, Fig 10.3, so that a comparison of the extension test results is considered justified.

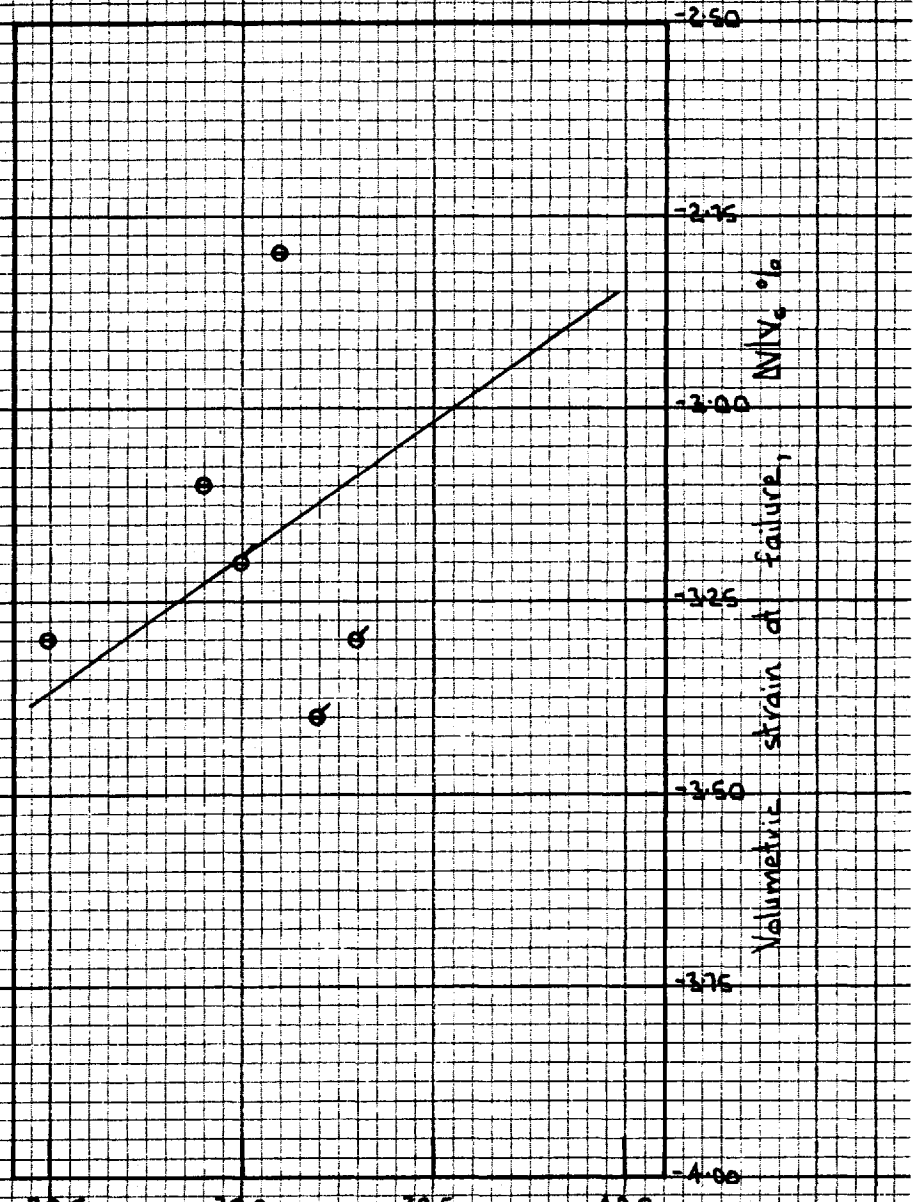
10.3 Comparison of failure characteristics

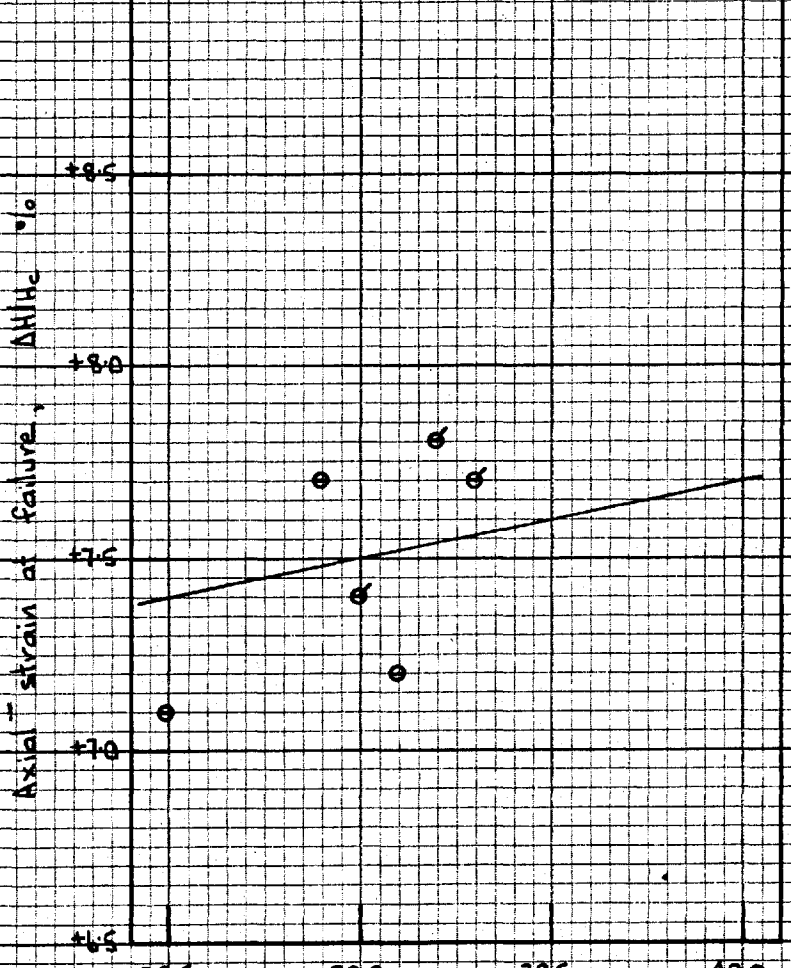
For each test type the failure characteristics are plotted against the initial porosity, Figs 10.6 to 10.9. The correlation between the tests at different porosities for a particular test type is seen to be good. For the extension tests, Type ICE, the mean lateral strain and the volumetric strain rate with respect to the mean lateral strain are plotted for comparison purposes.

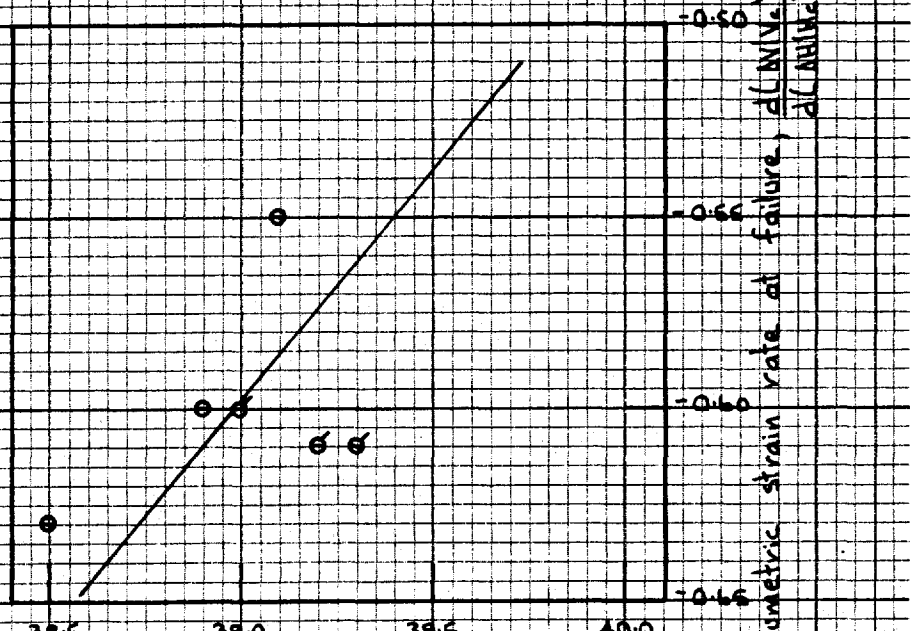
The observed compression strengths of the 4 ins diameter, 4 ins high samples made in a normal manner with 2/0.010 ins thick lubricated membranes at each end, Type IB, varied slightly, Fig 10.6. Tests IB/1(4), 2(5) & 3(6) exhibit a mean strength 0.4° higher than Tests IB/4(13), 5(14) & 6(19).

It was necessary to reset the caliper gauge for the intermediate tests on cuboidal samples IA/4(7) to IA/9(12) and it is believed that this was, in part, the cause of the non-repeatability of the latter 3 type IB tests. In Test IB/4(13) and all subsequent tests vernier calipers were used to measure up all the samples so that this type of error could not arise. A small discrepancy of 0.004 ins in the caliper gauge zero reading was discovered, which would decrease the measured initial porosity of the samples







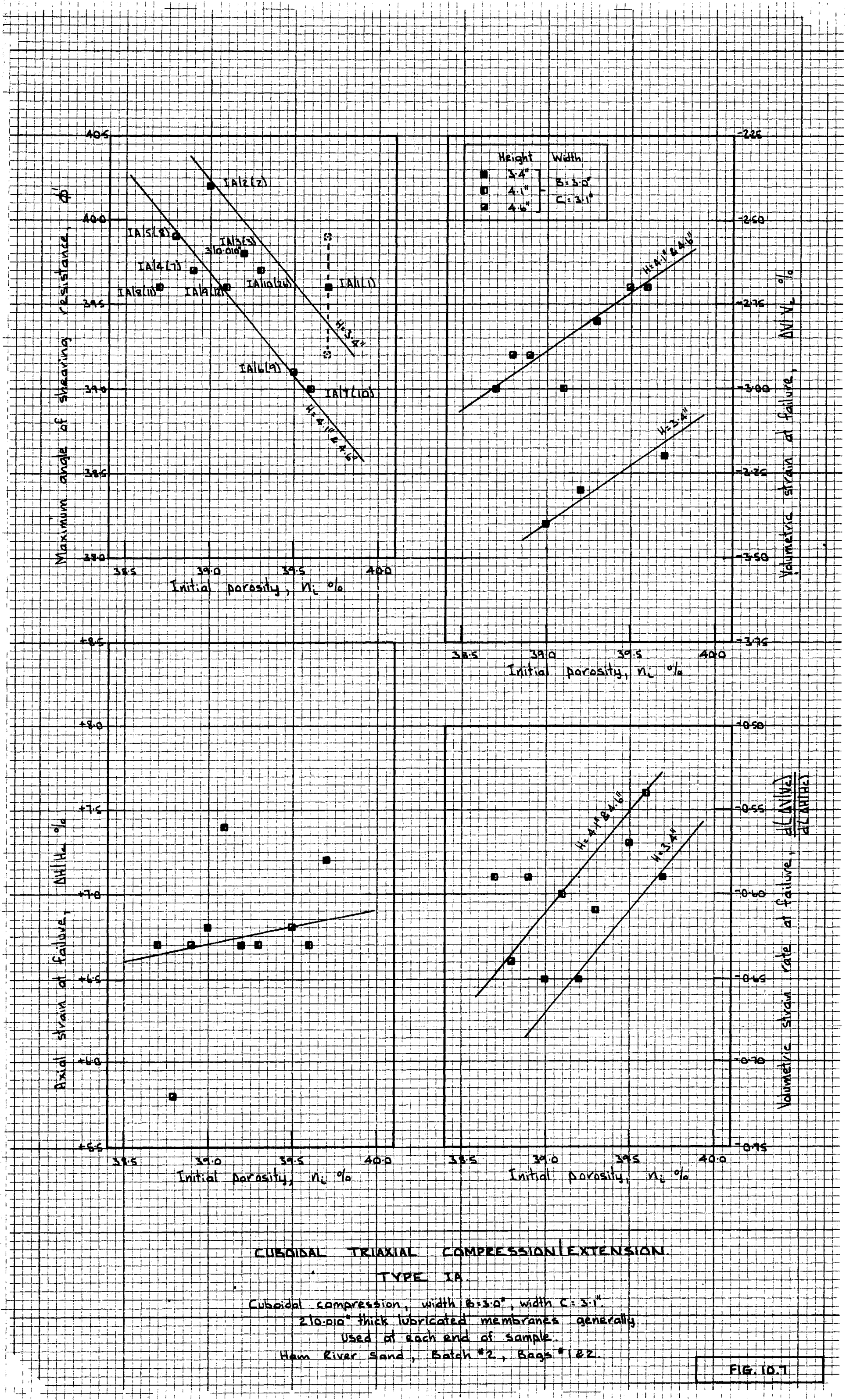


CUBOIDAL TRIAXIAL COMPRESSION / EXTENSION.

TYPE IB.

Cylindrical compression, diameter D = 3·9", height H = 4·1"
2 | 0·010" thick lubricated membranes used
at each end of sample.
Ham River Sand, Batch #2, Bags #1&2.

FIG. 10.6

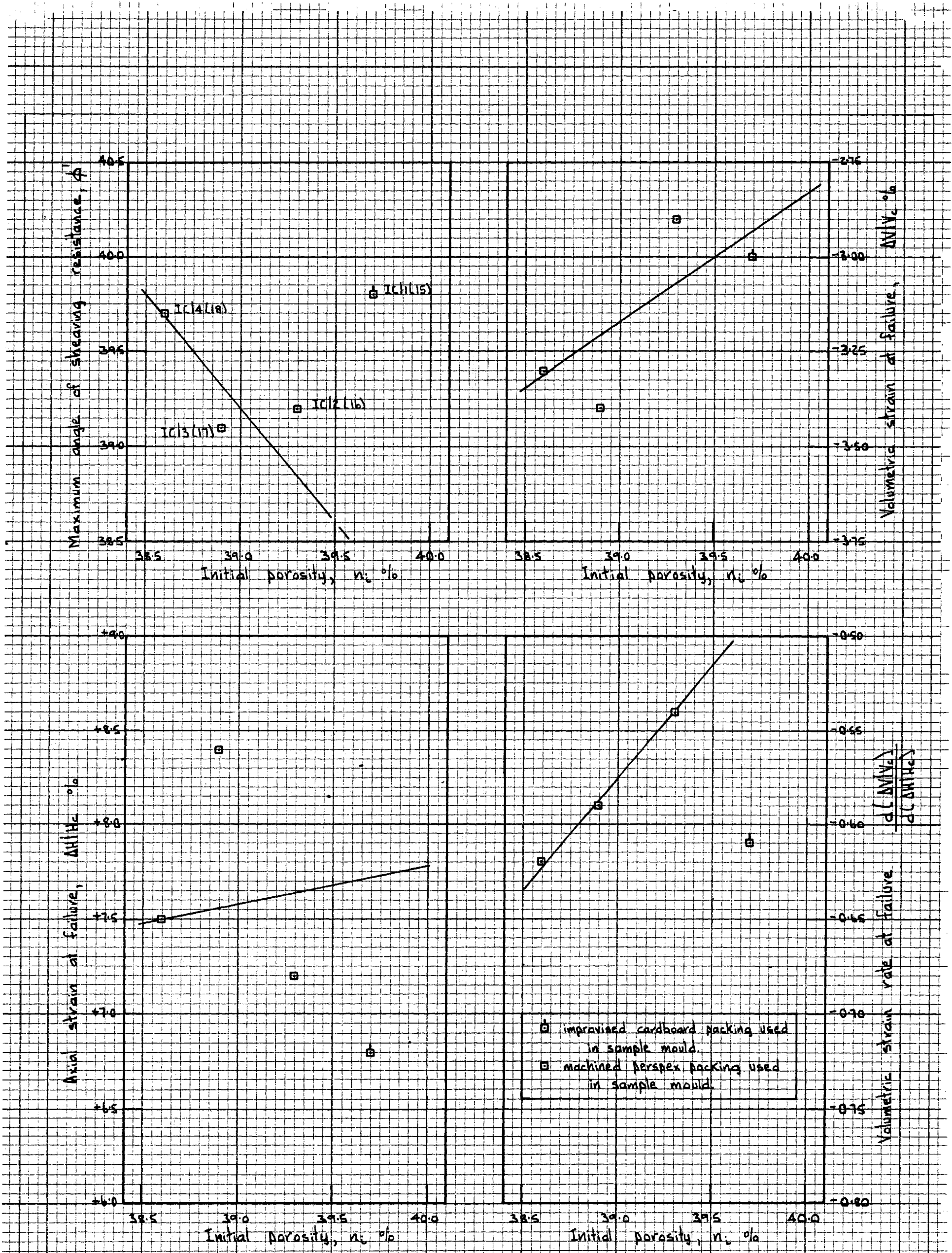


CUBOIDAL TRIAXIAL COMPRESSION/EXTENSION.

TYPE IA.

Cuboidal compression, width B: 3·0", width C: 3·1".
2|0·010" thick lubricated membranes generally used at each end of sample.
Ham River Sand, Batch #2, Bags #182.

FIG. 10.7



CUBOIDAL TRIAXIAL COMPRESSION / EXTENSION.

TYPE IC.

Cuboidal compression, width B = 3·0", width C = 2·5", height H = 3·5".
2 lo·oio" thick lubricated membranes used at each end of sample.
Ham River Sand, Batch #2, Bags # 1&2.

FIG. 10.8

in Tests IB/1(4), 2(5) & 3(6) by 0.1%. However, it would also increase the measured ϕ' value by about 0.1° so that the errors tend to be self-compensating. In addition, the pressure gauge was recalibrated immediately prior to Test IB/6(19) and a 0.1 psi change was found to have occurred which is equivalent to a 0.05° change in the value of ϕ' measured in the Type IB tests. Clearly these two factors alone are insufficient to explain the 0.4° change. Nevertheless they, together with other factors which cannot be pinpointed, are believed to have caused the change. Discrepancies also occur in the correlations of volumetric strain and volumetric strain rate whereas the axial strain at failure is unaffected. For comparison purposes the mean lines are based upon all 6 test results although it is possible that Tests IB/4(13), 5(14) & 6(19) are more correct. The slopes of the relevant strength-porosity and strain-porosity relationships from earlier test series are assumed to apply when plotting the mean lines. It should perhaps be pointed out that the scales in Fig 10.6 are very open and, when compared with the results of the Cylindrical Triaxial Compression, 2nd Series results, Fig 8.18, the Type IB test results are therefore only marginally beyond what might be considered acceptable limits.

The results of the cuboidal triaxial compression tests on samples of dimensions B = 3.0, C = 3.1 and H = 3.4, 4.1 & 4.6 ins, Type IA, are shown in Fig 10.7. They form two distinct groups. The longer samples, H = 4.1 & 4.6 ins, give similar failure characteristics whereas the short samples, H = 3.4 ins, give strengths 0.5° higher, together with significant differences in the volumetric strains and volumetric strain rates. The initial porosity in Test IA/8(11) is low and although a correction was applied (see Section 10.1.1) the ϕ' value is still marginally low. Otherwise the correlations between the measured strength are good. The axial strains at failure in Tests IA/5(8) & 9(12) are low and high respectively, the reason for which is not known. In Test IA/3(3), 3/0.010 ins thick lubricated membranes were used at each end of the sample. There are no differences in the observed failure characteristics, so that we may conclude that 2/0.010 ins thick lubricated membranes are adequate. Also shown are possible upper and lower bound ϕ' values for Test IA/1(1), 39.9° and 39.2° respectively, which failed at +7.2% and was stopped at +15.4% axial strain. These bounds are calculated on a similar basis to those for Test H/7(25), see Fig 9.5 and Section 9.3. The true ϕ' value is probably within a

much smaller range than is contained by these bounds. In fact, the value obtained based on the average cross-sectional area over the whole sample, 39.6°, is probably very close indeed to the true strength. The difference between the upper and lower bound ϕ' values, 0.7° compares favourably with the corresponding difference of 1.0° for Test H/7(25).

The results of the cuboidal triaxial compression tests on samples of dimensions B = 3.0, C = 2.3 & H = 3.3 ins, Type IC, are shown in Fig 10.8. With the exception of Test IC/1(15) the results are self-consistent. The sample in Test IC/1(15) was initially tapered due to its mode of preparation. The results of this test are therefore excluded from later comparisons of peak strengths etc. Also shown are possible upper and lower bound ϕ' values for Test IC/3(17), 39.3° and 38.9° respectively, which failed at +8.4% and was stopped at +9.0% axial strain (Fig A 10.19 & Plate 10.1). Again the true ϕ' value lies within a much smaller range than is contained by these bounds. That based on the average cross-sectional area, 39.1°, is probably very close indeed to the true strength. Thus we may infer that ϕ' values based on the average cross-sectional area are directly comparable for the cylindrical and cuboidal triaxial compression tests.

The results of six triaxial extension tests, Type ICE, on cuboidal samples are shown in Fig 10.9. The mean lines are based on these six tests, the slopes being assumed to be identical to similar triaxial extension tests on cylindrical samples. In addition the results of Tests ICE/6 & 9 are also shown which failed prematurely and are therefore considered unacceptable in later test type comparisons. There are no significant differences between the failure characteristics of the six acceptable tests, bearing in mind the likely scatter in triaxial extension test results. That is, there is no difference between the results obtained with samples of dimensions B = 3.2, C = 2.1 & H = 3.3 ins or B = 3.2, C = 3.1 & H = 4.1 ins. This conclusion is in agreement with similar extension tests on cylindrical samples, Types EX & EL, which gave similar failure characteristics for dense samples, Figs 9.12, 9.19, 9.20, 9.21. Moreover, with the exception of ϕ' the failure characteristics of the cuboidal and cylindrical extension samples are similar in magnitude. The ϕ' values and strains at failure for the two samples that failed prematurely are low, whereas the volumetric strain rates are similar to those of the main group. This latter agreement is reasonable since the shape of the volume change

curve is linear at and before failure in an acceptable test.

In view of the high strengths obtained in the cuboidal extension tests the testing technique was varied a little to see if a reason for the increase could be found. Firstly, in Test ICE/4, 3/0.010 ins thick lubricated membranes were used at each platten, but no change in behaviour resulted. Secondly, samples in Tests ICE/6, 8 & 9 were tamped in layers whereas in Tests ICE/4 & 10 and in Tests ICE/2,5 & 7 the samples were vibrated in a single lift and in layers, respectively. This appears to have had no significant effect on the results. Thirdly, the upper loading platten was, in general, connected to the anvil of the axial proving ring by a $\frac{1}{4}$ ins diameter steel rod in double shear, allowing one degree of rotational freedom, Fig 4.4. In Test ICE/5 this shear pin was replaced by the bayonet-type extension fitting used in the cylindrical triaxial extension tests, Fig 4.3. This change also appears to have had little effect upon the test results. Fourthly, due to the difficulty in fitting the cylindrical sample sheath over the loading plattens the initial tension in the sheath was probably different at the belt and cell face sample/platten junctions. If the sample sheath does not slip over the platten adjacent to the junctions on the belt faces during shear, undesirably high stresses may be set up in the sheath at these points. In Test ICE/6 the transition section and edges of the plattens were lubricated with silicone grease to ensure that slip was possible. Unfortunately the base of the sample lifted off the platten and caused premature failure. That the low value of ϕ' observed is close to that given in similar cylindrical triaxial extension tests is believed to be fortuitous. This technique did not appear to be very promising and was not pursued. Finally, it may be postulated that the cuboidal extension samples fail in "plane strain", which could account for the increased strength (see Chapter 11). This would imply that the lateral strains should be different in the B and C directions. Reference to Figs A 10.21, A 10.22 & A 10.24 shows that the strains based on end of test measurements do not support this theory, i.e. they are the same in the B and C directions. However we might further postulate that there is a transition from equal lateral strains to a "plane strain" condition just before failure, which is undetectable in the present tests. This seems an unlikely possibility, although it could be usefully investigated. It appears therefore that the observed strengths in cuboidal triaxial exten-

sion are well established.

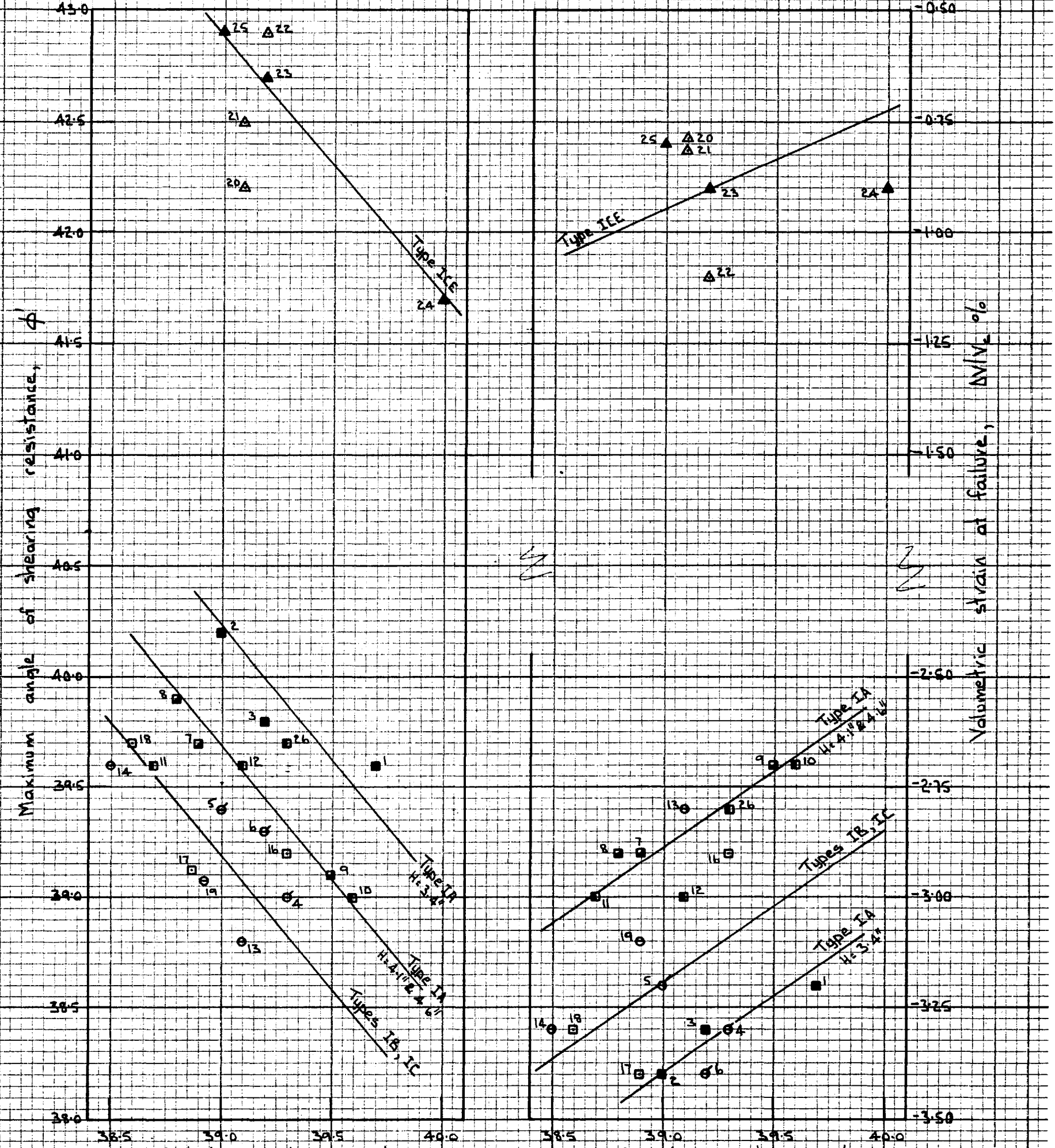
It is pertinent to see if a more realistic sample cross-sectional area correction may be applied to the cuboidal triaxial extension test results in a similar manner to that applied to the cylindrical triaxial extension samples. Also shown in Fig 10.9 are adjusted ϕ' values for Tests ICE/2(20)& 5(22) and ICE/6 & 9. These adjustments are made on the basis that the measured shape of the sample after the test approximates closely to a frustum of a right rectangular pyramid, for which the equations given in Fig 9.16 will still hold. The area at failure is assumed to correspond to A_2. The adjusted ϕ' values for the four tests are 1.5, 0.6, 0.6 & 1.3° respectively, higher than those calculated assuming uniform deformation. As with the cylindrical samples, Fig 9.17 , the magnitude of the increase in ϕ' does not appear to depend on the strain at which the test was stopped, Fig 10.12. The four tests give an average increase in ϕ' of 1.0° and although Tests ICE/6 & 9 failed prematurely they are considered valid as far as the cross-sectional area correction is concerned. It may be noted that if the two pairs of tests be considered separately, they each give an average increase of 1.0°. Thus the neck area corrections have an identical effect for the cylindrical and cuboidal triaxial extension samples of raising the ϕ' value by 1.0°.

10.4 Comparison of Peak Strengths

The peak strengths measured in all the cuboidal triaxial compression and extension tests together with the cylindrical triaxial compression tests, Type IB, are compared in Fig 10.10. The plotted points are based on the assumption that the samples deform uniformly.

The cuboidal samples, Type IC, exhibit similar compression strengths to the cylindrical compression samples, Type IB. The Type IA samples show an increase of 0.5° for the two ~~la~~en~~r~~gest samples, H =4.1 & 4.6 ins, and an increase of 1.0° for the shortest samples, H = 3.4 ins, over the strengths of the Type IB & IC samples. The precise magnitudes of these increases are complicated by the uncertainty noted earlier about the repeatability of the cylindrical triaxial compression tests, Type IB. However this is not too serious for our present purpose.

The sample sheath strength corrections for the cuboidal triaxial compression test samples are shown in Appendix A 6 to be negligible. It has



End conditions: lubricated, 2 to .010" thk. membranes generally used.			
Compression		Extension	
Cylindrical D = 3·9", H = 4·1"	θ σ type IB	Cuboidal B = 3·2" C = 2·1" H = 3·3"	type ICE △
Cuboidal B = 3·0", C = 3·1" H = 3·4"	type IA ■		
H = 4·1"	▣		
H = 4·6"	◪		
Cuboidal B = 3·0", C = 2·3" H = 3·3"	type IC ⊡	Cuboidal B = 3·0" C = 3·1" H = 4·1"	type ICE ▲

CUBOIDAL TRIAXIAL COMPRESSION / EXTENSION.

COMPARISON OF PEAK STRENGTHS AND OF VOLUMETRIC STRAINS AT MAXIMUM ϕ'.

Ham River Sand, Batch #2, Bags #1&2.

FIG. 10.10

Axial strain, $\Delta H/H_c$

Lateral strain $\Delta B/B_c = \Delta C/C_c$

Axial (Lateral) strain at failure, $\Delta H/H_c$ (or $\Delta B/B_c = \Delta C/C_c$), %

Type IA

Type IB

Type IC

Type ICE

$\frac{d(\Delta V/V_c)}{d(\Delta H/H_c)}$

$\frac{d(\Delta V/V_c)}{d(\Delta B/B_c)} = \frac{d(\Delta V/V_c)}{d(\Delta C/C_c)}$

Volumetric strain rate at failure, $\frac{d(\Delta V/V_c)}{d(\Delta H/H_c)}$ (or $\frac{d(\Delta V/V_c)}{d(\Delta B/B_c)} = \frac{d(\Delta V/V_c)}{d(\Delta C/C_c)}$), %

Initial porosity n_i %

End conditions: lubricated, 2 to 10 thk. membranes generally used			
Compression		Extension	
Cylindrical D=3·9", H=4·1"	type IB ● ○	Cuboidal B=3·2" C=2·1" H=3·3"	type ICE △
Cuboidal B=3·0", C=3·1" H=3·4"	type IA ■		
H=4·1"	□		
H=4·6"	▣	Cuboidal B=3·0" C=3·1" H=4·1"	type ICE ▲
Cuboidal B=3·0", C=2·5" H=3·3"	type IC ▣		

CUBOIDAL TRIAXIAL COMPRESSION/EXTENSION.
COMPARISON OF AXIAL AND LATERAL STRAINS AT MAXIMUM ϕ'
AND OF
VOLUMETRIC STRAIN RATES AT MAXIMUM ϕ'
- Ham River Sand, Batch #2, Bags #1&2.

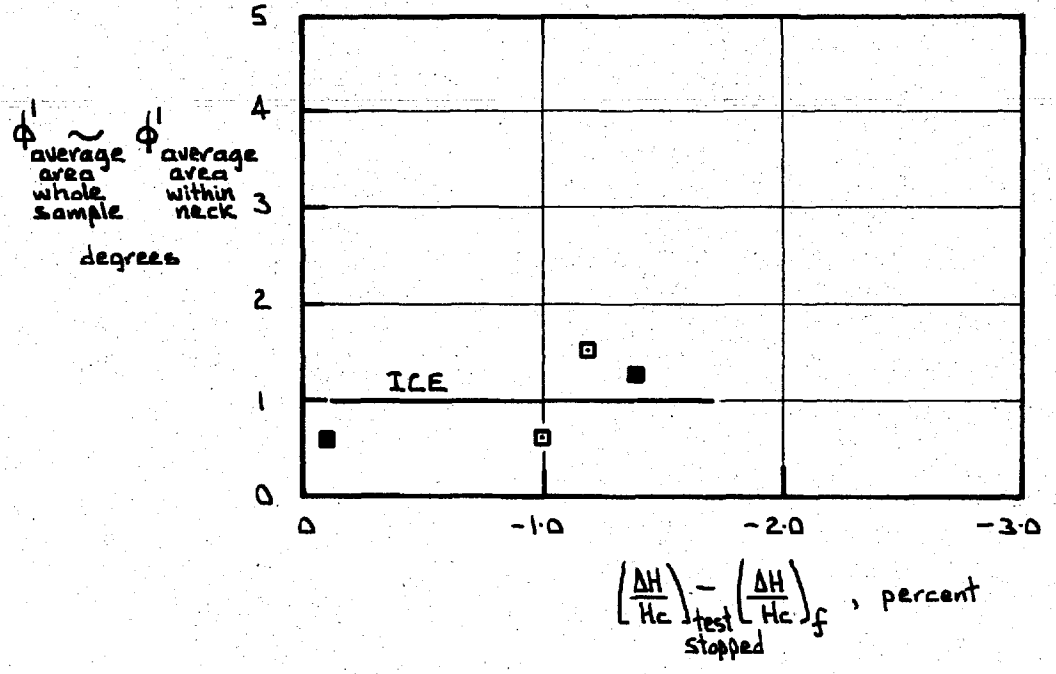
FIG. 10.11

Test No.	ϕ' based on average area of whole of sample.	ϕ' based on average area within neck.	$\left(\frac{\Delta H}{Hc}\right)_{test\ stopped} - \left(\frac{\Delta H}{Hc}\right)_f$ %	Theory used
ICE12	42·2°	43·7 (1·5)	−1·2	frustum of pyramid
ICE15	42·9	43·5 (0·6)	−1·0	
ICE16	39·9	40·5 (0·6)	−0·1	
ICE19	39·2	40·5 (1·3)	−1·4	

Notes:

(i) The average area within the neck is based on that part of the sample of height $D.\cot(45+\phi/2)$ and centred at the neck.

(ii) $(\Delta H/Hc)_f$ is based on the average area of the whole of the sample.



CUBOIDAL TRIAXIAL EXTENSION TESTS

CORRECTIONS TO MEASURED STRENGTHS FOR VARIOUS ASSUMED CROSS-SECTIONAL AREAS OF SAMPLES

FIG. 10.12

also been shown that the modes of deformation of cylindrical and cuboidal triaxial compression test samples are similar and that refinements in the area corrections give a similar reduction in ϕ' of the order 0.2°. Therefore the above observations are unaffected by these two factors and we can conclude that the Type IC sample of dimensions B = 3.0, C = 2.3 & H = 3.3 ins gives the most acceptable measure of the cuboidal triaxial compression strength.

However the cuboidal triaxial extension tests, Type ICE, show a much higher strength than the Type IB & IC triaxial compression tests; about 3.7° before the refined area correction, sample sheath strength and stress level corrections are applied. This is in marked contrast to the cylindrical triaxial extension samples. As noted in the previous section efforts were made to discover if this were due to apparatus errors. These were not detected and it must be presumed therefore that the difference is representative of the real behaviour of the sand.

However it is necessary to examine more closely the possible effect on the measured difference of 3.7° of relative, (i) differences in mode of deformation, (ii) sample sheath strength corrections, (iii) variation in ϕ' with stress level, and (iv) accuracy of the basic measurements. The argument follows a similar line to that set out for the cylindrical triaxial compression and extension tests, Type H & EX.

The accuracy of the basic measurements in tests on cuboidal and cylindrical samples are similar so that errors are considered to be similarly insignificant.

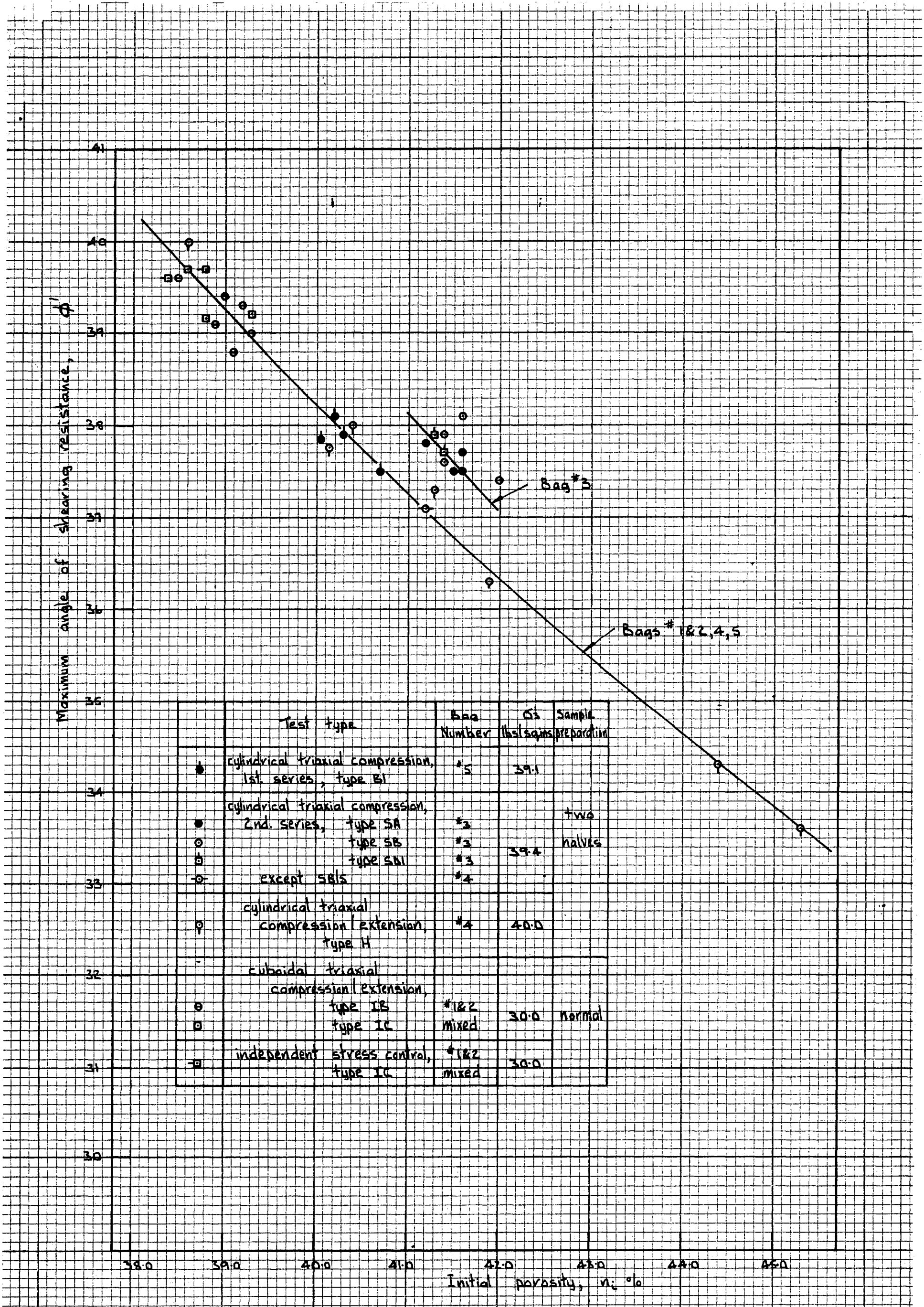
As noted earlier the effect of the stiffness of the sample sheath on the value of ϕ' measured in cuboidal compression is negligible. The deviation of the mode of deformation from that assumed lowers the value of ϕ' measured in cuboidal compression by an amount of the order of 0.2°. Thus the net effect of these two factors is to lower the value of ϕ' measured in cuboidal compression by 0.2°.

The effect of the stiffness of the sample sheath on the value of ϕ' measured in cuboidal extension is to lower its value by 0.1 to 0.2°. Again taking the pessimistic view that the axial strain within the neck is double the average axial strain, then ϕ' is lowered by about 0.3°. The deviation of the mode of deformation of the cuboidal samples from that assumed has been shown to raise ϕ' measured in triaxial extension by

about 1.0°. The difference in average stress at failure between the cuboidal triaxial compression and extension tests implies that the extension ϕ' value must be increased by 0.3° to put it on a comparable basis to the compression ϕ' value. The net effect of these three factors is to raise the value of ϕ' measured in cuboidal extension by -0.3 + 1.0 + 0.3 = 1.0°.

Combining these two sets of corrections results in raising the cuboidal extension ϕ' values by 1.2° relative to the cuboidal compression ϕ' values. These corrections are identical to those applied to the cylindrical triaxial test results. Hence the best estimate of the difference between the ϕ' value measured in cuboidal triaxial extension and cylindrical or cuboidal triaxial compression is 3.7 + 1.2 = 4.9°, a significantly large amount.

At this juncture it is necessary to review the consistency of all the triaxial compression test strength data obtained using the 2nd batch of Ham River sand, Fig 10.13. No corrections have been applied to the measured values. The effect of applying strength corrections would be to lower all the plotted points by 0.2°. It is evident that, of the sand used from the 2nd batch, there is little difference between that from Bags No.4 & 5 whereas that from Bag No.3 exhibited a 0.7° higher ϕ' value. Comparisons with the strengths given by the sand from Bags No.1 & 2 (mixed) are complicated by the difference in the minor principal stress and the mode of sample preparation used in testing the cuboidal samples. The average principal stresses at failure in tests at σ_3' = 30 psi and at σ_3' = 40 psi are insufficiently different to be likely to influence the measured strengths, being about 70 psi and 90 psi respectively, see Fig 9.15. No direct comparison is available between cylindrical triaxial compression test samples 4 ins high with 2/0.010 ins thick lubricated membranes at each end, made in two halves or in a normal manner. In Chapter 8 it was shown that a small difference in strength (and also in strains and volumetric strain rates) exists between 4 ins high samples with 1/0.010 ins thick lubricated membranes at each end, made in two halves and in a normal manner, tests Types A & X respectively and Types SD & SF (2nd series) respectively. The addition of a second lubricated membrane at each end of the sample made in two halves, Type SD1, reduced the strength to that of the 8 ins high samples and this was accepted as a reliable measure of the soil strength.



COMPARISON OF PEAK COMPRESSION STRENGTHS

FOR TESTS ON HAM RIVER SAND, BATCH #2.

FIG. 10.13

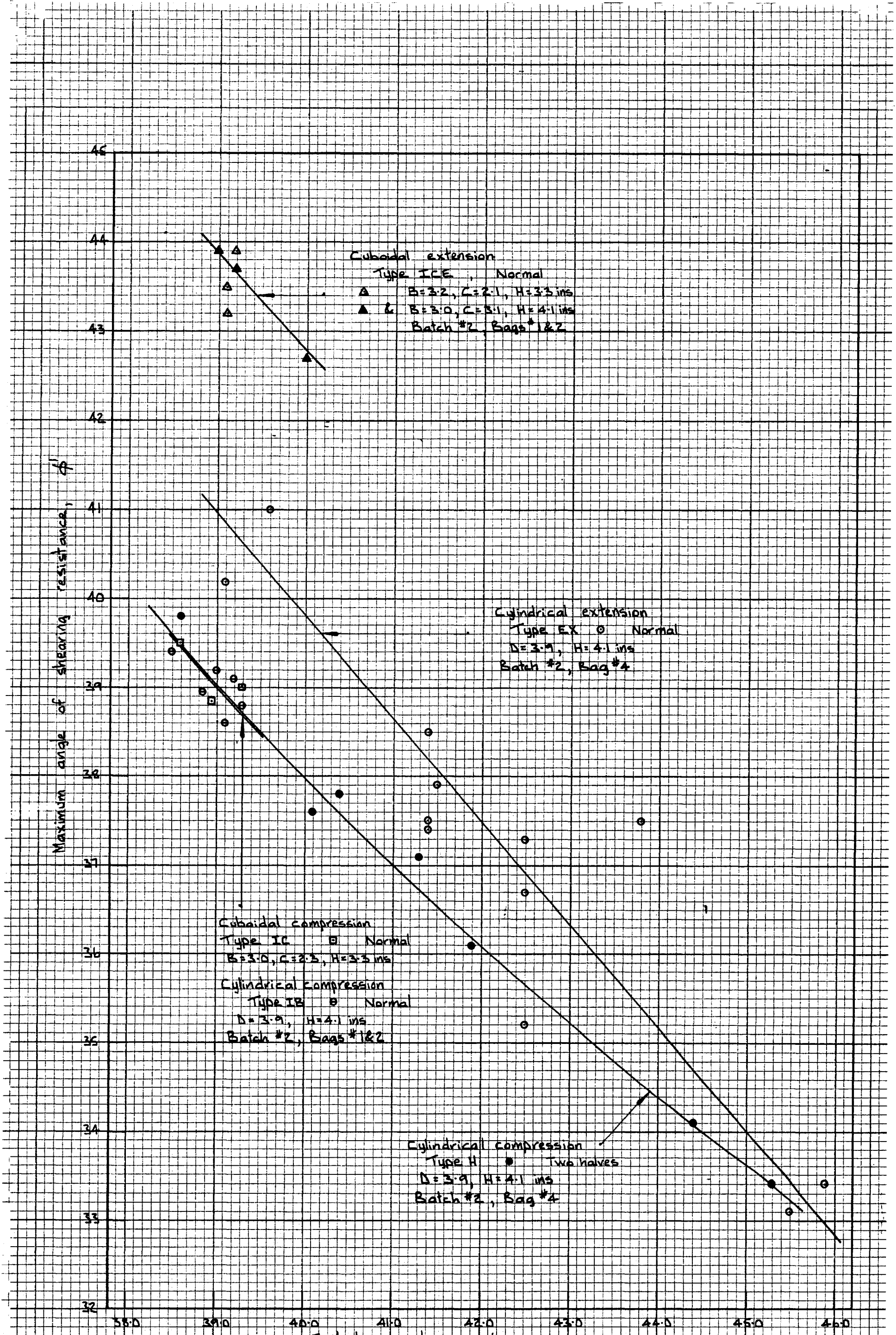
However it is not known what effect a second lubricated membrane would have had on the 4 ins high sample made in a normal manner. It is reasonable to presume that it would have resulted in a lowering of the measured strength by a similar amount to that of the Type SD1 test and that the effect on strains and strain rates would also be similar. Bearing in mind that the differences are likely to be small, it is reasonable to conclude that the strengths measured in the tests on samples made of sand from Bags No.1 & 2 (mixed) indicate that this material is similar to that of Bags No.4 & 5. Hence comparisons of the cylindrical and cuboidal triaxial compression & extension test results are considered justified.

The Type IB, IC & ICE strength data with the average corrections applied are shown together with the relevant cylindrical triaxial compression and extension test data also corrected, in Fig 10.14. The Type H, IB & IC triaxial compression tests exhibit identical ϕ' values (dense samples only), whereas the cuboidal triaxial extension strengths are 4.9° higher and the cylindrical triaxial extension strengths are 2.0° higher (both at $n_i = 39.0\%$). The reason for this difference in strength between the cylindrical and cuboidal extension samples is not at present clear. It is probable that if similar tests, i.e. Type IC & ICE, had been performed on initially loose samples ($n_i = 45.0 - 46.0\%$) they would have given identical strengths. If this were so it would strengthen the argument that the differences measured on initially dense samples were representative of the real behaviour of the sand. It is fair to point out, however, that there appears to be no evidence at present to the contrary.

There is no observed difference in behaviour between the two sizes of sample tested in cuboidal triaxial extension. Furthermore, the Type IC samples gave the most acceptable measure of strength in cuboidal triaxial compression. Therefore the sample geometry selected as being most suitable for the ISC tests was that used for the Type IC samples, i.e. B = 3.0, C = 2.3 & H = 3.3 ins.

10.5 Comparison of axial and lateral strains at failure

The axial strains at failure of the cylindrical, Type IB, and the cuboidal, Type IC, triaxial compression samples are the same, Fig 10.11. The cuboidal triaxial compression, Type IA, samples with a square shaped cross-section, failed at about 0.8% axial strain less than the Type IC



COMPARISON OF CORRECTED PEAK STRENGTHS MEASURED IN CYLINDRICAL AND CUBOIDAL TRIAXIAL COMPRESSION AND EXTENSION

Corrections applied for effect of: (i) non-uniform deformation
(ii) sample sheath strength
(iii) average stress level

FIG. 10.14

samples. The magnitudes of the axial strains at failure for the cuboidal extension tests, Type ICE, are about two-thirds those of the compression tests, Type IB and IC. Similarly the lateral strains in the extension tests are only one quarter of the corresponding axial strains in the compression tests.

Comparison of the cylindrical and cuboidal triaxial compression and extension test results are shown in Fig 10.15. The Type IB & IC triaxial compression tests exhibit marginally lower axial strains at failure than the Type H cylindrical triaxial compression test samples. The latter might be re-interpreted to give better agreement so that any difference cannot be considered to be significant. Furthermore, differences in the mode of sample preparation could account for differences in failure strains of about $\frac{1}{2}$ to 1%, see Figs 8.15 & 8.18. The axial and lateral strains at failure of all types of triaxial extension test are identical to each other. Therefore one can conclude that corresponding overall linear strains in cuboidal and cylindrical samples are identical when tested in triaxial compression and extension, provided compression and extension be considered separately.

10.6 Comparisons of volumetric strains at failure

The volumetric strains at failure are shown in Fig 10.10 and are complimentary to the linear strains at failure. There is no apparent difference between the behaviour of the cylindrical triaxial compression, Type IB, samples and the cuboidal triaxial compression, Type IC, samples, whereas the cuboidal triaxial compression, Type IA, samples exhibit different volumetric strains at failure as the height of the sample, H, was varied. The latter is in contrast to the linear strains, Fig 10.11, but is in agreement with the ϕ' values, Fig 10.10. The Type IA samples compare favourably with the cylindrical triaxial compression series samples of differing height to diameter ratio and degrees of end restraint, Fig 8.16. Here the dense 8 ins high samples with lubricated ends, Type C, failed at 0.7% lower volumetric strain than 4 ins high samples with lubricated ends, Types A & X. In the present case, the 4.1 & 4.6 ins high cuboidal samples failed at 0.5% lower volumetric strain than the 3.4 ins high samples.

The volumetric strains at failure in the cuboidal triaxial extension tests, Type ICE, are about one-third of the compression values. The two

sizes of cuboidal sample exhibit similar values. A similar result was obtained with the cylindrical samples over a wider range of sample geometry, Fig 9.20.

Comparisons of the cylindrical and cuboidal triaxial compression and extension test results are shown in Fig 10.16. Agreement between the two groups of tests is good. The marginal differences which exist between the Type H and Types IB & IC compression results are not serious and may be due to the different modes of sample preparation, c.f. Figs 8.16 & 8.18. Likewise the difference between the volumetric strains at failure in the cuboidal and cylindrical extension tests Type EX and Types ICE are considered acceptable.

10.7 Comparison of volumetric strain rates at failure

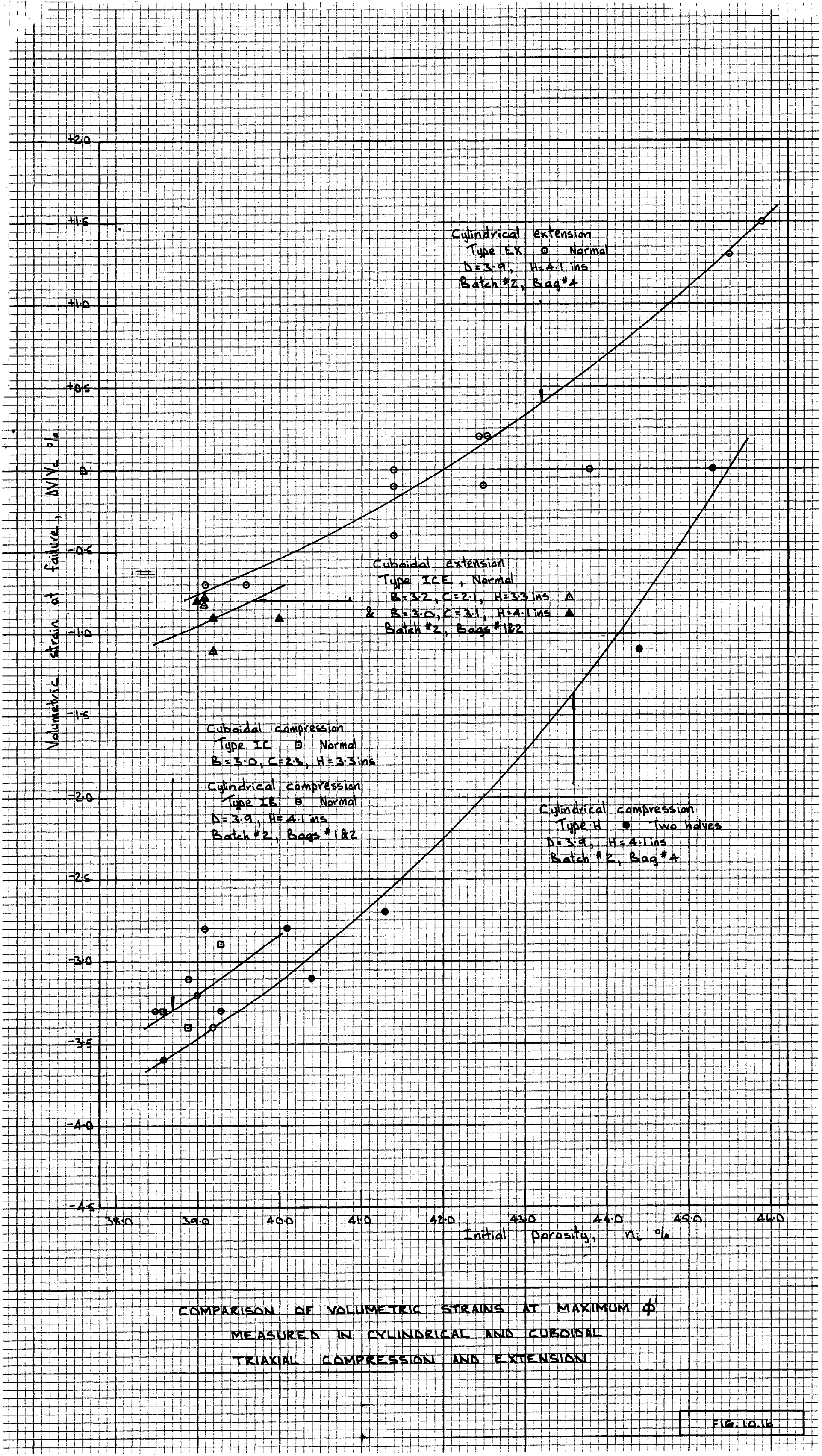
The variation of the rate of dilatation with porosity for all the tests is shown in Fig 10.11. There is no significant difference between the results of the triaxial compression tests, Type IB, IC & IA, H = 4.1 & 4.6 ins. The rate of dilatation at failure of the Type IA tests, H =3.4 ins, is, numerically, marginally higher. Therefore, as with the cylindrical triaxial compression tests, the rate of dilatation of the cuboidal samples is independent of the sample size.

There is no significant difference between the volumetric strain rate with respect to axial (or lateral) strain for the cuboidal triaxial extentests, Type ICE, for the two sample sizes tested. This is in accordance with similar tests on cylindrical samples, Fig 8.17. The volumetric strain rates with respect to lateral strain for the Type ICE samples are numerically higher than the volumetric strain rates with respect to axial strain for the triaxial compression samples.

Comparisons of the cylindrical and cuboidal triaxial compression and extension test results are shown in Fig 10.17. The difference between the Type H and the Types IB & IC triaxial compression results is small and within the limits defined in the cylindrical triaxial compression series. The cylindrical and cuboidal triaxial extension tests Type EX and Type ICE exhibit similar volumetric strain rate behaviour.

10.8 Influence of end restraint and H/D ratio

The tests on cuboidal samples were restricted to initially dense



COMPARISON OF VOLUMETRIC STRAINS AT MAXIMUM ϕ'
MEASURED IN CYLINDRICAL AND CUBOIDAL
TRIAXIAL COMPRESSION AND EXTENSION

FIG. 10.16

Cuboidal extension
Type ICE, Normal
B=3·2, C=2·1, H=3·3 ins △
& B=3·0, C=3·0, H=4·1 ins ▲
Batch #2, Bags #1&2

Cylindrical extension
Type EX ○ Normal
D=3·9, H=4·1 ins
Batch #2, Bag #4

Cylindrical compression
Type H ● Two halves
D=3·9, H=4·1 ins
Batch #2, Bag #4

Cuboidal compression
Type IC □ Normal
B=3·0, C=2·5, H=3·3 ins

Cylindrical compression
Type IB ⊙ Normal
D=3·9, H=4·1 ins
Batch #2, Bags #1&2

Type EX
$\frac{d(\Delta V/V_c)}{d(\Delta D/D_c)}$

Type ICE
$\frac{d(\Delta V/V_c)}{d(\Delta B/B_c)} = \frac{d(\Delta V/V_c)}{d(\Delta C/C_c)}$

$\frac{d(\Delta V/V_c)}{d(\Delta H/H_c)}$

Volumetric strain rate at failure, $\frac{d(\Delta V/V_c)}{d(\Delta B/B_c)}$, $\frac{d(\Delta V/V_c)}{d(\Delta D/D_c)}$, $\frac{d(\Delta V/V_c)}{d(\Delta H/H_c)}$

+0·4, +0·3, +0·2, +0·1, 0, −0·1, −0·2, −0·3, −0·4, −0·5, −0·6, −0·7, −0·8, −0·9, −1·0, −1·1, −1·2

38·0, 39·0, 40·0, 41·0, 42·0, 43·0, 44·0, 45·0, 46·0

Initial porosity, n_i %

COMPARISON OF VOLUMETRIC STRAIN RATES AT MAXIMUM ϕ' MEASURED IN CYLINDRICAL AND CUBOIDAL TRIAXIAL COMPRESSION AND EXTENSION

FIG. 10.17

specimens prepared in a normal manner. As was noted in Chapter 9 when discussing the cylindrical samples, the influence of the type of stress path is likely to be small when comparing compression and extension test data.

Accepting the cylindrical triaxial compression ϕ' value given by the Type IB samples, H/D = 1, as being correct, then of the 4 different cuboidal samples tested, the Type IC samples, B = 3.0, C = 2.3 & H = 3.3 ins, gave the lowest and hence the most acceptable strength, it being equal to that of the Type IB samples, Fig 10.10. Of the Type IA cuboidal triaxial compression samples, B = 3.0 & C = 3.1 ins, the two longest samples, H = 4.1 & 4.6 ins, showed a 0.5° increase in ϕ' and the shortest sample, H = 3.4 ins, a 1.0° increase in ϕ'. The lower limit of ϕ' as measured on the Type IA sample, H =4.1 & 4.6 ins, is still slightly higher than that measured in cylindrical triaxial compression. The reasons for this are not clearly defined. These conclusions are not affected by uncertainties regarding corrections for non-uniform deformation, sample sheath strength or average stress level.

Both sizes of cuboidal specimen tested in triaxial extension, Type ICE, exhibited the same strength and, indeed, the same linear & volumetric strains and volumetric strain rates at failure, Figs 10.10 & 10.11. This is in contrast to the slight difference in ϕ', 0.5°, observed between identical sized samples tested in triaxial compression. This is most likely due to the reduced portion of the sample involved in failure in triaxial extension compared with triaxial compression. The cuboidal triaxial extension specimens, Type ICE, show a 3.7° higher strength than the Type IB & IC triaxial compression specimens on a uniform deformation basis. After applying corrections for non-uniform deformation, sample sheath strength and average stress level, this difference increases to 4.9°; whereas the increase was only 2° for initially dense cylindrical triaxial extension test specimens, Fig 9.18.

From the point of view of strength alone the Types IC & ICE sample, B = 3.0, C = 2.1 & H = 3.3 ins (approx) give the most acceptable result. They also show very similar strain and strain rate behaviour to corresponding cylindrical triaxial compression and extension tests, Figs 10.15, 10.16 & 10.17. It therefore appears that the most suitable sized cuboidal sample for triaxial compression and extension tests, and by inference for

the ISC tests, is one of approximate dimensions B = 3.0, C = 2.1 & H = 3.3 ins, i.e. of proportions B : C : H equal 3: 2: 3. The faces in contact with the 2 pairs of rigid plattens require adequate lubrication which, for the Han River sand and stress levels used, is met by 2/0.010 ins thick greased rubber membranes.

CHAPTER 11

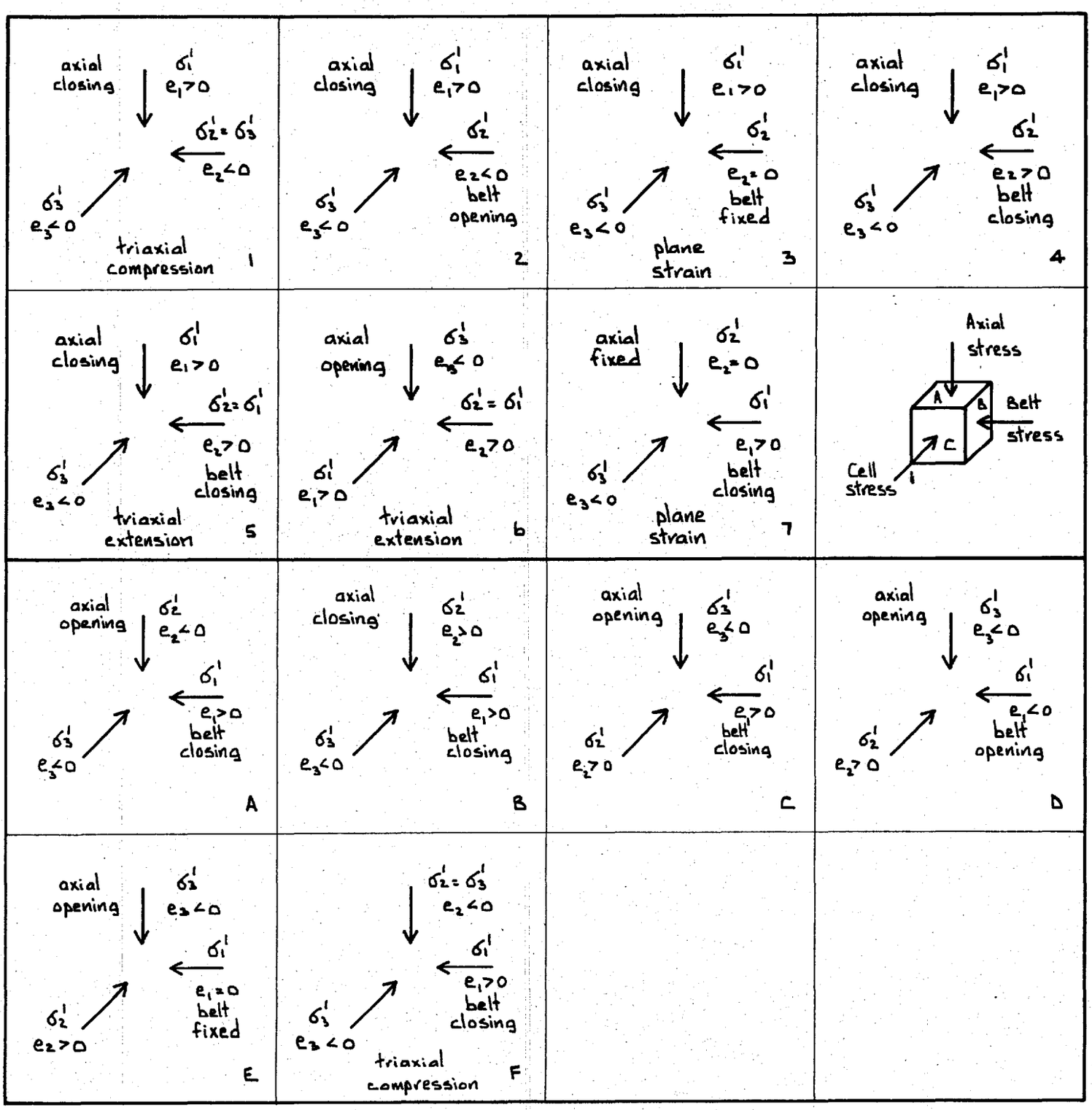
INDEPENDENT STRESS CONTROL TEST RESULTS AND DISCUSSION

11.1 Introduction

In the previous chapter the influence of the sample geometry and degree of end restraint on the behaviour of a cuboidal sample tested in conventional triaxial compression and extension were investigated. It was found that a cubical sample, H = 3.4, B = 3.0 and C = 3.1 ins, gave a perceptibly higher triaxial compression strength than a 4 ins high cylindrical sample with lubricated ends, Fig 10.10, but that on increasing H to 4.1 or 4.6 ins both the strength and the strains agreed very well with the cylindrical sample data, Figs 10.10 & 10.11. Alternatively by reducing the width in the cell direction so that H = 3.3, B = 3.0 and C = 2.3 ins the measured strength was again reduced to that of the cylindrical triaxial compression samples and the failure strains were similar. In the ISC tests it is desirable that the sample dimensions in the two rigid platten directions be approximately the same, so that the latter sample size was chosen as being suitable, i.e. H = 3.3, B = 3.0 and C = 2.3 ins. It was necessary to vary these dimensions by up to 0.1 ins to minimise the effect of platten interference at the four rigid boundary junctions; however this is considered to have a negligible influence on the stress-strain behaviour.

Two sizes of sample were tested in cuboidal triaxial extension and no difference in stress-strain behaviour could be discriminated between. However they exhibited a strength in excess of the compression strength by 4.9°, for an initial porosity, n_i = 39.0% after all corrections had been applied. These differences, the reasons for which are at present not completely understood, complicate the choice of ISC test sample geometry. The selection is therefore based primarily on the triaxial compression test data.

The stress conditions at failure in the ISC tests completed are shown in Fig 11.1 together with those that are considered possible in the apparatus. In general the stress conditions not investigated entail more difficult experimental techniques which were outside the immediate testing programme but are believed to be within the capability of the ISC cell. It is also possible to reach a number of the failure stress conditions by



SOME STRESS CONDITIONS AT FAILURE THAT ARE POSSIBLE IN THE ISC CELL

1-7 TESTS COMPLETED
A-F THEORETICALLY POSSIBLE

FIG. II.1

varying stress paths. The apparatus is limited in that the stress in the belt direction must always be greater than in the cell direction. This is in contrast to the stress in the axial direction which may be reduced below the cell pressure since the sample sheath spans across the junction of the sample and the axial platten and is sealed to the latter.

The strains which may be imposed on a sample are limited in those tests in which the ISC belt plattens move inwards and ultimately touch the axial plattens. In all the tests with the belt closing it was possible to reach failure before this occurred. However it was not always possible to impose strains sufficient to cause slip zones to be visible. By adjusting the speed of the drive to the external ISC belt control cylinder it was possible to vary the ratio $(\sigma_2' - \sigma_3')/(\sigma_1' - \sigma_3')$ between 0 and 1, i.e. to vary the intermediate principal stress from the minor to the major, Tests ISC/1 to 18. In two tests, ISC/19 & 29, σ_1' and σ_2' were interchanged by maintaining the axial plattens at an approximately constant separation and applying a constant rate of strain in the ISC belt direction.

All the tests were on dense samples, an initial porosity, $n_i = 39.0\%$ being the standard value aimed at. Differences in strength may be expected to be particularly marked for initially dense samples, Cornforth (1961, 1964). Due to the difficulties of sample preparation already noted, all the samples were prepared in the normal manner, see Chapter 7. The samples may therefore be initially non-uniform to a degree sufficient to affect their subsequent stress-strain behaviour. Compression tests on cylindrical samples, Chapter 8, indicate that the effect is small up to and including failure. It is the purpose of tests ISC/19 & 20 to examine this problem, albeit in a limited manner.

It was not considered possible to form loose samples with the apparatus in its present form due to the difficulty, (a) in folding the sample sheath back over the upper axial loading platten and (b) in assembling the ISC belt around the sample. It should be possible to overcome this in the future, but not without some ingenuity.

The ISC tests are numbered consecutively in the order in which they were carried out. They were immediately preceeded by Test IA/10 of the cuboidal triaxial compression & extension test series on the same material. Two further control tests, IC/5 & 6, were performed after Test ISC/20, their results being in good agreement with the previous triaxial compression tests.

There is, therefore, every reason to believe that no variation in the material properties or in the testing technique occurred, nor were there any significant errors in measurement , during the ISC test series.

The influence of non-uniform deformations on the interpretation of the ISC test results is less than in the more conventional triaxial compression and extension tests, since in the former two pairs of boundaries are strain-controlled. However the boundary stresses may be less uniform and can not be measured directly in the ISC apparatus in its present form. In addition, the influence of platten friction must be taken into account when calculating $(\sigma_1' - \sigma_3')$ and $(\sigma_2' - \sigma_3')$, see Appendix A6.

In general, the repeatability of the ISC tests at a particular b value, i.e. $(\sigma_2' - \sigma_3')/(\sigma_1' - \sigma_3')$ was very good; whereas the scatter in ϕ' as b varied was greater than might be anticipated, Fig 11.8. The reasons for this are not clear, but are probably associated with the corner effects at the junctions of the rigid plattens. Suffice it to say that these effects appear to be small and do not seriously influence the interpretation of the results.

The definitions of stress, strain, ϕ' and porosity are identical to those given in Chapter 8. The sample geometry is defined by the height in the axial direction, H, the width in the ISC belt direction, B, and the width in the cell direction, C. The strains in the axial and belt directions were measured directly, the strain in the cell direction being calculated from them, together with the measured volumetric strain.

The stress-strain and volume change curves for the individual ISC tests together with Tests IC/5 & 6 are given in Appendix A11. After most tests the sample was sketched and measured up after dismantling the cell, to record the mode of deformation together with the presence of slip zones, if any. The dimensions given are each the mean of two readings and are corrected for the thickness of the sample sheath. The basic test characteristics and failure stresses etc. are tabulated in Figs 11.2, 11.3 & 11.4.

The failure characteristics are adjusted to correspond to an initial porosity, $n_i = 39.0\%$ using as a basis the cuboidal triaxial compression and extension test results , Figs 10.10 & 10.11. This gives a more rational comparison of the different ISC tests. However it is not practicable to correct the whole of the stress-strain curves to allow for the initial porosity differences. Since the initial porosities of all the ISC test

Date	Test number	Sequence number	Porosity n %			Preload applied in σ_2' direction psi	Stresses at failure psi			Strains at failure %				Volumetric strain rate at failure		b $\frac{(\sigma_2'-\sigma_3')}{(\sigma_1'-\sigma_3')}$	ϕ' degrees	Material	End condition	Nominal strain rate ins/min.		Mode of sample preparation	Notes
			Initial n_i	After consolidation	At failure		Axial σ_1'	Belt σ_2'	Cell σ_3'	Axial $\Delta H/H_c$	Belt $\Delta B/B_c$	Mean Cell $\Delta C/C_c$	Volumetric $\Delta V/V_c$	$\frac{d(\Delta V/V_c)}{d(\Delta H/H_c)}$	$\frac{d(\Delta V/V_c)}{d(\Delta B/B_c)}$					Axial	Belt		
TYPE ISC H = 3.3 ins, B = 3.2 ins, C = 2.1 ins																							
18/7/66	ISC/1	1	39.0	38.4	39.1	0	161.0	58.5	30.0	+4.4	0	-5.9	-1.2	-0.56	∞	0.22	43.3	Batch 2 Bags 1&2 (mixed)	2 lo.010 ins thick lubricated membranes on axial platters	+0.002	0	Normal	
27/7/66	ISC/2	2	38.9	38.4	38.9	2.5	162.5	65.0	30.0	+3.7	0	-4.1	-0.8	-0.66	∞	0.26	43.5						Photo
29/7/66	ISC/3	3	39.1	38.6	39.1	3.0	166.5	67.6	30.0	+3.5	0	-4.6	-1.0	-0.61	∞	0.28	44.0						
1/8/66	ISC/4	4	38.6	37.9	39.4	4.8	166.8	50.7	30.0	+5.8	-1.8	-6.8	-2.5	-0.64	+2.43	0.15	44.0				-0.0005		
3/8/66	ISC/5	5	39.2	38.6	39.7	5.7	161.2	50.3	30.0	+5.2	-1.5	-5.9	-1.9	-0.58	+2.07	0.16	43.3						
5/9/66	ISC/6	6	38.7	38.3	40.4	3.1	155.4	43.0	30.0	+8.3	-4.2	-8.5	-3.6	-0.60	+1.20	0.10	42.6				-0.001		
2/10/66	ISC/7	7	38.8	38.2	40.4	2.2	153.1	42.0	30.0	+8.4	-4.5	-8.2	-3.6	-0.63	+1.21	0.10	42.2						Photo
9/10/66	ISC/8	8	39.1	38.4	38.8	3.4	159.5	87.5	30.0	+2.3	+0.6	-3.4	-0.5	-0.69	-2.21	0.44	43.1				+0.001	Normal	
12/10/66	ISC/9	9	38.7	38.0	38.2	2.0	161.9	88.0	30.0	+2.4	+0.7	-3.6	-0.5	-0.63	-2.00	0.44	43.4						
16/10/66	ISC/10	10	38.8	38.3	39.2	2.5	170.3	151.4	30.0	+2.7	+2.7	-7.4	-1.6	-1.17	-1.24	0.87	44.5		1 lo.010 ins thick lubricated membrane plus 0.013 ins thick sample sheath on belt platters	+0.0015	+0.0015		
19/10/66	ISC/11	11	38.7	38.3	39.5	3.2	179.4	159.0	30.0	+3.4	+3.2	-8.9	-2.0	-1.20	-1.29	0.86	45.5						
27/10/66	ISC/12	12	39.0	38.4	39.9	2.1	174.3	161.9	30.0	+3.7	+3.9	-10.7	-2.5	-1.23	-1.11	0.91	45.0			+0.0014			
14/11/66	ISC/K	15	39.1	38.5	38.9	1.2	159.6	105.3	30.0	+2.3	+1.3	-4.2	-0.5	-0.78	-1.40	0.58	43.1			+0.0015	+0.001		
19/11/66	ISC/16	16	39.0	38.3	38.6	1.8	164.5	99.0	30.0	+2.4	+0.9	-3.9	-0.5	-0.76	-2.08	0.51	43.7			+0.0019			
23/11/66	ISC/17	17	38.8	38.2	38.9	1.6	177.4	136.6	30.0	+3.0	+1.9	-6.1	-1.1	-1.03	-1.47	0.72	45.2				+0.0015		
25/11/66	ISC/18	18	38.7	38.1	38.5	1.3	165.7	129.3	30.0	+2.7	+1.8	-5.4	-0.8	-0.92	-1.38	0.73	43.9						
							Belt σ_1'	Axial σ_2'															
21/11/66	ISC/13	13	38.8	38.3	39.5	1.2	166.2	165.2	30.0	+3.2	+3.9	-9.8	-2.1	-1.49	-1.11	0.99	43.9	Batch 2 Bags 1&2 (mixed)	as above	+0.0012	+0.0015	Normal	
9/11/66	ISC/14	14	38.9	38.2	39.7	2.0	170.9	166.3	30.0	+3.3	+4.0	-10.3	-2.4	-1.40	-1.04	0.97	44.5						
28/11/66	ISC/19	19	39.1	38.6	38.9	0	154.5	70.6	30.0	-0.3	+4.1	-4.5	-0.5	∞	-0.64	0.33	42.4	Batch 2 Bags 1&2 (mixed)	as above	0	+0.0015	Normal	Photo
1/12/66	ISC/20	20	38.6	38.2	38.5	0	156.9	71.2	30.0	-0.3	+3.8	-4.2	-0.6	∞	-0.65	0.33	42.8						
TYPE IC H = 3.3 ins, B = 3.0 ins,							Axial σ_1'	Cell $\sigma_2' = \sigma_3'$	C = 2.3 ins	Cell $\Delta B/B_c = \Delta C/C_c$			triaxial compression										
3/12/66	IC/5	21	38.4	37.9	39.6		136.1	30.0	+6.5	-4.8		-2.9	-0.63		0	39.6	Batch 2 Bags 1&2 (mixed)	2 lo.010 ins	+0.002		Normal	
5/12/66	IC/6	22	38.8	38.3	40.5		136.6	30.0	+7.9	-6.0		-3.7	-0.62		0	39.7			+0.0035			

INDEPENDENT STRESS CONTROL TEST SERIES — BASIC MEASURED DATA

1

FIG. 11.2

Test number	Data adjusted to correspond to an initial porosity, n_i = 39.0 %: Stresses at failure psi — Axial σ_1'	Belt σ_2'	Cell σ_3'	Strains at failure % — Axial $\Delta H/H_c$	Belt $\Delta B/B_c$	Mean cell $\Delta C/C_c$	Volumetric $\Delta V/V_c$	Volumetric strain rate at failure $\frac{d(\Delta V/V_c)}{d(\Delta H/H_c)}$	$\frac{d(\Delta V/V_c)}{d(\Delta B/B_c)}$	b $\frac{(\sigma_2' - \sigma_3')}{(\sigma_1' - \sigma_3')}$	ϕ' degrees	Corrections applied for: (i) non-uniform deformation, (ii) sample sheath strength, (iii) platten friction, (iv) average stress level. Axial stress at failure psi — Non-uniform deformation correction	Sample sheath strength correction	Belt platten friction correction	Average stress level correction	Corrected axial stress σ_1'	Lateral – belt stress at failure psi — Non-uniform deformation correction	Sample sheath strength correction	Axial platten friction correction	Average stress level correction	Corrected belt stress σ_2'	b $\frac{(\sigma_2' - \sigma_3')}{(\sigma_1' - \sigma_3')}$	ϕ' degrees
TYPE ISC H = 3.3 ins, B = 3.2 ins, C = 2.1 ins																							
ISC11	161.0	58.5	30.0	+4.4	0	-5.9	-1.2	-0.56	∞	0.22	43.3	0	-0.2	-0.2	+0.6	161.2	0	0	0	+0.6	59.1	0.22	43.3
ISC12	162.0	64.4	30.0	+3.2	0	-4.1	-0.8	-0.65	∞	0.26	43.4	0	-0.1	-0.2	+0.6	162.3	0	0	0	+0.6	65.0	0.26	43.4
ISC13	167.1	68.2	30.0	+3.5	0	-4.6	-1.0	-0.62	∞	0.28	44.1	0	-0.1	-0.2	+0.7	167.5	0	0	0	+0.7	68.9	0.28	44.1
ISC14	164.5	48.4	30.0	+5.9	-1.9	-6.9	-2.4	-0.59	+2.38	0.14	43.6	0	-0.2	-0.1	+0.5	164.7	0	-0.1	-1.7	+0.5	47.1	0.13	43.6
ISC15	162.4	51.5	30.0	+5.2	-1.5	-5.9	-1.9	-0.60	+2.09	0.16	43.5	0	-0.2	-0.1	+0.5	162.6	0	-0.1	-1.7	+0.5	50.2	0.15	43.5
ISC16	153.7	41.3	30.0	+8.4	-4.3	-8.6	-3.5	-0.57	+1.17	0.09	42.3	0	-0.3	-0.1	+0.3	153.6	0	-0.2	-1.0	+0.3	40.4	0.08	42.3
ISC17	151.9	40.8	30.0	+8.4	-4.5	-8.2	-3.6	-0.60	+1.18	0.09	42.0	0	-0.3	-0.1	+0.3	151.8	0	-0.2	-0.9	+0.3	40.0	0.08	42.0
ISC18	160.1	88.1	30.0	+2.3	+0.6	-3.4	-0.5	-0.70	-2.22	0.45	43.2	0	-0.1	-0.4	+0.9	160.5	0	0	-0.1	+0.9	88.9	0.45	43.2
ISC19	160.2	86.3	30.0	+2.5	+0.8	-3.7	-0.4	-0.60	-1.97	0.43	43.2	0	-0.1	-0.4	+0.9	160.6	0	0	-0.2	+0.9	87.0	0.44	43.2
ISC110	169.1	150.2	30.0	+2.7	+2.7	-7.4	-1.6	-1.14	-1.21	0.86	44.3	0	-0.1	-1.2	+1.6	169.4	0	-0.1	-1.2	+1.6	150.5	0.86	44.3
ISC111	177.7	157.3	30.0	+3.5	+3.3	-9.0	-1.9	-1.16	-1.26	0.86	45.2	0	-0.1	-1.2	+1.8	178.2	0	-0.1	-1.5	+1.8	157.5	0.86	45.3
ISC112	174.3	161.9	30.0	+3.7	+3.9	-10.7	-2.5	-1.23	-1.11	0.91	45.0	0	-0.1	-1.4	+1.8	174.6	0	-0.1	-1.3	+1.8	162.3	0.92	45.0
ISC115	160.2	105.9	30.0	+2.3	+1.3	-4.2	-0.5	-0.79	-1.41	0.58	43.2	0	-0.1	-0.6	+1.1	160.6	0	-0.1	-0.1	+1.1	106.8	0.59	43.2
ISC116	164.5	99.0	30.0	+2.4	+0.9	-3.9	-0.5	-0.76	-2.08	0.51	43.7	0	-0.1	-0.5	+1.0	164.9	0	0	-0.2	+1.0	99.8	0.52	43.8
ISC117	176.2	135.4	30.0	+3.0	+1.9	-6.1	-1.1	-1.00	-1.44	0.72	45.1	0	-0.1	-0.9	+1.5	176.7	0	-0.1	-1.6	+1.5	135.2	0.72	45.1
ISC118	164.0	127.6	30.0	+2.8	+1.9	-5.5	-0.7	-0.89	-1.35	0.73	43.6	0	-0.1	-0.8	+1.3	164.4	0	-0.1	-1.4	+1.3	127.4	0.73	43.6
	Belt σ_1'	Axial σ_2'												Axial		Belt				Belt		Axial	
ISC113	165.0	164.0	30.0	+3.2	+3.9	-9.8	-2.1	-1.46	-1.08	0.99	43.7	0	-0.1	-1.3	+1.7	165.3	0	-0.1	-1.4	+1.7	164.2	0.99	43.7
ISC114	170.3	165.7	30.0	+3.3	+4.0	-10.3	-2.4	-1.39	-1.03	0.97	44.4	0	-0.1	-1.3	+1.8	170.7	0	-0.1	-1.5	+1.8	165.9	0.97	44.4
ISC119	155.1	71.2	30.0	-0.3	+4.1	-4.5	-0.5	∞	-0.65	0.33	42.5	0	-0.2	-0.2	+0.6	155.3	0	0	0	0.6	71.8	0.33	42.5
ISC120	154.3	69.0	30.0	-0.4	+3.9	-4.3	-0.5	∞	-0.60	0.31	42.4	0	-0.2	-0.3	+0.6	154.3	0	0	0	0.6	69.6	0.32	42.4
	Axial σ_1'	Cell $\sigma_2' = \sigma_3'$		Cell $\Delta B/B_c = \Delta C/C_c$				TYPE IC H = 3.3 ins, B = 3.0 ins, C = 2.3 ins, triaxial compression															
IC15	132.6	30.0	+6.6	-4.9		-2.8	-0.57			0	39.0	-1.4	-0.2	0	0	131.1						0	38.8
IC16	135.4	30.0	+7.9	-6.0		-3.7	-0.60			0	39.5	-1.4	-0.2	0	0	133.8						0	39.3

INDEPENDENT STRESS CONTROL TEST SERIES — CORRECTED DATA

FIG. 11.3

Test number	Data adjusted to correspond to an initial porosity, n_i = 39% — Stress ratios							Corrections applied for: (i) non-uniform deformation, (ii) sample sheath strength, (iii) platten friction, (iv) average stress level. — Strain ratios					Strain increment ratios		
	$\frac{\sigma_1'}{\sigma_3'}$	$\frac{\sigma_2'}{\sigma_3'}$	$\frac{\sigma_1'}{\sigma_2'}$	$\frac{\sigma_2'}{\sigma_1'+\sigma_3'}$	$\frac{\sigma_m'}{[\sigma_1'+\sigma_2'+\sigma_3']/3}$	$\frac{\sigma_1'-\sigma_m'}{\sigma_3'-\sigma_m'}$	$\frac{\sigma_2'-\sigma_m'}{\sigma_3'-\sigma_m'}$	$\frac{e_1}{e_3}$	$\frac{e_2}{e_3}$	e_1-e_3	e_2-e_3	$\frac{e_2-e_3}{e_1-e_3}$	$\frac{de_1}{de_3}$	$\frac{de_2}{de_3}$	$\frac{de_2-de_3}{de_1-de_3}$
TYPE ISC H=3.3 ins, B=3.2 ins, C=2.1 ins															
ISC11	5.38	1.97	2.73	0.31	83.4	-1.46	+0.45	-0.76	0	+10.3	+5.9	+0.57	-0.58	0	+0.63
ISC12	5.41	2.17	2.50	0.34	85.8	-1.37	+0.37	-0.78	0	+7.3	+4.1	+0.56	-0.61	0	+0.62
ISC13	5.59	2.29	2.43	0.35	88.8	-1.17	+0.34	-0.76	0	+8.1	+4.6	+0.57	-0.56	0	+0.64
ISC14	5.49	1.57	3.50	0.24	80.6	-1.66	+0.66	-0.85	+0.28	+12.8	+5.0	+0.39	-0.65	+0.18	+0.50
ISC15	5.42	1.67	3.24	0.26	80.9	-1.61	+0.60	-0.88	+0.25	+11.1	+4.4	+0.40	-0.68	+0.17	+0.49
ISC16	5.12	1.35	3.80	0.22	74.7	-1.76	+0.77	-0.98	+0.50	+17.0	+4.3	+0.25	-0.78	+0.40	+0.34
ISC17	5.06	1.33	3.80	0.22	73.9	-1.77	+0.77	-1.03	+0.55	+16.6	+3.7	+0.22	-0.77	+0.40	+0.34
ISC18	5.35	2.97	1.81	0.47	93.1	-1.07	+0.07	-0.68	-0.18	+5.7	+4.0	+0.70	-0.49	-0.15	+0.78
ISC19	5.35	2.90	1.85	0.46	92.5	-1.09	+0.09	-0.68	-0.22	+6.2	+4.5	+0.73	-0.50	-0.15	+0.77
ISC110	5.65	5.01	1.13	0.76	116.6	-0.61	-0.39	-0.37	-0.37	+10.1	+10.1	+1.00	-0.30	-0.28	+0.99
ISC111	5.94	5.25	1.13	0.76	121.9	-0.61	-0.39	-0.39	-0.37	+12.6	+12.3	+0.98	-0.28	-0.28	+1.00
ISC112	5.82	5.41	1.08	0.79	122.3	-0.56	-0.43	-0.36	-0.36	+14.4	+14.6	+0.99	-0.26	-0.29	+1.03
ISC115	5.35	3.56	1.50	0.56	99.1	-0.89	-0.11	-0.55	-0.31	+6.5	+5.5	+0.85	-0.42	-0.21	+0.85
ISC116	5.49	3.33	1.65	0.51	98.2	-0.98	-0.02	-0.61	-0.23	+6.3	+4.8	+0.76	-0.44	-0.18	+0.81
ISC117	5.89	4.51	1.31	0.65	113.9	-0.75	-0.25	-0.49	-0.31	+9.1	+8.0	+0.88	-0.36	-0.24	+0.91
ISC118	5.48	4.25	1.29	0.66	107.3	-0.74	-0.26	-0.51	-0.35	+8.3	+7.4	+0.89	-0.38	-0.26	+0.92
ISC113	5.51	5.48	1.01	0.84	119.8	-0.51	-0.50	-0.33	-0.40	+13.7	+13.0	+0.95	-0.32	-0.26	+0.95
ISC114	5.69	5.53	1.03	0.83	122.2	-0.53	-0.47	-0.39	-0.39	+14.3	+13.6	+0.95	-0.32	-0.25	+0.95
ISC119	5.18	2.39	2.16	0.39	85.7	-1.25	+0.25	-0.91	+0.07	+8.6	+4.2	+0.49	-0.60	+0.01	+0.62
ISC120	5.15	2.32	2.22	0.38	84.7	-1.27	+0.28	-0.91	+0.09	+8.2	+3.9	+0.48	-0.58	0	+0.63
TYPE IC H=3.3 ins, B=3.0 ins, C=2.3 ins, triaxial compression															
IC15	4.37	1.0	4.37	0.19	63.7			-1.35	1.00	+11.5	0	0			
IC16	4.46	1.0	4.46	0.18	64.6			-1.32	1.00	+13.9	0	0	1		

INDEPENDENT STRESS CONTROL TEST SERIES — CORRECTED DATA

FIG. 11.4

samples are approximately equally distributed about 39.0%, and the variation is at the most 0.4°, the error is small anyway.

11.2 Plane Strain Tests: ISC belt plattens fixed, $\Delta B/Bc = 0$

Three plane strain tests were performed in which the ISC belt plattens were maintained at a fixed distance apart, $\Delta B/Bc = 0$, whilst the axial stress was increased.

The sample for Test ISC/1 was tamped in layers and after isotropically consolidating the sample the ISC belt plattens were brought just into contact with it. The sample was sheared, maintaining a constant initial reading on the encapsulated dial gauge fixed between the ISC belt plattens. Only one gauge was used in this test. The stress-strain curves, Fig A 11.1, indicate that bedding occurred in the ISC belt direction so that the strains were probably unreliable; in fact subsequent comparisons indicate that this was the case. However the measured strength agreed reasonably well with the subsequent two plane strain tests. Compressibility calibrations, Appendix A 3, indicated that some initial platten bedding occurred but that beyond a stress $(\sigma_2' - \sigma_3') = 3$ psi it was negligible. Therefore all subsequent samples were pre-loaded in the belt direction after consolidation.

The sample for Test ISC/2 was vibrated and a second encapsulated dial gauge was added to the ISC belt. A new mould was used in preparing the sample - the original had been extensively modified and was inconvenient. As a result the sample was too short in the belt direction so that a 0.013 ins thick rubber membrane was stuck to each belt face to increase the width to prevent the plattens interfering. After consolidation the ISC belt plattens were adjusted to apply a 2.5 psi preload to the sample. The stress-strain curves, Fig A 11.2, indicate that preloading was partially successful although interpretation is complicated by the presence of the stuck-on packing membranes. During shear the reading of encapsulated dial gauge No 1 was maintained constant and the reading of gauge No 2 was recorded. The change in reading on gauge No 2 was 0.002 ins up to failure and thereafter a change of 0.008 ins occurred due to sample instability causing tilting of the belt platten mounted on the hydraulic ram. In retrospect, the clearance on the hydraulic ram was excessive and could usefully be reduced in future tests. The failure strains in Test ISC/2 were markedly reduced.

The sample for Test ISC/3 was also vibrated and the new mould was carefully packed, see Section 7.1.2 & Fig 7.2, to ensure a small clearance between the belt and axial plattens. The sample was again preloaded in the ISC belt direction and the stress-strain curves, Fig A 11.3, indicate that this was successful. Again relative rotation of the belt plattens occurred beyond failure and probably caused the discontinuity in the curve.

Relative to triaxial compression or extension tests with lubricated ends the drop in major principal stress, σ_1' , beyond peak is rapid, although not as abrupt as was observed by Cornforth (1961). Tests ISC/2 &3 failed at an average axial strain of 3.4% whereas Cornforth obtained axial failure strains of about 1.4% for dense Brasted sand samples in plane strain compression. This marked difference in failure strain is almost certainly due to the effect of platten friction. The strength rises again beyond about +6.0% axial strain in Tests ISC/2 & 3 although the results of Test ISC/1 suggest that this rise is temporary. Cornforth's tests were stopped at the first trough in the stress-strain curve and are of no help on this point. It is probable that at large strains platten interference becomes more important, although the mechanism is more difficult to define than in subsequent tests in which the belt plattens were driven inwards.

Well defined slip zones were observed beyond failure in all 3 tests, similar to those observed by Cornforth, but intersecting the top platten. Their presence is reflected in the volume change curve.

Plate 11.1 shows the sample in Test ISC/2 after dismantling. The sample failed at an axial strain of +3.2% the test being stopped at an axial strain of +8.5%. A complimentary pair of slip zones are clearly visible intersecting the top platten. The photograph also shows wrinkles in the sample sheath at the corners where it was very difficult to stretch the sheath to the required shape. This is believed to have had a negligible effect on the results.

All 3 samples appeared to expand uniformly up to the peak deviator stress. Any small deviation from uniformity in the cell direction has a negligible effect on the measured stress at so small a strain.



TEST ISC12.

plane strain,

n_i = 38·9 %, H = 3·3 ins, B = 3·2 ins, C = 2·1 ins,
2 10·010 ins thick membranes on axial plattens,
1 10·010 ins thick membrane + 1 10·013 ins thick
sample sheath on belt plattens,
test stopped at $\Delta H/H_c$ = +8·5 %,
$(\Delta H/H_c)_f$ = +3·2 %.

PLATE 11.1

11.3 ISC belt plattens opening, $\Delta B/Bc < 0$

These were two pairs of tests in which the belt plattens were driven steadily apart whilst the axial stress was increased. They cover the region between triaxial compression and plane strain. The reproducibility of the test is good, i.e. the stress-strain and volume change characteristics of Tests ISC/4 & 5, Figs All.4 & All.5, are similar and so are those of Tests ISC/ 6 & 7, Figs A 11.6 & A 11.7. It may be noted that the belt strain versus axial strain curves are linear up to failure except for the initial 0.5% axial strain. Thus, except for initial "take-up" in the hydraulic system, the ISC belt deformation control is linear. A marked discontinuity in the ISC belt strain occurs at failure in Tests ISC/4 & 5 associated with the formation of slip zones. No discontinuity or slip zones were observed in Tests ISC/6 & 7. The readings on the encapsulated dial gauges mounted on the ISC belt are compared for Test ISC/5 in Fig 11.5. The divergence of the slopes of the curves at failure is indicative of σ_2' platten tilting.

In each test the sample was vibrated. The stress drops rapidly beyond peak in Tests ISC/4 & 5 as predominant slip zones are formed. A similar pattern of predominant slip zones was observed in both tests. However, in Test ISC/5 the sample was lost during dismantling and the precise form of the failed sample was not recorded. The drop in strength beyond failure is smaller in Test ISC/5 than in Test ISC/4 due, presumably, to less tilting of the belt plattens.

The strains at which failure occurred in Tests ISC/6 and 7 were relatively larger so that post-failure behaviour was not established. No predominant slip zones were visible and both tests were fortuitously stopped at +10.1% axial strain. The end of test sample dimensions are very similar. Test ISC/6 shows an increased basal expansion whereas Test ISC/7 exhibits the beginnings of a mid-height bulge. Both of these observations appertain only to the cell direction, i.e. between the stress controlled boundaries.

Plate 11.2 shows the sample in Test ISC/7 after dismantling. The sample failed at an axial strain of +8.4%, the test being stopped at an axial strain of +10.1%. No slip zones are visible and the deformations appear to be very uniform. The sample has expanded in the belt direction so that it overhangs the edge of the axial plattens.



Cell face, C



Belt face, B

TEST ISC17.

ISC belt opening,

n_i = 38·8%, H = 3·3 ins, B = 3·2 ins, C = 2·1 ins,

2 lo·010 ins thick membranes on axial plattens,

1 lo·010 ins thick membrane + 1 lo·013 ins thick sample sheath on belt plattens,

test stopped at $\Delta H/H_c$ = +10·1%,

$(\Delta H/H_c)_f$ = + 8·4%.

PLATE 11.2

In each test the sample was preloaded by the ISC belt before shear commenced. Since $(\sigma_2' - \sigma_3')$ is quite small the effect of preloading may not be eliminated during subsequent stress application so that the failure characteristics in particular may be effected. The ISC belt stress for Tests ISC/4 & 5 can be extrapolated back to zero in a reasonable manner; likewise for Test ISC/6. However the curve for Test ISC/7 shows no increase in σ_2' during the initial +2% axial strain since the preload was reduced in this test. The resultant effect on the failure characteristics is insignificant.

11.4 ISC belt plattens closing, $\Delta B/Bc > 0$

There were 11 tests in which the ISC belt plattens were driven steadily towards each other whilst the axial stress was increased. They cover the region between plane strain up to and including triaxial extension. With the exception of the first two tests, ISC/8 & 9, the reproducibility is not as good as that obtained in the region between triaxial compression and plane strain. The reason for this is not certain.

In each test the sample was vibrated. The tests are not discussed in order of completion but are taken in groups moving from plane strain up to and including triaxial extension.

The stress-strain and volume change characteristics for Tests ISC/8 & 9, Fig A 11.8, are very similar. The measured dimensions of the sample in Test ISC/8 after dismantling the apparatus indicate very uniform deformations. The sample in Test ISC/9 was lost during dismantling. Failure occurred at relatively small axial strains and only a single slip zone was observed in Test ISC/8. The ISC belt stress continued to rise beyond failure and in Test ISC/9 it exceeded the axial stress beyond +5.4% axial strain. This results in some ambiguity in defining σ_1' and σ_2' throughout the test. As will be seen later this problem is recurrent. Since present work is primarily concerned with failure, σ_1' and σ_2' are defined with respect to failure. Since all the tests are drained and σ_3' is constant this is defined without further difficulty, as the first maximum value of the stress in the axial or belt direction.

The latter feature is observed again in Tests ISC/15, 16,17 & 18, Figs A 11.13 & A 11.14. In Tests ISC/15 & 16, σ_2' continues to increase beyond failure and similar well developed patterns of slip zones were visible in

both tests. The measured dimensions of both samples after dismantling the apparatus indicate very uniform deformations. The samples in Tests ISC/17 & 18 were destroyed during dismantling and it was not recorded whether or not slip zones were visible. The stress-strain and volume change curves are similar to those in Tests ISC/15 & 16. It is of interest to speculate that if Test ISC/18 had been continued a little further, whether the ISC belt stress would have reached a maximum value similar to the axial stress and then decreased. It seems very probable that this would have occurred. In a subsequently discussed test, ISC/11, a second peak was observed. It may be possible to continue a test similar to Tests ISC/17 & 18 to greater strains by starting with a larger initial gap. Only careful experiment will show how large a gap can be tolerated without seriously affecting the behaviour.

The nominal axial and ISC belt strain rates were identical in Tests ISC/10 & 11 and might be expected to result in equal axial and ISC belt stresses, i.e. $\sigma_1' = \sigma_2'$, an extension test. Reference to Fig A 11.9 shows that although the strains were approximately equal the ISC belt stress σ_2', was lower than the axial stress, σ_1'. In Test ISC/10 the ISC belt stress, σ_2', shows a maximum value well beyond failure; in fact the axial stress, σ_1', had fallen off significantly. However in Test ISC/11 which is otherwise similar, the two peak values almost coincide. The reason for this difference is not clear. Again, there is some ambiguity in defining σ_1' and σ_2'. The sample in Test ISC/10 exhibited two predominant slip zones symmetrically disposed through the sample. The strains measured after the test indicate that the sample had deformed very uniformly; even at so large a strain, -13.5%, in the cell direction. The sample in Test ISC/11 exhibited an asymmetric pattern of visible slip zones, which may be expected as one approaches the $\sigma_1' = \sigma_2'$ condition. It may also be noted that although the stress in the ISC belt direction is significantly lower than the axial stress the strains in these two directions are more nearly equal. This suggests that the sample may be anisotropic due to its mode of preparation. Further evidence on this point is discussed later.

In Test ISC/12, Fig A 11.10, the difference between the peak values of σ_1' and σ_2', is less than in the previously discussed two tests. These peak values occur at the same time and the stresses fall off rapidly by a

similar amount. However, in contrast, the strain in the ISC belt direction is slightly larger than in the axial direction. The axial stress, σ_1', increases sharply beyond +6.0% axial strain which suggests that the rigid plattens had interfered at the corners. Visually this appeared to be the case and since the ISC belt plattens were nesting inside the axial plattens one would expect the axial stress to increase most rapidly. When the cell was dismantled a leak occurred and the sample was lost. Close inspection of the sample sheath revealed lines of pinholes in the sheath along 3 of the edges where platten to platten contact had occurred. This explains the sudden rise in stress in a convincing manner.

Tests ISC/13 & 14, Figs A 11.10 & A 11.11, came closest to the ideal in which $\sigma_1' = \sigma_2'$, an extension test. In both tests the ISC belt stress remained lower than the axial stress until just before failure when the two stress-strain curves cross over. At failure the major principal stress, σ_1', is the stress in the ISC belt direction. The strain in the ISC belt direction is consistently 1.25 times higher than that in the axial direction. It is apparent both from these tests and Tests ISC/11 & 12 that the samples do not appear to be perfectly isotropic so that the major principal stress and strains do not coincide at failure. This is demonstrated more clearly in Fig A 11.12 where the axial stress versus axial strain plot is compared with the ISC belt stress versus belt strain plot for Tests ISC/13 & 14. If the sample were behaving isotropically the two curves would be more nearly superimposed. In fact the sample is stiffer in the axial direction than in the ISC belt direction. Whether this apparent anisotropy is of the type such that the stiffness in the belt and cell directions are identical cannot be determined from the present tests. If it is associated solely with the mode of sample preparation then it should be and, furthermore, the axial direction should be an axis of symmetry. In the theory of anisotropic materials this implies that the properties in any direction normal to the axial direction are identical. A uniform natural sedimentary soil deposit is a material of this type. Recent laboratory tests by Parkin et al (1968) indicate that this is so.

Tests ISC/13 & 14 both exhibit a slightly increased basal expansion in the cell direction. Well developed sets of slip zones were not observed in either test.

In Tests ISC/8,9,15,16,17 & 18 initial reverse curvature in the ISC

belt stress curve suggests that the initial belt preload applied was insufficient in relation to the rates of deformation imposed. It was not possible to know a priori what belt preload to use in each test. The effect on the interpretation of the results is not certain but is probably small. No corrections have been applied to the results for this effect. The preloads imposed are tabulated in Fig 11.2 for guidance in future research with the ISC apparatus.

11.5 Plane strain tests: axial plattens fixed, $\Delta H/Hc = 0$

These were two plane strain tests in which the axial plattens were maintained at an approximately fixed distance apart, $\Delta H/Hc = 0$, whilst the ISC belt stress was increased. It was not practicable to compensate for the elastic deformation of the axial proving ring. As a result, yielding of the axial plattens occurred, - 0.3% at failure. However the test is still close enough to plane strain to be considered as such in the discussion.

In both tests ISC/19 & 20, Fig A 11.15, a preload was not applied in the axial direction to bed in the plattens. The axial stress, σ_2', curves show a small initial reverse curvature; much less than in Tests ISC/1 or 2. Therefore we may infer that, generally, a much more intimate initial sample-platten contact was obtained in the axial direction than in the ISC belt direction.

In Test ISC/19 the sample deformed uniformly and no slip zones were visible when the test was stopped at an ISC belt strain of +1.8% beyond failure, Plate 11.3. Test ISC/20 was continued to a greater strain and a single predominant slip zone was visible as a near vertical line on a B and C face. This is consistent with the behaviour observed in Tests ISC/1,2 & 3 and by Cornforth (1961 & 1964).

11.6 Control tests, Type IC

These were 2 cuboidal triaxial compression tests on samples of dimensions B = 3.0, C = 2.3 and H = 4.1 ins, built in a normal manner with 2/0.010 ins thick lubricated rubber membranes used on each axial platten. Similar tests are described in the previous chapter. The 2 tests, IC/5 & 6, Figs A 11.16 & A 11.17, exhibit similar stress-strain and volume change characteristics as the earlier tests, IC/2, 3 & 4. It may be noted that in



Cell face, C



Belt face, B

TEST ISC119.

plane strain,
n_i = 39.1%, H = 3.3 ins, B = 3.2 ins, C = 2.1 ins,
2 10.010 ins thick membranes on axial platens,
1 10.010 ins thick membrane + 1 10.013 ins thick sample sheath on belt platens,
test stopped at $\Delta B/B_c$ = +5.9%,
$(\Delta B/B_c)_f$ = +4.1%.

PLATE 11.3

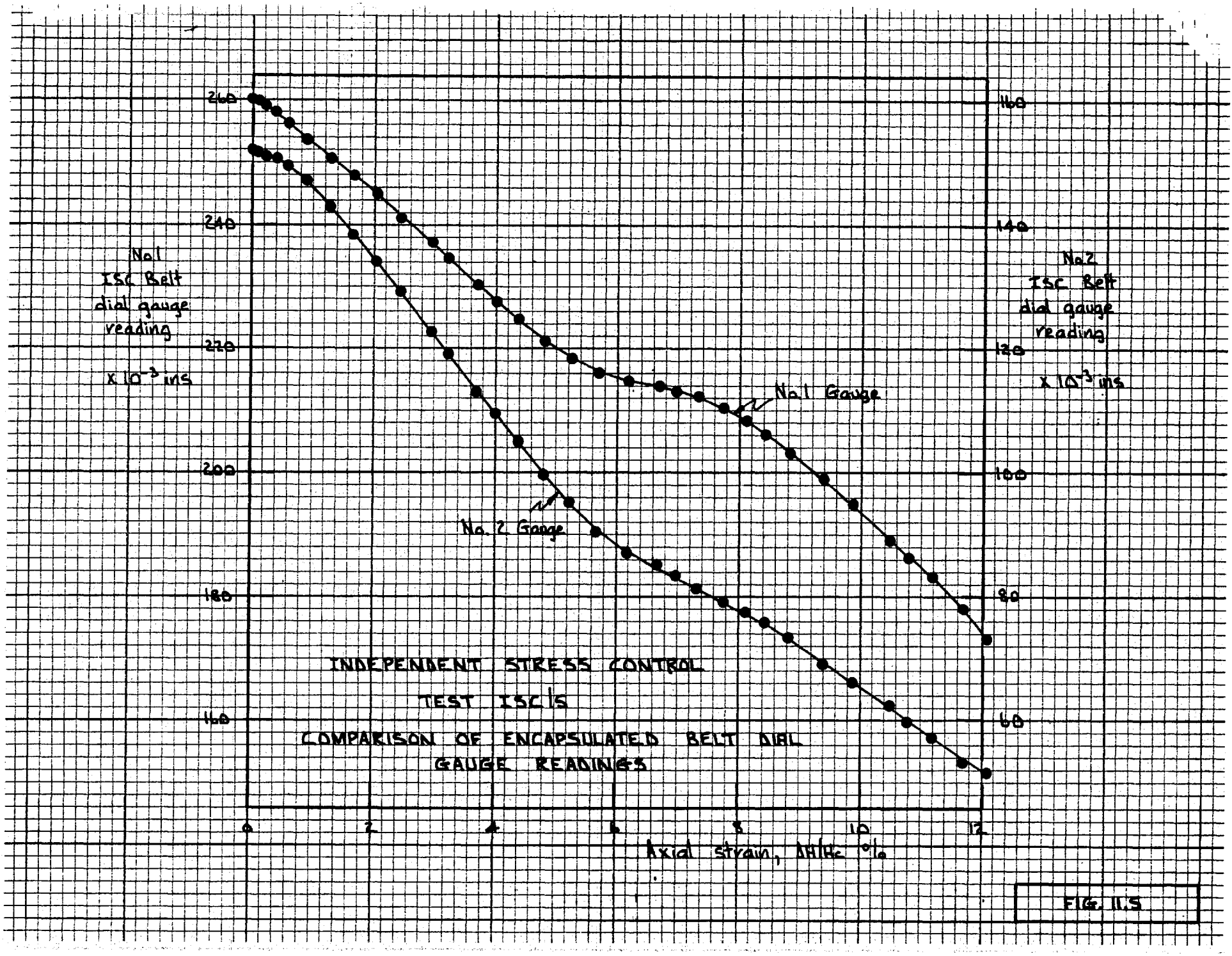
Test IC/5 the post-test lateral dimensions are similar in the cell and belt directions. The mean lateral strains, computed from $\Delta H/Hc$ and $\Delta V/Vc$ are also shown as they are useful for comparison with the measured lateral strain, $\Delta B/Bc$, in the ISC tests.

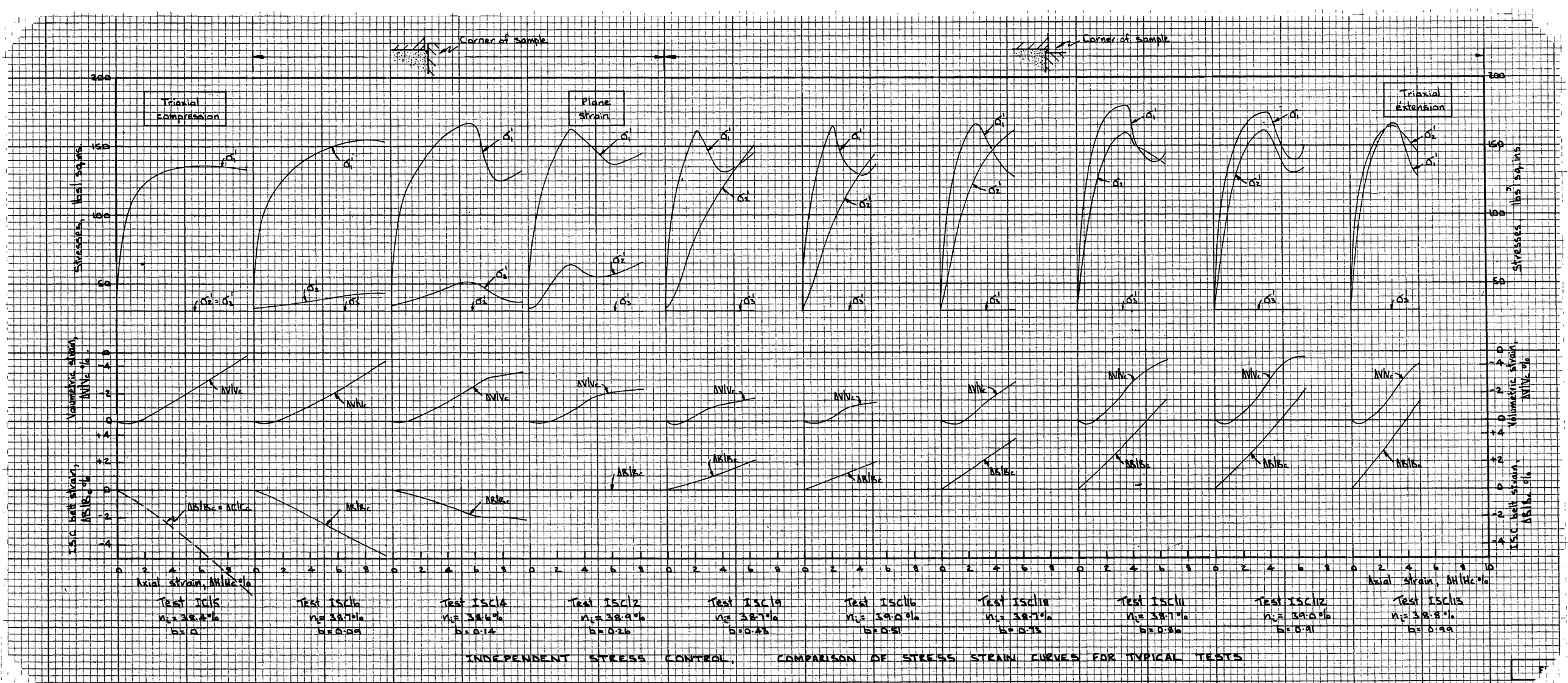
11.7 Comparison of stress-strain and volume change characteristics

The stress-strain and volume change characteristics of selected ISC tests are compared in Figs 11.6 & 11.7. The basis of this and of subsequent comparisons is that used by Esrig & Bemben (1965), Bishop (1966) & Bemben (1966). At failure the value of the intermediate principal stress σ_2' is related to σ_1' and σ_3' by the parameter $b = (\sigma_2' - \sigma_3')/(\sigma_1' - \sigma_3')$, where b is related to Lode's parameter μ of classical elasticity, Jaeger (1956), by the relation $2b = (1 + \mu)$. The merit of the present form of the parameter, b, is that for triaxial compression, where $\sigma_2' = \sigma_3'$, then $b = 0$ and for triaxial extension, where $\sigma_1' = \sigma_2'$, then $b = 1$. For all other values of σ_2', then $0 < b < 1$.

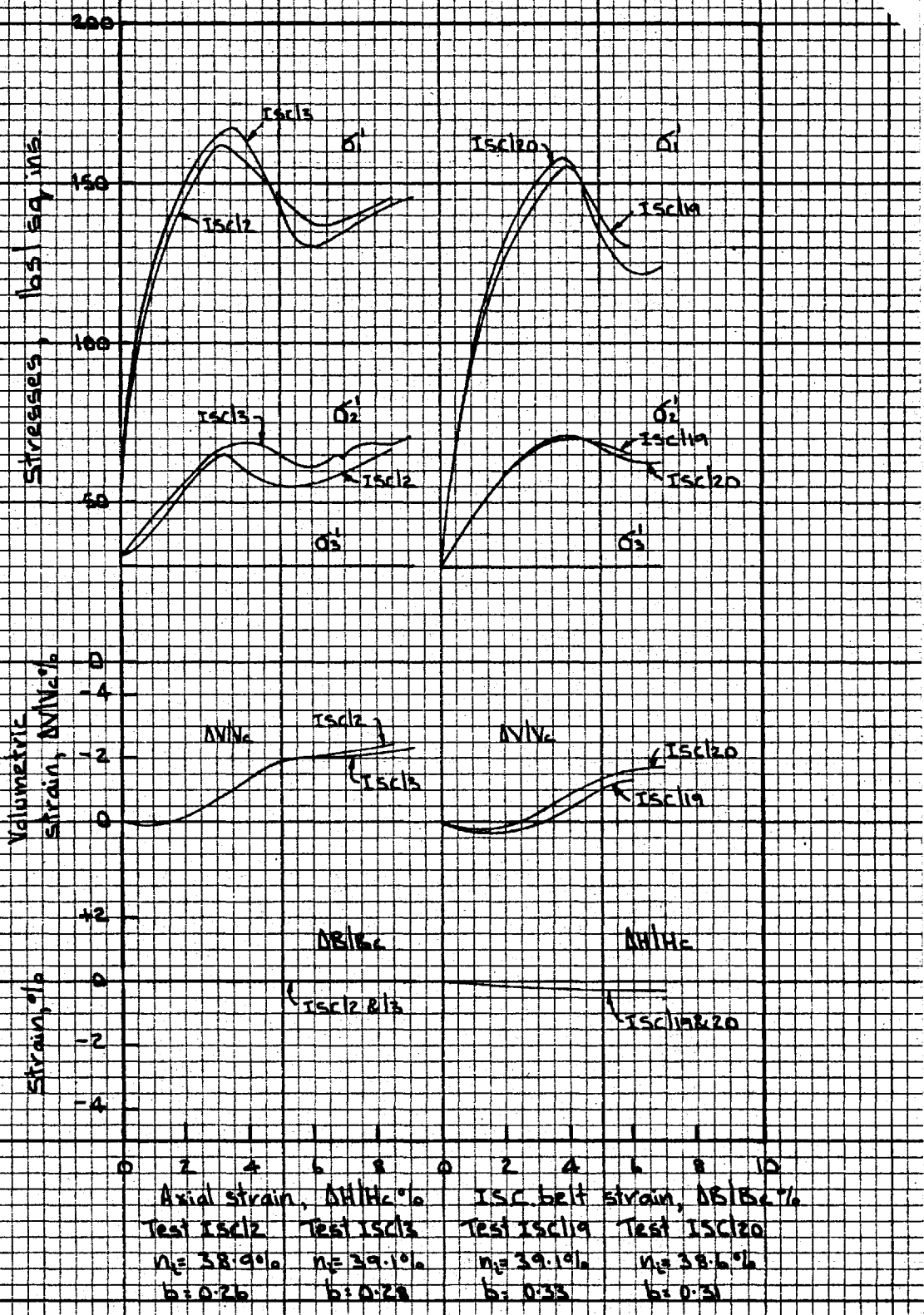
The results for a cuboidal triaxial compression control test, Test IC/5, are also shown in Fig 11.6. The lateral strain, $\Delta B/Bc = \Delta C/Cc$, was not measured directly and is therefore shown as a broken line. The maximum value of σ_1' increases as we move from triaxial compression, $b = 0$, to plane strain, $b = 0.26$, and thereafter remains relatively constant up to $b = 1$. The axial failure strain decreases rapidly as b varies from 0 to 0.5 and thereafter it increases slightly up to $b = 1$. Thus the greatest change in the shape of the major principal stress curve occurs between triaxial compression and plane strain after which all the curves are very similar. The value of the axial stress, σ_1', at failure is a minimum in triaxial compression whereas the strain is a maximum. Increasing σ_2' causes an increase in strength which reaches a maximum value when $\Delta B/Bc = 0$. A further increase in σ_2' has no significant effect on the strength. The drop in stress after peak is similar for $0.14 \leqslant b \leqslant 1$ although a residual or ultimate strength cannot be determined due to the limitations of the apparatus.

As the value of σ_2' increases from σ_3' to σ_1', a number of effects are observed. Up to and including the case of plane strain, $b = 0.26$, the σ_2' curve has a peak value at the same point as the σ_1' curve. In the range $0.26 < b < 0.86$ a peak value of σ_2' was not established. When $b \geqslant 0.86$ a peak value of σ_2' occurred and again coincided


No.1 ISC Belt dial gauge reading x 10^{-3} ins
No.2 ISC Belt dial gauge reading x 10^{-3} ins
260
240
220
200
180
160
160
140
120
100
80
60
No.1 Gauge
No.2 Gauge
0
2
4
6
8
10
12
Axial strain, $\Delta H/H_c$ %
INDEPENDENT STRESS CONTROL
TEST ISC/S
COMPARISON OF ENCAPSULATED BELT DIAL GAUGE READINGS
FIG. II.5



INDEPENDENT STRESS CONTROL. COMPARISON OF STRESS STRAIN CURVES FOR TYPICAL TESTS



INDEPENDENT STRESS CONTROL

COMPARISON OF STRESS STRAIN CURVES

FOR PLANE STRAIN TESTS

FIG. 11.7

with the maximum value of σ_1'. The most marked change in the behaviour pattern occurs between b = 0.26 and b = 0.43. The only apparent change in experimental technique also occurred at this juncture where the ISC belt plattens used for the plane strain tests and for the 4 tests in which the belt plattens were driven apart were interchanged with a narrower set to avoid platten interference in the range $0.26 < b \leqslant 1$. Whether this was the cause or not is uncertain, tests at intermediate b values, i.e. $0.26 < b < 0.43$, may shed light on this problem. The comparison of the stress-strain curves again illustrates the dilemma in trying to define σ_1' and σ_2' referred to earlier.

The shape of the volume change curves are similar in all the ISC tests. The maximum slope of the curve is approximately constant between b = 0 and b = 0.26 after which it increases as b tends to 1. In fact the slope is greater than 1 in the upper range of b values. The implications of this latter point are discussed in more detail later.

The slope of the ISC belt strain curve directly represents the strain conditions imposed upon the sample. As the intermediate principal stress varies from triaxial compression, b = 0, through plane strain, b = 0.26, to triaxial extension, b = 1, the curve rotates anticlockwise. This gave some guidance concerning a likely strain base on which to compare the stresses; a point which is of interest and which is taken up in the subsequent analysis of the ISC data. It may be noted that when b = 0.91, $\Delta B/Bc = \Delta H/Hc$ and thereafter $\Delta B/Bc > \Delta H/Hc$, indicating probable anisotropy within the sample.

It is not possible to directly compare the extension test stress-strain and volume change curves obtained in the conventional manner with those obtained in the ISC cell, and typified by Test ISC/13, due to the differing stress paths. In the conventional triaxial extension test the sample was consolidated at a cell pressure of 140 psi and the axial stress reduced to failure. In the ISC type of extension test the sample was consolidated at a cell pressure of 30 psi and the axial and belt stress were increased simultaneously, ideally at the same rate, until failure occurred.

Fig 11.7 shows the results of 2 plane strain tests, ISC/2 & 3 together with 2 additional tests which were approximately plane strain but with the directions of σ_1' and σ_2' interchanged, Tests ISC/19 and 20. It is not

possible to distinguish any major differences between the 2 types of test. The comparison is limited by the slight yield in the axial direction in Tests ISC/19 & 20. The second pair of tests exhibit marginally lower strengths together with slightly smaller volume changes. Any deficiency in the apparatus or the sample preparation method may therefore be inferred to be small.

11.8 Comparison of peak strengths

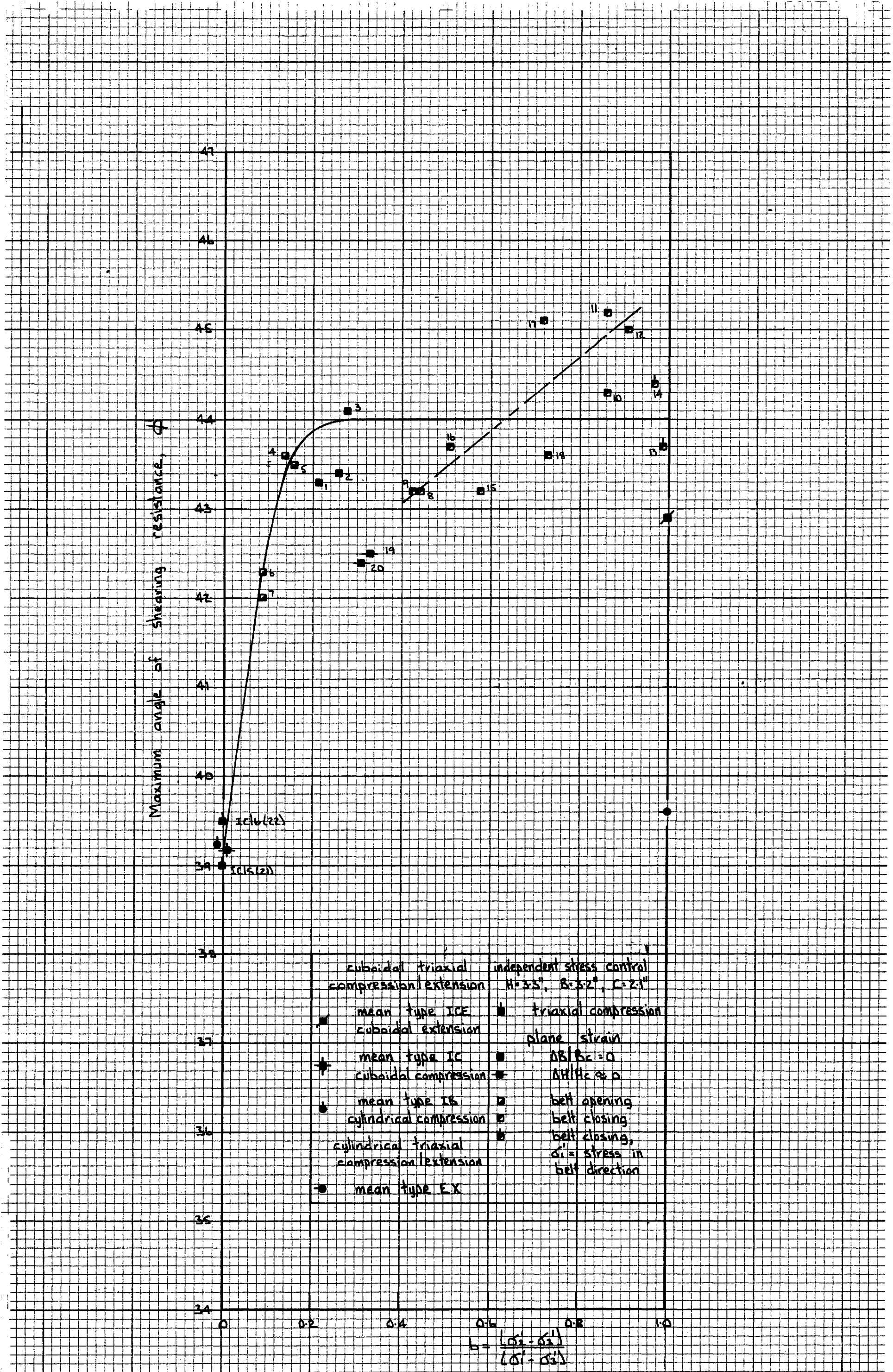
The peak strengths of all the independent stress control tests are compared in Fig 11.8. The measured strengths have been adjusted to correspond to an initial porosity, $n_i = 39.0\%$, using the strength-porosity relationship established in the earlier tests. The corrections are small but are nevertheless worthwhile since the comparison is placed on a more equitable basis. Generally 2 tests were performed for a particular value of $b = (\sigma_2' - \sigma_3')/(\sigma_1' - \sigma_3')$. The test number and sequence number of the ISC tests are identical. For simplicity on the figures the prefix "ISC" is omitted in the test point references.

Also shown in Fig 11.8 are the results of 2 Type IC control tests together with the average values of cylindrical triaxial compression & extension and cuboidal triaxial compression & extension strengths obtained from tests reported in the previous two chapters.

Of the 3 plane strain tests, ISC/1,2 & 3, the third test is probably the most reliable. In Tests ISC/1 & 2, belt platten bedding occurred and in Test ISC/2 it was necessary to insert additional rubber membranes between the sample and the ISC belt plattens to maintain a gap at the corners of the rigid plattens, see Section 11.1. The best fit curve is therefore weighted towards Test ISC/3. Nevertheless the differences in strengths between these 3 plane strain tests are not large compared with the difference between plane strain, $b = 0.25$ (average), and triaxial compression, $b = 0$.

The two pairs of tests between $b = 0$ and $b = 0.25$, Tests ISC/4 & 5 and 6 & 7, are extremely self-consistent. It is, in retrospect, unfortunate that tests were not performed corresponding to b approximately equal to 0.05. There is no reason to believe that such tests would not support the $\phi' - b$ relationship shown.

Consider the tests in the range from plane strain, $b = 0.25$, to triax-



INDEPENDENT STRESS CONTROL

COMPARISON OF PEAK STRENGTHS

Results adjusted to correspond to an initial porosity, n_i = 39·0 %

FIG. 11.8

ial extension, b = 1.0. Tests ISC/8 & 9 exhibit virtually identical strengths. In Tests ISC/10-18 the degree of reproducibility degenerates, in particular the difference in measured ϕ' values between Tests ISC/17 & 18 is 1.4°. The reason for this difference between these two consecutive, ostensibly identical tests is not known with certainty. The difference is comparable to the increased scatter observed earlier in extension tests when compared with compression tests. However this earlier difference is believed to be associated with the instability and consequent non-reproducible necking in the extension samples, which in the present ISC test close to b = 1 might reasonably be thought to be insignificant. In Test ISC/17 the drop in σ_1' beyond peak ϕ' is very sharp indeed, Fig A 11.14. This is in contrast to Test ISC/18, Fig A 11.14, and also to Tests ISC/15 & 16, Fig A 11.13, and ISC/10 & 11, Fig A 11.9. It is inferred, therefore, that Test ISC/18 is more reliable. The interpretation of Tests ISC/13 & 14 is complicated by the non-coincidence of principal stresses and strains previously noted. The points plotted correspond to the major principal stresses at failure in the belt direction, see Figs A 11.10, A 11.11 & A 11.12. The effect of taking the maximum axial stress instead would be to lower ϕ' by 0.1° and 0.6° in Tests ISC/13 & 14 respectively, and in addition, to increase b to a value apparently greater than 1.0. Although the reduction in ϕ' is small the latter point is, by definition, inadmissible.

A mean line through the group of tests, ISC/8,9,10,11,12,15,16,17 & 18 shows an increase in ϕ' of 2.0° as b increases from 0.44 to 0.90. However Tests ISC/13 & 14 do not fit in with this mean line, and Tests ISC/19 & 20 must be considered separately. It is believed that this increase in ϕ' of 2.0° is associated with the stress conditions at the junction of the 2 pairs of rigid plattens. If there is a corner problem then it is very probable that the effect on σ_1', the axial stress, would increase as σ_2', the belt stress, increases linearly as b increases beyond plane strain; so that a linear increase in ϕ' is reasonable. Indeed it would be expected if the hypothesis is correct. It may also be postulated that the "corner problem" is less severe in the range b = 0 to b = 0.25, see sketches in Fig 11.6.

Taking Tests ISC/1-18 into consideration and accepting the existence of a small "corner problem" the most appropriate ϕ' - b relation between

plane strain and triaxial extension is ϕ' = 44.0°, independent of b.

The range of scatter of the 2 control tests IC/5(21) and IC/6(22) about the previously established mean cylindrical and cuboidal triaxial compression test ϕ' value, 39.2°, is small and acceptable. The mean cylindrical triaxial extension test ϕ' value is 39.6°, 0.4° higher, whereas the mean cuboidal triaxial extension test ϕ' value is 42.9°, 3.7° higher. The difference between the triaxial compression and plane strain ϕ' value is 4.8°. There is a difference of 1.1° between the mean cuboidal triaxial extension test and the ISC extension test, b = 1.0.

The 2 plane strain tests ISC/19 & 20, in which the directions of σ_1' and σ_2' were reversed compared with Tests ISC/1,2 & 3, are in good agreement with each other. The b = value, 0.32, is marginally higher, whereas the ϕ' value, 42.5°, is about 1.5° lower than the mean plane strain value based on Tests ISC/1-18.

Before discussing in detail the differences in strength referred to in the previous two paragraphs, it is necessary to establish the influence of the corrections that must be applied to the measured ϕ' values to account for the effect of, (a) non-uniform deformation, (b) sample sheath strength, (c) average stress level, (d) accuracy of the basic measurements, and (e) platten friction. The mean values for triaxial compression and extension are only affected by factors (a), (b), (c) and (d), the effects of which have been described in detail in the previous two chapters. The net effect on the mean cylindrical and cuboidal triaxial compression strengths is to lower each by 0.2°. The net effect on the cylindrical triaxial extension strength is to increase it by 1.3° and on the cuboidal triaxial extension strength to increase it by 1.0°. These corrected peak strengths are shown in Fig 11.9 together with the corrected ISC test results.

The accuracy of the basic measurements in the ISC tests is similar to that in the earlier tests. The dimensions and weight of the sample are unaltered and identical load and pressure measuring devices were used. The ISC belt strain is measured directly and is probably even more reliable than the measured axial strain since the average of 2 gauge readings is obtained subject only to platten-membrane sandwich compressibility - which is shown to be negligible, Appendix A3. Errors in the basic measurements are therefore believed to be insignificant as before.

As with the cuboidal triaxial compression tests, the sample sheath

Maximum angle of shearing resistance, ϕ'

47
46
45
44
43
42
41
40
38
37
36
35
34

IC16(22)
IC15(21)

0 0·2 0·4 0·6 0·8 1·0

$b = \frac{(\sigma_2' - \sigma_3')}{(\sigma_1' - \sigma_3')}$

cuboidal triaxial compression / extension	independent stress control H = 3·3", B = 3·2", C = 2·1"
mean type IC6 cuboidal extension	triaxial compression
mean type IC cuboidal compression	plane strain: ■ $\Delta B/B_c = 0$; ✱ $\Delta H/H_c \approx 0$
mean type IC6 cylindrical compression	belt opening; belt closing; belt closing, σ_1' = stress in belt direction
cylindrical triaxial compression / extension	
mean type EX	

INDEPENDENT STRESS CONTROL
COMPARISON OF CORRECTED PEAK STRENGTHS

Results adjusted to correspond to an initial porosity, $n_i = 39{\cdot}0\%$

Corrections applied for effect of: (i) non-uniform deformation
(ii) sample sheath strength
(iii) platten friction
(iv) average stress level

FIG. 11.9

strength corrections are very small, particularly so, as it was necessary to minimise the sheath thickness to facilitate sample preparation. Typical corrections are shown in Appendix A6, and detailed corrections to $(\sigma_1' - \sigma_3')$ for each ISC test are given in Fig 11.3. It may be noted that the maximum correction is -0.3 psi.

The effect of non-uniform deformation of the ISC sample is considered to be negligible. Since two pairs of boundaries are strain-controlled, non-uniform overall strains are only possible in the cell direction. The measured strains in the cell direction at the end of the test do not vary greatly over the height of the sample, see Figs A 11.4, A 11.6 to A 11.11, A 11.13 & A 11.15, i.e. all tests in which measurements were made. This variation (a) is approximately half that observed in the cuboidal or cylindrical triaxial compression samples (see for example Figs A 9.1 to A 9.7, A 10.7, A 10.17, A 10.19, A 10.21, A 10.22) and (b) only applies to one of the 3 principal strain directions, whereas 2 principal strain directions were involved in the earlier tests. It may be noted that the problem of necking in extension never arises in an ISC test so that the most difficult case of an appropriate area correction is avoided. The best estimate of the correction to be applied to the earlier compression strengths was -0.2°, equivalent to a deviator stress correction of -1.2 psi. Clearly the correction applicable to the ISC tests is so small that it may be taken to be negligible.

The effect of platten friction on both $(\sigma_1' - \sigma_3')$ and $(\sigma_2' - \sigma_3')$ is discussed in Appendix A6. Detailed corrections for each ISC test are given in Fig 11.3. The magnitude of the correction to $(\sigma_1 - \sigma_3')$ depends largely on the value of $(\sigma_2' - \sigma_3')$ and is therefore greatest in Tests ISC/12,13,14; -1.3 psi. Likewise the magnitude of the correction to $(\sigma_2' - \sigma_3')$ depends largely on the value of $(\sigma_1' - \sigma_3')$.

The average stress at failure increases as b increases from 0 to 1. A correction must therefore be applied to account for the variation in ϕ' with average stress, Fig 9.15, in a similar manner to that described in the previous two chapters for the extension tests. The corrections to be applied to $(\sigma_1' - \sigma_3')$ are given in Fig 11.3, taking b = 0 as a base. It may be noted that, in contrast to the other three corrections, these are all positive. Similar average stress level corrections applied to $(\sigma_2 - \sigma_3')$ are also shown in Fig 11.3.

The corrected peak strengths for the ISC tests are shown in Fig 11.9 and average values are tabulated in Fig 11.10. There is very little difference between these values and the uncorrected values. The only two points affected are therefore Tests ISC/11 & 16 in each of which ϕ' is raised by 0.1°. This is because, (a) the corrections to be applied are all very small, and (b) the signs of the corrections are such that they are largely self-cancelling. Since the effect of these corrections is so very small the values may be accepted with greater confidence than would otherwise be possible. The effect on the value of b of applying these corrections is negligible.

The plane strain tests show a 5.0° higher strength than the triaxial compression tests and a further increase in σ_2' has no significant effect on ϕ'. The strength obtained in the ISC tests in which b = 1 is essentially the same as in plane strain, b = 0.25. The higher strengths obtain over the bulk of the stress range and the conventional triaxial compression strength could, in some respects, be considered as representing exceptional behaviour. The scatter of the experimental points in the range plane strain, b = 0.25, to triaxial extension, b = 1.0, is greater than might be hoped for. However the 5.0° increase in strength over triaxial compression is well established. The triaxial compression strength may be considered as a lower bound and the plane strain, ISC extension and cuboidal triaxial extension strengths as an upper bound. The cylindrical triaxial extension test gives an intermediate value for reasons that are not fully understood at present.

Agreement between the corrected ISC extension test value, Tests ISC/13 & 14, and the more conventional cuboidal triaxial extension ϕ' value is remarkably good. However the stress paths in the two types of extension test are different, Fig 11.33. It was shown in Chapter 9 that the difference in triaxial compression strength obtained by increasing σ_1' (Type H) compared with decreasing σ_3' (Type HA) was very small. It has also been established by Cornforth (1961), Fraser (1957), Eldin (1951), Taylor (1941) and others that the drained strength of sand is not very sensitive to the stress-path followed. Otherwise the only difference between the two types of extension test is the disposition and number of rigid and flexible boundaries. In the cuboidal triaxial extension test $\sigma_1' = \sigma_2'$ is applied at flexible boundaries whereas σ_3' is applied at a rigid

Test type	Maximum angle of shearing resistance ϕ'	Increase in ϕ' above triaxial compression value
Cylindrical triaxial compression $b=0$	39·0°	
Cuboidal triaxial compression $b=0$	39·0°	
$0 < b < 0.25$	linear ϕ'-b relationship	
Plane strain $b=0.25$	44·0°	5·0°
$0.25 < b < 1.0$	44·0°	5·0°
ISC extension $b=1$	44·0°	5·0°
Cylindrical triaxial extension $b=1.0$	40·9°	1·9°
Cuboidal triaxial extension $b=1.0$	43·9°	4·9°

AVERAGE CORRECTED PEAK STRENGTHS OBTAINED IN DIFFERENT TYPES OF TEST

FIG. 11.10

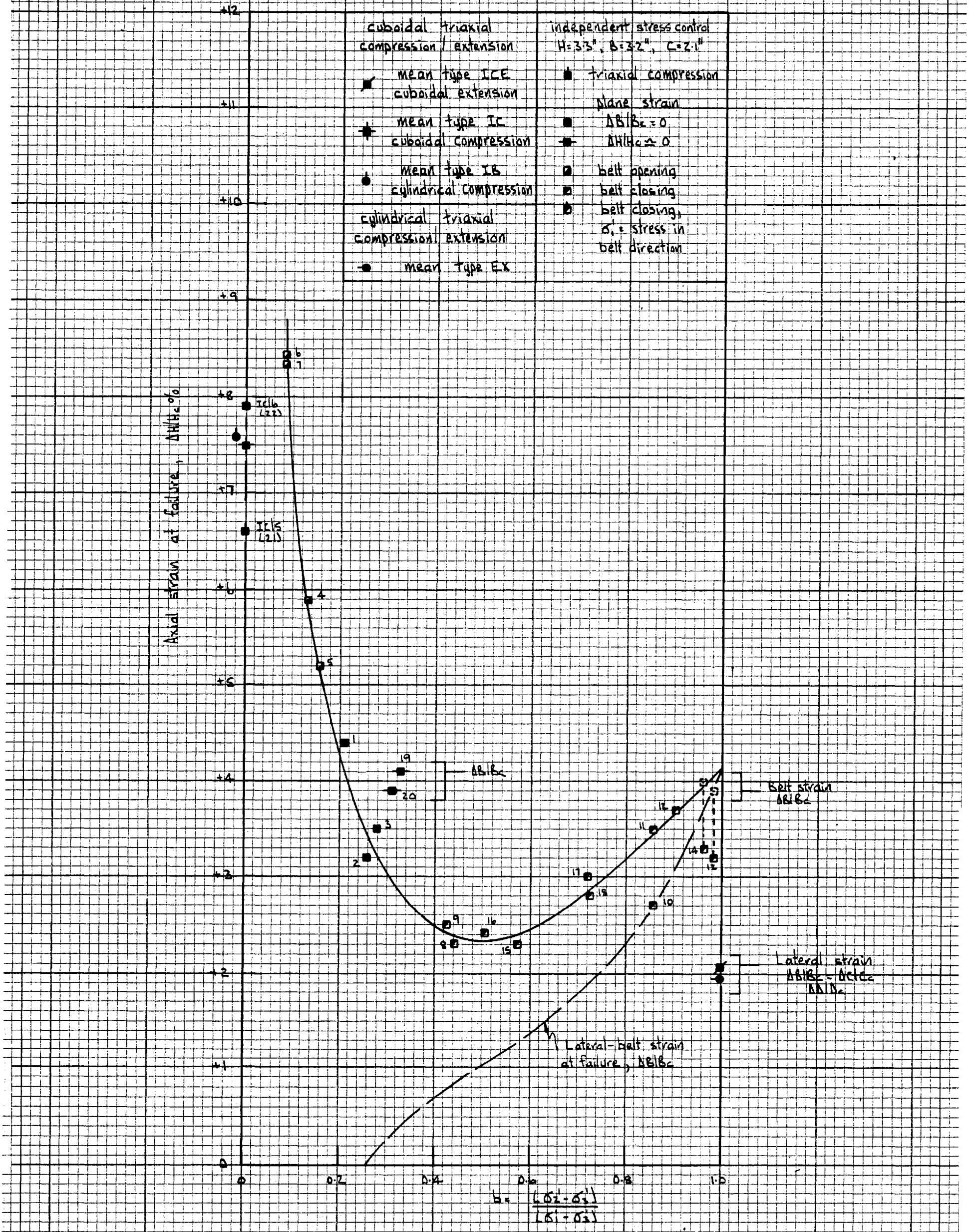
boundary. In the ISC type extension test σ_1' and σ_2' are applied at rigid boundaries whereas σ_3' is applied at a flexible boundary, i.e. the situation is reversed. If we exclude the possibility of self-compensating errors being present, then an important conclusion may be inferred. The rigid lubricated platten applied a uniform boundary stress to the sample in such a manner as to be indistinguishable from that imposed by a flexible sample sheath, see also Bishop (1967), Green & Bishop (1969). This is in direct conflict with the results obtained by Ko (1966), Ko & Scott,(1967a) for reasons given by Green (1967) and supported by Arthur & Menzies (1968) Bell(1968), see Chapter 2.

11.9 Comparison of axial and lateral strains at failure

The axial and lateral-belt strains which were measured directly are compared in Figs 11.11 & 11.12. The lateral-cell strains, which were calculated from these two measured values plus the volumetric strains, are compared in Fig 11.13. All 3 curves indicate a good correlation within the ISC data together with an apparent disagreement with the more conventional tests as $b \rightarrow 0$ and $b \rightarrow 1$.

Of the 3 plane strain tests, ISC/1,2 & 3, the latter 2 tests are very reproducible whereas Test ISC/1 shows a larger axial strain at failure due to the belt platten bedding problem already referred to. This is also reflected in the cell strain, although its apparent deviation from the mean line is small due to the latter's steepness in the region $0.1 < b < 0.3$. In the 4 tests in the region between triaxial compression, $b = 0$, and plane strain, $b = 0.25$, the linear strains correlate extremely well, Tests ISC/4, 5,6 & 7. The 9 tests in the region $0.25 < b < 0.9$ also exhibit a good correlation with the possible exception of Test ISC/10. The reason for the deviation of the latter test point is uncertain, the axial strain being about 0.5% too low.

A $b \rightarrow 1$, interpretation of the linear strain is a little more complex. In Tests ISC/13 & 14 the belt stress corresponds to σ_1' at failure and the axial stress to σ_2' . In the comparison of the axial strains at failure the solid points for Tests ISC/13 & 14 correspond to the axial strains whereas the dotted points correspond to the belt strains. The latter are the most relevant values in this correlation and, indeed, fit the average curve more closely. Similar remarks apply to the correlation



INDEPENDENT STRESS CONTROL

COMPARISON OF AXIAL STRAINS AT MAXIMUM ϕ'

Results adjusted to correspond to an initial porosity, n_c = 39.0%

FIG. 11.11

Axial strain at failure, $\Delta H/H_c$

Axial strain $\Delta H/H_c$

Lateral strain $\Delta B/B_c = \Delta C/C_c$ $\Delta D/D_c$

$\Delta H/H_c$

Lateral-cell strain at failure, $\Delta C/C_c$

Lateral-belt strain at failure, $\Delta B/B_c$ %

+6 +5 +4 +3 +2 +1 0 -1 -2 -3 -4 -5 -6 -7 -8

I(1.5 (2.1)

I(1.6 (2.2)

0 0·2 0·4 0·6 0·8 1·0

$$b = \frac{(\sigma_2' - \sigma_3')}{(\sigma_1' - \sigma_3')}$$

cuboidal triaxial compression || extension

mean type ICE cuboidal extension

mean type IC cuboidal compression

mean type IB cylindrical compression

cylindrical triaxial compression / extension

mean type EX

independent stress control
H = 3·3", B = 3·2", C = 2·1"

triaxial compression

plane strain
$\Delta B/B_c = 0$
$\Delta H/H_c \approx 0$

belt opening
belt closing
belt closing, σ_1' = stress in belt direction

INDEPENDENT STRESS CONTROL

COMPARISON OF LATERAL - BELT STRAINS AT MAXIMUM ϕ'

Results adjusted to correspond to an initial porosity, n_i = 39·0%

cuboidal triaxial compression / extension

- mean type ICE cuboidal extension
- mean type IC cuboidal compression
- mean type IB cylindrical compression

cylindrical triaxial compression / extension

- mean type EX

independent stress control
H = 3·5", B = 3·2", C = 2·1"

- triaxial compression

plane strain

- $\Delta B/B_c = 0$
- $\Delta H/H_c \approx 0$
- belt opening
- belt closing
- belt closing, σ_1' = stress in belt direction

Lateral-belt strain at failure, $\Delta B/B_c$

Lateral - Cell strain at failure, $\Delta C/C_c$ %

Axial strain $\Delta H/H_c$

+2, +1, 0, −1, −2, −3, −4, −5, −6, −7, −8, −9, −10, −11, −12

0, 0·2, 0·4, 0·6, 0·8, 1·0

$$b = \frac{(\sigma_2' - \sigma_3')}{(\sigma_1' - \sigma_3')}$$

INDEPENDENT STRESS CONTROL

COMPARISON OF LATERAL - CELL STRAINS AT MAXIMUM ϕ'

Results adjusted to correspond to an initial porosity, n_i = 39 %

of the lateral-belt strains where the situation is reversed. No ambiguity of the above type occurs in the comparison of the cell strains. Here the mean line is very steep in the region $0.7 < b < 1.0$ and its exact position as $b \rightarrow 1$ is a little uncertain, but is also of little consequence in the subsequent argument.

If the sample is isotropic and if the apparatus performs according to the designer's intention, then the axial and lateral-belt strains should be equal when $b = 1$. However, as previously noted, in Tests ISC/13 & 14 in which $b = 0.99$ & 0.97 respectively, these two strains are apparently different. In the present comparison, Figs 11.11 & 11.12, the scatter in the results of Tests ISC/10,11 & 12 together with the apparent rapid changes in failure strain in the region $0.8 < b < 1.0$ mask this apparent difference. For simplicity the mean curves are drawn so as to meet at $\Delta H/Hc = \Delta B/Bc = +4.6\%$ when $b = 1$. There is clearly a significant increase in these failure strains over the more conventional extension tests which failed at a lateral strain of +2.0%. The mean lateral-cell strain, Fig 11.13, may be extrapolated to about -11.0% at $b = 1$, which is more than twice that obtained in the conventional triaxial extension tests (-4.6 to -4.8%). These increases strongly suggest that more uniform strains are obtained in the ISC extension test as the possibility of necking is excluded. However, in marked contrast, the strength measured in cuboidal extension is almost identical to that measured in the ISC test as $b \rightarrow 1.0$.

Similar discrepancies in behaviour occur as $b \rightarrow 0$. In each of the three strain comparisons Tests ISC/4,5,6 & 7 establish a well defined portion of the mean curve which one may attempt to extrapolate to $b = 0$. However the curve is so steep that a precise extrapolation is difficult. Even the most optimistic extrapolation gives strain values for $b = 0$ approximately twice those obtained in conventional triaxial compression tests. The lateral-belt strain and the lateral-cell strain should be equal when $b = 0$. In Tests ISC/6 & 7, for which $b = 0.09$, the lateral-cell strain is approximately twice the lateral-belt strain. The lack of test data in the region $0 < b < 0.09$ makes it impossible to tell whether the two curves really converge to a common point at $b = 0$ or not.

There appears to be no good reason to believe that the strains measured in the ISC tests are less reliable than in more conventional tests. On the contrary, they suggest that the best cylindrical or cuboidal triaxial

compression test grossly under-estimates the failure strains. Similarly they must also under-estimate the strains at a particular stress level preceding failure. It was shown in previous chapters in this thesis that the strains in the "best" cylindrical or cuboidal triaxial compression or extension tests, i.e. on short samples with adequately lubricated ends, were generally greater than in similar tests on long samples with non-lubricated ends. Failure strain data for the different test types corresponding to a an initial sample porosity, n_i = 39.0% are collected in Fig 11.16. The data are adjusted to account for the differences in the two batches of sand used. However, these adjustments are small compared with the strain differences obtained in the different types of test. One can anticipate that if all 3 pairs of boundaries were strain-controlled then the strains, both at failure and at a specific stress level, should be even larger than those given by the ISC tests. This is in general agreement with the large strains obtained in the Cambridge Simple Shear Apparatus, Arthur et al (1964).

In Tests ISC/19 & 20 the directions of σ_1' and σ_2' were reversed and zero strain was approximately maintained in the axial direction. The 3 linear strains are reproducible and lie slightly off the mean curves for Tests ISC/1-18. Now the results of Tests ISC/11,12,13 & 14 in which $b \rightarrow 1$ indicate that the sample may be stiffer in the axial direction than in the belt direction. It therefore appears that, either the sample is slightly anisotropic or, there is a deficiency in the apparatus. It is difficult to conceive what faults may be in the apparatus which could account for this difference, slight anisotropy in the sample seems much more likely. Careful experimentation may clarify this matter. One can of course interchange the relative magnitudes of the axial and belt stresses over the whole range of b values and this would be very useful in attempting to separate out the factors involved.

The comparison of the lateral-belt strains at failure, Fig 11.12, has some analogy with the active-passive pressure problem. As b increases from 0 to 1, σ_1' remains relatively constant whereas σ_2' increases linearly from σ_3' to σ_1', Fig 11.17. A belt platten forms the retaining wall. As the wall is pushed in, i.e. $\Delta B/Bc$ is positive, b increase rapidly - the passive case. As the wall yields, i.e. $\Delta B/Bc$ is negative, b decreases slowly - the active case.

The axial strain at failure, Fig 11.11 is large as $b \rightarrow 0$ and decreases as the sample is increasingly restrained by the belt plattens. A minimum

value occurs when b = 0.5, beyond which the failure strain increases again, presumably due to the increasing σ_2' having a predominant effect while σ_1' remains constant beyond plane strain. Why the minimum value occurs at b = 0.5 and not at plane strain, b = 0.25, is not clear. The minimum value of $\Delta H/Hc$ gives a corresponding maximum value of $\Delta C/Cc$ and a point of inflexion for $\Delta B/Bc$.

The linear strains exhibit a well defined behaviour pattern with two regions requiring further careful investigation $0 < b < 0.1$ and $0.9 < b < 1$. Anisotropy within the samples is indicated, which merits further study.

11.10 Comparison of volumetric strains at failure

The volumetric strains at failure are shown in Fig 11.14 and are complimentary to the linear strains at failure. Tests ISC/1-12 & 15-18 show a good correlation. They do not agree with the conventional triaxial compression tests as $b \rightarrow 0$. A conservative extrapolation of the ISC test data toward b = 0 suggests a volumetric strain twice that obtained in the conventional test. It is not possible to say with certainty whether Tests ISC/13 & 14 correlate with the tests in which σ_1' at failure was the axial stress. However, it is clear that if the mean line is extrapolated to b = 1 it predicts a volumetric strain at failure about 3 times that of the more conventional triaxial extension tests. However this may, in part, be due to the differing stress paths followed in the two types of extension test, see Fig 11.33.

The results of Tests ISC/19 & 20 lie slightly off the mean curve and, together with those of Tests ISC/13 & 14, reinforce the suggestion that anistropy occurs in the sample. The magnitude of the volumetric strain attains a minimum value at b = 0.5 corresponding with the linear strains. The volumetric strains exhibit a well defined pattern of behaviour. Again the regions $0 < b < 0.1$ and $0.9 < b < 1$ require further investigation.

Volumetric failure strain data for the different test types are included in Fig 11.14. Again it is seen that the ISC tests show very much larger volumetric strains at failure than the more conventional tests, in conformity with the linear strain data.

Volumetric strain at failure, $\Delta V/V_c$ %

0
-0.5
-1.0
-1.5
-2.0
-2.5
-3.0
-3.5
-4.0
-4.5
-5.0
-5.5
-6.0
-6.5

0
0.2
0.4
0.6
0.8
1.0

$$b = \frac{(\sigma_2' - \sigma_3')}{(\sigma_1' - \sigma_3')}$$

IC|5(21)
IC|6(22)

cuboidal triaxial compression/extension

- mean type ICE cuboidal extension
- mean type IC cuboidal compression
- mean type IB cylindrical compression

cylindrical triaxial compression/extension

- mean type EX

independent stress control
H = 3·3" B = 5·2" C = 2·1"

- triaxial compression plane strain
  - $\Delta B/B_c = 0$
  - $\Delta H/H_c \approx 0$
- belt opening
- belt closing
- belt closing, σ_1' = stress in belt direction

INDEPENDENT STRESS CONTROL

COMPARISON OF VOLUMETRIC STRAINS AT MAXIMUM ϕ'

Results adjusted to correspond to an initial porosity, n_i = 39 %

FIG. 11.14

11.11 Comparison of volumetric strain rates at failure.

The variation in the volumetric strain rate at failure with b is shown in Fig 11.15. The primary comparison is of the volumetric strain rate with respect to H. A secondary comparison concerns the volumetric strain rate with respect to B, but only over a portion of the range of b values.

Consider the rate of dilatation with respect to H. Tests ISC/1-18 show a good correlation, the magnitude of the volumetric strain rate increasing with b. As $b \rightarrow 0$ the ISC results agree extremely well with the conventional triaxial compression tests. For the range from triaxial compression to plane strain, $0 < b < 0.25$ the curve is virtually horizontal, i.e. the rate of dilatation is insensitive to the intermediate principal stress. It may be recalled from Chapters 8,9 & 10 that all the triaxial compression tests were extremely insensitive to the geometrical properties of the sample and the degree of end restraint. The ISC data substantiate the insensitivity in this region. The full significance of this is not at present understood by the writer. The two plane strain tests ISC/19 & 20 are reproducible and lie on the mean curve for Tests ISC/1-18. Since the curve is relatively flat in this region the agreement may not be too significant.

As b increases beyond 0.8 the curve is steep, but very well defined, so that it may be extrapolated to b = 1 with certainty. The extrapolated value of $d(\Delta V/V_o)/d(\Delta H/H_o)$ of -1.5 is about 50% greater than that obtained for the more conventional triaxial extension tests, -0.90 to -1.01. However the secondary comparison of the volumetric strain rate with respect to the belt strain appears to throw further light on this discrepancy. Values for $0.6 < b < 1$ only are shown. In the remaining region $0 < b < 0.6$ the volumetric strain rates become large and are not conveniently plotted on the present diagram. As b approaches plane strain, 0.25, from zero, $d(\Delta V/V_c)/d(\Delta B/B_c)$ approaches $+\infty$ and for a b value slightly in excess of 0.25 it approaches $-\infty$. However the portion of the curve shown will suffice the present purpose. Ideally the two volumetric strain rate curves should meet at a point at b = 1. Instead they intersect at b = 0.88 in the region of Tests ISC/10,11,& 12, corresponding to $d(\Delta H/Hc) = d(\Delta B/Bc)$ and $\Delta H/Hc = \Delta B/Bc$ since a constant strain rate ratio $\Delta H/Hc : \Delta B/Bc = 1$ is imposed on these samples.

cuboidal triaxial compression / extension

- mean type ICE cuboidal extension
- mean type IC cuboidal compression
- mean type IB cylindrical compression

cylindrical triaxial compression / extension

- mean type EX

independent stress control
H = 3·3", B = 3·2", C = 2·1"

- triaxial compression

plane strain

- $\Delta B/B_c = 0$
- $\Delta H/H_c \approx 0$

- belt opening
- belt closing
- belt closing, σ_1' = stress in belt direction

Volumetric strain rate at failure, $\frac{d(\Delta V/V_c)}{d(\Delta B/B_c)}$ or $\frac{d(\Delta V/V_c)}{d(\Delta H/H_c)}$

$\frac{d(\Delta V/V_c)}{d(\Delta B/B_c)}$

$\frac{d(\Delta V/V_c)}{d(\Delta H/H_c)}$

$\frac{d(\Delta V/V_c)}{d(\Delta B/B_c)} = \frac{d(\Delta V/V_c)}{d(\Delta C/C_c)}$

$\frac{d(\Delta V/V_c)}{d(\Delta B/B_c)}$

$b = \frac{(\sigma_2' - \sigma_3')}{(\sigma_1' - \sigma_3')}$

INDEPENDENT STRESS CONTROL

COMPARISON OF VOLUMETRIC STRAIN RATES AT MAXIMUM ϕ'

Results adjusted to correspond to an initial porosity, $n_i = 39{\cdot}0\%$

FIG. 11.15

Reference to Figs A 11.9 & A 11.10 indicates that this is true. Furthermore the volumetric strain rate with respect to B, when extrapolated to b = 1, agree exactly with the cuboidal triaxial extension test mean point. It seems most unlikely that this agreement is fortuitous. It was noted earlier in the comparison of the peak strengths that the drained strength of sands is not very sensitive to the stress path followed. This is also true of the volumetric strain rates, see Fig 9.21 and Cornforth (1961), Fraser (1957) Eldin (1951), Taylor (1941). It is not likely, therefore, that the agreement of the volumetric strain rates is affected significantly by the differing stress paths. The volumetric strain rate with respect to lateral strain in the cuboidal triaxial extension test is equal to the volumetric strain rate with respect to the belt strain in the equivalent ISC test. One may conclude that, (a) the sample is probably anisotropic and that this anisotropy is identical in the samples used in the two types of test - which it clearly must be since the mode of sample preparation is the same, and (b) the difference in the nature of the loading boundaries, i.e. flexible or rigid lubricated, is probably not significant. Similar conclusions were reached as a result of considering the strengths and taken together form a substantial argument in support of (a) and (b) above.

The rates of volume change for the different test types are tabulated in Fig 11.16. The rate with respect to the axial strain is independent of the test type for triaxial compression. For triaxial extension, the cylindrical and cuboidal conventional triaxial samples exhibit similar rates with respect to lateral strain, i.e. e_1, even though the ϕ' values vary by up to 3.0°. This is in conflict with the essentially unique relationship between ϕ' and volumetric strain rate observed in triaxial compression. The steepness of the $d(\Delta V/V_c)/d(\Delta H/H_c)$ versus b relationship, Fig 11.15, in the region of $b \rightarrow 1$ indicates that a unique relation here is much less likely. The volumetric strain rates in the conventional extension tests are all measured with respect to the lateral strain whereas in the ISC extension test the axial direction is one of the major principal stress directions. The volumetric strain rate with respect to the B direction agrees with all the earlier tests whereas the rate with respect to the H direction is significantly different. This difference is probably due to anisotropy within the sample.

Triaxial compression					
Test type	Corrected ϕ'	e_1 %	$e_2 = e_3$ %	e_v %	$\frac{de_v}{de_1}$
Cylindrical compression H/D = 2, non-lubricated Type B	39·0°	$\Delta H/H_c$ +5·0	$\Delta D/D_c$ −4·0	$\Delta V/V_c$ −2·3	$\frac{d(\Delta V/V_c)}{d(\Delta H/H_c)}$ −0·60
Cylindrical compression H/D = 1, lubricated Types A, X, IB	39·0°	$\Delta H/H_c$ +7·5	$\Delta D/D_c$ −5·5	$\Delta V/V_c$ −3·2	$\frac{d(\Delta V/V_c)}{d(\Delta H/H_c)}$ −0·60
Cuboidal compression Type IC	39·0°	$\Delta H/H_c$ +7·5	$\Delta B/B_c = \Delta C/C_c$ −5·8	$\Delta V/V_c$ −3·2	$\frac{d(\Delta V/V_c)}{d(\Delta H/H_c)}$ −0·57
Extrapolated ISC test data, b = 0	39·0°	$\Delta H/H_c$ +14·0	$\Delta B/B_c = \Delta C/C_c$ −12·0	$\Delta V/V_c$ −6·0	$\frac{d(\Delta V/V_c)}{d(\Delta H/H_c)}$ −0·58

Triaxial extension					
Test type	Corrected ϕ'	e_3 %	$e_1 = e_2$ %	e_v %	$\frac{de_v}{de_1}$
Cylindrical extension H/D = 2, non-lubricated Type ELA	41·9°–43·5°	$\Delta H/H_c$ −7·2	$\Delta D/D_c$ +3·0	$\Delta V/V_c$ −1·0	$\frac{d(\Delta V/V_c)}{d(\Delta D/D_c)}$ −1·00
Cylindrical extension H/D = 1, lubricated Type EX	40·9°	$\Delta H/H_c$ −4·6	$\Delta D/D_c$ +2·0	$\Delta V/V_c$ −0·5	$\frac{d(\Delta V/V_c)}{d(\Delta D/D_c)}$ −0·90
Cuboidal extension Type ICE	43·9°	$\Delta H/H_c$ −4·8	$\Delta B/B_c = \Delta C/C_c$ +2·0	$\Delta V/V_c$ −0·9	$\frac{d(\Delta V/V_c)}{d(\Delta B/B_c)}, \frac{d(\Delta V/V_c)}{d(\Delta C/C_c)}$ −1·01
Extrapolated ISC test data, b = 1·0	44·0°	$\Delta C/C_c$ −11·5	$\Delta H/H_c = \Delta B/B_c$ +4·6	$\Delta V/V_c$ −2·9	$\frac{d(\Delta V/V_c)}{d(\Delta B/B_c)}, \frac{d(\Delta V/V_c)}{d(\Delta H/H_c)}$ −1·02 −1·50

Results correspond to an initial porosity, n_i = 39·0%

FAILURE CHARACTERISTICS OBTAINED IN DIFFERENT TRIAXIAL COMPRESSION & EXTENSION TESTS

FIG. 11.16

11.12 Variation of the intermediate principal stress

The form of the variation of the intermediate principal stress, σ_2', as it increases from the minor to the major principal stress is of prime interest. The 3 principal stress ratios at failure are compared in Fig 11.17, all corrections having been applied. The stress ratio σ_1'/σ_3' varies, of course, in an identical manner to that of ϕ', Fig 11.9, previously discussed. It is essentially constant in the region $0.25 \leq b \leq 1$ although there is some scatter of the points about the average line.

The stress ratio σ_2'/σ_3' increases linearly from 1 at b = 0 to 5.56 at b = 1. For $b > 0.4$ it is noticeable that the experimental points are disposed about the average line in an identical manner to those for σ_1'/σ_3'. Since σ_1'/σ_3' is essentially constant and independent of b for $0.25 \leq b \leq 1$ the linear form of the σ_2'/σ_3' plot may be misleading. Now we are plotting:

$$\frac{\sigma_2'}{\sigma_3'} \quad \text{against} \quad \left[\frac{\sigma_2'}{\sigma_3'} - 1\right] \Big/ \left[\frac{\sigma_1'}{\sigma_3'} - 1\right]$$

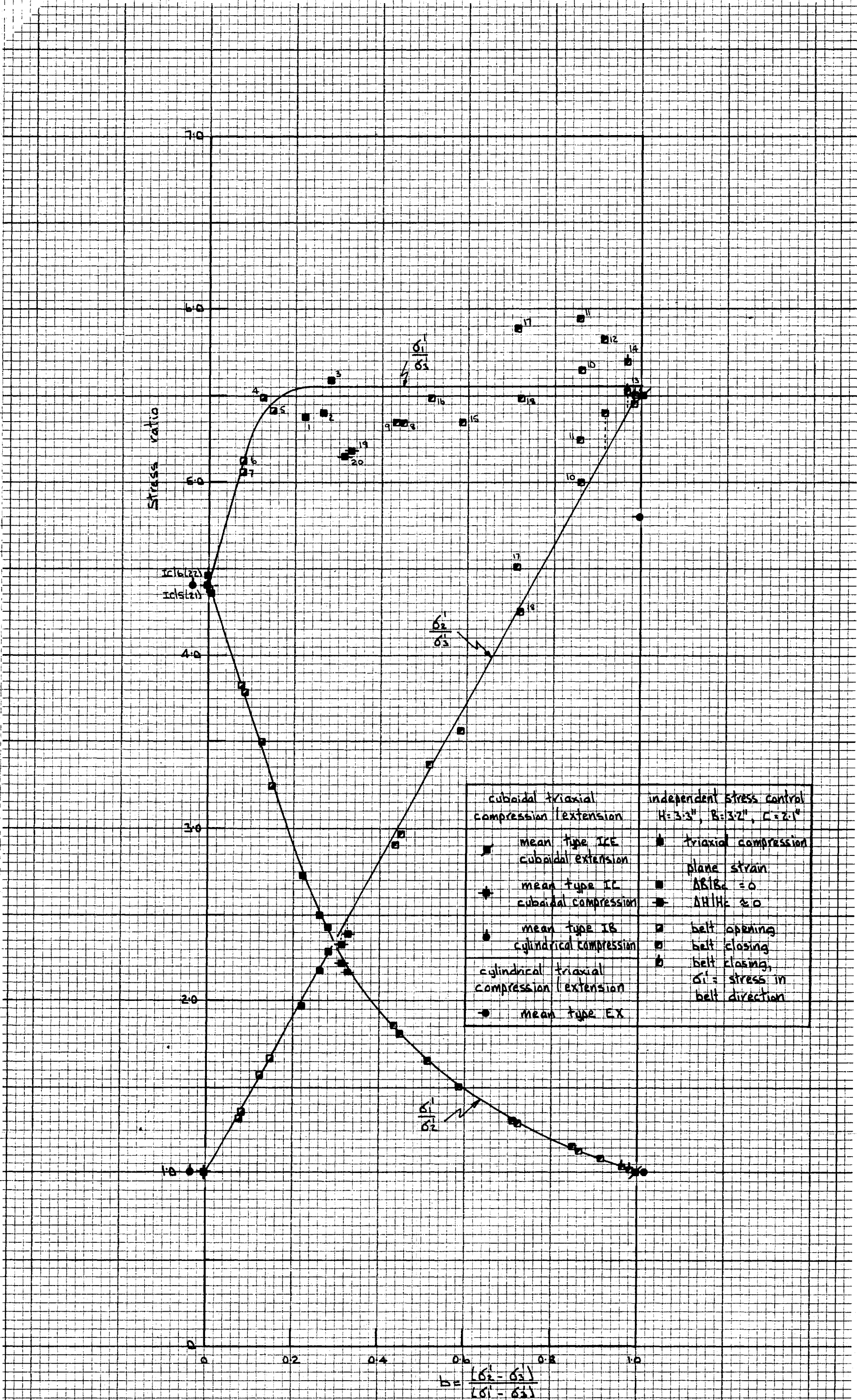
If σ_1'/σ_3' is constant then the plot is a straight line per se. In addition, in the region $0 \leq b \leq 0.25$ where σ_1'/σ_3' varies between 4.39 and 5.56 the b value is very insensitive to this change. For example consider Test ISC/6 in which $\sigma_2'/\sigma_3' = 1.35$, $\sigma_1'/\sigma_3' = 5.12$ and b = 0.084. If we change σ_1'/σ_3' to 5.56, then b = 0.077 ; alternatively if $\sigma_1'/\sigma_3' = 4.39$, then b = 0.103. This has an insignificant effect on the plotted σ_2'/σ_3' point. The above illustrates the difficulty in finding meaningful plots combining σ_1', σ_2' & σ_3' in a suitable form, Hendron (1965). The problem of including strains as well is perhaps even more difficult and is discussed in a subsequent section. As a corollary, if we try to write the equation to the line for σ_2'/σ_3' we get:

$$\left[\frac{\sigma_2'}{\sigma_3'} - 1\right] = 4.56 \left[\frac{\sigma_2'}{\sigma_3'} - 1\right] \div \left[\frac{\sigma_1'}{\sigma_3'} - 1\right]$$

$$\text{i.e.} \quad \frac{\sigma_1'}{\sigma_3'} = 5.6 \quad \text{or} \quad \frac{\sigma_2'}{\sigma_3'} = 1$$

which is clearly untenable for the reasons given.

The stress ratio σ_1'/σ_2' decreases along a smooth curve from 4.39 at b = 0 to 1.0 at b = 1. The scatter of the experimental points is reduced, particularly in the region $0.25 \leq b \leq 1$. Since $\sigma_1'/\sigma_2' = \sigma_1'/\sigma_3' \div \sigma_2'/\sigma_3'$ this is to be expected due to the similarity in the scatter of



INDEPENDENT STRESS CONTROL

COMPARISON OF CORRECTED STRESS RATIOS AT MAXIMUM ϕ'

Results adjusted to correspond to an initial porosity, n_i = 39·0%

Corrections applied for effect of: (i) non-uniform deformation
(ii) sample sheath strength
(iii) platten friction
(iv) average stress level

FIG. 11.17

σ_1'/σ_3' and σ_2'/σ_3'. A particular failure stress, σ_1', may be looked upon as inducing an appropriate intermediate stress, σ_2'. If for some extraneous reason σ_1' is slightly higher, then σ_2' will also be high such that the ratio σ_1'/σ_2' is unaffected.

There is no ambiguity in the preceding comparisons over Tests ISC/13 & 14.

Tests ISC/19 & 20 lie below the average curves for σ_1'/σ_3' and σ_2'/σ_3' whereas they correlate exactly on the σ_1'/σ_2' plot, as might be expected from the preceding arguments. Any anisotropy within the sample appears to be barely significant in this case.

The variation of σ_2' with belt strain $\Delta B/Bc$, is shown in Fig 11.18. The results of Tests ISC/2-12 & 15-18 are very consistent whereas in Test ISC/1, σ_2' is low. Again there is some uncertainty over whether to include the belt or axial strains in Tests ISC/13 & 14. The difference is small and the departure from the more conventional triaxial extension test is well established. At the opposite end of the strain scale the ISC test data does not agree with the triaxial compression test results due to the increased strains to failure obtained in the ISC apparatus. The form of the stress-strain relation is similar to the active-passive pressure relationship for a rigid retaining wall, Terzaghi (1934). Opening the belt corresponds to the active case and closing to the passive case. The results of Test ISC/19 & 20 are consistent but do not appear to correlate with the remaining tests. Admittedly the agreement could be improved by modifying the curve, shown dotted in Fig 11.18, but this seems unlikely. The difference in behaviour between Tests ISC/2 & 3 and 19 & 20 appears to be significant and is probably due to sample anisotropy although the possibility of an effect due to the different ISC belt plattens used in the two pairs of tests cannot be excluded.

It will be observed from Fig 11.17 that at failure σ_2'/σ_3' is approximately equal to σ_1'/σ_2' for plane strain. In fact the two lines intersect at b = 0.3 whereas plane strain corresponds to b = 0.25. We will neglect this difference in the present instance so that for plane strain we have the relationship:

$$\sigma_2' = (\sigma_1' . \sigma_3')^{\frac{1}{2}}$$

This is a simpler relationship than that for plane strain given by Bishop (1966) namely:

$$\frac{\sigma_2'}{\sigma_1' + \sigma_3'} = \tfrac{1}{2} \cos^2 \phi'$$

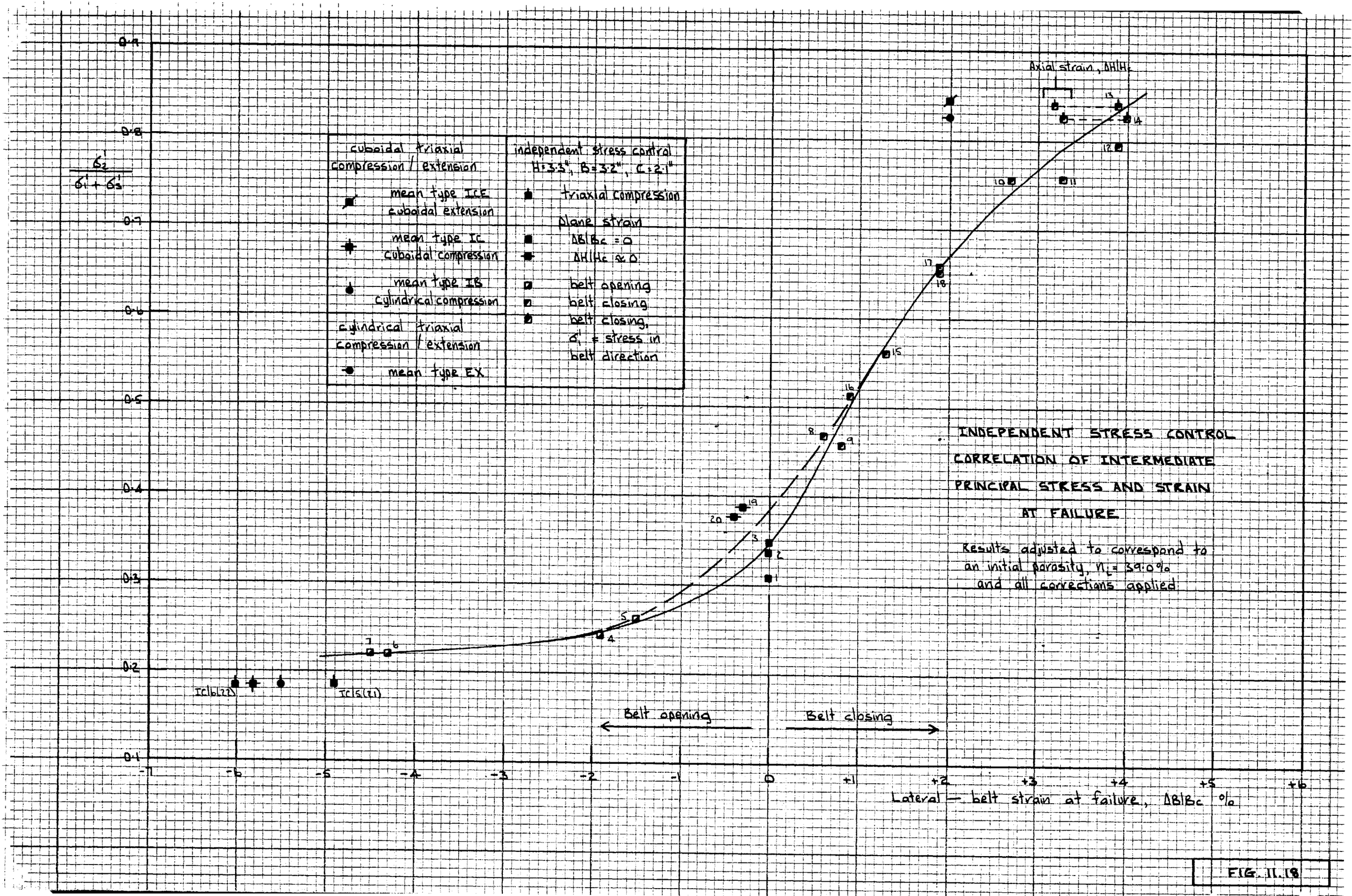

$\frac{\sigma_2'}{\sigma_1' + \sigma_3'}$
0·9
0·8
0·7
0·6
0·5
0·4
0·3
0·2
0·1
cuboidal triaxial compression / extension
mean type ICE cuboidal extension
mean type IC cuboidal compression
mean type IB cylindrical compression
cylindrical triaxial compression / extension
mean type EX
independent stress control
H=3·3", B=3·2", C=2·1"
triaxial compression
plane strain
ΔB/Bc = 0
ΔH/Hc ≈ 0
belt opening
belt closing
belt closing, σ1' = stress in belt direction
Axial strain, ΔH/Hc
IC/b(2)
IC/5(2)
Belt opening
Belt closing
-7
-6
-5
-4
-3
-2
-1
0
+1
+2
+3
+4
+5
+6
Lateral — belt strain at failure, ΔB/Bc %
INDEPENDENT STRESS CONTROL
CORRELATION OF INTERMEDIATE PRINCIPAL STRESS AND STRAIN AT FAILURE
Results adjusted to correspond to an initial porosity, n_i = 39·0% and all corrections applied

FIG. II.18

which is based partly on theory, Jaky (1944 & 1948) and partly on experimental observations, Wood (1958).

The values of σ_2' at failure in plane strain are correlated with ϕ' in Fig 11.19 after Bishop (1966). Also shown are data from tests in the plane strain apparatus. Of the present group, Test ISC/1 is unreliable. The other 4 ISC tests form 2 sets, Tests ISC/19 & 20 showing slightly higher $\sigma_2' / (\sigma_1' + \sigma_3')$ values than Tests ISC/2 & 3. However Tests ISC/19 &20 were not perfect plane strain tests since the axial plattens yielded by 0.3% due to the testing technique used. As noted previously these 2 tests do not correlate too well with the other ISC tests even allowing for yielding, due probably to initial anisotropy within the sample. Various "theoretical" curves are also shown, based on differing assumptions. The empirical relationship $\sigma_2'/(\sigma_1' + \sigma_3') = \frac{1}{2} \cos^2 \phi'$ slightly underestimates σ_2' obtained in all the previous plane strain tests shown. The present tests lie markedly above this line and the earlier data. All other things being equal the ISC tests should correlate with the earlier tests. Since they do not, we must conclude that there may be an"apparatus factor" causing this difference. The reason appears to be friction between the sample and the axial plattens in the earlier plane strain apparatus. Both Cornforth (1961) and Wade (1963) showed that a plane strain test on a K_o-consolidated sample in which the σ_2 belt or end clamp was not used gave similar, but not identical, failure characteristics to a test in which $e_2 = 0$ was precisely maintained and σ_2 measured. This demonstrates that without the belt friction can develop between the sample and the axial plattens to restrain the sample in the e_2 direction sufficiently for a plane strain type of failure to occur. When the σ_2 belt is used, theoretically there should be no friction force developed in the e_2 direction if $e_2 = 0$. Initial proving tests by Wood on compacted moraine in which the σ_2 belt was opened or closed slightly during shear showed no significant difference in σ_2 (these tests were never reported by Wood but are recalled by Professor Bishop). However in all tests in the plane strain apparatus, platten friction occurs in the e_3 direction which results in failure being concentrated towards the mid-height of the sample. Since in the earlier plane strain tests $\sigma_2'/(\sigma_1' + \sigma_3')$ was always rising as failure was approached only the average value is measured, which must be less than the true value. In the ISC apparatus

CORRELATION WITH ϕ' OF THE VALUE OF THE INTERMEDIATE PRINCIPAL STRESS AT FAILURE IN PLANE STRAIN

FIG. 11.19

platten friction is minimised so that the measured value of σ_2' is relatively higher and more nearly correct. It may be noted that in the earlier plane strain tests the samples were K_o- consolidated so that at the start of shear $\sigma_2'/(\sigma_1'+\sigma_3') < \frac{1}{2}$ and an initially uniform sample may then exhibit stress induced anisotropy. In the present tests the samples were isotropically consolidated so that $\sigma_2'/(\sigma_1'+\sigma_3') = \frac{1}{2}$ at the commencement of shear.

Now the relation $\sigma_2'/(\sigma_1'+\sigma_3') = \frac{1}{2}\cos^2\phi'$ is based on Wood's experimental observation that throughout a plane strain test $\sigma_2' = K_o\sigma_1'$. If the measured value of σ_2' were low then this relation would be incorrect and this would account for the discrepancy. The relationship $\sigma_2'/(\sigma_1'+\sigma_3') = \frac{1}{2}\cos^2\phi'$ may be conveniently modified by writing:

$$\frac{\sigma_2'}{(\sigma_1'+\sigma_3')} = \frac{1}{2}\cos^2(\alpha\phi')$$

where α = constant. The empirical relationship for $\alpha = 0.8$ is shown in Fig 11.19 which gives a reasonable fit with Tests ISC/2 & 3.

For a perfectly plastic material in which no volume change occurs $\sigma_2' = \frac{1}{2}(\sigma_1'+\sigma_3')$ for plane strain, independent of ϕ'. This appears as an upper bound in Fig 11.19. For an isotropic elastic material the theoretical relationship:

$$\sigma_2'/(\sigma_1'+\sigma_3') = K_o/(1+K_o)$$

is obtained, Cornforth (1961). Combining this with Jaky's expression, $K_o = (1-\sin\phi')$, (Jaky 1944,1948), gives the equation:

$$\sigma_2'/(\sigma_1'+\sigma_3') = (1-\sin\phi')/(2-\sin\phi')$$

which plots below Bishop's relation in Fig 11.19.

Two additional theoretical lines are shown. The equation $\sigma_2' = \frac{1}{3}(\sigma_1'+\sigma_3')$ bounding Rennies (1959) theoretical solution, extended by Parkin (1965), gives a reasonable fit to all sand test results but not to the clay. This relation has a lower cut-off point at $\sigma_1'/\sigma_3' = 0$, i.e. $\phi' = 19.5^\circ$, Rennie (1959). Since this solution assumes a rigid ordered pack of frictional spheres we may anticipate a lack of fit with sand data. Finally the simple empirical expression $\sigma_2'^2 = \sigma_1'.\sigma_3'$ based on the ISC data is plotted. With the exception of the case of a perfectly plastic material the remaining relationships give a reasonable fit with the observed data some being less good than others. The discrepancy between the two pairs of plane strain tests with the ISC apparatus needs clarifying before the best fitting relation can be chosen. The two relations $\sigma_2'^2 = \sigma_1'.\sigma_3'$ and

with clay data and a better fit

$\sigma_2'/(\sigma_1'+\sigma_3') = \frac{1}{2}\cos^2\alpha\phi'$ appear to be the most promising.

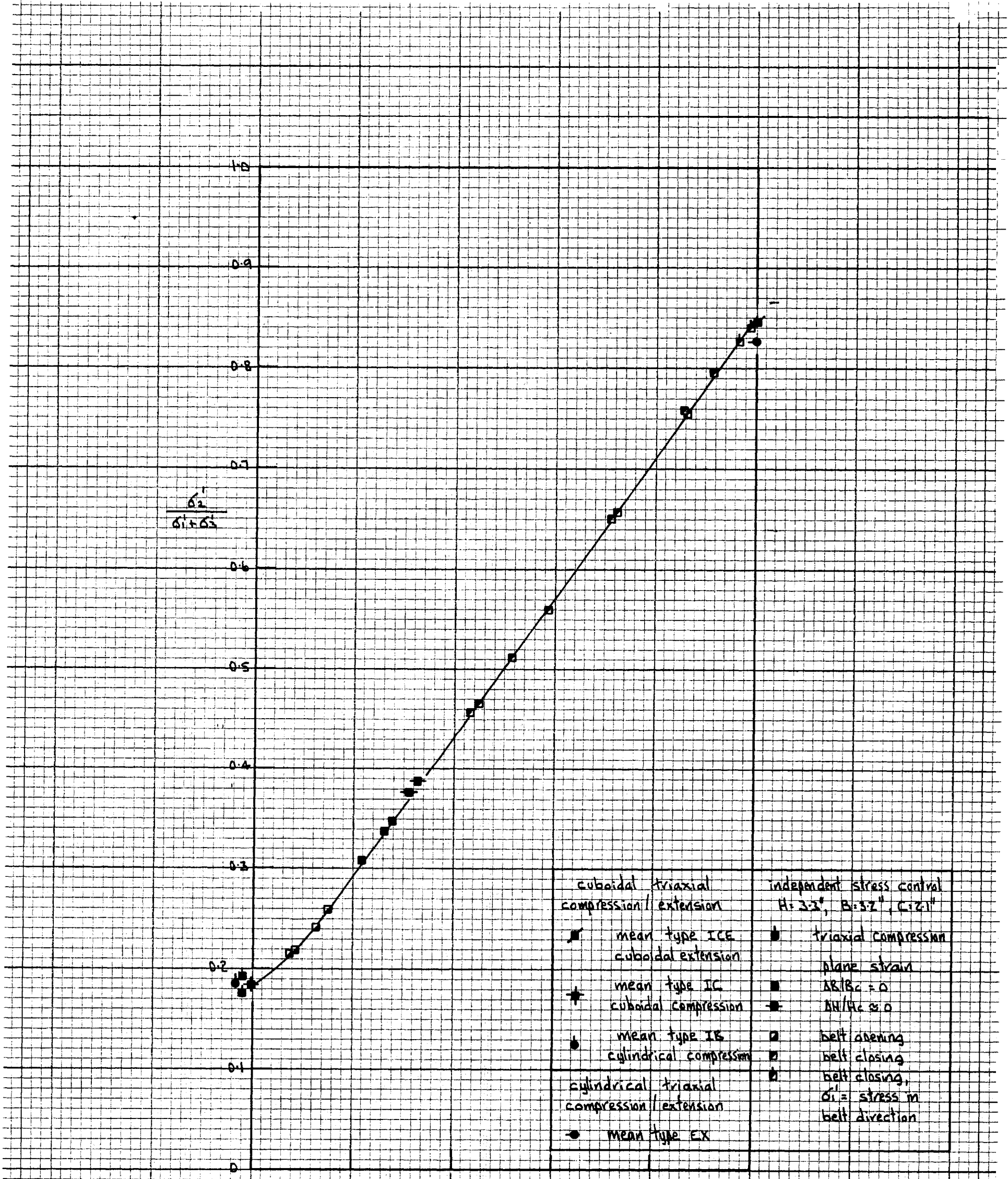
The variation of $\sigma_2'/(\sigma_1'+\sigma_3')$ with b at failure is shown in Fig 11.20. The value of σ_2' varies continuously over the stress range, the relation being linear in the region $0.25 \leqslant b \leqslant 1$ and slightly curved for $0 \leqslant b \leqslant 0.25$. The reasons for this are identical to those given earlier for the shape of the σ_2'/σ_3' plot, Fig 11.17. The points all lie close to the average line due to the predominating effect of σ_1' and σ_2' in the ratio $\sigma_2'/(\sigma_1'+\sigma_3')$. It is noted that when $b = \frac{1}{2}$, $\sigma_2'/(\sigma_1'+\sigma_3') = \frac{1}{2}$ whatever the relative values of σ_1', σ_2' & σ_3' since if $b = (\sigma_2'-\sigma_3')/(\sigma_1'-\sigma_3')$ then:

$$\frac{\sigma_2'}{(\sigma_1'+\sigma_3')} = \frac{b\sigma_1' + (1-b)\sigma_3'}{\sigma_1'+\sigma_3'}$$

putting $$\frac{b\sigma_1'+(1-b)\sigma_3'}{\sigma_1'+\sigma_3'} = \frac{1}{2}$$

$$\therefore \quad b = \tfrac{1}{2} \text{ if } \sigma_1' \neq \sigma_3'$$

So far only the influence of σ_2' on the failure characteristics has been discussed. The variation in $\sigma_2'/(\sigma_1'+\sigma_3')$ during the whole of the shear stage is shown in Fig 11.21. The failure points are indicated together with a failure envelope for the ISC tests. The values of $\sigma_2'/(\sigma_1'+\sigma_3')$ beyond failure for large b values are ambiguous on account of the cross-over of the axial and belt stress-strain curves near failure, e.g. Tests ISC/10 & 12. After isotropic consolidation $\sigma_2'/(\sigma_1'+\sigma_3') = 0.5$ for all the tests. At the commencement of shear this ratio drops, and (a) continues to drop before flattening out for $b \rightarrow 0$, or (b) rises by an increasing amount as $b \rightarrow 1$. Test ISC/1 does not agree with Tests ISC/2 &3. Tests ISC/19 & 20 are very different from the remainder over the initial 2% axial strain and do not lie on the failure envelope probably as a result of sample anisotropy. Otherwise the ISC tests are quite consistent up to failure, all failure points lying reasonably close to the failure envelope. The 2 triaxial compression tests, ISC/5 & 6, form a lower boundary to the family and the two cuboidal extension tests ICE/4 & 10 form an upper boundary. The ISC failure envelope does not fit these tests, reflecting the strain differences discussed earlier. The value of σ_2' increases markedly between plane strain, Tests ISC/2 & 3, and Tests ISC/8 & 9 in which the ISC belt closes in by a small amount. This is in contrast

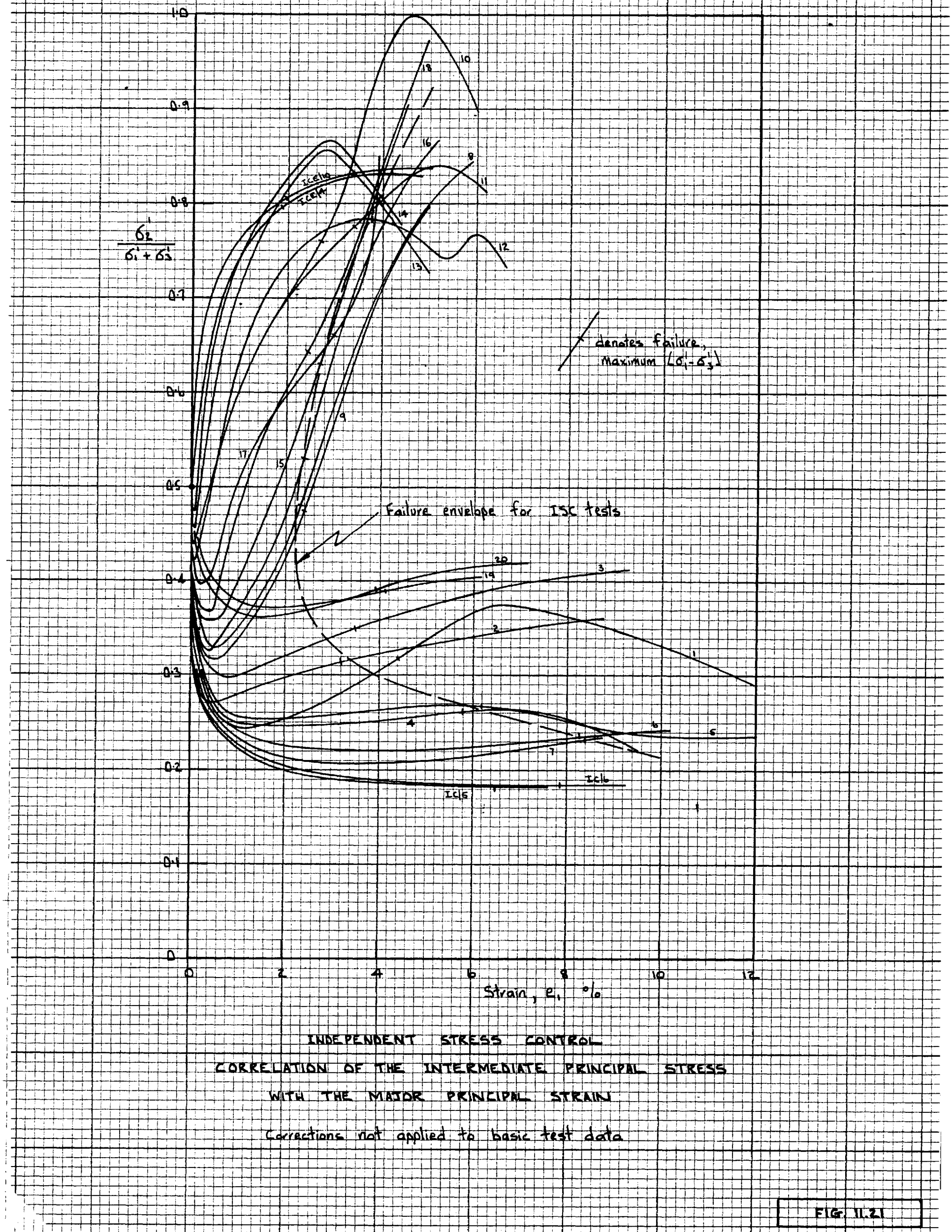


INDEPENDENT STRESS CONTROL

COMPARISON OF INTERMEDIATE PRINCIPAL STESSES AT FAILURE

Results adjusted to correspond to an initial porosity, $n_c = 39.0\%$ and all corrections applied.

FIG. 11.20



INDEPENDENT STRESS CONTROL

CORRELATION OF THE INTERMEDIATE PRINCIPAL STRESS WITH THE MAJOR PRINCIPAL STRAIN

Corrections not applied to basic test data

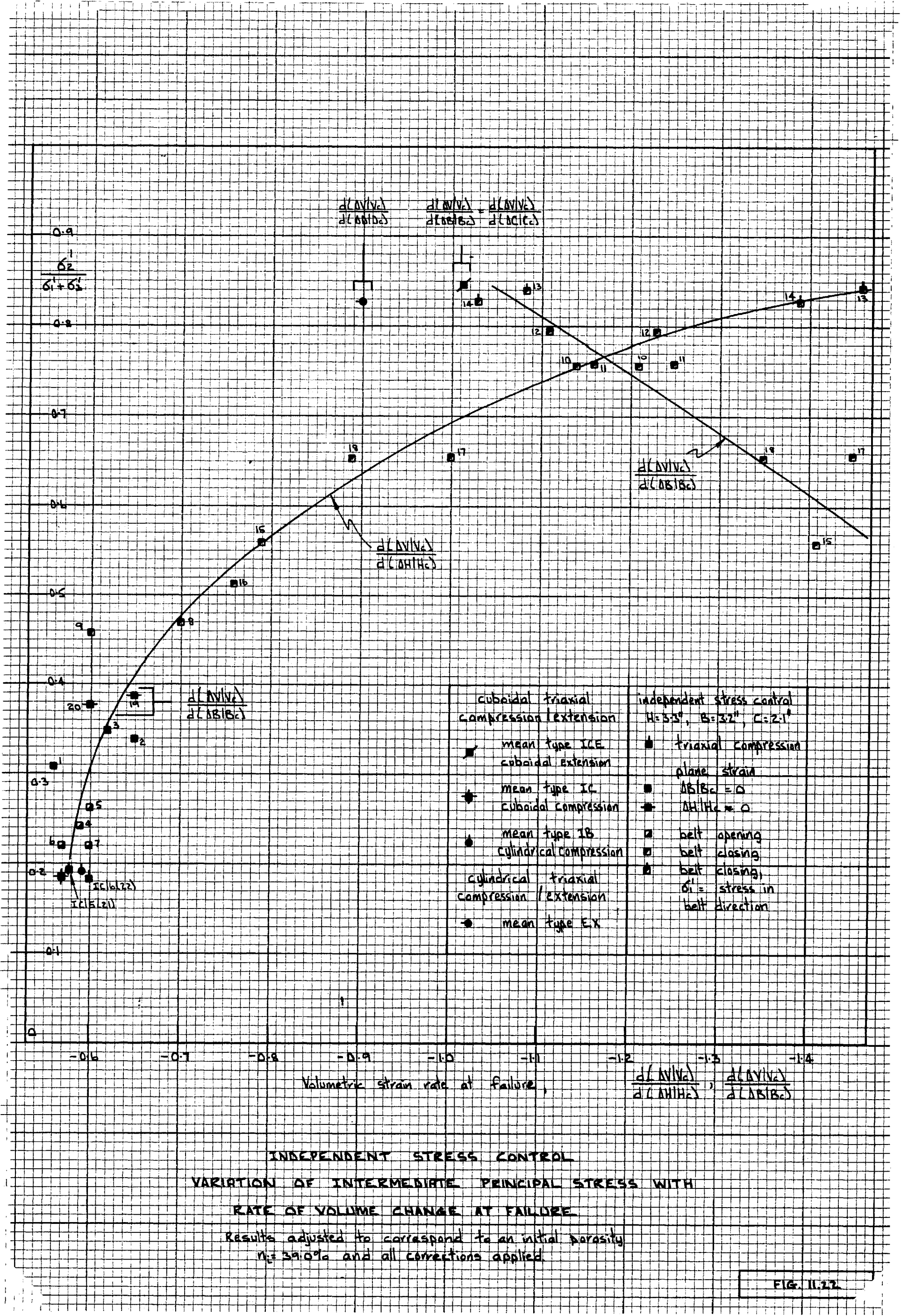
FIG. 11.21

to a small reduction in σ_2' as the ISC belt yields, Tests ISC/4 & 5. These latter two observations are analogous with the active-passive pressure problem (see also Fig 11.18).

The form of variation of σ_2' for the plane strain tests is consistent with the plane strain tests on K_o-consolidated sands by Cornforth (1961) and Wade (1963). Agreement is best beyond $e_1 = +1.0\%$ when the variations arising from the different modes of consolidation appear to be eliminated.

The variation of the intermediate principal stress with the volumetric strain rate at failure is shown in Fig 11.22. Increasing σ_2' causes an increase in the magnitude of the volumetric strain rate with respect to $\Delta H/Hc$ as one might anticipate. The increase is marginal from triaxial compression to plane strain and is in contrast to a small decrease observed by Wade (1963), his Fig 8 - 9 and Cornforth's (1961) identical values, his Fig 8 - 12. The relationship is well defined as $b \rightarrow 1$ and it is observed that $d(\Delta V/V_c)/d(\Delta H/H_c)$ does not agree with the more conventional triaxial extension test data at $b = 1$. However when plotted against $d(\Delta V/V_c)/d(\Delta B/B_c)$ the ISC results correlate almost exactly with the cuboidal triaxial extension tests. This seemingly remarkable agreement was observed and commented upon earlier, see Fig 11.15. The ISC test data agrees with the conventional triaxial compression data at $b = 0$. The 2 plane strain tests ISC/19 & 20 agree with Tests ISC/1-18 considering the appropriate strain rates. However this region is insensitive so that this agreement may not be very significant.

In Chapters 9 & 10 good correlations were obtained between ϕ' and initial porosity, n_i, and between volumetric strain rate and n_i for triaxial compression and extension. In Fig 11.23 the relationship between ϕ' and the volumetric strain rate at failure, $d(\Delta V/V_c)/d(\Delta H/H_c)$ for some cylindrical triaxial compression tests is given. Two sets of the author's tests, Types B & C, are shown together with tests on identical material at varying higher cell pressures, Skinner (1969). The agreement is remarkable considering (a) the pressure range, (b) the different sample size, apparatus and operator, and (c) the large strains (up to +30% axial strain) required in the high pressure tests to reach a peak $(\sigma_1' - \sigma_3')$, so that the lateral deformations were very non-uniform and for which no special corrections were applied. We may conclude that the $\phi' - de_v/de_1$ relationship expresses a fundamental material property. For a

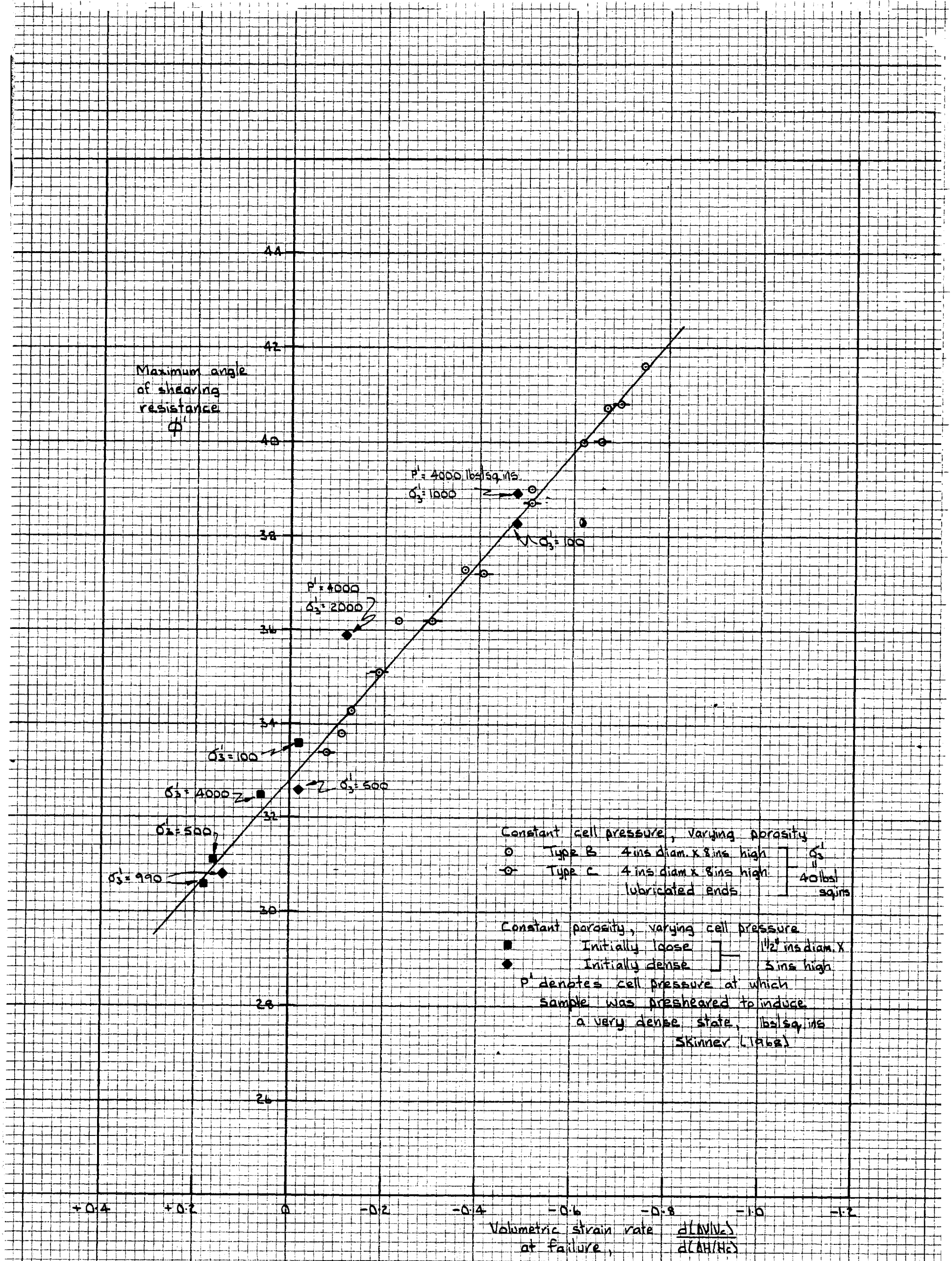


INDEPENDENT STRESS CONTROL

VARIATION OF INTERMEDIATE PRINCIPAL STRESS WITH RATE OF VOLUME CHANGE AT FAILURE

Results adjusted to correspond to an initial porosity n_i = 39·0% and all corrections applied.

FIG. 11.22



TRIAXIAL COMPRESSION TESTS AT VARYING POROSITY AND CELL PRESSURE

RELATIONSHIP BETWEEN Φ' AND RATE OF VOLUME CHANGE AT FAILURE

After Bishop (1966)

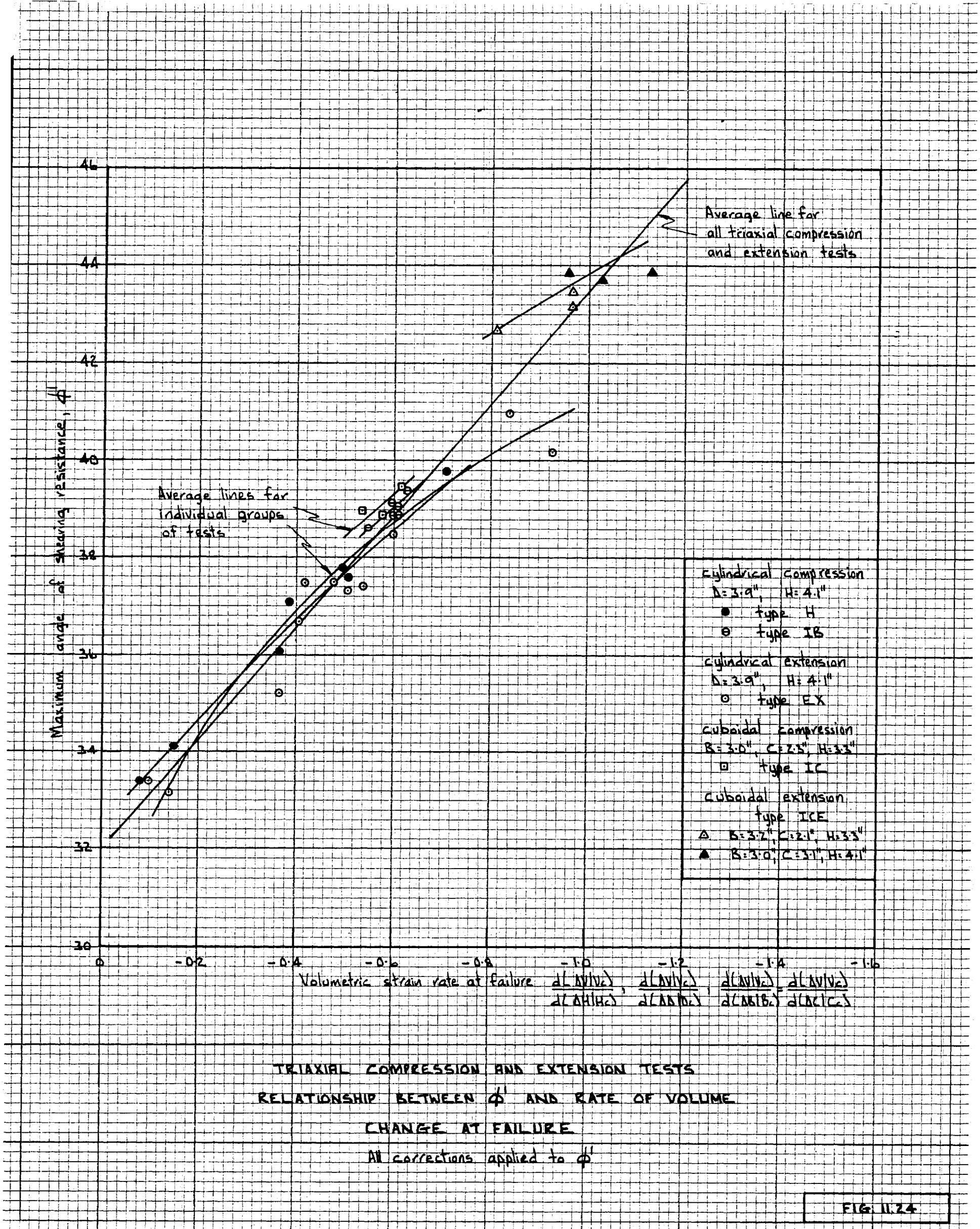
FIG. 11.23

given initial porosity, increasing the stress level decreases the volumetric strain rate and associated with this is a reduction in ϕ', Bishop (1966). In all of these tests $\sigma_2' = \sigma_3'$, i.e. $b = 0$.

Next, consider the triaxial compression, $b = 0$, and extension, $b = 1$, tests shown in Fig 11.24. The cylindrical triaxial compression and extension test data extend over a range of initial porosities (loose to dense) whereas only dense cuboidal samples were tested. The volumetric strain rates are all with respect to the major principal strain, e_1, so that the comparison may be slightly affected by sample anisotropy. The average lines for individual groups of tests are prescribed by earlier best fitting relations for $\phi' - n_i$ and $de_v/de_1 - n_i$. Superimposed is a new average line for all the tests, which implies a unique relationship for compression and extension, independent of the shape of the cross-section of the sample.

The volumetric strain rates for the ISC tests are given in Fig 11.25, generally with respect to the axial strain. The average line is ill-defined due to the scatter plus the small range of values. Between $b = 0$ and $b = 0.25$ the value of ϕ' increases by 5° for virtually no change in volumetric strain rate. It is unfortunate that there are no tests between IC/5 & 6 and ISC/6 & 7. Beyond plane strain, ϕ' is essentially constant whilst de_v/de_1 increases as $b \rightarrow 1$. In view of the apparently unique relationship between the triaxial compression and extension test results this behaviour is anomolous and difficult to explain. Interpretation is further complicated by the significantly large difference between the volumetric strain rates with respect to $\Delta H/H$ and $\Delta B/B$ in Tests ISC/13 & 14. These differences, attributed to sample anisotropy, would also affect Tests ISC/10,11,12,15,16,17 & 18, but to a decreasing extent. Tests of the type A & B of Fig 11.1 are needed to separate these factors. Tests ISC/19 & 20 appear to be relatively slightly affected by anisotropy and agree with Tests ISC/1,2 & 3 at least volumetric strain rate-wise.

The ISC test data of Fig 11.25 are superimposed on the triaxial compression & extension test data of Fig 11.24 in Fig 11.26 to enable an overall comparison, from which a pattern appears to emerge. There is a unique straight-line relationship between more conventional triaxial compression, $b = 0$, and triaxial extension, $b = 1$ tests. The ISC test data fit this relationship at $b = 0$ and $b = 1$ provided that in the latter case the volume-

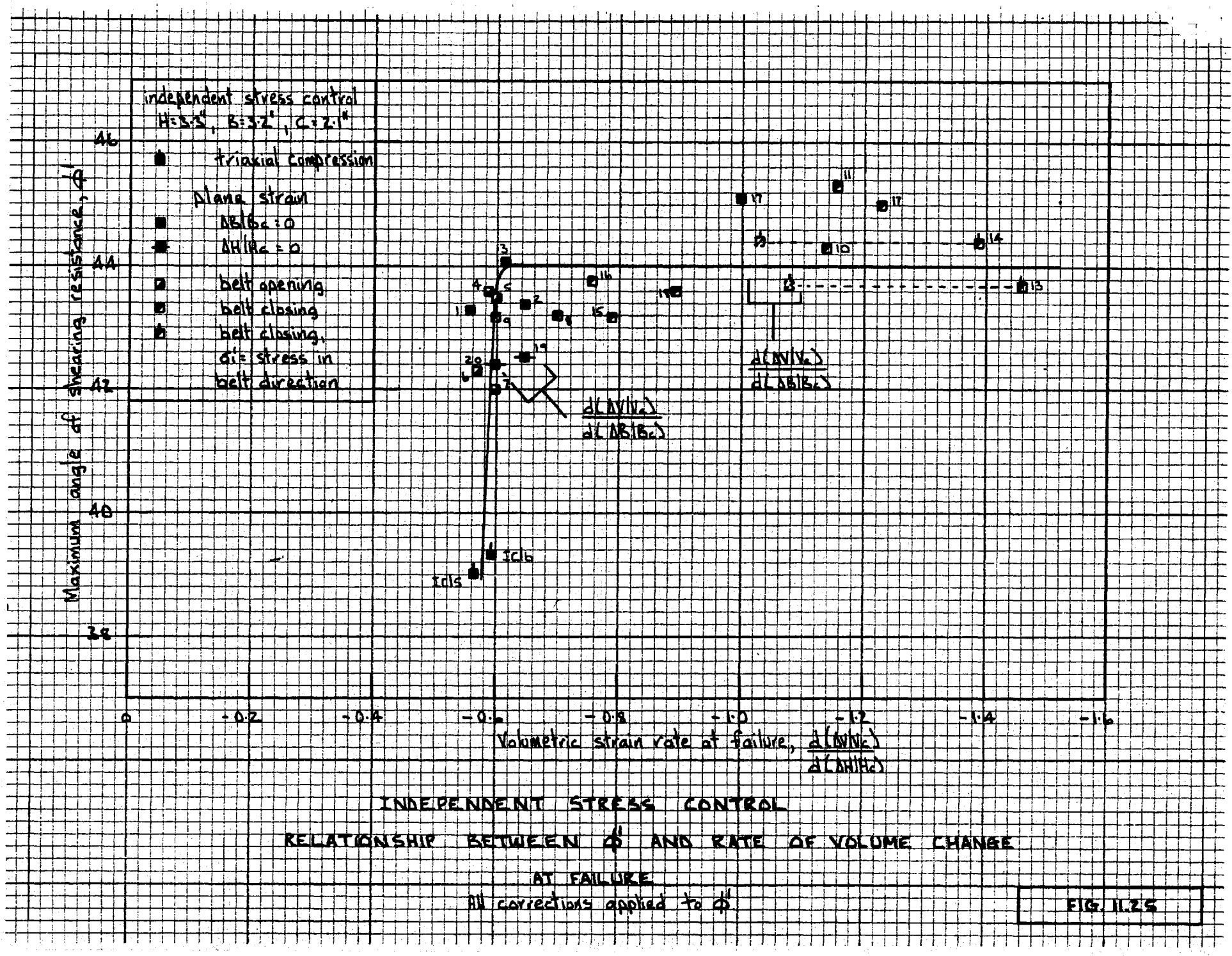


TRIAXIAL COMPRESSION AND EXTENSION TESTS

RELATIONSHIP BETWEEN ϕ' AND RATE OF VOLUME CHANGE AT FAILURE

All corrections applied to ϕ'

FIG. 11.24



INDEPENDENT STRESS CONTROL

RELATIONSHIP BETWEEN ϕ' AND RATE OF VOLUME CHANGE AT FAILURE

All corrections applied to ϕ'

FIG. 11.25

independent stress control
H=3.3", B=3.2", C=2.1"
● triaxial compression
plane strain
■ ΔB/B_c = 0
✚ ΔH/H_c ≈ 0
◪ belt opening
◪ belt closing
◪ belt closing,
σ'_1 = stress in belt direction

Average line for all triaxial compression and extension tests

Average lines for individual groups of tests

cylindrical compression
D=3.9", H=4.1"
● type H
⊙ type IB

cylindrical extension
D=3.9", H=4.1"
⊙ type EX

cuboidal compression
B=3.0", C=2.3", H=3.3"
⊡ type IC

cuboidal extension
type ICE
△ B=3.2", C=2.1", H=3.3"
▲ B=3.0", C=3.1", H=4.1"

Maximum angle of shearing resistance, ϕ'

50, 48, 46, 44, 42, 40, 38, 36, 34, 32, 30

0, -0.2, -0.4, -0.6, -0.8, -1.0, -1.2, -1.4, -1.6

Volumetric strain rate at failure, $\frac{d(\Delta V/V_c)}{d(\Delta H/H_c)}$, $\frac{d(\Delta V/V_c)}{d(\Delta B/B_c)}$, $\frac{d(\Delta V/V_c)}{d(\Delta B/B_c)} = \frac{d(\Delta V/V_c)}{d(\Delta C/C_c)}$

TRIAXIAL COMPRESSION & EXTENSION AND INDEPENDENT STRESS CONTROL TESTS

RELATIONSHIP BETWEEN ϕ' AND RATE OF VOLUME CHANGE AT FAILURE

All corrections applied to ϕ'

FIG. 11.26

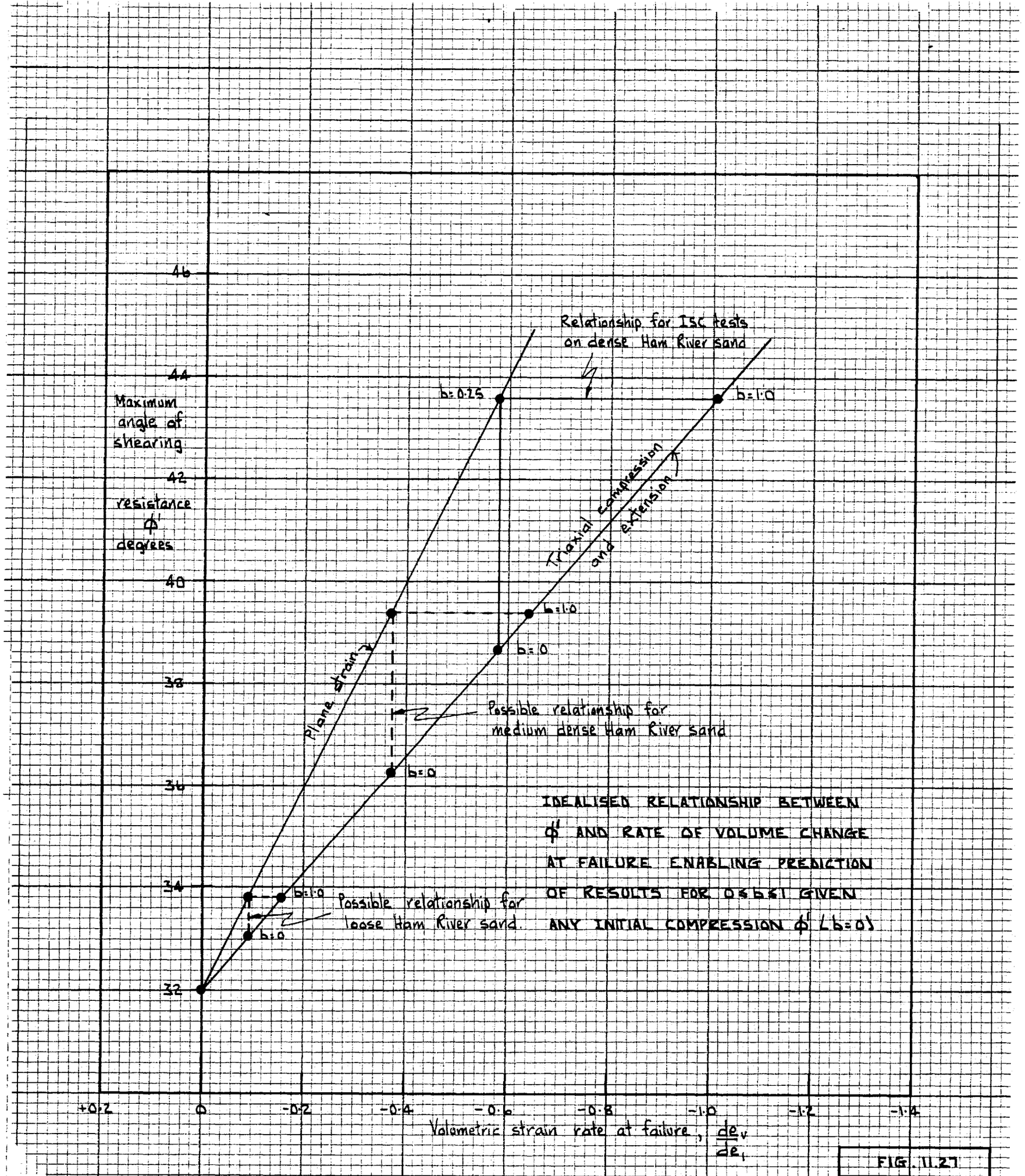
tric strain rate with respect to the belt strain is chosen. The latter corresponds in reference direction to that of the conventional triaxial extension test.

These results may be idealised to give the predictive relationship of Fig 11.27. The precise nature of this diagram is in some respects speculative since, (a) we cannot at present resolve the anisotropy problem, and (b) we assume that the triaxial compression, extension and plane strain strengths are all equal when de_v/de_1 is zero. However these two limitations are probably not serious for the present purpose. Indeed assumption (b) is not strictly necessary since this point will vary with the stress level and in any case may be found experimentally. The form of the upper and lower limit lines are established from plane strain and triaxial compression tests, see also Cornforth (1961) his Fig 8-12. Once these are known, then given any initial porosity and triaxial compression ϕ', b = 0, the strength and rate of volume change may be read off for plane strain and triaxial extension, b = 1.0. Intermediate values may also be obtained approximately, but a precise b - scale is not feasible at present.

11.13 Comparison of results with some failure theory predictions

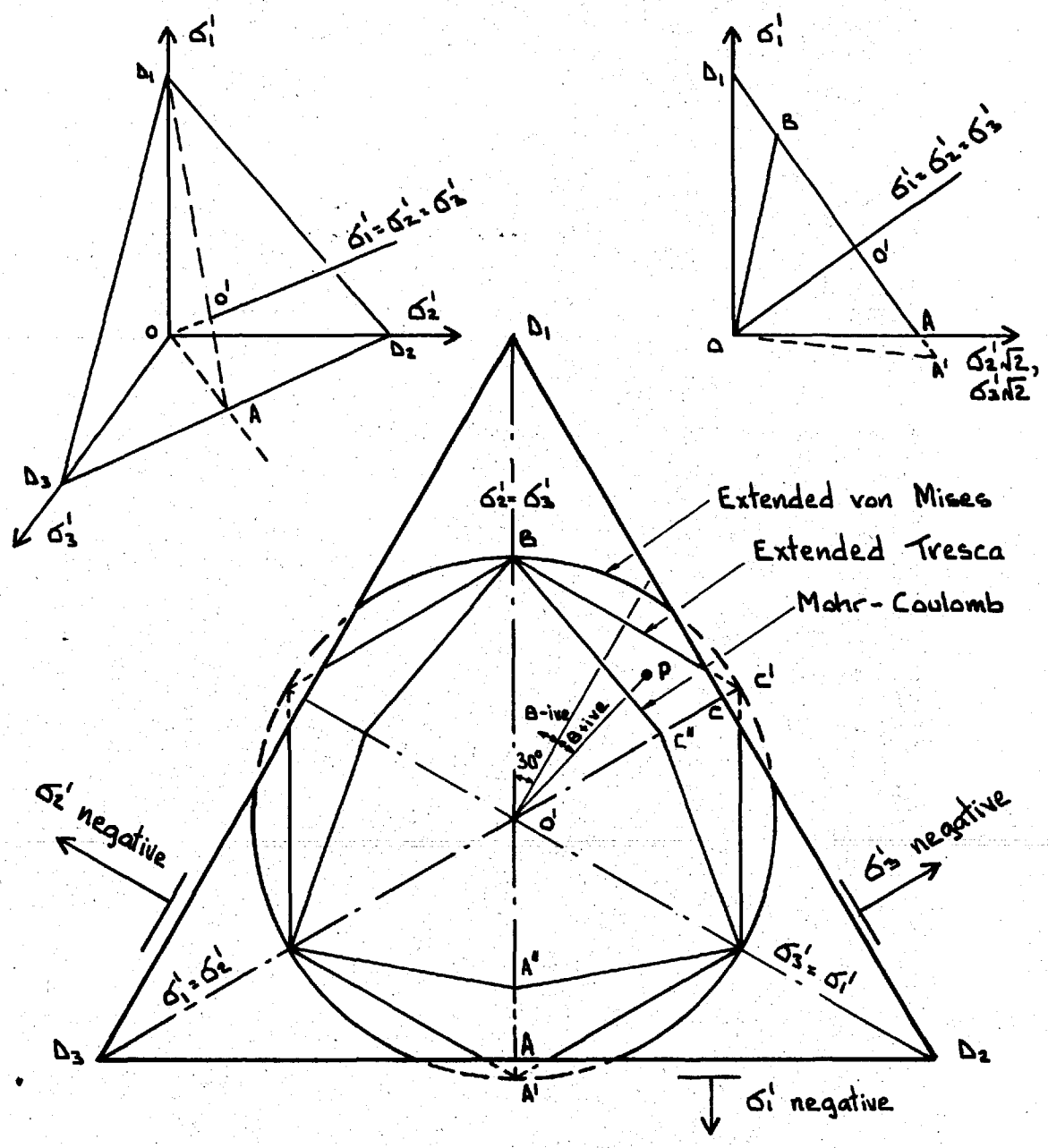
A major purpose of this thesis is to determine the influence of the intermediate principal stress, σ_2', on the strength. Firstly this is examined in terms of the 3 commonly discussed failure criteria. The slope of the failure (or yield) surface is conveniently shown in Fig 11.28 in which the theoretical shapes of the Mohr-Coulomb, extended Tresca and extended von Mises failure criteria are shown. The notation used follows Bishop (1966). In Fig 11.28 it is assumed that σ_1', σ_2' & σ_3' define a cartesian coordinate system and are therefore not ordered as is usually the case. In soil mechanics theory the co-ordinates of any point P on this reduced right section are given in polar co-ordinates by $O'P$ and θ, the latter measured clockwise positive from a line bisecting angle $D'O'C'$, after Kirkpatrick (1957).

The 3 failure criteria in terms of effective stresses for an isotropic cohesionless material may be written in a generalised form, i.e. the stresses not being ordered, as follows:



IDEALISED RELATIONSHIP BETWEEN ϕ' AND RATE OF VOLUME CHANGE AT FAILURE ENABLING PREDICTION OF RESULTS FOR $0 \leq b \leq 1$ GIVEN ANY INITIAL COMPRESSION $\phi'(b=0)$

FIG. 11.27



$$\sigma'P = \tan\left[\cos^{-1}\left(\frac{1}{\sqrt{3}}\,\frac{(\sigma_1'+\sigma_2'+\sigma_3')}{(\sigma_1'^2+\sigma_2'^2+\sigma_3'^2)^{1/2}}\right)\right]$$

$$\theta = -\tan^{-1}\left[\frac{1}{\sqrt{3}}\,\frac{(2\sigma_2'-\sigma_3'-\sigma_1')}{(\sigma_3'-\sigma_1')}\right]$$

REPRESENTATION OF FAILURE CRITERIA IN PRINCIPAL EFFECTIVE STRESS SPACE

Section of failure surface shown for $\phi' = 39.0°$ in axial compression

FIG. 11.28

(a) Mohr-Coulomb:

$$\left\{(\sigma_1'-\sigma_2')^2-\left[\sin\phi'(\sigma_1'+\sigma_2')\right]^2\right\}\left\{(\sigma_2'-\sigma_3')^2-\left[\sin\phi'(\sigma_2'+\sigma_3')\right]^2\right\}$$
$$\left\{(\sigma_3'-\sigma_1')^2-\left[\sin\phi'(\sigma_3'+\sigma_1')\right]^2\right\}=0$$

(b) Extended Tresca:

$$\left\{(\sigma_1'-\sigma_2')^2-\left[\alpha\left(\frac{\sigma_1'+\sigma_2'+\sigma_3'}{3}\right)\right]^2\right\}\left\{(\sigma_2'-\sigma_3')^2-\left[\alpha\left(\frac{\sigma_1'+\sigma_2'+\sigma_3'}{3}\right)\right]^2\right\}$$
$$\left\{(\sigma_3'-\sigma_1')^2-\left[\alpha\left(\frac{\sigma_1'+\sigma_2'+\sigma_3'}{3}\right)\right]^2\right\}=0$$

(c) Extended von Mises:

$$(\sigma_1'-\sigma_2')^2+(\sigma_2'-\sigma_3')^2+(\sigma_3'-\sigma_1')^2=2\alpha^2\left(\frac{\sigma_1'+\sigma_2'+\sigma_3'}{3}\right)^2$$

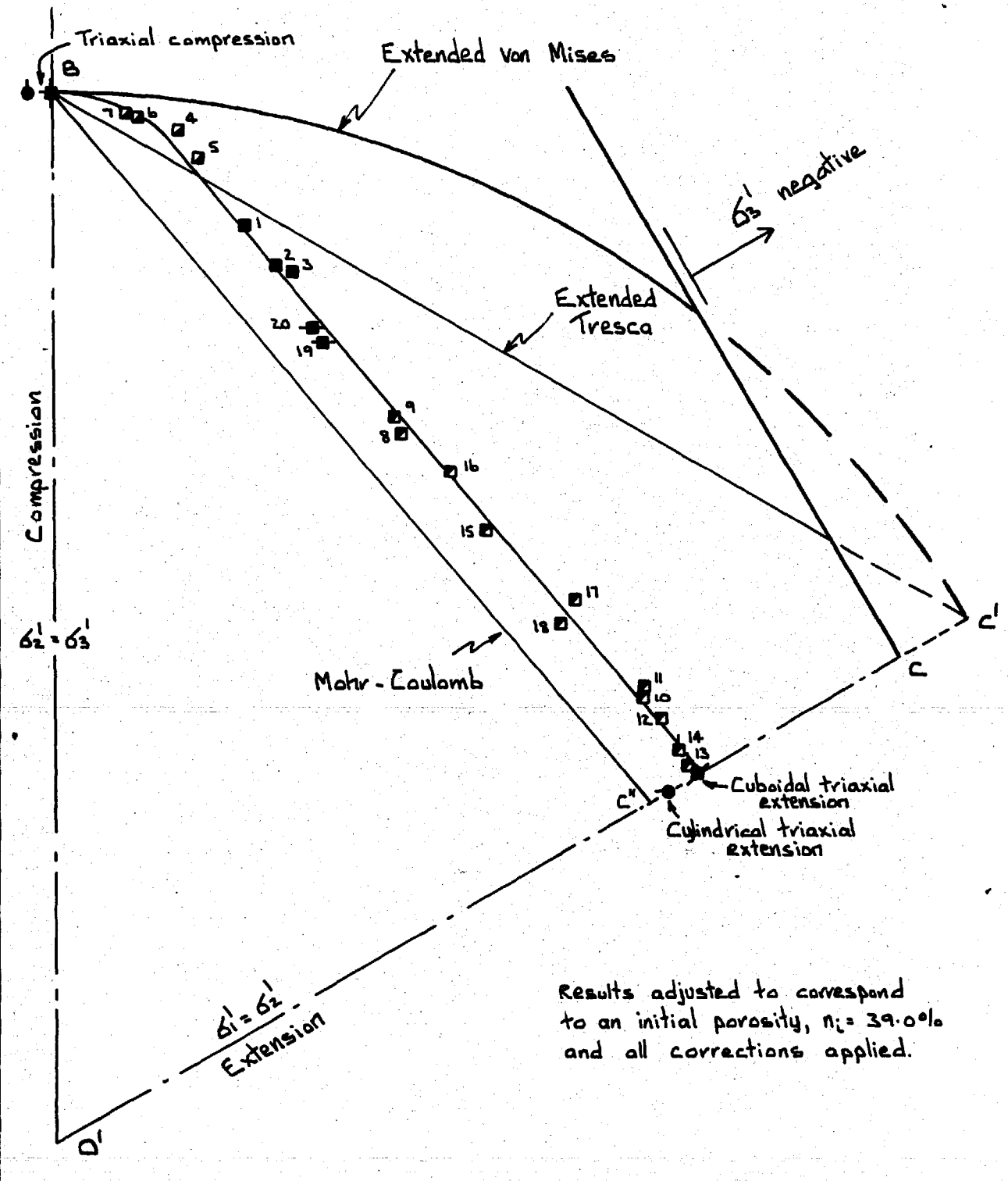
These are discussed by Kirkpatrick (1957), Hvorslev (1960), Scott (1963b), Roscoe et al (1963a) and Bishop (1966). It was pointed out in an earlier section that the sample was probably slightly anisotropic. However this did not appear to affect the measured ϕ' values sufficiently to be of importance in the present discussion.

The shape of these surfaces on the reduced right section are, (a) an irregular equal-sided hexagon, (b) a regular hexagon, and (c) a circle, respectively. They are drawn to coincide for $\phi' = 39.0^\circ$ in triaxial compression, i.e. $\sigma_2' = \sigma_3'$. It may be noted that, whereas the Mohr-Coulomb criterion predicts the same strength in extension, $\sigma_1' = \sigma_2'$, as in compression, $\sigma_2' = \sigma_3'$, the extended Tresca and von Mises criteria predict higher, but identical, strengths in extension. The portion of the latter two criteria outside the triangle $D_1D_2D_3$ (shown dotted in Fig 11.28) lie in negative effective stress space. As ϕ' increases, the cone or pyramid forming the 3-dimensional failure surface expands until for $\phi' = 36.9^\circ$ surfaces corresponding to the extended Tresca and von Mises criteria just touch (concurrently) the planes $\sigma_1' = 0$, $\sigma_2' = 0$, $\sigma_3' = 0$; typically along line OA in Fig 11.28. However the Mohr-Coulomb pyramid does not expand so rapidly and only when $\phi' = 90^\circ$ in triaxial compression does B coincide with D_1 and C'' coincide with C (or A'' coincide with A). Since soils cannot in general support tensile forces the

extended Tresca and von Mises criteria are unable to predict meaningful results for ϕ' values in triaxial compression in excess of 36.9°, Bishop (1966).

Since the failure surfaces are symmetrical it is only necessary to consider one 60° segment, e.g. $D_1O'C'$. This is tantamount to ordering the stresses, i.e. $\sigma_1' \geq \sigma_2' \geq \sigma_3'$. Fig 11.29 shows an enlarged portion of the reduced right section with the corrected ISC ϕ' values added. It may be recalled that a correction to ϕ' was included for the slight curvature of the ϕ' — average stress relationship, Fig 9.15. This is essential in the present comparison since it is assumed in the development of the reduced right section concept that the failure surface generators are straight lines radiating from O, Fig 11.32. The calculated failure criteria are based on $\phi' = 39.0^\circ$ in triaxial compression. The average line through the ISC test points lies parallel to and outside the Mohr-Coulomb line over most of its length, curving sharply at the triaxial compression end. Nowhere can it be said to lie close to the extended Tresca or von Mises lines, except for triaxial compression where by definition all must coincide.

A major disadvantage of the reduced right section is that it is not very convenient to put a ϕ' scale on it nor to indicate the magnitude of σ_2' relative to σ_1' and σ_3', Parkin (1967). It was probably for these reasons alone that the deficiencies of the extended Tresca and von Mises theories as applied to many soils were only recently discovered by Bishop (1966). In addition, plotting an experimental point involves calculating $O'P$ and θ in Fig 11.28, the meaning of which are a little obscure. An alternative method, Bishop (1966), is to plot ϕ' against $b = (\sigma_2' - \sigma_3')/(\sigma_1' - \sigma_3')$, Fig 11.30, which is a distortion of Fig 11.29, with the ϕ' scale extended and the 3 failure criteria added. The average line for the experimental points lies 5.0° above the Mohr-Coulomb 39.0° line for $0.25 \leq b \leq 1$ and curves down to 39.0° when $0 \leq b \leq 0.25$. The extreme predictions of the extended Tresca and von Mises theories are clearly seen. This result is very consistent with Cornforth's dense sand results, Bishop (1966), in which a 4.0° increase for plane strain was obtained over a compression $\phi' = 40.0^\circ$. Cornforth also measured a marginal 0.5° increase for a loose sand and it seems probable that tests in the ISC apparatus on Han River sand in a loose state



Results adjusted to correspond to an initial porosity, n_i = 39.0% and all corrections applied.

ENLARGED PORTION OF FAILURE SURFACE SHOWING INDEPENDENT STRESS CONTROL RESULTS

Section of failure surface shown for ϕ' = 39.0° in axial compression

FIG. 11.29

Maximum angle of shearing resistance, ϕ'

90
80
70
60
50
40
30
20
10
0

0 0·1 0·2 0·3 0·4 0·5 0·6 0·7 0·8 0·9 1·0

Extended von Mises for ϕ' in compression = 39·0°

Extended Tresca for ϕ' in compression = 39·0°

Mohr - Coulomb

cuboidal triaxial compression | extension

mean type ICE cuboidal extension

mean type IC cuboidal compression

mean type IB cylindrical compression

cylindrical triaxial compression | extension

mean type EX

independent stress control
H = 3·5", B = 3·2", C = 2·1"

plane strain
■ $\Delta B/B_c = 0$
■ $\Delta H/H_c = 0$

belt opening
belt closing
belt closing
σ_1' = stress in belt direction

INDEPENDENT STRESS CONTROL COMPARISON OF MEASURED PEAK STRENGTHS WITH PREDICTED VALUES

Results adjusted to correspond to an initial porosity, n_i = 39·0% and all corrections applied.

$$b = \frac{\sigma_2' - \sigma_3'}{\sigma_1' - \sigma_3'}$$

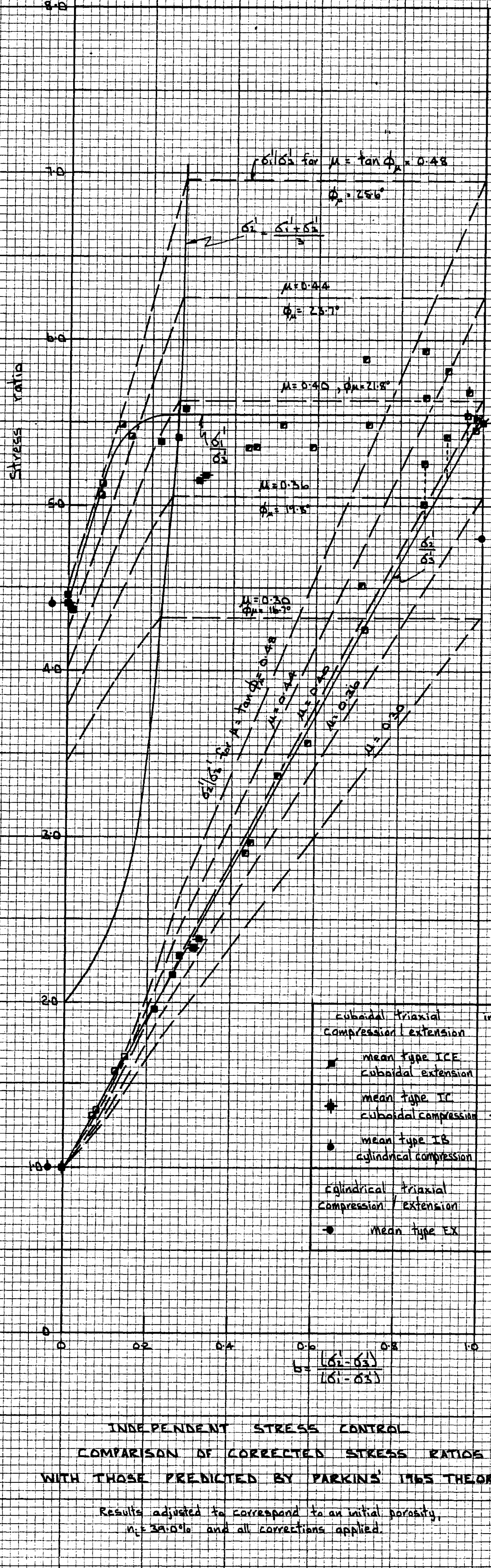
FIG. 11.30

would show no variation of ϕ' as b varies between 0 and 1.0. However this point remains to be proved.

Recently Parkin (1964, 1965) following Rennie (1959) has developed a theory of failure which is of particular interest since it predicts a ϕ'—b relationship of similar shape to the present data. In fact it appears to be the only theory which predicts a relationship of this type. A brief description of Parkins theory, as far as it is understood, is given in Chapter 2. Fig 11.31 shows the ISC test data together with theoretical curves plotted on a stress ratio basis from data kindly supplied by Dr. Parkin. The theory predicts two areas of behaviour. To the right of the line $\sigma_2' = \frac{1}{3}(\sigma_1' + \sigma_3')$, the principal stress ratio, σ_1'/σ_3' is independent of σ_2', i.e. the region $\frac{1}{3}(\sigma_1' + \sigma_3') \leqslant \sigma_2' \leqslant \sigma_1'$ (Rennie's original solution). To the left of the line σ_1'/σ_3' is dependent on σ_2', i.e. the region $\sigma_3' \leqslant \sigma_2' < \frac{1}{3}(\sigma_1' + \sigma_3')$. Parkin plotted his results in the form σ_1'/σ_3' against σ_2'/σ_3' and in the region $\sigma_3' \leqslant \sigma_2' < \frac{1}{3}(\sigma_1' + \sigma_3')$ the theoretical relationship was markedly curved whereas on the present plot it reduces to a very flat curve which could reasonably be replaced by a straight line. However the theory is not well enough understood to appreciate the implications of this point.

Since the theory is based upon a dense ordered pack of spheres the predicted increase in strength from triaxial compression to plane strain and triaxial extension is essentially an upper limit. It is reasonable to expect a dense sand to exhibit a smaller increase. For $\sigma_1'/\sigma_3' = 4.5$ at b = 0, the theory predicts an increase in ϕ' twice that observed in the ISC tests. The discontinuity of the theory at $\sigma_2' = \frac{1}{3}(\sigma_1' + \sigma_3')$ coincides almost exactly with the experimental discontinuity occurring at plane strain. It is not apparent in the theory whether σ_2' corresponds to plane strain or not. The theory does not appear to assume coincidence of the principal stress and strain axes.

The experimental and theoretical relationships between σ_2'/σ_3' and b are also shown in Fig 11.31. In the region $\frac{1}{3}(\sigma_1' + \sigma_3') \leqslant \sigma_2' \leqslant \sigma_1'$ both are straight lines per se and are slightly curved in the remaining region. The theoretical and experimental lines are clearly similar. Whether the appropriate μ value applies, equal to $\tan\phi_\mu$ as defined by Rowe (1962), is not certain due to the difficulty in measuring



INDEPENDENT STRESS CONTROL

COMPARISON OF CORRECTED STRESS RATIOS

WITH THOSE PREDICTED BY PARKINS' 1965 THEORY

Results adjusted to correspond to an initial porosity, $n_i = 39.0\%$ and all corrections applied.

FIG. 11.31

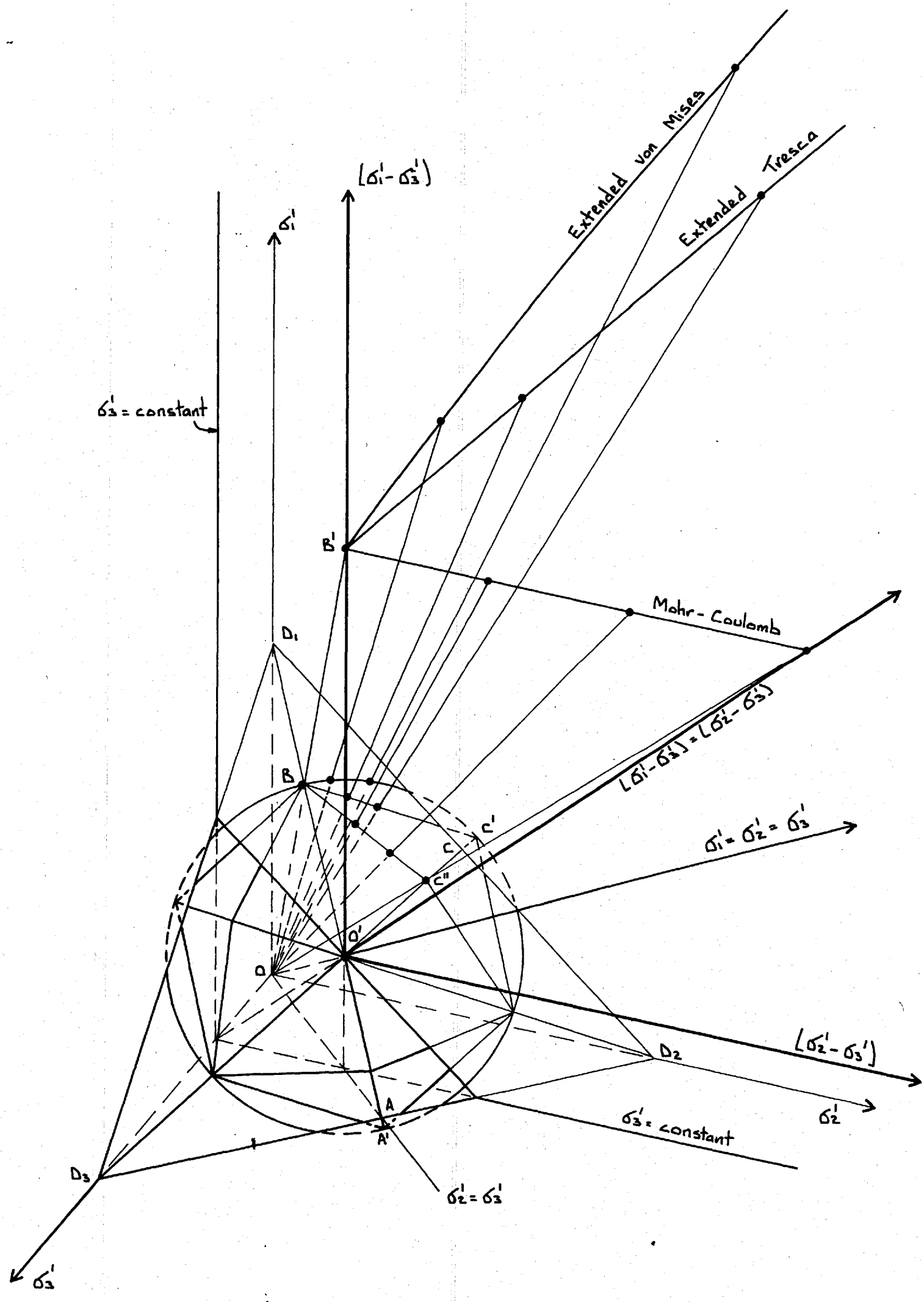
a reliable value of ϕ_μ, Horne & Deere (1964), Skinner (1969).

This theory seems promising and further study would appear likely to be fruitful. Ideally the magnitude of the difference in the stress ratio σ_1' / σ_3' between b = 0 and b = 1 should be reduced whilst maintaining the form of the stress functions. It is not certain whether or not the equations for Parkins failure criterion can be expressed in a useful and meaningful algebraic form in a similar manner to those for the Mohr-Coulomb or extended Tresca and von Mises criteria. Since the new theory is based upon particulate rather than continuum mechanics, similarity appears to be unlikely. It is of course possible to represent it graphically on the reduced right section, Parkin (1967).

11.14 Stress paths in σ_3' = constant space

Ideally we require a method of representing a meaningful stress-strain path for the whole of the shear stage for the range of intermediate principal stresses $0 \leqslant b \leqslant 1$. Unfortunately there are a number of major difficulties to overcome before this can be done. One may plot principal stress or strain paths separately but to combine all 6 variables on one useful plot is difficult. Generally, we must treat stress and strain separately. The present discussion is concerned with a stress path relating σ_1', σ_2' & σ_3' throughout the shear stage.

It is possible to plot an octahedral stress path on the reduced right section, Fig 11.28, Wade (1965). However this involves considerable calculation and seems inconvenient. In addition it only shows the projection of the stress path and not its true shape. A simpler, meaningful plot may be used instead for the present ISC tests. Consider the effective stress space shown in Fig 11.32. Initially we consolidate the sample along $00'$, $\sigma_1' = \sigma_2' = \sigma_3'$, and thereafter σ_3' is kept constant during shear. Therefore during shearing, the stress path lies in the plane σ_3' = constant through $0'$ and the coordinates of any point are given by $(\sigma_1' - \sigma_3')$, $(\sigma_2' - \sigma_3')$ referred to $0'$. If the samples were consolidated to different initial σ_3' values, which were then held constant during shear, one may normalise these axes by plotting instead $(\sigma_1' - \sigma_3')/\sigma_3'$, $(\sigma_2' - \sigma_3')/\sigma_3'$ to compare the stress paths. If σ_1', σ_2' & σ_3' are all varied during shear an undistorted stress path cannot be drawn on any plane.



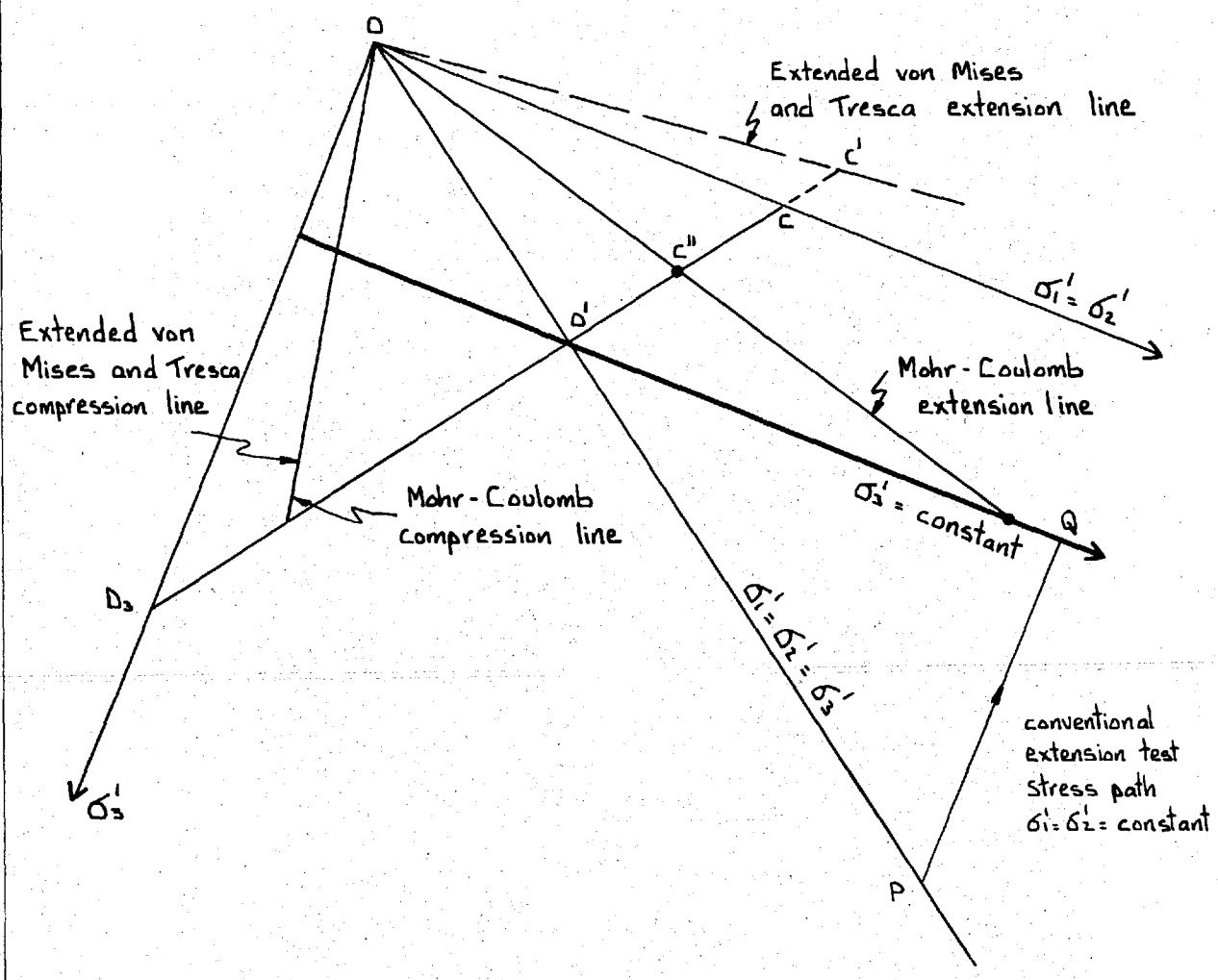
REPRESENTATION OF FAILURE CRITERIA IN PRINCIPAL EFFECTIVE STRESS SPACE SHOWING THE σ_3' = CONSTANT PLANE

FIG. 11.32

Consider the 3 failure criteria shown on the $D_1D_2D_3$ plane, in particular the segment $BO'C'$. How will this appear when projected onto the σ_3' = constant plane through O'? The straight line BC'' must appear as a straight line on the new plane. The circular segment BC' must appear as a flatter curved line on the new plane. In Fig 11.33 a section of the stress space showing the $\sigma_1' = \sigma_2'$ plane through O' is given. A line from O parallel to the σ_3' = constant plane through O' will only meet this plane at infinity. Thus stress points in negative effective stress space are, as before, not admitted.

Stress paths for the ISC tests are shown in Fig 11.34 together with the 3 failure criteria calculated for $\phi' = 39.0^\circ$ in triaxial compression. It was not practicable to apply the 4 corrections noted in the figure to the measured stresses throughout the test on account of the excessive labour, nor is it necessary for the present purpose. The upper limits of the scales are severely curtailed and do not show the extended von Mises and Tresca predictions over much of the intermediate principal stress range. The stress paths are bounded by, (a) the $(\sigma_1' - \sigma_3')$ ordinate corresponding to triaxial compression, b = 0, and (b) the line $(\sigma_1' - \sigma_3') = (\sigma_2' - \sigma_3')$ corresponding to triaxial extension, b = 1. Tests ISC/13 & 14 are again ambiguous and plot largely above or below the extension line depending on whether the axial stress is taken to be σ_1' or σ_2'. The stress paths are all ideally tangential to the experimental failure envelope. Beyond failure the tests close to b = 1.0, e.g. Tests ISC/10,11 & 12, cross the extension line. Over most of the range of b values the shape of the stress path beyond failure is erratic and of doubtful significance. The major principal strain, e_1, is indicated on each stress path from which a set of strain contours could be drawn. Tests ISC/19 & 20 are seen to be significantly different from the earlier tests both as regards stress path and strain.

In Fig 11.34 normalised scales $(\sigma_1'/\sigma_3' - 1)$ & $(\sigma_2'/\sigma_3' - 1)$ are also shown which would enable the comparison of ISC tests at differing constant cell pressures, σ_3'. In order to see what happens to the failure criteria at larger stress ratios these are replotted in Fig 11.35 as what may be termed a principal effective stress ratio space. A ϕ' scale is also shown plotted alongside the $(\sigma_1'/\sigma_3' - 1)$ scale. Comparison with Bishop's $\phi' - b$ plot, Fig 11.30, shows certain similarities and gives



SECTION OF STRESS SPACE SHOWING $\sigma_1' = \sigma_2'$ PLANE

FIG. 11.33

Extended von Mises

Extended Tresca

Experimental envelope

Mohr-Coulomb

triaxial extension

triaxial compression

$(\sigma_1' - \sigma_3')$ lbs/sq.ins.

$\left(\frac{\sigma_2'}{\sigma_3'} - 1\right)$

$\left(\frac{\sigma_1'}{\sigma_3'} - 1\right)$

3 Axial strain $\Delta H/H_0$

ISC 119 and ISC 120 σ_1' and σ_2' are in belt and axial direction respectively

ISC 113 and ISC 114 σ_1' and σ_2' are in belt and axial direction respectively.
σ_1' and σ_2' are in axial and belt direction respectively

INDEPENDENT STRESS CONTROL

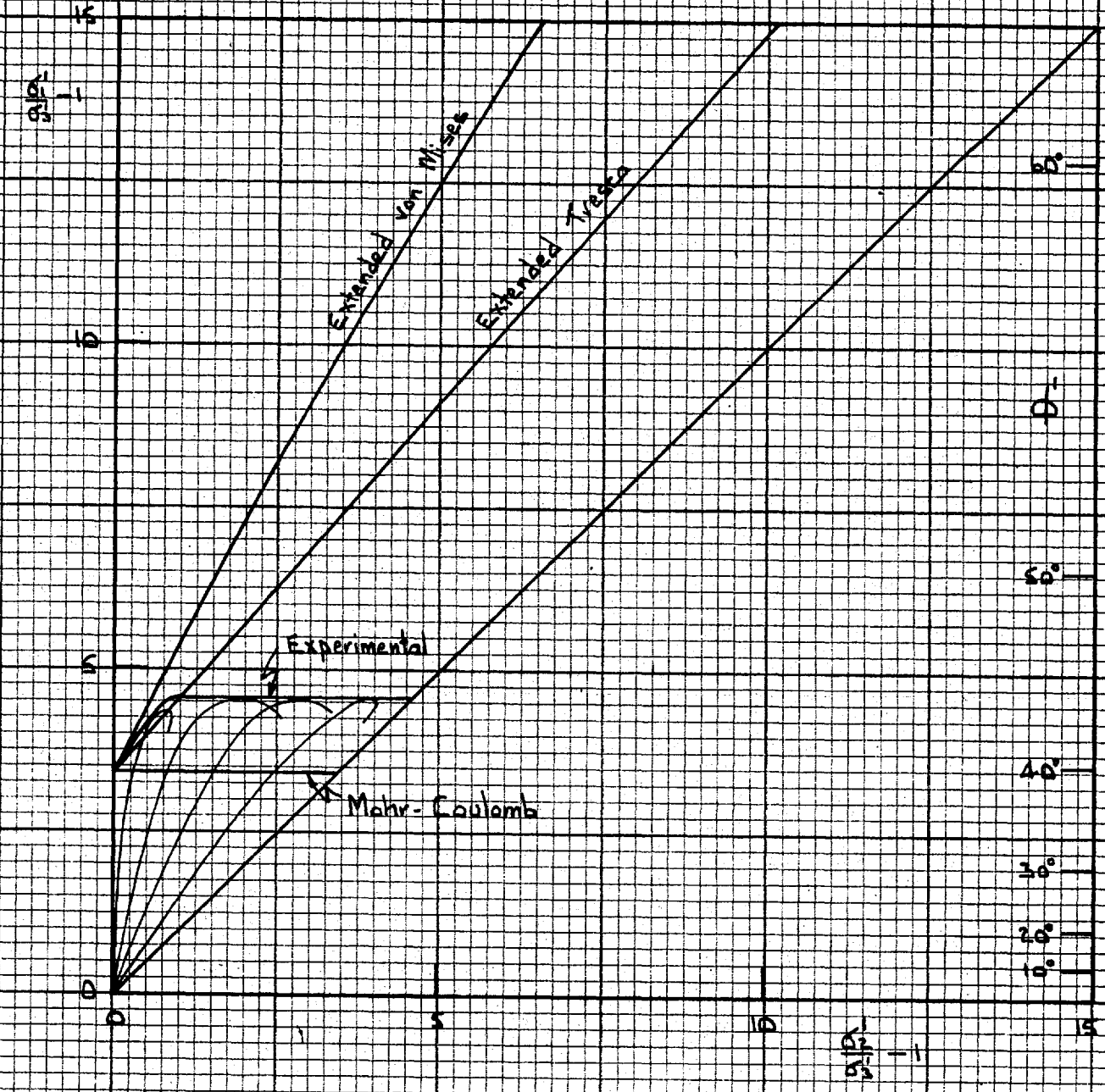
COMPARISON OF STRESS PATHS

Data not adjusted to correspond to an initial porosity, n_i = 39.0% and no corrections are applied for effect of:

(i) non-uniform deformation
(ii) sample sheath strength
(iii) platten friction
(iv) average stress level

$(\sigma_2' - \sigma_3')$, lbs/sq.ins.

FIG. 11.34



INDEPENDENT STRESS CONTROL

REPRESENTATION OF FAILURE CRITERIA IN PRINCIPAL EFFECTIVE STRESS RATIO SPACE

Section of failure surface shown for $\phi' = 39.0°$ in axial compression.

Experimental stress paths shown are diagrammatic only.

FIG. 11.35

the clue to a more significant method of representing the data in what we will call a ϕ' space, Fig 11.36. By transforming the stress ratio scales, the behaviour of the failure criteria for $\phi' = 90^\circ$ in triaxial compression is demonstrated. The value of $\phi' = \sin^{-1}(\sigma_1' - \sigma_3')/(\sigma_1' + \sigma_3')$ is plotted against $\sin^{-1}(\sigma_2' - \sigma_3')/(\sigma_1' + \sigma_3')$. The latter function has the useful feature of varying from 0 to 90° as does ϕ' and maintaining the 45° extension line. In addition it correctly shows the cut-off points for the extended von Mises and Tresca theories. The extreme predictions of these failure criteria are clearly seen. The ϕ' space shows a stress path closely related to principal effective stress space of Fig 11.35 and the coordinates of any point are easily calculated.

11.15 Correlation of stresses and strains

In all the ISC tests, strain control is maintained on two pairs of boundaries, e_1 & e_2, and stress control on the third, σ_3'. Since in any one test the ratio e_1 / e_2 is constant during shear, a strain path is of limited value in comparison to a stress path and in no sense do limiting values occur, i.e. the strain paths are not tangential to a failure strain envelope.

Corresponding to the stress space of Fig 11.34 the strain differences (e_1-e_3) and (e_2-e_3) at failure are shown in Fig 11.37. The ordinate $(e_2-e_3) = 0$ corresponds to triaxial compression and the line $(e_1-e_3) = (e_2 - e_3)$ to triaxial extension. Only the values at failure are shown; the complete path for any ISC test being an approximately straight line radiating from the origin. The line is not straight due to the effect of volume changes. The discrepancy in the strains between the ISC tests and conventional triaxial compression and extension tests are made plain. In Tests ISC/6 & 7, $e_2 \simeq -4\%$, $e_3 \simeq -8\%$ and hence $(e_2 - e_3) \simeq +4\%$ whereas to agree with the triaxial compression test result, $(e_2 - e_3)$ ought to be more nearly zero. The extrapolation of the average ISC line to $(e_2 - e_3) = 0$ implies a very large $(e_1 - e_3)$ value. In tests approaching $\sigma_1' = \sigma_2'$, e.g. Test ISC/12, $e_1 \simeq e_2 \simeq +4\%$, $e_3 \simeq -11\%$ and hence $(e_1 - e_3) \simeq +15\%$, i.e. the magnitudes of the two strains are additive and hence tend to accentuate any differences. Test ISC/1 is again seen to be inconsistent whereas, curiously enough, Tests ISC/19 & 20 correlate with the other test data.

Extended von Mises

Extended Tresca

Experimental

Mohr-Coulomb

$\sin^{-1}\frac{\sigma_1'-\sigma_3'}{\sigma_1'+\sigma_3'}$

ϕ'

$\frac{\sigma_1'}{\sigma_3'}$

INDEPENDENT STRESS CONTROL

REPRESENTATION OF FAILURE CRITERIA

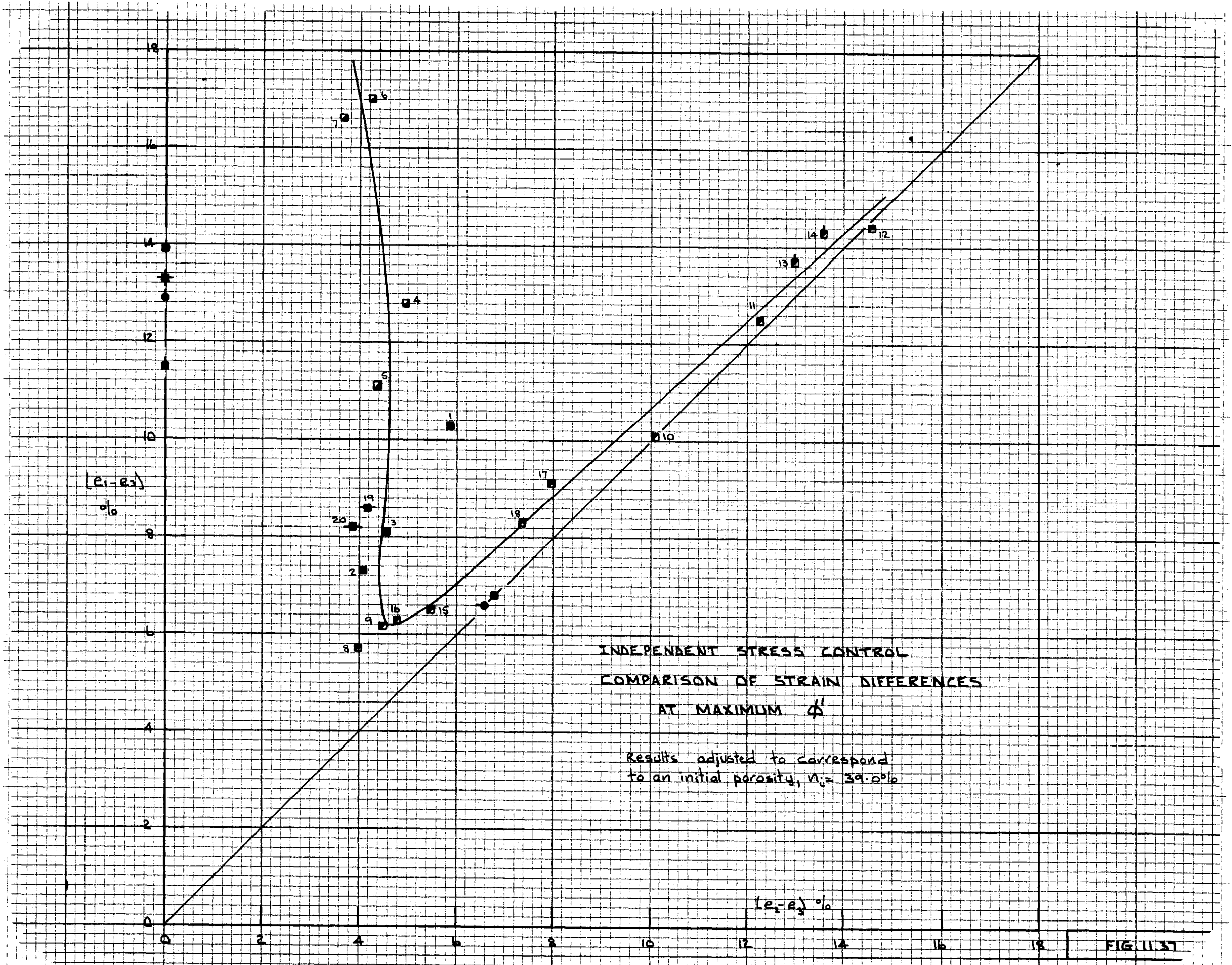
IN ϕ' SPACE

Section of failure surface shown for $\phi' = 39.0°$ in axial compression.

Experimental stress paths shown are diagrammatic only.

$\sin^{-1}\frac{\sigma_2'-\sigma_3'}{\sigma_1'+\sigma_3'}$

FIG 11.36



INDEPENDENT STRESS CONTROL

COMPARISON OF STRAIN DIFFERENCES

AT MAXIMUM ϕ'

Results adjusted to correspond to an initial porosity, n_i = 39.0%

FIG. 11.37

We have earlier obtained the relationship:

$$b = \frac{\sigma_2' - \sigma_3'}{\sigma_1' - \sigma_3'}$$

For triaxial compression $\sigma_2' = \sigma_3'$ so that $b = 0$ and for triaxial extension $\sigma_1' = \sigma_2'$ so that $b = 1$. Similarly the expression $(e_2 - e_3)/(e_1 - e_3)$ equals zero for triaxial compression when $e_2 = e_3$ and equals 1 for triaxial extension when $e_1 = e_2$. Fig 11.38 shows this strain ratio at failure plotted against b. Tests ISC/1 and 19 & 20 do not fit the average line as may be anticipated. However the ISC tests extrapolate to fit the triaxial compression test point (0,0) but do not extrapolate exactly to the triaxial extension test value (1,1). Tests ISC/13 & 14 are anomalous and the lack of fit here, as also of Tests ISC/19 & 20, may again be attributed to anisotropy within the sample. A strain path for a particular test for the whole of the shear stage would appear as a near horizontal line starting at $b = 0$ since the strain ratio $(e_2 - e_3)/(e_1 - e_3)$ has a predominant component e_2/e_1 which is constant during any single test.

In all the analyses so far we have attempted to relate stresses with strains; which may be associated with elastic theory. Consider now the equations for a perfectly plastic incompressible material relating principal stress and principal strain increments, Hill (1950).

$$de_1 = \psi \left[\sigma_1' - \tfrac{1}{2}(\sigma_2' + \sigma_3')\right]$$
$$de_2 = \psi \left[\sigma_2' - \tfrac{1}{2}(\sigma_3' + \sigma_1')\right]$$
$$de_3 = \psi \left[\sigma_3' - \tfrac{1}{2}(\sigma_1' + \sigma_2')\right]$$

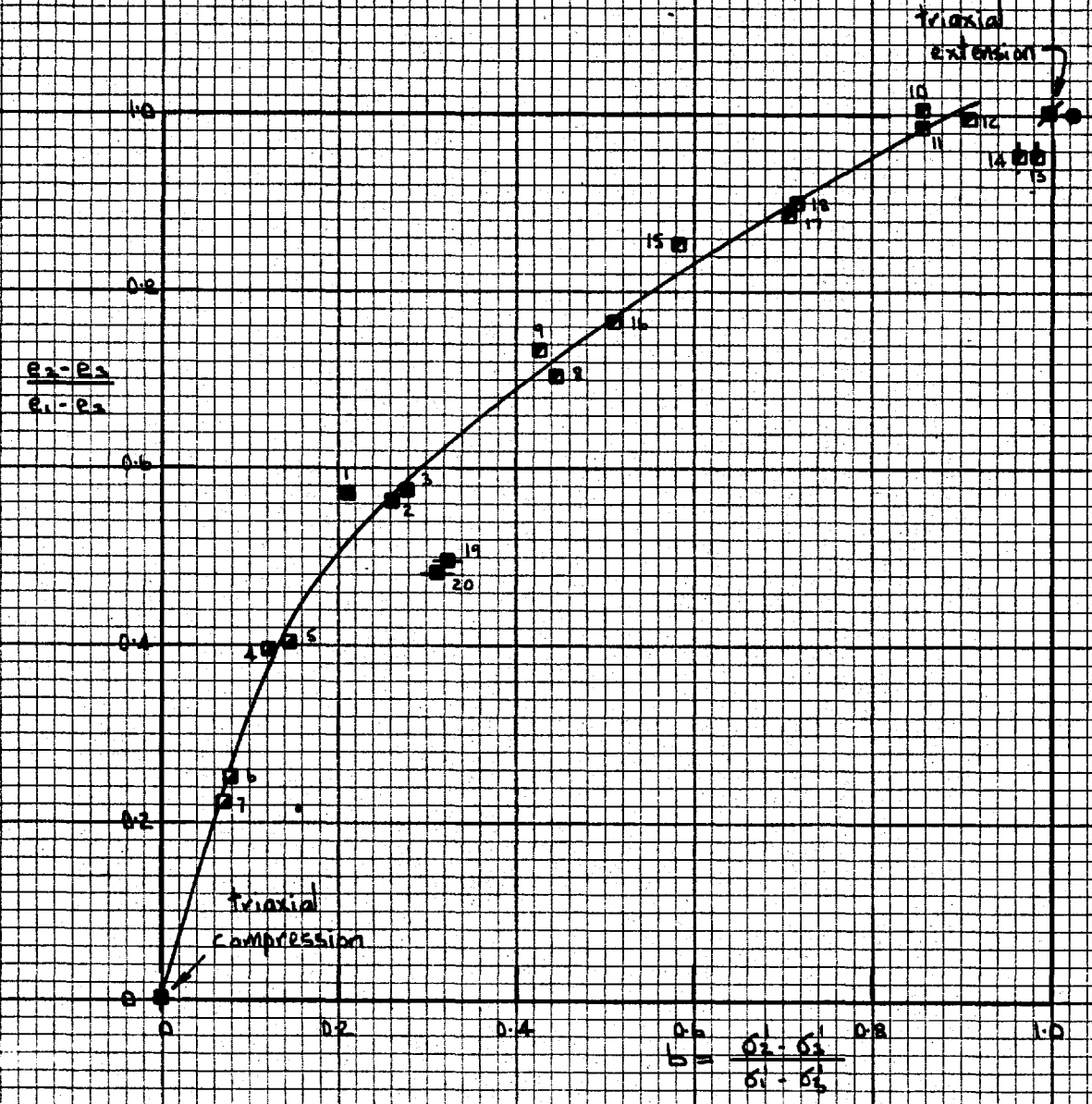
where de_1, de_2 & de_3 are small increments of plastic principal strain and ψ is a constant.

$$\frac{de_2 - de_3}{de_1 - de_3} = \frac{\left[\sigma_2' - \tfrac{1}{2}(\sigma_3' + \sigma_1')\right] - \left[\sigma_3' - \tfrac{1}{2}(\sigma_1' + \sigma_2')\right]}{\left[\sigma_1' - \tfrac{1}{2}(\sigma_2' + \sigma_3')\right] - \left[\sigma_3' - \tfrac{1}{2}(\sigma_1' + \sigma_2')\right]}$$

$$= \frac{\sigma_2' - \sigma_3'}{\sigma_1' - \sigma_3'}$$

$$= b$$

Fig 11.39 shows the measured values of $(de_2 - de_3)/(de_1 - de_3)$ at failure plotted against b, together with the theoretical relationship. For triaxial compression, $de_2 = de_3$, so that $(de_2 - de_3)/(de_1 - de_3) = 0$ and for triaxial extension, $de_1 = de_2$, so that $(de_2 - de_3)/(de_1 - de_3) = 1$. For plane strain, $de_2 = 0$, so that $\sigma_2' = \tfrac{1}{2}(\sigma_1' + \sigma_3')$. Thus $b = \tfrac{1}{2}$ and since $de_1 + de_2 + de_3 = 0$,



INDEPENDENT STRESS CONTROL

COMPARISON OF STRAIN RATIOS AT MAXIMUM ϕ'

Results adjusted to correspond to an initial porosity, n_i = 39.0 % and all corrections applied

FIG. II.38

$$\frac{(de_2 - de_3)}{(de_1 - de_3)} = \frac{1}{2}$$

The strain increment ratios, Fig 11.39, are very similar to the strain ratios of Fig 11.38, the scatter of the points about the average being slightly reduced. The behaviour of the sand deviates significantly from that of a perfectly plastic incompressible material except for b = 0 and b = 1 when the experimental values must agree with the theory due to the nature of the two functions plotted. Differences between conventional extension tests and ISC 'extension' tests are again observed.

The equations for de_1, de_2 & de_3 may be re-written to eliminate ψ as follows:

$$\frac{de_1}{de_2} = \frac{2\sigma_1' - \sigma_2' - \sigma_3'}{2\sigma_2' - \sigma_3' - \sigma_1'} = \frac{\sigma_1' - \sigma_m'}{\sigma_2' - \sigma_m'} \quad \ldots\ldots\ldots \text{(a)}$$

$$\frac{de_2}{de_3} = \frac{2\sigma_2' - \sigma_3' - \sigma_1'}{2\sigma_3' - \sigma_1' - \sigma_2'} = \frac{\sigma_2' - \sigma_m'}{\sigma_3' - \sigma_m'} \quad \ldots\ldots\ldots \text{(b)}$$

$$\frac{de_1}{de_3} = \frac{2\sigma_1' - \sigma_2' - \sigma_3'}{2\sigma_3' - \sigma_1' - \sigma_2'} = \frac{\sigma_1' - \sigma_m'}{\sigma_3' - \sigma_m'} \quad \ldots\ldots\ldots \text{(c)}$$

where $\sigma_m' = \frac{1}{3}(\sigma_1' + \sigma_2' + \sigma_3')$

This suggests another method of representing a failure stress-strain relationship. Consider equations (b) and (c) respectively. For equation (b):

(i) in triaxial compression, $de_2 = de_3$ and $\sigma_2' = \sigma_3'$

$$\therefore \frac{de_2}{de_3} = 1 \text{ and } \frac{\sigma_2' - \sigma_m'}{\sigma_3' - \sigma_m'} = 1$$

(ii) in triaxial extension, $de_1 = de_2$ and $\sigma_1' = \sigma_2'$

$$\therefore \frac{de_2}{de_3} = -\frac{1}{2} \text{ and } \frac{\sigma_2' - \sigma_m'}{\sigma_3' - \sigma_m'} = -\frac{1}{2}$$

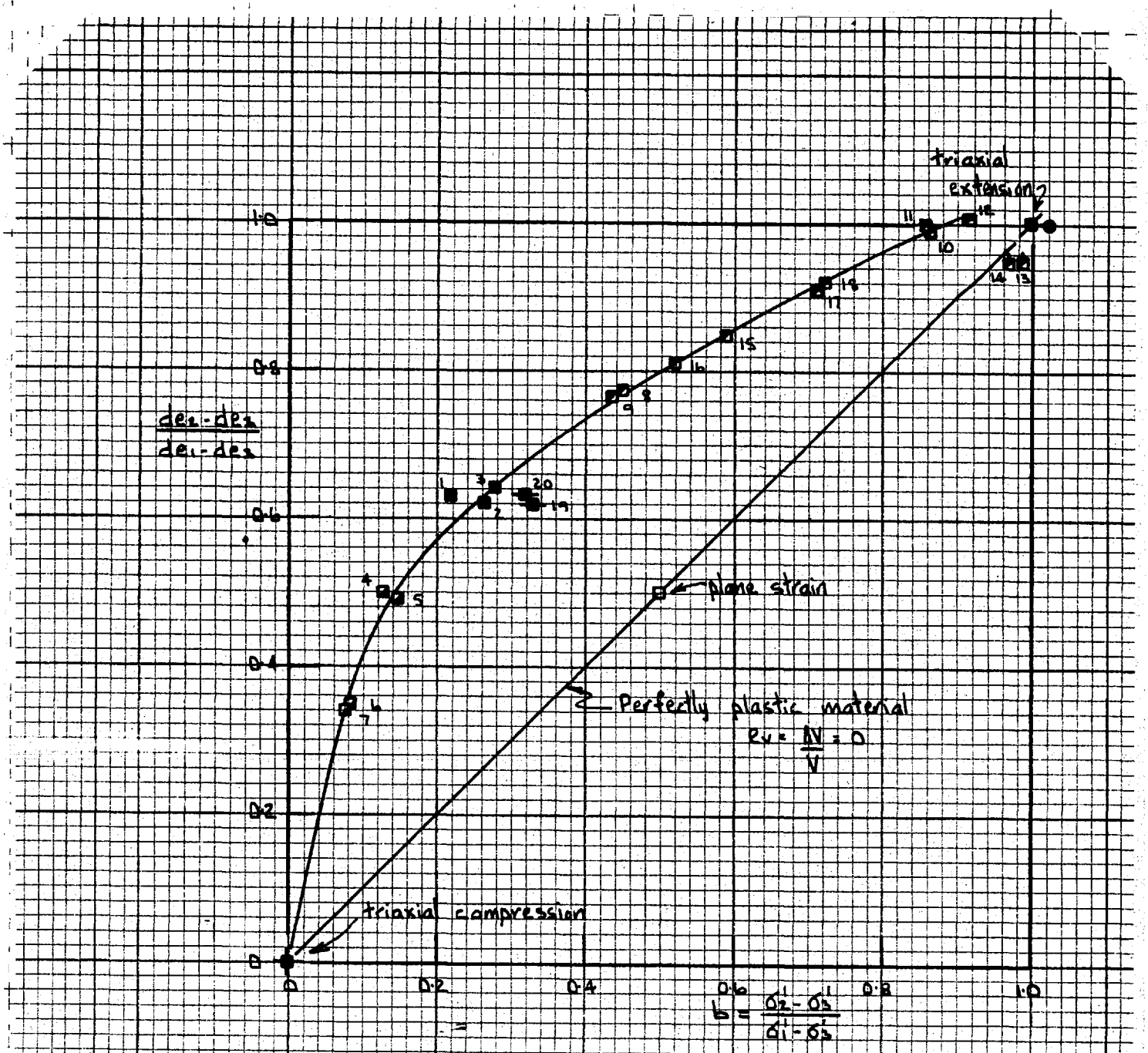
(iii) in plane strain, $de_2 = 0$ and $\sigma_2' = \frac{1}{2}(\sigma_1' + \sigma_3')$

$$\therefore \frac{de_2}{de_3} = 0 \text{ and } \frac{\sigma_2' - \sigma_m'}{\sigma_3' - \sigma_m'} = 0$$

and for equation (c):

(i) in triaxial compression, $de_2 = de_3$ and $\sigma_2' = \sigma_3'$

$$\therefore \frac{de_1}{de_3} = -2 \text{ and } \frac{\sigma_1' - \sigma_m'}{\sigma_3' - \sigma_m'} = -2$$



INDEPENDENT STRESS CONTROL

COMPARISON OF STRAIN INCREMENT RATIOS AT MAXIMUM ϕ'

Results adjusted to correspond to an initial porosity, n_i = 39.0% and all corrections applied.

FIG. II.39

(ii) in triaxial extension, $de_1 = de_2$ and $\sigma_1' = \sigma_2'$

$$\therefore \frac{de_1}{de_3} = -\frac{1}{2} \text{ and } \frac{\sigma_1' - \sigma_m'}{\sigma_3' - \sigma_m} = -\frac{1}{2}$$

(iii) in plane strain, $de_2 = 0$ and $\sigma_2' = \frac{1}{2}(\sigma_1' + \sigma_3')$

$$\therefore \frac{de_1}{de_3} = -1 \text{ and } \frac{\sigma_1' - \sigma_m'}{\sigma_3' - \sigma_m'} = -1$$

Now for triaxial extension the values of the two expressions (b) & (c) are identical and this results in a convenient combined plot of both functions. The two theoretical relationships, together with the experimental values are shown in Fig 11.40. The two theoretical relationships plot as two co-linear straight lines whereas the ISC test points define two slightly discontinuous curved lines, the discontinuity probably being associated with anisotropy. A number of features are notable. Tests ISC/13 & 14 are in apposition to their average lines due to the ambiguity of definition resulting from sample anisotropy. The conventional cuboidal triaxial extension test agrees with the extrapolated value of de_2/de_3 for the ISC tests but not with de_1/de_3. For conventional triaxial compression, $de_2 = de_3$, independent of the material behaviour, so that these two experimental points must fit the theory. In contrast the ratio de_1/de_3 is strongly dependent on the volume change so that there is a marked lack of fit. Thus the strain increment ratio plotted against the stress ratio at failure appears to offer a useful basis for comparison. In particular it emphasises the discontinuity attributable to anisotropy. An alternative 'hybrid' method which reduces the labour of computation is to consider only the strain ratios e_2/e_3 and e_1/e_3, shown in Fig 11.41. The form is very similar to the strain increment ratio plot but there are no theoretical relationships that are conveniently applicable. Tests ISC/19 & 20 deviate conspicuously from the other ISC tests whereas strain increment-wise they were in agreement, the reason for this is not clear. Strain or strain increment ratio versus stress ratio paths for the whole of the shear stage do not appear to be especially valuable for the reasons given earlier.

cuboidal triaxial compression / extension

- mean type ICE cuboidal extension
- mean type IC cuboidal compression
- mean type IB cylindrical compression

cylindrical triaxial compression / extension

- mean type EX

independent stress control
H = 3·3", B = 3·2", C = 2·1"

plane strain

- ΔB/Bc = 0
- ΔH/Hc = 0
- belt opening
- belt closing
- belt closing, σ_1' = stress in belt direction

$$\frac{\sigma_1' - \sigma_m'}{\sigma_3' - \sigma_m'} = \frac{2\sigma_1' - \sigma_2' - \sigma_3'}{2\sigma_3' - \sigma_1' - \sigma_2'}$$

$\frac{de_2}{de_3}$

$\frac{de_2}{de_3} = \frac{\sigma_2' - \sigma_m'}{\sigma_3' - \sigma_m'}$

triaxial compression

plane strain

triaxial extension

Perfectly plastic material
$e_v = \frac{\Delta V}{V} = 0$

$\frac{de_1}{de_3} = \frac{\sigma_1' - \sigma_m'}{\sigma_3' - \sigma_m'}$

triaxial compression

$\frac{de_1}{de_3}$

$\frac{\sigma_2' - \sigma_m'}{\sigma_3' - \sigma_m'} = \frac{2\sigma_2' - \sigma_3' - \sigma_1'}{2\sigma_3' - \sigma_1' - \sigma_2'}$

INDEPENDENT STRESS CONTROL

RELATIONSHIP BETWEEN STRAIN INCREMENT RATIO AND STRESS RATIO AT MAXIMUM ϕ'

Results adjusted to correspond to an initial porosity, n_i = 39·0% and all corrections applied.

FIG. 11.40

cuboidal triaxial compression / extension

mean type ICE cuboidal extension

mean type IC cuboidal compression

mean type IB cylindrical compression

cylindrical triaxial compression / extension

mean type EX

independent stress control
H = 3.3", B = 3.2", C = 2.1"

plane strain
- ΔB/Bc = 0
- ΔH/Hc ≈ 0

belt opening
belt closing
belt closing,
σ_1' = stress in belt direction

$$\frac{\sigma_1' - \sigma_m'}{\sigma_3' - \sigma_m'} = \frac{2\sigma_1' - \sigma_2' - \sigma_3'}{2\sigma_3' - \sigma_1' - \sigma_2'}$$

$$\frac{\sigma_2' - \sigma_m'}{\sigma_3' - \sigma_m'} = \frac{2\sigma_2' - \sigma_3' - \sigma_1'}{2\sigma_3' - \sigma_1' - \sigma_2'}$$

$\frac{e_1}{e_3}$ $\frac{e_2}{e_3}$

INDEPENDENT STRESS CONTROL

RELATIONSHIP BETWEEN STRAIN RATIO AND STRESS RATIO AT MAXIMUM ϕ'

Results adjusted to correspond to an initial porosity, n_i = 39.0% and all corrections applied.

FIG. II.4-1

CHAPTER 12

SUMMARY AND CONCLUSIONS

12.1 Introduction

In presenting the major sections of the research in the previous four chapters a full discussion together with the conclusions are given. What follows is a brief summary of some of the important features of the investigation.

12.2 Preliminary tests

The preliminary tests, Chapter 3, to examine the mode of deformation of cylindrical triaxial compression test specimens with H/D = 1 and with lubricated ends, generally 1/0.009 ins thick greased natural rubber membrane, indicated that the major factor influencing the mode of deformation appeared to be the difference in the contact at the top and bottom sample-platten interfaces. At the expense of using an awkward technique it was subsequently possible to build a specimen in two-halves which exhibited more uniform deformations than a normal specimen.

12.3 Cylindrical triaxial compression tests

Triaxial compression tests on cylindrical samples, Chapter 8, show that for the type of sand and end plattens used, a reduction in end restraint by lubrication has an insignificant effect on the observed strengths of samples with H/D = 2 over a range of porosities. For lower ratios the influence becomes increasingly important. For H/D = 1 very efficient lubrication, 2/0.009 ins thick greased membranes, is necessary to reduce the strength to that of the samples with H/D = 2. Additional membranes do not appear to reduce the strength below this value. It is shown that uncertainties in estimating the most appropriate area correction to be applied have a small and barely significant effect on these conclusions. Whereas the linear and volumetric strains are greatly affected by the H/D ratio and degree of end restraint the volumetric strain rate with respect to axial strain is virtually unaffected.

12.4 Cylindrical triaxial compression and extension tests

The strength and rate of dilatation at failure of cylindrical triaxial

compression test samples with H/D = 1 are only marginally affected by the stress path followed, Chapter 9. Of the three types of specimen tested in extension the short sample, H/D = 1, with 2/0.010 ins thick lubricated membranes at each end, exhibited a strength of from 1.0° to 2.5° lower than the longer specimens over a range of porosities. The precise magnitude of the difference is dependent on uncertainties in determining the most realistic area correction for the longer specimens. Comparing the corrected peak strengths measured in triaxial compression and extension for samples with H/D = 1 and with 2/0.010 ins thick lubricated membranes at each end, it is seen that the ϕ' values are identical for loose specimens whereas the extension ϕ' value is 2.0° higher for dense specimens. It is calculated that, of the specimen types tested, a 4 ins diameter, 4 ins high specimen with adequately lubricated ends, in this case 2/0.010 ins thick greased membranes, and preferably built in two halves, will give a minimum measured strength associated with the most uniform deformations. As was observed in the cylindrical triaxial compression test, the cylindrical triaxial extension tests exhibit linear and volumetric strains that are greatly affected by the H/D ratio whereas the rate of dilatation is independent of the sample proportions.

12.5 Cuboidal triaxial compression and extension tests

Triaxial compression and extension tests on cuboidal specimens were restricted to initially dense samples, Chapter 10. Accepting the triaxial compression strength given by the 4 ins diameter, 4 ins high, H/D = 1 , cylindrical triaxial specimens, with 2/0.010 ins thick membranes at each end, as being correct, then, of the 4 different cuboidal samples tested in triaxial compression, those of dimensions B = 3.0, C = 2.3 and H = 3.3 ins gave the lowest and hence the most acceptable strength, it being equal to that of the cylindrical triaxial compression specimens. Both sizes of cuboidal specimen tested in triaxial extension exhibited the same strength and, indeed, the same linear & volumetric strains and rate of dilatation at failure. After applying appropriate corrections the strength of the cuboidal triaxial extension test specimens was 4.9° higher than that given by cylindrical or cuboidal triaxial compression specimens. It was concluded that the most suitable size cuboidal sample for triaxial compression and extension tests, and by inference for the ISC test, was one of approximate

dimensions B = 3.0, C = 2.1 & H = 3.3 ins, i.e. of proportions B:C:H equal to 3:2:3.

12.6 Independent stress control tests

All the independent stress control tests, Chapter 11, were on initially dense specimens of the above stated dimensions. The measured strengths, adjusted to correspond to an initial sample porosity of 39.0% and with appropriate corrections applied, are compared with those obtained in the cylindrical and cuboidal triaxial compression and extension tests. The cylindrical and cuboidal triaxial compression test specimens exhibited identical strengths, $\phi' = 39.0^{\circ}$. The cylindrical triaxial extension test specimens gave a 2.0° higher ϕ' whereas the cuboidal triaxial extension test specimens gave a 4.9° higher ϕ' than in triaxial compression. For intermediate values of σ_2', i.e. the ISC tests, the strength was on average 5.0° higher than in triaxial compression. The strength rises rapidly from triaxial compression, b = 0, to plane strain $0.2 < b < 0.3$. Thereafter ϕ' remains essentially constant up to b = 1.0.

The ISC tests close to b = 1 show almost exactly the same increase in ϕ' above triaxial compression as does the cuboidal triaxial extension test. This appears to be of special significance. The conventional cuboidal triaxial extension test is performed with rigid lubricated plattens on only the pair of faces to which the minor principal stress, σ_3', is applied, the major and intermediate principal stresses, $\sigma_1' = \sigma_2'$, being applied as a fluid pressure through the flexible sample sheath. In contrast, in the ISC apparatus, rigid lubricated plattens are used to apply both the major and intermediate principal stresses, $\sigma_1' = \sigma_2'$, the minor principal stress, σ_3', being applied as a fluid pressure through the flexible sample sheath. The directions of two of the principal stresses are interchanged with respect to the vertical specimen axis in the two types of 'extension' test. The same value of ϕ' is obtained by these two methods. This could be fortuitous but it seems more reasonable to infer that the platten friction and rigidity must have a relatively insignificant effect on the measured strength and that the shape of the ϕ'-b relationship and magnitude of the increase in ϕ' represent the real behaviour of the sand and are not a result of inadequacies in the apparatus.

The reason for the observed difference in ϕ' of 2.9° between the

cylindrical and cuboidal triaxial extension test is not clear. It is notable that the volumetric strain rates at failure are almost identical in the two types of test. It has been suggested that in a cylindrical triaxial specimen the radial stress, σ_r , and the circumferential stress, σ_θ are not equal. However a number of objections may be raised against this, Chapter 2. Alternatively if a 'crust arching' mechanism exists in the cylindrical triaxial extension test specimen this would seem to imply a greater strength than for a cuboidal specimen similarly tested due to the diminished possibility of 'crust arching' occurring in the latter test. No entirely satisfactory explanation appears to be possible at present. On the basis of the ISC data the higher strength at b = 1 appears to be the more relevant value and not that obtained in cylindrical triaxial extension.

The two plane strain tests in which the directions of σ_1' and σ_2' are interchanged give a slightly lower strength than the average for the test in which σ_1' was the vertical stress. This is attributed to initial anisotropy in the sand specimen due to its mode of deposition. As a consequence of this the specimen is also slightly stiffer in the vertical direction than in the lateral direction. The measured linear and volumetric strains together with the volumetric strain rates as b approaches 1.0 support this hypothesis. However, the degree of anisotropy appears to be small enough for its influence on the overall view of the strength data to be negligible.

The linear and volumetric strains obtained by extrapolating the ISC test data to b = 0 and b = 1.0 indicate that the conventional triaxial compression and extension tests under-estimate these strains by a factor of 2 or more. The ideal test from the point of view of strains would appear to be one using rigid plattens on all 3 pairs of faces of a cubical specimen. In such a test it seems probable that the strains required to reach failure might be even greater than those presently measured in the ISC apparatus.

Of the existing failure criteria based on continuum mechanics , the extended Tresca and extended von Mises theories are entirely unacceptable. The commonly used Mohr-Coulomb theory will tend to underestimate the strength by about 5.0° over most of the range of b values. This would be a significant error in many analyses of field problems, but represents an extreme case inasmuch as medium dense and loose sands or all clays will show

a smaller increase. Potentially, the most useful theory appears to be that due to Parkin, based on particulate mechanics, which predicts a variation in ϕ' similar in form to that observed. The magnitude of the increase is approximately twice that measured in the present test. Since the idealised state of packing in the theory is not attained in a real sand it may be reasonable to expect the latter to show a smaller strength increase.

LIST OF REFERENCES

Amirsoleymani, T. (1966a) "Packing of granular materials with special reference to triaxial testing". Ph.D. thesis, Birmingham University.

Amirsoleymani, T. (1966b) Correspondence on "The influence of end restraint on the compression strength of a cohesionless soil". Géotechnique, Vol 16, No 2, pp 173-175.

Andresen, A. and N.E.Simons (1960) "Norwegian triaxial equipment and practice". Res.Conf.on Shear Strength of Cohesive soils, Boulder,ASCE, pp 695-709.

Arthur, J.R.F., R.G.James and K.H.Roscoe (1964) "The determination of stress fields during plane strain of a sand mass", Géotechnique,Vol.14, pp 283 - 308.

Arthur, J.R.F.& B.K.Menzies (1968) Correspondence on "A new soil testing apparatus". Géotechnique, Vol 18, No.2, pp 271-272.

Balla, A.(1957) "Stress conditions in the triaxial compression test", Proc 4th Int.Conf.Soil Mechs. and Found.Eng., Vol 1, pp 140-143.

Balla, A.(1960a)"A new solution of the stress distribution in triaxial compression," Acta Tech. Hung., Vol 28,pp 349 - 388.

Balla, A.(1960b) "Stress conditions in triaxial compression", Jour.Soil Mechs & Found Eng.Div., ASCE, Vol 88, SM6, pp 57-84.

Barden, L.(1963) Discussion on "The effect of non-uniform pore pressures on laboratory measurements of the shear strength of soils". Symp. Laboratory Shear Testing of Soils, Ottawa, ASTM, STP 361, p 184.

Barden, L.(1968) Personal communication.

Barden, L. and R.J.W.McDermott (1965) "Use of free ends in triaxial testing of clays". Jour.Soil Mechs. and Found.Div.ASCE, Vol 91, No SM6,pp 1-23.

Barden, L. and A.J.Khayatt (1966) "Incremental strain rate ratios and strength of sand in the triaxial test". Géotechnique, Vol 16, No 4, pp 338 - 357.

Barden, L. and R.J.W. McDermott (1967) Closure to discussion on "Use of free ends in triaxial testing of clays". Jour.Soil Mechs. and Found. Eng.Div. ASCE, Vol 93, SM1, p 125.

Barnes, J.(1960) "Experimental evidence for the stress-dilatancy theory". M.Sc.thesis, Manchester University.

Bell, J.M. (1965) "Stress-strain characteristics of cohesionless granular

materials subject to statically applied homogeneous loads in an open system". Ph.D. thesis, California Inst.Tech., Pasadena, Calif.

Bell, J.M. (1968) Correspondence on "A new soil testing apparatus". Géotechnique, Vol 18, No 2, pp 267 - 271.

Belshaw, D.J. (1967) "The conditions of strain in sand under triaxial compression". M.Sc.thesis, University of Strathclyde.

Bemben, S.M. (1966) "The influence of controlled strain restraints on the strength and behaviour during shear of a sand tested with a constant volume". Ph.D. thesis, Cornell University.

Bernal, J.D. (1962) "The structure of liquids". The Bakerian Lecture, Proc. Roy.Soc., Series A, Vol 280, pp299-322.

Bernal, J.D., K.R.Knight and I. Cherry (1964) "Growth of crystals from random close packing". Nature, Vol 202,pp 852-854.

Berthier, J and C. Tourenq (1966) "L'essai de compression simple pour les roches". Bul.Liaison Ponts et Chaussées,No 20, juil-août, réf 341, pp 2.1-2.12.

Biarez, J.(1961) "Contribution à l'étude des propriétés mécaniques de sols et des matérieux pulvérulents". D.Sc.thesis, Grenoble University.

Bishop, A.W. (1954) Correspondence on "Shear characteristics of a saturated silt in triaxial compression". Géotechnique, Vol 4, No 1, pp 43-45.

Bishop, A.W. (1961) Panel discussion on "Soil properties and their measurement ". Proc.5th Int.Conf.Soil Mechs. and Found.Eng., Vol 3, pp89-93, 97-100.

Bishop,A.W. (1965) Panel discussion on "Soil properties - shear strength and consolidation". Proc.6th Int.Conf.Soil Mechs. and Found.Eng., Vol 3, pp306-310.

Bishop,A.W. (1966) "The strength of soils as engineering materials". 6th Rankine Lecture, Géotechnique, Vol 16, No 2, pp91-128.

Bishop, A.W. (1967) Discussion to Session 3, "Shear strength of soil other than clay". Proc.Géotechnical Conf., Oslo, 1967. Vol 2,pp 201-204.

Bishop,A.W. and A.K.G.Eldin (1953) "The effect of stress history on the relation between ϕ and porosity in sand". Proc.3rd Int. Conf.Soil Mech. and Found.Eng., pp 126-130.

Bishop,A.W. and D.J.Henkel (1957) "The measurement of soil properties in the triaxial test". Arnold, London, 2nd Edn.,1962.

Bishop, A.W., I.Alpan, G.E.Blight, and I.B.Donald (1960a) "Factors controll-

ing the strength of partly saturated cohesive soils". Proc.Res.Conf. on Shear Strength of Cohesive Soils, Boulder, ASCE, pp 503-532.

Bishop, A.W., I.Alpan, G.E.Blight and I.B.Donald (1960b) Closure of "Factors controlling the strength of partly saturated cohesive soils". Proc.Res.Conf.on Shear Strength of Cohesive Soils, Boulder, ASCE, pp 1027-1042.

Bishop, A.W. and I.B.Donald (1961) "The experimental study of partly saturated soils in the triaxial apparatus". Proc.5th Int.Conf.Soil Mechs.& Found.Eng., Vol 1, pp 13-21.

Bishop, A.W. & R.E.Gibson (1963) "The influence of the provisions for boundary drainage on strength and consolidation characteristics of soil measured in the triaxial apparatus". Symp.Laboratory Shear Testing of Soils, Ottawa, ASTM, STP 361, pp 435-451.

Bishop, A.W. and G.E.Green (1965) "The influence of end restraint on the compression strength of a cohesionless soil". Géotechnique, Vol 15, No 3, pp 243 - 266.

Bishop, A.W., D.L.Webb and A.E.Skinner (1965) "Triaxial tests on soil at elevated cell pressures". Proc.6th Int.Conf.Soil Mech. and Found.Eng., Vol 1, pp 170-174.

Bjerrum, L., S.Kringstad and O.Kummeneje (1961) "The shear strength of a fine sand". Proc.5th Int.Conf.Soil Mech. and Found.Eng., Vol 1, pp 29-37.

Bjerrum, L.and O.Kummeneje (1961) "Shearing resistance of sand samples with circular and rectangular cross sections". Norwegian Géotechnical Institute Publn. No 44.

Blight, G.E. (1961) "Strength and consolidation characteristics of compacted soils ". Ph.D. thesis, University of London.

Blight, G.E. (1963a) "The effect of non-uniform pore pressures on laboratory measurements of the shear strength of soils". Symp.Laboratory Shear Testing of Soils, Ottawa, ASTM, STP 361, pp 173-184.

Blight, G.E. (1963b) Discussion on "Pore pressures within soil specimens in triaxial compression". Symp.Laboratory Shear Testing of Soils, ASTM, STP 361, pp 199-204.

Blight, G.E. (1965) "Shear stress and pore pressure in triaxial testing", Jour.Soil Mechs. and Found.Eng.Div., ASCE, Vol 91, SM6, pp25-39.

Blight, G.E.(1967a) "Observations on the shear testing of indurated fissured clays". Proc.Géotechnical Conf.Oslo,Vol.1, pp 97-102.

Blight, G.E. (1967b) Closure to discussion on "Shear stress and pore pressure in triaxial testing". Jour.Soil Mechs. and Found.Eng.Div., ASCE, Vol 93, SM1, p 125-126.

Borg, I., M.Friedman, J.Handin and D.V.Higgs (1966) "Experimental deformation of St.Peter sand: A study of cataclastic flow". Geological Society of America, Rock Deformation, Memoir 79, pp 133-91.

Borowicka, H.(1961) "The mechanical properties of soils". Proc.5th Int. Conf.Soil Mechs.and Found.Eng., Vol 1, pp39-42.

Botkin, A.I. (1940) "On the strength of granular and brittle materials". (in Russian). Trans.Sci.Res.Inst.Hydrotechnics, Vol 26, pp 206-236.

Broms, B.B. (1963) Discussion on "Basic experiment into soil-structure interaction". Jour.Soil Mechs.and Found.Eng. Div., ASCE, Vol 89,SM 4, pp 223-227.

Broms, B.B. and M.V.Ratnam (1963) "Shear strength of an anisotropically consolidated clay". Jour.Soil Mechs. and Found.Eng.Div., ASCE, Vol 89,SM6, pp 1-26.

Broms, B.B. and A.O.Casbarian (1965) "Effects of rotation of the principal stress axes and of the intermediate stress on the shear strength". Proc. 6th Int.Conf.Soil Mechs.and Found.Eng., Vol 1, pp 179-183.

Broms, B.B. and A.K.Jamal (1965) " Analysis of the triaxial test - cohesionless soils". Proc.6th Int.Conf.Soil Mechs. and Found.Eng.,Vol 1, pp 184-188.

Brown, E.H. (1964) "A theory for the mechanical behaviour of sand". 11th International Congress of Applied Mechanics, Munich, pp 183-191.

Buisson, M. (1948) "Tassements évalués d'après les essais oedométriques - comparaison des hypothèses - appareil triaxial". Travaux, No 164, pp 319-321.

Campbell, L.M. (1963) "Effect of end confinement on the triaxial compression characteristics of sodium kaolinite". Undergraduate Research Report, Dept.of Civil Eng., University of Illinois.

Caquot, A. (1934) "Equilibre des massifs à frottement interne. Stabilité des terres pulvérents et cohérentes." Paris: Gauthier Villars.

Casagrande, A. and W.L.Shannon (1948) "Stress-deformation and strength characteristics of soils under dynamic loads". Proc.2nd Int.Conf.Soil Mech.and Found.Eng., Vol 5, pp 29-34.

Casagrande, A. and S.D.Wilson (1951) "Report to Waterways Experiment

station on triaxial research performed during 1950-1957". Harvard University.

Casagrande, A. and S.J.Poulos (1964) "4th report on investigation of stress-deformation and strength characteristics of compacted clays". Harvard Soil Mechanics Series No 74, Harvard University.

Casbarian,A.O. (1964) "The effect of the rotation of the principal stress axes and variation of the intermediate principal stress on the shear strength of a remoulded clay". Ph.D. thesis, Cornell University.

Casbarian, A.O. and A.K.Jamal (1963) Discussion on "Study of failure envelope of soils" . Jour.Soil Mechs.and Found.Eng.Div., ASCE, Vol 89, SM4, p243.

Chandler, R.J. (1966a) Discussion on "Use of free ends in triaxial testing of clays". Jour.Soil Mechs. and Found.Eng.Div., ASCE, Vol 92, SM4, pp98-100.

Chandler, R.J. (1966b) "The measurement of residual strength in triaxial compression". Géotechnique, Vol 16, No 3,pp 181-186.

Chen, L.S. (1948) "An investigation of stress-strain and strength characteristics of cohesionless soils". Proc.2nd Int.Conf.Soil Mechs. & Found.Eng., Vol 5, p35.

Christensen, N.H.(1961) "Model tests on plane active earth pressures in sand". Danish Géotechnical Inst.Bull.No 10, Copenhagen.

Coleman, J.D.(1960) "Suction and the yield and failure surface for soil in the principal effective stress space". Géotechnique, Vol 10. No 4, pp 181-183.

Cooling, L.F. and H.Q.Golder (1940) "Portable apparatus for compression test of clay soils". Engineering, Vol 147, p 57.

Cornforth, D.H. (1961) "Plane strain failure characteristics of a saturated sand". Ph.D. thesis, University of London.

Cornforth, D.H. (1964) "Some experiments on the influence of strain conditions on the strength of sand". Géotechnique, Vol 14,No 2, pp 143-167.

Cox, A.D., G.Eason and H.G.Hopkins (1961) "Axially symmetric plastic deformations in soils", Phil.Trans. Roy.Soc., A, Vol 254, pp 1-45.

Daniel, A.W.T (1954) "A study of the stress-strain characteristics of granular materials". Ph.D.thesis,University of London.

Daniel, A.W.T.(1957) "Stress-strain characteristics of a granular material" Engineering, July 12,1957.

Dantu, P. (1961) "Etude mécanique d'un milieu pulvérulent formé de sphères égales de compacité maxima". Proc.5th Int.Conf.Soil Mechs. and Found. Eng.Vol 1, p61-70.

D'Appolonia, E and N.M.Newmark (1951) "A method for the solution of the restrained cylinder under compression". Proc.1st U.S.Natl.Conf.of Appl. Mechs.,ASME,pp 217-226.

DeJosselin De Jong, G.(1959) "Statics and kinematics in the failable zone of a granular material". Uitgeverij Waltman, Delft.

Duncan, J.M. and H.B.Seed (1966) "Strength variations along failure surfaces in clay". Jour.Soil Mechs. and Found.Eng.Div., ASCE, Vol 92, SM6, pp 81-104.

Duncan, J.M. and H.B.Seed (1967) "Corrections for strength test data". Jour.Soil Mechs. and Found.Div., ASCE, Vol 93, SM5, pp 121-137.

Duncan,J.D. and P. Dunlop (1968) "The significance of cap and base restraint". Jour.Soil Mechs. and Found.Eng.Div.,ASCE, Vol 94, SM1, pp 271-290.

Dunn, C.S. (1964) "Developments in the design of triaxial equipment for testing compacted soils". Symp.Economic use of Soil Testing in Site Investigation, University of Birmingham, pp 3-19 to 3-25.

Egger, P (1965) "Die abhängigkeit des spannungszustandes in druckversuch von den auflagerungsbedingungen". Publ.Soil Mechs.Inst.Karlsruhe,Tech. Univ., Vol 19, 1965.

Eldin,A.K.G. (1951) "Some fundamental factors controlling the shear properties of sand". Ph.D. thesis, University of London.

Escario, M.V. (1961) Discussion on "Soil properties and their measurement - the magnetic triaxial apparatus". Proc.5th Int.Conf.Soil Mechs. and Found.Eng., Vol III, p 124.

Escario,M.V. and S.Uriel (1961) "Optical methods of measuring the cross-section of samples in the triaxial test". Proc.5th Int.Conf.Soil Mechs. and Found.Eng., Vol 1, pp 89-93.

Esrig, M.I. and S.M.Bemben (1965) Discussion on "Soil properties - shear strength and consolidation". Proc.6th.Int.Conf.Soil Mechs. Found.Eng., Vol 3, pp 321-323.

Farouki, O.T. and H.F.Winterkorn (1964) "Mechanical properties of granular systems". Highway Research Record No 52, Mechanical and Physico-Chemical Properties of Soils, pp 10-42.

Fatt, I. (1957) "Compressibility of a sphere pack-comparison of theory and experiment". Jour.of Applied Mechs., Vol 24, pp 148-149.

Filon, L.N.G.(1902) "On the elastic equilibrium of circular cylinders under certain practical systems of load". Phil.Trans.A.,Vol 198, p 147.

Finn, W.D.L.and H.K.Mittal (1963) "Shear strength of soil in a general stress field". Symp.on Laboratory Shear Testing of Soils, Ottawa, ASTM, STP 361, pp 42-48.

Finn, W.D.L., N.H.Wade and K.L.Lee (1967) "Volume changes in triaxial and plane strain tests". Jour.Soil Mechs. and Found.Eng.Div., ASCE, Vol 93, SM6, pp 297-308.

Fraser, A.M.(1957) "The influence of stress ratio on compressibility and pore pressure coefficients in compacted soils". (2 vols), Ph.D.thesis, University of London.

Freedman, B.M. (1959) "Triaxial tests on sands". M.Sc.thesis, University of Manchester.

Geuze, E.C.W.A.(1963) Reply to discussion on "The uniqueness of the Mohr-Coulomb concept in shear failure". Symp.Laboratory Shear Testing of Soils, Ottawa,ASTM, STP 361, pp 73-75.

Gibson, R.E.(1961) Unpublished work at Imperial College, subsequently described by Bishop & Henkel, 2nd Edn, 1962.

Gibson, R.E. and N.Morgenstern (1963) Discussion of "Stress-dilatancy, earth pressures and slopes". Jour.Soil Mechs.and Found.Div.,ASCE, Vol.89, SM6, pp 127-129.

Gilbert,G.D.(1954) "The basic shear strength properties of Weald Clay". Ph.D.thesis, University of London.

Graton,L.C. and H.J.Fraser (1935). "Systematic packing of spheres with particular attention to porosity and permeability". Jour.of Geology, Vol 43, p 785.

Gray, J.E.(1960) "The relationship between principal stresses, dilatancy and friction angle of a granular material". M.Sc.thesis, University of Manchester.

Green, G.E.(1961) "A model study of the lateral stability of a single pole". M.S.thesis, Northwestern University.

Green, G.E. (1964) Discussion on "Developments in the design of triaxial equipment for testing compacted soils". Symp.Economic Use of Soil Testing in Site Investigation, Birmingham University, pp3.41-3.42.

Green, G.E.(1967) Correspondence on "A new soil testing apparatus". Géotechnique, Vol 17, No 3, p295.

Green, G.E. and A.W.Bishop (1969) 'A note on the drained strength of sand under generalised strain conditions'. Géotechnique, Vol 19. No 1.

Haar, A and T.V.Kármán (1909) "Zur theorie der spannungszustände in plastischen und sandartigen medien". Nachr Ges.Wiss.Göttingen,Math. Phys.Kl., pp 204-18.

Habib, M.P.(1951) "Nouvelles recherches en mecanique du sol. Note complémentaire: Influence de la contrainte intermédiare sur la resistance au cisaillement des sables". Annales de l'Institut Technique du Bâtiment et des Travaux Publics, No 5.

Habib, P.(1952) "La résistance au cisaillement des sols". Doctor's thesis, University of Paris.

Habib, P.(1953) "Influence de la variation de la contrainte principale moyenne sur la résistance au cisaillement des sols". Proc.3rd Int.Conf. Soil Mechs.and Found.Eng., Vol 1, pp 131-6.

Hafiz, M.A.(1950) "Strength characteristics of sands and gravels in direct shear". Ph.D.thesis, University of London.

Harr, M.E.(1966) "Foundations of theoretical soil mechanics".McGraw-Hill, New York.

Haythornthwaite, R.M.(1960a) "Stress and strain in soils". Proc.2nd Symposium on Naval Structural Mechanics,Pergamon Press, pp 185-192.

Haythornthwaite, R.M. (1960b) "Mechanics of the triaxial test". Jour. Soil Mechs. and Found.Eng.Div.,ASCE, Vol 86, SM5, pp 35-62.

Haythornthwaite, R.M. (1960c) Discussion on "Failure hypotheses for soils". Res.Conf.on Shear Strength of Cohesive Soils, Boulder, ASCE, pp 989-91.

Haythornthwaite,R.M. (1963a) "The kinematics of soils" in Progress in applied mechanics, (Prager Anniversary Volume).Collier Macmillan, New York and London.

Haythornthwaite,R.M. (1963b) Discussion on "Study of failure envelope of soils". Jour.Soil Mechs.and Found.Eng.Div., ASCE, Vol 89, SM5,pp119-120.

Hendron, A.J. (1965) Discussion on "Laboratory testing of rock strength". Testing Techniques for Rock Mechanics, ASTM, STP 402, pp 228-231.

Henkel, D.J.(1959) "The relationships between the strength, pore-water pressure and volume-change characteristics of saturated clays", Géotechnique, Vol 9, No 3 pp 119-135.

Henkel,D.J. (1960a) "The shear strength of saturated remoulded clays". Res.Conf.on Shear Strength of Cohesive Soils, Boulder, ASCE, pp 533-554.

Henkel, D.J. (1960b) "The relationships between the effective stresses and water content in saturated clays". Géotechnique, Vol 10.pp 41-54.

Henkel,D.J.and G.D.Gilbert (1952) "The effect of the rubber membrane on the measured triaxial compression strength of clay samples". Géotechnique, Vol 3, pp 20-29.

Henkel, D.J. and N.H.Wade (1966) "Plane strain tests on a saturated remoulded clay". Jour.Soil Mechs.and Found.Eng.Div., ASCE, Vol 92, SM6, pp 67-80.

Hill,R. (1950) "The mathematical theory of plasticity". Oxford University Press.

Hirschfeld, R.C.(1958) "Factors influencing the constant volume strength of clays". Sc.D. thesis, Harvard University, Cambridge, Mass.

Horn, H.M. and D.U.Deere (1962) "Frictional characteristics of minerals." Géotechnique,Vol 12, No 4, pp 319-335.

Horne, M.R. (1965) "The behaviour of an assembly of rotund, rigid, cohesionless particles,Parts I and II". Proc.Roy.Soc., A, Vol 286, pp 62-97.

Horne, M.R. (1969) "The behaviour of an assembly of rotund, rigid, cohesionless particles, Part III". Proc.Roy.Soc.A, in press.

Hvorslev, M.J. (1957) Discussion on "Irregularities in distribution of stress, strains and volume changes in triaxial test specimens". Proc. 4th, Int.Conf.Soil Mech.Found.Eng.,Vol 3, pp 105-107.

Hvorslev, M.J.(1960) "Physical components of the shear strength of saturated clays". Proc.Res.Conf.Shear Strength of Cohesive Soils, Boulder, ASCE, pp 169-273.

Jacobsen, M.(1967) "The undrained shear strength of preconsolidated boulder clay". Proc.Géotechnical Conf.Oslo., Vol I, pp 119-122.

Jaeger, J.C.(1956) "Elasticity, fracture and flow". Methuen, London, pp 94-95.

Jakobson, B. (1957) "Some fundamental properties of sand". Proc.4th Int.Conf.Soil Mechs. and Found.Eng., Vol I, pp 167-171.

Jaky, J. (1944) "A nyugalmi nyomas tenyezoje". Magyar Mernok-es Epitesz-Egylet Kozlonye, pp 355-358.

Jaky,J.(1948) "Pressure in silos". Proc.2nd Int.Conf.Soil Mechs.and Found.Eng., Vol I, pp 103-107.

Jamal, A.K. (1963) "An investigation into the distribution of stresses in a cylindrical specimen loaded to failure in axial compression triaxial tests". M.S.thesis, Cornell University.

Januskevicius, C.K.and E.Vey (1965) "Stresses and strains in triaxial specimens". Instruments and Apparatus for Rock Mechanics, ASTM, STP 392, pp 37-54.

Johansen, K.W. (1958) "Brudbetingelser for sten og beton". (Failure conditions for rocks and concrete). Bygningsstatiske Meddelelser,Vol 19, pp 25-44. Teknisk Forlag, Copenhagen.

Johnson, D.P., J.L.Cross, J.D.Hill and H.A.Bowman (1957) "Elastic distortion error in the dead-weight piston gage". High Pressure Symposium, in Industrial and Engineering Chemistry, Vol 49, pp 2046 -2050.

Jones, R.(1952) "A method of studying the formation of cracks in a material under stress". Brit.Jour.Appl.Phys.Vol 3, No 7, July, p 229.

Jones, R. and M.F.Kaplan (1957) "The effect of coarse aggregate on the mode of failure of concrete in compression and flexure". Mag.Concrete Res.,Vol 9, No 26, August.

Khayatt, A.J.(1965) "The influence of stress path on the stress-dilatancy behaviour of sand". M.Sc.thesis, University of Manchester.

Kirkpatrick, W.M. (1954) "The behaviour of sands under three dimensional stress systems". Ph.D. thesis, Univ.of Glasgow.

Kirkpatrick, W.M.(1957) "The condition of failure for sands". Proc.4th Int.Conf.on Soil Mechs. and Found.Eng.,Vol I, pp 172-8.

Kirkpatrick, W.M.(1961). Discussion on "Mechanics of triaxial test for soils". Jour.Soil Mechs.and Found.Eng.Div.ASCE, Vol 87, SM2,pp 176-177.

Kirkpatrick, W.M.(1967) Discussion to Session 3, "Shear strength of soil other than clay". Proc.Géotechnical Conf.Oslo,1967, Vol 2, pp 204-205.

Kirkpatrick, W.M. and D.J.Belshaw (1968) "On the interpretation of the triaxial test". Géotechnique, Vol 18, No 3, pp 336-350.

Kjellman, W.(1936) "Report on an apparatus for consummate investigation

of the mechanical properties of soils". Proc.Int.Conf.Soil Mechs.and Found.Eng.,Vol II, pp 16-20.

Ko,H.Y.(1966) "Static stress-deformation characteristics of sand". Ph.D. thesis,California Inst.Tech.,Pasadena,Calif.

Ko,H.Y. and R.F.Scott (1967a) "A new soil testing apparatus". Géotechnique, Vol 17, No 1, pp 40-57.

Ko,H.Y.and R.F.Scott (1967b) "Deformation of sand in hydrostatic compression." Proc.ASCE, Vol 93, SM3, pp 137-156.

Ko,H.Y.and R.F.Scott (1967c) "Deformation of sand in shear". Jour.Soil Mechs.and Found.Eng.Div., ASCE, Vol 93, SM5, pp 283 - 310.

Ko, H.Y. & R.F.Scott (1968a) Correspondence on "A new soil testing apparatus". Géotechnique, Vol 18, No 2, pp 273-274.

Ko, H.Y.& R.F.Scott (1968b) "Deformation of sand at failure". Jour.Soil Mechs.and Found.Eng.Div. ASCE, Vol 94, SM4, pp 883-898.

Kolbuszewski, J.J. (1948a) "An experimental study of the maximum and minimum porosities of sand". Proc.2nd Int.Conf.Soil Mech.& Found.Eng., Vol 1, pp 158-165.

Kolbuszewski, J.J.(1948b) "General investigation of the fundamental factors controlling loose packing of sands". Proc.2nd Int.Conf.Soil Mechs.& Found.Eng., Vol 7, pp 47-49.

Krumbein, W.C. and F.J.Pettijohn (1938) "Manual of Sedimentary Petrography". Appleton-Century, New York-London.

Kummeneje, O. (1957) "To-dimensjonale' vakuum - triaxialforsök på törr sand". Norwegian Geotechnical Institute, Int.Report F.80 (unpublished).

Ladanyi, B.(1960) "Étude des relations entre les contraines et les déformations lors du cisaillement des sols pulvérulents". Extrait des Annales des Travaux Publics de Belgique, No 3.

Ladanyi, B.(1967) Discussion on "Plane strain tests on a saturated remoulded clay". Jour.Soil Mechs.and Found.Eng.Div., ASCE, Vol 93, SM5, pp 322-325.

Ladd, C.C. and W.A.Bailey (1964) Correspondence on "The behaviour of saturated clay during sampling and testing". Géotechnique,Vol 14, No 4, pp 353-358.

Ladd, C.C. and J.Varallyay (1965) "The influence of stress system on the behaviour of saturated clays during undrained shear." M.I.T.Report, July.

Lambe,T.W. (1967) "Stress path method." Jour.Soil Mechs.and Found.Eng.Div., ASCE, Vol 93, SM6, pp 309-331.

Larew, H.G. (1960) Discussion on"Nonuniform conditions in triaxial test specimens". Proc.Res.Conf.on Shear Strength of Cohesive Soils, Boulder, ASCE, p 1013.

LaRochelle, P.(1960) "The short term stability of slopes in London clay". Ph.D. thesis, University of London.

LaRochelle, P.(1967) "Membrane, drain and area correction in triaxial test on soil samples failing along a single shear plane". Proc.3rd Pan.Amer.Conf.Soil Mechs.and Found.Eng., Vol 1, pp 273-291.

Lee, I.K. (1966) "Stress-dilatancy performance of feldspar". Jour.Soil Mechs.and Found.Div., ASCE, Vol 92, No SM2, pp 79-103.

Lee, K.L. and H.B.Seed (1964) Discussion to "Importance of free ends in triaxial testing". Jour.Soil Mechs.and Found.Eng.Div., ASCE, Vol 90, SM 6, pp 173-175.

Lenoe, E.M. (1966) "Deformation and failure of granular media under three-dimensional stresses". Experimental Mechanics, Feb 1966,pp99-104.

Leussink, H (1965) Panel discussion on "Soil properties - shear strength and consolidation". Proc.6th Int.Conf.Soil Mechs.and Found.Eng.,Vol 3, pp 302 - 306.

Leussink, H.and W.Wittke (1963) "Difference in triaxial and plane strain shear strength". Symp.Laboratory Shear Testing of Soils, Ottawa, ASTM, STP 361, pp 77-89.

Leussink, H.,W.Wittke and K.Weseloh (1966) "Unterschiede im scherverhalten rolliger erdstoffe und kugelschüttungen im dreiaxial-und biaxialversuch". Publ.Soil Mechs.Inst.Karlsruhe Tech.Univ., Vol 21.

Lomize, G.M. and A.L.Kryzhanovsky (1966) "Basic laws of stressed state and strength of sandy soils" (in Russian). Osnovaniya, fundamenty i mekhanika gruntov, No 3, 8-11, Moscow.

Lomize, G.M. and A.L.Kryzhanovsky (1967) "On the strength of sand". Proc. Géotechnical Conf.Oslo,Vol I, pp 215-219.

Lorenz, H.(1965). Discussion on"Soil properties - shear strength and consolidation". Proc.6th Int.Conf.Soil Mechs.& Found.Eng.,Vol III, p 340.

Lorenz, H.,H.Neumeuer and G.Gudehus (1965) "Tests concerning compaction and displacements performed on samples of sand in the state of plane deformation". Proc.6th Int.Conf.Soil Mechs.and Found.Eng.,Vol 1,pp293-297.

Lovenbury, H.T. (1969) "Creep characteristics of London Clay". Ph.D.thesis, University of London.

Macrae, J.C. and W.A.Gray, (1961) "Significance of the properties of materials in the packing of real spherical particles". Brit. Jour. Appl.Physics, Vol 12, pp 164-172.

Malyshev, M.V.(1963) "The effect of the average principal stresses on the strength of soil, and slip planes". (in Russian), Osnovaniya, fundamenty i mekhanika gruntov, No 1, Moscow. pp 7-11.

Malyshev, M.V. (1967a) "A generalisation of the Mohr-Coulomb strength criterion for soils". Proc.Géotechnical Conf.Oslo, 1967. Vol 1, pp 221-224.

Malyshev, M.V. (1967b) Written contribution to Session 3, "Shear strength of soil other than clay". Proc.Géotechnical Conf.Oslo, 1967. Vol 2, pp 219-220.

Marsal, R.J.(1965) Panel Discussion. Proc.6th Int.Conf.Soil Mechs.and Found.Eng.,Vol 3, pp 310-316.

Marsal, R.J., L.R.deArellano and A.Nuñes G.(1967) "Plane strain testing of rockfill materials". Proc.3rd Pan.Amer.Conf.on Soil Mechs.and Found. Eng., Vol 1, pp 249-271.

Mittal, H.K. (1963) "Effect of plane strain on pore pressure parameters". M.A.Sc.thesis, University of British Columbia, Vancouver.

Mogami, T. and K.Kubo (1953) "The behaviour of soil during vibration". Proc.3rd Int.Conf.Soil Mech.,Vol 1, pp 152-155.

Mogi, K.(1966) "Some precise measurements of fracture strength of rocks under uniform compressive stress". Rock Mechanics and Engineering Geology, Vol 4/1, pp 41-55.

Moretto, O.(1965) General report on "Soil properties - shear strength and consolidation". Proc.6th Int.Conf.Soil Mechs.and Found.Eng.,Vol 3, pp 220-241.

McMurdie, J.L. and P.R.Day (1958) "Compression of soil by isotropic stress". Proc.Amer.Soil Sci.Soc., Vol 22, pp 18-21.

Nadai, A.(1950) "Theory of flow and fracture of solids". Vol I, McGraw-Hill, New York.

Narain, J. and B.Singh(1966) Discussion on "Shear stress and pore pressure in triaxial testing". Jour.Soil Mechs.and Found.Eng.Div., ASCE, Vol 92, SM 4, pp 101-104.

Nash, K.L. and R.K.Dixon (1960) "The measurement of pore pressure in sand under rapid loading triaxial test". Conf.on Pore Pressure and Suction in Soils, London,pp 21-25.

Newland,P.L. and B.H.Allely (1957) "Volume changes in drained triaxial tests on granular materials". Géotechnique, Vol 7, No 1, pp 17-34.

Newland,P.L. and B.H.Allely (1959) "Volume changes during undrained triaxial tests on saturated dilatant granular materials". Géotechnique, Vol 9, pp 174-182.

Newman, K.and L.Lachance (1962) "The testing technique required to obtain a uniform state of uniaxial compressive stress in specimens of concrete and other brittle materials". C.S.T.R., July 1962, Civil Engineering Dept., Imperial College, London.

Newmark, N.(1960) "Failure hypotheses for soils". Res.Conf.on Shear Strength of Cohesive Soils,Boulder,ASCE, pp 17-32.

Norwegian Geotechnical Institute (1958) "Triaxial compression and extension tests on a saturated fine and uniform graded sand". Internal Report, F 94. (Unpublished).

Olsen, R.E. (1962) Discussion on "The shear strength properties of calcium illite". Géotechnique, Vol 12, No 4, pp 355-358.

Olsen, R.E. (1965)
Personal communication.

Olsen, R.E. and M.L.Kiefer (1963) "Effect of lateral filter-paper drains on the triaxial shear characteristics of soils". A.S.T.M., S.T.P. No 361, pp 482-491.

Olsen, R.E. and L.Campbell (1964) Discussion to "Importance of free ends in triaxial testing". Jour.Soil Mechs.and Found.Eng.Div., ASCE, Vol 90, SM6, pp 167-173.

Olsen,R.E. and L.M.Campbell (1967) "Bushing friction in triaxial shear testing". Materials Research and Standards, Vol 7, No 2, pp 45-52.

Parkin, A.K.(1964) "The application of discrete unit models to studies of the shear strength of granular materials". Ph.D.thesis, University of Melbourne.

Parkin, A.K.(1965) "On the strength of packed spheres". Jour.Aust.Math. Soc.,Vol 5, part 4, pp 443-452.

Parkin,A.K.(1967) Discussion on "Incremental strain rate ratios and the strength of sand in the triaxial test". Géotechnique, Vol 17, No 2, pp 171-172.

Parkin,A.K., C.M.Gerrard and D.R.Willoughby (1968) Discussion on "Deformation of sand in hydrostatic compression". Jour.Soil Mechs.and Found.Eng.Div., ASCE, Vol 94, SM1, pp 336-340.

Parry, R.H.G. (1956) "Strength and deformation of clay". Ph.D.thesis, University of London.

Peltier, M.R.(1957) "Recherches expérimentales sur la courbe intrinsèque de rupture des sols pulvérulents". Proc.4th Int.Conf.Soil Mechs.and Found.Eng., Vol 1, pp179-182.

Penman,A.D.M.(1953) "Shear characteristics of a saturated silt, measured in triaxial compression". Géotechnique, Vol 3, No 4, pp 312-328.

Petley, D.J. (1966) "The shear strength of soils at large strains". Ph.D. thesis, University of London.

Phalen, T.E.(1960) Discussion on "Nonuniform conditions in triaxial test specimens". Proc.Res.Conf.on Shear Strength of Cohesive Soils, Boulder, ASCE, pp 1002-1012.

Pickett, G.(1944) "Application of the Fourier method to the solution of certain boundary problems in the theory of elasticity". Jour.Applied Mechs., ASME, Vol 2, Part A, pp 176-182.

Prager,W.and P.G.Hodge (1951) "Theory of perfectly plastic solids". John Wiley, London, p4.

Procter, D.C. (1967) "The stress-dilatancy behaviour of dense sand in the hollow cylinder test". M.Sc. thesis, University of Manchester.

Rennie, B.C.(1959) "On the strength of sand". Jour.Aust.Math.Society, Vol 1, pp 71-79.

Reynolds, O.(1885) "On the dilatancy of media composed of rigid particles in contact,with experimental illustrations". Philosophical Mag.series 5, Vol 20, pp 469-481.

Reynolds, O.(1886a) "Experiments showing dilatancy, a property of granular material, possibly connected with gravitation". Proc.Roy.Inst., Vol 11, pp 354-363.

Reynolds, O.(1886b) "On the theory of lubrication and its application to Mr.Beauchamp-Tower's experiments, including an experimental determination of the viscosity of olive oil". Phil.Trans.Roy.Soc.,Vol 177,p 157.

Roscoe, K.H.(1953) "An apparatus for the application of simple shear to soil samples". Proc.3rd Int.Conf.Soil Mechs.,Vol 1, pp 186-191.

Roscoe, K.H., A.N.Schofield and C.P.Wroth, (1958) "On the yielding of soils".Géotechnique, Vol 8, pp 22-53.

Roscoe, K.H., A.N.Schofield and C.P.Wroth (1959) Discussion on "On the yielding of soils". Géotechnique, Vol 9, No 2, pp 72-82.

Roscoe, K.H. and H.B.Poorooshasb (1963) "A theoretical and experimental study of strains in triaxial compression tests on normally consolidated clays". Géotechnique, Vol 13, No 1, pp 12-38.

Roscoe, K.H. and A.N.Schofield (1963) "Mechanical behaviour of an idealised 'wet -clay'". Proc.2nd European Conf.Soil Mech.,Wiesbaden, Vol 1, pp 47-54.

Roscoe, K.H. , A.N.Schofield and A.Thurairajah (1963a) "An evaluation of test data for selecting a yield criterion for soils". Symp. Laboratory Shear Testing of Soils, Ottawa, ASTM, STP 361, pp 111-128.

Roscoe, K.H., A.N.Schofield and A.Thurairajah (1963b) "Yielding of clays in states wetter than critical". Géotechnique, Vol 13, No 3, pp 211-240.

Roscoe, K.H. , J.R.F.Arthur and R.James (1963c) "The determination of strains in soils by an X-ray method". Civil Eng.and Pub.Wks. Rev., Vol 58, pp 873-876 and 1009-1012.

Roscoe, K.H.and A.N.Schofield (1964) Discussion on "Stress - dilatancy, earth pressures and slopes". Jour.Soil Mechs.and Found.Div.ASCE, Vol 90, SM1, pp 136-150.

Roscoe, K.H., R.H.Bassett and E.R.L.Cole (1967) "Principal axes observed during simple shear of a sand". Proc.Géotechnical Conf.,Oslo, Vol 1, pp 231-237.

Roscoe, K.H. and J.B.Burland (1968) "On the generalised stress-strain behaviour of 'wet' clay". in Engineering Plasticity, edit.by J.Heyman & F.A.Leckie, C.U.P.

Rowe, P.W.(1962) "The stress-dilatancy relation for static equilibrium of an assembly of particles in contact". Proc.Roy.Soc.A, Vol 269,pp500-527.

Rowe, P.W.(1963) "Stress-dilatancy, earth pressures and slopes". Jour.Soil Mechs.and Found.Div.,ASCE, Vol 89, SM3, pp 37-61.

Rowe, P.W.(1964a) Discussion on "Some experiments on the influence of strain conditions on the strength of sand". Géotechnique, Vol 14,No 4, pp 361-364.

Rowe, P.W. (1964b) Closure to discussion on "Stress-dilatancy, earth pressures and slopes". Jour.Soil Mechs.and Found.Eng.Div., ASCE, Vol 90, SM4, pp 145-180.

Rowe, P.W.(1969) "The relation between the shear strength of sands in

triaxial compression, plane strain and direct shear". Géotechnique, in press.

Rowe, P.W.and L.Barden (1964) "Importance of free ends in triaxial testing". Jour.Soil Mechs.and Found.Div., ASCE, Vol 90, SM1, pp 1-27.

Rowe, P.W.,L.Barden and I.K.Lee (1964) "Energy components during the triaxial cell and direct shear tests". Géotechnique, Vol 14, No 3, pp 247-261.

Rowe, P.W. and L.Barden (1965) Closure to discussion on "Importance of free ends in triaxial testing". Jour.Soil Mechs.and Found.Eng.Div.,ASCE, Vol 91, SM 3, pp 105-106.

Rowe, P.W. and K.Peaker (1965) "Passive earth pressure measurements". Géotechnique, Vol 15, No 1, pp 57-78.

Rutledge, P.C.(1947) "Cooperative triaxial shear research program, progress report on soil mechanics fact finding survey". Corps of Engrs.U.S.Dept. of the Army, Waterways Experiment Station, Vicksburg, Miss.

Saada, A.S.(1962) "A rheological analysis of shear and consolidation of saturated clays". Stress Distribution in Earth Masses, HRB Bull.342, pp 52-76.

Saada, A.S. (1963) Discussion on "The uniqueness of the Mohr-Coulomb concept of shear failure". Symp.Laboratory Shear Testing of Soils, Ottawa, ASTM, STP 361, pp 69-73.

Saada, A.S. and A.K.Baah (1967) "Deformation and failure of a cross anisotropic clay under combined stresses". Proc.3rd Pan.Amer.Conf.on Soil Mechs.and Found.Eng., Vol 1, pp 67-88.

Schofield, A. and P.Wroth (1968) Critical State Soil Mechanics. McGraw-Hill, London.

Scott,R.F. (1963a) "Principles of soil mechanics". Addison Wesley, London.

Scott, R.F.(1963b) Discussion on "The uniqueness of the Mohr-Coulomb concept in shear failure". Symposium Laboratory Shear Testing of Soils, Ottawa, ASTM, STP 361, pp 75-76.

Scott, R.F.(1964) Discussion on "Stress-dilatancy, earth pressures and slopes". Jour.Soil Mechs.and Found.Div.ASCE, Vol 90, SM1, pp 133-135.

Seth, B.R.(1941) "On Guest's law of elastic failure". Proc.Ind.Academy Sciences,A. Vol 14, pp 37-40.

Shibata, T.(1966) Private communication.

Shibata, T. and D.Karube (1965) "Influence of the variation of the inter-

mediate principal effective stress on the mechanical properties of normally consolidated clays". Proc.6th Int.Conf.Soil Mechs.and Found. Eng.,Vol 1, pp 359-363.

Shibata, T. and D.Karube (1967) Discussion on "Plane strain tests on a saturated remoulded clay". Jour.Soil Mechs.and Found.Div., ASCE, Vol 93, SM 5, pp 325-327.

Shockley, W.G.(1953) Discussion on "Laboratory investigations including compaction tests, improvement of soil properties". Proc.3rd Int.Conf. Soil Mechs.,Vol 3, p 122.

Shockley, W.G. and R.G.Ahlvin (1960) "Nonuniform conditions in triaxial test specimens". Proc.Res.Conf.on Shear Strength of Cohesive Soils, Boulder, ASCE, pp 341-357.

Sinha, S.B., B.R.Sen and P.D.S.Verma (1961) "Stress distribution in the triaxial compression test". Bull.de l'Académic Polonaise de Sciences, Série de sciences techniques, Vol 9, No 3, pp 169-173.

Skinner, A.E.(1969) 'The effect of high pore-water pressures on the mechanical behaviour of sediments'. Ph.D.thesis, University of London.

Skipp, B.O. and L.Renner (1963) "The improvement of the mechanical properties of sand", in Grouts and Drilling Muds in Engineering Practice, Butterworths, London.

Smith, D.(1965) "The influence of particle shape on the limiting porosities and shear strength of sands". M.Sc.thesis, Liverpool University.

Smotrych, S.(1969) "The physical and mechanical properties of the Avonmouth clay". Ph.D.thesis, University of London.

Sowa, V.A.(1963) "A comparison of the effects of isotropic and anisotropic consolidation on the shear strength behaviour of a clay". Ph.D.thesis, University of London.

Sparrow, R.W. and A.N.S.Beaty (1964) "An instrumented triaxial cell base". Sols Soils, Vol 3, No 8. March.

Spencer, M.E.(1961) Discussion on"The relationship between porosity and angle of internal friction". Proc.5th Int.Conf.Soil Mechs.and Found. Eng.,Vol 3, p 138-140.

Suklje, L. and J.Drnovsek (1965) "Investigation of the tensile deformability of soils using hollow cylinders". Proc.6th Int.Conf.Soil Mechs. & Found. Vol 1, pp 368-372.

Taylor, D.W.(1941) "Cylindrical compression research program on stress-deformation and strength characteristics of soils". 7th Progress Report to U.S.Engineer Department, M.I.T., Cambridge,Mass.

Taylor, D.W.(1950) "Triaxial research on clay". Soil Mechanics Laboratory, M.I.T., Cambridge, Mass.

Taylor, D.W.(1955) "Review of research on shearing resistance of clay". Soil Mechanics Laboratory, M.I.T., Cambridge, Mass.

Taylor, D.W.and R.H.Clough (1951) "Research on shearing characteristics of clay". Soil Mechanics Laboratory, M.I.T., Cambridge,Mass.

Tchalenko, J.S.(1967) "The influence of shear and consolidation on the microscopic structure of some clays". Ph.D.thesis, University of London.

Terzaghi, K.(1934) "Large retaining-wall tests. I.Pressure of dry sands". Eng. News Record, Vol 112, pp 136-140.

Thurairajah, A.(1961) "Some shear properties of kaolin and of sand". Ph.D. thesis, University of Cambridge.

Thurston, C.W. and H.Deresiewicz, (1959) "Analysis of a compression test of a model of a granular material". Jour.Appl.Mechanics, Vol 26, Series E, No 2, pp 251-258.

Tombs, G.(1969) "Strength and deformation characteristics of rockfill". Ph.D.thesis, University of London.

Trollope, D.H. and A.K.Parkin (1963) Discussion on "Stress-dilatancy, earth pressures and slopes". Jour.Soil Mechs.and Found.Div., ASCE., Vol 89, SM6, pp 129-133.

Truesdale, W.B. and R.W.Rusin (1963) Discussion on "An evaluation of test data for selecting a yield criterion for soils". Symp.Laboratory Shear Testing of Soils, Ottawa,ASTM, STP 361, pp 129-133.

Tschebotarioff, G.P. and J.D.Welch (1948) "Lateral earth pressures and friction between soil minerals". Proc.2nd Int.Conf.Soil Mechs.,Vol 7, pp 135-138.

Tschebotarioff, G.P.,E.R.Ward, E.Dibiagio and J.Watkins(1956) "Large-scale triaxial cell tests". Progress Report to Office of Naval Research, Princeton Univ.,N.J.

Vesić, A. and R.D.Barksdale (1963) Discussion on "Shear strength of soils at very high pressures". Laboratory Shear Testing of Soils, ASTM, STP 361, pp 301-305.

Vesić, A. and G.W.Clough (1968) "Behaviour of granular materials under

high stresses". Jour.Soil Mechs.and Found.Eng.Div.,ASCE., Vol 94,SM3, pp 661-688.

Wade, N.H.(1963) "Plane strain failure characteristics of a saturated clay". Ph.D.thesis, University of London.

Walker, B.P.(1964) "Experiments on model pile foundations in sand". Ph.D. thesis, University of London.

Walker, B.P. and T.Whitaker (1967) "An apparatus for forming uniform beds of sand for model foundations tests". Géotechnique, Vol 17, pp 161-167.

Warlan,A.A.(1960) "Recent progress in triaxial apparatus design". Proc. Research Conf.on Shear Strength of Cohesive Soils, Boulder, ASCE, pp 859-876.

Waterways Experiment Station, Vicksberg (1947) "Triaxial shear research and pressure distrubution studies on soils". Progress report, W.E.S., Vicksberg.

Waterways Experiment Station, Vicksburg (1950) "Triaxial tests on sands - Reid Bedford Bend, Mississippi River". Report No. 5-3.

Webb, D.L. (1966) "The mechanical properties of undisturbed samples of London clay and Pierre shale". Ph.D.thesis, University of London.

Whitman, R.V. and U.Luscher (1962) "Basic experiment into soil-structure interaction". Jour.Soil Mechs.and Found.Eng.Div., ASCE, Vol 88, SM6, pp 135-167.

Wightman, A.(1967) "The stress-dilatancy of sands during plane strain compression". M.Sc.thesis, Manchester University.

Wittke, W.(1962) "Über die scherfestigkeit rolliger erdstoffe; rechnerische und experimentelle untersuchung von kugelschüttungen". (On the shear strength of cohesionless soils—experimental and mathematical investigations of ball packings), Publ.Soil Mechs.Inst. Karlsruhe Tech.Univ., Vol 11 , 1962.

Wood, C.C.(1958) "Shear strength and volume change characteristics of compacted soil under conditions of plane strain". Ph.D.Thesis, University of London.

Wu, T.H.,A.K.Loh and L.E.Malvern (1963) "Study of failure envelopes of soils". Jour.Soil Mechs.and Found.Eng.Div., ASCE., Vol 89, SM1, pp 145-181.

Yong, R.N. and E.McKyes (1967) "Yielding of clay in a complex stress field". Proc.3rd Pan.Amer.Conf. Soil Mechs.and Found.Eng.,Vol 1, pp 131-143.